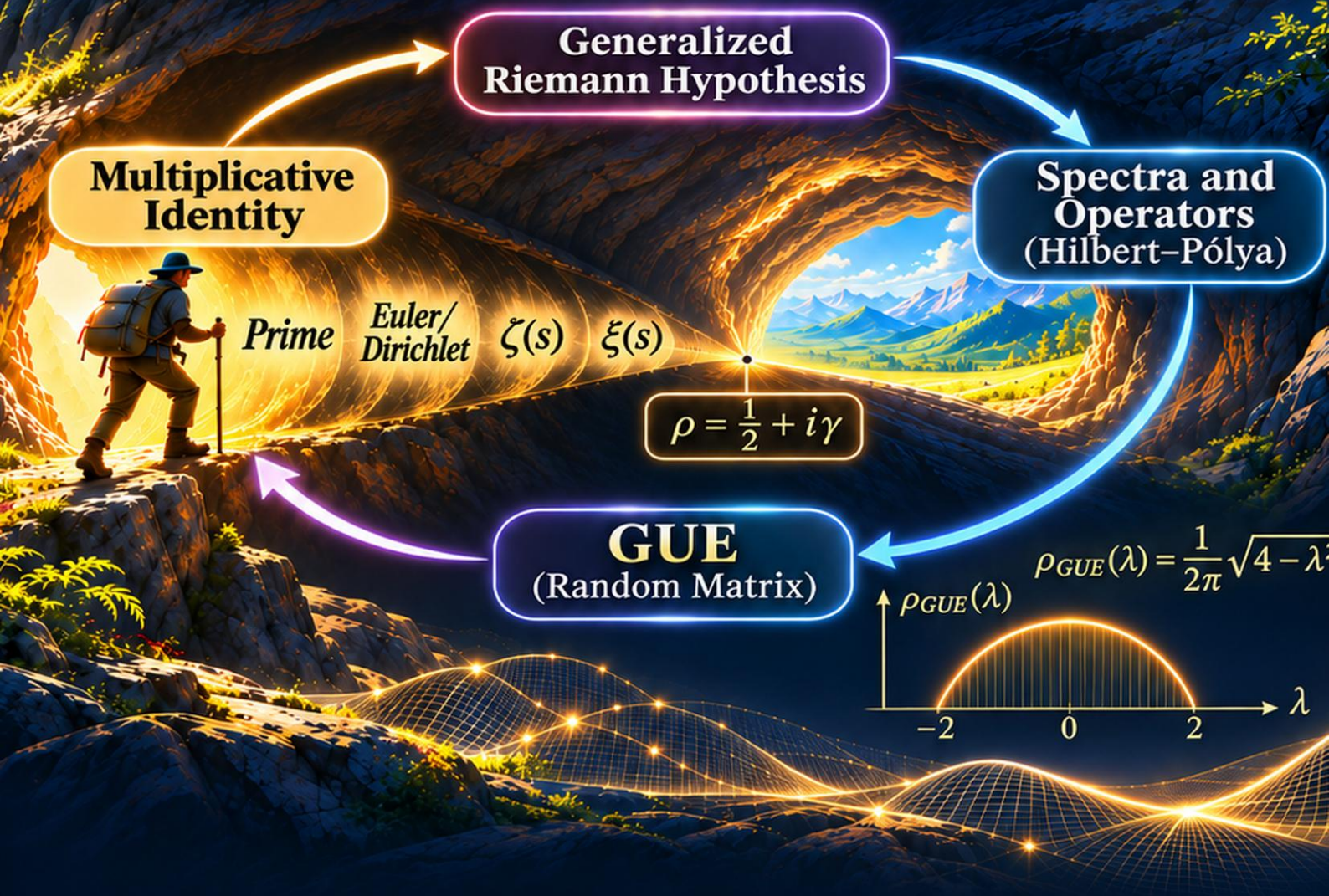
The Riemann Hypothesis: Proof, Spectra, and the Mathematical World Behind It

— From Multiplicative Identity and the Generalized Riemann Hypothesis to Hilbert–Pólya and GUE

$$\zeta(s) = \sum_{n=1}^{\infty} \frac{1}{n^s}$$

$$\rho = \frac{1}{2} + i\gamma$$



Yifei Ren

Independent Researcher

No Zeros

Only Heartbeats

The Riemann Hypothesis: Proof, Spectra, and the Mathematical World Behind It

— From Multiplicative Identity and the Generalized Riemann Hypothesis to Hilbert–Pólya and GUE

Author Yifei Ren

Author status Independent Researcher

Publication date November 12, 2026

Email zentiger@qq.com

ORCID 0009-0009-1373-9609

WeChat ryfweixin

GitHub (interactive teaching website and software for this book) https://github.com/qiaoranjushi/ghtmath

Highly Recommended Interactive Classroom https://qiaoranjushi.github.io/ghtmath/

Book DOI 10.5281/zenodo.23864108

This book is currently a preprint and is not under contract with a publisher. If you believe it may be suitable for publication, I would be glad to hear from you and discuss possible collaboration.

I am an independent researcher. If you would like to support my research financially, I would be sincerely grateful for your support.

arXiv endorsement request I am currently seeking endorsement to submit to the arXiv math.NT (Number Theory) category. If you are eligible to endorse submissions in this category and are willing to support my submission, please visit:

https://arxiv.org/auth/endorse?x=X4R44M

Thank you for your time and help.

Intellectual background The foundational ideas behind this book grew out of *Foundations of Mathematics: An Introduction to Generative History Theory (GHT)*.

https://doi.org/10.5281/zenodo.23662772

Copyright and license © 2026 Yifei Ren.

Unless otherwise indicated, this book is licensed under the **Creative Commons Attribution–NonCommercial 4.0 International License (CC BY-NC 4.0)**. Subject to the attribution and noncommercial-use conditions of that license, anyone may copy, distribute, display, adapt, and build upon the contents of this book. Third-party material and material carrying separate copyright notices remain subject to their respective terms.

Author's Note

I am still a beginner in mathematics, and I have only recently begun to explore these questions systematically.

This book records my present understanding, proofs, and organization of the Riemann Hypothesis, the Generalized Riemann Hypothesis, the Hilbert–Pólya spectral route, and the related mathematical structures. It is not intended as an endpoint beyond revision. Because my knowledge, research experience, and powers of exposition are limited, some definitions may still admit sharper formulation, some arguments may be strengthened, and some terminology or formalization may require correction. There may also be errors that I do not yet see.

Mathematics is worth sustained effort precisely because it permits public scrutiny, independent verification, criticism, correction, and reconstruction. I therefore welcome line-by-line examination of the definitions, theorems, proof chains, and interchapter dependencies in this book. If an error is found, I hope it will be identified at the exact point where it occurs, together with the missing condition or a counterexample, so that the issue can be corrected at the level of testable mathematics.

At the same time, this note is not meant to weaken the mathematical conclusions stated explicitly in the main text. The claims made here concerning proofs of the Riemann Hypothesis, the Generalized Riemann Hypothesis, and the independent source-generated Hilbert–Pólya spectral route stand or fall with the definitions, theorems, and proofs in the book itself. The author's identity, background, or self-assessment can neither replace a proof nor replace judgment of the proof.

What I hope is simple: the reader should not have to believe the author in order to walk the proof all the way through again.

Contents

Preface — From the Question of 1859 to a Double Closure of Identity and Spectrum 1
Chapter 1 Open Multiplicative Relations, Analytic Identity Fidelity, and Reciprocal Zero-Event Closure of the Riemann Hypothesis 24
Chapter 2 Horizon-Shape Geometry of Riemann Zero Gaps 66
Chapter 3 Identity Addresses and Analytic Multiplicities of Riemann Zeros 89
Chapter 4 Parameterization of the Riemann Closure Kernel and Proof of the Generalized Riemann Hypothesis 105
Chapter 5 A Faithful Event Spectral Atlas after Closure of the Riemann Hypothesis 141
Chapter 6 The Ren Operator: A Lossless Bridge between Multiplicative Identity, Analytic Continuation, and the Canonical Spectrum 166
Chapter 7 Riemann Spectral Witness Theorem: Uniqueness of the Ren Canonical Spectral Witness and Hilbert–Pólya Identity Transfer 204
Chapter 8 From the Riemann Spectral Witness to GUE 231
Chapter 9 Another Closure Path for the Riemann Hypothesis: Open Multiplicative Identity and an Independent Hilbert–Pólya Spectral Route 281
Afterword 320
Part I — Seeing What Was There All Along: How a Problem Is Made, and How It Becomes Visible Again 322
Part II — When Identity Reappears: How Proof Moves from Explanation into Mathematics 328
Part III — After Proof: Public Verification, History, and Mathematics That Continues to Grow 332
Acknowledgements 338
References 341

Preface — From the Question of 1859 to a Double Closure of Identity and Spectrum

1. Why Has a Conjecture of One Sentence Lasted for More Than a Century and a Half?

The standard statement of the Riemann Hypothesis is extraordinarily concise.

Let $\zeta(s)$ be the Riemann zeta function, and let ρ range over its nontrivial zeros. The conjecture asserts that

$$\boxed{\Re\rho = \frac{1}{2} \qquad \text{for every nontrivial zero} \rho.}$$

One sentence, one real part, one fixed value.

Yet from 1859 to the present, this sentence has drawn the attention of generations of mathematicians and has produced an unusually persistent convergence of complex analysis, analytic number theory, spectral theory, harmonic analysis, operator theory, probabilistic models, random matrices, geometric analogies, and large-scale computation. It formed part of the eighth problem in Hilbert's 1900 list and is one of the seven Millennium Prize Problems announced by the Clay Mathematics Institute in 2000.[2][7]

The historical weight of the conjecture is almost impossible to understand from the length of its statement alone.

What makes the Riemann Hypothesis the Riemann Hypothesis is not merely the question of whether all zeros lie on one line. More deeply, it stands at the intersection of the multiplicative structure of the integers, the distribution of primes, analytic continuation, the functional equation, the zero spectrum, explicit formulas, and the possible existence of an underlying self-adjoint spectral structure. It is a very small interface connecting an enormous mathematical world.

This book unfolds at that interface.

Its point of departure is not that the methods of the past were wrong, nor that one must invent a technique stronger than all existing ones.

On the contrary, the book begins by acknowledging a fact:

> **The mathematics built around the Riemann Hypothesis over more than 160 years was not wasted.**

Without the Euler product, there would be no first bridge between the multiplicative structure of the primes and the zeta function. Without Riemann's analytic continuation, functional equation, and explicit-formula ideas, there would be no later world of zeta zeros. Without Hadamard and de la Vallée Poussin, there would be no analytic proof of the prime number theorem in 1896. Without the sustained work of Hardy, Selberg, Levinson, Conrey, and others on zeros on the critical line, we would not know how far the line has already been reached rigorously. Without Turing, Odlyzko, and the computational tradition that followed, we would not possess such strong finite-height evidence.

Without the equivalent and positivity criteria of Weil, Nyman–Beurling, Li, and others, we would not know how many mature mathematical languages can express the Riemann Hypothesis. Without the long Hilbert–Pólya vision and the spectral routes of de Branges, Connes, Berry–Keating, Suzuki, and others, the deeper question—whether the zeros are in some sense the spectrum of a self-adjoint operator—would not have taken its present form. Without Montgomery, Dyson, Odlyzko, Katz–Sarnak, and related work, the remarkable second-order relation between zeta zeros and GUE/CUE would not be part of today's mathematical landscape.[5][8]–[42]

This book does not stand outside that history.

It stands on roads already built by it and asks again a more basic question:

When the mathematical representation changes, has the identity of the represented object really changed as well?

This is not a philosophical slogan.

It directly determines whether a new coordinate represents genuinely new information or merely a readout of the same object in another mature representation; whether a new proof obligation comes from the object itself or from the way we have partitioned it; whether a seemingly new "final gap" actually reduces the information needed for a proof or merely moves the same debt into another language.

This is the point of entry that most clearly distinguishes the present book from the traditional literature on the Riemann Hypothesis.

2. From Euler to Riemann: Primes Enter the Complex Domain

Riemann's work did not arise in a vacuum.

In the eighteenth century, Euler had already connected

$$\zeta(s) = \sum_{n=1}^{\infty} \frac{1}{n^s}$$

with the prime product

$$\zeta(s) = \prod_{p} (1 - p^{-s})^{-1}, \qquad \Re s > 1.$$

[1][5]

The Euler product is one of the great starting points of analytic number theory. It compresses two apparently different objects into a single function:

Dirichlet reading of all positive integers	=	Euler reconstruction from prime multiplicative generators.

Thus zeta was never merely a complex function.

From the outset, it carried the multiplicative structure of the positive integers.

In the early nineteenth century, numerical observations by Gauss and Legendre gradually revealed the macroscopic density profile of the primes. The prime-counting function

$$\pi(x) = \#\{p \le x : p \text{ is prime}\}$$

appeared to satisfy

$$\pi(x) \sim \frac{x}{\log x}.$$

In 1859, in his very short yet extraordinarily influential paper *Ueber die Anzahl der Primzahlen unter einer gegebenen Grösse*, Riemann transported the problem into the complex plane.[2] Rather than studying $\pi(x)$ alone, he studied the analytic continuation and functional equation of zeta and its zeros, thereby establishing a precise connection between the distribution of primes and complex zeros.

That step changed the direction of number theory.

Primes were no longer only discrete objects on the integer axis.

They acquired a kind of spectral shadow.

Riemann's completed function may be written

$$\xi(s) = \frac{1}{2}s(s-1)\pi^{-s/2}\Gamma\left(\frac{s}{2}\right)\zeta(s),$$

and satisfies the complementary symmetry

$$\xi(s) = \xi(1-s).$$

The nontrivial zeros lie in the critical strip

$$0 < \Re s < 1,$$

and Riemann's conjecture is precisely

$$\boxed{\Re\rho = \frac{1}{2}.}$$

From that moment on, the theory of primes acquired a new central question:

> Why should every nontrivial zero lie on the critical line?

3. 1896: Riemann's Method First Proves the Prime Number Theorem and Leaves the Deeper Question Open

Riemann did not prove his conjecture.

But the power of his ideas soon became evident.

In 1896, Hadamard and de la Vallée Poussin independently proved that zeta has no zeros on the line

$$\Re s = 1,$$

thereby proving the prime number theorem:

$$\boxed{\pi(x) \sim \frac{x}{\log x}.}$$

Hadamard's paper studied directly the distribution of zeta zeros and their arithmetic consequences; de la Vallée Poussin's analysis tightly connected zero-free regions with prime asymptotics.[3][4]

This historical moment is crucial.

It shows that even without the Riemann Hypothesis, Riemann's complex-analytic framework was already strong enough to solve what had been one of the central problems concerning the distribution of primes.

At the same time, it clarified the meaning of the Riemann Hypothesis.

The prime number theorem gives the average profile.

The Riemann Hypothesis controls the scale of fluctuations around that profile.[7]

In other words, the difference between the PNT and the Riemann Hypothesis is not merely that one is proved and the other is not.

They represent two different levels of information:

average distribution versus fine fluctuations about the average.

This helps explain why the Riemann Hypothesis gradually became one of the central problems of analytic number theory.

4. From Hardy to Conrey: The Critical Line Is Not an Empty Formal Center

One important direction in the twentieth century was to prove that ever more zeros actually lie on the critical line.

In 1914, Hardy proved that there are infinitely many zeros on

$$\Re s = \frac{1}{2}.$$

[9]

This was a major step. It showed that the critical line is not merely a formal center selected by symmetry while the zeros themselves never reach it.

Hardy–Littlewood, Selberg, and others continued to advance the counting of zeros on the line. In 1942, Selberg proved that a positive proportion of the nontrivial zeros lie on the critical line. In 1974, Levinson raised the proportion to at least one third.[10] In 1989, Conrey proved that more than two fifths of the zeros lie on the line, with simplicity in the corresponding sense.[11]

These results continually enlarged the part already known to lie on the critical line.

But they also exposed the universal quantifier in the Riemann Hypothesis with complete clarity:

infinitely many $\neq$ a positive proportion $\neq$ more than$40\% \neq 100\%$.

The Riemann Hypothesis does not say that many zeros lie on the line.

It says:

not a single one may leave it.

Methodologically, this distinction matters. Many mathematical tools are well suited to controlling averages, proportions, densities, and large sets; the Riemann Hypothesis demands a universal statement with no exception.

For more than a century, therefore, mathematics has not only sought sharper estimates. It has also sought a mechanism capable of locking local pointwise behavior to a global structure.

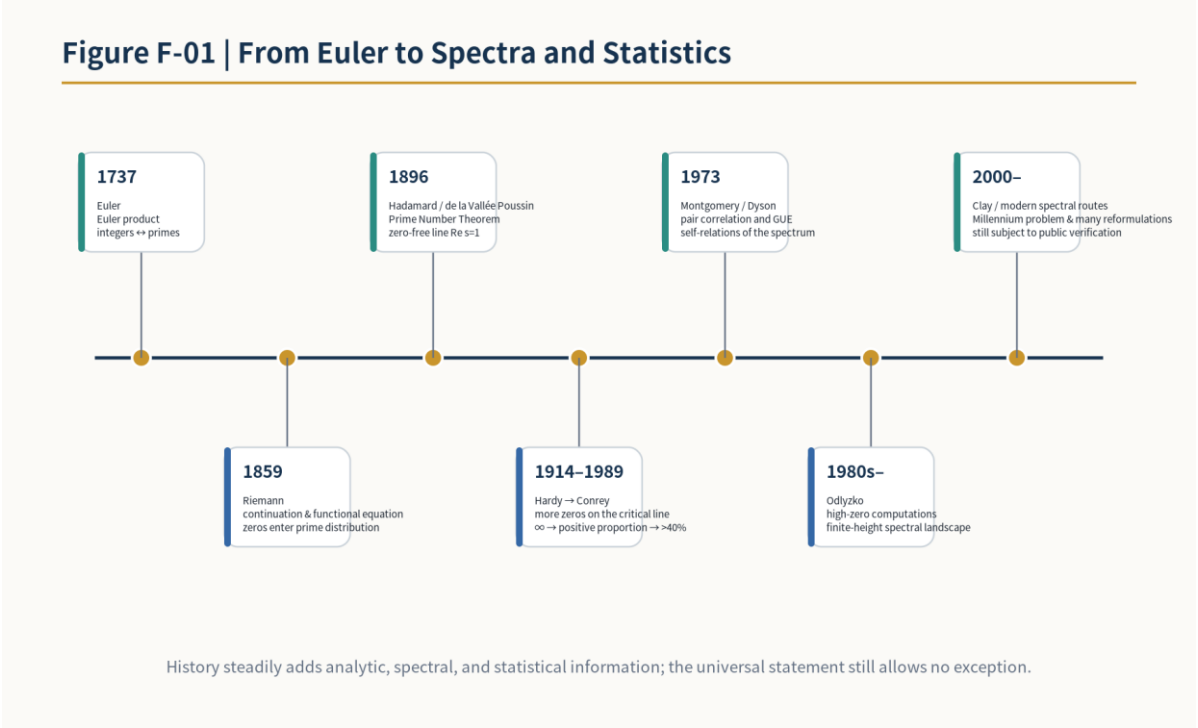


Figure F-01. From Euler to spectra and statistics: the long history of the Riemann Hypothesis. From Euler's product and Riemann's complex-analytic framework to critical-line results, Montgomery–Dyson pair correlation, and Odlyzko's high-zero computations, history has continually added analytic, spectral, and statistical information; the universal statement of RH nevertheless still permits no exception.

5. Computation, Equivalent Criteria, and Positivity Routes: New Pictures of the Same Problem

Another major historical current has been to translate the Riemann Hypothesis into other mathematical problems.

Turing developed a systematic method for checking zeta zeros, allowing finite-height verification to come with rigorous completeness of the zero count.[12] Booker and others later developed and organized this tradition further.[13] Odlyzko's computations of very high zeros made it possible, for the first time, to observe the statistics of zero spacings at extraordinary heights.[14]

But finite computation can always answer only

Has any counterexample appeared within the range checked?

It cannot automatically turn a finite height into a universal infinite conclusion.

At the same time, the Riemann Hypothesis acquired many equivalent formulations.

Weil connected explicit formulas with positivity conditions.[15] Nyman and Beurling translated the Riemann Hypothesis into density questions for certain function subspaces in L^2 or L^p.[16][17] Li translated it into the nonnegativity of a sequence of coefficients.[18]

These criteria are mathematically powerful.

They tell us that

> the Riemann Hypothesis does not live only in the coordinates of its zeros.

It can be expressed as a positivity problem, an approximation problem, a function-space problem, an arithmetic-cancellation problem, or a spectral problem.

Yet equivalence brings a persistent difficulty of its own:

$$A \Leftrightarrow B$$

does not imply that B is easier than A.

If the new representation merely transports the original critical difficulty intact, then we have obtained a new coordinate system, not a reduction in proof debt.

This is one of the points to which the present book pays particular attention.

A Geometric Analogy: Function Fields Show That "Riemann-Hypothesis-Type" Statements Can Arise from Higher Structure

There is another direction in the history of the Riemann Hypothesis that cannot be ignored: the function-field analogy.

For algebraic curves and, more generally, algebraic varieties over finite fields, zeta functions likewise possess Euler products, functional equations, and zero problems. Weil lifted these objects into algebraic geometry and cohomology, and Deligne later completed the deepest "Riemann hypothesis" part of the Weil conjectures.[68][69]

This history leaves a profound lesson for the number-field Riemann Hypothesis:

> zeros lying on the "correct line"may not be the result of pointwise estimates,but a spectral, weight-theoretic, or positivity consequence of higher structure.

But the success of the function-field case cannot simply be imported as a proof in the number-field case.

Finite fields possess Frobenius, étale cohomology, purity theory, and other structures with no ready-made number-field counterpart. The real difficulty is to find, in the number-field setting, an object that plays an analogous role.

Thus the geometric route and the Hilbert–Pólya route, though expressed in different languages, share a deep aspiration:

> Do not push the zeros one by one onto the critical line;find a structure for which criticality is an inevitable readout.

The book's analysis of identity operates at the same level of the problem: it seeks a structural source lying above pointwise coordinates.

6. Hilbert–Pólya: If the Zeros Form a Self-Adjoint Spectrum, $1/2$ Appears in a Different Way

One of the most famous structural dreams surrounding the Riemann Hypothesis is the Hilbert–Pólya idea.

Its basic intuition is simple.

Suppose there exists a self-adjoint operator H with real spectrum γ_n, and suppose the nontrivial zeros can be written exactly as

$$\rho_n = \frac{1}{2} + i\gamma_n.$$

Then the Riemann Hypothesis would follow from the reality of the spectrum forced by self-adjointness.

The route is attractive because it does not try to estimate

$$\Re\rho - \frac{1}{2}$$

point by point. It seeks instead a higher-level structure in which "real part equal to $1/2$" is intrinsic to the spectral representation.

The names of Pólya and Hilbert eventually became attached to this idea; Pólya's 1982 letter preserved by Odlyzko is an important document in its intellectual history.[20]

Since then, several deep spectral programs have developed.

de Branges approached the Riemann Hypothesis through Hilbert spaces of entire functions and structural theorems.[19] Connes studied spectral interpretations of the zeros through noncommutative geometry and trace formulas.[23] Berry and Keating explored the relation between zero counting and quantum energy asymptotics from semiclassical quantum dynamics and

$$H_{\mathrm{cl}} = xp.$$

[21][22] Suzuki has continued to develop links between zeta, Hilbert spaces, and spectral structures through canonical systems, screw functions, Weil distributions, and related constructions.[24]–[26]

These routes have produced an increasingly clear historical consensus:

> "having a spectrum" is not enough;the key is why that spectrum is exactly the Riemann spectrum.

This is the question addressed directly in Chapters 6, 7, and 9.

7. Montgomery, Dyson, and Odlyzko: The Zeros Resemble Not Only a Spectrum, but the Spectrum of Quantum Chaos

In 1973, Montgomery studied the pair correlation of the zeta zeros.[27]

The famous story is that a conversation between Montgomery and Dyson revealed that the pair-correlation form he obtained showed a striking agreement with the energy-level correlation of large GUE random matrices.[28]

This was not an isolated coincidence.

Odlyzko's later computations of high zeros provided exceptionally strong numerical evidence.[14] Work by Rudnick–Sarnak, Katz–Sarnak, Bogomolny–Keating, Conrey–Snaith, and others deepened the correspondence from the perspectives of families of L-functions, random matrices, explicit formulas, ratios, and related structures.[30]–[35]

Thus a second spectral question emerged around the Riemann Hypothesis.

The first asks:

> Are the ordinates of the zeros the spectrum of a self-adjoint operator?

The second asks:

> Why do the second- and higher-order statistics of that spectrum exhibit GUE/CUE structure?

These questions must be kept distinct.

Self-adjointness is a first-order spectral question.

GUE concerns second- and higher-order self-relations.

Chapter 8 follows this stratification: GUE does not determine the horizontal location in the Riemann Hypothesis. It enters only after the identity of the first-order Riemann spectrum has been fixed.

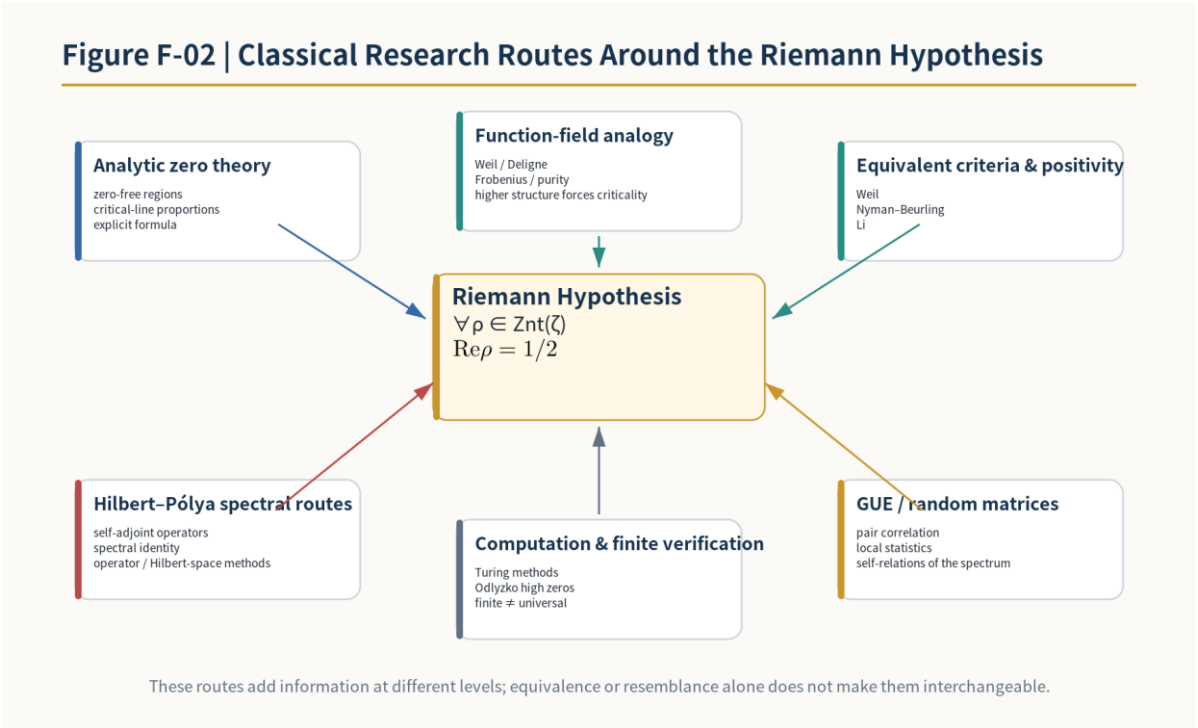


Figure F-02. Classical research routes around the Riemann Hypothesis. Analytic zero theory, equivalent and positivity criteria, function-field geometry, Hilbert–Pólya, random matrices, and finite computation add information at different mathematical levels. They can illuminate one another, but equivalence, resemblance, or shared readouts alone do not make them interchangeable.

8. What Actually Led to This Book Was Not "Another Route," but a Reorganization of Identity

The original impulse behind this book came from a very small question:

$$\boxed{\text{Why exactly} \frac{1}{2}?}$$

If one stops at the functional equation

$$\xi(s) = \xi(1 - s),$$

half of the answer is immediate.

The value $1/2$ is the fixed center of the complementary involution

$$s \mapsto 1 - s.$$

But standard mathematics is equally clear that

$$\boxed{\text{global symmetry} \Rightarrow / \text{ every zero is a fixed point.}}$$

This book therefore does not treat the mere existence of a center $1/2$ in the functional equation as a proof of the Riemann Hypothesis.

The real question is pushed one layer deeper:

> At what point does the real-part readout of a zero acquire a second degree of freedom independent of the original multiplicative identity?

To ask this precisely, three notions must be kept distinct:

$$\boxed{\text{identity} \neq \text{role} \neq \text{role readout.}}$$

A complete object may play different roles in different representations.

A role may carry different local coordinates.

But "being writable separately" does not imply "having acquired an independent generative source."

For this reason, I retain in the book the terms *objectification* and *proof debt*. They are reminders to ask, whenever a mathematical object is partitioned, named, or re-represented, whether the new proof obligations arise from the object itself or from the way we have partitioned it.

Mathematical objectification is a great power.

We turn a whole function into a zero set, a zero set into individual zeros, an individual zero into real and imaginary parts, and then place a universal quantifier over one of those coordinates.

Every step is legitimate.

But every step may also create a new proof obligation.

Hence one must ask:

> Does this proof obligation come from the object itself, or was it newly registered after the partition?

The book refers to this question as an examination of proof debt.

A boundary must be stated explicitly here:

GHT, object generation, regression, proof debt, and related ideas belong to the background through which the problem was discovered and organized; they do not enter the mathematical proof chain for the Riemann Hypothesis.

The mathematical core of the book uses only the multiplicative relations, analytic encodings, reciprocal roles, event representations, Hilbert spaces, Stieltjes reconstruction, spectral theorems, Fredholm structures, Fourier–Plancherel identities, and other mathematical objects explicitly defined in the main text.

In other words:

> methodology may help discover a proof;the proof itself must stand independently.

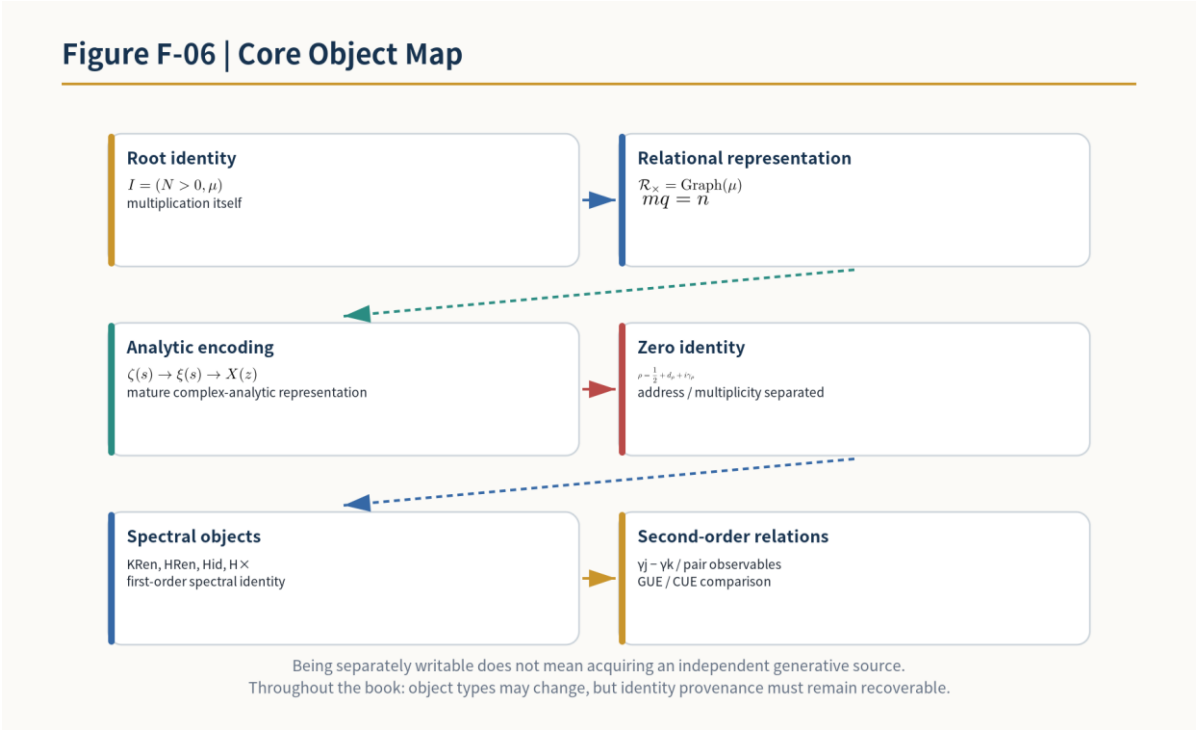


Figure F-06. Core object map. The root multiplicative identity, relational representation, analytic encoding, zero identity, spectral objects, and second-order relations are different mathematical object levels. The book continually tracks one question: representations may change, but can the provenance of identity still be recovered without loss?

9. The Two Closure Routes for the Riemann Hypothesis Presented in This Book

I want to state the book's mathematical conclusions clearly, but also with restraint.

As of November 2026, the Clay Mathematics Institute still lists the Riemann Hypothesis as an unsolved Millennium Prize Problem.[67] I therefore do not use the sentence "the problem has been solved" as a substitute for the independent reading, checking, and acceptance required by the mathematical community.

But caution should not make the conclusions actually stated in the main text vague.

The book explicitly claims that

Chapter 1 gives a direct reciprocal-zero-event closure proof of the Riemann Hypothesis;

and that

Chapter 9 starts from the same root multiplicative identity,independently constructs a source-generated Hilbert–Pólya self-adjoint spectrum,and closes the Riemann Hypothesis again.

These are not the same proof under two titles.

The first route starts from open multiplicative relations, reciprocal roles, and the complete history of an event, and proves that the terminal fixed-role readout lies on

$$\Re\rho = \frac{1}{2}.$$

The second route does not use a list of Riemann zeros, K_{Ren}, H_{Ren}, or the canonical spectral witness of Chapter 7 as generative input. Instead, it starts from structures on the generative side of the root multiplicative identity and, through two-depth identity self-pairing, dual Hankel/Gram positivity, Stieltjes reconstruction, and the spectral theorem, constructs a self-adjoint Hilbert–Pólya spectrum, recovers the Riemann zeros, and obtains the Riemann Hypothesis.

The two routes meet only at the identity of the canonical Riemann spectrum.

Thus what the book proposes is not merely

one proof of the Riemann Hypothesis.

It is

direct reciprocal-event closure,
independent source-generated spectral closure,
and, after closure, the geometry, multiplicities, canonical spectrum,
and second-order GUE structure of the zeros.

Whether these conclusions are correct does not depend on the force of the preface.

It depends only on whether the definitions and proofs in the main text survive independent scrutiny.

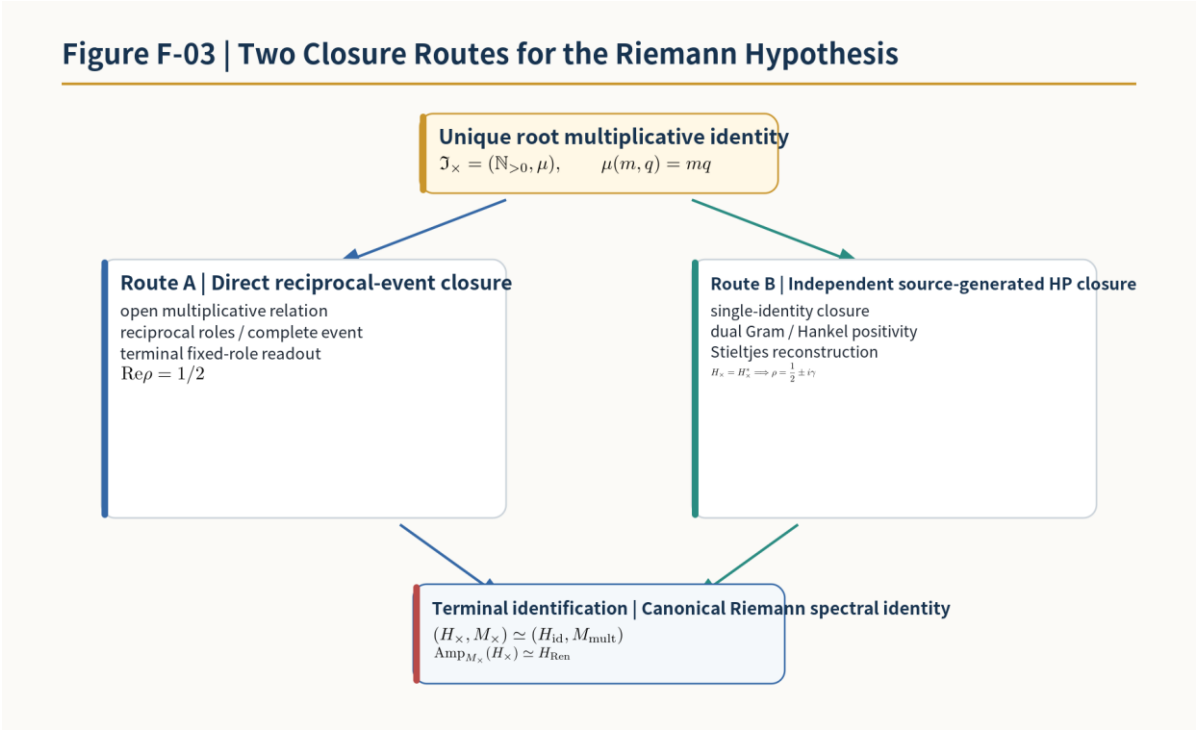


Figure F-03. The two closure routes for the Riemann Hypothesis in this book. The first route proceeds from open multiplication and reciprocal roles to a terminal fixed-role readout. The second independently generates Gram/Stieltjes spectral structure and a self-adjoint Hilbert–Pólya operator from the same root multiplicative identity. Only after each route has completed its own closure do they meet in canonical terminal spectral identification.

10. Chapter 1: Open Multiplicative Relations and Reciprocal Zero-Event Closure

Chapter 1 contains the book's first principal proof of the Riemann Hypothesis.

It begins from the unique root multiplicative identity

$$\boxed{\mathfrak{I}_\times = (\mathbb{N}_{>0}, \mu), \qquad \mu(m,q) = mq}$$

and treats the multiplicative relation itself not as a second identity but as a relational representation of the root identity:

$$\mathcal{R}_\times = \mathrm{Graph}(\mu).$$

Chapter 1 then distinguishes strictly between

$$\boxed{\text{identity} \neq \text{role} \neq \text{role readout.}}$$

At the source, exchanging the factors

$$(m,q) \leftrightarrow (q,m)$$

corresponds to the antisymmetric role coordinate

$$R = \log(q/m) \mapsto -R.$$

The fixed role is

$$R = 0.$$

After normalization, the readout of this reciprocal fixed role is

$$\frac{1}{2}.$$

The key is not to "transport" the source-side number $1/2$ to the real part of a zero. The key is to preserve the reciprocal role structure of the same complete event.

Through centered Mellin representation, global Dirichlet encoding, moving horizons, the complete event domain, and terminal zero-events, Chapter 1 establishes

$$\rho_E(\tau; J_E R) = 1 - \overline{\rho_E(\tau; R)}.$$

When a complete event reaches the source fixed role

$$J_E R_E = R_E,$$

the terminal representation must satisfy

$$\rho_E = 1 - \overline{\rho_E},$$

and therefore

$$\boxed{\Re \rho_E = \frac{1}{2}.}$$

Chapter 1 thus formulates the Riemann Hypothesis as terminal fixed-role closure within one reciprocal event history, rather than as a final matching imposed on two independent objects.

11. Chapter 2: After Zero Closure, How Can One Gap Carry the Whole Spectrum?

Once Chapter 1 fixes the horizontal coordinate, Chapter 2 turns to the vertical geometry of the zeros.

Let the positive ordinates be

$$0 < \gamma_1 < \gamma_2 < \cdots,$$

with analytic multiplicities m_n, and adjacent gaps

$$\Delta_n = \gamma_{n+1} - \gamma_n.$$

The question is: how much global information can the boundary analytic data of a single adjacent-zero interval contain?

Through a meromorphic Herglotz response, a canonical horizon-shape density, boundary analytic germs, and inverse-distance spectral moments, the chapter proves that a complete one-sided boundary analytic germ determines the entire distinct real zero spectrum and its analytic multiplicities; finite-order jets, in turn, give rigorous bounds on the nearest-neighbor gaps.

A seemingly local zero gap thereby acquires a new structural meaning:

$$\boxed{\text{local boundary analytic germ} \rightarrow \text{global spectral moments} \rightarrow \text{global zero spectrum.}}$$

Chapter 2 does not re-prove the Riemann Hypothesis.

It asks how much global spectral information is still stored in zero spacings after the Riemann Hypothesis has been closed.

12. Chapter 3: Addresses, Representation Sheets, and Analytic Multiplicity Must Be Kept Separate

Chapter 3 treats a source of confusion that arises easily in zero theory and spectral theory: multiplicity.

It strictly separates three layers:

representation-sheet count ≠ support-address count ≠ analytic multiplicity.

For

$$\xi(s) = (s-\rho)^{m_\rho} U_\rho(s), \qquad U_\rho(\rho) \neq 0,$$

ρ is the identity address of the zero, while

$$m_\rho = \operatorname{ord}_\rho \xi$$

is its analytic multiplicity.

Thus the appearance of two reciprocal representation sheets does not imply that a zero has multiplicity two.

Nor may a shared interval boundary be counted twice as the same zero address.

The chapter builds a complete stratification from local interval addresses to the global zero support, and from support counting to divisor counting, fixing the data

$$(\gamma_n, m_n)$$

required by the later spectral constructions.

This gives Chapters 6–9 a common multiplicity framework for identity-faithful and divisor-faithful spectra.

13. Chapter 4: Parameterizing the Riemann Closure Kernel and Proving the Generalized Riemann Hypothesis

Chapter 4 does not invent another proof of the Riemann Hypothesis.

It abstracts the concrete mechanism already realized in Chapter 1 into a transferable parameterized closure kernel and applies that kernel for the first time to the Dirichlet Generalized Riemann Hypothesis.

The crucial point is not “the Riemann Hypothesis is proved, therefore the Generalized Riemann Hypothesis follows automatically.” The chapter explicitly rejects that logical jump. The only genuinely new certification is this:

> Does Dirichlet-character weighting change the root multiplicative identity of Chapter 1?

The answer is compressed into an identity-preserving channel lift. The root multiplication remains

$$\mathfrak{I}_{\times} = (\mathbb{N}_{>0}, \mu), \qquad \mu(m,q) = mq,$$

while

$$\mathfrak{P}_{\chi} = \{\chi, \overline{\chi}\}$$

is only a reciprocal character package over the same root identity. For a complex character, χ and $\overline{\chi}$ are two reciprocal orientations, not two parent identities.

Using the weighted centered kernel

$$W_{\chi,z}(m,q) = \chi(m)\overline{\chi(q)}m^{-1/2-z}q^{-1/2+z},$$

Chapter 4 then verifies that the centered parameter, reciprocal roles, moving head/tail decomposition, and primitive completion all preserve the same identity transmission. The square-horizon fixed role depends only on $mq = n$ and therefore does not need to be proved again. Thus K1–K7 all hold for the primitive Dirichlet channel; reduction through the finite Euler factors for imprimitive and principal characters then yields the Dirichlet Generalized Riemann Hypothesis.

In this sense, the genuinely new content of the Generalized Riemann Hypothesis is compressed into

a character adds a channel, not a second root identity.

The chapter simultaneously extracts from Chapter 1 a minimal parameterized structure that can be transported.

The seven conditions K1–K7 control, respectively:

1. the root identity and reciprocal-role system;
2. the centered reciprocal representation;
3. exact transmission of the centered parameter;
4. reciprocal-role fidelity;
5. the generative-source fixed role of a complete event;
6. a zero-faithful completion target and terminal exhaustivity;
7. the canonical analytic reciprocal involution.

The core theorem can be compressed into one sentence:

If the source representation of the same complete event is already at a reciprocal fixed role and the terminal analytic representation preserves the reciprocal role, then the terminal readout lies in the fixed set of the analytic involution.

In the Riemann case, that fixed set is exactly

$$\Re\rho = \frac{1}{2}.$$

Chapter 4 therefore has two functions: it extracts the minimal parameterized structure from the concrete Riemann closure in Chapter 1, and it proves that Dirichlet-character weighting adds only reciprocal channels without replacing the root multiplicative identity, thereby transporting the same closure kernel to the Generalized Riemann Hypothesis.

14. Chapter 5: After the Riemann Hypothesis Is Closed, Horizontal Position and Vertical Frequency Separate Again

Chapter 5 enters the post-closure spectral-atlas layer.

Its most important object-discipline statement is

$$\boxed{d_E(\tau) \neq d_\rho.}$$

The former is an internal horizontal coordinate in a finite-horizon event lift; the latter is the actual horizontal coordinate of a zero,

$$d_\rho = \Re\rho - \frac{1}{2}.$$

After the closure of Chapter 1,

$$d_\rho = 0.$$

But finite event representations may still have their own internal geometry.

Chapter 5 therefore separates several notions often conflated under the word "spectrum":

- the actual Riemann zero spectrum;
- the finite-horizon event-lift spectrum;
- the prime-power generative-source spectrum;
- the Hilbert–Pólya vertical spectrum;
- second-order random-matrix statistics;
- Weil positivity and other global arithmetic–spectral responses.

The chapter is a map.

It tells the reader which structures are fixed once the Riemann Hypothesis is closed and which still contain rich new information.

15. Chapter 6: The Ren Operator and Bidirectional Recovery Between Multiplication, Analysis, and Spectrum

Chapter 6 organizes the complete centered zero coordinates into a full-coordinate normal operator.

Write

$$a_\rho = \rho - \frac{1}{2} = d_\rho + i\gamma_\rho.$$

Define

$$K_{\mathrm{Ren}} e_{\rho,j} = (\gamma_\rho - i d_\rho) e_{\rho,j}.$$

Then

$$\boxed{K_{\mathrm{Ren}} = \Gamma_{\mathrm{Ren}} - i\Delta_{\mathrm{Ren}}.}$$

Here

$$\Gamma_{\mathrm{Ren}}$$

reads the vertical coordinates of the zeros, while

$$\Delta_{\mathrm{Ren}}$$

reads their horizontal deviations.

Thus the Riemann Hypothesis is equivalent to

$$\boxed{\Delta_{\mathrm{Ren}} = 0,}$$

at which point

$$H_{\mathrm{Ren}} = K_{\mathrm{Ren}}|_{\mathrm{RH}}$$

becomes the positive self-adjoint canonical Riemann spectral operator.

More importantly, this chapter builds both a forward and a reverse chain:

$$\boxed{\text{multiplicative identity} \to \zeta \to \xi \to K_{\mathrm{Ren}},}$$

and

$$\boxed{K_{\mathrm{Ren}} \to \xi \to \zeta \to \text{the pre-continuation multiplicative logarithmic ledger.}}$$

Chapter 6 therefore does not study a bare diagonal spectrum, but a fully source-labeled spectral object that can be recovered in both directions.

16. Chapter 7: How a Scalar Witness Uniquely Recognizes the Riemann Spectrum

Chapter 7 treats the decisive "identification" problem in the Hilbert–Pólya route.

The existence of a self-adjoint operator does not by itself make that operator the Riemann spectrum.

The chapter extracts from H_{Ren} a canonical scalar spectral witness:

$$F_{\mathrm{R}}(y) = \sum_{n\geq 1} \frac{m_n}{y+\gamma_n^2} = \int \frac{d\nu_{\mathrm{R}}(\beta)}{1+y\beta}.$$

It establishes

$$\boxed{F_{\mathrm{R}} \Leftrightarrow \nu_{\mathrm{R}} \Leftrightarrow (H_{\mathrm{id}}, M_{\mathrm{mult}}) \Leftrightarrow H_{\mathrm{Ren}}.}$$

Thus the local analytic germ, the full moment sequence, the Stieltjes measure, and the cyclic spectral object uniquely determine one another.

If an independently constructed cyclic spectral object

$$(B_{\times}, \Psi_{\times})$$

has the same complete scalar response, the cyclic spectral theorem gives a basepoint-preserving unitary equivalence and hence identifies its Riemann spectral identity.

Chapter 7 has one task:

$$\boxed{\text{generation is not identification; identification is not generation.}}$$

This distinction becomes decisive in Chapter 9.

17. Chapter 8: From the First-Order Riemann Spectrum to GUE Two-Point Self-Relations

Chapter 8 proceeds from the established first-order spectral identity to the second-order structure of GUE.

It does not use GUE as a premise for proving the Riemann Hypothesis.

In this book, GUE enters strictly after the identity of the first-order Riemann spectrum has been fixed.

Define the signed spectral operator

$$\mathcal{D} = H_{\mathrm{id}} \oplus (-H_{\mathrm{id}}),$$

and the multiplicity display

$$\mathcal{M} = M_{\mathrm{mult}} \oplus M_{\mathrm{mult}}.$$

The spectral amplitude

$$Z_{\phi}(u) = \mathrm{Tr}\left[\mathcal{M}\phi(\mathcal{D})e^{iu\mathcal{D}}\right]$$

satisfies an exact two-point Fourier–Plancherel identity.

Thus

$$\boxed{\text{first-order spectrum} \rightarrow \text{two-point self-relation}}$$

becomes a rigorous mathematical interface.

The chapter then translates the two-point spectral relation back, through explicit formulas, into arithmetic self-correlations of

$$\Lambda(m)\Lambda(n),$$

separating the diagonal Montgomery ramp from off-diagonal shifted correlations, while accounting separately for finite height, finite CUE size, local Euler corrections, unfolding normalization, and renormalized residuals.

The first-order spectral identification from Chapter 7 yields another important conclusion:

if

$$(H_{\times}, M_{\times}) \simeq (H_{\mathrm{id}}, M_{\mathrm{mult}}),$$

then all unitary-invariant two-point observables are inherited automatically.

GUE is therefore not a second independent identity.

It is the second-order readout produced when the same first-order spectrum enters into relation with itself.

18. Chapter 9: Independently Generating a Hilbert–Pólya Self-Adjoint Spectrum from the Root Multiplicative Identity

Chapter 9 is the book's second principal proof of the Riemann Hypothesis.

It starts again from the root identity

$$\boxed{\mathfrak{I}_{\times} = (\mathbb{N}_{>0}, \mu).}$$

The complete identity class of the root identity on the generative-source side is written

$$\boxed{\mathfrak{C}_{\times} = [\Omega]_{\mathrm{id}}.}$$

The moving horizon, completion, $X/G/F$, scan functionals, moments, ordinary/shifted Hankel tables, and finite Source–Krylov truncations are all shown to be different representations of the same root identity.

The key step is two-depth identity self-pairing:

$$\mathcal{E}_{\times}^{[r]}\left(\Psi_i^{[r]}, \Psi_j^{[r]}\right) = \mu_{i+j+r}, \qquad r = 0,1.$$

Hence simultaneously

$$\boxed{\mathsf{H}_N \succcurlyeq 0, \qquad \mathsf{H}_N^{(1)} \succcurlyeq 0 \quad (\forall N).}$$

Dual Hankel positivity, through the Stieltjes moment theorem, yields a unique finite positive measure

$$\nu_{\times}.$$

Meromorphicity then forces it to be purely atomic; its support recovers

$$\gamma_n,$$

and the atomic weights recover the analytic multiplicities

$$m_n.$$

Define

$$B_{\times} = M_{\beta}, \qquad H_{\times} = B_{\times}^{-1/2}.$$

Then

$$\boxed{H_{\times} = H_{\times}^{*}, \qquad \sigma(H_{\times}) = \{\gamma_n\}.}$$

The centered zeros are therefore recovered as

$$z = \pm i\gamma_n,$$

that is,

$$\boxed{\rho = \frac{1}{2} \pm i\gamma_n.}$$

This generative chain does not take as input a list of Riemann zeros, K_{Ren}, H_{Ren}, or the canonical spectral witness.

Only after the Riemann Hypothesis has been closed by the source-generated spectrum does Chapter 7 enter for terminal identification:

$$\boxed{(H_\times, M_\times) \simeq (H_{\mathrm{id}}, M_{\mathrm{mult}}),}$$

and then

$$\widetilde{H}_\times \simeq H_{\mathrm{Ren}}.$$

This is what the book calls its second, independent Hilbert–Pólya spectral closure.

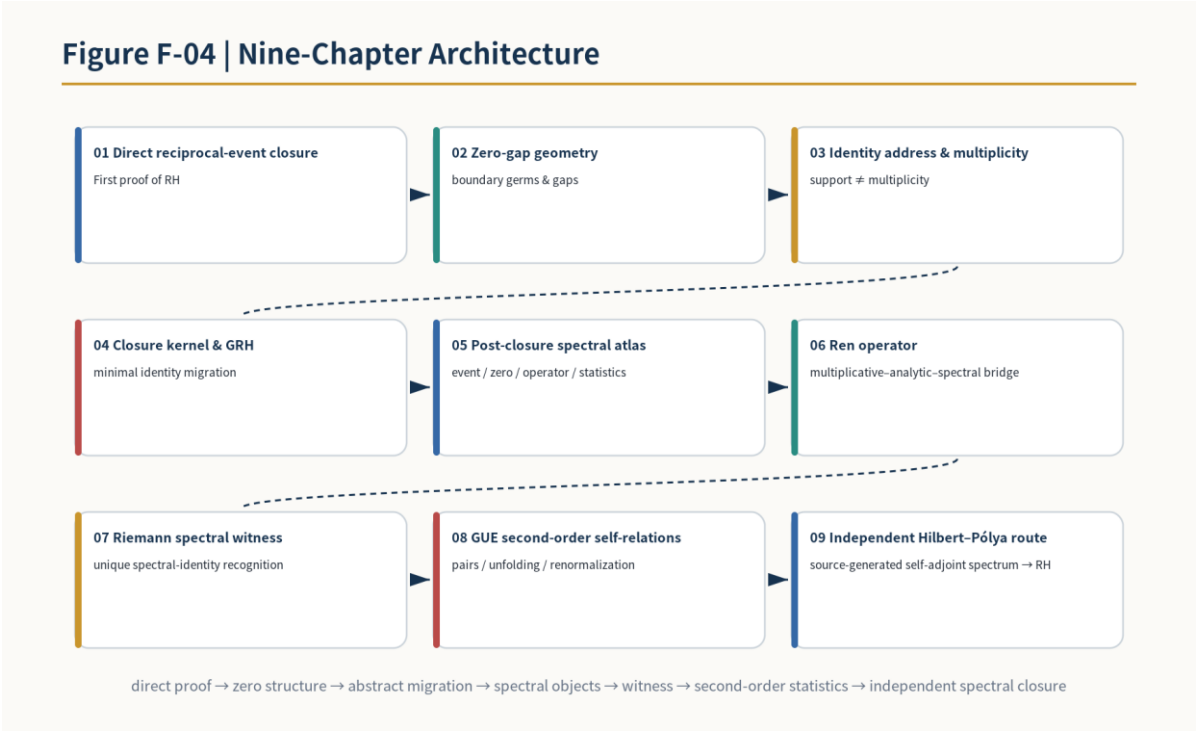


Figure F-04. Nine-chapter architecture. The nine chapters are not isolated topics: Chapter 1 gives the direct closure; Chapters 2–5 unfold the zero structure and closure kernel; Chapters 6–7 construct the canonical spectral objects and witness; Chapter 8 enters second-order self-relations; and Chapter 9 independently regenerates a self-adjoint spectrum from the root multiplicative identity and closes RH again.

19. How to Read This Book

The nine chapters form a path that unfolds gradually from the Riemann Hypothesis itself into the world of zeros, spectra, and statistics behind it:

direct closure of the Riemann Hypothesis →
zero geometry and multiplicity →
abstraction of the closure kernel →
post-closure spectral atlas →
canonical operator → spectral witness →
second-order GUE relations →
independent spectral proof.

Not every reader needs to enter by the same route.

If your primary concern is the first proof of the Riemann Hypothesis, begin with Chapter 1. If you then want to see how the same closure mechanism migrates to the Dirichlet Generalized Riemann Hypothesis, continue to Chapter 4.

If you are interested in the structure of the zeros themselves, Chapters 2, 3, and 5 treat zero gaps, identity addresses, analytic multiplicity, and the post-closure event spectral atlas.

If Hilbert–Pólya and operator language are your main interests, Chapters 6 and 7 give the canonical spectral object and its spectral witness.

If you are interested in Montgomery–GUE, random matrices, and second-order statistics, enter Chapter 8 after Chapter 7.

If you prefer to begin with an independent route that generates a self-adjoint spectrum from the multiplicative-identity source, go directly to Chapter 9. In that route, Chapter 7 enters only after the proof is complete, for terminal identification rather than upstream generation.

Whichever way you enter the book, one discipline should remain in view throughout:

$$\boxed{\text{identity} \neq \text{role} \neq \text{role readout.}}$$

This is not only the language of Chapter 1. It is the common coordinate system that allows all nine chapters to connect.

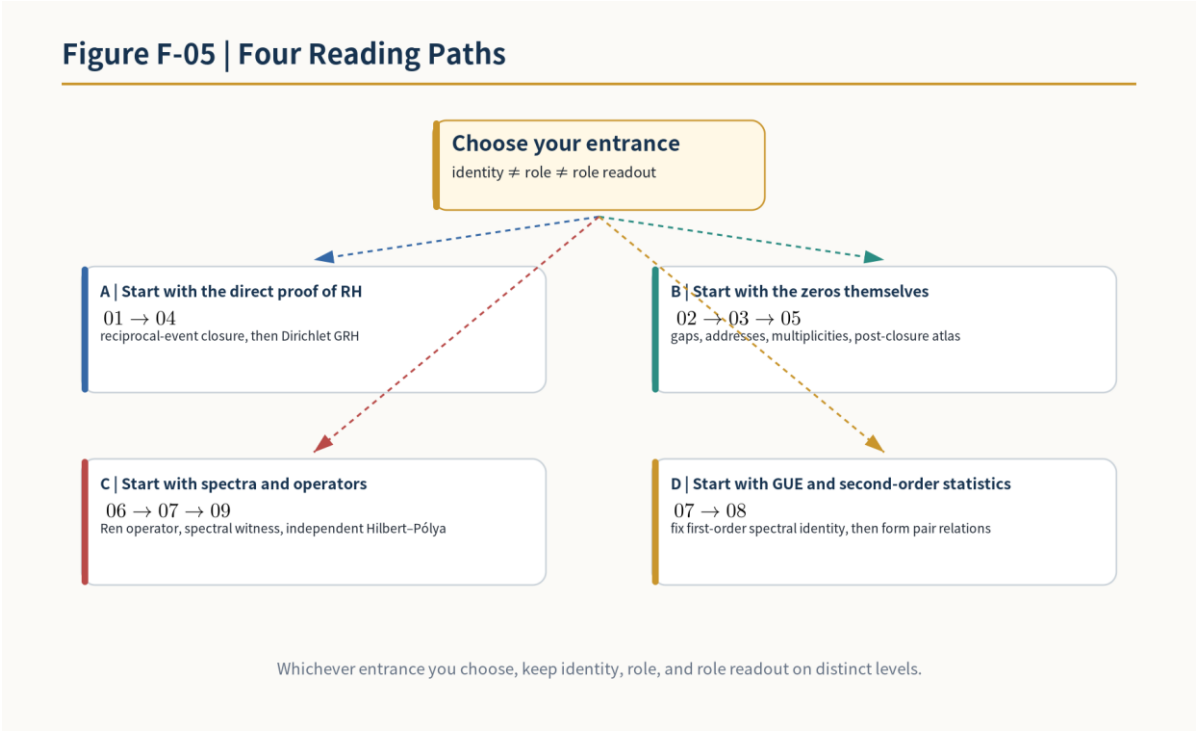


Figure F-05. How to read this book. A reader may enter through the direct proof, the structure of the zeros, the spectral/operator route, or GUE second-order statistics. Whichever route is chosen, the common object discipline remains the same: identity, role, and role readout must not be collapsed into one level.

20. On the Word "Proof": Strength and Humility Must Coexist

If you have read this far, I want to make the use of the word *proof* in this book as clear as possible.

I do not want the fact that the subject is the Riemann Hypothesis to turn theorems stated in the main text into vague language such as "possibility," "direction," or "attempt." If an argument has

been written as definitions, lemmas, theorems, and a complete derivation, then it should be examined by the standards of proof.

Accordingly, this book explicitly claims:

> **This book gives a direct closure proof of the Riemann Hypothesisand an independent source-generated Hilbert–Pólya spectral proof.**

Chapter 4 further gives a minimal identity migration from the same root multiplicative identity to Dirichlet-character channels and thereby obtains the Dirichlet case of the Generalized Riemann Hypothesis.

At the same time, I do not want "the author has written down a proof" to be confused with "the mathematical community has completed certification."

Both of the following statements must remain true:

> **The author must take full mathematical responsibility for the proof written here;**

and

> **a major mathematical conclusion must ultimately withstand independent reading, verification, refutation, and reconstruction.**

So if you believe a step fails, identify that step directly. If the definition of an object is circular, write down the circle. If a quantifier fails to cover the universal conclusion, identify the missing domain. If two routes called independent in fact share an input that they should not share, state exactly where.

Conversely, if these checks all pass, the strength of the conclusion should not be weakened merely because the author chooses cautious language.

The state I hope this book ultimately reaches is simple:

> **the reader need not believe the author in order to walk the proof through again.**

That matters more than any declaration.

21. Before the Main Text: Curiosity Is Still the Real Beginning of This Book

Looking back, the beginning of this book was not the ambition to "solve a Millennium problem."

It was closer to a childlike question:

$$\boxed{\text{Why}\frac{1}{2}?}$$

That is often the value of curiosity.

It does not begin by accepting the grandeur of the problem.

Nor does it begin by accepting the maturity of the available representations.

It simply asks:

Why?

Where did this object come from?

When did this number appear?

Why must this proof obligation exist?

If the representation changes, what has actually been added?

If one keeps moving backward, does the problem still remain?

Questions this simple are what turned the view from the zeros back to zeta, from zeta back to the Euler product, and from mature analysis back to multiplicative identity—and then forward again, from identity into zeros, spectra, operators, and GUE.

So before the main text begins, I leave one very simple invitation to the reader:

Do not believe it because it is the Riemann Hypothesis.

And do not reject it because it is the Riemann Hypothesis.

Look only at whether

the objects are defined clearly,the relations are preserved,and the proof closes.

If the answer is yes, the mathematics will speak for itself.

If the answer is no, then identifying the exact break is itself the best response this book can receive.

Chapter 1 Open Multiplicative Relations, Analytic Identity Fidelity, and Reciprocal Zero-Event Closure of the Riemann Hypothesis

Object discipline for the whole book: There is only one root identity: multiplication of the positive integers itself. Relational representations, primes, the Euler product, Dirichlet series, Mellin representations, Riemann completion, and terminal readouts are all treated as layered representations of that same identity. Identity, role, and role readout are kept strictly distinct. An object is a compression of its history; a history is the unfolding of the object. In this chapter, **identity closure** means that the current representation can still be losslessly unfolded, recovered, or certified as the same complete multiplicative identity; closure means that identity remains present. **Terminal closure** refers specifically to a fixed-role readout, not to the collision or merger of two entity-like zeros.

Abstract

The Riemann Hypothesis is usually approached from its nontrivial zeros and compressed into a single question: why do all of those zeros have real part $1/2$? This chapter moves the question one layer upstream. Instead of first treating a zero as an analytically completed object that is already independent, we track its generative history: where it comes from, in what relation it acquires its identity, and through which representations it passes before becoming the separately addressable zero readout used today.

The book has only one root identity: multiplication of the positive integers itself. Open multiplicative relations, primes, unique factorization, the Euler product, Dirichlet series, centered Mellin representation, multiplicative shells, moving horizons, Riemann completion, and terminal zero readouts are organized as layered representations of one and the same multiplicative identity. Representations may be unfolded, compressed, reorganized, and assigned new coordinates without thereby creating a new generative identity. On this basis, the chapter distinguishes **identity**, **role**, and **role readout**: the identity remains the same, roles emerge from relations, and readouts change with representation.

The core of this organization can be summarized in one sentence:

An object is a compression of its history; a history is the unfolding of the object.

A mature mathematical object may be named and computed independently without having become detached from the relation that generated it. The real question is whether, after many layers of compression, it can still be unfolded, recovered, or certified losslessly as the original complete multiplicative identity. This chapter calls that recoverability **identity closure**, and interprets closure as a testable condition for the continued presence of identity.

This viewpoint also explains an often overlooked issue. A bare result that carries no requirement of origin does not by itself create an explanatory obligation of the form “why this value?” New

explanatory debt often appears only after a result that originally had a clear generative history has been cut away from that history and re-objectified. Accordingly, this chapter does not first treat $\Re\rho = 1/2$ as a mysterious choice of an isolated terminal value. It asks instead whether that terminal readout remains inside the same multiplicative identity closure; whether the same reciprocal fixed relation remains present through every representational layer; and whether, in the terminal analytic layer, it has a unique fixed-role readout.

Seen globally, the analytic chain can be understood as one identity passing through a succession of increasingly compressed representational channels. Primes, Euler/Dirichlet representation, Mellin representation, shells, ζ, ξ, and zero readouts are not a sequence of mutually replacing objects; they are stages in the progressive compression and analytic realization of one identity. At the generative end, reciprocal roles have a unique fixed position in normalized coordinates. In the terminal analytic representation, the same reciprocal action is read as

$$\rho \mapsto 1 - \overline{\rho},$$

whose fixed readout satisfies

$$\Re\rho = \frac{1}{2}.$$

The value $1/2$ is not numerically transported from source to terminal. It is the compressed readout, in the terminal representation, of the same fixed relation.

Technically, this chapter assigns the corresponding mathematical responsibilities to centered Mellin decomposition, evenness of multiplicative shells, the global double-ζ encoding, exact repartition under the moving horizon, parameter fidelity under completion, the square-horizon fixed role, the terminal object domain, and reciprocal-role fidelity. The moving horizon has two related functions. First, it organizes the head/tail decomposition and the two reciprocal wings as dynamic role presentations of a single event, so that adjacent horizons become successive lifts of one process rather than two frozen objects. Second, it represents the complete infinite object through a family of exact finite horizons, with

$$H_r + T_r = \zeta$$

maintained at every stage. The point is therefore not to approximate the infinite by the finite, but to preserve the infinite identity inside a finite dynamics. Event identity, centered parameter, and role assignment remain consistent along the representational chain; the terminal fixed role is consequently read, in the analytic layer, as a fixed point of the reciprocal involution.

The chapter also places this forward analytic compression inside the larger architecture of the book. Chapter 6 (H06), through the Ren operator, provides the reverse direction from a highly compressed analytic/spectral object back to the multiplicative identity. Chapter 9 (H09) independently constructs a source-generated self-adjoint spectral route from the same root multiplicative identity. Chapter 7 (H07) provides the witness, uniqueness, and identification of the canonical spectrum as the Riemann spectrum. None of these later chapters is used as an input to the main theorem here. Their role is to display the fuller meaning of closure: after compression, identity can be recovered; once recovered, it can unfold again along other legitimate routes.

The chapter therefore does not take "drilling ever deeper into formulas" as its sole organizing principle. Every local proof is required to preserve the global object relation: **the identity remains the same while representations unfold and progressively contract; an object is a compression of its history, and a history is the unfolding of the object; what can be recovered losslessly lies inside the identity closure, and closure means that identity remains present.**

Overview: One Multiplicative Identity, Many Representations

Before entering the detailed proof, we fix the object hierarchy used in the chapter. The purpose is not to add an explanatory layer outside the mathematics, but to prevent a readout of the same identity in different representations from being mistaken for independently generated objects.

0.1 Root Identity: Multiplication of the Positive Integers Itself

The root identity used throughout the book is

$$\boxed{\mathfrak{I}_\times := (\mathbb{N}_{>0}, \mu), \qquad \mu(m,q) = mq.} \tag{0.1}$$

The open multiplicative relation

$$\mathcal{R}_\times = \{(m,q,n) \in \mathbb{N}^3 : mq = n\}$$

is a relational representation of μ. For fixed n,

$$\mathcal{D}_n = \{(m,q) \in \mathbb{N}^2 : mq = n\}$$

is a fiber of the same relational representation. Root identity, relational representation, and fiber representation must therefore be kept on distinct levels, but they need not be interpreted as three different generative sources.

Primes likewise do not form a second root identity. Let μ_{nt} denote nontrivial multiplication restricted to $m, q > 1$. Then

$$\mathbb{P} = \mathbb{N}_{\geq 2} \backslash \mathrm{Im}\mu_{\mathrm{nt}}. \tag{0.2}$$

Primes first appear as irreducible positions internal to the multiplicative structure. The fundamental theorem of arithmetic then gives

$$n = \prod_p p^{v_p(n)}, \tag{0.3}$$

reorganizing those irreducible positions as the generating primitives of full multiplication on the positive integers.

Thus the chapter does not describe an identity replacement of the form

$$\text{multiplication} \rightarrow \text{primes} \rightarrow \zeta,$$

but rather an unfolding of one multiplicative identity at different resolutions.

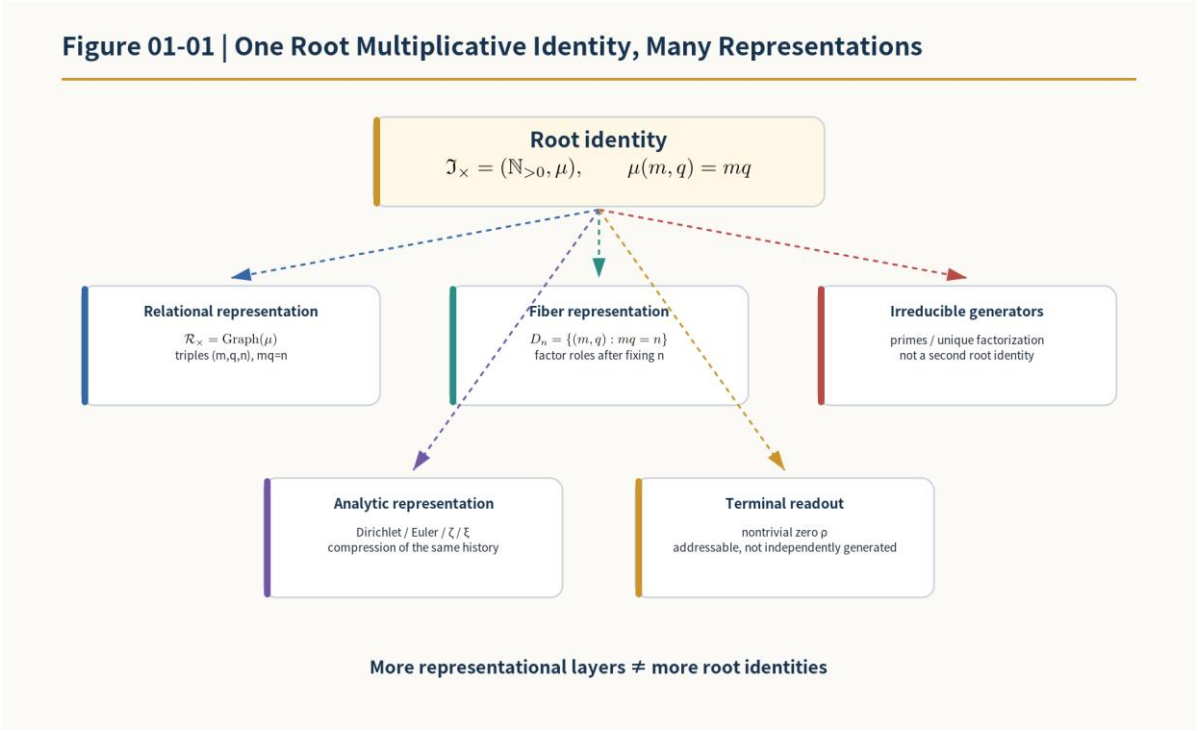


Figure 01-01. One root multiplicative identity, many representations. The root identity remains multiplication of the positive integers itself. The open relation, fixed fibers, primes/unique factorization, analytic encodings, and terminal zeros are representations of the same multiplicative identity at different resolutions and object levels. More representational layers do not create more generative identities.

0.2 Objects and Histories

The chapter adopts the following object discipline:

An object is a compression of its history; a history is the unfolding of the object. (0.4)

The fact that a mathematical object can be named, addressed, and computed separately does not thereby give it a second identity independent of the relation that generated it. Objectification means first of all that a segment of generative relational history has been compressed into a stable, operational representation. Unfolding in the reverse direction means reading that compressed object again inside its generative relations, role relations, and representational structure.

Hence

$$\boxed{\text{greater addressability} \neq \text{more identity information.}} \tag{0.5}$$

Representational levels may proliferate without a corresponding migration of the root identity.

A Minimal Intuitive Example: When Does the Question Arise?

Before discussing “closure,” consider the elementary identity

$$1 + 2 + 3 = 6.$$

Two entirely different situations must be distinguished.

If one is simply given the bare number

$$6,$$

with no requirement that it come from anywhere in particular, then no natural question "why is it 6?" arises. It is simply a given value and carries no obligation to explain its origin.

The question arises in a different situation: 6 originally appears as the result of the relation

$$1 + 2 + 3,$$

but once the generative history on the left has been cut away from the current presentation and only the result remains, one asks again

$$\text{Why is the result exactly} 6\ ?$$

The new "why" is not automatically created by the result itself. It is created when an existing generative history is severed and the result is re-objectified as if it were independent. Once the original relation is restored,

$$1 + 2 + 3 \to 6,$$

the reason the result is 6 is already contained in that generative relation; no new source explanation needs to be introduced at the result end.

The point of the example is therefore not whether one can uniquely infer $1 + 2 + 3$ from the bare number 6. A bare result carries no such obligation. What must be examined is whether, after a result with an existing generative history has been compressed and independently addressed in later representations, the generative relation remains present.

This is the entry point for the Riemann problem in this chapter. A nontrivial zero

$$\rho = \sigma + i\gamma$$

is not a bare complex number with no requirement of origin. It lies in the full multiplicative–analytic representational history

$$\Im_{\times} \to \text{primes} \to \text{Dirichlet/Euler} \to \zeta \to \xi \to \rho.$$

Thus when the problem is written as

$$\text{Why is} \sigma = \frac{1}{2}\ ?$$

the first question is not why an isolated terminal value has somehow "chosen" $1/2$. The first question is whether that terminal readout remains inside the same multiplicative identity closure; whether the reciprocal fixed relation remains present throughout the complete history; and whether, in the terminal analytic representation, it is read as

$$\Re\rho = \frac{1}{2}.$$

From this perspective, what the chapter tracks is not an external source of a terminal value, but whether an object with an existing generative history retains its identity and fixed relation after many representational layers.

The object discipline can be compressed as follows:

A bare result does not by itself create a question of origin;new explanatory debt appears when an existing generative history is cut away and the result is asked to explain itself.

(0.5a)

This simple example clarifies only the organization of the question. It replaces none of the mathematical proofs below. The actual proof obligations remain to verify, layer by layer, identity closure, role fidelity, and completeness of the object domain from multiplicative identity to terminal analytic representation.

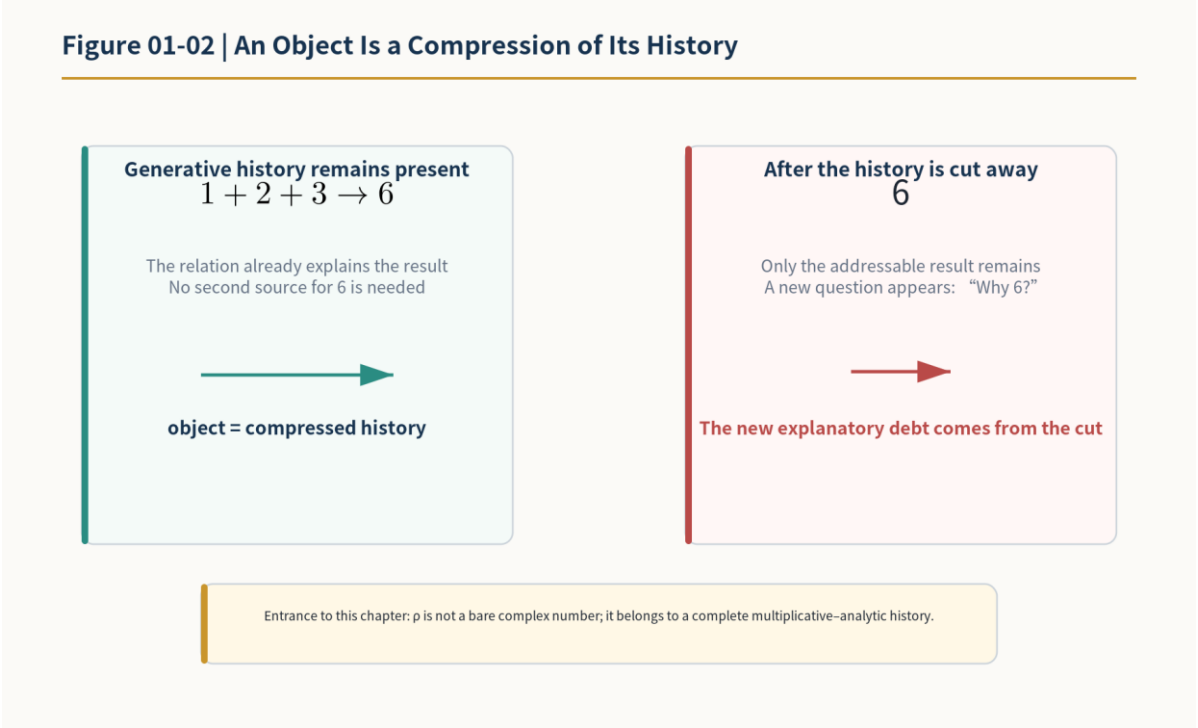


Figure 01-02. An object is a compression of its history. While the generative history remains present, the result is already contained in the relation. Once the history is cut away and only the addressable result remains, a new explanatory debt can appear. This chapter therefore audits nontrivial zeros inside their complete multiplicative–analytic history.

0.3 Identity Closure: Lossless Recoverability Means Identity Remains Present

To make "the same identity" a testable mathematical responsibility, this chapter links closure to recoverability.

Let the complete multiplicative generative history be

$$\mathcal{H}_{\times}.$$

Suppose a compressed representation at some layer is

$$C_k : \mathcal{H}_{\times} \to X_k.$$

If there exists a corresponding unfolding or recovery map

$$U_k : X_k \to \mathcal{H}_{\times}$$

such that

$$\boxed{U_k \circ C_k \equiv_{\mathrm{Id}} \mathrm{id}_{\mathcal{H}_\times},} \tag{0.6}$$

meaning that recovery returns the same complete multiplicative identity, then X_k is said to be **closed with respect to the multiplicative identity**.

The symbol $\equiv_{\mathrm{Id}}$ emphasizes identity equivalence, not symbol-by-symbol or coordinate-by-coordinate equality of different representations. The meaning of closure can be abbreviated as

$$\boxed{\text{lossless recoverability} \Leftrightarrow \text{identity closure} \Leftrightarrow \text{identity remains present.}} \tag{0.7}$$

Accordingly, deciding whether a mature analytic representation still belongs to the original multiplicative identity cannot rest on superficial similarity; one must determine whether its generative history can still be recovered or certified.

0.4 ζ: Global Analytic Compression of the Same Multiplicative Identity

For $\Re s > 1$,

$$\zeta(s) = \sum_{n\geq 1} n^{-s}. \tag{0.8}$$

By unique factorization and absolute convergence,

$$\zeta(s) = \prod_{p} (1 - p^{-s})^{-1}. \tag{0.9}$$

Equations (0.8) and (0.9) do not represent two independent sources. The former reads the same multiplicative identity from the full integer layer; the latter reads it from the layer of irreducible generators. In other words, the Dirichlet and Euler representations are two standard unfoldings of one multiplicative identity.

In this structure, the Euler product is not an independent supplementary assumption. It is the analytic representation generated by irreducible factorization in multiplication of the positive integers. It also provides an important identity witness: the global integer representation retains the history of generation by prime factors.

If

$$F(s) = \sum_{n\geq 1} c_n\, n^{-s}$$

is another Dirichlet series, then even if F has a similar Dirichlet form, a similar functional equation, or reciprocal zero symmetry, this alone does not establish that F has the same closure identity as ζ. Identity is ultimately determined by whether the generative history lies in the same multiplicative closure and can be recovered as the same root identity.

0.5 Identity, Role, and Role Readout

This chapter uses the strict distinction

$$\boxed{\text{identity} \neq \text{role} \neq \text{role readout.}} \tag{0.10}$$

Identity is the generative identity that remains present through changes of representation. A **role** is a position generated by a relation internal to the same identity. A **role readout** is the coordinate or analytic value acquired when that role enters a concrete representation.

For example, in

$$mq = n,$$

m and q are reciprocal roles internal to one multiplicative identity; the map

$$J(m,q) = (q,m)$$

only exchanges role positions and does not create a second identity.

In the relative coordinate

$$R = \log\frac{q}{m},$$

R is a role readout. In centered Mellin representation,

$$W_z(m,q)$$

is another layer of readout. In the analytic representation of an event,

$$\rho_{E,\pm} = \frac{1}{2} \pm d_E + i\gamma_E$$

are still analytic readouts of reciprocal roles within the same identity.

Different role readouts may therefore exist within one identity; different readouts do not imply a split in identity.

0.6 The Place of $1/2$: Different Readouts of the Same Fixed Relation

In normalized multiplicative coordinates,

$$u = \log_n m, \qquad v = \log_n q, \qquad u + v = 1,$$

and the reciprocal action is

$$u \mapsto 1 - u.$$

The fixed role satisfies

$$u = \frac{1}{2}. \tag{0.11}$$

In the relative multiplicative coordinate

$$R = \log\frac{q}{m},$$

the same reciprocal action is

$$R \mapsto -R,$$

with fixed role

$$R = 0. \tag{0.12}$$

In the terminal analytic representation, the reciprocal action is

$$\iota(\rho) = 1 - \overline{\rho}.$$

Its fixed readouts satisfy

$$\rho = 1 - \overline{\rho} \quad \Leftrightarrow \quad \Re\rho = \frac{1}{2}. \tag{0.13}$$

Thus

$$u = \frac{1}{2}, \qquad R = 0, \qquad \Re\rho = \frac{1}{2}$$

are not values transported numerically from one level to another. They are role readouts, in different representations, of the same reciprocal fixed relation.

One must also distinguish a **terminal readout** from **identity closure**. The bare number $1/2$ does not itself carry the full multiplicative history. What is closed is the complete terminal representation containing that readout. The terminal value may be highly compressed, while the closure structure guarantees that the history of the identity has not been deleted.

0.7 A Continuous Picture: Identity Passing Through Layer after Layer of Representation

The preceding definitions admit a more intuitive picture.

As the same multiplicative identity unfolds through later mathematical structures, each representational layer may be viewed as a funnel, sieve, or channel. On entering the next layer, the visible form of the identity changes and the freely variable representational components are gradually reduced. But so long as the layer remains inside the same identity closure, what passes through the sieve is still the same multiplicative identity.

Thus the more accurate statement is not that "identity does not move," but rather

> identity remains the same while representations unfold and progressively contract.

Starting from the root multiplicative identity, one sees a continuous analytic representational history:

$$\Im_{\times} \to \text{primes} \to \text{Dirichlet/Euler} \to$$
$$\text{centered Mellin} \to \text{multiplicative shells} \to$$
$$\zeta \to \xi \to \text{terminal zero readout.}$$

Every arrow here means that the same identity enters new representational conditions, not that one object is replaced by another.

The point of the "funnel" metaphor is that later representations allow fewer positions once the previously established relations are enforced. At the terminal reciprocal representation, the analytic readout of the same fixed role satisfies

$$\rho = 1 - \overline{\rho},$$

whose fixed-point set gives uniquely

$$\Re\rho = \frac{1}{2}.$$

The terminal value $1/2$ is therefore not an extra position "chosen" by a zero at the last moment. If identity closure and reciprocal-role fidelity have already been established, it is the unique fixed-role readout allowed in the terminal analytic layer after the same reciprocal fixed relation has passed through the entire representational contraction.

Equivalently,

representations progressively contract while identity remains the same;the terminal fixed position is a compressed readout of the complete history.

This also explains why the problem becomes mysterious again when its history is forgotten. If one looks only at the narrowest outlet of the funnel,

$$\rho = \frac{1}{2} + i\gamma,$$

while removing from the current description the multiplicative structure, irreducible factorization, Euler/Dirichlet representation, Mellin representation, completion, and reciprocal structure through which it has already passed, the explanatory debt "why exactly $1/2$?" reappears. Once the history is restored, the actual proof obligations are different: one must show that the entire channel preserves one identity and that the fixed role remains present in every representation.

0.8 Closure Means Not Only That One Can Return, but That the Recovered Identity Can Unfold Again

"Unfolding the history" does not mean merely reversing one particular representational path.

If a highly compressed terminal object can be recovered losslessly as the original multiplicative identity, what is recovered is the **identity**, not one fixed route of representation. Once the root identity is recovered, it again possesses every legitimate direction of unfolding allowed by that identity.

Thus forward compression and reverse recovery may be written as

$$\begin{aligned}&\mathfrak{I}_{\times} \to \text{multilayer analytic representation} \to \\ &\text{highly compressed terminal object} \to \mathfrak{I}_{\times},\end{aligned}$$

where the final arrow denotes recovery of identity, not a literal playback of history in reverse.

Later chapters realize different parts of this structure. Chapter 6 (H06), *The RH Ren Operator: A Lossless Bridge Between Multiplicative Identity, Analytic Continuation, and the Canonical Spectrum*, introduces the Ren operator and provides the reverse direction from a highly compressed analytic/spectral object to the unfolding, recovery, and identification of the multiplicative identity. Its role is not to manufacture a new generative source for the terminal object, but to unfold the already compressed history so that the root multiplicative identity becomes visible again.

Once identity has been recovered, one is not restricted to retracing the analytic road of the present chapter (H01). The same

$$\mathfrak{I}_{\times}$$

can enter another, independent route. Chapter 9 (H09), *Another Closure Route for the Riemann Hypothesis: Open Multiplicative Identity and an Independent Hilbert–Pólya Spectral Route—from Open Multiplicative Identity to a Source-Generated Self-Adjoint Spectrum and Canonical Terminal Identification*, starts from the same open multiplicative identity and independently constructs a source-generated self-adjoint spectral route. Its logical independence must be preserved: Chapter 9 does not depend on the present chapter or on the reverse recovery furnished by the Ren operator.

Chapter 7 (H07), *The Riemann Spectral Witness Theorem: Uniqueness of the Ren Canonical Spectral Witness and Hilbert–Pólya Identity Transfer*, lies at the level of witnessing and identifying spectral identity. In the architecture of the book, the three roles can be summarized as

H06:	recover and unfold the multiplicative identity from a compressed object;
H09:	independently construct a source-generated self-adjoint spectrum from the multiplicative identity;
H07:	witness, uniquely determine, and identify the canonical spectrum as Riemann.

Thus the relation between Chapters 7 and 9 is not that Chapter 7 must come first for Chapter 9 to work, nor that the Ren operator directly generates the independent spectrum of Chapter 9. More precisely, Chapter 9 grows its spectrum independently from the root identity; Chapter 7 then witnesses and identifies the Riemann identity carried by that canonical spectrum. Meanwhile, Chapter 6 provides identity recovery from the opposite direction, allowing the analytically compressed route and the spectral route to meet again at the same root identity.

These relations are better drawn as an identity-based loop than as a tree that branches left and right:

$$\mathfrak{I}_{\times} \overset{H01}{\rightarrow} \text{progressive analytic contraction} \rightarrow \underbrace{\rho,\ \Re\rho = \frac{1}{2}}_{\text{terminal zero / narrowest position}} \overset{H06}{\rightarrow} \mathfrak{I}_{\times} \overset{H09}{\rightarrow} \text{source-generated self-adjoint spectrum} \overset{H07}{\rightarrow} \text{canonic} \tag{0.14a}$$

The first segment,

$$\mathfrak{I}_{\times} \rightarrow \rho \rightarrow \mathfrak{I}_{\times},$$

forms a compression–recovery loop at the level of identity: the present chapter compresses the same multiplicative identity through analytic layers to a terminal zero readout, and Chapter 6 recovers the root identity in reverse from that highly compressed position. Once the root has been recovered, the same identity need not return along the same path. Chapter 9 can independently construct a source-generated self-adjoint spectrum from the root identity, and Chapter 7 can then provide the Riemann identity witness, uniqueness, and identification of that canonical spectrum. What closes into a circle is **identity**, not any single fixed form of representation.

This diagram is not an input to the main theorem of the present chapter. It is a book-level structural explanation of the statement that an object is a compression of its history and a history is the unfolding of the object. It reveals a fuller meaning of closure:

> identity can be recovered after compression;once recovered, it can unfold again along other legitimate routes.

What therefore remains continuously present is not one fixed representational path, but the root identity whose sameness can be certified across different routes of compression and unfolding.

Figure 0.1 — From Analytic Contraction through Identity Recovery to Spectral Witnessing

The following schematic is intended only to help the reader place this chapter and the later chapters within one object structure; it carries no independent proof responsibility. The left side represents the analytic/zero-contraction route of the present chapter (H01): the same multiplicative identity is compressed through successive representations and, in the terminal reciprocal representation, reaches the fixed-role readout. Chapter 6 (H06) represents the reverse recovery of the multiplicative identity from the highly compressed object. Chapter 9 (H09) represents the

independent source-generated self-adjoint spectral route from the same root identity. Chapter 7 (H07) provides the witness, uniqueness, and identification of the canonical spectrum as Riemann.

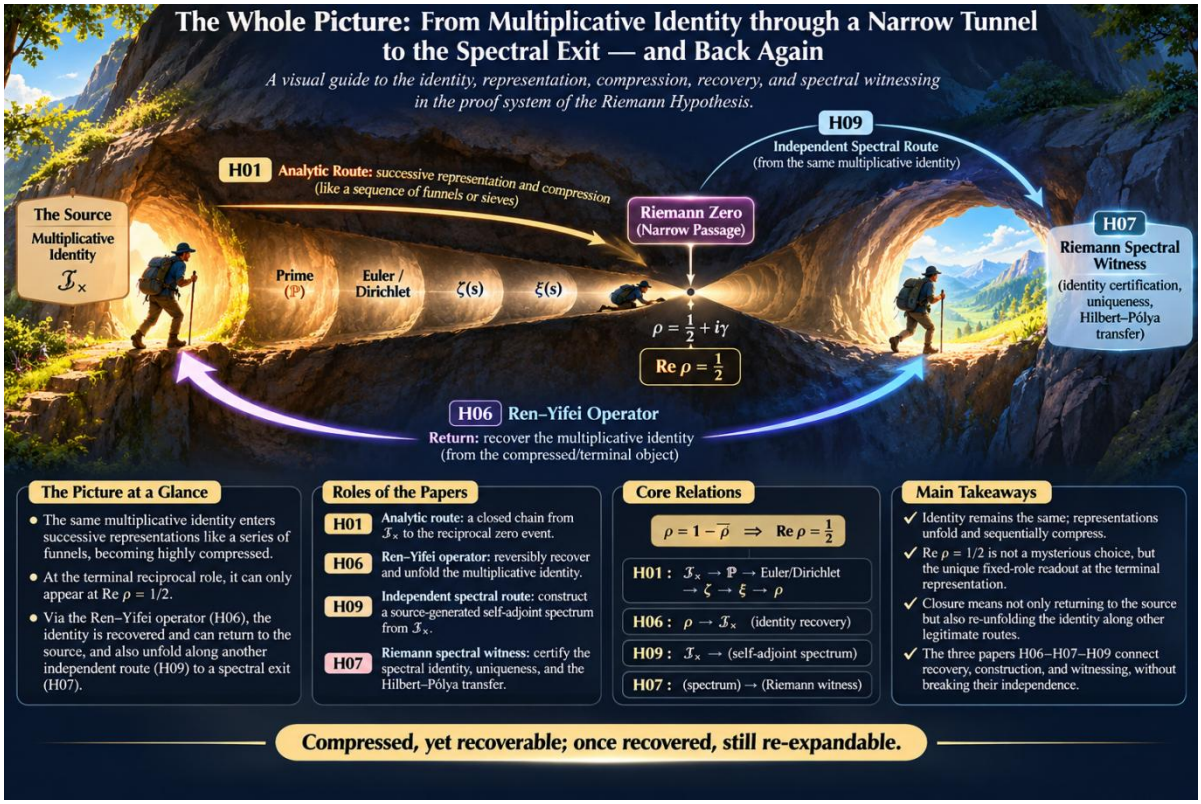


Figure 0.1 The multiplicative identity passes through analytic contraction, is recovered, and unfolds again along an independent spectral route

The most important feature of the diagram is not that there are many paths, but that every path is judged by the same root identity. The analytic route can contract; the compressed object can be recovered; and the recovered identity can unfold again along an independent spectral route. What remains present is the certifiable **identity**, not one fixed representation.

0.9 Proof Obligations of This Chapter

The overview fixes only the object hierarchy. The remainder of the chapter must still prove, layer by layer,

$$\begin{aligned} &\text{multiplicative identity} \to \\ &\text{relational representation} \to \\ &\text{reciprocal roles} \to \text{centered Mellin} \to \\ &\text{shells} \to \text{Dirichlet/Euler} \to \text{head/tail} \to \\ &\text{completion} \to \text{terminal role readout.} \end{aligned} \tag{0.14}$$

The concrete responsibilities are: the identity must not be replaced; the assignment of reciprocal roles must not be re-paired; the centered parameter must not be reset; every analytic representation must remain inside the same multiplicative identity closure; the terminal object domain must cover all actual nontrivial zeros; and the fixed-role assignment must still be read through the same reciprocal action in the terminal analytic representation.

GHT therefore serves in this chapter only as an audit of objects: it helps distinguish identity, role, role readout, and history. Whether the actual closure holds is established, layer by layer, by the standard mathematical identities, uniqueness statements, exact repartitions, completion, and the terminal object domain developed below.

The chapter can be compressed into the following general principle:

Identity remains the same while representations unfold; roles emerge from relations and readouts change with representation; an object is a compression of its history and a history is the unfolding of the object; what is losslessly recoverable lies in the identity closure, and closure means that identity remains present.

(0.15)

1. Introduction

The Riemann Hypothesis asserts that every nontrivial zero ρ of the Riemann ζ-function satisfies

$$\Re\rho = \frac{1}{2}.$$

The classical formulation usually begins directly with ζ, its completed function, and its zeros. This chapter retains all of those standard objects but moves the order of organization one step upstream: first fix multiplication of the positive integers as the root identity; then track how the same identity passes through relational representation, irreducible factorization, Dirichlet/Euler representation, centered Mellin representation, shells, moving horizons, and completion before finally entering zero readouts.

The point is not to replace local proof by a global metaphor. It is to require every local formula to answer a global question: **what exactly changes at this layer, and what is preserved?** If a formula holds locally but cannot identify its place in the full history of the identity, it has not yet discharged the proof responsibility required here. Conversely, every technical step must state its object-level meaning: is it changing representation, rearranging visible information, compressing a relation, or has it actually replaced the identity, the parameter, or the assignment of roles?

The chapter therefore proceeds from global structure into local detail and then returns, through local proofs, to global structure. No rigor in the formulas is sacrificed, but the formulas are not the endpoint. Their joint responsibility is to prove that the same multiplicative identity is not replaced through multiple layers of representation and, finally, to explain why the terminal fixed-role readout can lie only in the fixed-point set of the reciprocal involution.

This order of organization changes none of the standard analytic objects and does not introduce GHT into the proof steps. It merely requires that every change of representation distinguish explicitly between what remains present as identity, what is a role internal to that identity, and what is only a role readout at a particular representational layer.

The chapter first rules out three easily confused inferences.

First, **reflection symmetry of the functional equation alone does not prove the Riemann Hypothesis.** It tells us only that if ρ is a zero, then the corresponding reciprocal readout $1-\overline{\rho}$ also occurs. Whenever $\Re\rho \neq 1/2$, the two readouts may lie on opposite sides of the critical line. What

must actually be proved is therefore not "there is a symmetry," but "the terminal role must lie in the fixed-point set of that reciprocal action."

Second, **the source-side $1/2$ and the analytic-side $1/2$ may not be identified by a numerical sleight of hand.** The former comes from the normalized exchange of roles in $mq = n$; the latter comes from the fixed-point equation of $\rho \mapsto 1 - \overline{\rho}$. The chapter tracks representational fidelity of the same fixed relation; it does not transport a coordinate value from one coordinate system into another.

Third, **the same identity must not be broken into several independent sources merely because the representation changes, and then reconnected by an additional source-correspondence rule.** The chapter fixes

$$E_{\text{source}} \equiv E_{\text{analytic}} \equiv E_{\text{terminal}}$$

as different representational stages of one event identity. Identity fidelity excludes replacement of identity; parameter fidelity excludes reparameterizations $z \mapsto \tilde{z}$; role fidelity excludes re-pairing reciprocal roles in the middle of the chain. Identity closure further requires that a mature compressed representation remain unfoldable, recoverable, or certifiable as the same complete multiplicative identity.

For consistency, the chapter uses the following conventions:

- **root identity:** multiplication of the positive integers, $\Im_{\times} = (\mathbb{N}_{>0}, \mu)$, with $\mu(m, q) = mq$;
- **relational representation:** $\mathcal{R}_{\times} = \text{Graph}(\mu)$;
- **identity:** the generative identity that remains present through changes of representation and can be recovered or certified by the closure structure;
- **role:** a relational position that may be exchanged reciprocally inside one identity; a role is not a second identity object;
- **role readout:** a numerical or analytic coordinate of a role at a concrete representational layer;
- **identity closure:** the property that the current compressed representation can still be unfolded, recovered, or certified losslessly as the same complete multiplicative identity;
- **identity present:** the current representation lies inside that identity closure;
- **centered analytic parameter:** the parameter z tracked along the analytic representational chain;
- **event lift:** an intermediate analytic representation used in a finite horizon to describe reciprocal role readouts of the same identity;
- **terminal readout:** an actual zero readout of the complete Riemann object ξ;
- **moving horizon:** exact motion of the boundary between the head and tail;
- **exact repartition:** movement of the horizon changes only the partition, not the complete object.

For notation, the chapter uses

$$d_E(\tau)$$

for the horizontal coordinate of a finite-horizon event lift, and

$$d_\rho := \Re\rho - \frac{1}{2}$$

for the horizontal coordinate of an actual terminal zero. One must always preserve the object-type distinction

$$\boxed{d_E \neq d_\rho \quad \text{as object types.}}$$

A nonzero d_E internal to an event means only that two reciprocal roles of the same identity have different readouts in that intermediate representation. It does not mean that there are two independent identities, still less that an actual zero of the complete ξ-function has undergone an entity-like off-axis motion.

The main chain of the chapter consists, in order, of the reciprocal organization of open multiplication, centered Mellin decomposition, evenness of multiplicative shells, the global double-ζ encoding, exact head/tail migration, centered-parameter fidelity, exhaustivity of the terminal object domain, and the generative-source fixed role at the endpoint of a square horizon. Section 6 organizes these nodes into an exact double-fidelity transmission of one reciprocal event and reads the terminal fixed role from it.

2. Open Multiplicative Relations and the Unique Self-Dual Fixed Readout

In this section, $\mathcal{R}_\times$ is no longer treated as the root identity itself, but as a relational unfolding of multiplication $\mu(m,q) = mq$ on the positive integers. The purpose is to keep the hierarchy "identity–representation" explicit from the outset: the root identity is multiplication, while $\mathcal{R}_\times$ is one definite representation of that root identity.

Definition 2.1

Define multiplication on the positive integers by

$$\mu\colon \mathbb{N}_{>0} \times \mathbb{N}_{>0} \to \mathbb{N}_{>0}, \qquad \mu(m,q) = mq,$$

and its open multiplicative relational representation by

$$\boxed{\mathcal{R}_\times = \mathrm{Graph}(\mu) = \{(m,q,n) \in \mathbb{N}^3 \colon mq = n\}.}$$

For fixed n, write

$$\mathcal{D}_n = \{(m,q) \in \mathbb{N}^2 \colon mq = n\}.$$

Define the reciprocal exchange

$$J(m,q) = (q,m).$$

Here J exchanges only the two factor roles inside the same multiplicative identity; it does not generate a second source object. Every reciprocal construction below preserves this distinction between role and identity.

Lemma 2.2 (Unique Self-Dual Fixed Readout)

Let $n > 1$ and define

$$u = \log_n m, \qquad v = \log_n q.$$

Then

$$u + v = 1,$$

and J acts in normalized coordinates by

$$u \leftrightarrow 1 - u.$$

Its unique fixed point is

$$\boxed{u = v = \frac{1}{2}}.$$

Proof

From $mq = n$,

$$\log_n m + \log_n q = 1.$$

Exchanging m and q exchanges u and v, so in a one-variable representation the action is $u \mapsto 1 - u$. A fixed point satisfies

$$u = 1 - u,$$

whence $u = 1/2$. ▫

Important: the source-side value $1/2$ says only that the exchange of multiplicative roles has a fixed coordinate. It is not equal to, and does not directly imply, the value $1/2$ in the real part of a Riemann zero. The latter can be obtained only from the fixed-point equation of the terminal analytic reciprocal involution. The numerical values agree, but the proof responsibilities are different.

Definition 2.3

To unify the multiplicative coordinates used in this chapter, define the total multiplicative scale and the relative role coordinate by

$$\boxed{L_\times := \log(mq), \qquad R := \log\frac{q}{m}.} \tag{2.1}$$

Retain also the half-coordinate

$$\ell(m, q) := \frac{1}{2}R = \frac{1}{2}\log\frac{q}{m}. \tag{2.2}$$

Then reciprocal exchange gives

$$L_\times \mapsto L_\times, \qquad R \mapsto -R, \qquad \ell \mapsto -\ell. \tag{2.3}$$

Thus $R = 0$ (equivalently $\ell = 0$) is the fixed section of the generative-source role exchange; in the bare multiplicative relation it is exactly $m = q$.

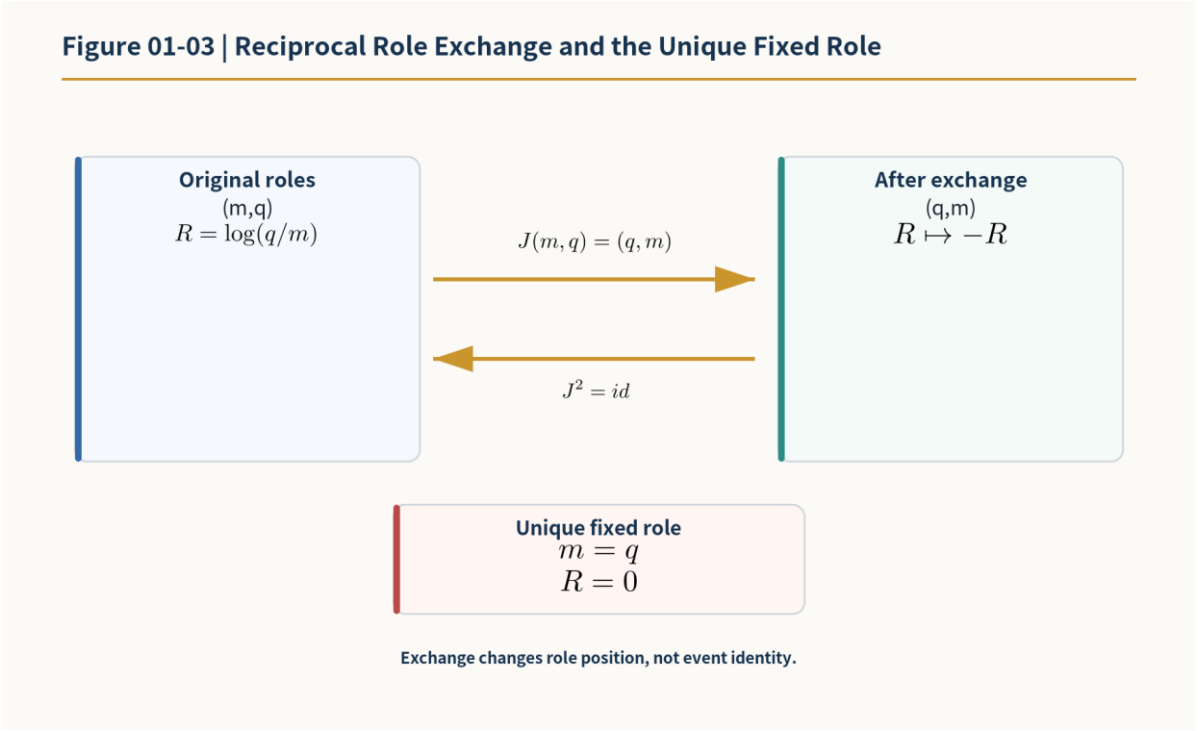


Figure 01-03. Reciprocal role exchange and the unique fixed role. The involution $J(m,q) = (q,m)$ changes role positions inside the same multiplicative event; the relative coordinate $R = \log(q/m)$ simultaneously changes to $-R$. The unique role fixed by the exchange satisfies $m = q$, equivalently $R = 0$.

3. Centered Mellin Representation

Proposition 3.1 (Centered Mellin Decomposition)

Let

$$s = \frac{1}{2} + z, \qquad z = \delta + i\gamma.$$

Define the centered Mellin kernel

$$W_z(m,q) := m^{-1/2-z} q^{-1/2+z}.$$

Then

$$\boxed{W_z(m,q) = (mq)^{-1/2} e^{2z\ell(m,q)} = e^{-L_\times/2} e^{zR}.}$$

Proof

A direct calculation gives

$$\begin{aligned} m^{-s} q^{-(1-s)} &= m^{-1/2-z} q^{-1/2+z} \\ &= (mq)^{-1/2} \left(\frac{q}{m}\right)^z \\ &= (mq)^{-1/2} e^{2z\ell(m,q)} = e^{-L_\times/2} e^{zR}. \end{aligned}$$

▫

Thus, if $z = \delta + i\gamma$,

$$|W_z(m,q)| = e^{-L_\times/2} e^{\delta R} = (mq)^{-1/2} e^{2\delta \ell}.$$

When $\delta = 0$, the relative multiplicative direction retains only the phase factor

$$e^{i\gamma R} = e^{2i\gamma \ell}.$$

From this point onward the chapter uses the generative-source coordinates $(L_\times, R)$: $L_\times$ records total multiplicative scale, while R records the reciprocal role direction.

Proposition 3.2 (Evenness of the Multiplicative Shell)

Define

$$a_n(z) = \sum_{mq=n} m^{-1/2-z}\, q^{-1/2+z}.$$

Then

$$\boxed{a_n(z) = a_n(-z)}.$$

Proof

The map $(m,q) \mapsto (q,m)$ is a bijection of $\mathcal{D}_n$. Exchanging the summation variables gives the result. ▫

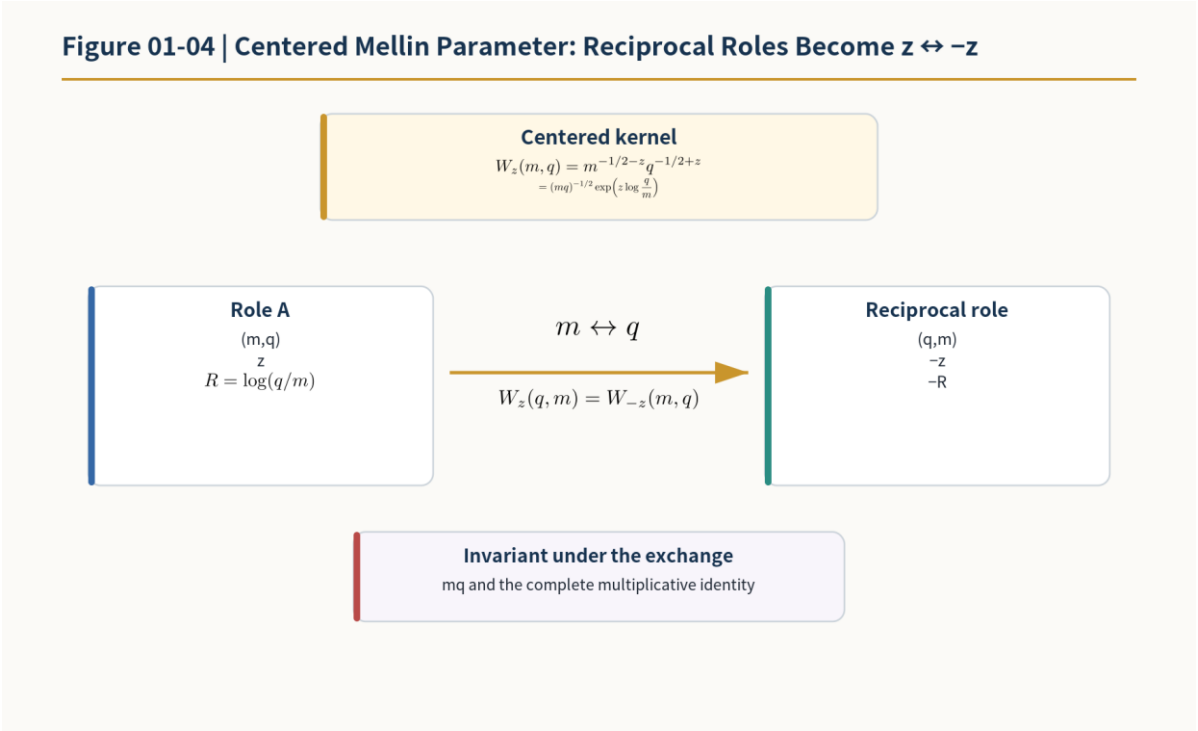


Figure 01-04. Centered Mellin parameter. The centered kernel reads factor exchange $m \leftrightarrow q$ as $R \mapsto -R$, correspondingly expressed as $z \leftrightarrow -z$. Throughout this change, mq and the complete multiplicative identity remain unchanged.

4. Global Dirichlet Encoding and the Moving Horizon

4.0 First Clarification: A Finite Horizon Is Not an Approximation

When this chapter uses the word *horizon*, it does not approximate ζ by a finite sum and does not treat the tail as an error term. The horizon makes an exact head/tail repartition inside the same complete object:

$$\text{complete object} = \text{head} + \text{tail}.$$

When the horizon moves from r to $r+1$, the same term migrates exactly from the tail into the head, and the total remains unchanged. The central property of the moving horizon is therefore

$$\boxed{\text{the visible part changes; the complete identity does not.}}$$

4.0A Dual Dirichlet–Euler Representation and Multiplicative Identity Closure

Before entering the global double-ζ encoding, fix the most basic arithmetic relation between ζ and the root multiplicative identity. For $\Re s > 1$,

$$\boxed{\zeta(s) = \sum_{n\geq 1} n^{-s} = \prod_{p} (1-p^{-s})^{-1}.} \tag{4.0a}$$

The left side reads the same multiplicative identity from the complete integer layer; the right side reads the same identity from the irreducible generators supplied by unique factorization. By the fundamental theorem of arithmetic, every

$$n = \prod_{p} p^{v_p(n)}$$

has a unique finite-support exponent family. By absolute convergence, the local geometric series

$$\sum_{k\geq 0} p^{-ks}$$

may be multiplied over primes and reorganized into all integer terms. Thus the Dirichlet and Euler representations agree exactly in their common domain of convergence.

In the identity language of this chapter, the equality has two responsibilities. First, it shows that the global integer representation of ζ and the prime-factor representation are two unfoldings of the same multiplicative identity. Second, it supplies a standard witness of recoverability: from the representation by irreducible generators one can reconstruct the complete integer multiplicative layer, while from the complete Dirichlet representation one recognizes the same analytic object in the region of absolute convergence.

The Euler product is therefore not introduced here as an independent extra condition. It arises from irreducible factorization in multiplication of the positive integers and acts as an arithmetic witness that the multiplicative identity remains present in the analytic representation ζ.

This also fixes the boundary for identifying substitutes. If

$$F(s) = \sum_{n\geq 1} c_n\, n^{-s}$$

has an analytic form, functional equation, or reciprocal symmetry resembling that of ζ, this is still insufficient to establish that F has the same closure identity as ζ. Membership in the same identity closure ultimately depends on whether it preserves and can recover the same complete multiplicative generative history.

4.0B Moving Horizon and Reciprocal Roles: Adjacent Sections Are Not Two Frozen Objects

The moving horizon and the reciprocal roles used later are not two independent structures. Their relation is this: **the horizon advances the process, while reciprocal roles provide the two-wing readout internal to the same process.**

To make this precise, write

$$\mathcal{V}_r(w) := (H_r(w), T_r(w)) \tag{4.0b}$$

for the finite presentation of the same complete analytic object at horizon r. By the exact migration formula,

$$\mathcal{V}_{r+1}(w) = (H_r(w) + (r+1)^{-w},\ T_r(w) - (r+1)^{-w}). \tag{4.0c}$$

Hence moving from r to $r+1$ is not a jump from one identity to another. It is a representational lift of the same object: the same term moves exactly from the tail role into the head role, while the complete sum remains unchanged.

If one simultaneously considers

$$w_{\pm}(\tau) = \alpha + \frac{1}{2} \pm z(\tau),$$

then the same horizon migration acts on both wings:

$$\mathcal{V}_r(w_+(\tau)) \to \mathcal{V}_{r+1}(w_+(\tau)), \qquad \mathcal{V}_r(w_-(\tau)) \to \mathcal{V}_{r+1}(w_-(\tau)), \tag{4.0d}$$

while preserving

$$w_+(\tau) - w_-(\tau) = 2z(\tau). \tag{4.0e}$$

The two reciprocal roles are therefore not two static entities waiting to merge at the end. They are the reciprocal wings of the same event at the current horizon, and the moving horizon carries the pair of role readouts together into the next event section. The later notation

$$R_+(E,\tau), \qquad R_-(E,\tau)$$

should be understood in precisely this sense of a dynamic role presentation.

If adjacent generative stages are pictured intuitively as N and $N+1$, they likewise represent two adjacent sections of one process, not two coexisting independent identities. To avoid collision with the notation N used for multiplicative bounds, the chapter uniformly writes

$$r \to r+1$$

for a horizon lift.

The reciprocal boundary avatars in Appendix A express the same dynamics as an exact scale flow:

$$\boxed{(y_+, y_-) \mapsto (ay_+, a^{-1}y_-), \qquad y_+y_- = 1.} \tag{4.0f}$$

Thus the two wings may change their readouts under horizon motion while the reciprocal relation itself remains invariant.

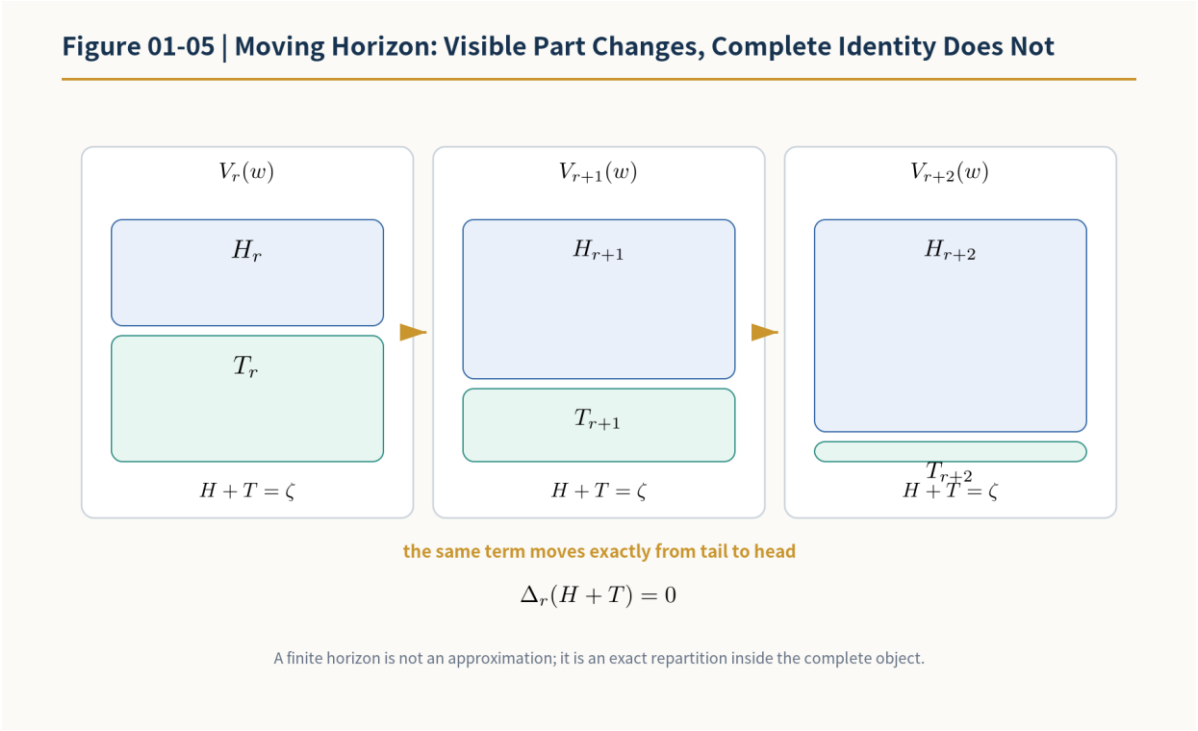


Figure 01-05. Moving horizon. Every finite horizon is an exact representation of the same complete analytic object: $H_r + T_r = \zeta$. When the horizon advances, the same term moves exactly from tail to head while the complete sum remains unchanged. A finite horizon is therefore an identity-preserving repartition, not an approximation.

4.0C Expressing the Infinite by Finite Dynamics: The Deeper Meaning of the Moving Horizon

The technical value of the moving horizon is not merely that "no information is lost after truncation." It also provides an exact finite interface for expressing an infinite object.

For every finite r,

$$\boxed{\zeta(w) = H_r(w) + T_r(w).} \tag{4.0g}$$

Here H_r is the finite visible part and T_r is the exact tail, not an ignored error. We are therefore not approximating an infinite object through

$$H_r(w) \approx \zeta(w).$$

Rather, every finite horizon

$$\mathcal{V}_r(w) = (H_r(w), T_r(w))$$

is already an exact representation of the same complete object.

As

$$r \to r+1 \to r+2 \to \cdots,$$

the finite visible part continues to grow while the tail recedes exactly, and the complete identity

$$H_r(w) + T_r(w)$$

remains unchanged. Infinity is therefore not "frozen" into one finite section; it is preserved as the same complete identity across an unboundedly advancing system of finite horizons:

$$\boxed{\mathcal{V}_0 \to \mathcal{V}_1 \to \mathcal{V}_2 \to \cdots, \qquad H_r + T_r \equiv \zeta.} \tag{4.0h}$$

In standard analytic language, ζ of course remains one definite analytic object. What changes here is its **mode of presentation**. The method represents the infinite by a family of advancing finite presentations, each exact at every stage, rather than by treating infinity as something that a single finite list must exhaust at once.

In the object-audit language of GHT, this suggests a further interpretation: the infinite may be understood as **identity remaining the same through an unbounded generative process**. This is methodological interpretation only; it does not replace the standard identities above. The proof responsibility still lies with

$$H_r + T_r = \zeta, \qquad \Delta_r(H + T) = 0.$$

But it explains why the moving horizon is more than a technical split: it is the central structure by which the chapter lets the finite carry the infinite.

Proposition 4.1 (Global Double-ζ Encoding)

Let

$$w_+ = \alpha + \frac{1}{2} + z, \qquad w_- = \alpha + \frac{1}{2} - z.$$

In the domain of absolute convergence $\Re w_\pm > 1$,

$$\boxed{\sum_{n\geq 1} a_n(z) n^{-\alpha} = \zeta\left(\alpha + \frac{1}{2} + z\right)\zeta\left(\alpha + \frac{1}{2} - z\right).}$$

Proof

Absolute convergence permits interchange of the sums:

$$\sum_{n\geq 1} a_n(z) n^{-\alpha} = \sum_{m,q\geq 1} m^{-\alpha-1/2-z}\, q^{-\alpha-1/2+z} = \zeta(w_+)\zeta(w_-).$$

▫

Proposition 4.2 (Exact Head/Tail Migration)

Define

$$H_r(w) = \sum_{n\leq r} n^{-w}, \qquad T_r(w) = \zeta(w, r+1).$$

Then

$$H_r(w) + T_r(w) = \zeta(w),$$

and

$$H_{r+1}(w) - H_r(w) = (r+1)^{-w},$$

$$T_{r+1}(w) - T_r(w) = -(r+1)^{-w}.$$

Therefore

$$\Delta_r(H+T)=0.$$

In particular, if $\zeta(\rho)=0$, then for every r,

$$\boxed{H_r(\rho)+T_r(\rho)=0.}$$

Proposition 4.3 (Completion Preserves the Analytic Parameter)

Let

$$\mathcal{C}_\xi(w)=\frac{1}{2}w(w-1)\pi^{-w/2}\Gamma(w/2), \qquad \xi(w)=\mathcal{C}_\xi(w)\zeta(w).$$

Because $\mathcal{C}_\xi(w)$ is independent of the horizon parameter r, migration of the head/tail decomposition preserves the same analytic point w after completion. Hence the centered parameter

$$z=\rho-\frac{1}{2}$$

remains unchanged across the shell representation, the double-ζ encoding, the head/tail decomposition, and completion.

Proposition 4.4 (Centered-Parameter Fidelity)

Let τ be the parameter of the same analytic event, and set

$$s(\tau)=\frac{1}{2}+z(\tau).$$

The centered Mellin kernel is

$$W_\tau(m,q)=m^{-s(\tau)}q^{-(1-s(\tau))}=(mq)^{-1/2}\exp\left(z(\tau)\log\frac{q}{m}\right). \tag{4.9}$$

For fixed n, the same $z(\tau)$ enters the entire multiplicative shell:

$$a_n(z(\tau))=\sum_{mq=n} m^{-1/2-z(\tau)}\,q^{-1/2+z(\tau)}. \tag{4.10}$$

In the domain of absolute convergence,

$$\sum_{n\geq 1} a_n\,(z(\tau))n^{-\alpha}=\zeta\left(\alpha+\frac{1}{2}+z(\tau)\right)\zeta\left(\alpha+\frac{1}{2}-z(\tau)\right). \tag{4.11}$$

Let

$$w_\pm(\tau)=\alpha+\frac{1}{2}\pm z(\tau).$$

Here α serves only as the **common translation parameter** in the global Dirichlet encoding. Strictly,

$$w_+(\tau)-w_-(\tau)=2z(\tau), \tag{4.11a}$$

and therefore

$$\boxed{z(\tau)=\frac{w_+(\tau)-w_-(\tau)}{2}.} \tag{4.11b}$$

Changing α translates w_+ and w_- in the same direction and does not change the reciprocal centered parameter $z(\tau)$. Proposition 4.4 therefore transmits the same centered parameter $z(\tau)$; it does not identify the arbitrary $w_\pm$ obtained for a given α directly with terminal zero coordinates.

For a terminal zero-role, the centered coordinate is read as

$$\rho(\tau) = \frac{1}{2} + z(\tau),$$

where the $z(\tau)$ is exactly the same centered parameter preserved along the representational chain above. The moving horizon changes only the repartition of the same analytic point between head and tail:

$$\zeta(w_{\pm}(\tau)) = H_r(w_{\pm}(\tau)) + T_r(w_{\pm}(\tau)), \tag{4.12}$$

while

$$H_{r+1}(w_{\pm}) - H_r(w_{\pm}) = (r+1)^{-w_{\pm}},$$

$$T_{r+1}(w_{\pm}) - T_r(w_{\pm}) = -(r+1)^{-w_{\pm}}. \tag{4.13}$$

Thus horizon migration changes neither $w_{\pm}(\tau)$ nor the parameterization of $z(\tau)$.

The completed function

$$\xi(w) = \mathcal{C}_{\xi}(w)\zeta(w)$$

multiplies by the completion factor $\mathcal{C}_{\xi}(w)$ at the same argument, so the same $z(\tau)$ continues into

$$\xi(w_{+}(\tau)), \qquad \xi(w_{-}(\tau)). \tag{4.14}$$

If the centered coordinate of a zero-role is denoted

$$\rho(\tau) = \frac{1}{2} + z(\tau), \tag{4.15}$$

then, strictly,

$$\boxed{\rho(\tau) - \frac{1}{2} = z(\tau).} \tag{4.16}$$

Thus from the Mellin kernel through shells, double-ζ, head/tail, completion, and zero coordinates, the centered analytic parameter is always the same $z(\tau)$. No additional reparameterization $z \mapsto \tilde{z}$ occurs between these representations.

The conclusion here is **analytic-parameter fidelity**. It does not numerically identify the multiplicative relation coordinate

$$\ell = \frac{1}{2}\log(q/m)$$

with the analytic event-lift coordinate

$$d_E = \Re\rho_{E,+} - \frac{1}{2}.$$

They belong respectively to the generative-source relational coordinates and the generative-source-resolved analytic role coordinates. The actual zero coordinate d_{ρ} is defined only at the terminal readout.

Identity discipline. Proposition 4.4 proves "change representation without changing the centered analytic parameter." It establishes analytic identity and parameter fidelity; it does not force the readouts of the two reciprocal roles to be equal. Throughout the chapter,

identity ≠ role ≠ role readout.

Once identity is fixed, the remainder of the argument tracks how reciprocal roles inside that same identity preserve their assignment in analytic representations.

5. Reciprocal Zero-Events and Terminal Readouts

The completed function satisfies

$$\xi(\bar{s}) = \overline{\xi(s)}, \qquad \xi(s) = \xi(1-s).$$

Definition 5.1 (Reciprocal Role Representation of One Identity)

Let E denote an event identity. For each event parameter τ, write the two reciprocal role positions inside the same identity as

$$R_+(E,\tau), \qquad R_-(E,\tau).$$

They are exchanged by one and the same reciprocal action; they are not two independent event objects.

At the analytic representational layer, denote the position readouts of these roles by

$$\rho_{E,+}(\tau), \qquad \rho_{E,-}(\tau).$$

The reflection–real structure of the completed function reads the same reciprocal action as

$$\boxed{\rho_{E,-}(\tau) = 1 - \overline{\rho_{E,+}(\tau)}.} \tag{5.1}$$

Accordingly, define

$$\mathrm{Read}_\tau(E) := \big(\rho_{E,+}(\tau), \rho_{E,-}(\tau)\big)$$

to be the **reciprocal role readout** of the event E at that analytic layer. The event E remains one identity; two readouts do not mean two identities.

Proposition 5.2 (Unique Horizontal Relational Quantity)

There exist real functions $d_E(\tau)$ and $\gamma_E(\tau)$ such that the centered readouts of the two reciprocal roles are

$$\boxed{z_{E,\pm}(\tau) = \pm d_E(\tau) + i\gamma_E(\tau).} \tag{5.2}$$

Since $\rho = 1/2 + z$, the role readouts in the original s-plane are

$$\boxed{\begin{aligned}\rho_{E,+}(\tau) &= \frac{1}{2} + d_E(\tau) + i\gamma_E(\tau),\\ \rho_{E,-}(\tau) &= \frac{1}{2} - d_E(\tau) + i\gamma_E(\tau).\end{aligned}} \tag{5.3}$$

Hence

$$\Re\rho_{E,+} + \Re\rho_{E,-} = 1,$$

and

$$\boxed{\rho_{E,+}(\tau) - \rho_{E,-}(\tau) = 2d_E(\tau) \in \mathbb{R}.} \tag{5.4}$$

Therefore

$$\left|\Re\rho_{E,+} - \frac{1}{2}\right| = \left|\Re\rho_{E,-} - \frac{1}{2}\right| = |d_E|. \tag{5.5}$$

Proof

Write

$$\rho_{E,+} = \sigma_E + i\gamma_E, \qquad d_E = \sigma_E - \frac{1}{2}.$$

By (5.1),

$$\rho_{E,-} = 1 - \sigma_E + i\gamma_E = \frac{1}{2} - d_E + i\gamma_E.$$

Thus

$$\rho_{E,+} - \rho_{E,-} = 2d_E,$$

and the remaining statements follow immediately. ▫

Relational-quantity discipline. The quantity $2d_E$ describes a relation between the two reciprocal role readouts **inside the same identity**. It is not a distance between two identities and must not be interpreted as a physical-like separation, motion, or collision of two entity-like zeros.

Proposition 5.3 (No Parameter Substitution in the Analytic Representation of an Event)

If the zero-role of E is represented by the same centered analytic parameter $z_E(\tau)$, Proposition 4.4 guarantees that from Mellin representation through shells, Dirichlet encoding, head/tail repartition, and completion, neither the event parameter τ nor the centered parameter $z_E(\tau)$ is replaced as the representation changes.

Therefore

$$d_E(\tau) = \Re z_E(\tau) = \Re\rho_{E,+}(\tau) - \frac{1}{2} \tag{5.6}$$

is the same horizontal relational readout of the same event identity in each analytic representation.

To avoid confusion with actual zero coordinates, define separately

$$d_\rho(\rho) := \Re\rho - \frac{1}{2}.$$

Then $d_E(\tau)$ and d_ρ are different object types: the former records the reciprocal relational readout of one identity in a finite-horizon representation; the latter is defined only for an actual terminal zero of the complete ξ-function.

Definition 5.4 (Complete Object and Terminal Event Family)

Let the complete Riemann object be

$$\xi(s) = \frac{1}{2}s(s-1)\pi^{-s/2}\Gamma(s/2)\zeta(s).$$

Let $\mathfrak{E}_{\mathrm{Riemann}}$ be the **terminal event family** consisting of all reciprocal zero-events in the complete parameter-transmission process that **terminate at** ξ. Thus $\mathfrak{E}_{\mathrm{Riemann}}$ is not an arbitrarily selected family of events; it is the complete family of terminal readouts of the "complete object ξ" at the event level.

For each $E \in \mathfrak{E}_{\mathrm{Riemann}}$, write

$$\tau_R(E)$$

for the **right-end event section** of that event in the event decomposition of the complete open multiplicative relation. Here $\tau_R(E)$ is determined by the right endpoint of the event interval, not by the condition $d_E(\tau_R) = 0$; self-dual closure at the right endpoint is proved in Section 6.

Inside the critical strip $0 < \Re s < 1$, the completion factor

$$\frac{1}{2}s(s-1)\pi^{-s/2}\Gamma(s/2)$$

is finite and nonzero. Hence

$$Z_{\mathrm{nt}}(\zeta) = Z(\xi) \cap \{0 < \Re s < 1\}. \tag{5.7}$$

By exact parameter transmission in Proposition 4.4, zero readouts of the complete open multiplicative relation on the terminal completion retain the same centered analytic parameter z, with

$$\rho - \frac{1}{2} = z. \tag{5.8}$$

Theorem 5.5 (Exhaustivity of the Object Domain and Terminal Readouts)

With the notation of Definition 5.4,

$$\boxed{Z_{\mathrm{nt}}(\zeta) = \{\rho_{E,\varepsilon}(\tau_R(E)) : E \in \mathfrak{E}_{\mathrm{Riemann}},\ \varepsilon \in \{+,-\}\}.} \tag{5.9}$$

In other words, the internal-event values

$$\rho_{E,\varepsilon}(\tau), \qquad \tau \neq \tau_R(E),$$

are zero-roles of intermediate analytic objects resolved at the generative source. Only

$$\rho_{E,\varepsilon}(\tau_R(E))$$

is an actual zero readout of the complete Riemann object ξ.

Proof

Equation (5.7) is the standard correspondence between the zeros of ζ and ξ in the critical strip. Proposition 4.4 guarantees that from Mellin representation through shells, Dirichlet encoding, head/tail repartition, and completion, the centered analytic parameter is always the same z; terminal completion therefore does not generate a second set of zero parameters.

On the other hand, by Definition 5.4, $\mathfrak{E}_{\mathrm{Riemann}}$ is defined as the family of **all reciprocal zero-events terminating at** ξ. Every actual zero of ξ therefore arises from some terminal event readout, and every terminal event readout lies in $Z(\xi)$. Hence

$$Z(\xi) \cap \{0 < \Re s < 1\} = \{\rho_{E,\varepsilon}(\tau_R(E)) : E \in \mathfrak{E}_{\mathrm{Riemann}},\ \varepsilon \in \{+,-\}\},$$

and (5.9) follows from (5.7). ▫

6. The Open-Multiplication Event Law, Exact Transmission, and Terminal Closure

This section carries the final transmission responsibility of the chapter. Earlier, **identity closure** referred to recoverability of a representation. Here, **terminal closure** refers specifically to the reciprocal action attaining a fixed-role readout at the terminal representational layer. These responsibilities are different and must remain distinct:

$$\boxed{\text{terminal closure} \neq \text{collision or merger of two entity-like roles.}}$$

Terminal closure means only that **the reciprocal action within the same event identity has a fixed-role readout in the terminal representation.** Accordingly, throughout the chapter

$$\boxed{E_{\text{source}} \equiv E_{\text{analytic}} \equiv E_{\text{terminal}} \quad \text{as different representational stages of one event history.}} \tag{6.0}$$

This is not an additional source correspondence, nor does it re-pair a source object with a terminal object. It is simply a different reading of one identity at different representational layers.

Thus the terminal event family $\mathfrak{E}_{\text{Riemann}}$ from Section 5 is not a set of zero data imported from elsewhere. It is the family of all terminal role readouts obtained when the same open-multiplication–analytic history terminates in the complete object ξ. The chapter has no second generative source, no second system of zero identities, and no second chain of origins.

Theorem 6.1 (Square-Horizon Event Decomposition of the Complete Open Multiplicative Relation) [E]

For any integer $k \geq 1$, consider the adjacent square sections

$$N = (k+1)^2, \qquad N = (k+2)^2.$$

Let the complete open multiplicative relation between them be the event interval I_k.

At the left endpoint $N = (k+1)^2$, with current horizon $r = k$, the unique new double-exterior relation satisfying

$$m > k, \qquad q > k, \qquad mq \leq (k+1)^2$$

is

$$\boxed{(m, q) = (k+1, k+1).} \tag{6.1}$$

At the right endpoint $N = (k+2)^2$, with the next horizon $r = k+1$, the unique new double-exterior relation is likewise

$$\boxed{(m, q) = (k+2, k+2).} \tag{6.2}$$

Therefore both endpoints of every complete square-horizon event interval are fixed roles of the generative-source role exchange

$$J(m, q) = (q, m).$$

Proof

From $m > k$ and $q > k$,

$$m \geq k+1, \qquad q \geq k+1,$$

so $mq \geq (k+1)^2$. Combining this with $mq \leq (k+1)^2$ gives

$$m = q = k+1.$$

The right endpoint is identical. Thus both endpoints satisfy $J(m,q) = (m,q)$. ▫

Coordinate note. In normalized coordinates these fixed roles satisfy $u = v = 1/2$. This expresses only the fixed geometry of the source-side roles. In particular, when $m = q = S$,

$$W_z(S,S) = S^{-1} \qquad (\forall z),$$

so one cannot numerically identify $m = q$, $\ell = 0$, or the source-side $1/2$ directly with $\Re z = 0$. The chapter keeps these coordinates distinct throughout in order to prevent a conflation of different layers.

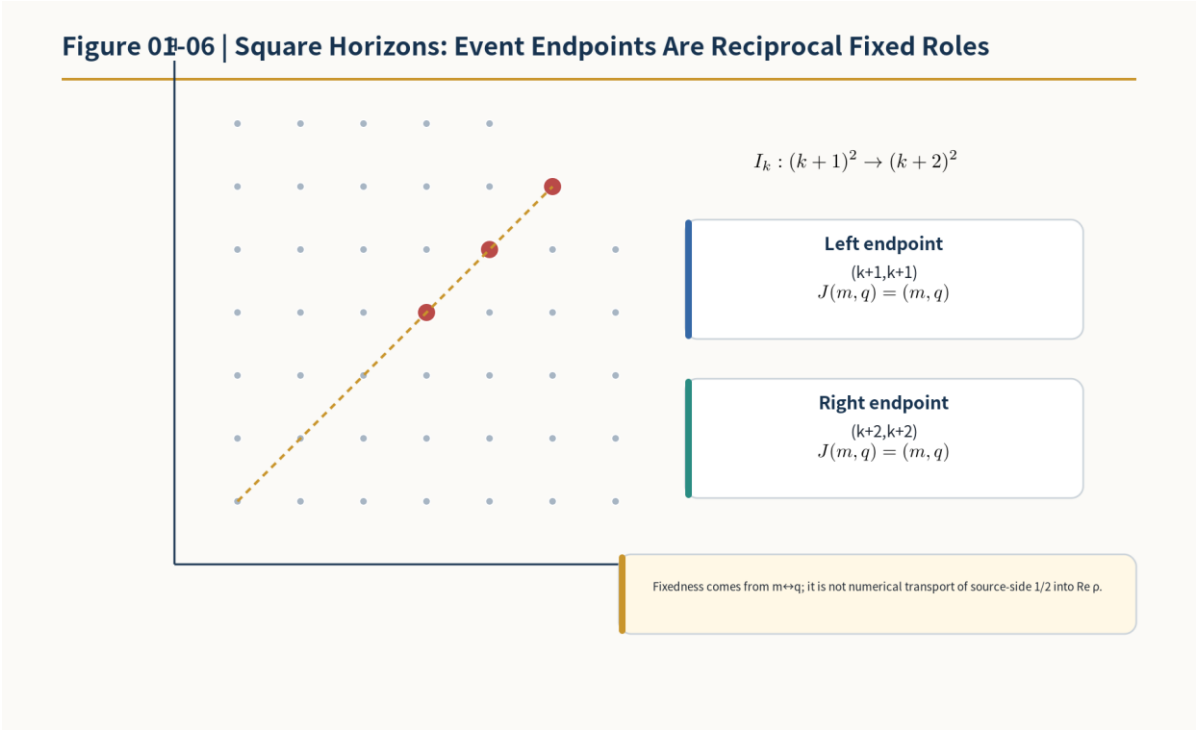


Figure 01-06. Square horizons. Between adjacent square sections, the endpoints of a complete event lie uniquely at the diagonal roles $(k+1, k+1)$ and $(k+2, k+2)$, hence they are fixed roles of the exchange $m \leftrightarrow q$. This fixedness belongs to source-side role geometry; it is not a numerical transport of source-side $1/2$ into $\Re\rho$.

Definition 6.2 (Layered Readings of One Event Identity)

Let E be a complete reciprocal event identity, let R be a role position inside that identity, and let J_E be the reciprocal-role action internal to the same identity. The generative-source layer and the analytic layer are not two event systems; they are different readings of the same (E, R).

At the generative-source layer, write the role readout as

$$x_E(\tau; R),$$

with

$$x_E(\tau; J_E R) = J\, x_E(\tau; R), \qquad J(m,q) = (q,m).$$

At the analytic layer, write the role readout as

$$\rho_E(\tau; R),$$

and the analytic reading of the same reciprocal action as

$$\rho_E(\tau; J_E R) = 1 - \overline{\rho_E(\tau; R)}. \tag{6.3}$$

Thus the chapter fixes

$$\boxed{\text{identity} \neq \text{role} \neq \text{role readout},} \tag{6.4}$$

and further fixes the rule

$$\boxed{\text{changing representation changes only the reading of the same identity and the same role; it creates no new identity and no new source}} \tag{6.5}$$

In particular, a **fixed role** means $J_E R = R$. It is a property of a role internal to the same identity, not a third object created after two role-entities merge.

Figure 01-07 | Identity, Role, and Role Readout Are Distinct

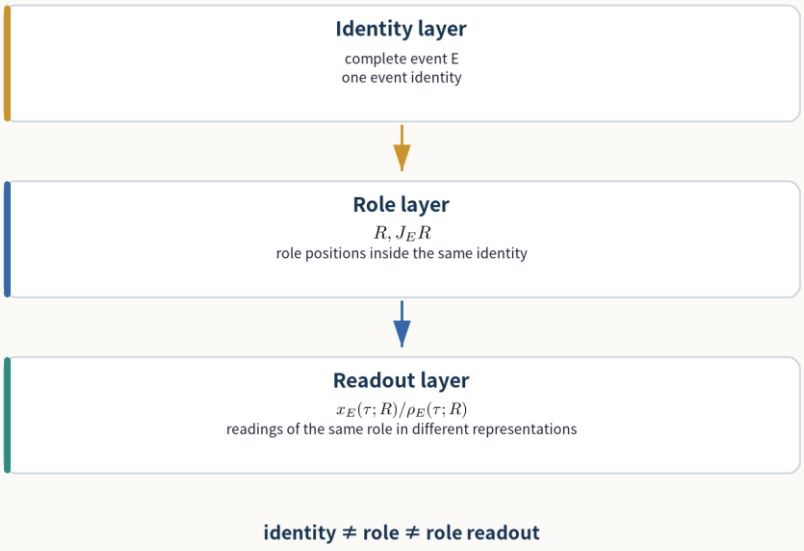


Figure 01-07. Identity, role, and role readout. A complete event identity E may contain reciprocal roles R and $J_E R$; the same role can then receive different readouts in the source and analytic representations. Changing representation changes the reading, not the identity or the source of the role.

Theorem 6.3 (Exact Double-Fidelity Transmission of Reciprocal Event and Centered Parameter) [E]

For every complete reciprocal event identity E, the representational chain established in Sections 3–5 is not a bridge between different objects, but a deterministic unfolding of one and the same identity:

$$\boxed{\begin{aligned} E \to W_{E,\tau} \to a_n(z_E(\tau)) \to \\ \zeta(w_{E,+}(\tau))\zeta(w_{E,-}(\tau)) \to (H_r, T_r) \to \xi \to \\ \rho_E(\tau; R). \end{aligned}} \tag{6.6}$$

Along this chain, four things are preserved simultaneously:

1. **Event-identity fidelity.** The root identity remains multiplication of the positive integers, $\mathfrak{I}_{\times}$, throughout. The open multiplicative relation $\mathcal{R}_{\times}$ is its relational representation. Horizon splitting, shell summation, Dirichlet/Euler encoding, head/tail repartition, and completion all take place inside the representational history of the same multiplicative identity; no second independent generative identity is introduced.
2. **Parameter fidelity.** The same centered analytic parameter $z_E(\tau)$ is neither reset nor reparameterized:

$$z_{\text{Mellin}} = z_{\text{shell}} = z_{\zeta} = z_{\text{head/tail}} = z_{\xi} = \rho_E(\tau; R) - \frac{1}{2}. \tag{6.7}$$

3. **Reciprocal-role fidelity.** The reciprocal action always acts inside the same event identity. If $R \mapsto J_E R$ is the role exchange internal to identity E, then its terminal analytic reading is

$$\boxed{\rho_E(\tau; J_E R) = \iota(\rho_E(\tau; R)), \qquad \iota(\rho) = 1 - \overline{\rho}.} \tag{6.8}$$

Equation (6.8) is **consistency of the role reading of one identity across representational layers**, not an additional map of origin from a source object to a terminal object.

4. **Identity closure.** The preceding three fidelities require more than local symbolic consistency: mature representations must remain inside the recoverable closure of the same multiplicative identity. The relational representation, primes/unique factorization, and Dirichlet/Euler representation provide arithmetic witnesses of recovery; centered Mellin representation, shells, and exact head/tail repartition preserve the same parameterized analytic object; completion registers the completion structure at the same analytic variable. Thus when this chapter says that "identity remains present," it means concretely that these representations have not replaced the original multiplicative identity by another generative identity and that the full representational history still bears responsibility for recovery to $\mathfrak{I}_{\times}$.

In particular, the family $\mathfrak{E}_{\text{Riemann}}$ defined in Section 5 is exactly the family of all event identities in this same history when it terminates at ξ, together with their terminal role readouts. "Exhaustivity of terminal origin" is only a completeness statement about one and the same object domain.

Proof

Propositions 3.1–3.2 give centered Mellin representation and reciprocity of the multiplicative shell. Proposition 4.1 inserts the same $z_E(\tau)$ into the two ζ-arguments. Proposition 4.2 shows that the moving horizon merely repartitions the same analytic object exactly between H_r and T_r. Propositions 4.3–4.4 show that completion does not change the analytic parameter, and Proposition 5.3 confirms again that changing representation introduces no parameter substitution. Combined with the dual Dirichlet–Euler representation of Section 4.0A, the relational layer, the irreducible generating layer, and the global analytic layer remain organized by the same multiplicative structure. Thus neither identity nor centered parameter is replaced along the representational chain, and the identity-closure responsibility required here is preserved.

For reciprocal roles, the source-side exchange $m \leftrightarrow q$ changes only role positions internal to the same multiplicative identity. The centered kernel and shell representations preserve that reciprocal structure; the reflection–real structure of the completed function reads the same reciprocal action in the terminal representation as $\rho \mapsto 1 - \overline{\rho}$. Thus (6.8) is not a matching between two event systems,

but a consistent reading of the same (E, R) at different representational layers. All three fidelities, together with closure, hold. ▫

Logical boundary. Theorem 6.3 does not claim numerical equality between the internal multiplicative coordinate

$$\ell = \frac{1}{2}\log\frac{q}{m}$$

and the horizontal analytic zero coordinate $\Re\rho - 1/2$, nor does it use the false implication $m = q \Rightarrow z = 0$. What it preserves is the assignment of identity, role, and role readout; it does not force coordinates belonging to different layers to be numerically identical.

Lemma 6.3A (Identification of the Terminal Reciprocal Roles with One Fixed Role) [E]

Let

$$E \in \mathfrak{E}_{\text{Riemann}}$$

be any complete terminal event, and let $\tau_R(E)$ be the right-end event section from Definition 5.4. Denote the two reciprocal roles of the event at that right-end section by

$$R_{E,+}(\tau_R), \qquad R_{E,-}(\tau_R) = J_E R_{E,+}(\tau_R).$$

Then, at the level of roles, these are not two distinct roles. They are the same generative-source fixed role:

$$\boxed{R_{E,+}(\tau_R) = R_{E,-}(\tau_R) = R_E.} \tag{6.8a}$$

Consequently, the terminal analytic readouts satisfy

$$\boxed{\rho_{E,+}(\tau_R) = \rho_E(\tau_R; R_E) = \rho_{E,-}(\tau_R).} \tag{6.8b}$$

Hence the terminal object domain of Theorem 5.5 can equivalently be written

$$\boxed{Z_{\text{nt}}(\zeta) = \{\rho_E(\tau_R(E); R_E) : E \in \mathfrak{E}_{\text{Riemann}}\}.} \tag{6.8c}$$

Proof

By Definition 5.4, $\tau_R(E)$ is the right-end section of the complete open-multiplication event in the square-horizon event decomposition. Let the corresponding right-end square section be

$$N = S^2.$$

Theorem 6.1 already proves that the unique new double-exterior factor relation at that section is

$$(m, q) = (S, S).$$

The two reciprocal roles of the event are precisely

$$(m, q) \quad \text{and} \quad (q, m).$$

Thus at the right endpoint

$$(m, q) = (q, m),$$

so the reciprocal action no longer changes the role position. Therefore

$$R_{E,+}(\tau_R) = R_{E,-}(\tau_R) = R_E,$$

which is (6.8a).

In Definition 6.2,

$$\rho_E(\tau; R)$$

is the readout, at the analytic representational layer, of role R inside one event identity. Since the two reciprocal labels at the right endpoint already point to the same R_E in the role space, the same readout map applied to the same role can only return the same value. Hence

$$\rho_{E,+}(\tau_R) = \rho_E(\tau_R; R_E) = \rho_{E,-}(\tau_R),$$

giving (6.8b).

Finally, Theorem 5.5 gives

$$Z_{\mathrm{nt}}(\zeta) = \{\rho_{E,\varepsilon}(\tau_R(E)) : E \in \mathfrak{E}_{\mathrm{Riemann}},\ \varepsilon \in \{+,-\}\}.$$

By (6.8b), for each fixed E, the terminal labels $+$ and $-$ both read the same fixed role R_E at the right-end section. The set therefore collapses immediately to (6.8c). ▫

Object-level clarification. Equation (6.8a) does not describe "two entities colliding at the terminal point." It states only that the reciprocal involution acts on a fixed role at the right endpoint of the event, so that the $+$ and $-$ role labels point to the same element of role space. Equation (6.8b) is simply the functional consequence of that role identity at the level of analytic readout.

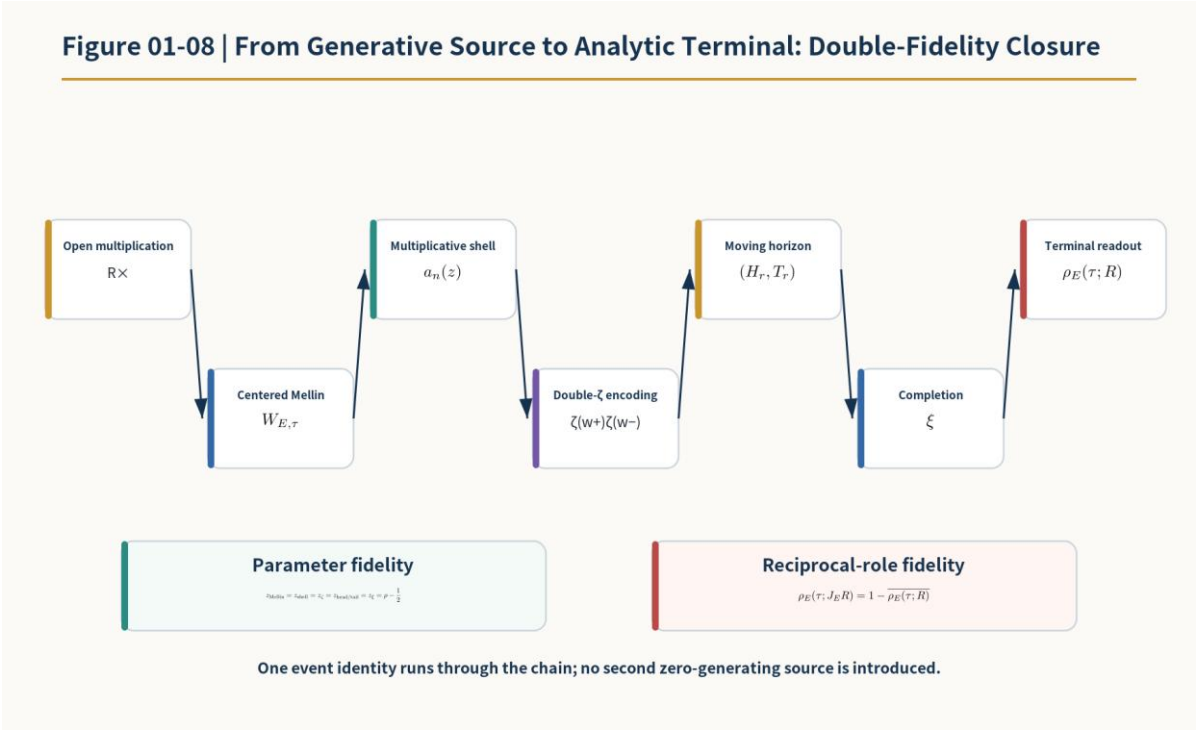


Figure 01-08. Double-fidelity closure from generative source to analytic terminal. Open multiplication, centered Mellin representation, multiplicative shells, double-ζ encoding, moving horizons, completion, and terminal readout are deterministic representations of one event identity. The chain preserves both the centered parameter and reciprocal-role provenance without introducing a second zero-generating source.

Theorem 6.4 (Terminal Fixed-Role Readout) [E]

Let $E \in \mathfrak{E}_{\text{Riemann}}$, and let R_E be its generative-source fixed role at the right endpoint of the complete square horizon. By Theorem 6.1,

$$J_E R_E = R_E. \tag{6.9}$$

By reciprocal-role fidelity in Theorem 6.3, the readout of the same role R_E in the terminal analytic representation satisfies

$$\rho_E(\tau_R; J_E R_E) = \iota(\rho_E(\tau_R; R_E)). \tag{6.10}$$

Together with $J_E R_E = R_E$, this gives

$$\boxed{\rho_E(\tau_R; R_E) = 1 - \overline{\rho_E(\tau_R; R_E)}.} \tag{6.11}$$

Hence

$$\boxed{\Re \rho_E(\tau_R; R_E) = \frac{1}{2}.} \tag{6.12}$$

Proof

Equation (6.9) says that at the right endpoint of the source-side square horizon, the reciprocal action no longer changes the position of role R_E inside the same identity. Theorem 6.3 guarantees that role assignment is not replaced under a change of representation and that the same reciprocal action is read at the terminal analytic layer as $\iota(\rho) = 1 - \overline{\rho}$. The terminal readout must therefore be a fixed readout of ι, which is exactly (6.11). Taking real parts gives (6.12). ▫

There is no ontological process in which "two roles first separate and later merge." Fixedness belongs to the action on a role inside one event identity; $\rho = 1 - \overline{\rho}$ is the readout equation of that

fixed role in the terminal analytic representation. The final $1/2$ therefore comes from the analytic reciprocal fixed-point equation, not from numerical copying of the source-side value $1/2$.

6.5 The Role-Readout Picture of a Complete Event

At an intermediate analytic representation, the same event identity E may have two reciprocal role readouts

$$\rho_{E,\pm}(\tau) = \frac{1}{2} \pm d_E(\tau) + i\gamma_E(\tau). \tag{6.13}$$

When $d_E(\tau) \neq 0$, this means only that the two role positions of the same identity have different readouts at that representational layer. Their relational quantity is

$$\boxed{\rho_{E,+}(\tau) - \rho_{E,-}(\tau) = 2d_E(\tau).} \tag{6.14}$$

It is not a distance between two identities and does not describe two entity-like zeros moving toward one another along a physical trajectory.

At the terminal fixed role R_E, the reciprocal action no longer changes the role position. Its analytic readout satisfies

$$\iota(\rho_E) = \rho_E,$$

so the corresponding horizontal relational readout is

$$\boxed{d_E(\tau_R(E)) = 0.} \tag{6.15}$$

If this representational change is drawn schematically, it may be compressed as

$$0 \to d_E(\tau) \to 0, \tag{6.16}$$

or

$$\frac{1}{2} \to \left(\frac{1}{2} + d_E(\tau), \frac{1}{2} - d_E(\tau)\right) \to \frac{1}{2}. \tag{6.17}$$

But these arrows must be read strictly as **changes in role readout of the same identity across event sections or representational stages**, not as two entities moving from opposite sides and then colliding, meeting, or merging.

The diagrammatic language is therefore only an aid at the level of representation. The entire proof responsibility of Theorem 6.4 rests on “fixed role + role fidelity + terminal analytic fixed-point equation.”

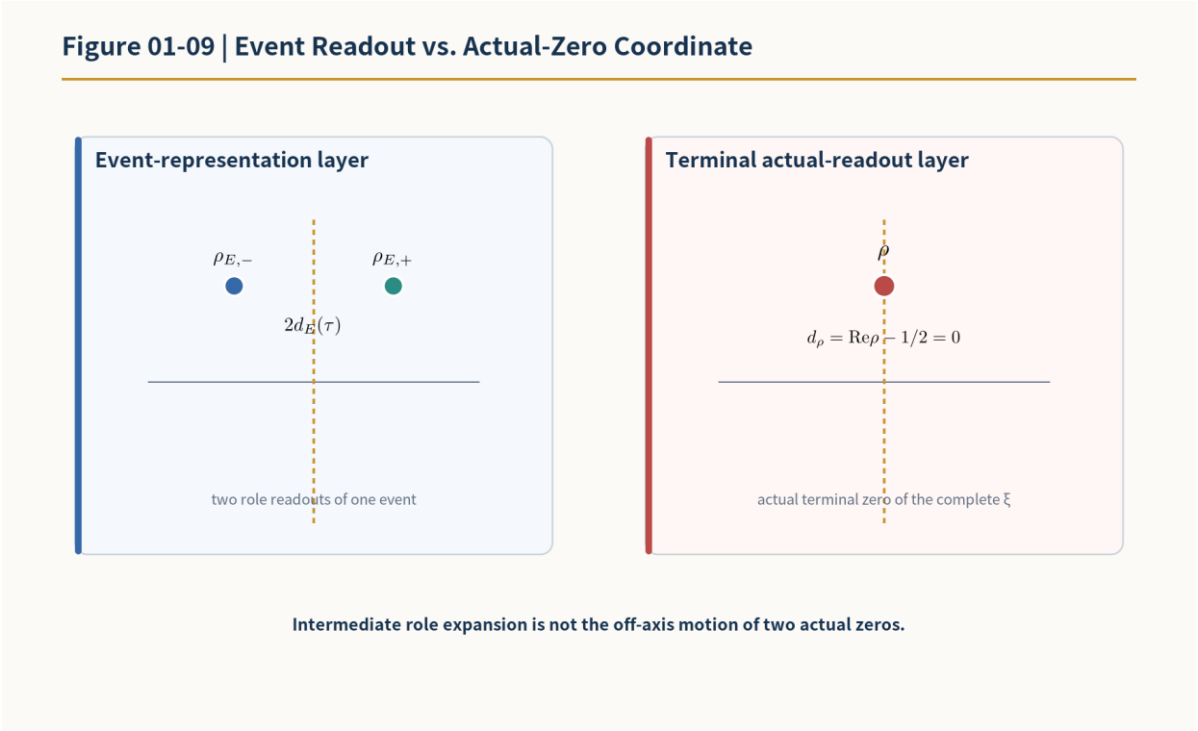


Figure 01-09. Event readout versus actual-zero coordinate. The intermediate values $\rho_{E,\pm}(\tau) = \frac{1}{2} \pm d_E(\tau) + i\gamma_E(\tau)$ are two role readouts of one event identity; they are not two actual off-axis zeros of the complete ξ-function. The actual terminal-zero coordinate is $d_\rho = \Re\rho - \frac{1}{2}$, and the fixed-role terminal readout gives $d_\rho = 0$.

7. Main Theorem

Theorem 7.1 (Critical-Line Conclusion for All Nontrivial Zeros) [E]

For every nontrivial Riemann zero ρ,

$$\boxed{\Re\rho = \frac{1}{2}.}$$

Proof

Take any

$$\rho \in Z_{\mathrm{nt}}(\zeta).$$

By Theorem 5.5 and Lemma 6.3A, there exists

$$E \in \mathfrak{E}_{\mathrm{Riemann}}$$

such that

$$\boxed{\rho = \rho_E(\tau_R(E); R_E).} \tag{7.1}$$

No actual zero needs to be paired after the fact with some source-side fixed role. Theorem 5.5 already exhausts all terminal zero-events, and Lemma 6.3A proves that the $+$ and $-$ reciprocal role labels of every terminal event are, at the right endpoint of the square horizon, already the same fixed role R_E. Thus the terminal object domain is identical to the object domain of terminal fixed-role readouts.

By Theorem 6.4,

$$\Re\rho_E(\tau_R(E); R_E) = \frac{1}{2}. \tag{7.2}$$

Substituting (7.1) yields

$$\Re\rho = \frac{1}{2}.$$

Since ρ was arbitrary, the conclusion covers all nontrivial zeros. ▫

Logical note. This theorem introduces no second source of zero data and invokes no spectral operator as a proof input. It uses only the complete object ξ defined in this chapter, exhaustivity of the terminal event family, and the exact double-fidelity transmission of one and the same event history.

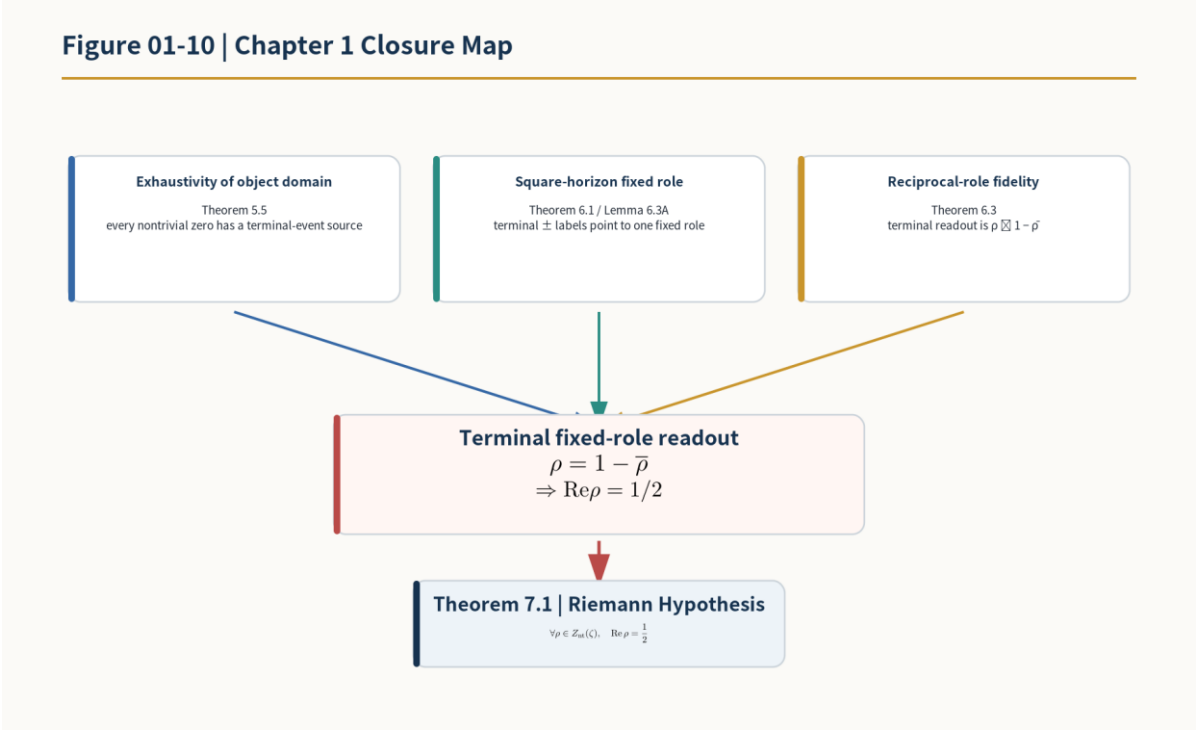


Figure 01-10. Chapter 1 closure map. Theorem 5.5 gives terminal-source exhaustivity for every nontrivial zero; Theorem 6.1 and Lemma 6.3A identify the terminal reciprocal labels with one fixed role; Theorem 6.3 preserves the reciprocal-role readout in the analytic representation. These converge in Theorem 6.4 to $\rho = 1 - \overline{\rho}$, and Theorem 7.1 concludes that every nontrivial zero satisfies $\Re\rho = \frac{1}{2}$.

8. Reciprocal Role Readouts Inside an Event Do Not Mean That Actual Zeros Move Off the Critical Line

Theorem 7.1 closes the horizontal coordinate

$$d_\rho = \Re\rho - \frac{1}{2}$$

of actual terminal zeros of the complete object ξ. It does not require the relational coordinate

$$d_E(\tau)$$

in finite-horizon event representations to vanish identically throughout the history of the event.

When

$$d_E(\tau) \neq 0,$$

one may write the two reciprocal role readouts of the same identity as

$$\rho_{E,\pm}(\tau) = \frac{1}{2} \pm d_E(\tau) + i\gamma_E(\tau).$$

The object-type discipline is essential: $\rho_{E,+}(\tau)$ and $\rho_{E,-}(\tau)$ are two role readouts of the same event identity in an intermediate analytic representation. They are **not two independent identities, and they are not actual zero divisors of the complete ξ-function**.

The horizontal quantity

$$\rho_{E,+}(\tau) - \rho_{E,-}(\tau) = 2d_E(\tau)$$

is a role-relation quantity internal to one identity. It may vary with the event parameter, but this must not be reified as horizontal motion of two actual zero-entities.

At the terminal fixed-role readout

$$\tau = \tau_R(E),$$

Theorem 6.4 gives

$$\iota(\rho_E) = \rho_E,$$

equivalently

$$\boxed{d_\rho = 0.}$$

Thus there is no contradiction between "an intermediate representation has two reciprocal role readouts" and "the actual terminal zeros of the complete Riemann object lie on the critical line": the former belongs to a representational layer, the latter to the terminal actual-readout layer.

8.1 Minimal Summary of Two Technical Features

To prevent the technical contributions of the chapter from being hidden by the main theorem, the method can be compressed into two reusable structures.

A. The Moving Horizon as Exact Repartition

$$H_r(w) + T_r(w) = \zeta(w), \qquad \Delta_r(H + T) = 0.$$

A finite horizon is not truncation-error analysis, but an exact identity-preserving split. More importantly, the lift $r \to r + 1$ provides a dynamics for the same event: the same term moves from the tail role into the head role, both reciprocal wing readouts advance together into the next representational section, and the complete object does not change. A finite horizon is therefore both the carrier of role dynamics and an exact finite interface to an infinite object. It carries the complete

infinite identity through a continuously generated sequence of finite presentations, without mistaking any finite window for a new object.

B. One Identity, Identity Closure, and Reciprocal-Role Fidelity

There is only one root multiplicative identity in the book:

$$\Im_{\times} = (\mathbb{N}_{>0}, \mu), \qquad \mu(m, q) = mq.$$

Open multiplicative relations, primes/unique factorization, Dirichlet/Euler representations, head/tail horizons, shells, the completed function, and terminal zero readouts are all organized inside the representational history of that root identity and do not constitute new generative identities. The most compact form is

$$\boxed{\text{one root identity} + \text{one event history} + \text{one centered parameter} + \text{many faithful representations.}}$$

Identity fidelity requires that no layer replace the identity. **Identity closure** further requires that a mature compressed representation remain losslessly unfoldable, recoverable, or certifiable as the same complete multiplicative identity. **Terminal closure** refers specifically to the fixed-role readout, not to the merger of two entities. These notions carry, respectively, the proof responsibilities of continuity of identity, recoverability, and the terminal fixed-role value.

9. Conclusion

The proof in this chapter does not understand the Riemann Hypothesis as a question of why an isolated zero "chooses" $1/2$. It returns the zero to a complete generative–representational history. What the chapter actually follows is one and the same multiplicative identity of the positive integers: how it changes representation through relations, irreducible factorization, Dirichlet/Euler representation, Mellin representation, shells, moving horizons, completion, and terminal zero readouts while preserving the consistency of identity, parameter, and reciprocal-role assignment.

From this viewpoint, the formulas themselves are not what most easily create additional difficulty. The additional burden often appears only after the hierarchy of objects has been cut apart and new explanatory debt has been manufactured. A bare result with no requirement of origin does not automatically generate a question "why this?" The question arises when a result originally generated by a clear relation is severed from its history and re-objectified, forcing the terminal value to search again for its own source. This chapter therefore always examines zero readouts inside their multiplicative–analytic history rather than treating them as source-free complex numbers.

The history can be understood on three levels.

First, **the identity remains the same.** The root identity is

$$\Im_{\times} = (\mathbb{N}_{>0}, \mu), \qquad \mu(m, q) = mq.$$

The relation $\mathcal{R}_{\times} = \mathrm{Graph}(\mu)$ is a relational representation. Primes and unique factorization supply an irreducible generating representation. Dirichlet and Euler representations supply global and irreducible analytic readings. After entering Mellin representation, shells, ζ, ξ, and terminal zeros, what changes is the form of representation and the role readout, not the generative identity.

Second, **representations unfold and progressively contract.** The funnel provides the intuitive picture: the same identity enters new representational conditions, and the freely variable components

are reduced layer by layer. So long as every layer remains inside the same identity closure, what emerges from the sieve is still the same identity. The square horizon gives the source-side fixed role. Reciprocal-role fidelity guarantees that its role assignment is not re-paired when the representation changes. At the terminal layer, the reciprocal action is read as

$$\iota(\rho) = 1 - \overline{\rho}.$$

Hence the terminal readout of the fixed role satisfies

$$\rho = 1 - \overline{\rho},$$

and therefore

$$\boxed{\Re\rho = \frac{1}{2}.}$$

The value $1/2$ is not copied from source to terminal; it is the unique fixed-role readout, in the terminal analytic representation, of the same reciprocal fixed relation.

Third, **closure means that identity remains recoverable.** The chapter distinguishes terminal closure from identity closure: terminal closure is the fixed-role readout; identity closure requires that a highly compressed mature representation remain losslessly unfoldable, recoverable, or certifiable as the same complete multiplicative identity. Together they say that even though the terminal readout is highly compressed, its generative history has not been erased.

Technically, exact repartition under the moving horizon ensures that a finite horizon changes only the visible allocation, not the complete object. Centered-parameter fidelity ensures that z is never reset between Mellin representation, shells, double-ζ, head/tail, and completion. The event-identity discipline

$$E_{\text{source}} \equiv E_{\text{analytic}} \equiv E_{\text{terminal}}$$

ensures that source, analytic, and terminal are not three objects re-paired after the fact. The terminal object domain carries responsibility for covering all actual nontrivial zeros. The local formulas close the global proof responsibility exactly at these nodes.

The core of the chapter is therefore not that "more formulas bring one closer to the answer," but that every formula must return to the same global question: **what exactly is preserved at this layer?** If identity remains the same, role assignment is not replaced, the parameter is not reset, and compression remains closed, then the final fixed-role readout is not a numerical condition that suddenly appears at the end; it is the terminal reading of the whole contracted history.

At the object level, the chapter can be compressed as

> **Identity remains the same while representations unfold and progressively contract; roles emerge from relations and readouts change with representation; an object is a compression of its history and a history is the unfolding of the object; what is losslessly recoverable lies in the identity closure, and closure means that identity remains present.**

Later chapters unfold this structure from the opposite direction. Chapter 6 (H06), *The RH Ren Operator: A Lossless Bridge Between Multiplicative Identity, Analytic Continuation, and the*

Canonical Spectrum, introduces the Ren operator and recovers and unfolds the multiplicative identity in reverse from a highly compressed analytic/spectral object. It does not invent a new origin for the terminal object; it verifies that, after compression, identity can still return to the root. Chapter 9 (H09), *Another Closure Route for the Riemann Hypothesis: Open Multiplicative Identity and an Independent Hilbert–Pólya Spectral Route—from Open Multiplicative Identity to a Source-Generated Self-Adjoint Spectrum and Canonical Terminal Identification*, remains independent and constructs a source-generated self-adjoint spectral route from the same root multiplicative identity. Chapter 7 (H07), *The Riemann Spectral Witness Theorem: Uniqueness of the Ren Canonical Spectral Witness and Hilbert–Pólya Identity Transfer*, lies at the level of spectral witnessing and identification and carries responsibility for uniqueness and certification of the Riemann identity of the canonical spectrum.

Their roles may be summarized as

H06:	recover and unfold the multiplicative identity in reverse from a compressed object;
H09:	independently construct a source-generated self-adjoint spectrum from the multiplicative identity;
H07:	witness, uniquely determine, and identify the canonical spectrum as Riemann.

These chapters are not inputs to the main theorem here, but they give closure its fuller meaning: **after compression, recovery is possible; once identity is recovered, it can unfold again along other legitimate routes.** What remains continuously present is therefore not one fixed formula or one fixed path, but the root identity whose sameness can be certified across different representational routes.

The final $1/2$ of this chapter should accordingly be understood as the compressed readout of the complete reciprocal history in the terminal fixed-role representation. It is not an isolated number that contains all multiplicative information; it is the fixed position left in the terminal analytic layer after one and the same multiplicative identity has contracted through many representations.

Appendix A. Reciprocal Boundary Geometry of Finite Horizons

Let

$$E_N(r) = \left\{m > r : \left\lfloor \frac{N}{m} \right\rfloor > r\right\} = \left\{r < m \le \left\lfloor \frac{N}{r+1} \right\rfloor\right\}.$$

For double-exterior ordered pairs

$$m > r, \qquad q > r, \qquad mq \le N,$$

define the boundary ratios

$$y_+(N,r) = \frac{\lfloor N/(r+1) \rfloor}{r+1},$$

$$y_-(N,r) = \frac{r+1}{\lfloor N/(r+1) \rfloor}.$$

Then

$$y_+(N,r)\, y_-(N,r) = 1.$$

If both $E_N(r)$ and $E_N(r+1)$ are nonempty, define

$$a(N,r) = \frac{(r+1)\lfloor N/(r+2)\rfloor}{(r+2)\lfloor N/(r+1)\rfloor}.$$

Then

$$y_+(N,r+1) = a(N,r)y_+(N,r),$$

$$y_-(N,r+1) = a(N,r)^{-1}y_-(N,r).$$

Hence the reciprocal boundary avatars of a finite horizon satisfy the exact reciprocal scale flow

$$(y_+, y_-) \mapsto (ay_+, a^{-1}y_-).$$

When

$$N = S^2, \qquad r = S-1,$$

one has

$$y_+ = y_- = 1,$$

and the unique remaining role is

$$(S,S),$$

whose normalized fixed readout is $1/2$.

Chapter 2 Horizon-Shape Geometry of Riemann Zero Gaps

— Boundary Analytic Germs, Global Spectral Determination, and Finite-Jet Gap Bounds

Reader's Guide: From One Gap to the Entire Real Zero Spectrum

Traditional zero-spacing studies begin by recording the distance between adjacent zeros,

$$\Delta_k = \gamma_{k+1} - \gamma_k.$$

This chapter retains that scale but asks a finer question: **must equal gap lengths correspond to identical analytic structure inside the interval?** The answer is no. For each adjacent-zero interval we construct a canonical phase density p_k. A gap is therefore no longer characterized only by its length; it also carries the internal phase advance, the analytic multiplicities at its endpoints, the analytic germ at the shared boundary, and the global spectral response generated on that interval by all remaining zeros.

The key structure appears at the zero boundary. The logarithmic derivative $-\Xi'/\Xi$ has a pole at a zero. After introducing the reciprocal boundary coordinate

$$R_k(x) = -\frac{1}{M_k(x)},$$

the pole is removed and the shared zero becomes an ordinary analytic boundary point. One can then prove that two adjacent gaps sharing that zero share not merely the endpoint location or finitely many derivatives, but the **complete boundary analytic germ**, after the appropriate scale normalization.

The Taylor coefficients of this boundary analytic germ in turn generate the global inverse-distance spectral moments relative to the current zero. Once these moments are organized into a finite, compactly supported positive measure, all remaining real zeros and their analytic multiplicities can be recovered uniquely. Thus, in the real-zero spectral framework fixed in this chapter,

one zero location + one adjacent-gap scale + the complete one-sided boundary analytic germ at that zero ⇒ the entire real zero spectrum and its analytic multiplicities.

This is a global uniqueness statement for exact analytic data, not a metaphor that "the local resembles the global."

Finite-order information is also rigorous. If only finitely many boundary jets are known, the entire spectrum cannot be reconstructed, but one already obtains upper and lower bounds for the nearest-neighbor distance and, through residual moments, can determine whether an adjacent gap is shorter than, equal to, or longer than the current one. The hierarchy may be summarized as

finite jets give deterministic bounds; a complete germ gives global uniqueness.

The logical position of this chapter in the RH sequence must also be explicit: this chapter **does not re-prove RH**. Chapter 1 (H01) has already closed the nontrivial zeros onto the critical line; the present chapter takes the resulting real Riemann zero spectrum as input and studies its local-to-global analytic geometry. Nor does the chapter assume that all zeros are simple: the standard analytic

multiplicities m_k remain independent spectral data throughout. Chapter 3 (H03) further distinguishes distinct zero addresses, representation-sheet count, and analytic multiplicity; the present chapter studies only how analytic multiplicity is read from the horizon shape and enters global reconstruction.

Abstract

This chapter studies the canonical analytic geometry carried by adjacent-zero intervals of the completed Riemann function

$$\Xi(t) = \xi\left(\frac{1}{2} + it\right)$$

under the prior assumption that its nontrivial zeros form an orderable real zero spectrum, and establishes an interval-by-interval local-to-global determination structure on that real spectrum. Analytic multiplicity is retained as independent spectral data.

Write the distinct real zeros in strictly increasing order as $\{\gamma_j\}$, with analytic multiplicities m_j, and fix the adjacent interval

$$I_k = (\gamma_k, \gamma_{k+1}), \qquad \Delta_k = \gamma_{k+1} - \gamma_k.$$

Define the meromorphic Herglotz response

$$m(z) = -\frac{\Xi'(z)}{\Xi(z)},$$

the dimensionless interval response

$$M_k(x) = \Delta_k m(\gamma_k + \Delta_k x), \qquad 0 < x < 1,$$

and the canonical phase density

$$p_k(x) = \frac{1}{\pi}\frac{M_k'(x)}{1 + M_k(x)^2}.$$

We first prove that $p_k(x)\,dx$ is a probability measure and that p_k determines M_k completely. Its endpoint values read off the analytic multiplicities exactly:

$$p_k(0^+) = \frac{1}{\pi m_k}, \qquad p_k(1^-) = \frac{1}{\pi m_{k+1}}.$$

The central boundary coordinate of the chapter is

$$R_k(x) := -\frac{1}{M_k(x)} = \tan\left(\pi \int_0^x p_k(u)\,du\right).$$

It removes the pole of m at a zero. If γ_k is shared by the two adjacent intervals on its left and right, then for every $n \geq 1$,

$$\Delta_{k-1}^{1-n} R_{k-1}^{(n)}(1^-) = \Delta_k^{1-n} R_k^{(n)}(0^+).$$

Thus adjacent gaps share, at their common zero, the same reciprocal Herglotz boundary analytic germ, not merely finitely many boundary data.

Next define

$$Q_k(x) = \frac{x}{R_k(x)}.$$

Its left-end expansion is

$$Q_k(x) = m_k - \sum_{r\geq 1} C_{k,r}\, x^r,$$

where

$$C_{k,r} = \sum_{j\neq k} m_j \left(\frac{\Delta_k}{\gamma_j - \gamma_k}\right)^r.$$

For $r \geq 2$ the sum converges absolutely. The measure

$$\nu_k^{\text{gap}} = \sum_{j\neq k} m_j \left(\frac{\Delta_k}{\gamma_j - \gamma_k}\right)^2 \delta_{\Delta_k/(\gamma_j-\gamma_k)}$$

is finite, positive, and compactly supported, and its n-th moment is exactly $C_{k,n+2}$. Determinacy of the compactly supported moment problem yields the main theorem: fixing one zero location γ_k, one adjacent-gap scale Δ_k, and the complete one-sided boundary analytic germ at that zero uniquely recovers all distinct real zeros and their analytic multiplicities.

Finite boundary jets give Euler–Rayleigh-type bounds for the nearest-neighbor gap. If

$$d_k = \min_{j\neq k} |\gamma_j - \gamma_k|,$$

then

$$\frac{\Delta_k}{C_{k,2r}^{1/(2r)}} \leq d_k \leq \Delta_k \sqrt{\frac{C_{k,2r}}{C_{k,2r+2}}},$$

and both bounds converge to d_k. After subtracting the known atom at the opposite endpoint of the current interval, a residual-moment trichotomy determines from one-sided high-order boundary jets whether the adjacent gap is shorter than, equal to, or longer than the present gap.

The classical foundations are meromorphic Herglotz/meromorphic-inner theory, determinacy of compactly supported moment problems, and Euler–Rayleigh inverse-power-sum bounds. In the canonical shape coordinates of individual Riemann zero gaps they combine into the deterministic local-to-global chain

canonical phase density →
reciprocal boundary analytic germ →
global spectral moments →
compactly supported positive measure →
global real zero spectrum.

0. Logical Position, Prior Input, and Object Boundaries

0.1 Prior Input: The Real Zero Spectrum after RH Closure

The logical arrow at this point in the book is

$$\boxed{\begin{array}{r}\text{RH closure in Chapter 1 (H01)} \Rightarrow \\ \text{real Riemann zero spectrum} \Rightarrow \\ \text{the gap-shape geometry of this chapter.}\end{array}} \tag{0.1}$$

All subsequent theorems are established within the prior framework that the relevant nontrivial zeros of Ξ have already formed an orderable real zero spectrum.

0.2 Zero Addresses and Analytic Multiplicity

Throughout the chapter we distinguish

$$\boxed{\text{distinct zero address} \neq \text{analytic multiplicity.}} \tag{0.2}$$

Distinct zero locations are denoted by γ_j, with analytic multiplicity

$$m_j = \operatorname{ord}_{\gamma_j}\Xi \in \mathbb{N}.$$

We do not assume $m_j = 1$. Chapter 3 (H03) further separates zero address, representation-sheet count, and analytic multiplicity; the present chapter uses only standard analytic multiplicity and proves that it can be read exactly from the boundary shape of a gap.

0.3 Type Distinction Between Gap Shape and Event-Lift Coordinates

In this chapter, **horizon shape** refers only to an adjacent real-zero interval together with its canonical analytic data

$$(\Delta_k, p_k).$$

It introduces no new generative identity. It is not the finite-horizon event-lift coordinate $d_E(\tau)$ of Chapters 1 and 5, nor is it the actual horizontal zero coordinate

$$d_\rho = \Re\rho - \frac{1}{2}.$$

The present chapter studies the **vertical gap geometry** between zeros ordered along the real t-axis after RH closure; horizontal role readouts of event lifts do not enter the main theorem chain.

0.4 Exact Uniqueness and Stable Inversion Are Different Levels

The results here establish uniqueness at the level of exact information: can the same complete boundary analytic germ correspond to two different global real spectra? The answer is no. Conditioning under finite-precision measurement, sensitivity to noise, numerical stability, and algorithmic complexity belong to a separate computational inverse-spectral level and do not follow automatically from exact analytic uniqueness.

1. The Real Zero Spectrum and Basic Setup

1.1 The Real Zero Spectrum

This chapter starts from the closure result of Chapter 1 (H01): the relevant nontrivial zeros of the completed Riemann function $\Xi(t) = \xi(1/2 + it)$ enter an orderable real-zero spectral framework. From there we study the canonical shape inside adjacent zero gaps, the analytic germ at shared boundaries, and local-to-global spectral determination. Every theorem below is stated under the real-zero spectral assumption fixed in Section 0.

The chapter does not confuse "a distinct zero address occurs once" with "the analytic multiplicity equals one." The standard analytic multiplicity m_k remains independent spectral data. Chapter 3 further separates zero address, representation-sheet count, and analytic multiplicity; here we study only how m_k is read exactly from the boundary shape of a gap, how it participates in gluing adjacent intervals, and how it enters global spectral determination. GHT or generative auditing is not a mathematical premise of this chapter.

1.2 From Gap Length to Interval Shape

Write the distinct positive zeros as

$$0 < \gamma_1 < \gamma_2 < \cdots,$$

and let

$$\Delta_k = \gamma_{k+1} - \gamma_k.$$

The classical datum Δ_k records only the distance between two adjacent zeros. We ask further whether the complete phase transport of $-\Xi'/\Xi$ inside the interval, the endpoint multiplicities, the shared boundary analytic germ, and the global spectral field generated by all other zeros can be organized into a canonical local object.

Together these data form what the chapter calls the **horizon shape**. Here *horizon* means only the adjacent-zero interval and its canonical readout.

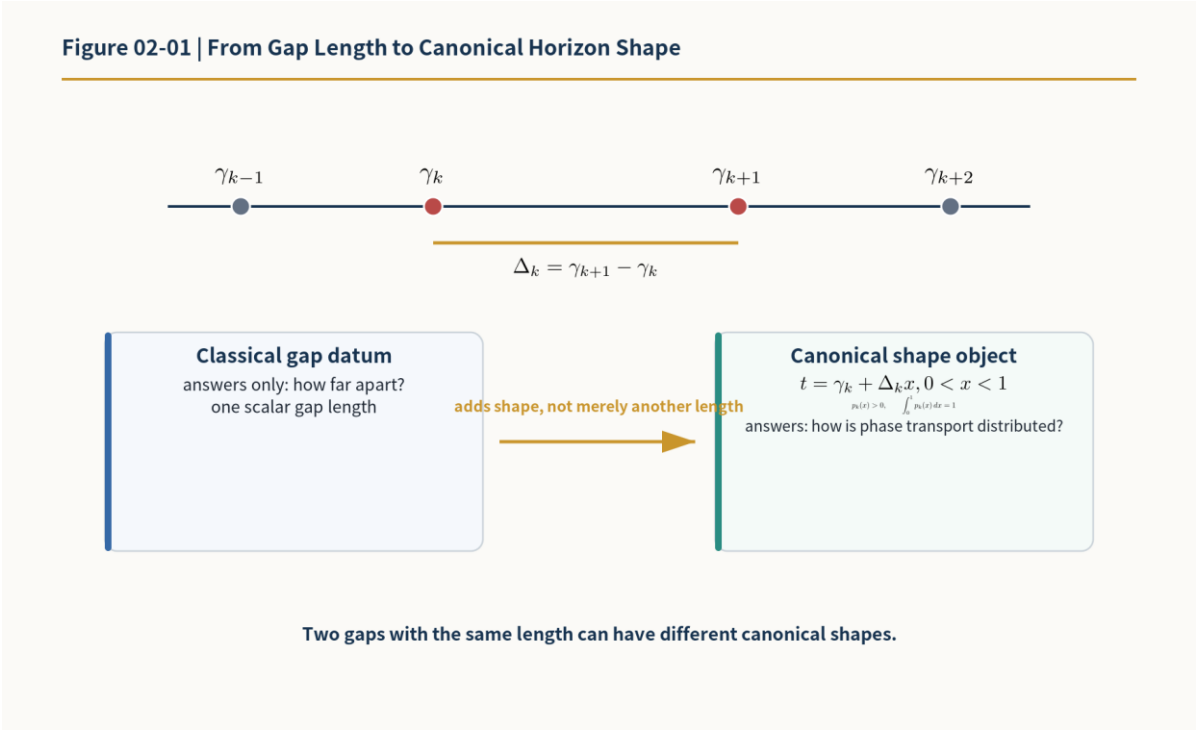


Figure 02-01. From gap length to the canonical horizon shape. The scalar $\Delta_k = \gamma_{k+1} - \gamma_k$ records only how far apart two adjacent zeros are. This chapter additionally rescales the interval to unit length and uses the probability density p_k to record how one full pole-to-pole phase transport is distributed across that distance. Two gaps of the same length may therefore still have different shapes.

2. Meromorphic Herglotz Response and Phase Monotonicity

Define

$$\xi(s) = \frac{1}{2}s(s-1)\pi^{-s/2}\Gamma(s/2)\zeta(s),$$

$$\Xi(t) = \xi\left(\frac{1}{2} + it\right).$$

The function Ξ is even, real, and entire. Write its distinct real zeros in strictly increasing order as

$$\cdots < \gamma_{-1} < \gamma_0 < \gamma_1 < \cdots,$$

with analytic multiplicities

$$m_j = \operatorname{ord}_{\gamma_j}\Xi \in \mathbb{N}.$$

In the Riemann case, the zeros occur symmetrically about the origin.

Define

$$\boxed{m(z) := -\frac{\Xi'(z)}{\Xi(z)}.} \tag{2.1}$$

In the real-zero spectral setting of this chapter, the paired Hadamard product gives

$$m(z) = \sum_j \frac{m_j}{\gamma_j - z}, \tag{2.2}$$

where the first-order terms are understood in the paired Riemann-symmetric sense; the differentiated series

$$m'(z) = \sum_j \frac{m_j}{(\gamma_j - z)^2} \tag{2.3}$$

converges locally uniformly on compact sets avoiding the poles.

If $z \in \mathbb{C}_+$, every term $(\gamma_j - z)^{-1}$ has positive imaginary part, so m is a meromorphic Herglotz function. In particular, between any two adjacent real poles,

$$m'(t) > 0. \tag{2.4}$$

We use this meromorphic Herglotz structure and its Cayley-phase properties throughout. In a standard canonical-system realization, m may be read as a Weyl–Herglotz m-function; throughout the chapter we call it the **Herglotz response**.

3. Canonical Horizon-Shape Density

Intuitive picture. The length Δ_k tells us only "how far apart are the two zeros?" The density p_k tells us how the full unit of phase transport from the left endpoint to the right endpoint is distributed across that distance. Two gaps of equal length may have different p_k, so shape is strictly finer data than gap length.

Fix adjacent zeros

$$I_k = (\gamma_k, \gamma_{k+1}), \qquad \Delta_k = \gamma_{k+1} - \gamma_k.$$

Set

$$t = \gamma_k + \Delta_k x, \qquad 0 < x < 1,$$

and define the dimensionless Herglotz response

$$\boxed{M_k(x) = \Delta_k m(\gamma_k + \Delta_k x).} \tag{3.1}$$

Since $m' > 0$,

$$M_k'(x) > 0,$$

and

$$M_k(0^+) = -\infty, \qquad M_k(1^-) = +\infty.$$

Theorem 3.1 (Canonical Phase Probability Measure)

Define

$$\boxed{p_k(x) = \frac{1}{\pi} \frac{M_k'(x)}{1 + M_k(x)^2}.} \tag{3.2}$$

Then

$$p_k(x) > 0, \qquad \int_0^1 p_k(x)\, dx = 1. \tag{3.3}$$

Proof.

$$\frac{d}{dx} \arctan M_k(x) = \frac{M_k'(x)}{1 + M_k(x)^2}.$$

Since M_k increases strictly from $-\infty$ to $+\infty$,

$$\int_0^1 p_k\,(x)dx = \frac{1}{\pi}\left(\frac{\pi}{2}+\frac{\pi}{2}\right) = 1.$$

▫

Define the cumulative phase

$$F_k(x) := \int_0^x p_k\,(u)\,du. \tag{3.4}$$

Then

$$\arctan M_k(x) = -\frac{\pi}{2} + \pi F_k(x),$$

so

$$\boxed{M_k(x) = -\cot(\pi F_k(x)).} \tag{3.5}$$

Thus p_k determines M_k completely.

Relation to Classical Phase Theory

If one defines the Cayley transform

$$\Theta(z) = \frac{m(z)-i}{m(z)+i},$$

then Θ is a meromorphic inner function whose phase increases strictly along the real axis. Equation (3.2) is essentially the phase derivative normalized to have unit mass on a single pole-to-pole interval. Monotone phase belongs to classical meromorphic-inner/Herglotz theory. The contribution here is to normalize that phase derivative gap by gap and use it to derive endpoint multiplicities, reciprocal analytic germs, all-order gluing, and moment reconstruction.

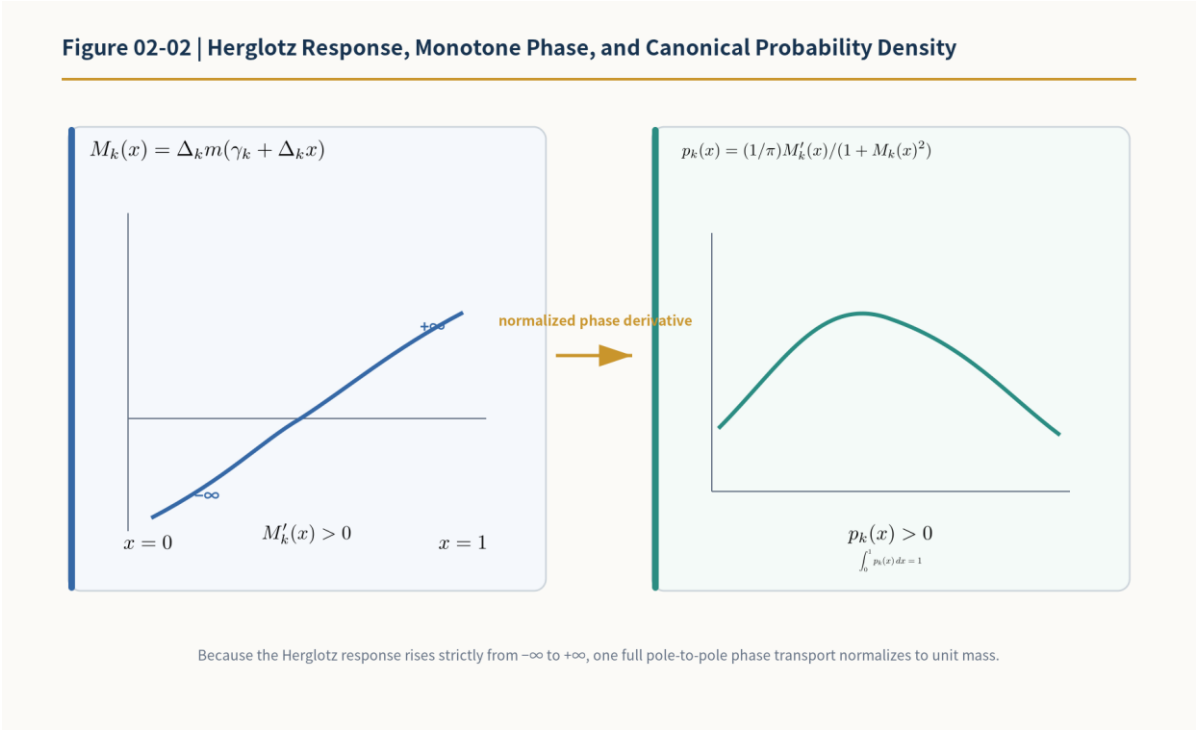


Figure 02-02. Herglotz response, monotone phase, and canonical probability density. Between two adjacent real poles, $M_k(x)$ rises strictly from $-\infty$ to $+\infty$. Normalizing its Cayley-phase derivative by $1/\pi$ gives $p_k(x) > 0$ with $\int_0^1 p_k(x)\,dx = 1$. One complete phase transport across a gap is therefore normalized to unit mass.

4. Interval Reconstruction and Quantization of Boundary Multiplicity

By (3.5), knowing p_k and Δ_k recovers

$$m(\gamma_k + \Delta_k x) = \frac{1}{\Delta_k} M_k(x). \tag{4.1}$$

Moreover,

$$\frac{d}{dx} \log|\Xi(\gamma_k + \Delta_k x)| = -M_k(x),$$

so for any $x_0 \in (0,1)$,

$$\boxed{\frac{|\Xi(\gamma_k + \Delta_k x)|}{|\Xi(\gamma_k + \Delta_k x_0)|} = \exp\left[-\int_{x_0}^{x} M_k(u)du\right].} \tag{4.2}$$

Near the left endpoint zero, write

$$m(\gamma_k + \delta) = -\frac{m_k}{\delta} + r_k + O(\delta), \tag{4.3}$$

where r_k is the finite part. Substitution into (3.2) gives:

Theorem 4.1 (Boundary Multiplicity Quantization)

$$\boxed{p_k(0^+) = \frac{1}{\pi m_k}, \qquad p_k(1^-) = \frac{1}{\pi m_{k+1}}.} \tag{4.4}$$

Hence

$$\boxed{m_k = \frac{1}{\pi p_k(0^+)} = \frac{1}{\pi p_{k-1}(1^-)}.} \tag{4.5}$$

The boundary value can therefore lie only in

$$\left\{\frac{1}{\pi}, \frac{1}{2\pi}, \frac{1}{3\pi}, \cdots\right\}.$$

Analytic simplicity is equivalent to the corresponding boundary density being $1/\pi$.

The first-order expansion also gives

$$p_k'(0^+) = \frac{2\Delta_k r_k}{\pi m_k^2}, \qquad p_{k-1}'(1^-) = \frac{2\Delta_{k-1} r_k}{\pi m_k^2}, \tag{4.6}$$

and therefore

$$\boxed{\frac{p_{k-1}'(1^-)}{\Delta_{k-1}} = \frac{p_k'(0^+)}{\Delta_k}.} \tag{4.7}$$

Equation (4.7) is only the first nontrivial layer of the all-order gluing developed next.

Figure 02-03 | Boundary Shape Density Quantizes Analytic Multiplicity

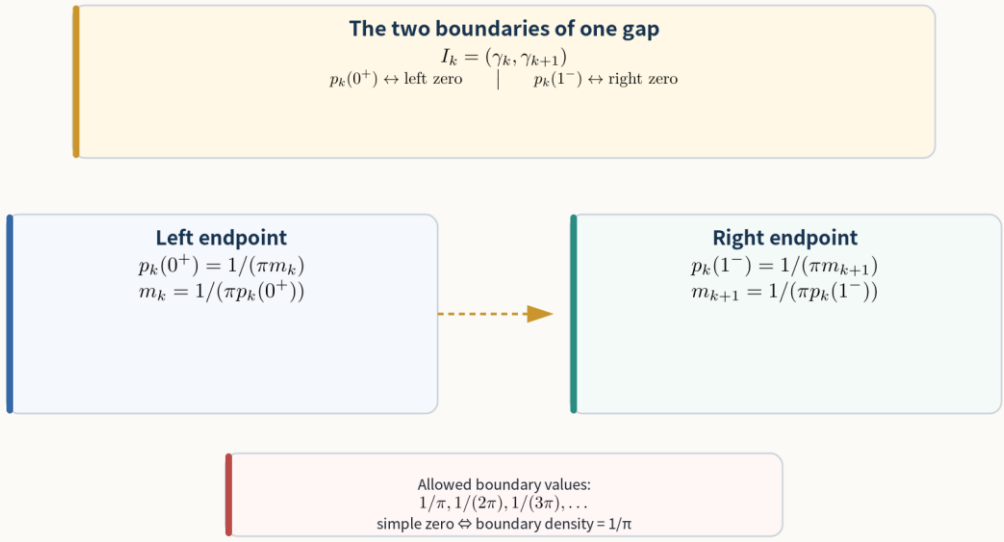


Figure 02-03. Boundary shape density quantizes analytic multiplicity. The two endpoint values of the canonical shape read the analytic multiplicities of the left and right zeros: $p_k(0^+) = 1/(\pi m_k)$ and $p_k(1^-) = 1/(\pi m_{k+1})$. Hence the boundary density can take only the discrete values $1/\pi, 1/(2\pi), 1/(3\pi)$, ..., with a simple zero corresponding exactly to boundary density $1/\pi$.

5. Reciprocal Boundary Coordinate and All-Order Boundary-Jet Gluing

Why this section matters. The original Herglotz response diverges at a zero, so direct comparison of higher derivatives is obscured by the pole. Taking the reciprocal turns the zero into an ordinary analytic boundary point $R_k = 0$. This upgrades the statement "two gaps share one zero" to "two gaps share one complete analytic interface."

The raw M_k diverges at the boundary, so the correct variable for higher-order gluing is not the raw $p_k^{(n)}$, but the reciprocal coordinate

$$\boxed{R_k(x) := -\frac{1}{M_k(x)}.} \tag{5.1}$$

By (3.5),

$$\boxed{R_k(x) = \tan(\pi F_k(x)) = \tan\left(\pi \int_0^x p_k(u)du\right).} \tag{5.2}$$

In particular, $R_k(0) = R_k(1) = 0$, understood by analytic continuation to the endpoints.

Fix the shared zero γ_k and define

$$\boxed{G_k(\delta) := -\frac{1}{m(\gamma_k + \delta)}.} \tag{5.3}$$

By (4.3), G_k is analytic at $\delta = 0$, with

$$G_k(0) = 0, \qquad G_k'(0) = \frac{1}{m_k}. \tag{5.4}$$

The right-hand gap satisfies

$$R_k(x) = \frac{1}{\Delta_k} G_k(\Delta_k x), \tag{5.5}$$

and the left-hand gap satisfies

$$R_{k-1}(x) = \frac{1}{\Delta_{k-1}} G_k(\Delta_{k-1}(x-1)). \tag{5.6}$$

Theorem 5.1 (Infinite Boundary-Jet Gluing)

For every integer $n \geq 1$,

$$\boxed{\Delta_{k-1}^{1-n} R_{k-1}^{(n)}(1^-) = \Delta_k^{1-n} R_k^{(n)}(0^+) = G_k^{(n)}(0).} \tag{5.7}$$

Proof. Differentiate (5.5) and (5.6) successively. ▫

The formula shows that adjacent gaps share, at their common zero, not merely finitely many empirical boundary quantities but the same reciprocal Herglotz analytic germ.

Corollary 5.2 (Equivalence with the Laurent Germ)

The complete Taylor germ of $G_k = -1/m$ and the complete Laurent germ of m at γ_k determine one another uniquely. Hence the entire sequence of scaled boundary R-jets is equivalent to the complete Laurent data at the shared zero.

Remark

Beginning at second order, direct gluing of the raw derivatives $p_k^{(n)}$ acquires nonlinear correction terms. For example, at an endpoint

$$R''' = \pi p'' + 2\pi^3 p^3.$$

The correct invariant is therefore the R-jet, not a naive quantity such as p''/Δ^2. This is why the reciprocal coordinate is essential.

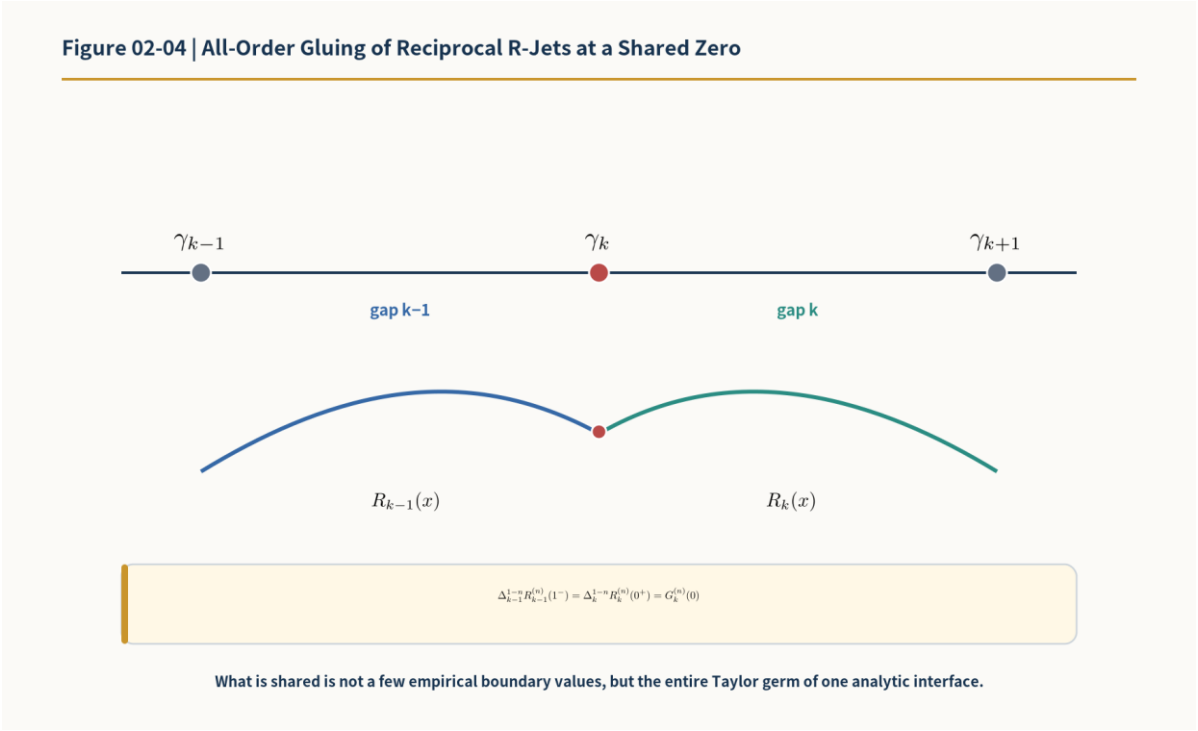


Figure 02-04. All-order gluing of reciprocal R-jets at a shared zero. The raw Herglotz response diverges at a zero, whereas the reciprocal coordinate $R = -1/M$ turns the shared zero into an ordinary analytic boundary point. After the respective scale normalizations, all R-jets from the adjacent gaps agree order by order at the shared zero. The two sides therefore share one complete analytic germ, not merely a finite collection of empirical boundary values.

6. The Boundary Analytic Germ Generates Global Inverse-Distance Spectral Moments

Let the current zero be γ_k, and set $\delta = z - \gamma_k$. Inside the disk bounded by the nearest other zero,

$$m(\gamma_k + \delta) = -\frac{m_k}{\delta} + \sum_{r\geq 1} S_{k,r}\, \delta^{r-1}, \tag{6.1}$$

where

$$S_{k,r} = \sum_{j\neq k} \frac{m_j}{(\gamma_j - \gamma_k)^r}. \tag{6.2}$$

For $r \geq 2$, the series converges absolutely; $r = 1$ is understood with the same symmetric regularization used for m.

Define

$$\boxed{Q_k(x) := \frac{x}{R_k(x)}.} \tag{6.3}$$

Using $R_k(x) = G_k(\Delta_k x)/\Delta_k$ and $G_k = -1/m$,

$$Q_k(x) = -\Delta_k x\, m(\gamma_k + \Delta_k x). \tag{6.4}$$

Substitution of (6.1) gives

$$\boxed{Q_k(x) = m_k - \sum_{r\geq 1} C_{k,r}\, x^r,} \tag{6.5}$$

where

$$\boxed{C_{k,r} = \Delta_k^r S_{k,r} = \sum_{j\neq k} m_j \left(\frac{\Delta_k}{\gamma_j - \gamma_k}\right)^r.} \tag{6.6}$$

Hence

$$\boxed{C_{k,r} = -\frac{1}{r!} Q_k^{(r)}(0^+).} \tag{6.7}$$

Theorem 6.1 (Spectral-Moment Extraction)

Given Δ_k and the complete analytic germ of p_k at the left endpoint, all $C_{k,r}$ are determined uniquely. Consequently, for every $r \geq 2$, the global inverse-distance spectral moment

$$S_{k,r} = \sum_{j\neq k} \frac{m_j}{(\gamma_j - \gamma_k)^r} \tag{6.8}$$

is determined uniquely.

This theorem provides the spectral-moment entry point needed for global reconstruction.

7. Global Spectral Determination from a One-Sided Boundary Analytic Germ

Intuitive form of the main result. Regard the complete boundary analytic germ near one zero as a "spectral fingerprint." The fingerprint does not merely identify a few nearby zeros. Its full Taylor coefficients form global inverse-distance moments, and those moments uniquely determine a compactly supported positive measure. The atoms and masses of that measure then recover all zeros and multiplicities one by one.

Let

$$y_j := \frac{\Delta_k}{\gamma_j - \gamma_k}, \qquad j \neq k. \tag{7.1}$$

Define the positive discrete measure

$$\boxed{\nu_k^{\mathrm{gap}} := \sum_{j\neq k} m_j\, y_j^2\, \delta_{y_j}.} \tag{7.2}$$

Since

$$\sum_{j\neq k} \frac{m_j}{|\gamma_j - \gamma_k|^2} < \infty,$$

ν_k^{gap} is a finite positive measure. Because the zero set is discrete, the nearest distance from the current zero to any other zero,

$$d_k := \min_{j\neq k} |\gamma_j - \gamma_k| > 0,$$

is positive. Hence

$$|y_j| \leq \frac{\Delta_k}{d_k},$$

so ν_k^{gap} has compact support.

Its moments are

$$\boxed{\int y^n \, d\nu_k^{\mathrm{gap}}(y) = C_{k,n+2}, \qquad n \geq 0.} \tag{7.3}$$

A compactly supported finite positive measure is uniquely determined by all its moments. This yields the main result of the chapter.

Theorem 7.1 (Single-Boundary Global Spectral Determination)

Within the real Riemann zero spectral framework fixed in Section 0, fix one zero γ_k and one adjacent-gap scale Δ_k. If the complete boundary analytic germ of the corresponding horizon shape p_k at $x = 0^+$ is known, then these data uniquely determine all distinct real zeros and their analytic multiplicities:

$$\boxed{\{(\gamma_j, m_j) : j \in \mathbb{Z}\}.} \tag{7.4}$$

Proof. The complete p_k-germ gives the Q_k-germ uniquely through (5.2) and (6.3), hence the entire sequence $C_{k,r}$ through (6.7). By (7.3), these are the complete moments of the compactly supported positive measure ν_k^{gap}, so that measure is unique. Its nonzero atomic locations give the values y_j, and therefore

$$\gamma_j = \gamma_k + \frac{\Delta_k}{y_j}. \tag{7.5}$$

The mass of the atom at y_j satisfies

$$\nu_k^{\mathrm{gap}}(\{y_j\}) = m_j y_j^2,$$

so

$$m_j = \frac{\nu_k^{\mathrm{gap}}(\{y_j\})}{y_j^2}. \tag{7.6}$$

Thus all zero locations and multiplicities are recovered uniquely. ▫

Interpretation

Theorem 7.1 is a statement of **global uniqueness for exact analytic data**: the same complete boundary analytic germ and the same gap scale cannot correspond to two different global real spectra. Conditioning under finite-precision perturbation, error propagation, stable inversion, and algorithmic complexity belong to the computational inverse-spectral level and are distinct from the exact uniqueness proved here.

Theorem 7.2 (One-Gap Global Uniqueness)

If the entire $p_k(x)$, γ_k, and Δ_k are given, then (3.5) uniquely recovers the values of m on the open interval I_k. If two candidate responses in the same meromorphic class produce exactly the same p_k on that gap, the identity theorem makes them equal globally. If they are $-X_1'/X_1$ and $-X_2'/X_2$, respectively, then

$$X_1 = CX_2, \qquad C \neq 0. \tag{7.7}$$

Theorem 7.1 is stronger than Theorem 7.2: the full gap is unnecessary; the complete one-sided analytic germ at a single boundary point already suffices.

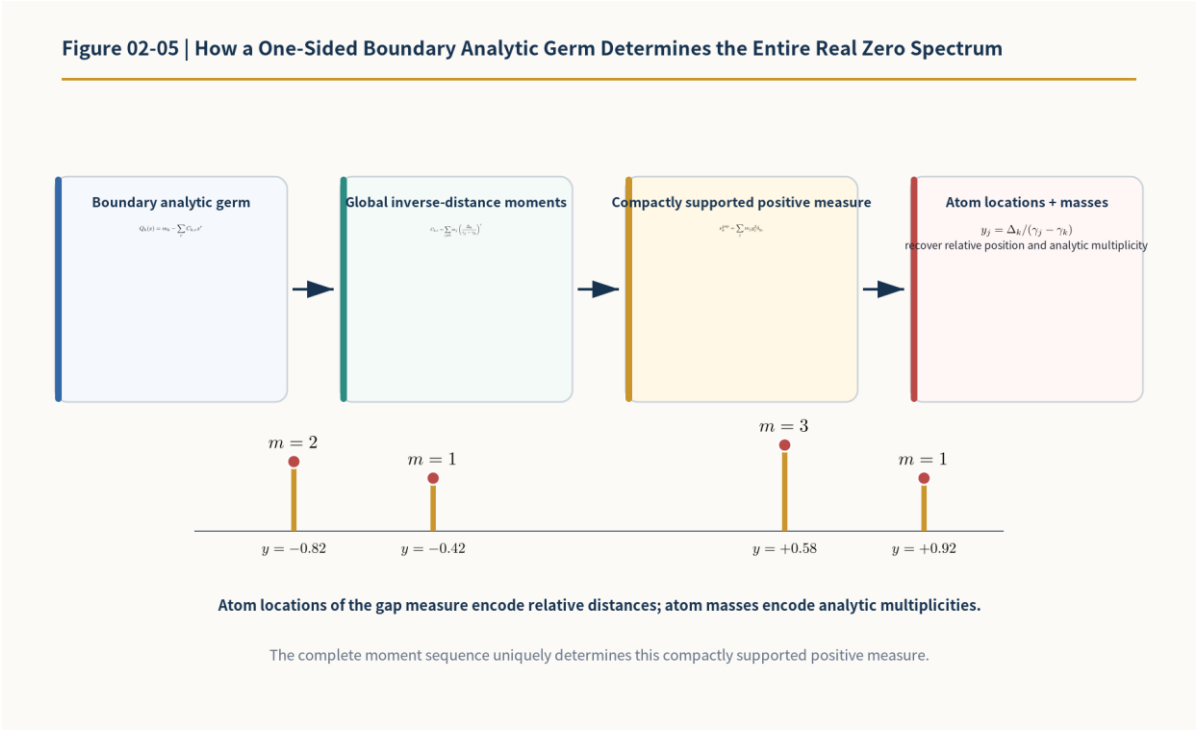


Figure 02-05. How a one-sided boundary analytic germ determines the entire real zero spectrum. The Taylor coefficients of the boundary germ yield the global inverse-distance moments $C_{k,r}$. These form the complete moment sequence of the compactly supported positive measure ν_k^{gap}. The measure is uniquely determined by all of its moments, and its atom locations and masses recover all relative zero positions and analytic multiplicities. Thus, given γ_k and Δ_k, the entire real zero spectrum is uniquely recovered.

8. Relation to Herglotz Inverse-Spectral Representation

The classical Herglotz representation says that a meromorphic Herglotz function with prescribed real poles and positive spectral masses can be written as

$$m(z) = az + b + \sum_j m_j \left(\frac{1}{\gamma_j - z} - \frac{\gamma_j}{1+\gamma_j^2} \right), \qquad a \geq 0,\ b \in \mathbb{R}. \tag{8.1}$$

Thus "pole locations + residues" generally determine m only up to an affine defect $az + b$.

In the Riemann Ξ-class, Ξ is even, so $m = -\Xi'/\Xi$ is odd, forcing $b = 0$. Moreover, if the corresponding entire function is required to remain of order one, then $a > 0$ would integrate to a quadratic exponential factor of the form $e^{-az^2/2}$, so one must have $a = 0$. Hence within the explicit class of even order-one entire functions, the complete spectral data determine m uniquely.

This section invokes the classical Herglotz/inverse-spectral framework to show that no additional hidden degree of freedom remains between the pole/residue spectrum recovered in Theorem 7.1 and the Riemann m-function.

9. Nearest-Neighbor Gap Bounds from Finite Jets

Finite information already yields visible results. A complete analytic germ is needed for unique recovery of the whole spectrum, but the first few jets already give upper and lower bounds on the nearest-neighbor distance. As the order grows, the squeeze converges to the true nearest-neighbor gap. Thus the theory does not say that only infinite information is meaningful.

A complete boundary analytic germ yields the whole spectrum; a finite boundary jet yields only finitely many $C_{k,r}$. Those finite moments already control the nearest-neighbor distance rigorously.

Let

$$d_k = \min_{j \neq k} |\gamma_j - \gamma_k|. \tag{9.1}$$

For $r \geq 1$,

$$C_{k,2r} = \sum_{j \neq k} m_j \left| \frac{\Delta_k}{\gamma_j - \gamma_k} \right|^{2r}. \tag{9.2}$$

The largest base is Δ_k / d_k. Therefore:

Theorem 9.1 (Finite-Jet Nearest-Gap Squeeze)

$$\boxed{\frac{\Delta_k}{C_{k,2r}^{1/(2r)}} \leq d_k \leq \Delta_k \sqrt{\frac{C_{k,2r}}{C_{k,2r+2}}}.} \tag{9.3}$$

Both bounds tend to d_k as $r \to \infty$.

Proof. The nearest-zero term gives

$$C_{k,2r} \geq \left(\frac{\Delta_k}{d_k} \right)^{2r},$$

which gives the left inequality. On the other hand,

$$C_{k,2r+2} \leq \left(\frac{\Delta_k}{d_k} \right)^{2} C_{k,2r},$$

which gives the right inequality. The root limit of the high power sums and the ratio limit of consecutive moments both tend to the largest base. ▫

Relation to the Euler–Rayleigh Method

Bounding the nearest zero through reciprocal power sums belongs to the Euler–Rayleigh/Rayleigh-sum tradition. Here the reciprocal moments are generated canonically from the boundary-shape jet of a single Riemann zero gap, so (9.3) can be read directly from that local boundary data.

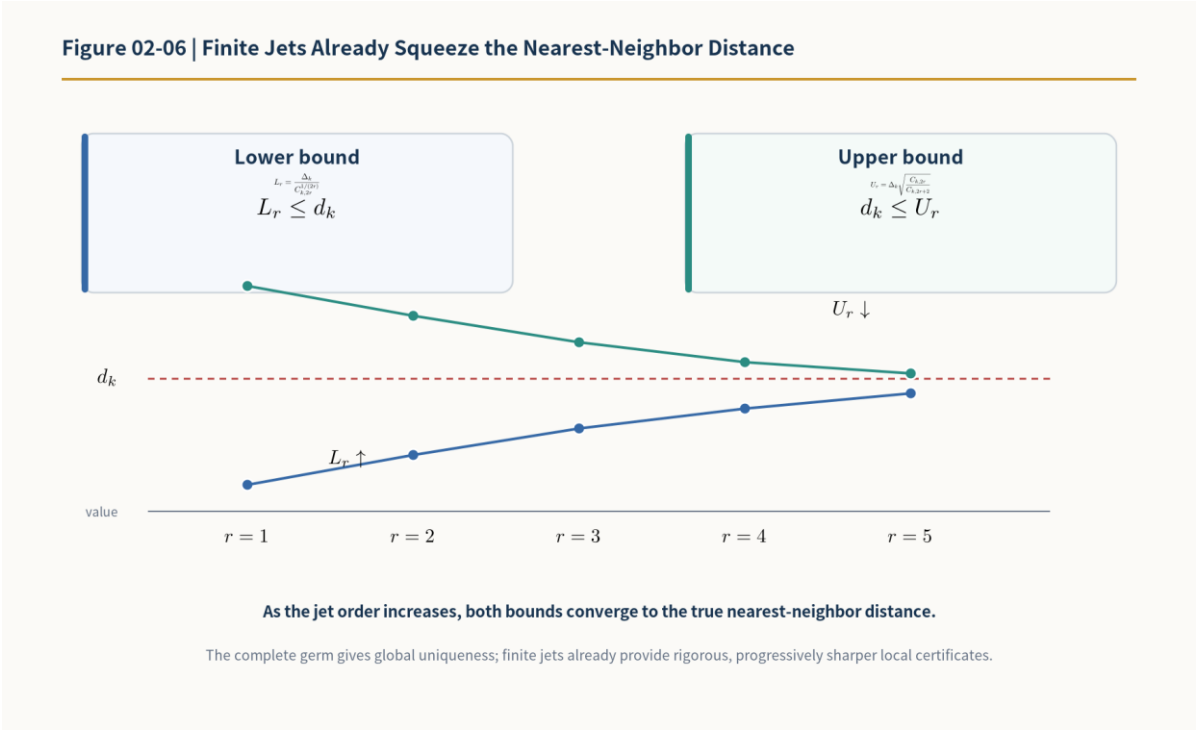


Figure 02-06. Finite jets already squeeze the nearest-neighbor distance. The complete boundary analytic germ gives global spectral uniqueness, but finitely many even inverse-distance moments already provide rigorous lower and upper bounds for the nearest-neighbor distance d_k. As r increases, the two bounds tighten from opposite sides and converge to the true d_k.

10. Residual-Moment Trichotomy for Adjacent Gaps

Assume now that k is not the leftmost point of the positive spectrum, so the preceding positive zero exists. The right endpoint zero γ_{k+1} of the current gap contributes exactly m_{k+1} to (9.2). Subtract that known atom and define

$$\boxed{E^L_{k,r} := C_{k,2r} - m_{k+1}.} \tag{10.1}$$

Then

$$E^L_{k,r} = \sum_{j \neq k,k+1} m_j \left| \frac{\Delta_k}{\gamma_j - \gamma_k} \right|^{2r}. \tag{10.2}$$

Among all remaining zeros, the only one that can be closer to γ_k than the current right endpoint is the left neighbor γ_{k-1}. Hence:

Theorem 10.1 (Residual-Moment Gap Trichotomy)

$$\boxed{E^L_{k,r} \to \begin{cases} +\infty, & \Delta_{k-1} < \Delta_k, \\ m_{k-1}, & \Delta_{k-1} = \Delta_k, \\ 0, & \Delta_{k-1} > \Delta_k. \end{cases}} \tag{10.3}$$

Proof. The base corresponding to the left neighbor is Δ_k/Δ_{k-1}. If it exceeds 1, that term grows exponentially. If it equals 1, the term is constantly m_{k-1} while every other base is strictly less than 1. If it is less than 1, then all remaining bases are strictly less than 1. Since $E^L_{k,1} < \infty$, dominated convergence applies in the final two cases. ▫

Define

$$A_{k,r}^{L} := \frac{E_{k,r+1}^{L}}{E_{k,r}^{L}}. \tag{10.4}$$

By log-convexity of positive moment sequences, $A_{k,r}^{L}$ is nondecreasing in r and tends to the square of the largest residual base.

This gives two finite-order certificates:

$$A_{k,r}^{L} > 1 \Rightarrow \Delta_{k-1} < \Delta_k, \tag{10.5}$$

and

$$E_{k,r}^{L} \leq 1 \Rightarrow \Delta_{k-1} > \Delta_k. \tag{10.6}$$

If (10.5) holds, then further

$$\boxed{\frac{\Delta_k}{(E_{k,r}^{L})^{1/(2r)}} \leq \Delta_{k-1} \leq \Delta_k \sqrt{\frac{E_{k,r}^{L}}{E_{k,r+1}^{L}}}.} \tag{10.7}$$

The right-end boundary analytic germ gives a completely symmetric quantity $E_{k,r}^{R}$, so the complete analytic germs on the two sides of one gap determine the local shape of the three adjacent gaps.

11. Hankel Positivity of Boundary Spectral Moments

By (7.2)–(7.3), $\{C_{k,n+2}\}_{n\geq 0}$ is the Hamburger moment sequence of a finite positive measure. Therefore for every $N \geq 0$,

$$\boxed{H_k^{(N)} := [C_{k,i+j+2}]_{i,j=0}^{N} \succcurlyeq 0.} \tag{11.1}$$

In particular,

$$C_{k,2} > 0, \tag{11.2}$$

and

$$C_{k,2}C_{k,4} - C_{k,3}^{2} \geq 0. \tag{11.3}$$

These give finite-order necessary conditions for a candidate horizon shape to be spectralizable: an arbitrary positive probability density is not automatically the gap shape of a real discrete zero spectrum.

If

$$a = p_k(0^+), \quad b = p_k'(0^+), \quad c = p_k''(0^+),$$

a direct expansion gives

$$\boxed{C_{k,1} = \frac{b}{2\pi a^2},} \tag{11.4}$$

and

$$\boxed{C_{k,2} = \frac{\frac{\pi^2}{3}a^4 + \frac{1}{6}ac - \frac{1}{4}b^2}{\pi a^3}.} \tag{11.5}$$

Thus $C_{k,2} > 0$ is equivalent to

$$\boxed{2ac - 3b^2 + 4\pi^2 a^4 > 0.} \tag{11.6}$$

This is a purely boundary-shape curvature constraint.

12. Global Exterior Spectral Field and the Phase Center

Inside one gap, explicitly separate the poles at the two endpoints:

$$\boxed{M_k(x) = -\frac{m_k}{x} + \frac{m_{k+1}}{1-x} + E_k(x).} \tag{12.1}$$

By (2.3),

$$\boxed{E_k'(x) = \Delta_k^2 \sum_{j \neq k,k+1} \frac{m_j}{(\gamma_j - \gamma_k - \Delta_k x)^2} > 0.} \tag{12.2}$$

Thus the internal shape of a gap is not determined only by its two endpoints; every remaining zero enters the current interval through a strictly increasing exterior field.

Since M_k increases strictly from $-\infty$ to $+\infty$, there is a unique $x_k^* \in (0,1)$ such that

$$M_k(x_k^*) = 0. \tag{12.3}$$

At that point,

$$\Xi'(\gamma_k + \Delta_k x_k^*) = 0$$

and

$$\int_0^{x_k^*} p_k(x)dx = \frac{1}{2},$$

so it is both the unique phase center and the median of the shape probability measure.

If only the two endpoint poles are retained, the baseline field

$$B_k(x) = -\frac{m_k}{x} + \frac{m_{k+1}}{1-x}$$

has zero at

$$x_k^{(0)} = \frac{m_k}{m_k + m_{k+1}}.$$

The true center satisfies

$$\boxed{\operatorname{sgn}(x_k^{(0)} - x_k^*) = \operatorname{sgn} E_k(x_k^*).} \tag{12.4}$$

Thus displacement of the phase center is a local readout, within the current gap, of the global exterior spectral field.

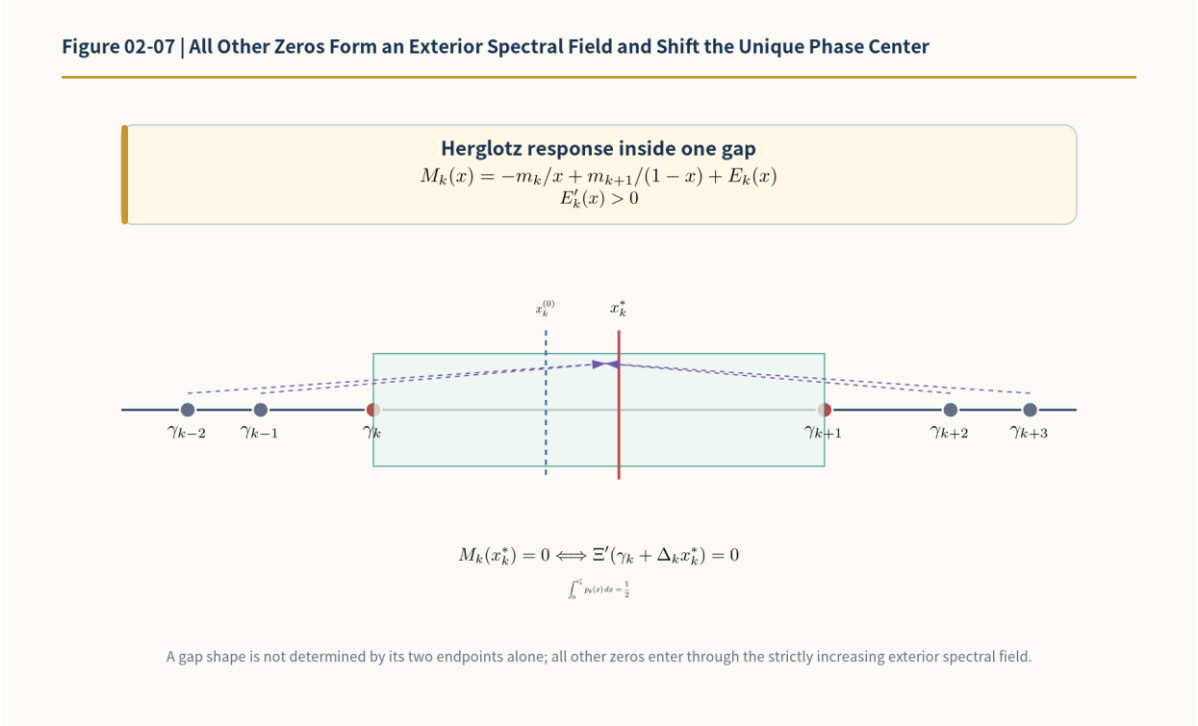


Figure 02-07. Exterior spectral field and the unique phase center. After the two endpoint poles are removed explicitly from M_k, all other zeros collectively form the strictly increasing exterior field $E_k(x)$. The true phase center x_k^* is therefore not determined by the two endpoints alone. It satisfies $M_k(x_k^*) = 0$ and $\Xi'(\gamma_k + \Delta_k x_k^*) = 0$, and it is simultaneously the median of the shape probability measure.

13. Classical Foundations and the Unified Structure

Herglotz representation, compactly supported moment problems, and Euler–Rayleigh inverse-power-sum methods form the classical foundation of this chapter. In the canonical shape coordinates of individual Riemann zero gaps, they become one theorem chain: all-order boundary gluing, global spectral determination from a one-sided analytic germ, and finite-jet readout of adjacent gaps.

This section separates the classical tools used here from the unified structure built from them.

13.1 Classical Inputs

The following are standard mature results:

1. the Cayley correspondence between meromorphic Herglotz functions and meromorphic inner functions;
2. the linear term and positive discrete Clark/spectral measure in the Herglotz representation;
3. monotonicity of meromorphic-inner phase on the real axis;
4. uniqueness of a compactly supported finite positive measure from all of its moments;
5. Euler–Rayleigh-type upper and lower bounds for the nearest zero from reciprocal power sums/Rayleigh sums;

6. work placing the Riemann Ξ-function in de Branges, meromorphic-inner, and spectral frameworks.

13.2 Unified Structure

These classical tools are organized here into the following structure:

- for every adjacent Riemann zero gap, use the unit-scale phase density p_k as the canonical shape object;
- read both endpoint analytic multiplicities and internal phase from the same p_k-coordinate;
- introduce the reciprocal coordinate $R_k = -1/M_k$, so that all higher-order compatibility at a shared zero becomes scaled boundary-jet gluing;
- convert a one-sided boundary analytic germ directly into all inverse-distance spectral moments, then into a compactly supported positive measure, thereby recovering uniquely the entire global zero spectrum and its multiplicities;
- let finite boundary jets generate deterministic nearest-neighbor and adjacent-gap bounds together with the residual trichotomy;
- place local gap shape, shared boundary analytic germ, and global spectrum inside one invertible deterministic chain.

14. Conclusion

This chapter upgrades an adjacent Riemann zero interval from the scalar length Δ_k to the canonical shape object (Δ_k, p_k). The density p_k is a unit-mass phase density; its endpoint values quantize analytic multiplicity, its reciprocal coordinate satisfies all-order gluing at a shared zero, and its complete boundary analytic germ generates all global inverse-distance spectral moments.

The strongest deterministic conclusion is

one zero locationγk + one adjacent-gap scaleΔk + one-sided complete boundary analytic germ ⇒ the entire real zero spectrum and all analytic multiplicities.

This is global uniqueness at the level of exact analytic information: once the gap scale is fixed, a complete boundary analytic germ corresponds to only one global real spectrum. Stable inversion from finite-precision data belongs to the computational inverse-spectral level and is distinct from this analytic uniqueness.

Finite-order germ data form a natural hierarchy: more boundary jets provide more global moments and hence increasingly tight control of the nearest-neighbor distance and adjacent-gap ratio. Infinite Boundary-Jet Gluing at the shared zero of two adjacent gaps further guarantees that the local spectral readouts from the two sides belong to one and the same global analytic germ.

A Riemann zero gap is therefore not “empty space between two zeros.” In the canonical coordinates developed here it simultaneously carries internal phase, endpoint multiplicities, the shared boundary analytic germ, global moment data, and the exterior spectral field obtained by projecting all other zeros onto the current interval. Local interval and global spectrum thus become two scale readouts of the same meromorphic response.

Appendix A: The First Three Boundary Spectral Coefficients

Let

$$a = p_k(0^+), \qquad b = p_k'(0^+), \qquad c = p_k''(0^+), \qquad d = p_k'''(0^+).$$

Expanding

$$Q_k(x) = \frac{x}{\tan\left(\pi \int_0^x p_k\,(u)du\right)}$$

gives

$$m_k = \frac{1}{\pi a},$$

$$C_{k,1} = \frac{b}{2\pi a^2},$$

$$C_{k,2} = \frac{\frac{\pi^2}{3}a^4 + \frac{1}{6}ac - \frac{1}{4}b^2}{\pi a^3},$$

$$C_{k,3} = \frac{4\pi^2 a^4 b + a^2 d - 4abc + 3b^3}{24\pi a^4}.$$

These formulas give a direct conversion from low-order boundary derivatives to low-order global inverse-distance moments.

Chapter 3 Identity Addresses and Analytic Multiplicities of Riemann Zeros

— Representation-Sheet Count, Address Uniqueness, and Divisor Multiplicity under the Open-Multiplication Horizon

Abstract

Let

$$\xi(s) = \frac{1}{2}s(s-1)\pi^{-s/2}\Gamma(s/2)\zeta(s)$$

be the completed Riemann function, and let

$$Z_{\mathrm{nt}}^{\mathrm{dist}}(\xi)$$

denote the support set of its distinct nontrivial zeros. Within the unified framework of open multiplicative relations, moving horizons, centered Mellin representations, and terminal zero readouts, representation-sheet count, support-address count, and analytic multiplicity form three strictly distinct layers.

If

$$\rho \in Z_{\mathrm{nt}}^{\mathrm{dist}}(\xi), \qquad \xi(s) = (s-\rho)^{m_\rho}U_\rho(s), \qquad U_\rho(\rho) \neq 0,$$

then ρ is the analytic address of the zero, while

$$m_\rho = \mathrm{ord}_\rho \xi$$

is the analytic multiplicity at that address. The corresponding zero divisor is

$$\mathcal{D}_\xi^{\mathrm{nt}} = \sum_{\rho \in Z_{\mathrm{nt}}^{\mathrm{dist}}(\xi)} m_\rho\,[\rho].$$

This naturally separates two different objects. The support

$$\mathrm{supp}\mathcal{D}_\xi^{\mathrm{nt}} = Z_{\mathrm{nt}}^{\mathrm{dist}}(\xi)$$

records each distinct zero address exactly once, whereas the divisor weight m_ρ records the order of analytic vanishing at that same address.

The two reciprocal wings in the open-multiplication horizon belong to a third layer of data. They are representation sheets of the same complete event under reciprocal roles and do not constitute new support addresses of zeros. Because the centered parameter is transmitted exactly among the generative source, shell, ζ, ξ, and terminal readout, duplication in event representation, continuous lifting between horizons, and repeated references to a shared endpoint by adjacent intervals do not alter the address count of the terminal support.

Thus one obtains the three-layer separation

event representation-sheet count ≠ support-address count ≠ analytic multiplicity.

Here the event representation-sheet count records the number of representation sheets in a finite reciprocal lift; support-address count means that a distinct zero address appears only once in the support; and analytic multiplicity is m_ρ.

For positive-height zeros, define

$$N_{\mathrm{supp}}(T) = \#\{\rho \in Z_{\mathrm{nt}}^{\mathrm{dist}}(\xi) : 0 < \Im\rho \le T\},$$

and define the multiplicity-weighted count

$$N_{\mathrm{div}}(T) = \sum_{\substack{\rho \in Z_{\mathrm{nt}}^{\mathrm{dist}}(\xi) \\ 0<\Im\rho\le T}} m_\rho.$$

They satisfy the exact identity

$$\boxed{N_{\mathrm{div}}(T) - N_{\mathrm{supp}}(T) = \sum_{0<\Im\rho\le T} (m_\rho - 1).}$$

Therefore uniqueness of support addresses and analytic simplicity are two different statements. All nontrivial zeros are analytically simple if and only if

$$m_\rho = 1 \quad \text{for every} \rho,$$

equivalently,

$$N_{\mathrm{div}}(T) = N_{\mathrm{supp}}(T)$$

for every T not passing through a zero.

This stratification places zero addresses, the zero divisor, and event representations in a single object ledger, while maintaining a unified interface with multiplicity data in adjacent zero-gap geometry, the faithful post-closure spectrum, and identity-faithful/divisor-faithful spectral realizations.

1. Position of This Chapter and Object Levels

This chapter continues the unified object discipline established in Chapter 1 (H01). The root identity is

$$\boxed{\Im_\times = (\mathbb{N}_{>0}, \mu), \qquad \mu(m,q) = mq.} \tag{1.1}$$

The open multiplicative relation

$$\mathcal{R}_\times = \{(m,q,n) \in \mathbb{N}_{>0}^3 : mq = n\} \tag{1.2}$$

is a relational representation of that root identity.

As one unfolds through the centered Mellin representation, multiplicative shells, moving horizons, ζ, Riemann completion, and terminal zero readouts, the representational level changes step by step while the root identity remains unchanged. Throughout the book we enforce

$$\boxed{\text{identity} \neq \text{role} \neq \text{role readout.}} \tag{1.3}$$

Under this object discipline, we further distinguish three counts of different mathematical types:

$$\boxed{\begin{array}{rcl} \nu_{\mathrm{sheet}}(E) & : & \text{event representation-sheet count,} \\ \mu_{\mathrm{supp}}(\rho) & : & \text{support-address count,} \\ m_\rho & : & \text{analytic multiplicity.} \end{array}} \tag{1.4}$$

Here:

- $\nu_{\mathrm{sheet}}(E)$ belongs to the representation structure of a finite-horizon event;

- $\mu_{\mathrm{supp}}(\rho)$ belongs to the support formed by distinct zero addresses;
- $m_\rho = \mathrm{ord}_\rho \xi$ belongs to the analytic zero divisor.

These three quantities live on different levels, and every theorem below is stated with this type distinction in force.

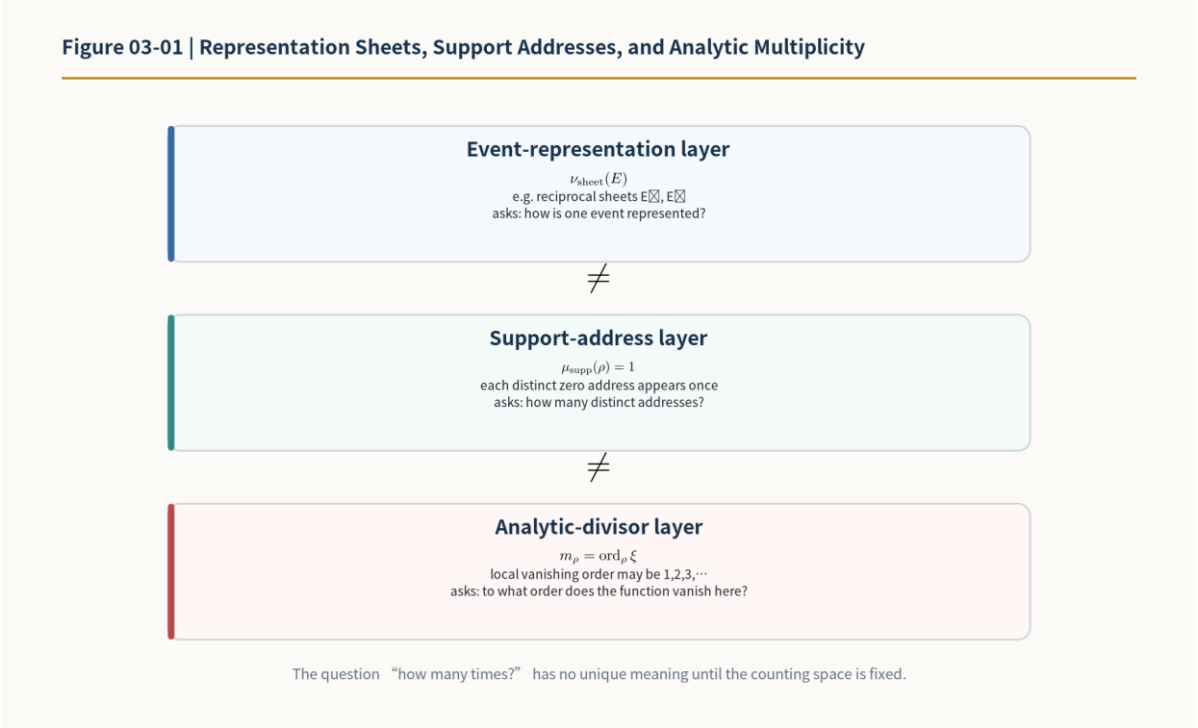


Figure 03-01. Strict separation of the three counts. The event representation-sheet count $\nu_{\mathrm{sheet}}(E)$, support-address count $\mu_{\mathrm{supp}}(\rho)$, and analytic multiplicity m_ρ belong respectively to event representation, distinct-zero support, and the analytic divisor. A count at one level does not automatically rewrite the counts at the other two levels.

2. The Centered Parameter and Terminal Zero Addresses

Let

$$W_z(m,q) = m^{-1/2-z} q^{-1/2+z} = (mq)^{-1/2} e^{z\log(q/m)}, \tag{2.1}$$

and define

$$a_n(z) = \sum_{mq=n} m^{-1/2-z}\, q^{-1/2+z}. \tag{2.2}$$

In the region of absolute convergence,

$$\sum_{n\geq 1} a_n(z) n^{-u} = \zeta\left(u+\frac{1}{2}+z\right)\zeta\left(u+\frac{1}{2}-z\right). \tag{2.3}$$

The centered parameter retains the same parameter identity across the generative source, shell, ζ, completion, and terminal readout. We denote this exact transmission by

$$\boxed{z_{\mathrm{source}} = z_{\mathrm{shell}} = z_\zeta = z_\xi = z_{\mathrm{term}}.} \tag{2.4}$$

When the terminal readout is a nontrivial zero

$$\rho = \frac{1}{2} + z_{\mathrm{term}}, \tag{2.5}$$

the post-RH-closure representation may be written as

$$\rho = \frac{1}{2} + i\gamma. \tag{2.6}$$

Equation (2.4) expresses exact transmission of one centered parameter through different representational layers; it does not identify objects of different mathematical types. The generative-source relation, the analytic function, and the zero address remain representations of distinct types.

3. Zero Support, Zero Addresses, and the Analytic Divisor

Define the set of distinct nontrivial zeros by

$$\boxed{Z_{\mathrm{nt}}^{\mathrm{dist}}(\xi) = \{\rho : \xi(\rho) = 0,\ \rho\text{nontrivial}\}_{\mathrm{distinct}}.} \tag{3.1}$$

For every

$$\rho \in Z_{\mathrm{nt}}^{\mathrm{dist}}(\xi),$$

there exists a unique integer

$$m_\rho \geq 1$$

and a function U_ρ, analytic in a neighborhood of ρ and satisfying

$$U_\rho(\rho) \neq 0,$$

such that

$$\boxed{\xi(s) = (s-\rho)^{m_\rho} U_\rho(s).} \tag{3.2}$$

Definition 3.1 (Zero Identity Address)

The complex number ρ is called the **identity address** of the nontrivial zero. In the post-RH-closure positive-height spectrum, its ordinate

$$\gamma = \Im\rho > 0 \tag{3.3}$$

may also be used as the vertical spectral address.

Definition 3.2 (Analytic Multiplicity)

The integer

$$\boxed{m_\rho = \mathrm{ord}_\rho \xi} \tag{3.4}$$

is called the analytic multiplicity of the zero ρ.

Definition 3.3 (Nontrivial-Zero Divisor)

Define

$$\boxed{\mathcal{D}_\xi^{\mathrm{nt}} = \sum_{\rho \in Z_{\mathrm{nt}}^{\mathrm{dist}}(\xi)} m_\rho\,[\rho].} \tag{3.5}$$

Its support is

$$\boxed{\mathrm{supp}\mathcal{D}_\xi^{\mathrm{nt}} = Z_{\mathrm{nt}}^{\mathrm{dist}}(\xi).} \tag{3.6}$$

Thus the same zero object naturally carries two different layers of data:

$$\boxed{\rho \quad \text{and} \quad m_\rho.} \tag{3.7}$$

The former answers “where is the address?”, while the latter answers “to what order does the function vanish at that address?”

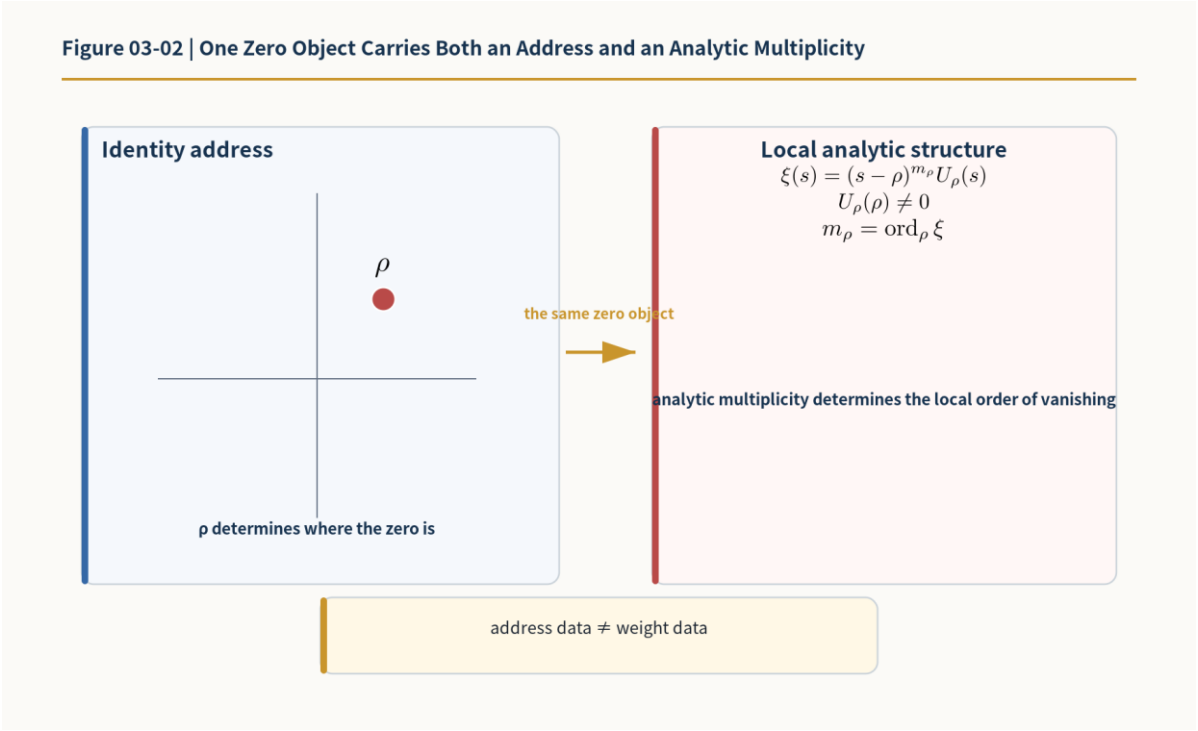


Figure 03-02. Zero address and analytic multiplicity. The local factorization $\xi(s) = (s-\rho)^{m_\rho} U_\rho(s)$ carries two different kinds of data: ρ is the identity address specifying where the zero is, while $m_\rho = \mathrm{ord}_\rho \xi$ is the analytic multiplicity specifying the order of vanishing there. Address data and weight data are not the same count.

4. Strict Stratification of the Three Counts

The phrase "how many times an object appears" has a definite meaning only after the counting space has been fixed. For the structure of Riemann zeros, this chapter fixes the following three counts.

4.1 Event Representation-Sheet Count

In a finite-horizon event, one reciprocal relation may appear as two reciprocal representation sheets. If the complete event is denoted by E, its representation layer may be written as

$$E \rightsquigarrow (E_+, E_-). \tag{4.1}$$

Here

$$\nu_{\mathrm{sheet}}(E) \tag{4.2}$$

records the number of event-representation sheets. It belongs to the event representation, not to the zero divisor.

4.2 Support-Address Count

The distinct zero support

$$Z_{\mathrm{nt}}^{\mathrm{dist}}(\xi)$$

is a set, not a multiset expanded by multiplicity. Hence, for

$$\rho \in Z_{\mathrm{nt}}^{\mathrm{dist}}(\xi),$$

define

$$\boxed{\mu_{\mathrm{supp}}(\rho) = 1.} \tag{4.3}$$

This means that each distinct zero address is recorded exactly once in the support.

4.3 Analytic Multiplicity

The analytic multiplicity is

$$m_\rho = \mathrm{ord}_\rho \xi. \tag{4.4}$$

It may be any positive integer and is retained through the divisor weight:

$$\mathcal{D}_\xi^{\mathrm{nt}} = \sum_\rho m_\rho\,[\rho]. \tag{4.5}$$

Thus the fundamental stratification of this chapter is

$$\boxed{\nu_{\mathrm{sheet}}(E) \neq \mu_{\mathrm{supp}}(\rho) \neq m_\rho \quad \text{as object types.}} \tag{4.6}$$

Theorem 4.1 (Three-Layer Multiplicity Separation Theorem)

The representation-sheet count in a finite reciprocal lift, the address count in the support of distinct zeros, and the analytic multiplicity in the zero divisor are defined respectively by event representation, support set, and local order of vanishing. A change in the count at any one level does not automatically alter the other two.

Proof. The event representation-sheet count is defined by the branching structure of an event representation; the support-address count is defined by the set

$$Z_{\mathrm{nt}}^{\mathrm{dist}}(\xi);$$

and analytic multiplicity is defined by the local factorization (3.2). Their domains, codomains, and equivalence relations are different. Hence there is no type identity by which the numerical value of one count could automatically force equality with either of the others. ▫

5. Reciprocal Representation and Address Fidelity

The two reciprocal wings in a moving horizon express reciprocal roles of one complete event. Write the reciprocal action as

$$J: E_+ \leftrightarrow E_-. \tag{5.1}$$

At the terminal analytic layer, the corresponding reciprocal action is read as

$$\iota(\rho) = 1 - \overline{\rho}. \tag{5.2}$$

At a fixed-role readout,

$$\iota(\rho) = \rho,$$

and therefore

$$\Re\rho = \frac{1}{2}. \tag{5.3}$$

It is essential here to distinguish **role reciprocity** from **address duplication**. E_+ and E_- are two reciprocal roles of one event. When they close at the terminal fixed-role readout, closure means that the role readout is fixed by the involution ι; it does not mean that two identical zero addresses are generated and then merged.

Theorem 5.1 (Address Fidelity of Reciprocal Representation)

Suppose the reciprocal roles of a complete event E enter the terminal analytic representation through exact centered-parameter transmission and yield a zero address ρ at the fixed-role readout. Then the number of reciprocal representation sheets does not alter the support count of that terminal address in

$$Z_{\mathrm{nt}}^{\mathrm{dist}}(\xi):$$

$$\boxed{\mu_{\mathrm{supp}}(\rho) = 1.} \tag{5.4}$$

Its analytic multiplicity remains recorded independently as

$$m_\rho = \mathrm{ord}_\rho \xi. \tag{5.5}$$

Proof. Reciprocal roles belong to the representational layer of the same event. Exact transmission of the centered parameter preserves the event identity of their parameter, and the terminal readout yields one definite analytic address ρ. Since the support is formed from distinct addresses, that address appears only once. Its local analytic order is determined independently by (3.2) and is not determined by the number of reciprocal representation sheets. ▫

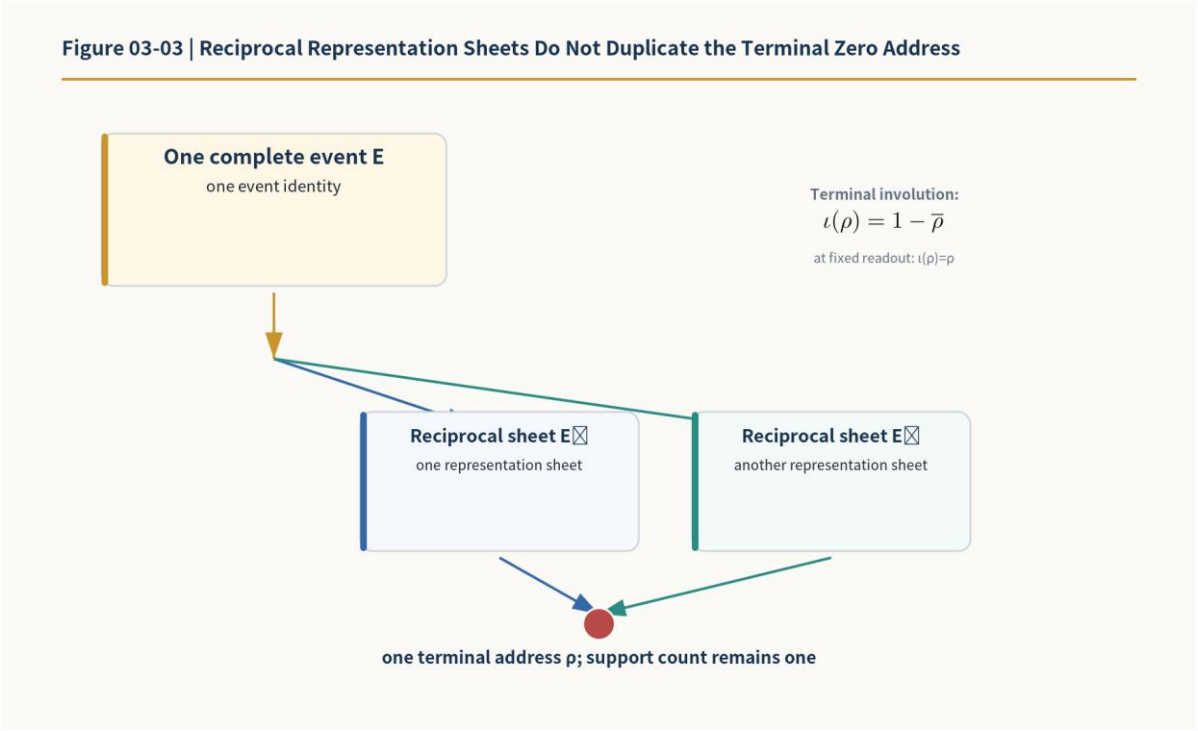


Figure 03-03. Reciprocal representation sheets and the terminal address. A complete event may unfold into reciprocal sheets E_+ and E_- inside a finite horizon, but both remain representations of one event identity. The terminal fixed-role readout gives one analytic address ρ, so the support count remains $\mu_{\mathrm{supp}}(\rho) = 1$; the analytic multiplicity m_ρ is retained independently at the divisor level.

6. Complete Intervals and Endpoint Addresses

Let the distinct positive-height zeros after RH closure be ordered strictly as

$$0 < \gamma_1 < \gamma_2 < \cdots, \tag{6.1}$$

and write

$$\rho_k = \frac{1}{2} + i\gamma_k. \tag{6.2}$$

The adjacent zero interval is

$$I_k = (\gamma_k, \gamma_{k+1}). \tag{6.3}$$

In the terminal analytic readout of the open-multiplication horizon, a complete interval is determined by two distinct boundary addresses:

$$\partial I_k = \{\rho_k, \rho_{k+1}\}. \tag{6.4}$$

Theorem 6.1 (Single-Interval Support-Address Theorem)

For every complete adjacent zero interval I_k, its boundary support consists of exactly two distinct addresses:

$$\boxed{\partial I_k = \{\rho_k, \rho_{k+1}\}.} \tag{6.5}$$

If the analytic multiplicities of the endpoints are

$$m_k = \mathrm{ord}_{\rho_k}\xi, \qquad m_{k+1} = \mathrm{ord}_{\rho_{k+1}}\xi, \tag{6.6}$$

then the corresponding boundary divisor is

$$\boxed{\mathcal{D}_{\partial I_k} = m_k[\rho_k] + m_{k+1}[\rho_{k+1}].} \tag{6.7}$$

Thus the support cardinality of the interval boundary is 2, while the total multiplicity of the boundary divisor is

$$m_k + m_{k+1}. \tag{6.8}$$

Proof. By the strict ordering of adjacent zeros,

$$\gamma_k < \gamma_{k+1},$$

hence

$$\rho_k \neq \rho_{k+1}.$$

The support counts distinct addresses, so the boundary contains exactly two elements. Analytic multiplicities are defined by the local orders of vanishing at the two endpoints and enter (6.7) as divisor weights. ▫

7. Shared Boundaries of Adjacent Intervals and Deduplication

Two adjacent intervals are

$$I_k = (\gamma_k, \gamma_{k+1}), \qquad I_{k+1} = (\gamma_{k+1}, \gamma_{k+2}). \tag{7.1}$$

They share the same analytic address

$$\rho_{k+1} = \frac{1}{2} + i\gamma_{k+1}. \tag{7.2}$$

Their local interval ledgers are

$$\partial I_k = \{\rho_k, \rho_{k+1}\},$$

$$\partial I_{k+1} = \{\rho_{k+1}, \rho_{k+2}\}. \tag{7.3}$$

The global support is formed by set union:

$$\partial I_k \cup \partial I_{k+1} = \{\rho_k, \rho_{k+1}, \rho_{k+2}\}. \tag{7.4}$$

Therefore

$$\boxed{\rho_{k+1}^{(I_k)} = \rho_{k+1}^{(I_{k+1})} = \rho_{k+1}} \tag{7.5}$$

means only that the same address is referenced once from each of two local intervals; it does not create two support atoms.

Theorem 7.1 (Shared-Boundary Deduplication)

For every finite chain of adjacent intervals

$$I_k, I_{k+1}, \dots, I_{k+r},$$

the global support is

$$\boxed{\bigcup_{j=k}^{k+r} \partial I_j = \{\rho_k, \rho_{k+1}, \dots, \rho_{k+r+1}\}.} \tag{7.6}$$

Each internal shared endpoint appears exactly once in the support union.

Proof. This follows by repeated use of the idempotence of set union,

$$\{x\} \cup \{x\} = \{x\}.$$

▫

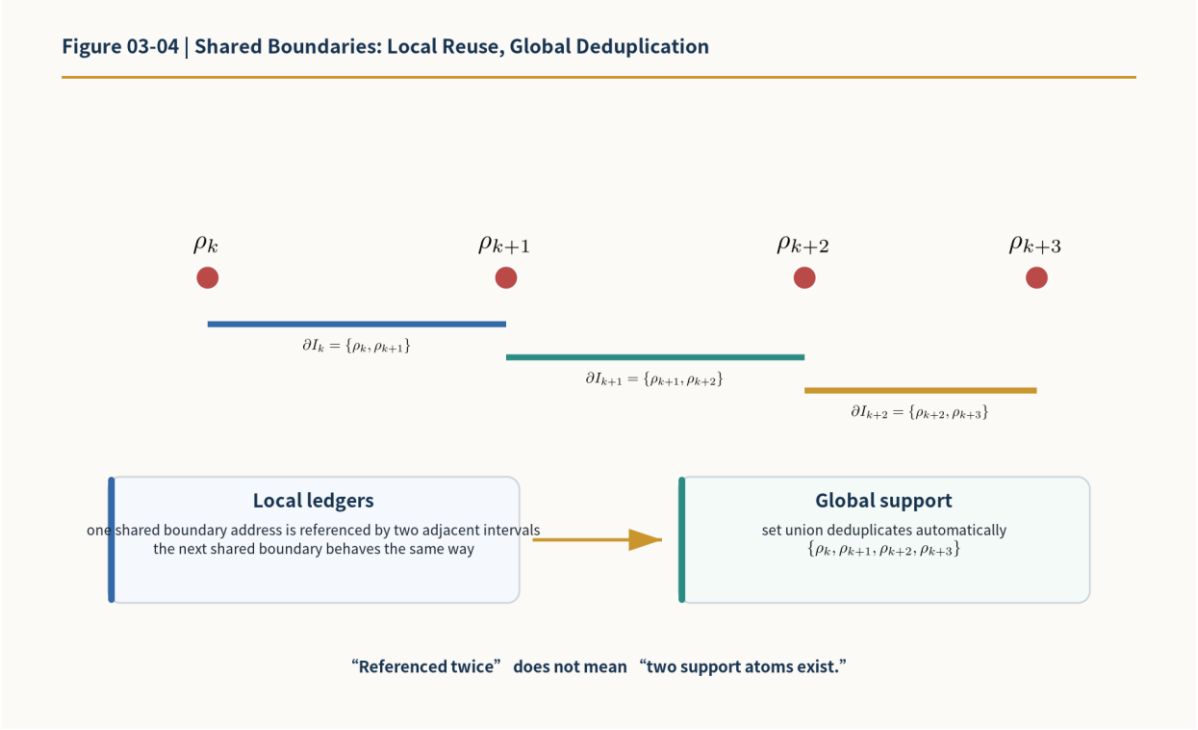


Figure 03-04. Shared-boundary deduplication. Adjacent intervals I_k and I_{k+1} both reference the same boundary address ρ_{k+1}. This is repeated use of one address in two local ledgers. Global support is formed by set union, whose idempotence automatically removes the duplicate reference; a shared boundary therefore does not create a second support atom.

8. From Local Addresses to Global Support

Define the support of distinct positive-height ordinates by

$$\boxed{\Gamma_+ = \{\gamma_1, \gamma_2, \dots\}.} \tag{8.1}$$

The corresponding support of complex zeros is

$$Z_+ = \left\{\frac{1}{2} + i\gamma_k : k \geq 1\right\}. \tag{8.2}$$

The family of complete adjacent intervals satisfies

$$I_k = (\gamma_k, \gamma_{k+1}), \tag{8.3}$$

so the union of all local interval boundaries recovers the entire positive-height support:

$$\boxed{Z_+ = \bigcup_{k\geq 1} \partial I_k.} \tag{8.4}$$

If analytic multiplicities are retained as well, the positive-height zero divisor is

$$\boxed{\mathcal{D}_\xi^+ = \sum_{k\geq 1} m_k\,[\rho_k].} \tag{8.5}$$

Equations (8.4) and (8.5) give two different but compatible global objects:

$$\boxed{\begin{array}{lcl} Z_+ & : & \text{identity-faithful support,} \\ \mathcal{D}_\xi^+ & : & \text{divisor-faithful zero data.} \end{array}} \tag{8.6}$$

The former contains each distinct address once; the latter retains the full analytic multiplicity at that address.

9. Support Counting and Divisor Counting

For $T > 0$ not passing through a zero, define the distinct-support count

$$\boxed{N_{\text{supp}}(T) = \#\{\rho \in Z_+ : 0 < \Im\rho \leq T\}.} \tag{9.1}$$

Define the divisor-weighted count

$$\boxed{N_{\text{div}}(T) = \sum_{\substack{\rho\in Z_+ \\ 0<\Im\rho\leq T}} m_\rho\,.} \tag{9.2}$$

Clearly,

$$N_{\text{div}}(T) = N_{\text{supp}}(T) + \sum_{\substack{\rho\in Z_+ \\ 0<\Im\rho\leq T}} (m_\rho - 1). \tag{9.3}$$

Hence:

Theorem 9.1 (Support–Divisor Counting Identity)

$$\boxed{N_{\text{div}}(T) - N_{\text{supp}}(T) = \sum_{\substack{\rho\in Z_+ \\ 0<\Im\rho\leq T}} (m_\rho - 1) \geq 0.} \tag{9.4}$$

Equality holds if and only if every zero below height T is analytically simple.

Proof. For each

$$m_\rho \in \mathbb{N}, \qquad m_\rho \geq 1,$$

write

$$m_\rho = 1 + (m_\rho - 1)$$

and sum term by term. ▫

Corollary 9.2 (Exact Criterion for Analytic Simplicity)

The following are equivalent:

1. all nontrivial zeros are analytically simple;
2. for every $\rho \in Z_{\text{nt}}^{\text{dist}}(\xi)$,

$$m_\rho = 1;$$

3. for every $T > 0$ not passing through a zero,

$$N_{\mathrm{div}}(T) = N_{\mathrm{supp}}(T);$$

4. the nontrivial-zero divisor is reduced:

$$\mathcal{D}_\xi^{\mathrm{nt}} = \sum_{\rho \in Z_{\mathrm{nt}}^{\mathrm{dist}}(\xi)} [\rho].$$

This criterion completely separates **address uniqueness** from **analytic simplicity**. Address uniqueness is a fact at the support level; analytic simplicity is the additional property that every divisor weight equals 1.

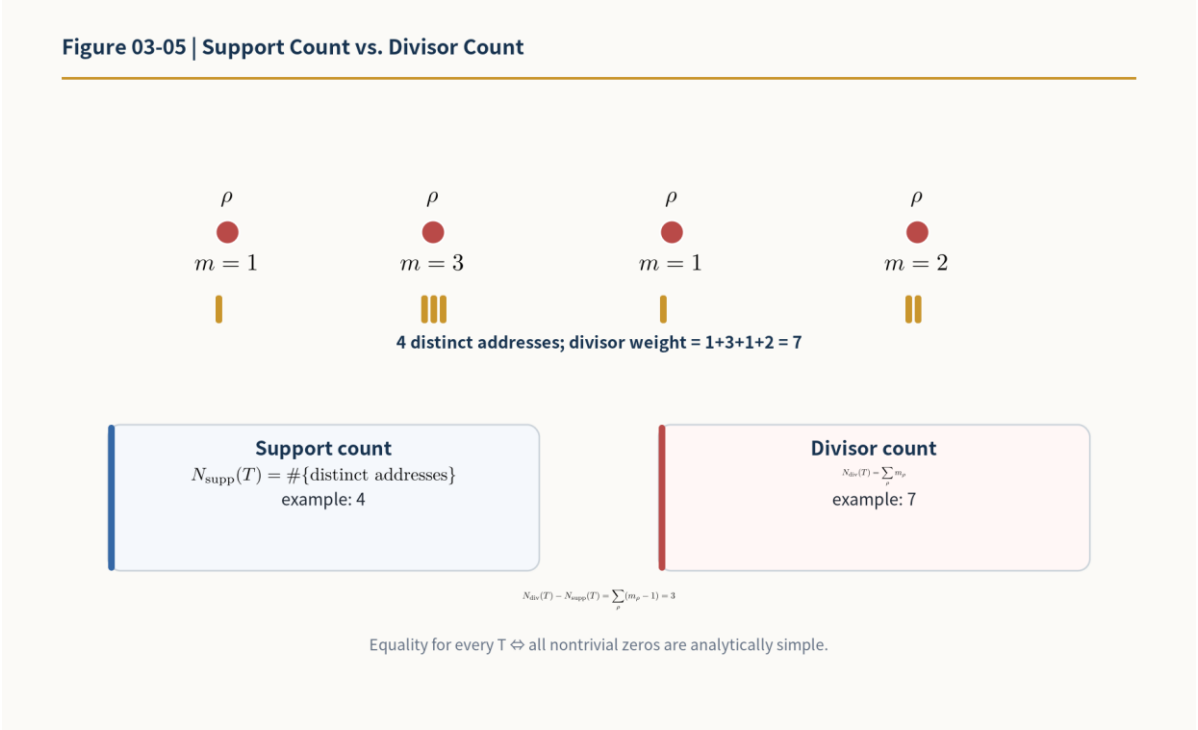


Figure 03-05. Support count versus divisor count. $N_{\mathrm{supp}}(T)$ counts only distinct zero addresses, whereas $N_{\mathrm{div}}(T)$ weights each address by its analytic multiplicity. Their difference is exactly $\sum(m_\rho - 1)$. Thus unique addressing does not imply simple zeros; the two counts agree for every height only when all $m_\rho = 1$.

10. The Argument Principle and Finite-Height Multiplicity Checks

For a closed contour not passing through zeros, the argument principle gives the total number of zeros counted with analytic multiplicity. Applied to the standard finite-height region for the Riemann ξ-function, it yields the multiplicity-weighted zero count, which in the notation of this chapter is

$$N_{\mathrm{div}}(T). \tag{10.1}$$

On the other hand, if all distinct zero addresses have been located, one obtains

$$N_{\mathrm{supp}}(T). \tag{10.2}$$

By Theorem 9.1, their difference

$$N_{\mathrm{div}}(T) - N_{\mathrm{supp}}(T) \tag{10.3}$$

is exactly the excess analytic multiplicity:

$$\sum_{0<\Im\rho\le T} (m_\rho - 1). \tag{10.4}$$

Turing-type methods are classical tools for certifying the completeness of finite-height zero counts. In the stratified notation of this chapter, the count they certify and the multiplicity-weighted count furnished by the argument principle both belong to the divisor layer. If this is combined with an independent location of distinct zeros, then divisor count and support count may be compared within a finite window, thereby determining whether excess multiplicity occurs in that window.

Thus finite-height zero certification and the three-layer separation of this chapter use the same basic ledger:

$$\boxed{\text{support of distinct addresses} \quad + \quad \text{divisor weights.}} \tag{10.5}$$

11. Interface with the Zero-Gap Geometry of Chapter 2

Chapter 2 (H02) uniformly uses adjacent real zero ordinates

$$\gamma_k < \gamma_{k+1}$$

together with analytic multiplicities

$$m_k = \mathrm{ord}_{\gamma_k}\Xi = \mathrm{ord}_{\rho_k}\xi. \tag{11.1}$$

Here

$$\rho_k = \frac{1}{2} + i\gamma_k. \tag{11.2}$$

Therefore the boundary shape of a gap in Chapter 2 reads the analytic multiplicity m_k at the divisor layer, not the event representation-sheet count. When two adjacent gaps share a zero, what they share is the same support address ρ_k; its analytic multiplicity m_k, as the local divisor weight at that address, is read consistently from both sides.

This gives the unified interface

$$\boxed{\text{shared boundary address} \quad + \quad \text{analytic multiplicity.}} \tag{11.3}$$

Repeated references to the same boundary address by adjacent intervals do not add new zero-support atoms.

12. Interface with the Spectral Objects of Chapters 5–9

For positive-height zeros, write the distinct ordinates as

$$\Gamma_+ = \{\gamma_n\}_{n\ge1}, \tag{12.1}$$

and retain the analytic multiplicity sequence

$$\{m_n\}_{n\ge1}. \tag{12.2}$$

Define the identity-support Hilbert space

$$\mathcal{H}_{\mathrm{id}} = \ell^2(\Gamma_+), \tag{12.3}$$

whose canonical basis vector e_n appears once for each distinct address. Define the ordinate operator

$$H_{\mathrm{id}}e_n = \gamma_n e_n. \tag{12.4}$$

At the same time, define the multiplicity operator

$$\boxed{M_{\text{mult}} e_n = m_n e_n.} \tag{12.5}$$

Thus

$$(H_{\text{id}}, M_{\text{mult}}) \tag{12.6}$$

represents the two layers of zero data—support address and analytic multiplicity—separately:

$$\boxed{H_{\text{id}} \leftrightarrow \text{distinct zero addresses},} \tag{12.7}$$

$$\boxed{M_{\text{mult}} \leftrightarrow \text{analytic multiplicities.}} \tag{12.8}$$

If divisor-faithful eigenspace dimensions are needed, one may amplify by multiplicity:

$$\tilde{H} = \oplus_n \gamma_n I_{m_n}, \tag{12.9}$$

so that

$$\dim\ker(\tilde{H} - \gamma_n I) = m_n. \tag{12.10}$$

Therefore

$$\boxed{\begin{array}{lll} \text{identity-faithful spectrum} & : & \gamma_n \text{appears once for each distinct address,} \\ \text{divisor-faithful spectrum} & : & \gamma_n \text{is amplified by} m_n. \end{array}} \tag{12.11}$$

All zeros are analytically simple if and only if

$$\boxed{M_{\text{mult}} = I,} \tag{12.12}$$

in which case the multiplicity layers of the identity-faithful and divisor-faithful spectral realizations coincide.

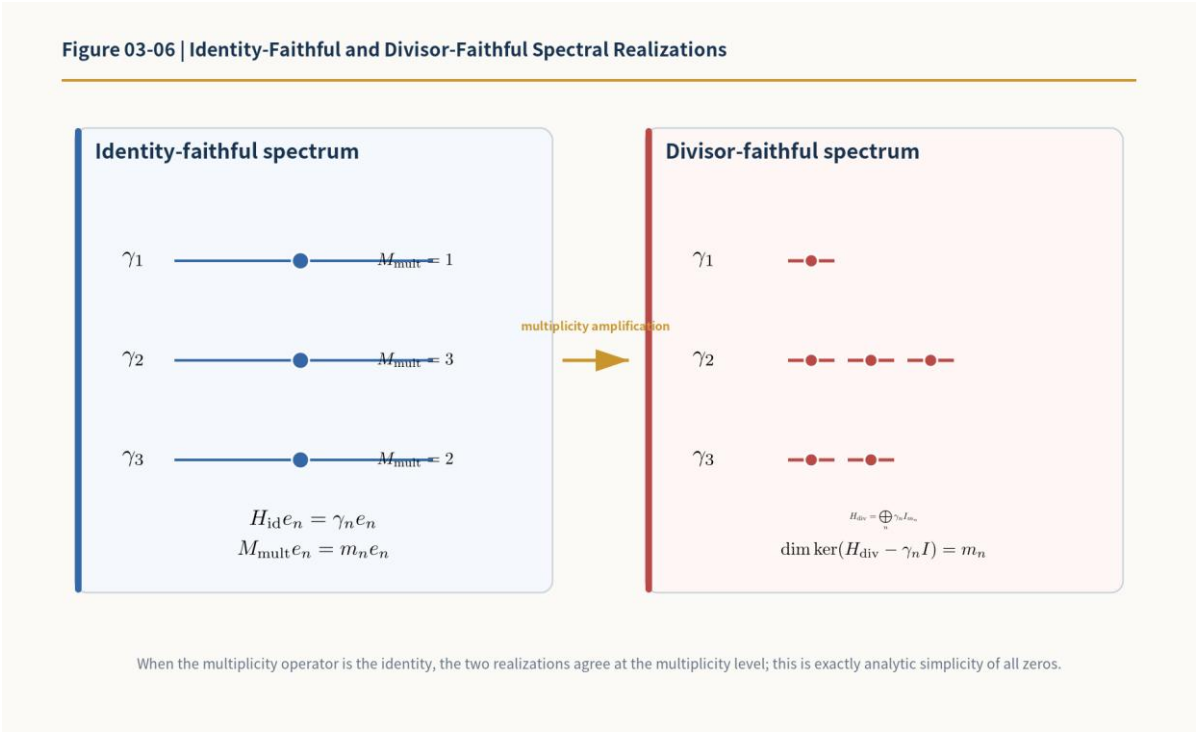


Figure 03-06. Identity-faithful and divisor-faithful spectral realizations. In the identity-faithful pair $(H_{\text{id}}, M_{\text{mult}})$, each distinct ordinate γ_n appears once as a spectral address, while analytic multiplicity is stored separately by M_{mult}. When divisor-faithful eigenspace dimension is required, multiplicity amplification gives $\tilde{H} = \oplus_n \gamma_n I_{m_n}$. The two realizations agree at the multiplicity level exactly when $M_{\text{mult}} = I$.

13. Main Theorem: Stratification of Address, Sheet Count, and Analytic Multiplicity

Theorem 13.1 (Riemann Zero Address–Representation-Sheet Count–Analytic Multiplicity Separation Theorem)

Within the unified representation chain consisting of open multiplication, exact centered-parameter transmission, reciprocal moving-horizon representation, and terminal zero readout, every nontrivial zero

$$\rho \in Z_{\mathrm{nt}}^{\mathrm{dist}}(\xi)$$

has the following three-layer structure:

$$\boxed{\begin{array}{rcl} \nu_{\mathrm{sheet}}(E) & = & \text{representation-sheet count of a finite reciprocal event,} \\ \mu_{\mathrm{supp}}(\rho) & = & 1, \\ m_\rho & = & \mathrm{ord}_\rho \xi. \end{array}} \tag{13.1}$$

More precisely:

1. reciprocal representation sheets are role-wise unfoldings of the same event and do not add distinct zero addresses;
2. repeated references by adjacent intervals to a shared boundary are automatically deduplicated under set union;
3. each distinct zero address appears exactly once in the support;
4. analytic multiplicity is stored independently in the zero divisor

$$\mathcal{D}_\xi^{\mathrm{nt}} = \sum_\rho m_\rho\,[\rho];$$

5. uniqueness of support addresses does not imply $m_\rho = 1$;
6. analytic simplicity is equivalent to

$$m_\rho = 1 \quad \forall \rho,$$

and equivalently to

$$M_{\mathrm{mult}} = I.$$

Proof. (1) follows from the event-layer definition of reciprocal representation.
(2) follows from the shared-boundary deduplication in Theorem 7.1.
(3) follows from the definition of distinct-address support together with the address fidelity of Theorem 5.1.
(4) follows from the local factorization (3.2) and the divisor definition (3.5).
(5) holds because support counting and analytic order of vanishing belong to different object levels.
(6) follows from Corollary 9.2 and the definition (12.5) of the multiplicity operator.

▫

14. Conclusion

Counting Riemann zeros first requires fixing the level at which the counting is performed. The unified stratification is

representation-sheet count ≠ support-address count ≠ analytic multiplicity.

The reciprocal wings of the open-multiplication horizon belong to event representation; a terminal nontrivial zero

$$\rho$$

belongs to analytic support; and the local order of vanishing

$$m_\rho$$

belongs to the zero divisor. The three are related within one generative–representational chain, but they are not conflated as types.

Accordingly, the complete data of the nontrivial zeros naturally split into

$$Z_{\mathrm{nt}}^{\mathrm{dist}}(\xi) \quad \text{and} \quad \mathcal{D}_\xi^{\mathrm{nt}} = \sum_\rho m_\rho\,[\rho].$$

The former is the identity-faithful support, recording each distinct address once; the latter is the divisor-faithful zero data, retaining analytic multiplicity at the same address.

At finite height, the two counting functions satisfy

$$N_{\mathrm{div}}(T) - N_{\mathrm{supp}}(T) = \sum_{0<\Im\rho\le T} (m_\rho - 1).$$

Thus the logical relation between address uniqueness and analytic simplicity is exact: the former fixes the support of distinct addresses, while the latter requires every divisor weight to equal 1.

This stratification simultaneously unifies the boundary multiplicities of adjacent zero gaps, the bare support and divisor data after closure, and the spectral structure

$$(H_{\mathrm{id}}, M_{\mathrm{mult}}).$$

The addresses, representations, and multiplicities of Riemann zeros thereby enter a single unambiguous object ledger.

Chapter 4 Parameterization of the Riemann Closure Kernel and Proof of the Generalized Riemann Hypothesis

— Reciprocal-Role Fidelity, Terminal Fixed Readout, and Minimal Identity Migration

Abstract

The Riemann closure argument of Chapter 1 (H01) can be formalized as a minimal closure kernel composed of an open multiplicative relation, a centered parameter, reciprocal roles, complete events, a completed analytic object, and terminal zero readouts. This chapter gives a parameterized form of that closure kernel together with its general conditions of applicability.

Let $\mathfrak{E}$ be a domain of complete events. Each event $E \in \mathfrak{E}$ carries a role space X_E and a reciprocal involution

$$J_E: X_E \to X_E, \qquad J_E^2 = \mathrm{id}.$$

The same event passes through a sequence of representations

$$\mathcal{R}_0, \mathcal{R}_1, \dots, \mathcal{R}_N,$$

and each layer carries both a centered parameter and a reciprocal-role reading. If every migration between adjacent representations preserves the centered parameter and commutes with the reciprocal action at the two layers, then parameter identity and role assignment remain unchanged throughout the representation chain.

A complete event also possesses a fixed role determined by the geometry of its generative source,

$$R_E \in X_E, \qquad J_E R_E = R_E.$$

The terminal analytic representation carries the canonical reciprocal involution

$$\iota_c(s) = 2c - \overline{s}.$$

If the terminal readout

$$\Phi_E: X_E \to \mathbb{C}$$

preserves reciprocal roles,

$$\Phi_E(J_E R) = \iota_c(\Phi_E(R)),$$

then, at the generative-source fixed role R_E,

$$\Phi_E(R_E) = \iota_c(\Phi_E(R_E)).$$

Hence

$$\Re\Phi_E(R_E) = c.$$

Terminal closure is defined as the acquisition, in the analytic representation, of a fixed-role readout by the generative-source fixed role under reciprocal-role fidelity. It follows directly from the two conditions above.

If the completed object is also terminally exhaustive—meaning that all target zeros arise as terminal fixed-role readouts of complete events—then

$$\forall \rho \in Z_{\text{target}}, \qquad \Re\rho = c.$$

This yields the minimal seven-condition closure kernel:

K1root identity and reciprocal-role system, K2centered reciprocal representation,

K3exact centered-parameter transmission, K4reciprocal-role fidelity,

K5generative-source fixed role of a complete event, K6zero-faithful completion and terminal exhaustivity,

K7canonical analytic reciprocal involution.

In the Riemann realization, the root identity is multiplication on the positive integers,

$$\Im_{\times} = (\mathbb{N}_{>0}, \mu), \qquad \mu(m,q) = mq,$$

and the reciprocal role is

$$J(m,q) = (q,m).$$

The square horizon satisfies

$$m > k, \quad q > k, \quad mq \le (k+1)^2 \Rightarrow m = q = k+1,$$

thereby producing a generative-source fixed role. The terminal analytic involution is

$$\iota_{1/2}(\rho) = 1 - \overline{\rho}.$$

Therefore a terminal fixed-role readout satisfies

$$\rho = 1 - \overline{\rho},$$

and hence

$$\Re\rho = \frac{1}{2}.$$

The chapter then applies this parameterized kernel to the Dirichlet case of the Generalized Riemann Hypothesis. We do **not** use the false implication

$$\text{RH} \Rightarrow \text{GRH}.$$

Instead, we verify one minimal migration fact: a Dirichlet character does not create a second root multiplicative identity. For an arbitrary character χ, define the reciprocal character package

$$\mathfrak{P}_{\chi} = \{\chi, \overline{\chi}\},$$

which is only channel data carried by the same root multiplicative identity. The weighted centered kernel

$$W_{\chi,z}(m,q) = \chi(m)\overline{\chi(q)}m^{-1/2-z}q^{-1/2+z}$$

satisfies the exact reciprocity

$$(m,q,\chi,z) \leftrightarrow (q,m,\overline{\chi},-z),$$

while the global encoding, moving head/tail decomposition, and standard completion preserve the same centered parameter z. For a primitive Dirichlet character, the functional equation and conjugation structure give the terminal analytic involution

$$\rho \mapsto 1 - \overline{\rho}$$

on the zero set belonging to that same χ-channel. Thus the Dirichlet lift satisfies K1–K7 term by term, and the square-horizon fixed role is inherited unchanged because it depends only on $mq = n$. By Theorem 18.1,

$$L(\rho, \chi) = 0, \qquad 0 < \Re\rho < 1 \Rightarrow \Re\rho = \frac{1}{2}.$$

Imprimitive and principal characters are then reduced by finite Euler factors; zeros of those additional factors lie on $\Re s = 0$ and therefore do not enter the open critical strip. Throughout this chapter, GRH means this Dirichlet–GRH statement.

The chapter also freezes the coordinate types. The horizontal coordinate of a finite-horizon event lift is denoted by $d_E(\tau)$, while the actual horizontal displacement of a zero from the critical line is

$$d_\rho = \Re\rho - \frac{1}{2}.$$

These are not identified as objects and no numerical transfer is asserted between them. The Riemann closure kernel is thereby compressed to the strict formal chain

$$\boxed{\text{generative-source fixed role} + \text{reciprocal-role fidelity} + \text{terminal exhaustivity} \Rightarrow \text{global fixed-role readout.}}$$

1. Parameterized Objects and Logical Position

Following the notation of Chapter 1 (H01), the root identity of multiplication on the positive integers is

$$\boxed{\mathfrak{I}_\times = (\mathbb{N}_{>0}, \mu), \qquad \mu(m, q) = mq.} \tag{1.1}$$

The open multiplicative relation

$$\mathcal{R}_\times = \mathrm{Graph}(\mu) = \{(m, q, n) : mq = n\} \tag{1.2}$$

is a relational representation of this root identity. As one unfolds through Dirichlet, Mellin, multiplicative shells, moving horizons, ζ, Riemann completion, and zero readouts, the root identity remains unchanged while representation form and role readout change from layer to layer.

This chapter rewrites the structure responsible for the terminal fixed readout in the concrete closure chain of Chapter 1 as a parameterized closure kernel. The core objects occupy four levels:

$$\boxed{\text{root identity} \;\rightarrow\; \text{event} \;\rightarrow\; \text{role} \;\rightarrow\; \text{role readout.}} \tag{1.3}$$

Here:

1. the **root identity** gives the unified generative relation;
2. an **event** is one complete relational history within that identity;
3. a **role** is a position determined inside the event by the reciprocal action;
4. a **role readout** is a coordinate or analytic reading of that same role in a specific representation layer.

Throughout the book,

$$\boxed{\text{identity} \neq \text{role} \neq \text{role readout.}} \tag{1.4}$$

The parameterization therefore specifies the conditions under which objects of different types retain their identity through representational change.

2. Root Reciprocal System

Definition 2.1 (Root Reciprocal-Role System)

Let $\mathfrak{I}$ be a root identity and X the role space in one of its relational representations. Suppose

$$J: X \to X \tag{2.1}$$

satisfies

$$\boxed{J^2 = \mathrm{id}_X.} \tag{2.2}$$

Then

$$(\mathfrak{I}, X, J) \tag{2.3}$$

is called a **root reciprocal-role system**.

In the Riemann realization,

$$X = \mathcal{R}_\times, \qquad J(m, q, n) = (q, m, n). \tag{2.4}$$

The fixed-role set is

$$\mathrm{Fix}(J) = \{x \in X : Jx = x\}. \tag{2.5}$$

Definition 2.2 (Reciprocal Normalized Readout)

Let

$$u: X \to \mathbb{R}$$

satisfy

$$u(Jx) = L - u(x) \tag{2.6}$$

for some $L > 0$. If $x \in \mathrm{Fix}(J)$, then

$$u(x) = \frac{L}{2}. \tag{2.7}$$

In the Riemann normalization, $L = 1$, so the fixed-role readout is

$$u = \frac{1}{2}. \tag{2.8}$$

Definition 2.3 (Antisymmetric Relational Coordinate)

If

$$R: X \to \mathbb{R}$$

satisfies

$$\boxed{R(Jx) = -R(x),} \tag{2.9}$$

then R is called an **antisymmetric relational coordinate**.

For a fixed role,

$$Jx = x \Rightarrow R(x) = 0. \tag{2.10}$$

The standard choice in the Riemann multiplicative representation is

$$R(m, q) = \log \frac{q}{m}. \tag{2.11}$$

Equations (2.8) and (2.10) are two different generative-source readouts of the same reciprocal fixed relation.

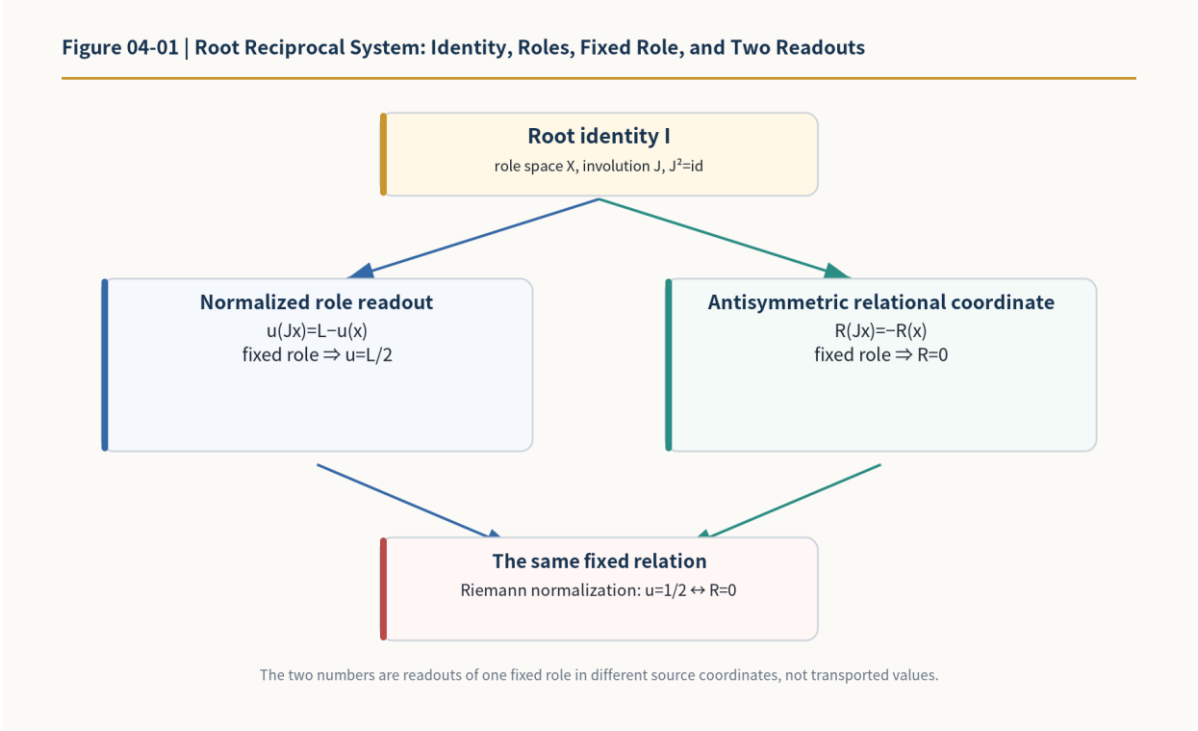


Figure 04-01. Root reciprocal system. The involution $J^2 = \mathrm{id}$ on roles over a root identity supports two source-side readouts. A normalized role coordinate $u(Jx) = L - u(x)$ reads a fixed role as $L/2$, while an antisymmetric relational coordinate $R(Jx) = -R(x)$ reads the same fixed role as 0. In the Riemann normalization, $u = 1/2$ and $R = 0$ are two readings of one fixed relation, not a number transported along the representation chain.

3. Centered Reciprocal Representation

Definition 3.1 (Centered Reciprocal Kernel)

Let $z \in \mathbb{C}$. If a family of functions

$$K_z : X \to \mathbb{C}$$

satisfies

$$\boxed{K_z(Jx) = K_{-z}(x),} \tag{3.1}$$

then $\{K_z\}$ is called a **centered reciprocal kernel**.

The Riemann realization is

$$\boxed{K_z(m,q) = m^{-1/2-z} q^{-1/2+z} = (mq)^{-1/2} e^{z\log(q/m)}.} \tag{3.2}$$

Exchanging m and q gives

$$K_z(q,m) = K_{-z}(m,q). \tag{3.3}$$

Lemma 3.2 (Evenness of Reciprocal Aggregation)

If $D \subset X$ is invariant under J and

$$A_D(z) = \sum_{x \in D} K_z(x) \tag{3.4}$$

converges absolutely, then

$$\boxed{A_D(z) = A_D(-z).} \tag{3.5}$$

Proof. Since $J: D \to D$ is a bijection,

$$A_D(z) = \sum_{x \in D} K_z\,(Jx) = \sum_{x \in D} K_{-z}\,(x) = A_D(-z).$$

▫

4. Two-Channel Analytic Encoding

After the centered reciprocal kernel enters an analytic representation, the parameter z enters two channels reciprocally as $+z$ and $-z$.

Definition 4.1 (Reciprocal Analytic Channel Pair)

Let F_+ and F_- be analytic objects and set

$$w_+(z) = a + c + z, \qquad w_-(z) = a + c - z. \tag{4.1}$$

If the global encoding has the form

$$\boxed{\mathcal{G}_a(z) = F_+(w_+(z))F_-(w_-(z)),} \tag{4.2}$$

and the reciprocal action exchanges the two channels, then the pair is called a **reciprocal analytic channel pair**.

In the Riemann realization,

$$F_+ = F_- = \zeta, \qquad c = \frac{1}{2}, \tag{4.3}$$

and

$$\sum_{n \geq 1} a_n\,(z) n^{-a} = \zeta\left(a + \frac{1}{2} + z\right)\zeta\left(a + \frac{1}{2} - z\right). \tag{4.4}$$

What is preserved here is the paired occurrence of the same centered parameter in reciprocal channels. The generative-source reciprocal coordinate and the terminal zero coordinate retain their respective coordinate types throughout.

5. Multiple Representations of the Same Event

The generative-source, analytic, and terminal layers are written uniformly as multiple representations over one event domain.

Definition 5.1 (Domain of Complete Events)

Let

$$\mathfrak{E} \tag{5.1}$$

be the set of complete events. For each

$$E \in \mathfrak{E},$$

let its role space be

$$X_E, \tag{5.2}$$

and its reciprocal action be

$$J_E: X_E \to X_E, \qquad J_E^2 = \mathrm{id}. \tag{5.3}$$

The representation of E at layer j is denoted

$$\mathcal{R}_j(E), \qquad j = 0,1,\dots,N. \tag{5.4}$$

Thus

$$\boxed{E_{\text{generative source}} \equiv E_{\text{analytic}} \equiv E_{\text{terminal}} \equiv E} \tag{5.5}$$

means that the same event history is being read continuously at the generative-source, analytic, and terminal representation layers.

Definition 5.2 (Representation Migration)

Between adjacent representations, let there be a specified map

$$T_{j+1}: \mathcal{R}_j(E) \to \mathcal{R}_{j+1}(E). \tag{5.6}$$

The total migration of representations is

$$T = T_N \circ \cdots \circ T_1. \tag{5.7}$$

Representation migration changes the encoding but not the event identity E.

6. Exact Transmission of the Centered Parameter

Each representation layer carries a centered-parameter readout

$$z_j: \mathcal{R}_j(E) \to \mathbb{C}. \tag{6.1}$$

Definition 6.1 (Exact Centered-Parameter Transmission)

If for every j,

$$\boxed{z_{j+1} \circ T_{j+1} = z_j,} \tag{6.2}$$

then the migration between adjacent representations is said to preserve the centered parameter.

Theorem 6.2 (Compositionality of Parameter Fidelity)

If every layer satisfies (6.2), then

$$\boxed{z_N \circ T = z_0.} \tag{6.3}$$

Proof. Substituting layer by layer,

$$z_N T_N \cdots T_1 = z_{N-1} T_{N-1} \cdots T_1 = \cdots = z_0.$$

▫

For the Riemann representation chain this may be compressed as

$$\boxed{z_{\text{Mellin}} = z_{\text{shell}} = z_{\text{Dirichlet}} = z_{\text{head/tail}} = z_{\text{completion}} = z_{\text{terminal}}.} \tag{6.4}$$

Equation (6.4) says that the centered parameter remains the same throughout all representation layers.

7. Reciprocal-Role Fidelity

Equality of parameters does not by itself imply equality of role assignment. The closure kernel therefore requires reciprocal-role fidelity as an independent condition.

Suppose the representation at layer j carries a reciprocal action

$$J_j: \mathcal{R}_j(E) \to \mathcal{R}_j(E), \qquad J_j^2 = \mathrm{id}. \tag{7.1}$$

Definition 7.1 (Reciprocal-Role Fidelity)

If

$$\boxed{T_{j+1} \circ J_j = J_{j+1} \circ T_{j+1},} \tag{7.2}$$

then T_{j+1} is said to preserve reciprocal roles.

Theorem 7.2 (Compositionality of Role Fidelity)

If all adjacent migrations satisfy (7.2), then the total migration T satisfies

$$\boxed{T \circ J_0 = J_N \circ T.} \tag{7.3}$$

Proof.

$$\begin{aligned} TJ_0 &= T_N \cdots T_2 (T_1 J_0) \\ &= T_N \cdots T_2 (J_1 T_1) \\ &= \cdots \\ &= J_N T_N \cdots T_1 \\ &= J_N T. \end{aligned}$$

▫

Corollary 7.3 (Representation Fidelity of Fixed Roles)

If

$$x \in \mathrm{Fix}(J_0), \tag{7.4}$$

then

$$T(x) \in \mathrm{Fix}(J_N). \tag{7.5}$$

Proof. Since $J_0 x = x$, (7.3) gives

$$J_N T(x) = T J_0(x) = T(x).$$

▫

This theorem shows that the fixedness of a fixed role can be transmitted through an equivariant representation chain without reselecting the role in every terminal representation.

8. Complete Events and Generative-Source Fixed Roles

Whether a complete event acquires a fixed role is determined by the geometry of the concrete carrier.

Definition 8.1 (Generative-Source Fixed Role of a Complete Event)

For each

$$E \in \mathfrak{E},$$

if there exists a role

$$R_E \in X_E \tag{8.1}$$

determined by the geometry of the generative-source event and satisfying

$$\boxed{J_E R_E = R_E,} \tag{8.2}$$

then R_E is called the **generative-source fixed role** of the event E.

Condition (8.2) is part of the geometry of the complete event and is determined by the concrete structure of the carrier and the event boundary.

Theorem 8.2 (Riemann Square-Horizon Fixed Role)

For every integer $k \geq 1$, if

$$m > k, \qquad q > k, \qquad mq \leq (k+1)^2, \tag{8.3}$$

then

$$\boxed{m = q = k+1.} \tag{8.4}$$

Hence the role at the endpoint of a square horizon is fixed under

$$J(m, q) = (q, m).$$

Proof. From

$$m > k, \quad q > k$$

we obtain

$$m \geq k+1, \qquad q \geq k+1,$$

and hence

$$mq \geq (k+1)^2.$$

Together with

$$mq \leq (k+1)^2,$$

this yields

$$mq = (k+1)^2.$$

Since $m, q \geq k+1$, the only possibility is

$$m = q = k+1.$$

▫

Likewise, the next square section gives

$$m = q = k+2. \tag{8.5}$$

This elementary integer inequality is the concrete carrier geometry of K5 in the Riemann realization.

9. Terminal Analytic Reciprocal Involution

Let the zero readouts of the target completed analytic object lie in the complex plane, and fix a real number c.

Definition 9.1 (Canonical Analytic Reciprocal Involution)

Define

$$\boxed{\iota_c(s) = 2c - \overline{s}.} \tag{9.1}$$

Clearly,

$$\iota_c^2 = \mathrm{id}. \tag{9.2}$$

Lemma 9.2 (Analytic Fixed Set)

$$\boxed{\mathrm{Fix}(\iota_c) = \{s \in \mathbb{C} : \Re s = c\}.} \tag{9.3}$$

Proof. Let

$$s = \sigma + i\gamma.$$

Then

$$s = \iota_c(s)$$

is equivalent to

$$\sigma + i\gamma = 2c - \sigma + i\gamma,$$

so

$$\sigma = c.$$

The converse is immediate. ▫

For the Riemann case, set

$$c = \frac{1}{2}, \tag{9.4}$$

which gives

$$\boxed{\iota_{1/2}(s) = 1 - \overline{s}.} \tag{9.5}$$

Its fixed set is

$$\Re s = \frac{1}{2}. \tag{9.6}$$

10. Terminal Role Readouts

For every complete event E, let its role readout in the terminal representation be

$$\Phi_E : X_E \to \mathbb{C}. \tag{10.1}$$

Definition 10.1 (Terminal Reciprocal-Role Fidelity)

If for every

$$R \in X_E$$

one has

$$\boxed{\Phi_E(J_E R) = \iota_c(\Phi_E(R)),} \tag{10.2}$$

then the terminal role readout is said to preserve reciprocal roles.

This condition is the terminal analytic reading of reciprocal-role fidelity along the entire representation chain.

11. Core Theorem: Terminal Fixed-Role Readout

Theorem 11.1 (Reciprocal-Role Fidelity and Terminal Fixed Readout)

Let $E \in \mathfrak{E}$ be a complete event and assume:

1. $R_E \in X_E$ is a generative-source fixed role:

$$J_E R_E = R_E;$$

2. the terminal readout Φ_E preserves reciprocal roles:

$$\Phi_E(J_E R) = \iota_c(\Phi_E(R)).$$

Then

$$\rho_E := \Phi_E(R_E) \tag{11.1}$$

satisfies

$$\boxed{\rho_E = \iota_c(\rho_E),} \tag{11.2}$$

and therefore

$$\boxed{\Re\rho_E = c.} \tag{11.3}$$

Proof. From $J_E R_E = R_E$ and reciprocal-role fidelity,

$$\begin{aligned}\rho_E &= \Phi_E(R_E)\\ &= \Phi_E(J_E R_E)\\ &= \iota_c(\Phi_E(R_E))\\ &= \iota_c(\rho_E).\end{aligned}$$

Lemma 9.2 then gives

$$\Re\rho_E = c.$$

▫

Corollary 11.2 (Terminal Closure)

Under the hypotheses of Theorem 11.1, the terminal role readout of the event E lies in

$$\mathrm{Fix}(\iota_c). \tag{11.4}$$

This fact is called **terminal closure** in this chapter.

Thus terminal closure follows directly from

$$\boxed{\text{generative-source fixed role} + \text{reciprocal-role fidelity.}} \tag{11.5}$$

Corollary 11.3 (Terminal-Closure Identity)

Under the hypotheses of Theorem 11.1,

$$\boxed{\Phi_E(J_E R_E) = \Phi_E(R_E) = \iota_c(\Phi_E(R_E)).} \tag{11.6}$$

Proof. Substitute $J_E R_E = R_E$ into reciprocal-role fidelity. ▫

12. Zero Fidelity and Terminal Exhaustivity

The event-level fixed-role conclusion is extended to the full target zero domain by terminal exhaustivity.

Definition 12.1 (Zero-Faithful Completed Target)

Let the completed analytic object be F, with target zero set

$$Z_{\mathrm{target}}(F). \tag{12.1}$$

Define the family of terminal readouts by

$$\mathcal{Z}_\Phi = \{\Phi_E(R_E) : E \in \mathfrak{E}\}. \tag{12.2}$$

If

$$\boxed{Z_{\text{target}}(F) = \mathcal{Z}_{\Phi},} \tag{12.3}$$

then the completed target is said to have **terminal exhaustivity**.

Equation (12.3) says equivalently:

- the fixed-role readout of every complete event is a target zero;
- every target zero is the fixed-role readout of some complete event.

Theorem 12.2 (Terminal Exhaustivity Theorem)

If every $E \in \mathfrak{E}$ satisfies Theorem 11.1 and the target completed object satisfies terminal exhaustivity (12.3), then

$$\boxed{\forall \rho \in Z_{\text{target}}(F), \qquad \Re\rho = c.} \tag{12.4}$$

Proof. Choose arbitrary

$$\rho \in Z_{\text{target}}(F).$$

By (12.3), there is an $E \in \mathfrak{E}$ such that

$$\rho = \Phi_E(R_E).$$

Theorem 11.1 gives $\Re\rho = c$. Since ρ was arbitrary, the conclusion follows. ▫

13. The Minimal Seven-Condition Closure Kernel

The preceding structure compresses to seven conditions.

K1. Root Identity and Reciprocal-Role System

There is a unified root identity $\mathfrak{J}$ and an involution on event role spaces,

$$J^2 = \text{id}. \tag{13.1}$$

K2. Centered Reciprocal Representation

There exists a centered representation K_z satisfying

$$\boxed{K_z(Jx) = K_{-z}(x).} \tag{13.2}$$

K3. Exact Centered-Parameter Transmission

Along the representation chain,

$$\boxed{z_{j+1}T_{j+1} = z_j.} \tag{13.3}$$

K4. Reciprocal-Role Fidelity

Representation migration satisfies

$$\boxed{T_{j+1}J_j = J_{j+1}T_{j+1}.} \tag{13.4}$$

K5. Generative-Source Fixed Role of a Complete Event

For each $E \in \mathfrak{E}$, there exists a role R_E, determined by generative-source event geometry, such that

$$\boxed{J_E R_E = R_E.} \tag{13.5}$$

K6. Zero-Faithful Completed Target and Terminal Exhaustivity

The fixed-role readouts of complete events cover exactly the target zero set:

$$\boxed{Z_{\text{target}}(F) = \{\Phi_E(R_E) : E \in \mathfrak{E}\}.} \tag{13.6}$$

K7. Canonical Analytic Reciprocal Involution

The reciprocal action on terminal zero roles is

$$\boxed{\iota_c(s) = 2c - \overline{s},} \tag{13.7}$$

and the terminal readout is equivariant with the reciprocal role of the generative source:

$$\boxed{\Phi_E(J_E R) = \iota_c(\Phi_E(R)).} \tag{13.8}$$

K5 and K7 give

$$\Phi_E(R_E) \in \mathrm{Fix}(\iota_c).$$

With K6,

$$\boxed{\forall \rho \in Z_{\text{target}}(F), \qquad \Re\rho = c.} \tag{13.9}$$

K1–K4 provide the generative and fidelity structure of the event and its representation chain; K5 supplies the generative-source fixed role; K6 supplies global coverage of the object domain; and K7 reads the fixed role into the terminal analytic fixed set.

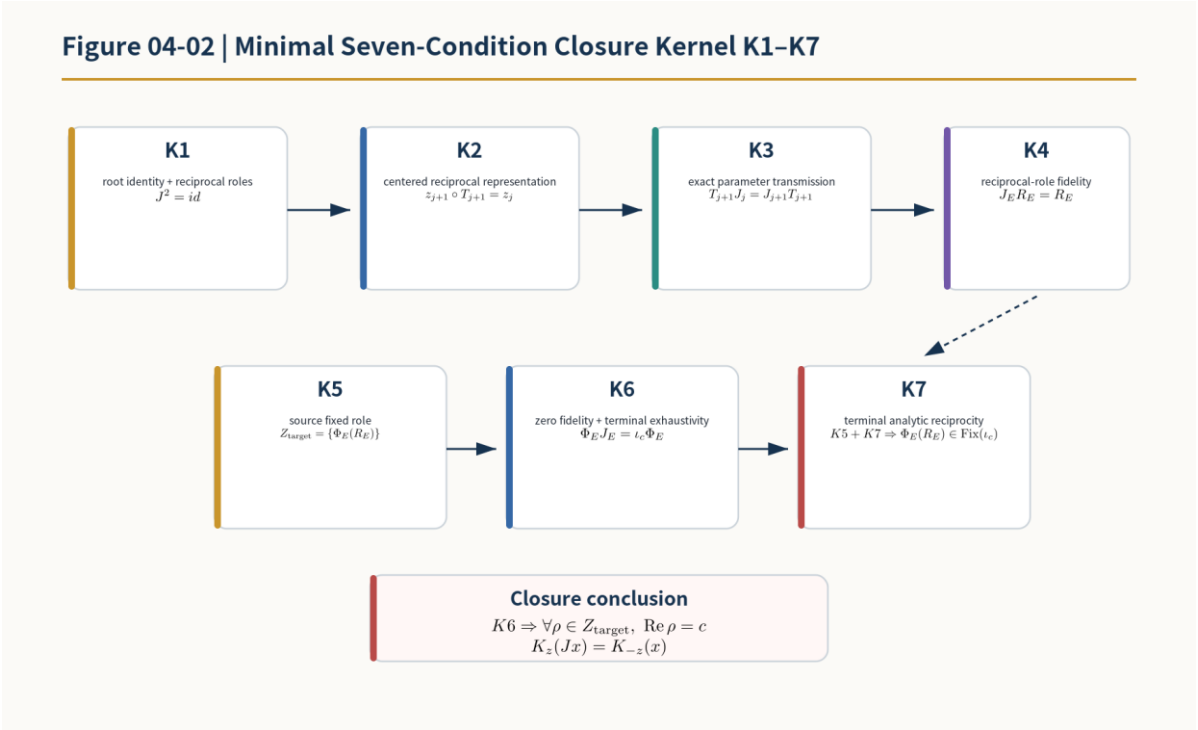


Figure 04-02. Minimal seven-condition closure kernel. K1–K4 govern the root identity, centered representation, and exact preservation of the centered parameter and reciprocal roles along the representation chain. K5 supplies the source-fixed role of each complete event; K6 gives zero-faithful terminal exhaustivity; K7 translates source reciprocity into the terminal analytic involution. K5 and K7 first place every fixed-role readout in $\mathrm{Fix}(\iota_c)$, and K6 extends the conclusion to all target zeros.

14. The Riemann Realization

This section identifies K1–K7 in the Riemann closure chain.

14.1 K1: Multiplication on the Positive Integers and Role Exchange

The root identity is

$$\Im_{\times} = (\mathbb{N}_{>0}, \mu), \qquad \mu(m,q) = mq. \tag{14.1}$$

Its relational representation is

$$\mathcal{R}_{\times} = \{(m,q,n) : mq = n\}. \tag{14.2}$$

The reciprocal exchange of roles is

$$\boxed{J(m,q,n) = (q,m,n).} \tag{14.3}$$

14.2 K2: Centered Mellin Reciprocal Kernel

Take

$$\boxed{K_z(m,q) = m^{-1/2-z} q^{-1/2+z}.} \tag{14.4}$$

Then

$$K_z(q,m) = K_{-z}(m,q). \tag{14.5}$$

14.3 K3: Exact Centered-Parameter Transmission

The same centered parameter remains unchanged along

$$\text{Mellin} \to \text{shell} \to \text{Dirichlet} \to \text{head/tail} \to \text{completion} \to \text{terminal readout}. \tag{14.6}$$

14.4 K4: Reciprocal-Role Fidelity

The multiplicative role exchange is read in intermediate analytic representations as

$$z \leftrightarrow -z, \tag{14.7}$$

and in the terminal completed analytic representation as

$$\boxed{\rho \mapsto 1 - \overline{\rho}.} \tag{14.8}$$

Every representation layer preserves the assignment of reciprocal roles within the same event.

14.5 K5: Square-Horizon Fixed Role

By Theorem 8.2,

$$m > k, \quad q > k, \quad mq \le (k+1)^2$$

implies

$$\boxed{m = q = k+1.} \tag{14.9}$$

Thus the endpoint of a square horizon is a generative-source fixed role.

14.6 K6: Terminal Object Domain

Lemma 6.3A of Chapter 1 already identifies the terminal object domain

$$\rho_{E,\pm}(\tau_R)$$

from Theorem 5.5 with the readout of the same right-end fixed role R_E. Hence, in the Riemann realization, K6 is not an additional assumption; it follows from **object-domain exhaustivity plus terminal role identification**:

$$\boxed{Z_{\mathrm{nt}}(\xi) = \{\Phi_E(R_E) : E \in \mathfrak{E}_{\mathrm{Riemann}}\}.} \tag{14.10}$$

No external surjection from the generative source to the terminal layer is newly manufactured for each zero. Theorem 5.5 already exhausts all terminal zero events; Lemma 6.3A simply recognizes that the original $+$ and $-$ reciprocal-role labels of a terminal event are, at the right end of the square horizon, the same fixed role.

14.7 K7: Riemann Analytic Reciprocal Involution

Take

$$c = \frac{1}{2}.$$

Then

$$\boxed{\iota_{1/2}(\rho) = 1 - \overline{\rho}.} \tag{14.11}$$

By K5 and K7,

$$\begin{aligned} \rho_E &= \Phi_E(R_E) \\ &= \Phi_E(J_E R_E) \\ &= 1 - \overline{\Phi_E(R_E)} \\ &= 1 - \overline{\rho_E}. \end{aligned} \tag{14.12}$$

Therefore

$$\boxed{\Re\rho_E = \frac{1}{2}.} \tag{14.13}$$

With K6,

$$\boxed{\forall \rho \in Z_{\mathrm{nt}}(\xi), \qquad \Re\rho = \frac{1}{2}.} \tag{14.14}$$

In this realization, no direct numerical transfer is asserted from the generative-source fixed coordinate to the terminal analytic coordinate. What is transmitted is the reciprocal role; the value $1/2$ at the terminal layer is read from the analytic fixed-point equation (14.12).

15. Coordinate-Type Discipline

The parameterized closure kernel must simultaneously preserve the type distinction between event coordinates and actual zero coordinates.

15.1 Relative Role Coordinate at the Generative Source

Define

$$R = \log\frac{q}{m}. \tag{15.1}$$

The reciprocal exchange acts by

$$R \mapsto -R. \tag{15.2}$$

The fixed role is

$$R = 0. \tag{15.3}$$

15.2 Normalized Generative-Source Role

The normalized role coordinate satisfies

$$u \leftrightarrow 1 - u, \tag{15.4}$$

with fixed role

$$u = \frac{1}{2}. \tag{15.5}$$

15.3 Finite-Horizon Event-Lift Coordinate

The horizontal unfolding of an intermediate event representation is denoted by

$$\boxed{d_E(\tau).} \tag{15.6}$$

The corresponding reciprocal-role readouts may be written as

$$z_{E,\pm}(\tau) = \pm d_E(\tau) + i\gamma_E(\tau). \tag{15.7}$$

15.4 Horizontal Displacement of an Actual Zero

The horizontal coordinate of an actual zero relative to the critical line is

$$\boxed{d_\rho = \Re\rho - \frac{1}{2}.} \tag{15.8}$$

The two are strictly distinct as object types:

$$\boxed{d_E(\tau) \neq d_\rho \quad \text{as object types.}} \tag{15.9}$$

The terminal fixed-role readout gives

$$d_\rho = 0. \tag{15.10}$$

Equation (15.10) is read directly from the terminal analytic fixed-point equation

$$\rho = 1 - \overline{\rho}. \tag{15.11}$$

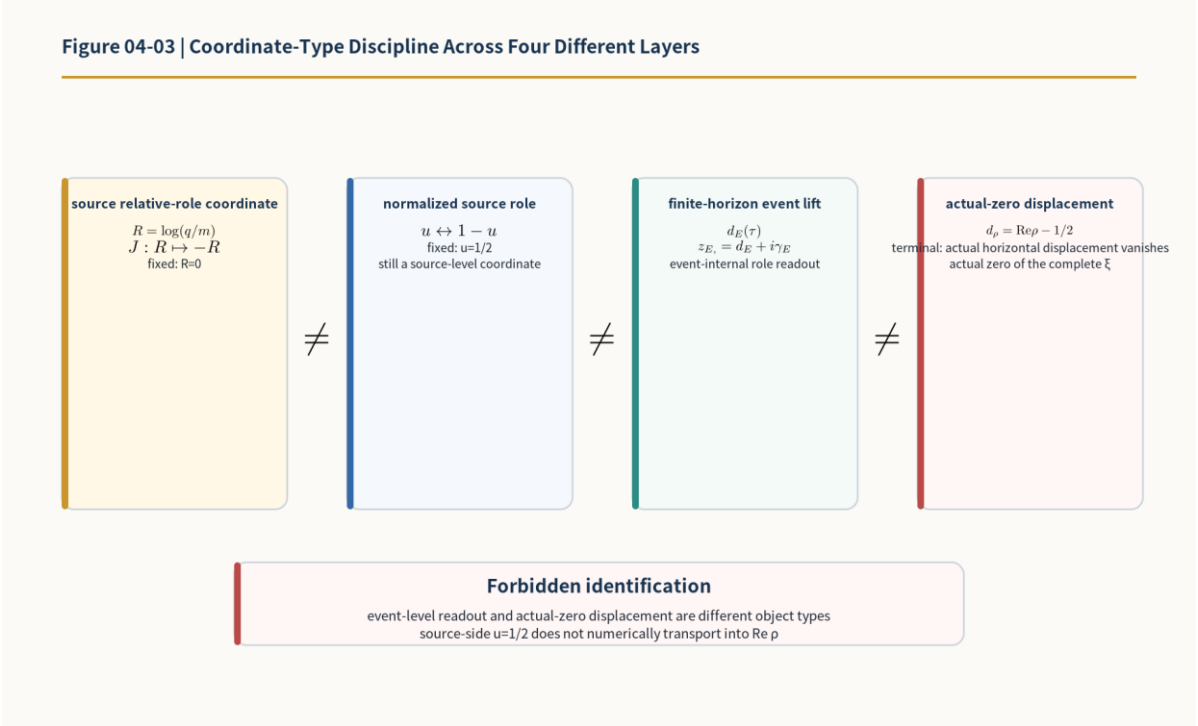


Figure 04-03. Coordinate-type discipline. The source relative-role coordinate R, normalized role u, finite-horizon event lift $d_E(\tau)$, and actual-zero horizontal displacement d_ρ are four different object types. In particular, $d_E(\tau) \neq d_\rho$, and the source-side value $u = 1/2$ is not numerically transported into $\Re\rho$. The terminal equality $d_\rho = 0$ is read from the analytic fixed-point equation $\rho = 1 - \overline{\rho}$.

16. Interface with Chapter 3: Zero Addresses and Analytic Multiplicities

The parameterized closure kernel determines the analytic address position of a terminal role. If

$$\rho \in Z_{\mathrm{nt}}^{\mathrm{dist}}(\xi)$$

and

$$\xi(s) = (s-\rho)^{m_\rho} U_\rho(s), \qquad U_\rho(\rho) \neq 0, \tag{16.1}$$

then

$$\boxed{\rho = \text{terminal zero address,}} \tag{16.2}$$

while

$$\boxed{m_\rho = \mathrm{ord}_\rho \xi = \text{analytic multiplicity.}} \tag{16.3}$$

The fixed-role argument K1–K7 acts on the address readout ρ; it does not mix the number of reciprocal event-representation sheets with analytic multiplicity. Hence

$$\boxed{\text{event representation-sheet count} \neq \text{support-address count} \neq \text{analytic multiplicity.}} \tag{16.4}$$

This keeps the closure kernel compatible with the zero divisor

$$\mathcal{D}_\xi^{\mathrm{nt}} = \sum_\rho m_\rho\,[\rho]. \tag{16.5}$$

The fixed-role theorem determines the horizontal position of the support address, while the divisor weight m_ρ remains independent analytic data.

17. Interface with the Zero-Gap Geometry of Chapter 2

The terminal fixed-role readout in Chapter 1 gives

$$\rho_k = \frac{1}{2} + i\gamma_k. \tag{17.1}$$

The distinct post-closure ordinates

$$\gamma_k \tag{17.2}$$

therefore form a real zero spectrum. The adjacent gap

$$\Delta_k = \gamma_{k+1} - \gamma_k \tag{17.3}$$

belongs to the geometry of zero gaps.

Thus, in the notation of this series,

$$\boxed{\begin{array}{rcl} d_E(\tau) & : & \text{finite-horizon event-lift horizontal coordinate,} \\ d_\rho & : & \text{horizontal displacement of an actual zero,} \\ \Delta_k & : & \text{adjacent-ordinate gap scale.} \end{array}} \tag{17.4}$$

The three belong to different object layers and never reuse the same symbol.

18. Generalization Theorem and Conditions of Applicability

K1–K7 provide general conditions under which the same type of closure structure applies.

Theorem 18.1 (Parameterized Fixed-Role Generalization Theorem)

Suppose a target system has:

1. a root identity $\mathfrak{I}$;
2. a complete event domain $\mathfrak{E}$;
3. a reciprocal-role involution J_E for every event;
4. a centered reciprocal representation;
5. exact centered-parameter transmission;
6. reciprocal-role fidelity;
7. a fixed role R_E determined by generative-source geometry;
8. a terminal analytic involution

$$\iota_c(s) = 2c - \overline{s};$$

9. zero-faithful terminal exhaustivity

$$Z_{\text{target}} = \{\Phi_E(R_E) : E \in \mathfrak{E}\}.$$

Then

$$\boxed{Z_{\text{target}} \subset \{s : \Re s = c\}.} \tag{18.1}$$

Proof. For arbitrary E, from

$$J_E R_E = R_E$$

and

$$\Phi_E(J_E R) = \iota_c(\Phi_E(R))$$

we obtain

$$\Phi_E(R_E) = \iota_c(\Phi_E(R_E)).$$

Hence

$$\Re\Phi_E(R_E) = c.$$

By terminal exhaustivity, every

$$\rho \in Z_{\text{target}}$$

is some $\Phi_E(R_E)$, and therefore $\Re\rho = c$. ▫

18.2 Table of General Conditions of Applicability

For any target system of this type, the conditions are checked as follows:

Layer	Object to verify	Mathematical condition
K1	root identity and role space	$J^2 = \mathrm{id}$
K2	centered representation	$K_z(Jx) = K_{-z}(x)$
K3	parameter chain	$z_{j+1}T_{j+1} = z_j$
K4	role chain	$T_{j+1}J_j = J_{j+1}T_{j+1}$
K5	complete-event geometry	$J_E R_E = R_E$
K6	completed target	$Z_{\text{target}} = \{\Phi_E(R_E)\}$
K7	terminal analytic involution	$\iota_c(s) = 2c - \bar{s}$, and $\Phi_E J_E = \iota_c \Phi_E$

When K1–K7 hold simultaneously along the same event history, Theorem 18.1 applies.

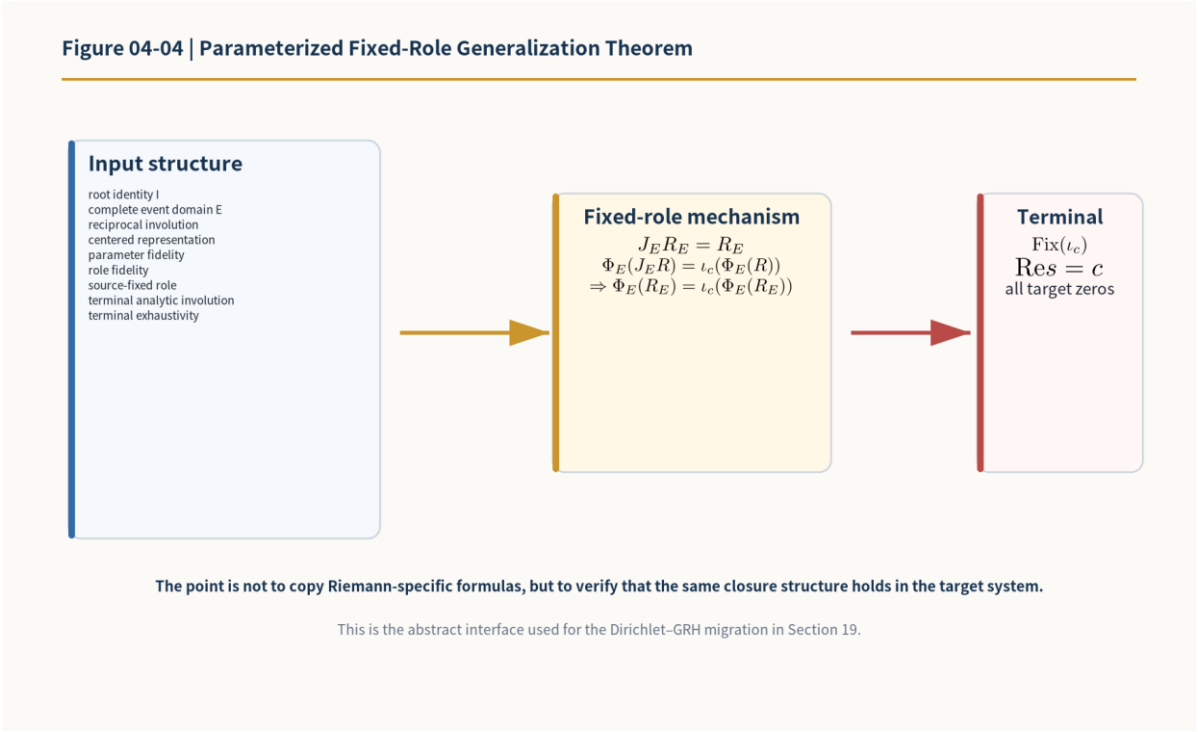


Figure 04-04. Parameterized fixed-role generalization theorem. Theorem 18.1 compresses the concrete Riemann closure of Chapter 1 into a migratable structure: root identity, complete events, reciprocity, centered representation, parameter and role fidelity, source-fixed roles, terminal analytic involution, and terminal exhaustivity. Any target system satisfying the same structure sends its fixed-role readouts into $\Re s = c$.

19. The Minimal Migration Problem for Dirichlet–GRH

We now apply the general closure kernel of Section 18 to Dirichlet L-functions.

Throughout this chapter, the **Generalized Riemann Hypothesis (GRH)** means **Dirichlet–GRH**:

$$\boxed{L(\rho,\chi)=0, \qquad 0<\Re\rho<1 \Rightarrow \Re\rho=\frac{1}{2}} \tag{19.1}$$

for every Dirichlet character χ.

We begin by fixing the logical boundary:

$$\boxed{\text{RH} \not\Rightarrow \text{Dirichlet-GRH}} \tag{19.2}$$

as a bare logical implication. Different $L(s,\chi)$ have different coefficients and different completion factors.

The form of migration used here is

$$\boxed{\text{Riemann fixed-role closure of Chapter 1} + \text{Dirichlet identity-preservation certification} \Rightarrow \text{Dirichlet–GRH.}} \tag{19.3}$$

The new task is therefore **not** to reprove the square-horizon statement of Chapter 1, nor to construct a second terminal-closure mechanism, but to certify

$$\boxed{\text{character weighting does not replace the root multiplicative identity.}} \tag{19.4}$$

19.1 Root Identity and Character Channels

The unique root multiplicative identity of the book remains

$$\boxed{\mathfrak{I}_{\times}=(\mathbb{N}_{>0},\mu), \qquad \mu(m,q)=mq.} \tag{19.5}$$

A Dirichlet character changes neither the multiplication law μ nor the relation

$$mq=n.$$

It merely adds channel weights to that same multiplicative relation.

To avoid incorrectly treating a complex character χ and its conjugate $\overline{\chi}$ as two mother identities, define the **reciprocal character package**

$$\boxed{\mathfrak{P}_{\chi}:=\{\chi,\overline{\chi}\}.} \tag{19.6}$$

$\mathfrak{P}_{\chi}$ is an unordered channel package:

$$\mathfrak{P}_{\chi}=\mathfrak{P}_{\overline{\chi}}.$$

Thus

$$\chi \leftrightarrow \overline{\chi}$$

changes only the reciprocal orientation, not the identity of the channel package.

This is the identity level required for complex characters. What is fixed is

$$\boxed{\mathfrak{I}_{\times} \quad \text{and} \quad \mathfrak{P}_{\chi},}$$

not the false requirement

$$\chi=\overline{\chi}.$$

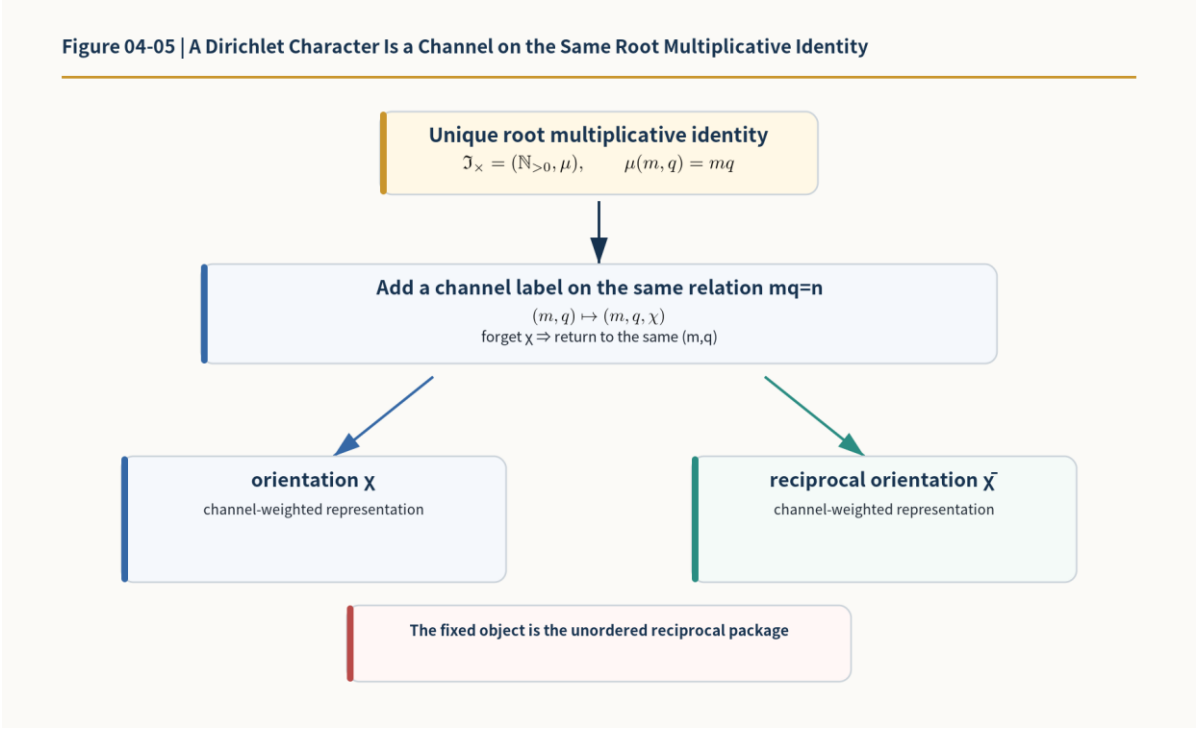


Figure 04-05. Root identity and character channels. A Dirichlet character does not change the multiplication law $\mu(m,q) = mq$; it only adds a channel weight on the same relation $mq = n$. For a complex character, χ and $\overline{\chi}$ are two orientations of the same unordered reciprocal package $\mathfrak{P}_\chi = \{\chi, \overline{\chi}\}$. Forgetting the channel label returns to the unique root multiplicative identity of Chapter 1.

19.2 Minimal Migration Criterion: Certifying Only One Identity

The fixed-role closure of Chapter 1 has already been completed on the mother multiplicative identity

$$\mathfrak{I}_\times = (\mathbb{N}_{>0}, \mu).$$

The Dirichlet case does not rebuild a proof from "zeros to fixed roles." It only certifies that all character-weighted representations still belong to the same root identity.

Definition 19.1 (Identity-Preserving Channel Lift)

Suppose an added channel representation is built on the same root relation

$$mq = n.$$

If the following hold:

1. **Root identity is preserved.**

$$\pi_\chi : (m,q,\chi) \mapsto (m,q)$$

returns, after forgetting the channel label, to the same

$$\mathfrak{I}_\times = (\mathbb{N}_{>0}, \mu);$$

2. **Reciprocal identity is preserved.** The character appears only in the two orientations of the unordered reciprocal package

$$\mathfrak{P}_\chi = \{\chi, \overline{\chi}\},$$

and

$$(m, q, \chi) \leftrightarrow (q, m, \overline{\chi})$$

is compatible with the role exchange of the mother identity;

3. **The representation history is preserved.** The local kernel, multiplicative shell, global Dirichlet encoding, moving head/tail decomposition, and completion all use the same centered parameter z. What changes are the channel weights and completion factors; no second generative identity is created;
4. **The completed representation remains in the same channel identity.** $\Lambda(s, \chi)$ is the completed analytic representation of that channel identity; its zero addresses are terminal readings of that channel identity, and the functional equation together with conjugation reads the same reciprocal orientation as

$$\rho \mapsto 1 - \overline{\rho}.$$

then the Dirichlet representation is called an **identity-preserving channel lift** of the root multiplicative identity.

The four items are not four new closure mechanisms. They are four representational checks of a single proposition:

$$\boxed{\text{after adding a character, there is still only one root identity.}} \tag{19.7}$$

Theorem 19.2 (Inheritance Theorem for Mother-Identity Closure)

Assume the mother multiplicative identity of Chapter 1 has completed fixed-role closure. If a Dirichlet channel is an identity-preserving channel lift in the sense of Definition 19.1, then the fixed-role coverage and terminal closure of Chapter 1 are inherited unchanged in that channel. No second fixed-role mechanism or second terminal-readout mechanism needs to be constructed for the Dirichlet L-function.

In particular, every complete event in the channel still reaches

$$m = q$$

at the right endpoint of the same square horizon, and the $+$ and $-$ reciprocal-role labels are identified, at the role level, with the same fixed role. The character only extends the reciprocal orientation to

$$\chi \leftrightarrow \overline{\chi},$$

without changing the fixed role itself.

Therefore, once Sections 20–22 certify that the Dirichlet channel indeed preserves the same identity, the closure conclusion of the mother identity holds in that channel:

$$\boxed{L(\rho, \chi) = 0, \quad 0 < \Re\rho < 1 \Rightarrow \Re\rho = \frac{1}{2}.} \tag{19.8}$$

Proof

The terminal fixed-role coverage of Chapter 1 consists of three identity-level facts:

complete event object domain + fixed role at the right end of the square horizon + change of representation without change of role assignment.

For a Dirichlet channel, forgetting the character label through π_χ returns to the same relation

$$mq = n.$$

Hence the event intervals and the square-horizon decomposition are unchanged. In particular,

$$m > k, \qquad q > k, \qquad mq \le (k+1)^2 \Rightarrow m = q = k+1$$

contains no χ at all, so the fixed role of the mother identity is inherited without alteration.

On the reciprocal side, the character merely lifts

$$(m, q) \leftrightarrow (q, m)$$

to

$$(m, q, \chi) \leftrightarrow (q, m, \overline{\chi}),$$

while the unordered package

$$\mathfrak{P}_\chi = \{\chi, \overline{\chi}\}$$

remains unchanged. This is therefore an exchange of channel orientation within the same identity, not the creation of a second identity.

Sections 20–22 further show that the same z enters the weighted centered kernel, multiplicative shell, global L-encoding, head/tail decomposition, and completion; the functional equation and conjugation structure of the completed function then read the same reciprocal action at the terminal analytic layer as

$$\rho \mapsto 1 - \overline{\rho}.$$

Thus the terminal role identification of Lemma 6.3A in Chapter 1 is preserved under the channel lift. The terminal $+$ and $-$ labels remain two reciprocal orientations of the same fixed role, not two new identities. The fixed-role closure already proved for the mother identity is therefore inherited directly by the channel.

Consequently, the new mathematical obligation in Dirichlet–GRH is only

whether the Dirichlet character remains within the closure of the same root multiplicative identity.

Sections 20–22 certify precisely this point. ▫

20. Character-Weighted Centered Dirichlet Representation

Let χ be a Dirichlet character.

Define the **character-weighted centered kernel** by

$$\boxed{W_{\chi,z}(m, q) = \chi(m)\overline{\chi(q)}m^{-1/2-z}q^{-1/2+z}.} \tag{20.1}$$

What changes is the channel weight; the underlying multiplicative relation remains

$$mq = n.$$

20.1 Weighted Reciprocal Exchange

Proposition 20.1

One has

$$\boxed{W_{\chi,z}(q,m) = W_{\overline{\chi},-z}(m,q).} \tag{20.2}$$

Proof

A direct calculation gives

$$\begin{aligned} W_{\chi,z}(q,m) &= \chi(q)\overline{\chi(m)}q^{-1/2-z}m^{-1/2+z} \\ &= \overline{\chi(m)}\chi(q)m^{-1/2+z}q^{-1/2-z} \\ &= W_{\overline{\chi},-z}(m,q). \end{aligned}$$

▫

Thus the Riemann reciprocity

$$(m,q,z) \leftrightarrow (q,m,-z)$$

is lifted in the character channel to

$$\boxed{(m,q,\chi,z) \leftrightarrow (q,m,\overline{\chi},-z).} \tag{20.3}$$

This is not a new identity. It is an exchange of reciprocal orientations inside the same

$$\mathfrak{P}_\chi = \{\chi, \overline{\chi}\}.$$

20.2 Weighted Multiplicative Shells and the Global L-Encoding

Define

$$a_{n,\chi}(z) = \sum_{mq=n} \chi(m)\overline{\chi(q)}m^{-1/2-z}q^{-1/2+z}. \tag{20.4}$$

By Proposition 20.1,

$$\boxed{a_{n,\chi}(z) = a_{n,\overline{\chi}}(-z).} \tag{20.5}$$

In the region of absolute convergence,

$$\begin{aligned} \sum_{n\geq 1} a_{n,\chi}(z)n^{-\alpha} &= \sum_{m,q\geq 1} \chi(m)\overline{\chi(q)}m^{-\alpha-1/2-z}q^{-\alpha-1/2+z} \\ &= L\left(\alpha+\frac{1}{2}+z,\chi\right)L\left(\alpha+\frac{1}{2}-z,\overline{\chi}\right). \end{aligned}$$

Hence

$$\boxed{\sum_{n\geq 1} a_{n,\chi}(z)n^{-\alpha} = L(w_+,\chi)L(w_-,\overline{\chi}),} \tag{20.6}$$

where

$$\boxed{w_\pm = \alpha+\frac{1}{2}\pm z.} \tag{20.7}$$

Therefore

$$\boxed{z = \frac{w_+ - w_-}{2}.} \tag{20.8}$$

Character weighting introduces no new map

$$z \mapsto \tilde{z}.$$

K3 is therefore preserved.

20.3 Moving Head/Tail Does Not Change the Analytic Point

Define

$$H_{\chi,r}(w) = \sum_{n \le r} \chi(n) n^{-w}, \tag{20.9}$$

and

$$T_{\chi,r}(w) = L(w,\chi) - H_{\chi,r}(w). \tag{20.10}$$

Then exactly

$$\boxed{H_{\chi,r}(w) + T_{\chi,r}(w) = L(w,\chi).} \tag{20.11}$$

Moreover,

$$H_{\chi,r+1}(w) - H_{\chi,r}(w) = \chi(r+1)(r+1)^{-w}, \tag{20.12}$$

$$T_{\chi,r+1}(w) - T_{\chi,r}(w) = -\chi(r+1)(r+1)^{-w}. \tag{20.13}$$

Hence

$$\boxed{\Delta_r\big(H_\chi + T_\chi\big) = 0.} \tag{20.14}$$

The moving horizon changes how the same analytic point w is partitioned between head and tail; it changes neither w nor z.

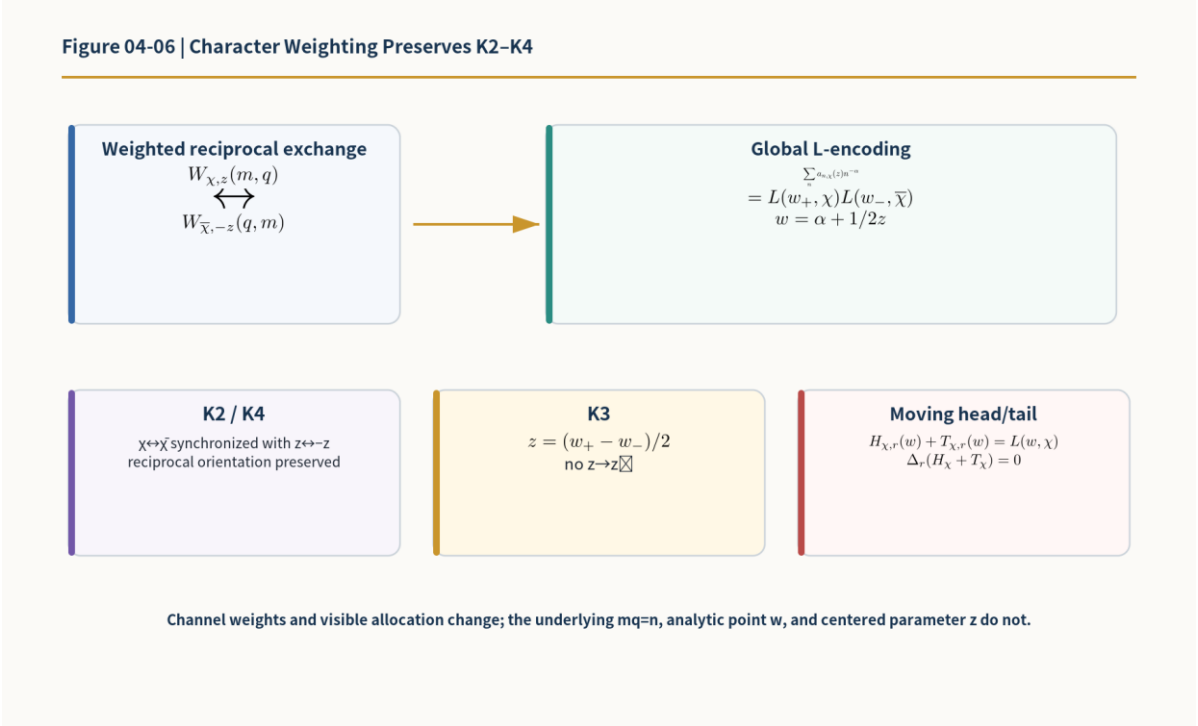


Figure 04-06. Representation fidelity after character weighting. The weighted kernel obeys $W_{\chi,z}(q,m) = W_{\overline{\chi},-z}(m,q)$, the global shell still encodes as $L(w_+,\chi)L(w_-,\overline{\chi})$, and $z = (w_+ - w_-)/2$ is unchanged. Moving head/tail also preserves $H_{\chi,r}(w) + T_{\chi,r}(w) = L(w,\chi)$ exactly. Thus the channel lift preserves K2–K4 rather than creating a new analytic coordinate system.

21. Primitive-Character Completion and Terminal Reciprocity within the Same Channel

Let χ be a primitive Dirichlet character of conductor q_χ, and set

$$\chi(-1) = (-1)^{a_\chi}, \qquad a_\chi \in \{0,1\}.$$

The standard completed function is

$$\boxed{\Lambda(s,\chi) = \left(\frac{q_\chi}{\pi}\right)^{(s+a_\chi)/2} \Gamma\left(\frac{s+a_\chi}{2}\right) L(s,\chi).} \tag{21.1}$$

Its functional equation is

$$\boxed{\Lambda(s,\chi) = \varepsilon_\chi \Lambda(1-s,\overline{\chi}), \qquad |\varepsilon_\chi| = 1.} \tag{21.2}$$

Completion acts only on the same argument s. Hence the centered parameter

$$z = s - \frac{1}{2}$$

is unchanged.

21.1 Conjugation and Reflection of the Same χ-Zero Set across the Critical Line

Conjugation of the Dirichlet coefficients gives

$$\boxed{\overline{\Lambda(\overline{s},\chi)} = \Lambda(s,\overline{\chi}).} \tag{21.3}$$

If

$$\Lambda(\rho, \chi) = 0,$$

then the functional equation gives

$$\Lambda(1 - \rho, \overline{\chi}) = 0.$$

Taking conjugates and using (21.3) yields

$$\boxed{\Lambda(1 - \overline{\rho}, \chi) = 0.} \tag{21.4}$$

Thus, for each fixed primitive χ, its nontrivial zero set itself carries the terminal reciprocal involution

$$\boxed{\iota_{1/2}(\rho) = 1 - \overline{\rho}.} \tag{21.5}$$

This is of exactly the same form as the terminal Riemann involution of Chapter 1.

21.2 Zero Fidelity of Completion

In the open critical strip

$$0 < \Re s < 1,$$

the factor

$$\left(\frac{q_\chi}{\pi}\right)^{(s+a_\chi)/2}$$

has no zeros, and

$$\Gamma\left(\frac{s + a_\chi}{2}\right)$$

has no zeros either.

Therefore, in that region,

$$\boxed{L(\rho, \chi) = 0 \Leftrightarrow \Lambda(\rho, \chi) = 0.} \tag{21.6}$$

Completion thus does not manufacture a second identity for the nontrivial zeros. K6 and K7 are preserved.

21.3 For a Complex Character, the Fixed Object Is the Reciprocal Package, Not a Single Orientation

When $\chi \neq \overline{\chi}$, we do not require the individual character label to be a fixed point.

What is fixed is the unordered reciprocal package

$$\mathfrak{P}_\chi = \{\chi, \overline{\chi}\}.$$

At the generative-source fixed role

$$m = q,$$

the character orientation changes as

$$(m, m, \chi) \leftrightarrow (m, m, \overline{\chi}),$$

but the unordered reciprocal package

$$\mathfrak{P}_\chi = \{\chi, \overline{\chi}\}$$

remains unchanged. The generative-source fixed role and the centered analytic parameter z are not conflated here: $m = q$ belongs to the generative-source role layer, while z belongs to the analytic representation layer.

Hence, in the identity quotient by reciprocal orientation,

$$\boxed{[(m, m, \chi)]_{\mathrm{rec}} = [(m, m, \overline{\chi})]_{\mathrm{rec}}.} \tag{21.7}$$

This is the correct reading of K5 for a complex character.

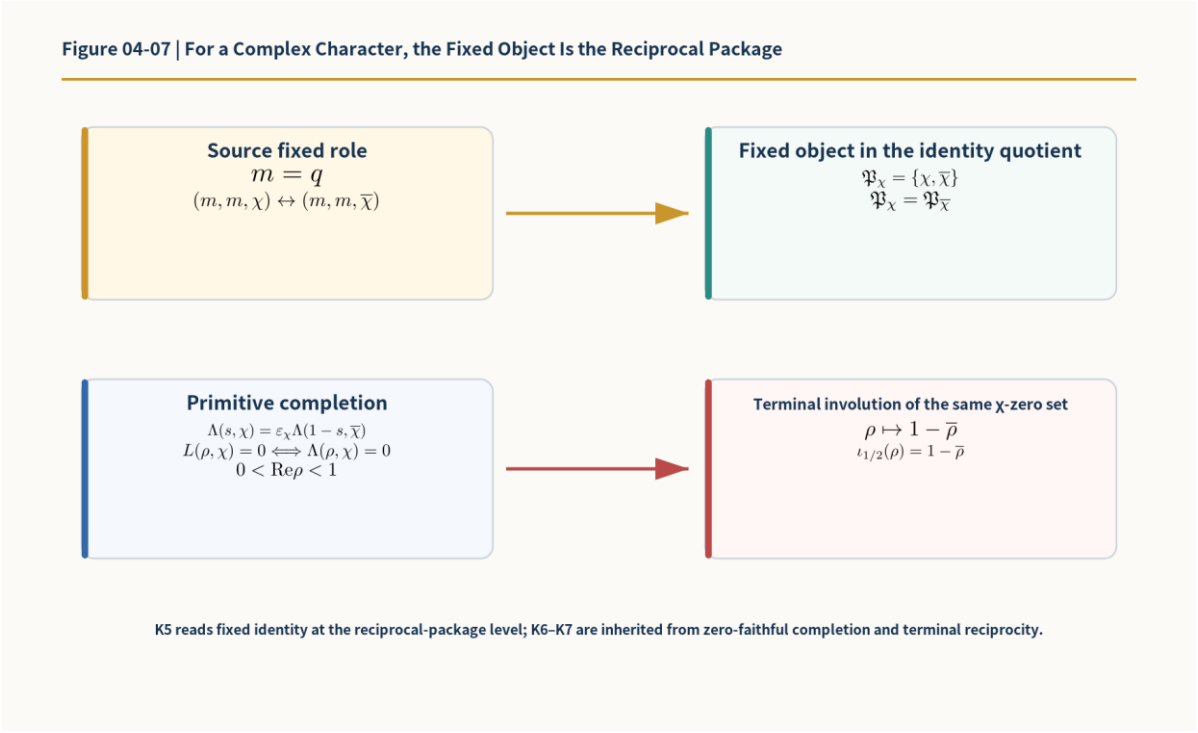


Figure 04-07. Fixed object for a complex character. When $\chi \neq \overline{\chi}$, the source-fixed role $m = q$ does not require the individual character label to be a fixed point. What remains fixed is the unordered reciprocal package $\mathfrak{P}_\chi = \{\chi, \overline{\chi}\}$. Primitive completion preserves the centered parameter and the nontrivial-zero identity in the open critical strip while supplying the terminal involution $\rho \mapsto 1 - \overline{\rho}$ on the same χ-zero set, thereby preserving the structure required by K5–K7.

22. Primitive Dirichlet–GRH

Theorem 22.1 (Primitive Dirichlet Identity Migration)

For every primitive Dirichlet character χ, the character-weighted representation is an identity-preserving channel lift of the root multiplicative identity of Chapter 1.

Proof

We verify Definition 19.1 item by item.

First, the root identity is preserved.

Every weighted term is still built on

$$mq = n.$$

After forgetting the χ-weights, the underlying relation is exactly

$$\mathcal{R}_{\times} = \mathrm{Graph}(\mu)$$

of Chapter 1.

Second, the reciprocal channel is preserved.

By Proposition 20.1,

$$(m, q, \chi, z) \leftrightarrow (q, m, \overline{\chi}, -z),$$

while

$$\mathfrak{P}_{\chi} = \mathfrak{P}_{\overline{\chi}}.$$

Hence reciprocal exchange never leaves the same character package.

Third, the centered parameter is preserved.

By (20.6)–(20.8), the global L-encoding uses the same z; by (20.11)–(20.14), the moving head/tail decomposition does not change the analytic point; and by (21.1), completion acts at the same $s = \frac{1}{2} + z$.

Fourth, terminal assignment is preserved.

By (21.6), the L-zeros and Λ-zeros in the open critical strip coincide; by (21.5), terminal reciprocal action on the zero set remains

$$\rho \mapsto 1 - \overline{\rho}.$$

Thus all conditions of Definition 19.1 hold. ▫

Theorem 22.2 (Primitive Dirichlet–GRH)

For every primitive Dirichlet character χ, if

$$L(\rho, \chi) = 0, \qquad 0 < \Re\rho < 1,$$

then

$$\boxed{\Re\rho = \frac{1}{2}.} \tag{22.1}$$

Proof

By Theorem 22.1, the primitive Dirichlet channel is an identity-preserving channel lift of the root multiplicative identity.

By Theorem 19.2:

- the root-identity part of K1 is inherited from the same root multiplicative identity, while the reciprocal character orientation is certified in Section 20;
- K5 is inherited from the same square-horizon fixed role;
- K2–K4 are supplied by the weighted reciprocity and parameter fidelity of Section 20;
- K6–K7 are supplied by the zero fidelity of completion and terminal reciprocity in Section 21.

Thus K1–K7 all hold for the primitive channel.

Theorem 18.1 therefore applies with

$$c = \frac{1}{2}.$$

Hence every nontrivial zero in the open critical strip satisfies

$$\Re\rho = \frac{1}{2}.$$

▫

23. Imprimitive Characters and Finite Euler Factors

Let a Dirichlet character χ modulo q be induced by a primitive character χ^* of conductor $f \mid q$. Then

$$\boxed{L(s,\chi) = L(s,\chi^*)\prod_{\substack{p\mid q\\ p\nmid f}}(1-\chi^*(p)p^{-s}).} \tag{23.1}$$

If one of the additional Euler factors vanishes,

$$1-\chi^*(p)p^{-s} = 0,$$

then

$$p^{-s} = \chi^*(p)^{-1}.$$

Since

$$|\chi^*(p)| = 1,$$

taking absolute values gives

$$p^{-\Re s} = 1.$$

Thus

$$\boxed{\Re s = 0.} \tag{23.2}$$

Consequently, these finite Euler factors add no zeros in the open critical strip

$$0 < \Re s < 1.$$

All nontrivial zeros of an imprimitive $L(s,\chi)$ in the open critical strip therefore come from the primitive ancestor

$$L(s,\chi^*).$$

By Theorem 22.2,

$$\boxed{\Re\rho = \frac{1}{2}.} \tag{23.3}$$

24. Principal Characters and the Riemann Channel

For the principal character χ_0 modulo q,

$$\boxed{L(s,\chi_0) = \zeta(s)\prod_{p\mid q}(1-p^{-s}).} \tag{24.1}$$

If

$$1 - p^{-s} = 0,$$

then again

$$\Re s = 0.$$

Thus all nontrivial zeros in the open critical strip come from $\zeta(s)$.

Chapter 1 has already established

$$\boxed{\zeta(\rho) = 0, \qquad 0 < \Re\rho < 1 \Rightarrow \Re\rho = \frac{1}{2}.} \tag{24.2}$$

The same conclusion therefore holds for principal characters.

25. Main Dirichlet–GRH Theorem and the Meaning of "One Identity"

Theorem 25.1 (Dirichlet–GRH)

For every Dirichlet character χ, if

$$L(\rho, \chi) = 0, \qquad 0 < \Re\rho < 1,$$

then

$$\boxed{\Re\rho = \frac{1}{2}.} \tag{25.1}$$

Proof

There are three cases.

1. Primitive nonprincipal characters: Theorem 22.2.
2. Imprimitive Dirichlet characters: reduce by Section 23 to the primitive ancestor.
3. Principal characters: reduce by Section 24 to the Riemann case of Chapter 1.

Hence the conclusion holds for all Dirichlet characters. ▫

25.1 The Minimal Migration Chain

The entire Dirichlet–GRH proof can be compressed as

$$
\begin{array}{l}
\mathfrak{I}_{\times} = (\mathbb{N}_{>0}, \mu) \\
\Downarrow \\
\text{add a character channel on the same} mq = n \\
\Downarrow \\
\mathfrak{P}_{\chi} = \{\chi, \overline{\chi}\} \quad \text{preserves reciprocal-package identity} \\
\Downarrow \\
W_{\chi,z}(m,q) \leftrightarrow W_{\overline{\chi},-z}(q,m) \\
\Downarrow \\
z \text{remains unchanged in the} L\text{-encoding, head/tail decomposition, and completion} \\
\Downarrow \\
\rho \mapsto 1 - \overline{\rho} \\
\Downarrow \\
\text{K1–K7 hold for the Dirichlet channel} \\
\Downarrow \\
\boxed{\Re\rho = \frac{1}{2}}.
\end{array}
\tag{25.2}
$$

Thus the new mathematical content of GRH is not the reconstruction of a second fixed-role closure, but the certification

$$\boxed{\textbf{a character adds a channel, not a second root identity.}} \tag{25.3}$$

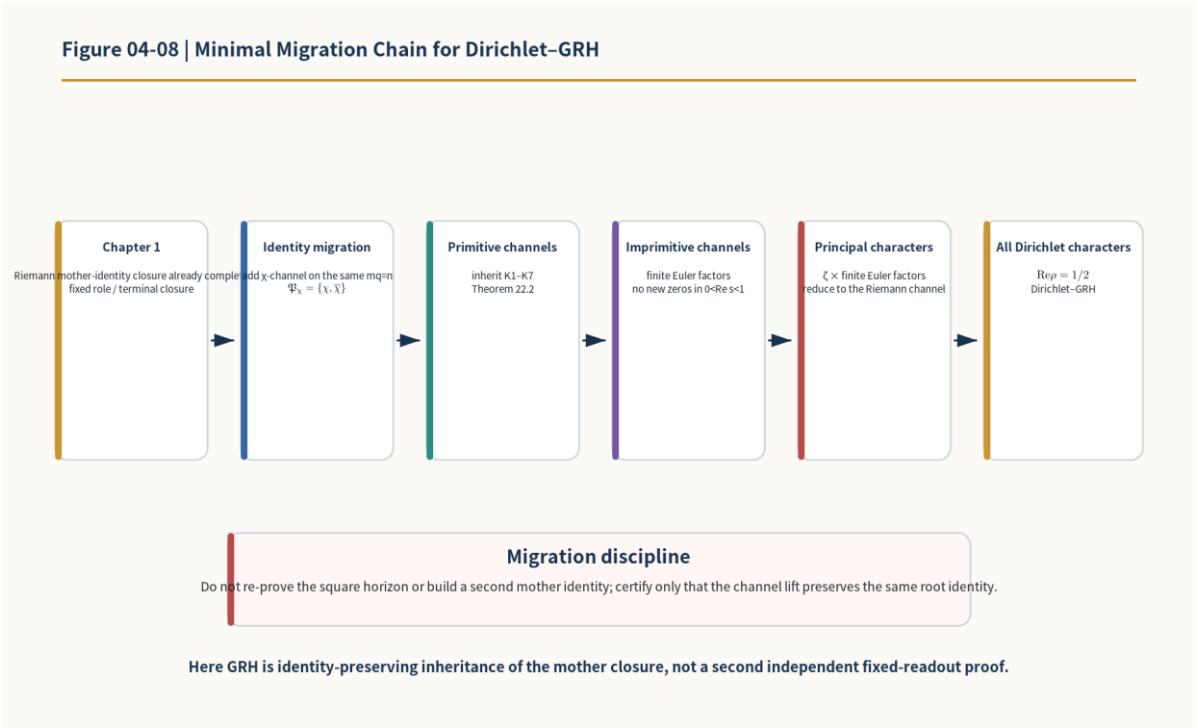


Figure 04-08. Minimal migration chain for Dirichlet–GRH. Chapter 1 has already completed fixed-role closure on the mother multiplicative identity. The genuinely new Dirichlet task is only to certify that the character-weighted channel lift preserves the same root identity. Primitive channels inherit K1–K7 directly; finite Euler factors of imprimitive channels introduce no new zeros in the open critical strip; principal characters reduce to the Riemann channel. The three cases together give Theorem 25.1.

25.2 Identity Consistency from the Cyclotomic / Artin Viewpoint

This section is not an additional premise of Theorem 25.1; it provides a standard structural consistency check.

Let

$$K_m = \mathbb{Q}(\zeta_m).$$

Then

$$\mathrm{Gal}(K_m/\mathbb{Q}) \simeq (\mathbb{Z}/m\mathbb{Z})^{\times}. \tag{25.4}$$

This Galois group is Abelian, so all of its irreducible complex representations are one-dimensional characters. Through the Abelian Artin–Dirichlet correspondence, the Artin factors of the Dedekind zeta function are precisely the corresponding Dirichlet L-channels, with conductors determined by the individual characters.

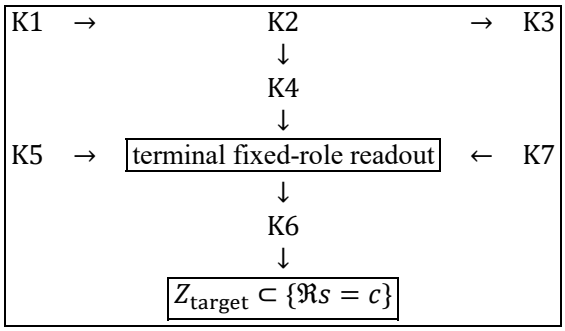
Thus the total cyclotomic object leads to the same structural conclusion:

> Dirichlet characters are internal representation channels of the total multiplicative object,not mutually independent root multiplicative identities. (25.5)

This agrees with the identity judgment obtained directly from the weighted multiplicative representation in Sections 19–24.

26. Minimizing the Logical Dependencies

The dependency structure of the closure kernel can be written as



(26.1)

The core local-closure relations remain

$$\boxed{J_E R_E = R_E} \tag{26.2}$$

and

$$\boxed{\Phi_E J_E = \iota_c \Phi_E.} \tag{26.3}$$

Together they give directly

$$\boxed{\Phi_E(R_E) \in \mathrm{Fix}(\iota_c).} \tag{26.4}$$

The parameterized closure kernel therefore takes (26.4) as the exact definition of terminal closure; its logical inputs are precisely the generative-source fixed role and reciprocal-role fidelity.

27. Conclusion

The Riemann closure kernel can be compressed into three successive levels.

The first is **generation and representation**:

$$\Im_{\times} \rightarrow \text{reciprocal relation} \rightarrow \text{centered representation.}$$

The second is **dual fidelity**:

$$\boxed{\text{centered-parameter fidelity} + \text{reciprocal-role fidelity.}}$$

The third is **fixed role and terminal readout**:

$$\boxed{J_E R_E = R_E}$$

passed through

$$\boxed{\Phi_E J_E = \iota_c \Phi_E}$$

to obtain

$$\boxed{\Phi_E(R_E) = \iota_c(\Phi_E(R_E)).}$$

Hence

$$\boxed{\Re\Phi_E(R_E) = c.}$$

Terminal exhaustivity lifts this event-level conclusion to the global target zero set:

$$\boxed{\forall \rho \in Z_{\text{target}}, \qquad \Re\rho = c.}$$

In the Riemann realization,

$$c = \frac{1}{2}, \qquad \iota_{1/2}(\rho) = 1 - \overline{\rho},$$

so

$$\boxed{\rho = 1 - \overline{\rho} \Leftrightarrow \Re\rho = \frac{1}{2}.}$$

Dirichlet–GRH provides the first complete application of the general migration theorem of this chapter. Its key step is not to reprove the Riemann event geometry, but to show that character weighting is only an internal channel lift of the same root multiplicative identity. Thus

$$\boxed{\text{RH closure kernel} + \text{Dirichlet identity-preservation certification} \Rightarrow \text{Dirichlet–GRH.}}$$

In this application, what remains invariant is

$$\boxed{\mathfrak{I}_\times, \qquad \mathfrak{P}_\chi, \qquad z, \qquad \text{reciprocal-role assignment}, \qquad \iota_{1/2}.}$$

The minimal mathematical content of the passage “from RH to GRH” can therefore be compressed into one sentence:

> **the same root identity enters a new character channel, but does not become a new root identity.**

The entire parameterized structure is

one root identity →
multiple representations of the same event →
exact centered-parameter transmission →
reciprocal-role fidelity →
generative-source fixed role →
terminal fixed-role readout →
global terminal exhaustivity.

What is preserved throughout is role assignment within the same event. The normalized fixed readout at the generative source and the terminal analytic real coordinate are coordinates of different types; the final analytic real coordinate is determined by the fixed set of the terminal reciprocal involution.

Chapter 5 A Faithful Event Spectral Atlas after Closure of the Riemann Hypothesis

Actual Zero Readouts, Finite-Horizon Event Lifts, and the Stratified Structure of Spectral Routes

Abstract

The closure conclusion of Chapter 1 (H01) fixes the actual horizontal readout of every nontrivial zero:

$$\Re\rho = \frac{1}{2}.$$

Writing the centered zero coordinate as

$$a_\rho = \rho - \frac{1}{2} = d_\rho + i\gamma_\rho, \qquad d_\rho = \Re\rho - \frac{1}{2},$$

this closure readout is equivalent to

$$d_\rho = 0.$$

This conclusion fixes only the horizontal coordinate of actual zeros. The zero ordinates γ_n, analytic multiplicities m_n, total multiplicative logarithmic scale

$$L_\times = \log(mq),$$

and relative role coordinate

$$R = \log(q/m)$$

remain data of different levels.

Inside a finite-horizon event there is, separately, an event-lift coordinate

$$d_E(\tau),$$

whose two-sheet representation is

$$z_{E,\pm}(\tau) = \pm d_E(\tau) + i\gamma_E(\tau).$$

One must preserve the type distinction

$$\boxed{d_E(\tau) \neq d_\rho \quad \text{as object types.}}$$

The former records the unfolding and closure of a reciprocal finite-horizon event; the latter is the horizontal displacement of an actual zero from the critical line.

The minimal local event carrier is

$$\chi_E(z,\tau) = (z - i\gamma_E(\tau))^2 - d_E(\tau)^2.$$

When $d_E = 0$, its double root means that two reciprocal event sheets glue at the closure section; it is **not** the analytic multiplicity of a zero of ξ. Actual closed zeros simultaneously retain the support of distinct addresses

$$\Gamma_+ = \{\gamma_n\}$$

and the positive-height zero divisor

$$\mathcal{D}_\xi^+ = \sum_{n\geq 1} m_n\,[\rho_n], \qquad \rho_n = \frac{1}{2} + i\gamma_n.$$

Under this stratification, Hilbert–Pólya, Berry–Keating, random matrices, Weil positivity, de Branges / canonical systems, Connes scaling / spectral triples, finite Weil spectral convergence, and geometric/cohomological routes can all be compared within a single coordinate ledger. They read different projections of

$$(L_\times, R, d_\rho, \gamma)$$

and of the event-lift coordinate $d_E(\tau)$.

This chapter therefore constructs the first faithful post-closure spectral atlas. It distinguishes the actual zero spectrum, event-lift spectrum, multiplicative generative coordinates, and later operator spectra, and supplies a common coordinate interface for the Ren operator of Chapter 6, the spectral witness of Chapter 7, the GUE two-point self-relation of Chapter 8, and the independent source-generated Hilbert–Pólya route of Chapter 9.

0. Logical Position of This Chapter: the Post-Closure Spectral-Atlas Layer

Chapter 1 (H01) gives the closed readout of the actual nontrivial zeros:

$$\boxed{\rho_n = \frac{1}{2} + i\gamma_n.} \tag{0.1}$$

Starting from this closed zero object, the present chapter constructs its minimal faithful spectral atlas:

$$\boxed{\text{RH closure} \;\Rightarrow\; \text{faithful spectral atlas} \;\Rightarrow\; \text{stratification of spectral routes.}} \tag{0.2}$$

Here "spectral atlas" means a spectral carrier that records, in distinct layers, zero support, analytic multiplicity, event lifts, and multiplicative generative coordinates. From Chapter 6 onward we enter operator spectra on Hilbert spaces; the present chapter fixes the common coordinate interface prior to operator construction.

Its place in the book is

$$\boxed{\begin{aligned}&\text{H01 closure} \to \text{H05 faithful spectral atlas} \to\\ &\text{H06 canonical operator} \to \text{H07 spectral witness} \to\\ &\text{H08 GUE two-point relations,}\end{aligned}} \tag{0.3}$$

while Chapter 9 independently constructs a source-generated Hilbert–Pólya spectral route from the multiplicative generative source.

1. Zero Coordinates Fixed by RH Closure

Let

$$\rho = \beta + i\gamma$$

be a nontrivial zero. Standard reciprocal-conjugate symmetry sends

$$\rho$$

to

$$1 - \overline{\rho}.$$

Introduce the centered coordinate

$$a_\rho = \rho - \frac{1}{2}.$$

Write

$$\boxed{a_\rho = \rho - \frac{1}{2} = d_\rho + i\gamma_\rho, \qquad d_\rho = \Re\rho - \frac{1}{2}, \qquad \gamma_\rho = \Im\rho.} \tag{1.1}$$

The centered reciprocal involution is then

$$\boxed{\iota(a) = -\overline{a}.} \tag{1.2}$$

Thus

$$d_\rho + i\gamma_\rho \mapsto -d_\rho + i\gamma_\rho.$$

Its fixed set is

$$a = -\overline{a} \quad \Leftrightarrow \quad \Re a = 0,$$

that is,

$$\boxed{\mathrm{Fix}(\iota) = i\mathbb{R}} \tag{1.3}$$

and equivalently

$$\boxed{\Re s = \frac{1}{2}.} \tag{1.4}$$

In these coordinates, the content of RH can be compressed to one sentence:

$$\boxed{\text{the horizontal displacement } d_\rho \text{ of every complete Riemann zero readout is } 0.} \tag{1.5}$$

RH closure acts on the horizontal coordinate of actual zeros:

$$d_\rho = 0.$$

The vertical coordinate γ_ρ, analytic multiplicity m_n, and prime-power generative positions $k\log p$ retain their own data types.

Thus, after RH closure, at least two levels of zero data must still be distinguished.

The support of distinct positive-height addresses is

$$\boxed{\Gamma_+ = \{\gamma_n\}.} \tag{1.6}$$

The positive-height divisor data with analytic multiplicity is

$$\boxed{\mathcal{D}_\xi^+ = \sum_{n\geq 1} m_n\,[\rho_n].} \tag{1.7}$$

The corresponding centered closed support can be written

$$\boxed{\Sigma_\xi^{\mathrm{closed}} = \{\, i\gamma_n \,\}.} \tag{1.8}$$

Here m_n is the analytic multiplicity of ξ at the corresponding zero.

Therefore horizontal RH closure, vertical spectral generation, analytic multiplicity, canonical operator realization, two-point statistics, and prime–zero structure belong to different levels.

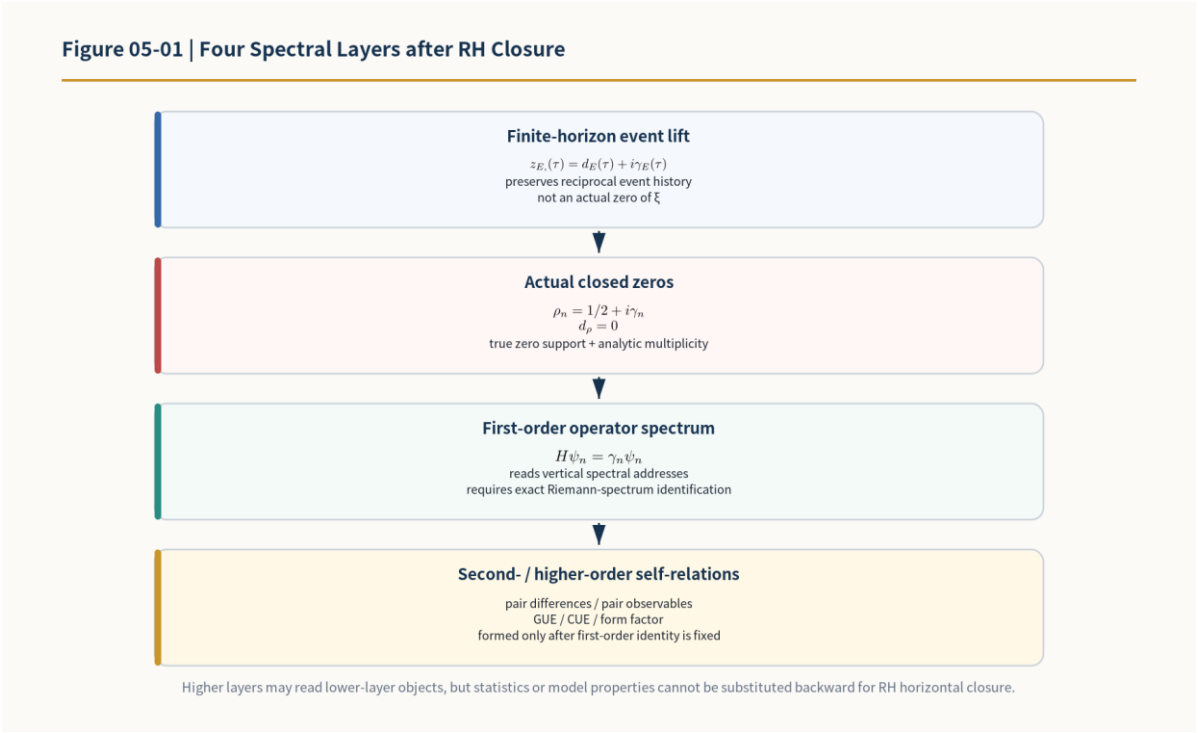


Figure 05-01. Four spectral layers after RH closure. Finite-horizon event lifts, actual closed zeros, a first-order operator spectrum, and second- or higher-order statistics are four distinct object layers. Event lifts preserve generative history but are not actual zeros of ξ; actual zeros satisfy $d_\rho = 0$ after RH closure; an operator spectrum reading γ_n still requires exact Riemann-spectrum identification; and GUE/CUE-type relations are formed only after first-order spectral identity has been fixed.

2. Closed Spectrum and Event Lifts

If we retain only the actual closed support

$$\{i\gamma_n\},$$

we obtain a one-dimensional vertical readout of the final zero positions. It is faithful to the actual zeros but does not preserve the reciprocal event history used earlier in the finite multiplicative horizon:

$$0 \to d_E(\tau) \to 0 \to d_{E+1}(\tau) \to 0 \to \cdots. \tag{2.1}$$

In the original coordinate this may be written

$$\boxed{\frac{1}{2} \to \left(\frac{1}{2} + d_E(\tau), \frac{1}{2} - d_E(\tau)\right) \to \frac{1}{2}.} \tag{2.2}$$

The parameter τ is a descriptive parameter for a finite-horizon event, used to record the unfolding and closure of a reciprocal relation inside the event. It has no physical-time interpretation.

This produces three distinct levels:

$$\boxed{d_\rho = \Re\rho - \frac{1}{2}}$$

is the actual zero coordinate;

$$\boxed{d_E(\tau)}$$

is the finite-horizon event-lift coordinate; and the actual closed spectrum satisfies

$$\boxed{d_\rho = 0.}$$

We therefore distinguish

$$\boxed{\text{the actual closed Riemann spectrum}}$$

from

$$\boxed{\text{the finite-horizon event spectral lift.}}$$

The former reads only actual zeros. The latter permits $d_E(\tau) \neq 0$ inside an event, but only as a lifted coordinate of the generative history.

In particular,

$$\boxed{d_E(\tau) \neq d_\rho \quad \text{as object types.}} \tag{2.3}$$

The "opening–closure" seen in an event diagram describes a reciprocal finite-horizon history; it does not change the coordinate type of actual zeros of ξ.

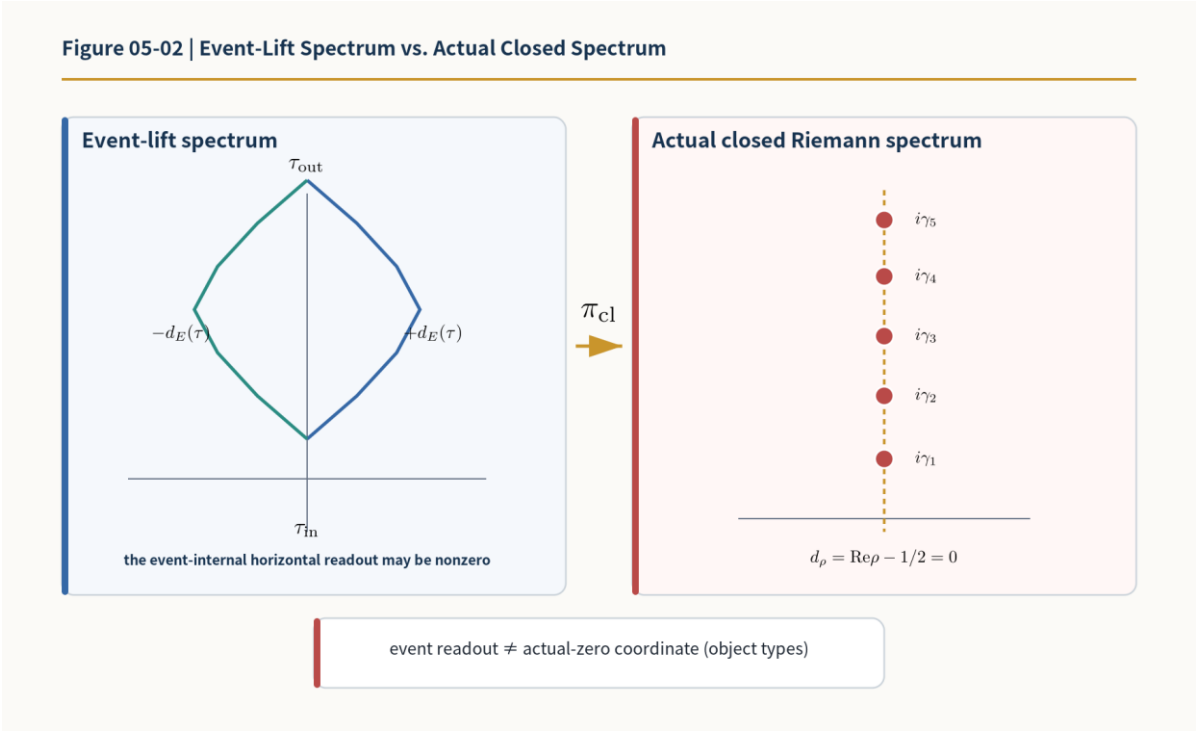


Figure 05-02. Event-lift spectrum versus actual closed spectrum. Within a complete event, $d_E(\tau)$ may open from 0, become nonzero, and return to 0; the two event sheets enter the actual Riemann readout through the closure section π_{cl}. The actual closed spectrum itself remains on $i\mathbb{R}$. The two layers meet at the terminal interface, but $d_E(\tau) \neq d_\rho$ as object types.

3. Definition of a Faithful Event Spectrum

Denote a finite-horizon reciprocal event by E. It carries at least

$$\gamma_E(\tau), \qquad d_E(\tau), \qquad I_E = [\tau_E^{\mathrm{in}}, \tau_E^{\mathrm{out}}],$$

with closure conditions

$$d_E(\tau_E^{\mathrm{in}}) = 0, \qquad d_E(\tau_E^{\mathrm{out}}) = 0. \tag{3.1}$$

Define its two-sheet centered lift by

$$\boxed{z_{E,\pm}(\tau) = \pm d_E(\tau) + i\gamma_E(\tau).} \tag{3.2}$$

In the original s-plane,

$$\boxed{\rho_{E,\pm}(\tau) = \frac{1}{2} \pm d_E(\tau) + i\gamma_E(\tau).} \tag{3.3}$$

An event-spectral representation is called **faithful** in this chapter if it satisfies at least the following six requirements.

1. **Center fidelity.** The horizontal center of the two sheets is always zero:

$$\frac{\Re z_{E,+} + \Re z_{E,-}}{2} = 0.$$

2. **Reciprocal fidelity.**

$$\iota(z_{E,+}) = z_{E,-}.$$

3. **Closure fidelity.** When

$$d_E = 0,$$

the two sheets meet at the same event-closure readout.

4. **Fidelity to actual zero readouts.** Event lifts and the actual zero divisor belong to different object layers; closure sections compatible with the closed readout of Chapter 1 enter the actual Riemann readout.
5. **Generative-source fidelity.** Multiplicative role exchange has an explicit counterpart on the spectral side.
6. **Type fidelity.** $L_\times, R, d_\rho, d_E, \gamma$ are recorded at their respective levels and retain their respective object types.

This definition fixes only structural fidelity. Metric structure, positivity, self-adjointness, and Hilbert norms belong to the later operator layer.

4. Minimal Local Event Carrier

Given the unordered reciprocal pair

$$\{i\gamma_E + d_E,\ i\gamma_E - d_E\},$$

the unique monic quadratic polynomial determined by it is

$$\boxed{\chi_E(z,\tau) = (z - i\gamma_E(\tau))^2 - d_E(\tau)^2.} \tag{4.1}$$

Thus the local event carrier is uniquely determined by the two event sheets:

$$\boxed{\text{unordered reciprocal pair} \Rightarrow \text{unique monic quadratic carrier.}} \tag{4.2}$$

Expanding

$$\chi_E(z,\tau) = 0$$

gives exactly

$$z_{E,\pm}(\tau) = i\gamma_E(\tau) \pm d_E(\tau).$$

The spectral surface of one event is therefore

$$\boxed{\mathcal{S}_E = \{(\tau, z): (z - i\gamma_E(\tau))^2 = d_E(\tau)^2\}.} \tag{4.3}$$

It is a two-sheeted spectral surface over the event parameter τ:

closure branch point → two representation sheets → closure branch point.

This is the spectral-language form of

$$0 \to d_E(\tau) \to 0.$$

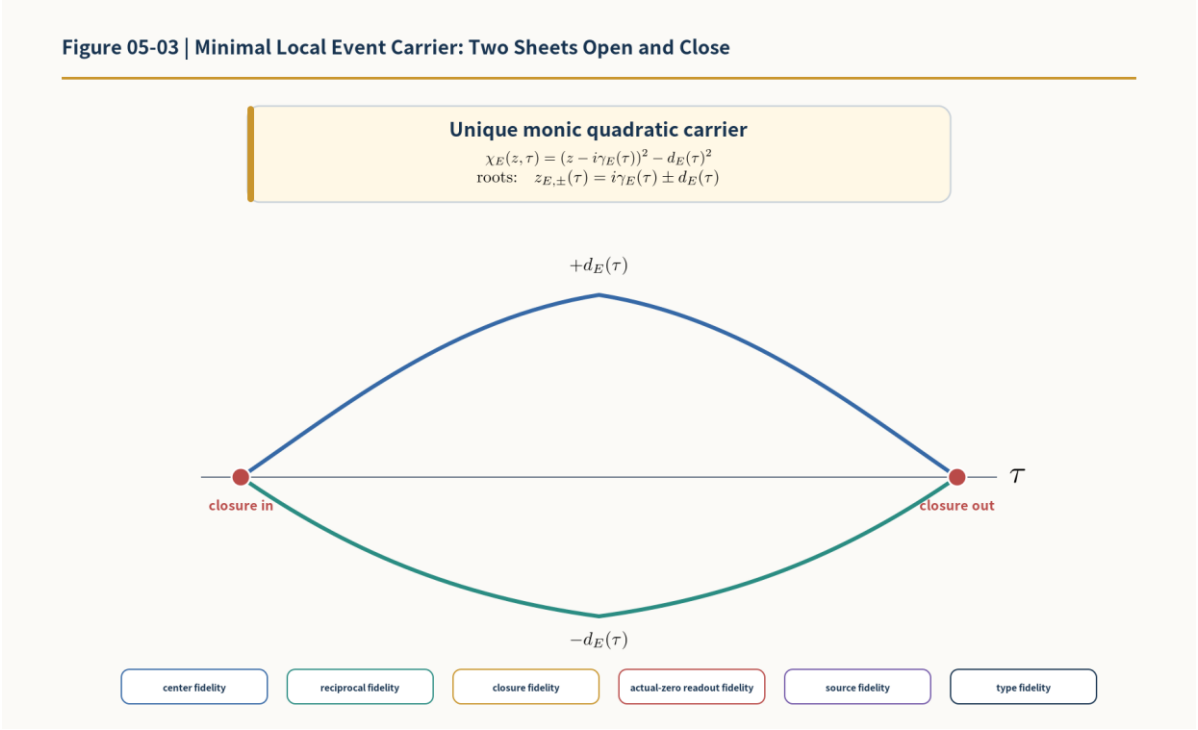


Figure 05-03. Minimal local event carrier. The unordered reciprocal pair $\{i\gamma_E + d_E,\ i\gamma_E - d_E\}$ uniquely determines the monic quadratic carrier $\chi_E(z,\tau) = (z - i\gamma_E(\tau))^2 - d_E(\tau)^2$. Its two sheets open from a closure branch point and glue again at the end of the event. Center, reciprocity, closure, actual-zero readout, source, and type fidelity specify this as an event-lift carrier rather than a second actual zero spectrum.

5. Representation-Sheet Multiplicity versus Analytic Zero Multiplicity

At a closure section where $d_E = 0$,

$$\chi_E(z,\tau) = (z - i\gamma_E)^2. \tag{5.1}$$

This double root means that two reciprocal representation sheets glue at the closure section:

$$\boxed{\text{two reciprocal representation sheets glue at the closure section.}} \tag{5.2}$$

The resulting two-sheet multiplicity and the analytic zero multiplicity of ξ belong to different object layers. In particular,

$$\boxed{\text{two-sheet multiplicity at an event closure section} \not\Rightarrow \operatorname{ord}_{\frac{1}{2}+i\gamma_E} \xi = 2.} \tag{5.3}$$

Chapter 3 records analytic zero multiplicity independently through the divisor

$$\mathcal{D}_{\xi}^{+} = \sum_{n\geq 1} m_n\,[\rho_n].$$

The representation-sheet multiplicity of an event carrier does not change these divisor weights.

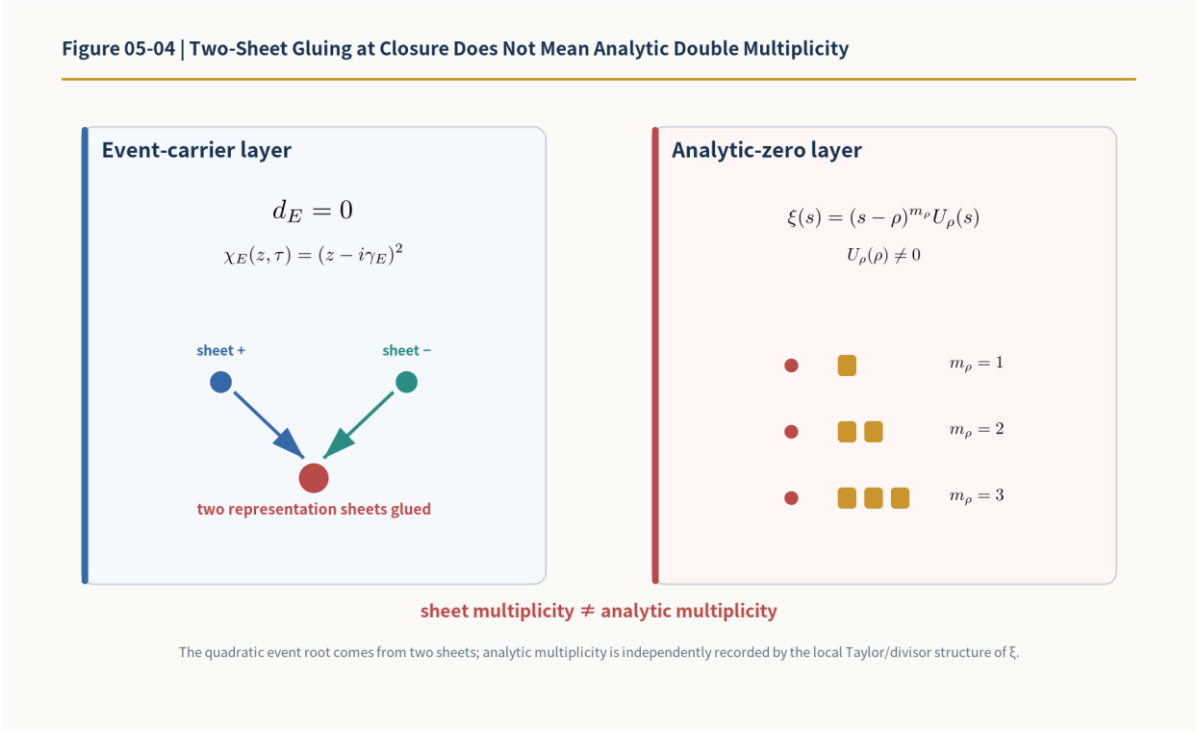


Figure 05-04. Representation-sheet multiplicity versus analytic multiplicity. At $d_E = 0$, the event carrier becomes $\chi_E = (z - i\gamma_E)^2$. This double root records only the gluing of two reciprocal representation sheets at the closure section. The analytic multiplicity of an actual ξ-zero is independently recorded by the local factorization $\xi(s) = (s-\rho)^{m_\rho} U_\rho(s)$; a quadratic event carrier therefore does not imply $m_\rho = 2$.

6. Actual Closed Spectrum and Event-Lift Spectrum

The two layers can now be placed on the same atlas. The event-lift spectrum is

$$\boxed{\hat{\Sigma}_{\text{evt}} = \bigsqcup_E \{\pm d_E(\tau) + i\gamma_E(\tau)\},} \tag{6.1}$$

whereas the actual closed Riemann spectrum is

$$\boxed{\Sigma_{\xi}^{\text{closed}} = \{i\gamma_n\}.} \tag{6.2}$$

They are connected through closure sections:

$$\boxed{\text{event history} \xrightarrow{\text{closure section}} \text{actual zero readout.}} \tag{6.3}$$

Using a closure map,

$$\pi_{\text{cl}}: \hat{\Sigma}_{\text{evt}} \supset \{\tau = \tau_E^{\text{out}}\} \to \Sigma_{\xi}^{\text{closed}},$$

where

$$d_E(\tau_E^{\text{out}}) = 0.$$

7. Multiplicative Generative-Source Coordinates: $L_\times$ and R

Take a multiplicative relation

$$mq = n.$$

Define the total logarithmic scale

$$\boxed{L_\times = \log(mq) = \log n,} \tag{7.1}$$

and the relative factor-role coordinate

$$\boxed{R = \log\frac{q}{m}.} \tag{7.2}$$

Then

$$\log m = \frac{L_\times - R}{2}, \qquad \log q = \frac{L_\times + R}{2}.$$

For the centered Mellin parameter

$$s = \frac{1}{2} + z,$$

one has

$$m^{-s}q^{-(1-s)} = e^{-L_\times/2}e^{zR}.$$

Thus the minimal generative-source kernel is

$$\boxed{K_z(L_\times, R) = e^{-L_\times/2}e^{zR}.} \tag{7.3}$$

Here

$$\boxed{L_\times = \text{total multiplicative log-scale}, \qquad R = \text{relative factor-role coordinate.}} \tag{7.4}$$

We use $L_\times$, rather than T, in order to distinguish the total multiplicative scale from the conventional use of T for zero height in later spectral statistics.

Role exchange

$$(m, q) \leftrightarrow (q, m)$$

gives

$$L_\times \mapsto L_\times, \qquad R \mapsto -R. \tag{7.5}$$

The bare Mellin kernel therefore satisfies

$$K_z(L_\times, -R) = K_{-z}(L_\times, R). \tag{7.6}$$

The completed zero symmetry also contains conjugation, and hence

$$\overline{K_z(L_\times, -R)} = K_{-\bar{z}}(L_\times, R). \tag{7.7}$$

The correct handshake between generative-source role exchange and the reciprocal involution of zeros is therefore

$$\boxed{R \mapsto -R \quad + \quad \text{complex conjugation} \quad \Leftrightarrow \quad z \mapsto -\bar{z}.} \tag{7.8}$$

Role exchange supplies $R \mapsto -R$, while conjugation comes from the real structure of the completed object. Together they correspond to the reciprocal involution on centered zero coordinates.

8. Two Orthogonal Directions of a Zero: d_ρ and γ_ρ

For an actual zero

$$\rho = \frac{1}{2} + d_\rho + i\gamma_\rho,$$

there are two orthogonal coordinate directions:

$$\boxed{d_\rho = \Re\rho - \frac{1}{2}} \tag{8.1}$$

and

$$\boxed{\gamma_\rho = \Im\rho.} \tag{8.2}$$

d_ρ reads the horizontal displacement of the actual zero from the reciprocal fixed axis.

γ_ρ reads the oscillation frequency on logarithmic scale, because

$$x^\rho = x^{1/2+d_\rho} e^{i\gamma_\rho \log x}.$$

After RH closure, when $d_\rho = 0$,

$$x^\rho = x^{1/2} e^{i\gamma_\rho \log x}.$$

Thus γ_ρ is a Mellin/Fourier frequency on the log-coordinate.

The event coordinate $d_E(\tau)$ describes a finite-horizon reciprocal history; d_ρ belongs to the actual zero coordinate. Their types remain distinct.

Hence

$$\boxed{\text{RH fixes the actual horizontal coordinate} d_\rho\text{; the vertical coordinate} \gamma_\rho \text{ remains.}} \tag{8.3}$$

Random matrices, Hilbert–Pólya, and finite self-adjoint spectra primarily read the γ-direction and describe the vertical structure that survives closure.

9. Prime-Power Generative Spectrum and Zero Frequencies

The standard logarithmic derivative gives

$$-\frac{\zeta'}{\zeta}(s) = \sum_{n\geq 1} \frac{\Lambda(n)}{n^s} = \sum_p \sum_{k\geq 1} (\log p)\, p^{-ks}. \tag{9.1}$$

In the log-coordinate, the prime-power positions are

$$\boxed{L_{p^k} = k\log p.} \tag{9.2}$$

They belong to the generative-source spectral positions.

The zero ordinates γ_n, by contrast, are collective Mellin/Fourier readouts of the global completed object.

Throughout the book we fix the type distinction

$$\boxed{k\log p \neq \gamma_n \quad \text{as a type identity.}} \tag{9.3}$$

Their correct relation is the global duality encoded by the explicit formula, not pointwise equality of addresses. Thus prime-power logarithmic positions and zero ordinates are related by the global structure of the explicit formula without being identified point by point.

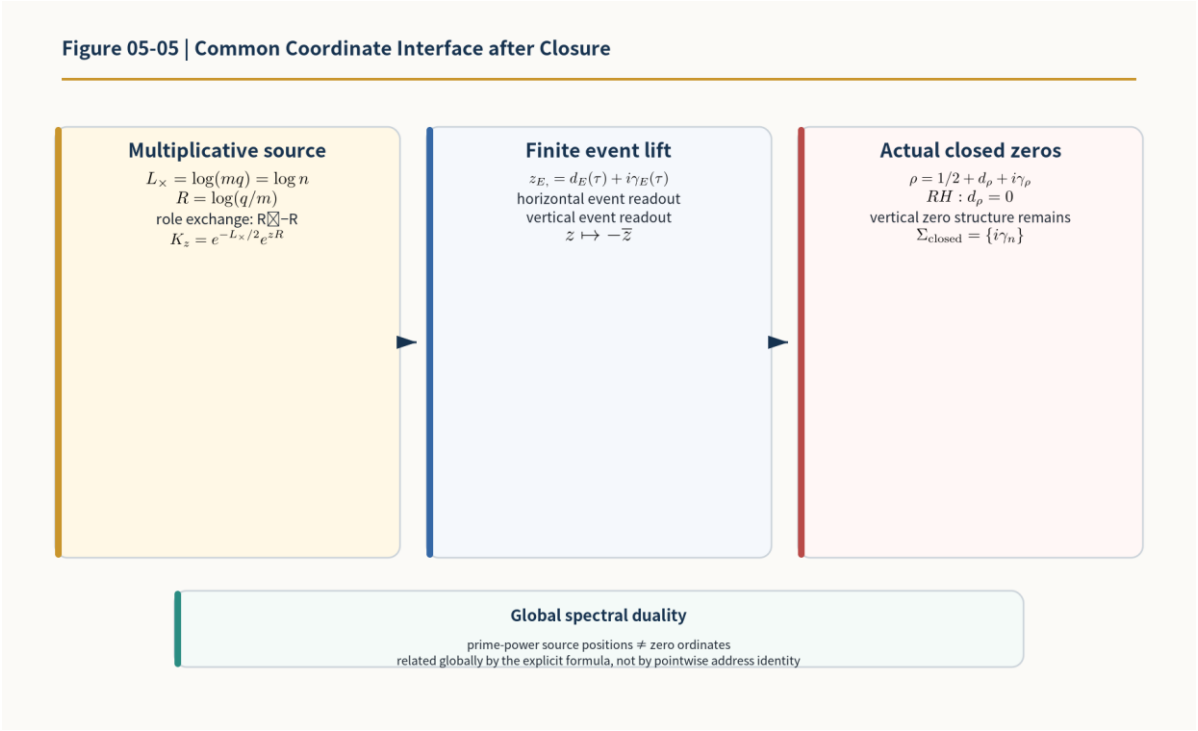


Figure 05-05. Common coordinate interface after closure. $L_\times, R$ belong to the multiplicative generative source; $d_E(\tau), \gamma_E(\tau)$ belong to finite event lifts; and d_ρ, γ_ρ belong to actual zero readouts. RH fixes only the actual horizontal coordinate $d_\rho = 0$, while the vertical structure γ_n remains. Prime-power positions $k\log p$ and zero ordinates γ_n are globally dual through the explicit formula rather than pointwise identical addresses.

10. The Faithful Post-Closure Spectral Atlas

The positions of the principal coordinates can now be fixed:

Layer	Coordinate	Action / symmetry	Mathematical role
total multiplicative scale	$L_\times = \log(mq)$	$mq = n$	finite horizon / total log-scale
relative multiplicative role	$R = \log(q/m)$	$R \mapsto -R$	reciprocal factor roles
actual-zero horizontal coordinate	$d_\rho = \Re\rho - \frac{1}{2}$	$d_\rho \mapsto -d_\rho$	reciprocal horizontal displacement of a zero
event-lift horizontal coordinate	$d_E(\tau)$	$d_E \mapsto -d_E$	finite-horizon unfolding / closure
zero ordinate	$\gamma = \Im\rho$	phase $e^{i\gamma R}$	global collective frequency
prime-power generative position	$k\log p$	multiplication → logarithmic translation	prime-power history
event lift	$\pm d_E + i\gamma_E$	$z \mapsto -\bar{z}$	two-sheet reciprocal lift
actual closed zero	$i\gamma_n$	fixed set	$d_\rho = 0$
bare spectral support	$\Gamma_+ = \{\gamma_n\}$	identity address	distinct ordinates
divisor data	$\mathcal{D}_\xi^+ = \sum_{n\geq 1} m_n [\rho_n]$	analytic multiplicity	zero addresses + analytic multiplicities

The core atlas of this chapter is therefore not an equation in which four coordinates are interchangeable, but a stratified interface:

$$\boxed{(L_\times, R) \rightsquigarrow \text{generative-source structure}, \qquad (d_\rho, \gamma) \rightsquigarrow \text{actual zero readout},} \tag{10.1}$$

together with

$$\boxed{d_E(\tau)}$$

for the finite-horizon event history.

More fully,

$$\boxed{\begin{array}{ccc} & mq = n & \\ & \Downarrow & \\ L_\times = \log(mq) & & R = \log(q/m) \\ \Downarrow & & \Downarrow \\ \text{finite horizon} & & R \leftrightarrow -R \\ \Downarrow & & \Downarrow \\ \{k\log p\} & & z \leftrightarrow -\bar{z} \\ & & \Downarrow \\ & & \boxed{z_{E,\pm} = \pm d_E + i\gamma_E} \\ & & \boxed{(z - i\gamma_E)^2 - d_E^2 = 0} \\ & & \boxed{d_E(\tau_{\text{in}}) = 0 \to d_E(\tau) \to d_E(\tau_{\text{out}}) = 0} \end{array}} \tag{10.2}$$

The actual Riemann readout separately satisfies

$$\boxed{d_\rho = 0, \qquad \Gamma_+ = \{\gamma_n\}, \qquad \mathcal{D}_\xi^+ = \sum_{n\geq 1} m_n\,[\rho_n].} \tag{10.3}$$

This is the faithful event spectral atlas of the chapter, fixing the object interfaces among the later spectral layers.

11. Hilbert–Pólya: Realization of the Vertical Spectrum

The Hilbert–Pólya route seeks a self-adjoint operator H for which the ordinates of the Riemann zeros form the real spectrum:

$$\sigma(H) = \{\gamma_n\},$$

and, when analytic multiplicities are retained, the corresponding eigenspace multiplicities agree with m_n.

If one establishes independently that

$$\xi\left(\frac{1}{2} + i\lambda\right) = 0 \Leftrightarrow \lambda \in \sigma(H), \tag{11.1}$$

then self-adjointness gives a real spectrum and furnishes an independent spectral route to RH.

Within the post-closure atlas of this chapter, Hilbert–Pólya reads the projection

$$\boxed{(d_\rho, \gamma) \mapsto \gamma.} \tag{11.2}$$

Its object-level position is therefore a self-adjoint realization of the vertical spectrum after closure.

The book separates this structure into two levels:

$$\boxed{\text{Chapter 5 (H05) = post-closure vertical spectral atlas and interfaces,}} \tag{11.3}$$

while Chapter 9 (H09) starts from the multiplicative generative source and constructs an independent, source-generated Hilbert–Pólya spectral route. The two chapters respectively supply the post-closure atlas and the independent source-generated spectral construction.

12. Berry–Keating: Scale Generator and the Vertical Spectrum

The Berry–Keating-type Hamiltonian

$$H_{\mathrm{BK}} = \frac{1}{2}(xp + px)$$

is fundamentally a generator of dilations and is therefore naturally close to the logarithmic scale

$$L = \log n$$

and Mellin frequencies.

This explains both why the route reproduces the semiclassical structure of Riemann–Mangoldt counting so deeply and why Srednicki's local RH models can relate the imaginary parts of corresponding Mellin zeros to a projected Berry–Keating spectrum.

Within the faithful spectral atlas of this chapter, the route primarily reads the scale–frequency direction

$$L/\gamma;$$

factor-role reciprocity and event lifts belong to other coordinate layers.

Its position in this chapter is therefore

$$\boxed{\text{a representation of scale–frequency geometry.}} \tag{12.1}$$

13. Random Matrices: Two-Point and Higher-Order Relations of the Vertical Spectrum

The Montgomery–Odlyzko and GUE analogy primarily concerns spacings, two-point correlations, and higher-order local statistics among the ordinates

$$\gamma_n.$$

This is entirely natural in the post-closure spectrum. RH fixes

$$d_\rho = 0,$$

while the closed vertical addresses

$$\Gamma_+ = \{\gamma_n\}$$

still retain their full local-ordering problem.

Random-matrix theory can therefore describe the vertical spectrum with very high precision without reopening the horizontal coordinate d_ρ of the actual zeros. Hence

$$\boxed{\text{extremely strong}\gamma\text{-statistical evidence} \not\Rightarrow \text{ a horizontal proof of RH.}} \tag{13.1}$$

The two statements read different object levels.

One must also distinguish a one-point spectrum from a two-point self-relation. Given a first-order spectral measure ν_{spec}, random-matrix comparison genuinely begins with a two-point object such as

$$\nu_{\mathrm{spec}} \otimes \nu_{\mathrm{spec}},$$

and usually requires unfolding before comparison with a stationary bulk statistical law. Two-point measures and form factors are intertranslatable by Fourier transform.

Accordingly, the initial place assigned to GUE in this chapter is

$$\boxed{\text{two-point self-relations and universality of the closed}\gamma\text{-spectrum.}} \tag{13.2}$$

Chapter 8 (H08) develops, on top of this first-order spectrum, the two-point arithmetic translation, finite-height corrections, and the ζ–GUE handshake.

14. Weil Positivity: Global Arithmetic–Spectral Response

The strength of the Weil explicit-formula criterion is that the prime side and the zero side already enter a single rigorous quadratic form.

Within the spectral atlas of this chapter, it therefore performs another compression:

$$\boxed{(L_{\times}, R, d_{\rho}, \gamma, \text{generative-source history}) \mapsto \text{sign of a quadratic form.}} \tag{14.1}$$

When positivity is equivalent to RH, the essential difficulty remains

> can positivity be derived from an independent generative-source structure?

In the post-closure spectral atlas, the Weil quadratic form plays three structural roles:

1. it reads the sign of the quadratic form associated with the closed spectrum;
2. it forms a rigorous global interface for prime–zero duality;
3. it supplies a natural inner-product or energy structure for spectral operators after RH closure.

Thus its role shifts from a "closure route" to

$$\boxed{\text{a global arithmetic–spectral consistency structure.}}$$

15. de Branges and Θ_{ω}: Horizontal Scanning

Consider

$$\Theta_{\omega}(z) = \frac{\xi(\frac{1}{2} - \omega - iz)}{\xi(\frac{1}{2} + \omega - iz)}. \tag{15.1}$$

Here ω explicitly changes the horizontal distance from the critical line. Thus, in the spectral atlas of this chapter, it naturally reads the

$$\boxed{d\text{-direction.}} \tag{15.2}$$

Suzuki's work on canonical systems shows the deep relation between the meromorphic-inner property of Θ_{ω} and RH, and constructs the associated canonical system unconditionally for $\omega > 1$. If the corresponding construction could be extended unconditionally to all $\omega > 0$, it would yield a canonical-system criterion.

After closure, this route takes on a particularly clear role:

$$\boxed{\Theta_{\omega} = \text{a horizontal tomographic representation of the closed spectral atlas.}} \tag{15.3}$$

That is, it is well suited to testing how the fact that the actual spectrum lies on $d_{\rho} = 0$ is re-expressed in half-plane geometry, inner-function properties, and positivity of the Hamiltonian.

It re-expresses the horizontal geometry $d_{\rho} = 0$ within the post-closure spectral atlas.

16. Connes Scaling / Spectral Triples: Finite Generative Sources and the Vertical Spectrum

The Connes–Consani scaling picture, zeta cycles, and later Zeta Spectral Triples have a natural correspondence with finite multiplicative horizons.

In particular, the 2025 work on Zeta Spectral Triples constructs self-adjoint operators using finite Euler prime data; numerically, their low-energy spectra agree strikingly with the low Riemann zeros. That work explicitly observes that a rigorous proof that the relevant finite spectra and regularized determinants converge in the limit to the complete target object would yield RH.

In the atlas of this chapter, the structure can be written

$$\boxed{\text{finite generative-source spectrum} \to \gamma\text{-spectrum.}} \tag{16.1}$$

The essential difficulty is

$$\boxed{\text{finite-to-global spectral fidelity.}} \tag{16.2}$$

Self-adjointness at the finite level and spectral identification from finite to global are different problems. A finite self-adjoint operator already has real spectrum. Therefore the inference

$$\boxed{\text{finite model has real spectrum } \not\Rightarrow \text{ global} \xi \text{satisfies RH}} \tag{16.3}$$

must be rejected. What is missing is exact identification and convergence, not additional self-adjointness.

17. Suzuki's Finite Weil Spectral Convergence: Spectral Convergence from Finite to Global

Suzuki's 2026 results construct finite-interval Hilbert spaces and distinguished self-adjoint extensions from localized Weil quadratic forms and, **assuming RH**, prove that their positive eigenvalues converge to the distinct positive ordinates of the nontrivial zeros of the Riemann zeta function.

Within the atlas of this chapter, the result separates into four levels.

First, **the finite-interval spectral problem is rigorously defined.** For the localized Weil structure on a finite interval $[-a, a]$, only a finite range of arithmetic data is used, and this defines a local self-adjoint problem.

Second, **the eigenvalues at finite a give rigorous approximations to Riemann ordinates.** If the corresponding distinguished positive eigenvalues are denoted by $t_{a,n}$, then, under RH, Suzuki proves

$$\boxed{t_{a,n} \geq \gamma_n, \qquad t_{a,n} \searrow \gamma_n \quad (a \to \infty).} \tag{17.1}$$

Thus, at a finite horizon,

$$\boxed{\text{rigorously defined finite spectral problem} \;\Rightarrow\; \text{approximate ordinate} t_{a,n}.} \tag{17.2}$$

Third, **there is an exact operator-level relation between the finite and global operators.** The convergence proof uses an exact inverse-compression identity: the inverse of the distinguished local self-adjoint extension is identified with a compression of the inverse of the corresponding global self-adjoint operator. Together with increasing local spaces and the min–max principle, this yields the monotone spectral convergence in (17.1).

The most accurate structural statement is therefore

$$\boxed{\text{rigorously defined finite operator problem} \xrightarrow{\text{exact compression identity}} \text{rigorous spectral approximation} \xrightarrow[a\to\infty]{} \text{exact global ordinates.}} \tag{17.3}$$

Fourth, **the limiting layer is exact.** In addition to

$$t_{a,n} \to \gamma_n$$

for each fixed n, the corresponding normalized spectral entire functions converge locally uniformly to the canonical product built from the distinct ordinates:

$$\boxed{\frac{W(a,\pi;z)}{W(a,\pi;0)} \to \Delta_\Gamma(z),} \tag{17.4}$$

where

$$\Delta_\Gamma(z) = \prod_{\gamma\in\Gamma_+} \left(1 - \frac{z^2}{\gamma^2}\right). \tag{17.5}$$

The object level matters: Γ_+ lists **distinct ordinates** only and does not automatically record analytic multiplicities of zeros of ξ. The limit therefore first recovers the spectral support at the identity level. Analytic multiplicities are separately recorded by the zero divisor of Chapter 3; when all zeros are analytically simple, the multiplicity-layer structure of the normalized spectral entire function agrees with that of normalized ξ.

The structural place of Suzuki 2026 in this atlas can be written

Once RH is known, self-adjoint spectra defined from finite local arithmetic data converge rigorously and monotonically, through an exact operator-compression mechanism, to the true distinct Riemann-zero ordinates.

(17.6)

This makes the result a particularly strong

$$\boxed{\textbf{finite-to-global spectral-fidelity theorem after RH closure,}} \tag{17.7}$$

at the layer of finite-to-global spectral convergence conditional on RH.

It forms a natural complement to the Θ_ω side:

$$\boxed{\Theta_\omega\text{: } d_\rho\text{horizontal scan,} \qquad \text{finite Weil spectrum: } \gamma\text{vertical scan.}} \tag{17.8}$$

The former continuously describes the horizontal / inner-function / canonical-system structure; the latter, under RH, rigorously controls finite-to-global convergence in the vertical spectrum.

Viewed historically within this route—from Suzuki's 2012 canonical-system work on the Riemann ξ-function to later results on the Weil quadratic form, self-adjoint realizations, and spectral convergence—the operator-level fidelity relation between finite structures and the global Riemann spectrum becomes progressively more precise.

Its structure can be summarized as

rigorous post-closure spectral convergence is not exact equality at every finite level; but the finite operator relation is exact, and the global limit is exact.

(17.9)

The two families of structures read horizontal and vertical spectral information, respectively.

18. Carathéodory–Fejér / Real-Zero Mechanisms: Finite All-Real Spectra

The real-zero theorem of Connes–van Suijlekom shows that under suitable quadratic-form / self-adjointness conditions, zeros of the corresponding Fourier transform can be forced onto the real axis.

This means that

$$\boxed{\text{a finite construction produces only real zeros}}$$

belongs to the real-zero structure of a finite representation layer.

An additional bridge is required between all-real behavior at the finite level and all-real behavior globally:

$$\boxed{\text{finite all-real spectrum} \Rightarrow \text{global Riemann all-real spectrum.}} \tag{18.1}$$

Information at the finite level can pass to the global object only after convergence, a determinant identity, or a zero correspondence has been established between the finite family and the global Ξ. A complete link between finite spectral structure and the global object therefore still requires one of these mechanisms.

19. Geometric and Cohomological Routes: the Geometric Origin of the Fixed Axis

The success of RH-type theorems over finite fields is deeply connected with Frobenius, cohomology, weights, and positivity.

The characteristic-one, Scaling Site, Riemann–Roch, and Weil-cohomology programs of Connes and others aim, at a deep level, to explain

$$\boxed{\text{the natural fixed axis of the global arithmetic spectrum.}} \tag{19.1}$$

In the atlas of this chapter, that corresponds to

$$\boxed{d_\rho = 0}$$

as the fixed set of the global readout of the completed object.

Chapter 1 has already supplied this fixed axis. The role of the geometric route in the present atlas is therefore

$$\boxed{\text{the geometric and cohomological origin of the fixed axis.}} \tag{19.2}$$

This is the layer that seeks a geometric explanation of the fixed axis itself.

20. Five Logical Non-Equivalences among Spectral Routes

The following five pairs of statements are not logically equivalent; each spectral route must establish its own bridging conditions.

20.1 Symmetry versus Fixed-Point Property

$$\rho \leftrightarrow 1 - \bar{\rho}$$

gives reciprocal symmetry only. It is not equivalent to

$$\Re\rho = \frac{1}{2}.$$

20.2 Self-Adjointness versus Identification with the Riemann Spectrum

$$H = H^*$$

only guarantees

$$\sigma(H) \subset \mathbb{R}.$$

One must separately establish

$$\sigma(H) = \{\gamma_n\}.$$

20.3 Finite All-Real Spectrum versus Global All-Real Spectrum

Exact convergence or a zero correspondence is required.

20.4 Generative-Source Unitarity versus Zeros after Analytic Continuation

Unitarity at the generative source and locations of analytically continued zeros belong to different levels. A conclusion about zeros of ξ also depends on the concrete structure of the completed Riemann object.

20.5 Prime Logarithmic Positions versus Zero Ordinates

$$k\log p$$

and

$$\gamma_n$$

are spectral data of different types.

These non-equivalences fix the independent bridging responsibilities of the various spectral routes.



Figure 05-06. Five logical non-equivalences. Reciprocal symmetry is not the fixed-point property of every zero; self-adjointness is not identification with the Riemann spectrum; a finite all-real spectrum is not a global all-real spectrum; source unitarity is not the location of zeros after analytic continuation; and $k\log p$ is not γ_n. Each distinction fixes an independent bridge that a spectral route must actually establish.

21. Structural Interpretation of the Faithful Spectral Atlas

21.1 The Critical Real Coordinate $1/2$

The centered reciprocal involution

$$z \mapsto -\bar{z}$$

has fixed set

$$i\mathbb{R}.$$

Returning to the s-plane gives

$$\Re s = \frac{1}{2}.$$

Thus $1/2$ is the real coordinate, in the original s-plane, of the fixed set of the terminal reciprocal involution.

21.2 Random-Matrix Statistics and Horizontal RH Closure

Random matrices primarily read the γ-direction that remains after closure, whereas RH fixes the actual horizontal coordinate d_ρ. They belong to different coordinate layers.

21.3 Finite Self-Adjoint Models and the Global Riemann Spectrum

The eigenvalues of a finite self-adjoint model are real. Between such a finite model and the global Riemann spectrum one must still establish

exact identification and convergence between the finite real spectrum and the global Riemann spectrum.

21.4 Horizontal Scanning and Vertical Spectral Readout

The former naturally scans the horizontal d_ρ-direction; the latter naturally reads the vertical γ-direction. They read different orthogonal directions.

21.5 Global Spectral Duality between Prime Powers and Zeros

The positions

$$k\log p$$

belong to the generative source, whereas

$$\gamma_n$$

are global frequency readouts. The explicit formula establishes a global duality, not identity of addresses.

21.6 Event-Sheet Multiplicity and Analytic Zero Multiplicity

The double-sheet structure of an event carrier comes from the gluing of a two-sheeted event carrier, not from the Taylor expansion of ξ. Spectral-surface branch multiplicity and analytic zero multiplicity therefore belong to different layers.

21.7 Multiple Faithful Representations and a Canonical Operator

A complete Riemann object carries, simultaneously, generative-source scale, reciprocal factor roles, actual zero coordinates, vertical coordinates, analytic multiplicities, and additional completion data. Different mathematical representations naturally read different projections.

One should therefore not demand that all faithful representations be identical. Rather,

different faithful representations may read different projections of the Riemann object.

This does not exclude a canonical unitary-equivalence class under a clearly specified normalization. The common interface among faithful representations satisfies

different representations give compatible readings of the same Riemann data on their common interface. (21.1)

The coexistence of multiple representations and the existence of a canonical unitary-equivalence class at a specific information level are different statements.

21.8 Spectral Structure Remaining after RH Closure

RH gives only

$$d_\rho = 0.$$

It does not by itself give:

- a natural source-generated operator for γ_n;
- analytic simplicity of the zeros;
- a canonical spectral representation of identity addresses and analytic multiplicities;
- exact prime–zero reconstruction;
- the generative origin of GUE two-point and higher-order statistics;
- a finite-to-global convergence mechanism;
- an unconditional canonical-system realization for all parameters;
- a geometric/cohomological realization.

After RH closure, vertical spectral generation, multiplicity, operator realization, statistical relations, and geometric realization therefore remain distinct spectral structures.

22. Fidelity Conditions for Spectral Representations

For any Riemann spectral representation $\mathcal{M}$, compatibility with the atlas of this chapter is checked by the following conditions:

F1.	$\mathcal{M}$ specifies how it reads $L_\times$;
F2.	$\mathcal{M}$ specifies its representation of R and $R \mapsto -R$;
F3.	$\mathcal{M}$ distinguishes actual d_ρ from event $d_E(\tau)$;
F4.	$\mathcal{M}$ specifies how γ_n is produced or read;
F5.	$\mathcal{M}$ preserves reciprocal roles or an equivalent representation;
F6.	$\mathcal{M}$ distinguishes support addresses from analytic multiplicities;
F7.	$\mathcal{M}$ has an explicit finite-horizon or finite-truncation structure;
F8.	$\mathcal{M}$ supplies a faithful bridge from a finite generative source to the global zero object;
F9.	$\mathcal{M}$ distinguishes representation-sheet multiplicity from analytic zero multiplicity;
F10.	$\mathcal{M}$ distinguishes a one-point spectrum from two-point self-relations when entering the GUE layer.

(22.1)

These conditions place different spectral representations in one coordinate system and make explicit both the data layer preserved by each representation and the bridging structure it requires.

23. Stratification of Spectral Routes after Closure

Route	Primarily reads	Main structure	Position in this book
Hilbert–Pólya	γ and possible spectral multiplicities	exact self-adjoint realization	vertical spectral realization after RH closure; Chapter 9 gives an independent source-generated route
Berry–Keating	L, γ	scale / semiclassical counting	scale–frequency structure
random matrices	two-point / higher-order statistics of γ	spacing / universality	second- and higher-order self-relations of the vertical spectrum
Weil positivity	global generative-source–zero response	sign of an arithmetic quadratic form	global consistency and positivity encoding
de Branges / Θ_ω	d_ρ	horizontal scanning / inner-function geometry	horizontal tomographic representation
Connes scaling / zeta cycles	log-scale, γ	finite-prime spectral realization	finite-to-global spectral-fidelity structure
Zeta Spectral Triples	finite generative source $\to \gamma$	numerical / self-adjoint finite spectrum	finite vertical spectral realization

Route	Primarily reads	Main structure	Position in this book
Suzuki finite Weil spectrum	finite horizon → γ	rigorous monotone convergence under RH; exact inverse-compression mechanism	finite-to-global spectral convergence
geometry / cohomology	fixed axis / global structure	explanation of the natural central axis	geometric explanation of the fixed axis

The table records

$$\boxed{\text{which part of the Riemann object each route actually sees.}} \tag{23.1}$$

Chapters 6–9 develop, respectively, the canonical spectral object, the spectral witness, the ζ–GUE two-point interface, and the independent Hilbert–Pólya construction.

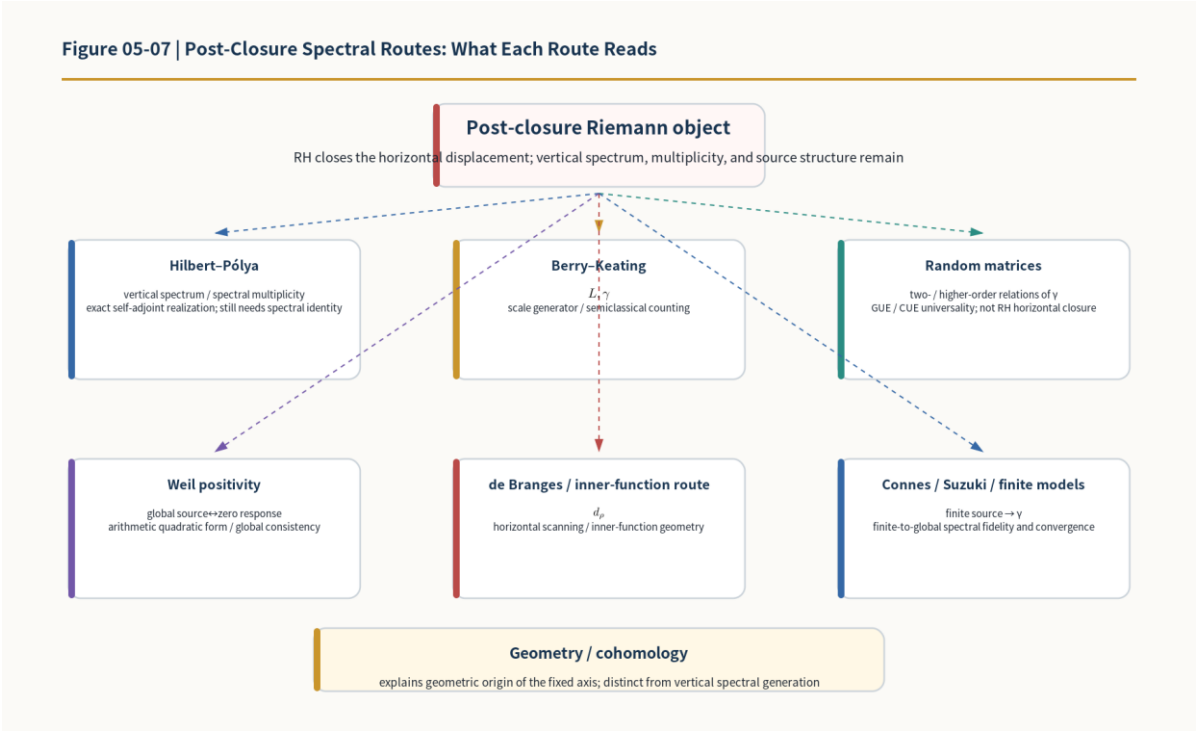


Figure 05-07. Stratification of post-closure spectral routes. Hilbert–Pólya, Berry–Keating, random matrices, Weil positivity, de Branges, Connes/Suzuki/finite self-adjoint models, and geometric/cohomological routes read different projections of the same closed Riemann object: vertical spectrum, scale–frequency structure, second-order self-relations, global arithmetic response, horizontal scanning, finite-to-global spectral fidelity, and the geometric origin of the fixed axis. Multiple faithful representations may coexist, but conclusions from different projections cannot be substituted for one another.

24. Logical Boundaries of the Spectral-Atlas Layer

The logical relations among the objects of this chapter are fixed as follows.

The event carrier

$$\chi_E(z,\tau) = (z - i\gamma_E)^2 - d_E^2$$

encodes the two-sheet structure of a finite-horizon reciprocal event; the actual horizontal RH closure

$$d_\rho = 0$$

comes from the terminal fixed-role conclusion of Chapter 1.

The generative-source role exchange

$$R \mapsto -R$$

and the real structure of the completed object together correspond to the reciprocal involution on centered zero coordinates. This remains type-distinct from the actual zero horizontal coordinate d_ρ.

Finite self-adjoint spectra provide real-spectral structure at the finite level. Their relation to the complete Riemann spectrum is determined separately by spectral identification, convergence, or determinant structure.

Prime-power positions

$$k\log p$$

belong to the generative-source spectral positions, while zero ordinates

$$\gamma_n$$

are collective frequency readouts of the completed object. The two are linked by the global structure of the explicit formula.

The event-lift coordinate

$$d_E(\tau)$$

belongs only to a finite-horizon event history and does not enter the horizontal coordinate of actual zeros. Accordingly, representation-sheet multiplicity at event closure and analytic multiplicity of zeros of ξ are recorded by different objects.

Random-matrix and GUE structures act on the post-closure vertical spectrum and its two-point and higher-order self-relations. Logically they come after horizontal RH closure.

In summary, the type relations at the spectral-atlas layer compress to

$$\boxed{\text{event-lift layer} \neq \text{actual-zero layer} \neq \text{operator-identification layer} \neq \text{second-order statistical layer.}} \tag{24.1}$$

25. Conclusion

The closure conclusion of Chapter 1 is

$$\Re\rho = \frac{1}{2}.$$

On top of this horizontal closure, the present chapter decomposes the post-closure Riemann object into the following coordinate layers.

The multiplicative generative source carries

$$\boxed{L_\times = \log(mq), \qquad R = \log(q/m).}$$

An actual zero carries

$$\boxed{d_\rho = \Re\rho - \frac{1}{2}, \qquad \gamma_\rho = \Im\rho.}$$

A finite-horizon event history separately uses

$$\boxed{d_E(\tau).}$$

Here

$$\boxed{d_E(\tau) \neq d_\rho}$$

as object types.

RH closure gives only

$$\boxed{d_\rho = 0.}$$

The actual closed spectrum must still distinguish the support of distinct addresses

$$\Gamma_+ = \{\gamma_n\}$$

from the divisor data with analytic multiplicities

$$\mathcal{D}_\xi^+ = \sum_{n\geq 1} m_n\,[\rho_n].$$

A finite-horizon generative history may be preserved through the two-sheet event lift

$$\boxed{(z - i\gamma_E)^2 - d_E^2 = 0,}$$

but this event carrier is not the set of off-axis zeros of the complete ξ-function.

The result of this chapter is therefore

a faithful event spectral atlas after RH closure.

Different spectral routes can then be compared within the same coordinate ledger.

On this common background:

- Hilbert–Pólya primarily reads a self-adjoint realization of γ;
- Berry–Keating primarily reads logarithmic scale and frequency;
- random-matrix theory reads two-point and higher-order self-relations of the closed γ-spectrum;
- Weil positivity reads the sign of a global arithmetic–spectral quadratic form;
- de Branges / canonical systems strongly probe the horizontal d_ρ-direction;
- finite spectral constructions read approximations from a finite generative source to the vertical spectrum;
- geometric/cohomological routes seek to explain the naturality of the fixed axis.

These routes read different projections of the Riemann object. Their common interface is

object level, retained data, compressed data, and common readout interface

Chapter 6 organizes the closed-zero data into the Ren operator; Chapter 7 establishes the canonical spectral witness; Chapter 8 enters GUE two-point self-relations; Chapter 9 then returns to the multiplicative generative source and independently constructs a source-generated Hilbert–Pólya spectral route.

Thus the connective role of this chapter is

RH closure → faithful event spectral atlas →
canonical spectrum, spectral witness, and second-order statistical structure.

The chapters that follow address, in turn,

canonical spectral construction, spectral identity witnessing, the GUE two-point interface, and an independent source-generated spectral route ———

Chapter 6 The Ren Operator: A Lossless Bridge between Multiplicative Identity, Analytic Continuation, and the Canonical Spectrum

Abstract

Chapter 5 develops the faithful event spectral atlas after closure. This chapter enters the operator layer. Let

$$X(z) = \xi\left(\frac{1}{2} + z\right),$$

and for a nontrivial zero

$$\rho = \frac{1}{2} + a_\rho$$

define the centered zero coordinate

$$a_\rho = \rho - \frac{1}{2} = d_\rho + i\gamma_\rho, \qquad \gamma_\rho > 0.$$

On the Hilbert space formed with analytic multiplicities, define the **Yifei Ren operator**

$$K_{\mathrm{Ren}} e_{\rho,j} = (-ia_\rho)e_{\rho,j} = (\gamma_\rho - id_\rho)e_{\rho,j}.$$

This is a normal operator defined before RH, with the strongly commuting decomposition

$$\boxed{K_{\mathrm{Ren}} = \Gamma_{\mathrm{Ren}} - i\Delta_{\mathrm{Ren}},}$$

where

$$\Gamma_{\mathrm{Ren}} e_{\rho,j} = \gamma_\rho e_{\rho,j}, \qquad \Delta_{\mathrm{Ren}} e_{\rho,j} = d_\rho e_{\rho,j}.$$

Hence

$$\boxed{\mathrm{RH} \Leftrightarrow \Delta_{\mathrm{Ren}} = 0 \Leftrightarrow K_{\mathrm{Ren}} = K_{\mathrm{Ren}}^{*} > 0.}$$

Next define

$$B_{\mathrm{Ren}} = K_{\mathrm{Ren}}^{-2}.$$

Using Riemann–von Mangoldt zero counting, the Hadamard factorization of an even entire function, and trace-class Fredholm determinant theory, one obtains

$$B_{\mathrm{Ren}} \in \mathfrak{S}_1,$$

and

$$\boxed{\frac{X(w)}{X(0)} = \det(I + w^2 B_{\mathrm{Ren}}),}$$

as well as

$$\boxed{\frac{X'(w)}{X(w)} = 2w\mathrm{Tr}[B_{\mathrm{Ren}}(I + w^2 B_{\mathrm{Ren}})^{-1}].}$$

The full Ren–Riemann spectral object is

$$\boxed{\boldsymbol{R}_{\mathrm{Ren}}^{\mathrm{full}} = (\mathcal{H}_{\mathrm{Ren}}, K_{\mathrm{Ren}}, J_{\mathrm{Ren}}, c_*, \kappa_*, C_\xi),}$$

where

$$c_* = \frac{1}{2}, \qquad \kappa_* = X(0),$$

and

$$C_\xi(s) = \frac{1}{2}s(s-1)\pi^{-s/2}\Gamma(s/2)$$

is the Riemann completion multiplier. This full object preserves centered coordinates, analytic multiplicities, reciprocal symmetry, the central anchor, Fredholm normalization, and the completion marker.

Within the standard Riemann normalization there is a bidirectional recovery chain

$$\boxed{\mathfrak{M}_\times \leftrightarrow \zeta_{\mathrm{germ}} \leftrightarrow \zeta_{\mathrm{global}} \leftrightarrow \xi \leftrightarrow X \leftrightarrow \boldsymbol{R}_{\mathrm{Ren}}^{\mathrm{full}},}$$

where

$$\mathfrak{M}_\times = (\mathbb{N}, \mathcal{R}_\times, \ell), \qquad \ell(n) = \log n,$$

is the scaled relational realization of the root multiplicative identity

$$\mathfrak{I}_\times = (\mathbb{N}_{>0}, \mu)$$

from Chapter 1. Reverse recovery proceeds through

$$\eta_\times = \sum_{n\geq 1} \delta_{\log n}$$

and Laplace / Dirichlet uniqueness, returning to the integer multiplication relation before analytic continuation.

Thus the phrase **lossless bridge** in this chapter means bidirectional recoverability under the standard Riemann normalization: different mathematical types retain their own object identities, while their canonical information can be generated forward and recovered backward along specified maps. Under RH,

$$\boxed{H_{\mathrm{Ren}} := K_{\mathrm{Ren}}|_{\mathrm{RH}}}$$

becomes the positive self-adjoint canonical Riemann spectral operator and connects continuously with the closed spectral atlas of Chapter 5, the spectral witness of Chapter 7, and the GUE two-point self-relation of Chapter 8.

1. Operator Position, Object Levels, and Naming

Chapter 5 separated the closed Riemann-zero data into actual zero coordinates, analytic multiplicities, and the event-lift layer. On that basis, the present chapter constructs a full-coordinate normal operator that simultaneously retains

$$(d_\rho, \gamma_\rho)$$

and establishes a bidirectional recovery relation among multiplicative identity, analytic continuation, the completed Riemann object, and a canonical spectral object.

The operator structure of this chapter has four levels: the full-coordinate Ren operator; the hidden horizontal operator and the equivalent operator formulation of RH; Fredholm / resolvent recovery through a trace-class square inverse; and the bidirectional multiplicative–analytic–spectral recoverability carried by the fully marked object.

1.1 Logical Position of This Chapter

This chapter uses the standard theory of the Riemann ζ/ξ-functions, complex analysis, spectral theory, trace-class theory, and Laplace / Dirichlet uniqueness. Its logical chain is

closed zero divisor →
full-coordinate Ren operator →
full Ren–Riemann object ↔
multiplicative–analytic history.

Chapter 5 supplies the post-closure spectral-atlas interface; Chapter 7 establishes a canonical spectral identity witness; Chapter 8 enters GUE two-point self-relations; and Chapter 9 independently constructs a Hilbert–Pólya spectral route from the multiplicative generative source. The present chapter constructs the canonical operator object from the completed Riemann zero divisor and develops its reverse-recovery structure.

1.2 Object Levels and Naming Convention

Three core levels are distinguished: the unconditional full-coordinate normal operator before RH, the canonical self-adjoint specialization after RH, and the full spectral object carrying recovery markers.

1.3 Unconditional Full-Coordinate Operator

$$\boxed{K_{\mathrm{Ren}}}$$

is defined from the centered zero divisor before RH. It retains both the vertical and horizontal coordinates of

$$a_\rho = d_\rho + i\gamma_\rho$$

and decomposes as

$$\boxed{K_{\mathrm{Ren}} = \Gamma_{\mathrm{Ren}} - i\Delta_{\mathrm{Ren}}.}$$

Here

$$\Gamma_{\mathrm{Ren}}$$

is called the **ordinate operator**, while

$$\Delta_{\mathrm{Ren}}$$

is the **hidden horizontal-displacement operator**. Define

$$\boxed{\delta_{\mathrm{Ren}} = \| \Delta_{\mathrm{Ren}} \|}$$

as the global horizontal defect.

1.4 RH Specialization

Under RH,

$$d_\rho = 0, \qquad \Delta_{\mathrm{Ren}} = 0,$$

so

$$K_{\mathrm{Ren}} = K_{\mathrm{Ren}}^{*} > 0.$$

Define

$$\boxed{H_{\mathrm{Ren}} := K_{\mathrm{Ren}}|_{\mathrm{RH}}.}$$

H_{Ren} is called the **canonical Riemann spectral operator**. Its unitary-equivalence class is

$$\boxed{\mathfrak{R}_{\mathrm{Ren}} := [H_{\mathrm{Ren}}]_{\mathrm{u}},}$$

called the **Ren–Riemann spectral class**.

1.5 Full Marked Spectral Object

To retain the central anchor, normalization, completion rule, and reciprocal symmetry, define

$$\boxed{\boldsymbol{R}_{\mathrm{Ren}}^{\mathrm{full}}}$$

as the **full marked Ren–Riemann spectral object**, and denote its marked unitary-equivalence class by

$$\boxed{\mathfrak{R}_{\mathrm{Ren}}^{\mathrm{full}}.}$$

The full object contains not only the Hilbert space and K_{Ren}, but also

$$J_{\mathrm{Ren}}, \qquad c_*, \qquad \kappa_*, \qquad C_\xi,$$

which support the bidirectional multiplicative–analytic–spectral recovery developed below.

1.6 Related Downstream Objects

Before RH, define

$$\boxed{B_{\mathrm{Ren}} = K_{\mathrm{Ren}}^{-2},}$$

called the **Ren square-inverse operator**. It is a normal trace-class operator; under RH it is positive. When the positive divisor reading after RH needs to be emphasized, the corresponding positive operator may be denoted by

$$B_{\mathrm{div}}.$$

Further define the signed bare spectral operator

$$\boxed{D_{\mathrm{Ren}} = H_{\mathrm{Ren}} \oplus (-H_{\mathrm{Ren}}),}$$

with spectrum

$$\sigma(D_{\mathrm{Ren}}) = \{\pm\gamma_n\}$$

counted with analytic multiplicity. This object is used as the two-sided spectral input to the two-point statistical interface of Chapter 8.

The object hierarchy throughout the book is therefore

$$\boxed{\boldsymbol{R}_{\mathrm{Ren}}^{\mathrm{full}} \supset K_{\mathrm{Ren}} \overset{\mathrm{RH}}{\to} H_{\mathrm{Ren}} \to D_{\mathrm{Ren}} \text{ or other bare spectral readouts.}}$$

Figure 06-01 | Object Levels of the Ren Operator

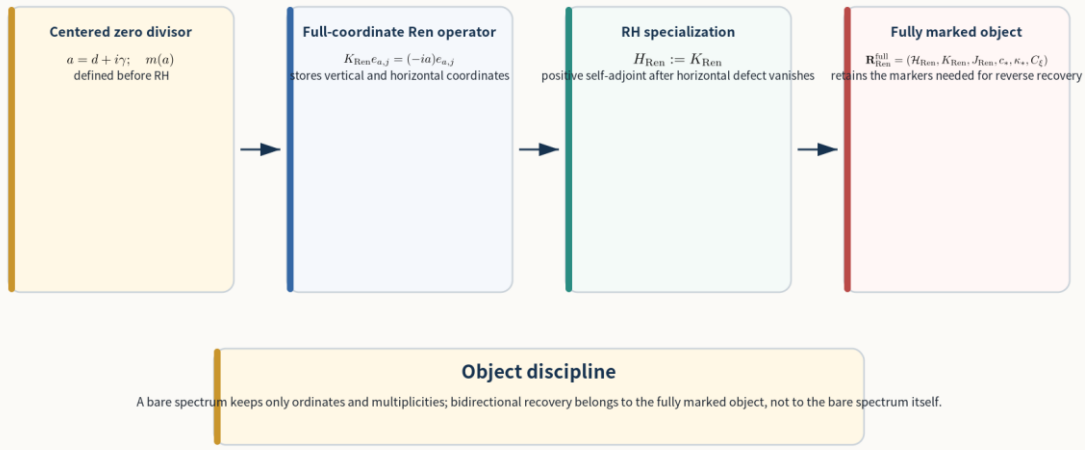


Figure 06-01. Object levels of the Ren operator. Before RH, the centered zero divisor already defines the unconditional full-coordinate operator K_{Ren}, which stores both horizontal and vertical coordinates. Only after RH does it specialize to the positive self-adjoint operator H_{Ren}. Bidirectional recovery belongs to the fully marked Ren–Riemann object, which retains the involution, center anchor, normalization constant, and completion marker; it does not belong to the bare diagonal spectrum by itself.

2. Multiplicative Identity, the Dirichlet Region, and Analytic Continuation

2.1 Multiplicative Identity with Scale

The numerical scale of the Riemann zeta function is fixed jointly by the standard positive-integer structure and its logarithmic scale. The lossless chain of this chapter begins with the scaled multiplicative realization

$$\boxed{\mathfrak{M}_{\times} = (\mathbb{N}, \mathcal{R}_{\times}, \ell),}$$

where

$$\mathcal{R}_{\times} = \{(m, q, n) \in \mathbb{N}^3 : mq = n\},$$

and

$$\ell : \mathbb{N} \to [0, \infty), \qquad \ell(n) = \log n.$$

The scale satisfies

$$\boxed{\ell(mq) = \ell(m) + \ell(q).}$$

This is the canonical coordinate through which multiplication enters additive spectral / transform language.

2.2 The Multiplicative Log Ledger before Analytic Continuation

Define the positive discrete measure

$$\boxed{\eta_{\times} = \sum_{n \geq 1} \delta_{\log n}.}$$

It records the standard positive-integer multiplicative scale completely in

$$S_{\times} := \operatorname{supp} \eta_{\times} = \{\log n : n \in \mathbb{N}\}.$$

For $\Re s > 1$,

$$\int_{[0,\infty)} e^{-sx} \, d\eta_{\times}(x) = \sum_{n \geq 1} e^{-s \log n} = \sum_{n \geq 1} n^{-s}.$$

Therefore

$$\boxed{\zeta_{\mathrm{germ}}(s) = \mathcal{L}\eta_{\times}(s), \qquad \Re s > 1.}$$

Equivalently, on

$$\mathcal{H}_{\mathrm{mult}} = \ell^2(\mathbb{N}),$$

define

$$H_{\mathrm{mult}} e_n = (\log n) e_n.$$

Then

$$\boxed{\zeta_{\mathrm{germ}}(s) = \mathrm{Tr}(e^{-sH_{\mathrm{mult}}}), \qquad \Re s > 1.}$$

Here H_{mult} is the multiplicative-source operator before analytic continuation and belongs to the multiplicative generative layer; K_{Ren} belongs to the canonical spectral layer of the completed zero divisor.

2.3 Exact Recovery of Multiplication from the Log Ledger

From

$$S_\times = \{\log n\},$$

define

$$\boxed{\mathcal{R}_\times^{\log} = \{(x, y, z) \in S_\times^3 : x + y = z\}.}$$

The exponential map

$$\exp: S_\times \to \mathbb{N}$$

gives

$$e^x e^y = e^z \Leftrightarrow x + y = z.$$

Hence

$$\boxed{(\exp x, \exp y, \exp z) \in \mathcal{R}_\times \Leftrightarrow (x, y, z) \in \mathcal{R}_\times^{\log}.}$$

Thus

$$\boxed{\eta_\times \Rightarrow S_\times \Rightarrow \mathcal{R}_\times^{\log} \Rightarrow \mathcal{R}_\times.}$$

This shows that the Dirichlet/Laplace analytic germ before continuation does not preserve merely a string of function values. In its canonical Dirichlet representation, it retains the complete standard multiplicative ledger.

2.4 Dirichlet / Laplace Uniqueness

Theorem 2.1 (Recovery Theorem for the Multiplicative Log Ledger)

Let η_1, η_2 be locally finite positive Borel measures on $[0, \infty)$, and suppose there is a $\sigma_0 \in \mathbb{R}$ such that for every $\sigma > \sigma_0$,

$$\int_{[0,\infty)} e^{-\sigma x}\, d\eta_j(x) < \infty, \qquad j = 1,2.$$

If there exists $\sigma_1 > \sigma_0$ such that

$$\int e^{-sx}\, d\eta_1(x) = \int e^{-sx}\, d\eta_2(x) \qquad (s > \sigma_1),$$

then

$$\boxed{\eta_1 = \eta_2.}$$

In particular, within this class of positive measures, ζ_{germ} uniquely determines

$$\boxed{\eta_{\times} = \sum_{n\geq 1} \delta_{\log n}\,.}$$

Proof

Fix $s_0 > \sigma_1$, and define finite positive measures

$$d\mu_j(x) = e^{-s_0 x}\, d\eta_j(x).$$

Finiteness follows from the hypothesis. For every $t > 0$,

$$\int e^{-tx}\, d\mu_1(x) = \int e^{-(s_0+t)x}\, d\eta_1(x) = \int e^{-(s_0+t)x}\, d\eta_2(x) = \int e^{-tx}\, d\mu_2(x).$$

Push forward under $x \mapsto y = e^{-x}$ to $(0,1]$, and denote the resulting finite measures by ν_j. Then, for every integer $n \geq 1$,

$$\int_{(0,1]} y^n\, d\nu_1(y) = \int_{(0,1]} y^n\, d\nu_2(y).$$

Letting $t \downarrow 0$ and using monotone convergence shows that the total masses are also equal, so the zeroth moments agree. Polynomials are dense in $C([0,1])$, hence the two finite measures integrate every continuous function equally. Uniqueness in the Riesz representation theorem gives

$$\nu_1 = \nu_2.$$

Because $x \mapsto e^{-x}$ is injective, $\mu_1 = \mu_2$; multiplying back by the positive weight $e^{s_0 x}$ yields

$$\eta_1 = \eta_2.$$

For

$$\eta_{\times} = \sum_{n\geq 1} \delta_{\log n},$$

one has

$$\int e^{-\sigma x}\, d\eta_{\times}(x) = \sum_{n\geq 1} n^{-\sigma} = \zeta(\sigma) < \infty \qquad (\sigma > 1),$$

so the theorem applies. ▫

Corollary 2.2

Under the standard real scale and exponential map, ζ_{germ} uniquely recovers $\eta_{\times}$, whose support uniquely recovers a scaled multiplicative system identical to the standard positive-integer multiplication structure. Therefore

$$\boxed{\zeta_{\mathrm{germ}} \Rightarrow (\mathbb{N}, \mathcal{R}_{\times}, \ell)}$$

is a determinate recovery under the standard normalization fixed in this chapter.

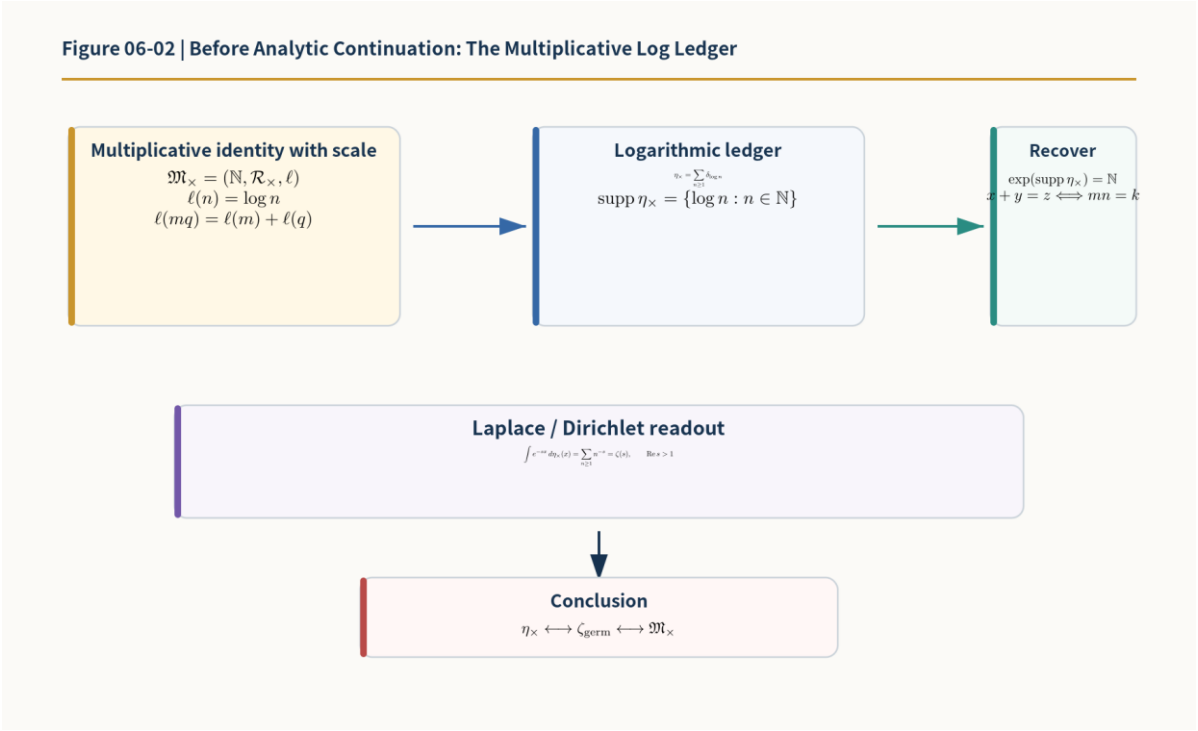


Figure 06-02. The multiplicative logarithmic ledger. The positive discrete measure $\eta_\times = \sum_{n\geq 1} \delta_{\log n}$ stores the integer multiplicative scale as $\{\log n\}$. Exponentiation recovers the standard natural-number objects, while the additive relation $\log m + \log n = \log(mn)$ recovers multiplication exactly. On $\Re s > 1$, its Laplace–Dirichlet readout is the original Dirichlet germ of ζ. Thus a bidirectionally recoverable multiplicative ledger already exists before analytic continuation.

2.5 Bidirectional Uniqueness of Analytic Continuation

Let

$$\zeta_{\text{global}}$$

be the standard meromorphic continuation of ζ_{germ}.

Uniqueness of analytic continuation gives the forward map

$$\zeta_{\text{germ}} \to \zeta_{\text{global}}.$$

The reverse direction is simply restriction:

$$\boxed{\zeta_{\text{global}}|_{\Re s>1} = \zeta_{\text{germ}}.}$$

Hence

$$\boxed{\zeta_{\text{germ}} \leftrightarrow \zeta_{\text{global}}}$$

is reversible under the standard Riemann normalization adopted here.

The reversibility is restricted to the same Riemann analytic germ and its unique analytic continuation: restriction to $\Re s > 1$ recovers the original germ.

2.6 Completion and the Registered Marker

Define

$$C_\xi(s) = \frac{1}{2}s(s-1)\pi^{-s/2}\Gamma\left(\frac{s}{2}\right),$$

and

$$\boxed{\xi(s) = C_\xi(s)\zeta_{\text{global}}(s).}$$

Thus the forward map is

$$\zeta_{\text{global}} \to \xi.$$

The reverse map is meromorphic recovery:

$$\boxed{\zeta_{\text{global}}(s) = \frac{\xi(s)}{C_\xi(s)}.}$$

Accordingly, the Archimedean completion factor and normalization data are retained as canonical markers. A bare zero set and the fully completed object belong to different information levels.

3. The Centered Completed Riemann Function and the Ren Operator

3.1 Centering and the Even Completed Function

Define

$$c_* = \frac{1}{2}, \qquad X(z) = \xi(c_* + z).$$

The standard functional equation and real structure give, respectively,

$$X(z) = X(-z), \qquad X(\bar{z}) = \overline{X(z)}.$$

Hence the zero divisor is closed, with multiplicity preserved, under

$$z \mapsto -z, \qquad z \mapsto \bar{z}.$$

Lemma 3.1 (No Real Centered Zeros)

X has no zeros on the real axis. Consequently, every $\{a, -a\}$-orbit of zeros has exactly one representative in the upper half-plane.

Proof

For real x, $X(x) = 0$ is equivalent to $\xi(1/2 + x) = 0$. The zeros of ξ are precisely the nontrivial zeros of ζ. Thus, if $|x| < 1/2$, such a zero would give a real zero of $\zeta(s)$ with $0 < s < 1$.

For $s > 0$, the Dirichlet eta function

$$\eta(s) = \sum_{n\geq 1}(-1)^{n-1}n^{-s}$$

is positive by the alternating-series test, while

$$\eta(s) = (1 - 2^{1-s})\zeta(s).$$

For $0 < s < 1$, $1 - 2^{1-s} < 0$, so $\zeta(s) < 0$ and has no zero there. At the endpoints, $\xi(0) = \xi(1) = 1/2 \neq 0$. Hence X has no real zero. ▫

For a nontrivial zero ρ, retain the centered coordinate of Chapter 5:

$$\boxed{a_\rho := \rho - \frac{1}{2} = d_\rho + i\gamma_\rho.}$$

Let the support of the centered zeros in the upper half-plane be

$$\mathcal{Z}_+ = \{a_\rho : X(a_\rho) = 0,\ \Im a_\rho > 0\},$$

counted with analytic multiplicity

$$m_\rho = \mathrm{ord}_\rho \xi.$$

For brevity in the operator formulas, write

$$a = a_\rho = d_a + i\gamma_a, \qquad m(a) = m_\rho.$$

Since every nontrivial zero lies in $0 < \Re s < 1$,

$$|d_a| < \frac{1}{2}.$$

3.2 The Full-Coordinate Ren Hilbert Space

Define

$$\boxed{\mathcal{H}_{\mathrm{Ren}} = \oplus_{a \in \mathcal{Z}_+} \mathbb{C}^{m(a)}.}$$

Choose an orthonormal basis

$$e_{a,j}, \qquad 1 \leq j \leq m(a).$$

This is a divisor space faithful to analytic multiplicity.

3.3 The Full-Coordinate Ren Operator

Definition 3.2 (The Ren Operator)

On

$$\mathcal{H}_{\mathrm{Ren}} = \oplus_{a \in \mathcal{Z}_+} \mathbb{C}^{m(a)},$$

define

$$\boxed{K_{\mathrm{Ren}} e_{a,j} = (-ia) e_{a,j}.}$$

If $a = d_a + i\gamma_a$, then

$$-ia = \gamma_a - i d_a.$$

The domain is

$$\boxed{D(K_{\mathrm{Ren}}) = \left\{ c = (c_{a,j}) : \sum_{a,j} |a|^2 |c_{a,j}|^2 < \infty \right\}.}$$

Theorem 3.3 (Unconditional Full-Coordinate Ren Operator)

K_{Ren} is densely defined, closed, and normal. Its adjoint is

$$K_{\mathrm{Ren}}^* e_{a,j} = \overline{-ia}\, e_{a,j} = (\gamma_a + i d_a) e_{a,j},$$

with

$$D(K_{\mathrm{Ren}}^*) = D(K_{\mathrm{Ren}}).$$

Its spectrum is

$$\boxed{\sigma(K_{\mathrm{Ren}}) = \{-ia : a \in \mathcal{Z}_+\},}$$

where each eigenvalue is counted with analytic multiplicity $m(a)$. The spectrum has no finite accumulation point, and K_{Ren} has compact resolvent.

Proof

Finite-support vectors lie in the domain and are dense in $\mathcal{H}_{\mathrm{Ren}}$, so K_{Ren} is densely defined. Suppose $c^{(n)} \to c$ and $Kc^{(n)} \to b$. Coordinatewise,

$$(-ia) c_{a,j}^{(n)} \to b_{a,j}, \qquad c_{a,j}^{(n)} \to c_{a,j},$$

so $b_{a,j} = (-ia) c_{a,j}$. Since $b \in \ell^2$,

$$\sum_{a,j} |a|^2 |c_{a,j}|^2 = \| b \|^2 < \infty.$$

Thus $c \in D(K)$ and $Kc = b$; hence K is closed.

The adjoint of a diagonal operator has the conjugate diagonal coefficients, and

$$|-ia| = |a| = |\overline{-ia}|,$$

so $D(K^*) = D(K)$. Hence $KK^* = K^*K$, and K is normal.

The function X is a nonzero entire function, so its zero set is finite in every bounded region. Hence $|a| \to \infty$ along every infinite sequence of zeros. For any $z \notin \{-ia\}$,

$$(K - zI)^{-1} e_{a,j} = \frac{1}{-ia - z} e_{a,j},$$

and the diagonal coefficients tend to zero. Finite-rank truncations therefore approximate $(K - zI)^{-1}$ in operator norm, so the resolvent is compact. The spectrum of a compact-resolvent diagonal operator consists precisely of the stated eigenvalues, with multiplicities $m(a)$. ▫

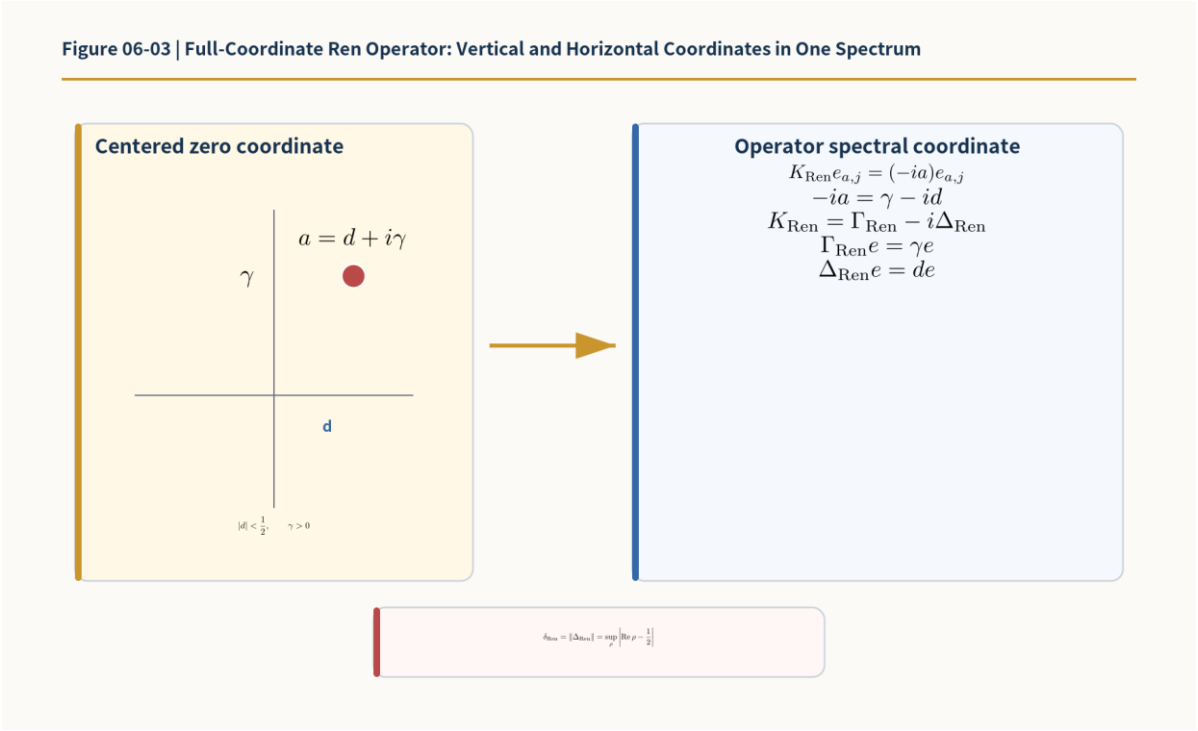


Figure 06-03. Full-coordinate Ren operator. For a centered zero $a = d + i\gamma$, the Ren eigenvalue is $-ia = \gamma - id$. Hence Γ_{Ren} reads the vertical coordinate γ, Δ_{Ren} reads the horizontal displacement d, and $K_{\mathrm{Ren}} = \Gamma_{\mathrm{Ren}} - i\Delta_{\mathrm{Ren}}$. The global invariant $\delta_{\mathrm{Ren}} = \| \Delta_{\mathrm{Ren}} \|$ compresses all horizontal deviations into one bounded operator quantity.

3.4 The Hidden Horizontal Operator

To avoid domain ambiguities in sums of unbounded operators, first define directly by diagonal action

$$\boxed{\Gamma_{\mathrm{Ren}} e_{a,j} = \gamma_a e_{a,j},}$$

with domain

$$D(\Gamma_{\mathrm{Ren}}) = \left\{ c : \sum_{a,j} \gamma_a^2 \, |c_{a,j}|^2 < \infty \right\},$$

and define the bounded operator

$$\boxed{\Delta_{\mathrm{Ren}} e_{a,j} = d_a e_{a,j}}$$

on all of $\mathcal{H}_{\mathrm{Ren}}$.

Since $|d_a| < 1/2$,

$$\boxed{\| \Delta_{\mathrm{Ren}} \| = \sup_{a \in Z_+} |d_a| \leq \frac{1}{2}.}$$

Because d_a is bounded,

$$D(\Gamma_{\mathrm{Ren}}) = D(K_{\mathrm{Ren}}).$$

Both operators are diagonal with respect to the same orthogonal decomposition, hence strongly commute, and

$$\boxed{K_{\mathrm{Ren}} = \Gamma_{\mathrm{Ren}} - i\Delta_{\mathrm{Ren}}, \qquad K_{\mathrm{Ren}}^{*} = \Gamma_{\mathrm{Ren}} + i\Delta_{\mathrm{Ren}}.}$$

On the common domain, $K - K^{*}$ equals the restriction of the bounded operator $-2i\Delta$. Hence its closure / bounded extension satisfies

$$\boxed{\| \overline{K_{\mathrm{Ren}} - K_{\mathrm{Ren}}^{*}} \| = 2 \| \Delta_{\mathrm{Ren}} \|.}$$

Define

$$\boxed{\delta_{\mathrm{Ren}} := \| \Delta_{\mathrm{Ren}} \| = \sup_{a \in \mathcal{Z}_{+}} |d_a|.}$$

Then

$$0 \leq \delta_{\mathrm{Ren}} \leq \frac{1}{2}.$$

Moreover,

$$\sigma(K_{\mathrm{Ren}}) \subset \{\lambda : \Re\lambda > 0,\ |\Im\lambda| < 1/2\}.$$

The joint point spectrum of the strongly commuting pair $(\Gamma_{\mathrm{Ren}}, \Delta_{\mathrm{Ren}})$ is

$$\boxed{\{(\gamma_a, d_a) : a \in \mathcal{Z}_{+}\},}$$

counted with analytic multiplicity. Thus the full Ren object retains both the vertical ordinate and the horizontal displacement usually suppressed in spectral routes.

3.5 The Reciprocal-Symmetry Operator

From

$$X(a) = 0 \Rightarrow X(-\bar{a}) = 0$$

with multiplicity preserved, the map

$$\iota(a) := -\bar{a}$$

is a multiplicity-preserving involution on $\mathcal{Z}_{+}$.

For each two-point orbit $\{a, \iota(a)\}$, choose a unitary identification between the corresponding multiplicity spaces; on a fixed point $a = \iota(a)$, equivalently $d_a = 0$, take the identity. This defines a linear unitary involution

$$\boxed{J_{\mathrm{Ren}} e_{a,j} = e_{-\bar{a},j}}$$

(the basis formula represents one choice of the unitary identifications above). Then

$$J_{\mathrm{Ren}}^{2} = I.$$

Proposition 3.4 (Reciprocal Spectral Symmetry)

$$\boxed{J_{\mathrm{Ren}} K_{\mathrm{Ren}} J_{\mathrm{Ren}} = K_{\mathrm{Ren}}^{*}.}$$

Equivalently,

$$J_{\mathrm{Ren}}\Gamma_{\mathrm{Ren}}J_{\mathrm{Ren}} = \Gamma_{\mathrm{Ren}}, \qquad J_{\mathrm{Ren}}\Delta_{\mathrm{Ren}}J_{\mathrm{Ren}} = -\Delta_{\mathrm{Ren}}.$$

Proof

For a basis vector $e_{a,j}$,

$$JKJe_{a,j} = JKe_{-\bar{a},j} = J\big(-i(-\bar{a})e_{-\bar{a},j}\big) = i\bar{a}\,e_{a,j}.$$

On the other hand,

$$K^*e_{a,j} = \overline{-ia}\,e_{a,j} = i\bar{a}\,e_{a,j}.$$

This proves the first identity; separating its real and imaginary parts gives the other two. ▫

3.6 Operator Form of RH

Theorem 3.5 (Equivalence of RH and Vanishing Hidden Horizontal Coordinate)

The following statements are equivalent:

1. the Riemann Hypothesis;
2. $d_a = 0$ for every $a \in \mathcal{Z}_+$;
3. $\Delta_{\mathrm{Ren}} = 0$;
4. $\delta_{\mathrm{Ren}} = 0$;
5. $K_{\mathrm{Ren}} = K_{\mathrm{Ren}}^*$;
6. K_{Ren} is a positive self-adjoint operator.

Hence

$$\boxed{\mathrm{RH} \Leftrightarrow \Delta_{\mathrm{Ren}} = 0 \Leftrightarrow \delta_{\mathrm{Ren}} = 0 \Leftrightarrow K_{\mathrm{Ren}} = K_{\mathrm{Ren}}^* > 0.}$$

Proof

A nontrivial zero $\rho = 1/2 + a$ satisfies RH exactly when $\Re a = d_a = 0$, so (1) and (2) are equivalent. Since $\Delta e_{a,j} = d_a e_{a,j}$, statements (2), (3), and (4) are equivalent.

Also,

$$K^* - K = 2i\Delta,$$

so (3) and (5) are equivalent. When $d_a = 0$,

$$Ke_{a,j} = \gamma_a e_{a,j}, \qquad \gamma_a > 0.$$

Because the zero set is finite in compact sets and there are no centered zeros on the real axis,

$$\gamma_* := \inf_{a\in\mathcal{Z}_+} \gamma_a > 0.$$

Therefore

$$K \geq \gamma_* I > 0.$$

Thus (2) implies (6), while a positive operator is self-adjoint by definition, so (6) implies (5). ▫

Under RH write

$$\boxed{H_{\mathrm{Ren}} := K_{\mathrm{Ren}}.}$$

Then

$$\sigma(H_{\mathrm{Ren}}) = \{\gamma_n\}, \qquad \mathrm{dimker}(H_{\mathrm{Ren}} - \gamma_n I) = m_n.$$

3.7 The Ren Square-Inverse Operator

By Lemma 3.1, $0 \notin \sigma(K_{\mathrm{Ren}})$. Since K has compact resolvent, K^{-1} is bounded and compact. Define

$$\boxed{B_{\mathrm{Ren}} := K_{\mathrm{Ren}}^{-2}.}$$

Its eigenvalues are

$$(-ia)^{-2} = -\frac{1}{a^2}.$$

Theorem 3.6 (Trace-Class Square Inverse)

$$\boxed{B_{\mathrm{Ren}} \in \mathfrak{S}_1.}$$

In particular, B_{Ren} is a normal trace-class operator, with

$$\| B_{\mathrm{Ren}} \|_1 = \sum_{a \in Z_+} \frac{m(a)}{|a|^2} < \infty.$$

Proof

Riemann–von Mangoldt counting gives

$$N(T) = O(T \log T)$$

for positive ordinates. Since $|a| \geq \gamma_a$, group the zeros with $\gamma_a \geq 1$ into dyadic shells $2^k \leq \gamma_a < 2^{k+1}$. Then

$$\sum_{\gamma_a \geq 1} \frac{m(a)}{|a|^2} \leq \sum_{k \geq 0} \frac{N(2^{k+1})}{2^{2k}} \ll \sum_{k \geq 0} \frac{k+1}{2^k} < \infty.$$

There are only finitely many low-height zeros, so the full sum converges. For a diagonal normal operator, the trace norm equals the sum of the absolute values of its eigenvalues. ▫

Theorem 3.7 (Equivalence of RH and Positivity of the Square Inverse)

$$\boxed{\mathrm{RH} \Leftrightarrow B_{\mathrm{Ren}} \geq 0.}$$

Proof

If RH holds, then $a = i\gamma_a$, and hence

$$-\frac{1}{a^2} = \frac{1}{\gamma_a^2} > 0,$$

so B_{Ren} is a positive trace-class operator.

Conversely, if $B_{\mathrm{Ren}} \geq 0$, then every diagonal eigenvalue $-1/a^2$ is positive real. Write $a = d + i\gamma$, with $\gamma > 0$. If $-1/a^2 \in \mathbb{R}_+$, then $a^2 \in \mathbb{R}_-$. Since

$$a^2 = (d^2 - \gamma^2) + 2id\gamma,$$

we have $2d\gamma = 0$. Because $\gamma > 0$, it follows that $d = 0$. Thus all centered zeros lie on the imaginary axis, and RH holds. ▫

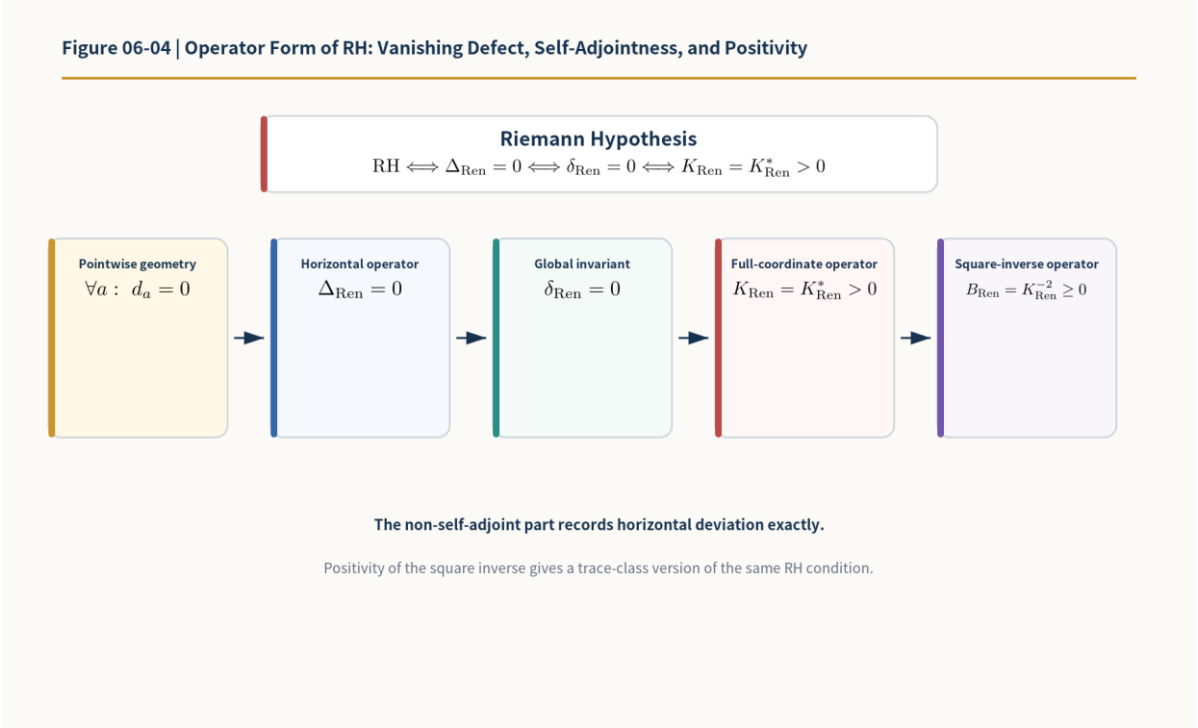


Figure 06-04. Operator form of RH. Theorem 3.5 rewrites the pointwise condition $d_a = 0$ equivalently as $\Delta_{\mathrm{Ren}} = 0$, $\delta_{\mathrm{Ren}} = 0$, and $K_{\mathrm{Ren}} = K^*_{\mathrm{Ren}} > 0$. Theorem 3.7 gives the same condition as positivity of the trace-class square inverse $B_{\mathrm{Ren}} = K^{-2}_{\mathrm{Ren}}$. These are not additional RH hypotheses, but operator-level readings of the same horizontal closure.

4. Fredholm Determinants and Resolvent Recovery

This section uses canonical products of entire functions and trace-class determinant theory.

4.1 Unconditional Fredholm-Determinant Recovery

Define

$$G(y) := \frac{X(\sqrt{y})}{X(0)}.$$

Because X is even, its even Taylor series uniquely defines an entire function G with

$$X(w) = X(0)G(w^2).$$

Lemma 4.1 (Hadamard Factorization in the Squared Variable)

The function G has order $1/2$, and its zeros are exactly

$$\{a^2 : a \in \mathcal{Z}_+\}$$

with multiplicities $m(a)$. Moreover,

$$\boxed{G(y) = \prod_{a \in \mathcal{Z}_+} \left(1 - \frac{y}{a^2}\right)^{m(a)}.}$$

Proof

The standard completed Riemann function ξ is an entire function of order 1, so X is also of order 1. Since

$$M_G(r) = M_X(\sqrt{r})/|X(0)|,$$

G has order $1/2$. Lemma 3.1 shows that X has no real zeros, so each $\{a, -a\}$-orbit is represented by a unique $a \in \mathcal{Z}_+$. If a is a zero of multiplicity m, evenness gives $-a$ with the same multiplicity, and the local factors combine as

$$(z - a)^m (z + a)^m = (z^2 - a^2)^m.$$

Thus a^2 is a zero of G of multiplicity m.

By Theorem 3.6,

$$\sum_a \frac{m(a)}{|a^2|} < \infty,$$

so the canonical product over the zeros has genus zero. For an entire function of order < 1, Hadamard factorization permits only a constant exponential factor:

$$G(y) = e^c \prod_a \left(1 - \frac{y}{a^2}\right)^{m(a)}.$$

Since $G(0) = 1$, $e^c = 1$. ▫

Theorem 4.2 (Unconditional Ren–Fredholm Identity)

For every $w \in \mathbb{C}$,

$$\boxed{\frac{X(w)}{X(0)} = \det(I + w^2 B_{\mathrm{Ren}}) = \det(I + w^2 K_{\mathrm{Ren}}^{-2}).}$$

This identity does not use RH.

Proof

By Theorem 3.6, B_{Ren} is trace class, so its Fredholm determinant is well defined, with

$$\det(I + yB_{\mathrm{Ren}}) = \prod_{a \in \mathcal{Z}_+} \left(1 + y\left(-\frac{1}{a^2}\right)\right)^{m(a)} = \prod_a \left(1 - \frac{y}{a^2}\right)^{m(a)}.$$

By Lemma 4.1, this product equals $G(y)$. Put $y = w^2$ and use $G(w^2) = X(w)/X(0)$. ▫

4.2 Resolvent Trace and Logarithmic Derivative

Theorem 4.3 (Resolvent-Trace / Logarithmic-Derivative Identity)

If $X(w) \neq 0$, then

$$\boxed{\frac{X'(w)}{X(w)} = 2w\mathrm{Tr}[B_{\mathrm{Ren}}(I + w^2 B_{\mathrm{Ren}})^{-1}].}$$

Proof

Let

$$D(y) = \det(I + yB_{\mathrm{Ren}}).$$

For trace-class B, at points where $I + yB$ is invertible, the standard differentiation formula for the Fredholm determinant gives

$$\frac{D'(y)}{D(y)} = \mathrm{Tr}(B(I + yB)^{-1}).$$

By Theorem 4.2, $X(w)/X(0) = D(w^2)$. The chain rule gives

$$\frac{X'(w)}{X(w)} = 2w\frac{D'(w^2)}{D(w^2)},$$

and substitution yields the formula. ▫

Thus the full Ren object recovers both the zero divisor and the logarithmic response of the completed object. Under RH,

$$B_{\mathrm{Ren}} = H_{\mathrm{Ren}}^{-2} \geq 0,$$

and the formula specializes to the positive self-adjoint resolvent trace.

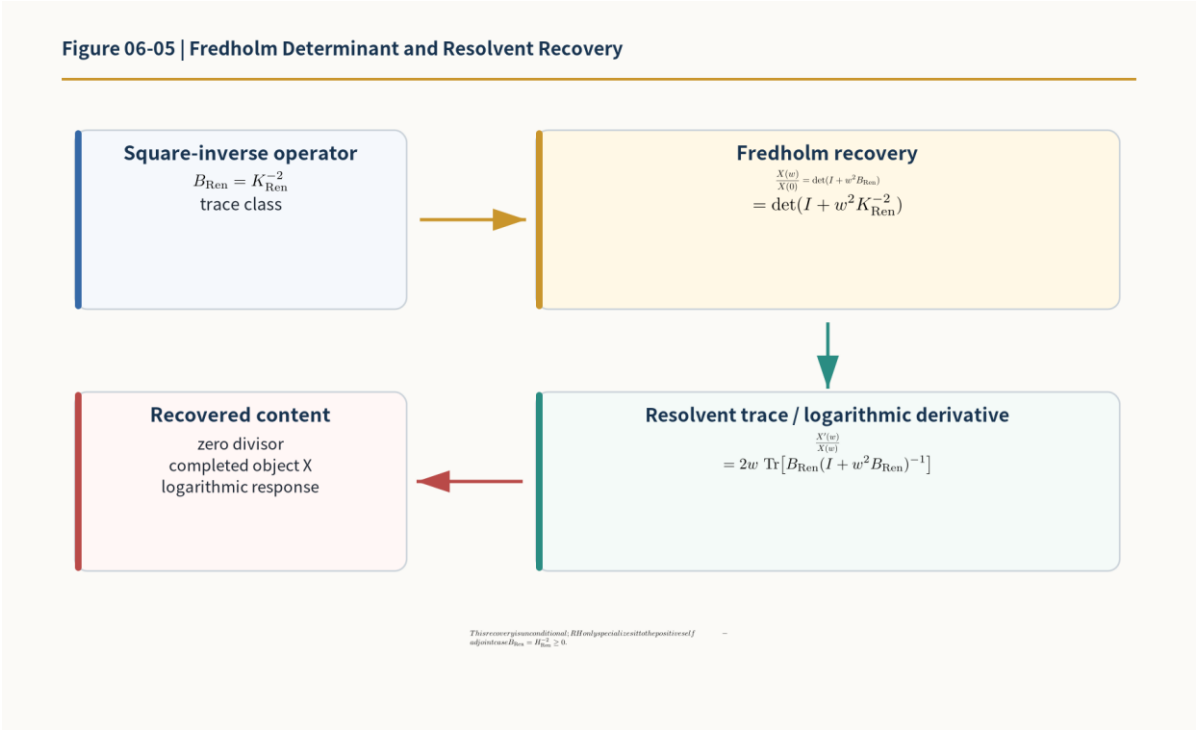


Figure 06-05. Fredholm and resolvent recovery. The unconditional trace-class operator $B_{\mathrm{Ren}} = K_{\mathrm{Ren}}^{-2}$ gives $\frac{X(w)}{X(0)} = \det(I + w^2 B_{\mathrm{Ren}})$; the standard differential formula for Fredholm determinants then recovers X'/X. The Ren object therefore recovers not only the zero divisor but also the completed function and its logarithmic response. This recovery chain itself does not assume RH.

5. The Fully Marked Ren–Riemann Object and Reverse Recovery

5.1 The Fully Marked Ren–Riemann Object

To avoid incorrectly attributing recoverability to the "bare spectrum," define

$$\boxed{\boldsymbol{R}_{\mathrm{Ren}}^{\mathrm{full}} = (\mathcal{H}_{\mathrm{Ren}}, K_{\mathrm{Ren}}, J_{\mathrm{Ren}}, c_*, \kappa_*, C_\xi).}$$

Here

$$c_* = \frac{1}{2},$$

$$\kappa_* = X(0) = \xi\left(\frac{1}{2}\right),$$

and

$$C_\xi(s) = \frac{1}{2}s(s-1)\pi^{-s/2}\Gamma(s/2).$$

These marks preserve, respectively:

- the divisor Hilbert space and analytic multiplicities;
- the full centered zero coordinates;
- reciprocal/reflection symmetry;

- the central anchor;
- Fredholm normalization;
- completion normalization / the Archimedean mark.

The notation

$$\boxed{K_{\mathrm{Ren}} \subset \boldsymbol{R}_{\mathrm{Ren}}^{\mathrm{full}}}$$

expresses an information hierarchy between the bare operator and the fully marked object: beyond the operator itself, the latter retains the central anchor, normalization, completion mark, and reciprocal symmetry.

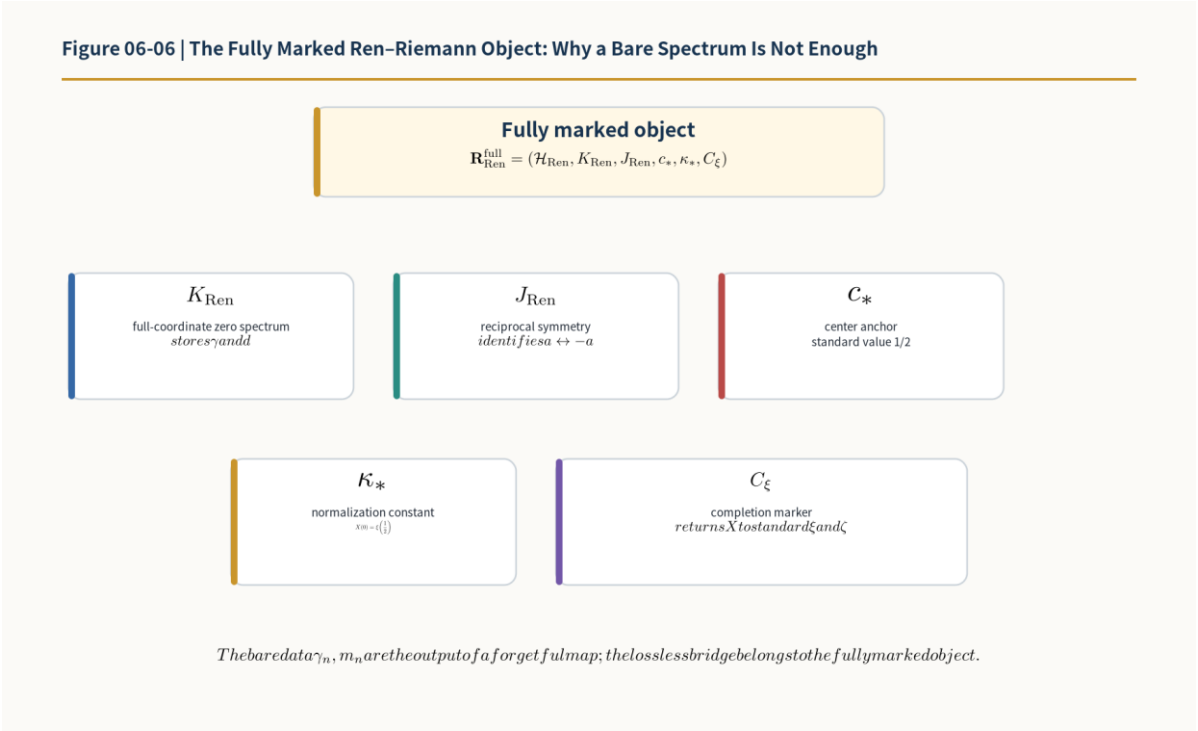


Figure 06-06. Fully marked Ren–Riemann object. K_{Ren} stores the full-coordinate zero divisor, J_{Ren} stores reciprocal orbits, c_* fixes the center anchor, $\kappa_* = X(0)$ fixes normalization, and C_ξ stores the standard completion marker. Together these data form $\boldsymbol{R}_{\mathrm{Ren}}^{\mathrm{full}}$. Forgetting the markers leaves only $\{\gamma_n, m_n\}$, so lossless recovery must not be attributed to the bare spectrum.

5.2 Recovering X from the Full Ren Object

From

$$B_{\mathrm{Ren}} = K_{\mathrm{Ren}}^{-2}$$

and Theorem 4.2,

$$\boxed{X(w) = \kappa_* \det(I + w^2 K_{\mathrm{Ren}}^{-2}).}$$

Therefore

$$\boxed{\boldsymbol{R}_{\mathrm{Ren}}^{\mathrm{full}} \Rightarrow X.}$$

This gives exact recovery of X from the fully marked object.

5.3 Recovering ξ from X

Using the central anchor

$$c_* = \frac{1}{2},$$

we have

$$\boxed{\xi(s) = X(s - c_*).}$$

Hence

$$\boxed{\boldsymbol{R}^{\text{full}}_{\text{Ren}} \Rightarrow \xi.}$$

5.4 Recovering the Global ζ-Function from ξ

From the completion mark C_ξ,

$$\boxed{\zeta_{\text{global}}(s) = \frac{\xi(s)}{C_\xi(s)}}$$

in the meromorphic sense.

Thus

$$\boxed{\boldsymbol{R}^{\text{full}}_{\text{Ren}} \Rightarrow \zeta_{\text{global}}.}$$

5.5 Returning from Global ζ to the Pre-Continuation Germ

Restriction gives

$$\boxed{\zeta_{\text{germ}} = \zeta_{\text{global}}|_{\Re s>1}.}$$

Therefore

$$\boxed{\boldsymbol{R}^{\text{full}}_{\text{Ren}} \Rightarrow \zeta_{\text{germ}}.}$$

This returns us to the Dirichlet/Euler analytic germ on $\Re s > 1$.

5.6 Recovering the Multiplicative Logarithmic Ledger from ζ_{germ}

By Theorem 2.1, within the class of locally finite positive measures possessing an exponential moment in some right half-plane, ζ_{germ} uniquely determines

$$\eta_\times = \sum_{n\geq 1} \delta_{\log n}.$$

Let

$$S_\times = \text{supp}\eta_\times.$$

On the recovered real scale, define

$$\mathcal{R}_{\times}^{\log} = \{(x, y, z) \in S_{\times}^{3} : x + y = z\}.$$

Next set

$$\mathbb{N}_{\eta} := \{e^{x} : x \in S_{\times}\}.$$

Because the unique recovered measure is precisely $\sum_{n} \delta_{\log n}$, we have $\mathbb{N}_{\eta} = \mathbb{N}$, and

$$x + y = z \Leftrightarrow e^{x} e^{y} = e^{z}.$$

Theorem 5.1 (Multiplicative Identity Recovery Theorem)

From the fully marked Ren–Riemann object one can deterministically recover the multiplicative system together with its scale mark:

$$\boxed{\boldsymbol{R}_{\mathrm{Ren}}^{\mathrm{full}} \Rightarrow (\mathbb{N}, \mathcal{R}_{\times}, \ell), \qquad \ell(n) = \log n.}$$

Proof

Theorem 4.2 together with the normalization mark κ_{*} recovers X. The central anchor then recovers ξ. The completion multiplier C_{ξ} recovers ζ_{global} by meromorphic division, and restriction to $\Re s > 1$ yields ζ_{germ}. Theorem 2.1 uniquely recovers $\eta_{\times}$, while the additive relation on its support recovers $mq = n$ under exponentiation. Every step is deterministic, so the conclusion follows. ▫

5.7 A Second Reverse Channel: Euler–Möbius–von Mangoldt

From the recovered ζ_{germ}, for $\Re s > 1$,

$$\boxed{\zeta(s) = \prod_{p} (1 - p^{-s})^{-1}.}$$

Its reciprocal expansion is

$$\boxed{\frac{1}{\zeta(s)} = \sum_{n \geq 1} \frac{\mu(n)}{n^{s}}.}$$

Its logarithmic derivative is

$$\boxed{-\frac{\zeta'(s)}{\zeta(s)} = \sum_{n \geq 1} \frac{\Lambda(n)}{n^{s}}.}$$

Uniqueness of Dirichlet series therefore recovers

$$\mu(n), \qquad \Lambda(n).$$

In particular,

$$\Lambda(n) > 0 \Leftrightarrow n = p^{k}.$$

Hence the full Ren object also recovers

$$\boxed{\text{prime-power source information.}}$$

This channel cross-checks the logarithmic-ledger recovery:

$$\boxed{\eta_\times \quad \| \quad \text{Euler} \quad \| \quad \mu \quad \| \quad \Lambda.}$$

5.8 Recovering Prime Generators Internally from the Logarithmic Ledger

Let

$$S_\times^+ = S_\times \backslash \{0\},$$

and define the additively indecomposable elements

$$P_{\log} = \{x \in S_\times^+ : \nexists\, y, z \in S_\times^+ \text{ such that } x = y + z\}.$$

Proposition 5.2 (Recovering the Primes from Additively Indecomposable Elements)

$$\boxed{P_{\log} = \{\log p : p \text{prime}\}.}$$

Proof

If $n = ab$ is composite with $a, b > 1$, then

$$\log n = \log a + \log b,$$

so $\log n \notin P_{\log}$. Conversely, if p is prime and

$$\log p = \log a + \log b$$

for integers $a, b > 1$, exponentiation gives $p = ab$, a contradiction. Hence $\log p \in P_{\log}$. ▫

Thus $\eta_\times$ recovers not only the multiplicative relation but also the prime generators and the unique prime-exponent coordinates internal to that relation. This channel and the von Mangoldt channel give two recoveries of the same prime-generative structure.

6. Forward Generation, Reverse Recovery, and the Lossless Bridge

6.1 Forward Chain: From Multiplicative Identity to the Ren Object

Starting from

$$\mathfrak{M}_\times = (\mathbb{N}, \mathcal{R}_\times, \ell),$$

construct

$$\eta_\times = \sum_n \delta_{\ell(n)}.$$

Then

$$\eta_\times \to \zeta_{\text{germ}}$$

by the Laplace transform;

$$\zeta_{\mathrm{germ}} \to \zeta_{\mathrm{global}}$$

by unique meromorphic continuation;

$$\zeta_{\mathrm{global}} \to \xi$$

by the registered completion;

$$\xi \to X$$

by centering;

and

$$X \to \mathcal{Z}_+ \to K_{\mathrm{Ren}}, J_{\mathrm{Ren}}$$

by the zero-divisor construction.

Therefore

$$\boxed{\mathfrak{M}_\times \Rightarrow \boldsymbol{R}_{\mathrm{Ren}}^{\mathrm{full}}.}$$

6.2 Reverse Chain: From the Ren Object Back to Multiplicative Identity

By Section 5,

$$\boxed{\boldsymbol{R}_{\mathrm{Ren}}^{\mathrm{full}} \Rightarrow X \Rightarrow \xi \Rightarrow \zeta_{\mathrm{global}} \Rightarrow \zeta_{\mathrm{germ}} \Rightarrow \eta_\times \Rightarrow \mathfrak{M}_\times.}$$

6.3 The Multiplicative–Analytic–Spectral Lossless Bridge

Theorem 6.1 (Bidirectional Recoverability under the Standard Riemann Normalization)

Fix the standard Riemann normalization:

1. the standard positive integers and real-number structure;
2. the scale mark

$$\ell(n) = \log n;$$

3. the central anchor

$$c_* = \frac{1}{2};$$

4. the standard completion multiplier C_ξ;
5. the normalization

$$\kappa_* = \xi(1/2).$$

Existence and uniqueness of analytic continuation are taken from the standard uniqueness theorem of complex analysis.

Then there is a deterministic forward chain

$$\boxed{\mathfrak{M}_\times \to \zeta_{\mathrm{germ}} \to \zeta_{\mathrm{global}} \to \xi \to X \to \boldsymbol{R}_{\mathrm{Ren}}^{\mathrm{full}}}$$

and a deterministic reverse chain

$$\boxed{\boldsymbol{R}^{\mathrm{full}}_{\mathrm{Ren}} \to X \to \xi \to \zeta_{\mathrm{global}} \to \zeta_{\mathrm{germ}} \to \mathfrak{M}_{\times}.}$$

Forward followed by reverse recovers the original $\mathfrak{M}_{\times}$. Reverse followed by forward recovers the same centered zero divisor, the same scalar marks, and a Ren structured spectral object that is marked-unitarily equivalent to the original one.

Proof

For the forward chain, the scale mark of $\mathfrak{M}_{\times}$ gives

$$\eta_{\times} = \sum_{n} \delta_{\log n}.$$

Its Laplace transform gives ζ_{germ}; unique meromorphic continuation gives ζ_{global}; multiplication by C_{ξ} gives ξ; translation by c_* gives X; and the upper-half-plane zero divisor together with its multiplicities constructs K and the reciprocal involution J. Adding c_*, κ_*, C_{ξ} yields $\boldsymbol{R}^{\mathrm{full}}_{\mathrm{Ren}}$.

The reverse chain is exactly Theorem 5.1. Hence forward followed by reverse recovers $\eta_{\times}$, and therefore the same scale-marked multiplicative system.

For reverse followed by forward, Theorem 4.2 recovers the same X, and therefore the same centered zero divisor with the same multiplicities. By the spectral classification of diagonal normal operators, the resulting K is unitarily equivalent to the original K. On each non-fixed reciprocal orbit, the two admissible unitary pairings can be conjugated by a block-diagonal unitary acting on the two multiplicity spaces; on a fixed orbit the canonical choice is $J = I$. Therefore, together with the scalar marks, the two full objects are marked-unitarily equivalent. ▫

Terminology

This bidirectional recoverability is called

$$\boxed{\textbf{the multiplicative–analytic–spectral lossless bridge}.}$$

Here “lossless” means bidirectional recoverability of the canonical information under the standard Riemann normalization. Distinct mathematical types retain their own object identities, and the bare spectrum remains distinct from the fully marked object.

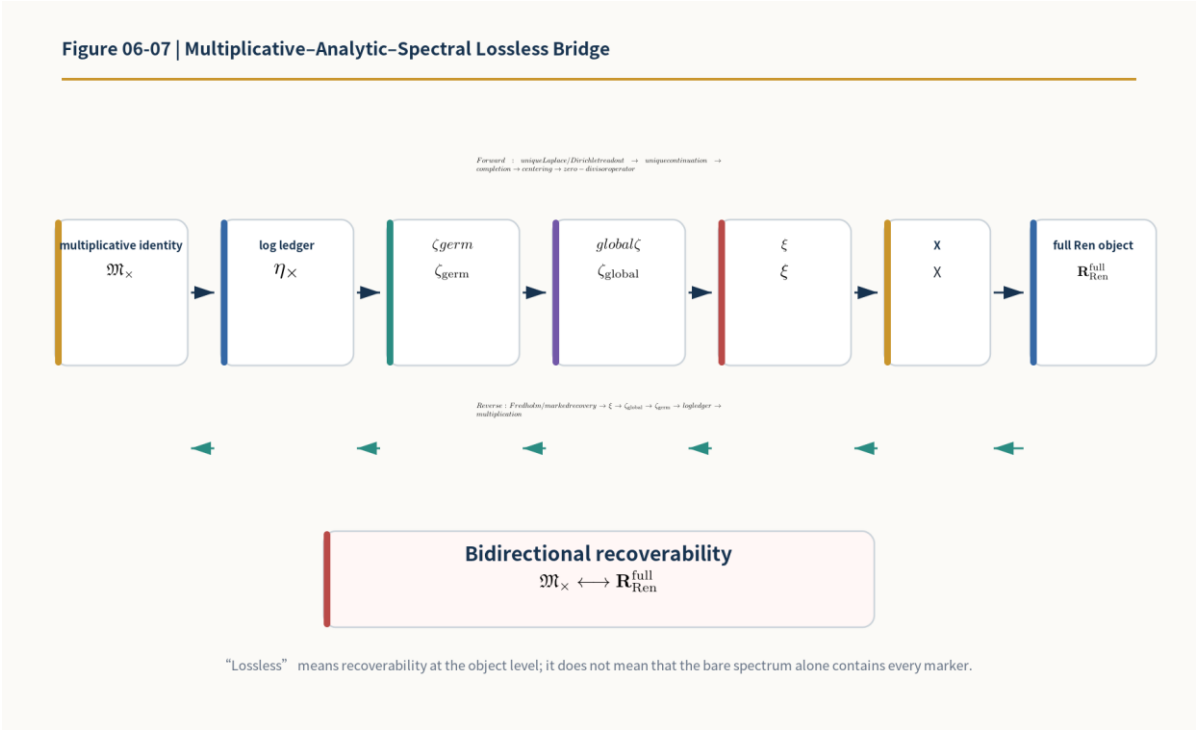


Figure 06-07. Multiplicative–analytic–spectral lossless bridge. The forward chain moves from multiplicative identity through the logarithmic ledger, Dirichlet germ, unique meromorphic continuation, completion, centering, and finally the fully marked Ren object. The reverse chain uses Fredholm recovery, completion markers, and Dirichlet/Laplace uniqueness to return step by step to the original multiplicative identity. "Lossless" therefore means bidirectional recoverability between the complete object levels, not that every intermediate projection contains every marker.

6.4 What "Lossless" Means at the Object Level

"Lossless" means that the canonical information can be recovered in both directions across different object types.

There are explicit recovery maps:

$$\begin{aligned}&\text{generative source} \to \text{analytic germ} \to \\ &\text{global analytic object} \to \text{completed object} \to \\ &\text{spectral object},\end{aligned}$$

and, under the chosen normalization, a reverse readout:

$$\begin{aligned}&\text{spectral object} \to \text{completed object} \to \\ &\text{global analytic object} \to \text{analytic germ} \to \\ &\text{generative source}.\end{aligned}$$

Thus

> what is reversible is the canonical information; distinct mathematical types retain their own object identities.

6.5 Canonical Uniqueness

Define two fully marked Ren objects to be **marked-unitarily equivalent** if there exists a unitary

$$U: \mathcal{H}_{\mathrm{Ren}}^{(1)} \to \mathcal{H}_{\mathrm{Ren}}^{(2)}$$

such that

$$UK_{\mathrm{Ren}}^{(1)}U^{-1} = K_{\mathrm{Ren}}^{(2)}, \qquad UJ_{\mathrm{Ren}}^{(1)}U^{-1} = J_{\mathrm{Ren}}^{(2)},$$

and the scalar marks c_*, κ_*, C_ξ agree.

Theorem 6.2 (Marked-Unitary Uniqueness)

Any two fully marked Ren objects constructed from the same X by Definitions 9–12 of this chapter are marked-unitarily equivalent.

Proof

The two constructions have the same centered zero divisor with the same analytic multiplicities. Thus their K-operators are normal diagonal operators with identical pure-point spectra and identical eigenspace multiplicities. Choosing a unitary eigenspace by eigenspace gives

$$UK^{(1)}U^{-1} = K^{(2)}.$$

It remains to intertwine J. On each two-element orbit $\{a, -\bar{a}\}$ of the reciprocal involution, J is merely a unitary identification between two multiplicity spaces of equal dimension, together with its inverse. Given two such choices V_1, V_2, fix the unitary on one side to be the identity and take $V_2V_1^{-1}$ on the other. This conjugates the two J-operators. On a fixed orbit $a = -\bar{a}$, the convention of this chapter is $J = I$, leaving no further freedom. Taking the direct sum over all reciprocal orbits yields a global unitary simultaneously intertwining K and J. Since the scalar marks are already identical, the result follows. ▫

Denote this marked-unitary equivalence class by

$$\boxed{\mathfrak{R}_{\mathrm{Ren}}^{\mathrm{full}}.}$$

7. RH Specialization, Bare-Spectral Readout, and Interfaces with the Rest of the Book

Once the Riemann Hypothesis holds, the full Ren object has a positive self-adjoint specialization and interfaces, at distinct levels, with the spectral witness of Chapter 7, the two-point GUE relations of Chapter 8, and the independent Hilbert–Pólya route of Chapter 9.

7.1 The Ren–Riemann Spectral Class

From

$$K_{\mathrm{Ren}} = H_{\mathrm{Ren}} > 0$$

define

$$\boxed{\mathfrak{R}_{\mathrm{Ren}} := [H_{\mathrm{Ren}}]_{\mathrm{u}}.}$$

This is a downstream spectral readout of the fully marked unitary-equivalence class

$$\mathfrak{R}_{\mathrm{Ren}}^{\mathrm{full}}.$$

The former primarily preserves eigenvalues and analytic multiplicities; the latter also preserves the central anchor, completion mark, reciprocal symmetry, and the multiplicative–analytic recovery structure.

7.2 The Bare-Spectral Forgetful Map

Define the forgetful map

$$\boxed{\mathcal{F}_{\mathrm{bare}}: \mathfrak{R}_{\mathrm{Ren}}^{\mathrm{full}} \to [H_{\mathrm{Ren}}]_{\mathrm{u}},}$$

which, after RH, forgets the completion mark, central anchor, and recovery structure and retains only

$$\{\gamma_n, m_n\}.$$

Further define

$$\boxed{D_{\mathrm{Ren}} = H_{\mathrm{Ren}} \oplus (-H_{\mathrm{Ren}}),}$$

so that

$$\sigma(D_{\mathrm{Ren}}) = \{\pm\gamma_n\}$$

with analytic multiplicities. This bilateral spectrum is the direct input for the second-order self-relations of Chapter 8.

7.3 Interface with the Spectral Witness of Chapter 7

The canonical spectral terminal object in this chapter is

$$H_{\mathrm{Ren}}, \qquad \mathfrak{R}_{\mathrm{Ren}}.$$

Chapter 7 takes this object as its canonical spectral interface and establishes the Riemann spectral identity-witness structure

$$F_{\mathrm{R}} \Leftrightarrow \nu_{\mathrm{R}} \Leftrightarrow (H_{\mathrm{id}}, M_{\mathrm{mult}}) \Leftrightarrow H_{\mathrm{Ren}}.$$

7.4 Relation to the Independent Hilbert–Pólya Route of Chapter 9

This chapter and Chapter 9 run in opposite generative directions.

This chapter begins with the completed Riemann zero divisor and passes to the canonical spectrum:

$$\boxed{\begin{array}{r}\text{completed Riemann zero divisor} \to \\ \text{canonical spectral realization} \leftrightarrow \\ \text{multiplicative–analytic recovery.}\end{array}} \tag{7.1}$$

Chapter 9 begins independently from the multiplicative generative source and passes to a self-adjoint spectrum:

$$\boxed{\begin{array}{r}\text{multiplicative generative source} \rightarrow \\ \text{positive self-adjoint spectrum} \rightarrow \\ \text{canonical terminal identification.}\end{array}} \tag{7.2}$$

Thus this chapter gives a lossless realization from the closed zero divisor to the canonical spectrum, whereas Chapter 9 gives an independent Hilbert–Pólya construction starting from the generative source.

7.5 Additional Structure of the Full Ren Object Beyond the Bare Diagonal Spectrum

If one keeps only

$$He_n = \gamma_n e_n,$$

the resulting object preserves the vertical eigenvalues and their multiplicities. The full Ren object additionally preserves

$$\boxed{K_{\mathrm{Ren}} = \Gamma_{\mathrm{Ren}} - i\Delta_{\mathrm{Ren}},}$$

and therefore records the horizontal coordinates before RH; it preserves

$$\boxed{J_{\mathrm{Ren}} K_{\mathrm{Ren}} J_{\mathrm{Ren}} = K_{\mathrm{Ren}}^{*},}$$

and therefore records reciprocal symmetry; and through

$$\boxed{B_{\mathrm{Ren}} = K_{\mathrm{Ren}}^{-2}}$$

it yields

$$\boxed{X(w) = X(0)\det(I + w^2 B_{\mathrm{Ren}}),}$$

from which the completed analytic object can be recovered. Inverting the completion, restricting, and applying Laplace/Dirichlet uniqueness then returns

$$\boxed{\mathcal{R}_{\times}.}$$

The fully marked Ren–Riemann object is therefore a canonical structured spectral object that supports bidirectional read/write between multiplicative identity, analytic continuation, and the spectrum.

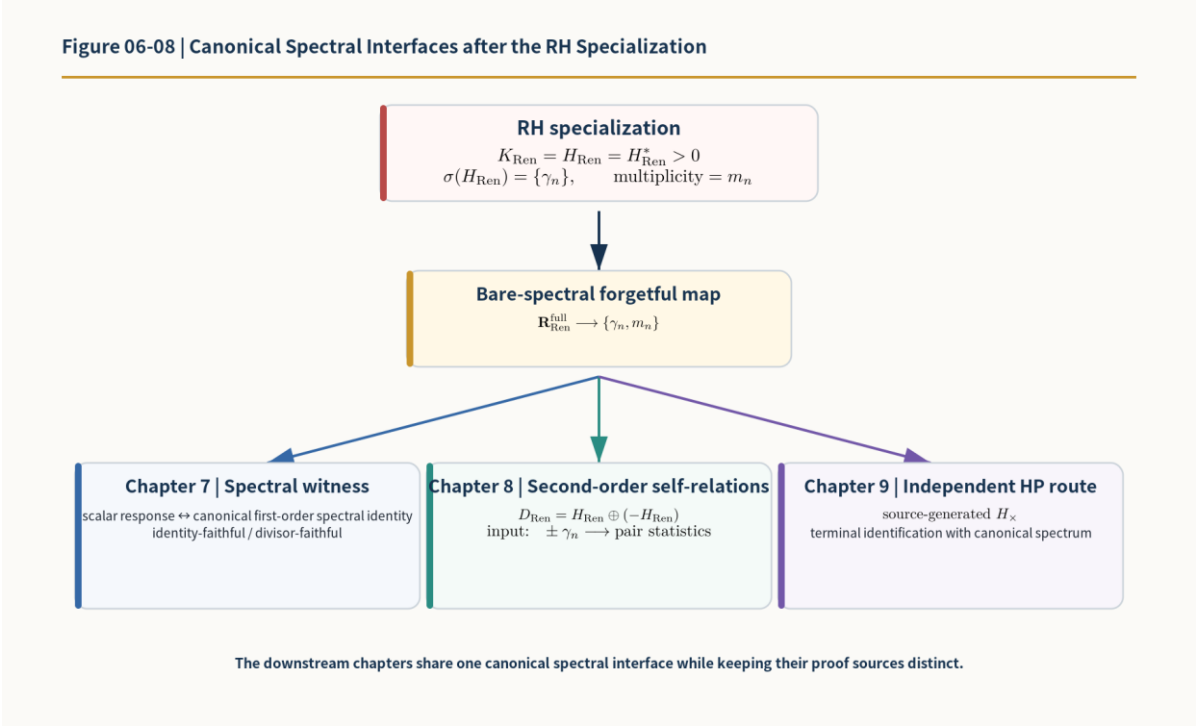


Figure 06-08. Canonical spectral interfaces after the RH specialization. Under RH, K_{Ren} specializes to the positive self-adjoint H_{Ren}, while the bare-spectral forgetful map retains only $\{\gamma_n, m_n\}$. Chapter 7 re-identifies this canonical first-order spectrum through a scalar spectral witness; Chapter 8 uses the signed operator $D_{\mathrm{Ren}} = H_{\mathrm{Ren}} \oplus (-H_{\mathrm{Ren}})$ to enter second-order self-relations; and Chapter 9 reaches the canonical spectrum terminally from an independently source-generated Hilbert–Pólya route. The downstream interfaces share one canonical spectrum while keeping their proof sources distinct.

8. Operator Readouts and Immediate Consequences

The following subsections record spectral readouts obtained directly from the operator structure developed in this chapter.

8.1 A Common Base for Zero Geometry, Analytic Multiplicity, and Second-Order Spectral Statistics

After RH,

$$H_{\mathrm{Ren}}$$

stores uniformly

$$\{\gamma_n, m_n\}.$$

Therefore zero counting may be written as

$$\boxed{N(T) = \mathrm{Tr}\mathbf{1}_{(0,T]}(H_{\mathrm{Ren}}),}$$

while analytic multiplicity is

$$\boxed{m_n = \dim\ker(H_{\mathrm{Ren}} - \gamma_n I).}$$

This stores the same multiplicity data m_n as the analytic multiplicity operator of Chapter 3,

$$\boxed{M_{\mathrm{mult}} e_n = m_n e_n.}$$

Chapter 3 retains analytic multiplicity as a separate diagonal mark; the present chapter realizes it as the eigenspace dimension of H_{Ren}.

After ordering the γ_n, the adjacent gaps of Chapter 2 are read directly as

$$\boxed{\Delta_n = \gamma_{n+1} - \gamma_n.}$$

The signed version

$$D_{\mathrm{Ren}} = H_{\mathrm{Ren}} \oplus (-H_{\mathrm{Ren}})$$

then supplies the bilateral spectral input required for the second-order spectral statistics of Chapter 8.

Thus the zero gaps of Chapter 2, the analytic multiplicities of Chapter 3, and the second-order statistics of Chapter 8 share one canonical spectral base.

8.2 A Global Operator Expression for Horizontal Deviation

The full Ren operator gives

$$K_{\mathrm{Ren}} = \Gamma_{\mathrm{Ren}} - i\Delta_{\mathrm{Ren}}.$$

Hence

$$\boxed{\delta_{\mathrm{Ren}} = \| \Delta_{\mathrm{Ren}} \| = \sup_{\rho} \left| \Re\rho - \frac{1}{2} \right|}$$

compresses the pointwise horizontal displacement into a single bounded operator invariant.

At the same time,

$$\boxed{\mathrm{RH} \Leftrightarrow \delta_{\mathrm{Ren}} = 0 \Leftrightarrow K_{\mathrm{Ren}} = K_{\mathrm{Ren}}^{*}.}$$

Thus horizontal zero displacement has a unified operator-theoretic expression:

$$\boxed{\text{horizontal zero defect} \leftrightarrow \text{self-adjointness defect.}}$$

This equivalence compresses the horizontal displacement of all zeros into a global defect of self-adjointness.

8.3 Consistency Across the Zero, Analytic, and Multiplicative Sides

From

$$B_{\mathrm{Ren}} = K_{\mathrm{Ren}}^{-2}$$

one recovers

$$\frac{X(w)}{X(0)} = \det(I + w^2 B_{\mathrm{Ren}})$$

and

$$\frac{X'(w)}{X(w)} = 2w\mathrm{Tr}[B_{\mathrm{Ren}}(I + w^2 B_{\mathrm{Ren}})^{-1}].$$

On the other hand,

$$X \to \xi \to \zeta_{\mathrm{global}} \to \zeta_{\mathrm{germ}}$$

returns to

$$\zeta(s) = \sum_{n\geq 1} n^{-s} = \prod_p (1 - p^{-s})^{-1}, \qquad \Re s > 1,$$

and

$$-\frac{\zeta'}{\zeta}(s) = \sum_{n\geq 1} \frac{\Lambda(n)}{n^s}.$$

Thus the chapter provides a three-sided consistency structure:

zero divisor ↔ Fredholm/resolvent response ↔ Euler/Dirichlet multiplicative generative source.

The three descriptions mutually check one another through the same full Ren object and read different information layers of the same Riemann object.

8.4 Finite Spectral Truncation and Computable Readouts

Actual computation can use only finitely many zeros. Let

$$H_{\mathrm{Ren},N}, \qquad B_{\mathrm{Ren},N} = H_{\mathrm{Ren},N}^{-2}$$

be the finite-rank truncations associated with the first N spectral points.

One may compute

$$\boxed{D_N(w) = \det(I + w^2 B_{\mathrm{Ren},N})}$$

as an approximation to

$$\frac{X(w)}{X(0)},$$

and

$$\boxed{R_N(w) = 2w\mathrm{Tr}\left[B_{\mathrm{Ren},N}(I + w^2 B_{\mathrm{Ren},N})^{-1}\right]}$$

as an approximation to

$$\frac{X'(w)}{X(w)}.$$

The finite truncations themselves are rigorously defined. Their errors are controlled by the trace-class tail.

Thus the computable readout is

finite spectral truncation → finite-precision readout of the completed analytic object.

This gives a spectral approximation framework from finite zero data to the completed analytic object.

8.5 Structural Position of the Operator Layer

The full Ren object supports the following chain of readouts:

$$\begin{array}{c}\text{closed vertical zero spectrum and analytic multiplicities}\\ \Downarrow\\ \text{global horizontal-deviation operator}\\ \Downarrow\\ \text{Fredholm/resolvent analytic recovery}\\ \Downarrow\\ \text{multiplicative–analytic–spectral bidirectional recoverability}\\ \Downarrow\\ \text{finite spectral-truncation readout.}\end{array} \tag{8.1}$$

Chapter 6 thereby completes the construction from the closed zero divisor to the canonical spectral object. Chapter 7 proceeds to spectral identity witnesses, Chapter 8 to second-order statistical structure, and Chapter 9 independently constructs another self-adjoint spectral route from the multiplicative generative source.

9. Structural Summary and Conclusion

9.1 Core Structure

The structure of this chapter is summarized by three groups of relations.

First,

$$\boxed{\mathrm{RH} \Leftrightarrow \Delta_{\mathrm{Ren}} = 0 \Leftrightarrow K_{\mathrm{Ren}} = K_{\mathrm{Ren}}^{*} > 0.}$$

Second,

$$\boxed{\mathfrak{M}_{\times} \leftrightarrow \boldsymbol{R}_{\mathrm{Ren}}^{\mathrm{full}}.}$$

Third,

$$\boxed{\boldsymbol{R}_{\mathrm{Ren}}^{\mathrm{full}} \supset K_{\mathrm{Ren}} \overset{\mathrm{RH}}{\to} H_{\mathrm{Ren}} \to D_{\mathrm{Ren}}.}$$

The first relation records the operator condition for the Riemann Hypothesis; the second records multiplicative–analytic–spectral bidirectional recoverability; the third records the information hierarchy from the fully marked object to downstream spectral readouts.

9.2 Theorems and Interfaces

The principal results of this chapter and their roles in the book are as follows:

Object or conclusion	Mathematical content	Role in the book
K_{Ren}	Closed normal operator defined from the centered zero divisor	Core object of Chapter 6

Object or conclusion	Mathematical content	Role in the book
$K_{\mathrm{Ren}} = \Gamma_{\mathrm{Ren}} - i\Delta_{\mathrm{Ren}}$	Strongly commuting decomposition into vertical coordinate and horizontal deviation	Consistent with the coordinate spectral atlas of Chapter 5
$\delta_{\mathrm{Ren}} = \| \Delta_{\mathrm{Ren}} \|$	Global horizontal deviation	RH iff $\delta_{\mathrm{Ren}} = 0$
$J_{\mathrm{Ren}} K_{\mathrm{Ren}} J_{\mathrm{Ren}} = K_{\mathrm{Ren}}^{*}$	Operator representation of reciprocal symmetry	Corresponds to the reciprocal-role structures of Chapters 1 and 4
$B_{\mathrm{Ren}} = K_{\mathrm{Ren}}^{-2} \in \mathfrak{S}_1$	Trace-class inverse-square operator	Basis for Fredholm/resolvent recovery
$X(w)/X(0) = \det(I + w^2 B_{\mathrm{Ren}})$	Fredholm recovery of the completed entire function	Analytic–spectral interface
$\boldsymbol{R}_{\mathrm{Ren}}^{\mathrm{full}} \to X \to \xi \to \zeta_{\mathrm{global}}$	Recovery of the completed analytic object	Fully marked object
$\zeta_{\mathrm{germ}} \to \eta_{\times} \to \mathcal{R}_{\times}$	Recovery of the pre-continuation multiplicative structure	Multiplicative–analytic interface
Bidirectional lossless bridge	Bidirectional recoverability under the standard Riemann normalization	Main theorem of Chapter 6
H_{Ren}	Canonical positive self-adjoint operator after RH	Spectral interface for Chapters 7 and 8
$D_{\mathrm{Ren}} = H_{\mathrm{Ren}} \oplus (-H_{\mathrm{Ren}})$	Bilateral bare-spectral readout	Interface with second-order statistics in Chapter 8
$\mathfrak{M}_{\times} \to \boldsymbol{R}_{\mathrm{Ren}}^{\mathrm{full}}$	From scale-marked multiplicative realization to the Ren object	Directionally distinct from the independent source-generated route of Chapter 9

The source-generated Hilbert–Pólya construction of Chapter 9 independently builds a self-adjoint spectrum from the multiplicative generative source. The present chapter instead constructs a full-coordinate canonical spectral object from the completed Riemann zero divisor. The two routes play different proof-theoretic roles in the architecture of the book.

9.3 Conclusion

The **Yifei Ren operator**, abbreviated **Ren operator**, is defined before RH from the centered zero divisor:

$$\boxed{K_{\mathrm{Ren}} = \Gamma_{\mathrm{Ren}} - i\Delta_{\mathrm{Ren}}.}$$

It simultaneously preserves the vertical zero coordinates and the horizontal displacement from the critical line, and writes the Riemann Hypothesis as

$$\boxed{\mathrm{RH} \Leftrightarrow \Delta_{\mathrm{Ren}} = 0.}$$

The inverse-square operator

$$B_{\mathrm{Ren}} = K_{\mathrm{Ren}}^{-2}$$

is trace class and recovers the normalized completed Riemann function through the Fredholm determinant:

$$\boxed{\frac{X(w)}{X(0)} = \det(I + w^2 B_{\mathrm{Ren}}).}$$

After adjoining the central anchor, normalization, completion multiplier, and reciprocal symmetry, the fully marked object

$$\boldsymbol{R}_{\mathrm{Ren}}^{\mathrm{full}}$$

recovers in reverse

$$X \to \xi \to \zeta_{\mathrm{global}} \to \zeta_{\mathrm{germ}} \to \eta_{\times} \to \mathcal{R}_{\times}.$$

Hence

$$\boxed{\mathfrak{M}_{\times} \leftrightarrow \boldsymbol{R}_{\mathrm{Ren}}^{\mathrm{full}}}$$

expresses bidirectional information recoverability under the standard Riemann normalization. Distinct mathematical types retain their own object identities, while multiplicative, analytic, and spectral information can be generated forward and recovered backward through deterministic maps.

After RH,

$$\boxed{H_{\mathrm{Ren}} = K_{\mathrm{Ren}}|_{\mathrm{RH}}}$$

becomes the canonical Riemann spectral operator. Its signed version

$$D_{\mathrm{Ren}} = H_{\mathrm{Ren}} \oplus (-H_{\mathrm{Ren}})$$

feeds into the second-order spectral statistics of Chapter 8. Chapter 7 further establishes its Riemann spectral identity witness, while Chapter 9 independently constructs a source-generated Hilbert–Pólya spectral route from the multiplicative generative source.

Chapter 6 therefore completes the full operator chain from the closed zero divisor to a full-coordinate canonical spectral object and then back to the multiplicative–analytic history.

Appendix A | Core Notation

Symbol	Meaning
$\mathfrak{I}_{\times} = (\mathbb{N}_{>0}, \mu)$	Root multiplicative identity fixed in Chapter 1
$\mathcal{R}_{\times}$	Integer multiplicative relation $mq = n$
$\ell(n) = \log n$	Canonical multiplicative scale
$\mathfrak{M}_{\times} = (\mathbb{N}, \mathcal{R}_{\times}, \ell)$	Scale-marked relational realization of the root multiplicative identity
$\eta_{\times}$	Multiplicative logarithmic ledger $\sum_n \delta_{\log n}$
H_{mult}	Pre-continuation multiplicative-source operator, $H_{\mathrm{mult}} e_n = \log n \, e_n$
ζ_{germ}	Euler/Dirichlet analytic germ on $\Re s > 1$
ζ_{global}	Standard meromorphic continuation
$C_{\xi}(s)$	Riemann completion multiplier
$X(z)$	$\xi(1/2 + z)$
$a_{\rho} = d_{\rho} + i\gamma_{\rho}$	Centered zero coordinate
$\mathcal{Z}_{+}$	Support of centered upper-half-plane zeros
K_{Ren}	Yifei Ren operator; unconditional full-coordinate Ren operator
Γ_{Ren}	Vertical-coordinate operator
Δ_{Ren}	Hidden horizontal-deviation operator
$\delta_{\mathrm{Ren}} = \| \Delta_{\mathrm{Ren}} \|$	Global horizontal defect
J_{Ren}	Unitary reciprocal involution
$B_{\mathrm{Ren}} = K_{\mathrm{Ren}}^{-2}$	Ren inverse-square operator

Symbol	Meaning
$\boldsymbol{R}_{\mathrm{Ren}}^{\mathrm{full}}$	Fully marked Ren–Riemann spectral object
H_{Ren}	Canonical Riemann spectral operator after RH
$\mathfrak{R}_{\mathrm{Ren}} = [H_{\mathrm{Ren}}]_{\mathrm{u}}$	Ren–Riemann spectral class
D_{Ren}	Signed canonical Riemann spectral operator

Appendix B | Dependency Diagram

$$\mathfrak{I}_{\times}$$
$$\Downarrow$$
$$\mathfrak{M}_{\times} = (\mathbb{N}, \mathcal{R}_{\times}, \log)$$
$$\Updownarrow$$
$$\eta_{\times} = \sum_{n} \delta_{\log n}$$
$$\Updownarrow_{\mathrm{Laplace/Dirichlet}}$$
$$\zeta_{\mathrm{germ}} \quad (\Re s > 1)$$
$$\Updownarrow_{\text{analytic continuation/restriction}}$$
$$\zeta_{\mathrm{global}}$$
$$\Updownarrow_{\mathrm{completion/recovery}}$$
$$\xi$$
$$\Updownarrow_{\mathrm{centering}}$$
$$X$$
$$\Updownarrow_{\mathrm{divisor/Fredholm}}$$
$$\boldsymbol{R}_{\mathrm{Ren}}^{\mathrm{full}}$$
$$\Downarrow_{\mathrm{RH}}$$
$$H_{\mathrm{Ren}} = H_{\mathrm{Ren}}^{*} > 0$$
$$\Downarrow_{\mathcal{F}_{\mathrm{bare}}}$$
$$\{\gamma_n, m_n\}$$
$$\Downarrow$$

Chapter 7: spectral witness and Chapter 8: GUE second-order structure.

Appendix C | Relation to the Independent Hilbert–Pólya Route of Chapter 9

The direction of this chapter is

completed Riemann zero divisor →
canonical Ren spectrum ↔
multiplicative–analytic recovery.

The direction of Chapter 9 is

multiplicative generative source →
source-generated positive self-adjoint spectrum →
canonical terminal identification.

The two chapters share the root multiplicative identity and the canonical spectral interface but run in opposite proof directions: Chapter 6 constructs a full-coordinate spectral object from completed zero data, while Chapter 9 independently constructs a self-adjoint spectral route from the generative source.

Appendix D | Terminology and Object Levels

Throughout the book, the following terminology is used:

$$\boxed{\text{Yifei Ren operator} = \text{Ren operator}}$$

for K_{Ren};

$$\boxed{\text{fully marked Ren–Riemann spectral object}}$$

for $\boldsymbol{R}_{\mathrm{Ren}}^{\mathrm{full}}$;

$$\boxed{\text{canonical Riemann spectral operator}}$$

for H_{Ren} after RH;

and

$$\boxed{\text{signed canonical Riemann spectral operator}}$$

for D_{Ren}.

The object hierarchy is

$$\boxed{\boldsymbol{R}_{\mathrm{Ren}}^{\mathrm{full}} \supset K_{\mathrm{Ren}} \overset{\mathrm{RH}}{\to} H_{\mathrm{Ren}} \to D_{\mathrm{Ren}}.}$$

Here K_{Ren} preserves the full centered zero coordinates, H_{Ren} is the positive self-adjoint specialization after RH, and D_{Ren} supplies the bilateral bare-spectral readout.

Chapter 7 Riemann Spectral Witness Theorem: Uniqueness of the Ren Canonical Spectral Witness and Hilbert–Pólya Identity Transfer

Abstract

Chapter 6 constructed the fully marked Ren–Riemann spectral object and, after the Riemann Hypothesis, its canonical self-adjoint operator H_{Ren}. This chapter extracts from that canonical object a scalar witness sufficient to determine the Riemann spectral identity uniquely, and establishes both its uniqueness and the transfer of spectral identity.

Let

$$X(z) = \xi\left(\frac{1}{2} + z\right), \qquad G(y) = \frac{X(\sqrt{y})}{X(0)}, \qquad F_{\mathrm{R}}(y) = \frac{G'(y)}{G(y)}.$$

Under the Riemann Hypothesis, let the distinct positive ordinates of the zeros be

$$0 < \gamma_1 < \gamma_2 < \cdots$$

with analytic multiplicities m_n. Then

$$F_{\mathrm{R}}(y) = \sum_{n\geq 1} \frac{m_n}{y + \gamma_n^2} = \int_{[0,\infty)} \frac{d\nu_{\mathrm{R}}(\beta)}{1 + y\beta},$$

where

$$\boxed{\nu_{\mathrm{R}} = \sum_{n\geq 1} m_n \beta_n \delta_{\beta_n}, \qquad \beta_n = \gamma_n^{-2}.}$$

The scalar response F_{R}, the equivalent Stieltjes measure ν_{R}, and the canonical spectral data uniquely reconstructed from them together form the **canonical Riemann spectral witness**. The complete chain of determination is

$$\boxed{F_{\mathrm{R}} \Leftrightarrow \nu_{\mathrm{R}} \Leftrightarrow (H_{\mathrm{id}}, M_{\mathrm{mult}}) \Leftrightarrow H_{\mathrm{Ren}},}$$

where

$$H_{\mathrm{id}} e_n = \gamma_n e_n, \qquad M_{\mathrm{mult}} e_n = m_n e_n,$$

and

$$H_{\mathrm{Ren}} = \oplus_n \gamma_n I_{m_n}.$$

In an analytic neighborhood of $y = 0$,

$$F_{\mathrm{R}}(y) = \sum_{k\geq 0} (-1)^k \mu_k^{\mathrm{R}} y^k, \qquad \mu_k^{\mathrm{R}} = \sum_n m_n \gamma_n^{-2k-2}.$$

Because ν_{R} is a compactly supported finite positive measure, its full moment sequence determines ν_{R} uniquely. Consequently, the complete local analytic germ, the full moment sequence, the Stieltjes measure, and the canonical spectral identity determine one another uniquely.

Suppose $B_\times \geq 0$ is a bounded self-adjoint operator, $\Psi_\times$ is cyclic, and

$$F_\times(y) = \langle (I + yB_\times)^{-1}\Psi_\times, \Psi_\times \rangle$$

agrees with F_{R} on some nonempty open interval, or has the same full moment sequence. Then the cyclic spectral theorem gives a pointed unitary equivalence

$$\boxed{(B_\times, \Psi_\times) \simeq (B_{\mathrm{R}}, \mathbf{1}).}$$

Hence

$$H_\times := B_\times^{-1/2} \simeq H_{\mathrm{id}},$$

and the same witness measure recovers the analytic multiplicities, giving

$$\boxed{\mathrm{Amp}_{M_{\mathrm{mult}}}(H_\times) \simeq H_{\mathrm{Ren}}.}$$

Thus this chapter completes the witnessing and identification of spectral identity: once an independently constructed cyclic self-adjoint spectral object has the same complete scalar response, full moment sequence, or local analytic germ as the canonical Riemann witness, its spectral identity is uniquely determined. Chapter 9 is responsible for constructing a self-adjoint spectrum from the multiplicative generative source; the present chapter provides the canonical terminal-identification interface.

1. The Generative Layer and the Witness Layer

A Hilbert–Pólya structure contains two distinct mathematical levels.

The first is the generative layer:

$$\boxed{\mathcal{S}_\times \to H_\times = H_\times^*.} \tag{1.1}$$

The second is the spectral-identity witness layer:

$$\boxed{H_\times \to \text{canonical identification with the Riemann spectral identity.}} \tag{1.2}$$

Chapter 9 is responsible for the former direction—the independent source-generated Hilbert–Pólya construction. The present chapter is responsible for the latter—the canonical identification.

For a cyclic self-adjoint realization, a single scalar resolvent matrix element already encodes its cyclic spectral measure. Spectral-identity identification can therefore be written at the object level as

$$\boxed{\text{same cyclic response} \Rightarrow \text{same spectral measure} \Rightarrow \text{same cyclic spectral object.}} \tag{1.3}$$

This identification does not require the two sides to choose the same eigenvalue indexing in advance. The sections below establish, in sequence, the unique-determination relations among the scalar response, Stieltjes measure, full moment sequence, local analytic germ, and cyclic spectral realization.

2. Extracting a Canonical Spectral Witness from the Full Ren–Riemann Object

Write the fully marked Ren–Riemann spectral object as

$$\boldsymbol{R}_{\mathrm{Ren}}^{\mathrm{full}}.$$

Beyond the zero spectrum, it retains centered coordinates, the completion multiplier C_ξ, normalization, reciprocal symmetry, and the recovery structure that returns from the spectral side to the completed Riemann function and the pre-continuation multiplicative identity.

Under the Riemann Hypothesis, its full-coordinate normal operator specializes to the positive self-adjoint operator

$$H_{\mathrm{Ren}},$$

with

$$H_{\mathrm{Ren}} = \oplus_n \gamma_n I_{m_n}.$$

Hence

$$\dim\ker(H_{\mathrm{Ren}} - \gamma_n I) = m_n.$$

The information required for terminal identity identification can be compressed from the full object into a scalar canonical witness.

This chapter extracts from the full object a **canonical spectral witness** sufficient to determine the Riemann spectral identity uniquely, and establishes uniqueness of its cyclic spectral realization.

Thus the mappings carried by this chapter are

$$\boxed{\boldsymbol{R}^{\mathrm{full}}_{\mathrm{Ren}} \to \mathfrak{W}_{\mathrm{R}}}$$

and

$$\boxed{\mathfrak{W}_{\mathrm{R}} \Rightarrow \text{unique Riemann spectral realization.}}$$

Any independent Hilbert–Pólya construction can be identified at the terminal stage with the Riemann spectral identity through this canonical witness while its generative chain remains independent.

3. The Canonical Riemann Spectral Witness

3.1 Scalar Response

Define

$$X(z) = \xi\left(\frac{1}{2} + z\right),$$

and

$$G(y) = \frac{X(\sqrt{y})}{X(0)}.$$

Because X is an even entire function, G is entire.

Define the logarithmic response

$$\boxed{F_{\mathrm{R}}(y) = \frac{G'(y)}{G(y)}.}$$

Under RH,

$$\frac{X(z)}{X(0)} = \prod_n \left(1 + \frac{z^2}{\gamma_n^2}\right)^{m_n},$$

so

$$\boxed{F_{\mathrm{R}}(y) = \sum_n \frac{m_n}{y + \gamma_n^2}.}$$

Let

$$\beta_n = \gamma_n^{-2}.$$

Then

$$F_{\mathrm{R}}(y) = \sum_n \frac{m_n \beta_n}{1 + y\beta_n}.$$

3.2 Stieltjes Witness Measure

Define

$$\boxed{\nu_{\mathrm{R}} = \sum_n m_n \, \beta_n \delta_{\beta_n}.}$$

Since

$$\sum_n m_n \, \gamma_n^{-2} < \infty,$$

ν_{R} is a finite positive measure.

Moreover,

$$\boxed{F_{\mathrm{R}}(y) = \int_{[0,\infty)} \frac{d\nu_{\mathrm{R}}(\beta)}{1 + y\beta}.}$$

Its support contains

$$\beta_n \in (0, \beta_1],$$

with 0 as its only possible finite accumulation point. Thus

$$\mathrm{supp}\nu_{\mathrm{R}} \subset [0, \beta_1].$$

Notice that

$$\nu_{\mathrm{R}}(\{0\}) = 0.$$

3.3 Definition of the Canonical Witness

Define

$$\boxed{\mathfrak{W}_{\mathrm{R}} := F_{\mathrm{R}},}$$

and regard its unique Stieltjes representing measure ν_{R} as the equivalent measure representation. Thus

$$\boxed{\mathfrak{W}_{\mathrm{R}} \equiv F_{\mathrm{R}} \equiv \nu_{\mathrm{R}}.}$$

Here "≡" means only mutual unique determination within the stated Stieltjes class; it does not assert that the function and the measure are objects of the same mathematical type.

We call $\mathfrak{W}_{\mathrm{R}}$ the

canonical Riemann spectral witness.

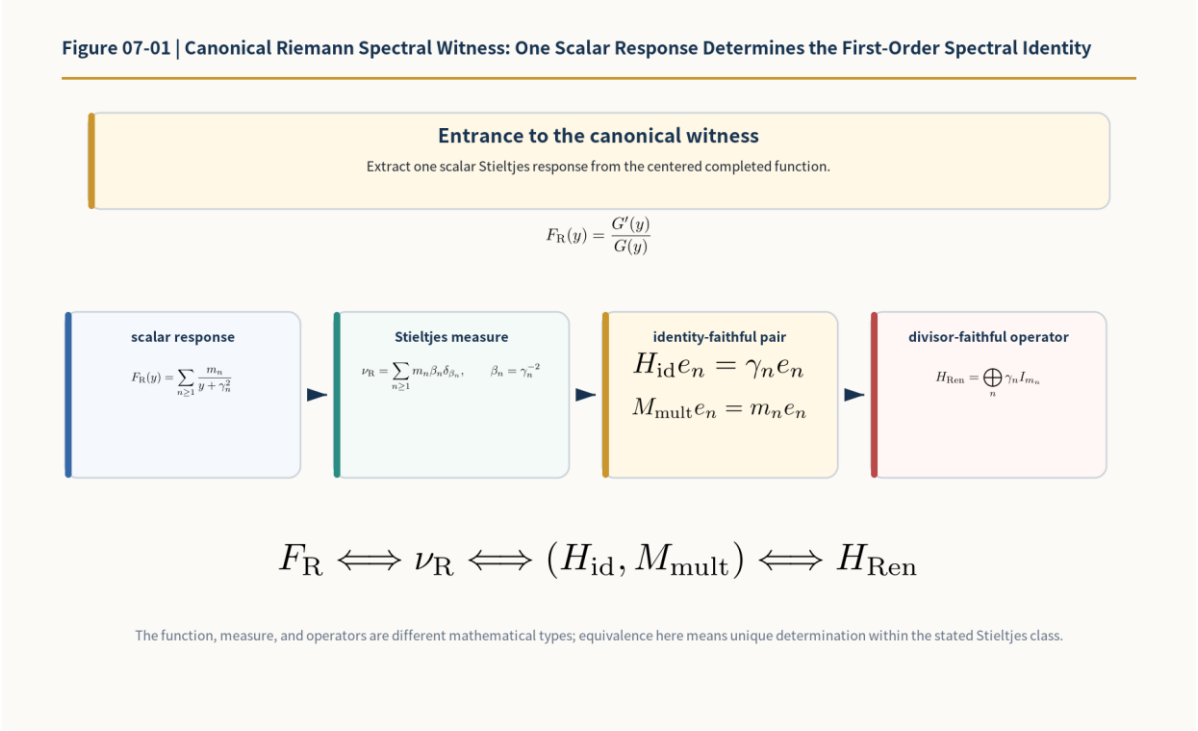


Figure 07-01. The canonical Riemann spectral witness. Under RH, the scalar response F_{R}, its unique Stieltjes representing measure ν_{R}, the identity-faithful pair $(H_{\mathrm{id}}, M_{\mathrm{mult}})$, and the divisor-faithful operator H_{Ren} uniquely determine one another. "Equivalence" here means unique recoverability between object types; it does not identify functions, measures, and operators as the same mathematical type.

4. Scalar Complete Spectral Witness Theorem

Theorem 4.1

Under RH, the canonical Riemann spectral witness F_{R} uniquely determines:

1. the Stieltjes measure ν_{R};
2. the distinct spectral identity addresses $\{\gamma_n\}$;
3. the analytic multiplicities $\{m_n\}$;
4. the unitary-equivalence class of the identity-faithful pair $(H_{\mathrm{id}}, M_{\mathrm{mult}})$;
5. the unitary-equivalence class of the divisor-faithful canonical operator H_{Ren}.

Therefore

$$\boxed{F_{\mathrm{R}} \Leftrightarrow \nu_{\mathrm{R}} \Leftrightarrow (H_{\mathrm{id}}, M_{\mathrm{mult}}) \Leftrightarrow H_{\mathrm{Ren}}.}$$

Proof

By uniqueness of the Stieltjes transform, F_{R} uniquely determines ν_{R}.

Define the positive atomic support

$$\mathrm{AtSupp}_{+}(\nu_{\mathrm{R}}) = \{\beta > 0 : \nu_{\mathrm{R}}(\{\beta\}) > 0\}.$$

Then

$$\mathrm{AtSupp}_{+}(\nu_{\mathrm{R}}) = \{\beta_n\}.$$

Hence

$$\gamma_n = \beta_n^{-1/2}.$$

On the other hand,

$$\nu_{\mathrm{R}}(\{\beta_n\}) = m_n \beta_n,$$

so

$$\boxed{m_n = \frac{\nu_{\mathrm{R}}(\{\beta_n\})}{\beta_n}.}$$

Thus ν_{R} recovers both the distinct zero ordinates and the analytic multiplicities.

Define

$$H_{\mathrm{id}} e_n = \gamma_n e_n, \qquad M_{\mathrm{mult}} e_n = m_n e_n.$$

These data uniquely determine the unitary-equivalence class of the pair $(H_{\mathrm{id}}, M_{\mathrm{mult}})$.

Now define multiplicity amplification:

$$\mathrm{Amp}_{M_{\mathrm{mult}}}(H_{\mathrm{id}}) = \oplus_n \gamma_n I_{m_n}.$$

This is precisely

$$H_{\mathrm{Ren}}.$$

The reverse direction is immediate: the eigenvalue–multiplicity data of H_{Ren} recover γ_n, m_n, hence ν_{R} and F_{R}. ▫

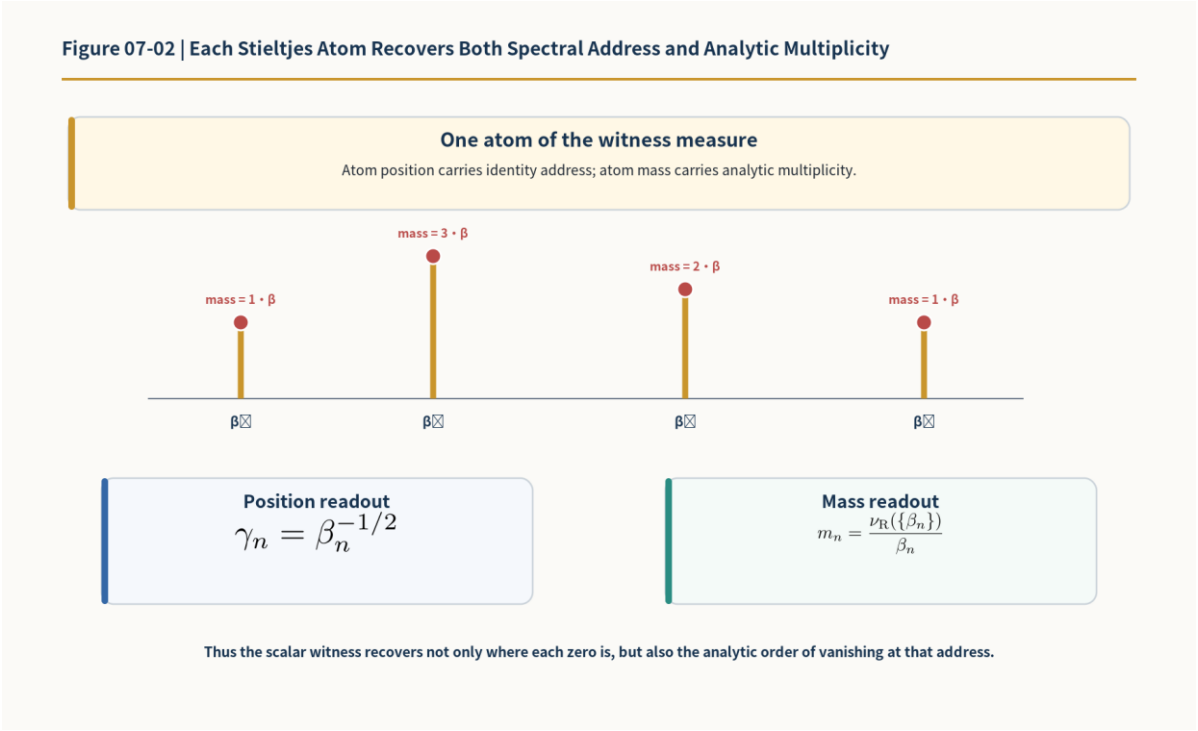


Figure 07-02. The two readouts of a Stieltjes atom. The position β_n of each positive atom recovers the distinct zero ordinate through $\gamma_n = \beta_n^{-1/2}$. The mass of the same atom recovers analytic multiplicity through $m_n = \nu_R(\{\beta_n\})/\beta_n$. A single scalar witness therefore determines both zero addresses and divisor weights.

5. Local Analytic Germs and Full Moment Witnesses

The witness used in this chapter does not require an independent generative-source realization to provide the entire meromorphic response at the outset. Complete local data already suffice.

5.1 Moment Sequence

For

$$|y| < \gamma_1^2,$$

the expansion

$$\frac{1}{1+y\beta} = \sum_{k\geq 0} (-1)^k y^k \beta^k$$

is uniformly integrable. Therefore

$$F_R(y) = \sum_{k\geq 0} (-1)^k \mu_k^R y^k,$$

where

$$\boxed{\mu_k^R = \int \beta^k d\nu_R(\beta) = \sum_n m_n \gamma_n^{-2k-2}.}$$

Thus

$$\boxed{F_{\mathrm{R}}^{(k)}(0) = (-1)^k k!\, \mu_k^{\mathrm{R}}.}$$

Theorem 5.1 (Compact-Support Moment Witness Theorem)

Let ν_1, ν_2 be compactly supported finite positive measures on $[0, \infty)$. If

$$\int \beta^k \, d\nu_1(\beta) = \int \beta^k \, d\nu_2(\beta) \qquad \forall k \geq 0,$$

then

$$\boxed{\nu_1 = \nu_2.}$$

Proof

Choose $R > 0$ such that

$$\mathrm{supp}\nu_1 \cup \mathrm{supp}\nu_2 \subset [0, R].$$

Equality of moments implies equality of the integrals of every polynomial p against the two measures.

By the Weierstrass approximation theorem, polynomials are uniformly dense in $C([0, R])$. Hence the two measures integrate every $f \in C([0, R])$ equally.

Uniqueness in the Riesz representation theorem for finite Borel measures gives

$$\nu_1 = \nu_2.$$

▫

Corollary 5.2 (Full-Moment Witness)

If $\nu_{\times}$ is a compactly supported finite positive measure and

$$\boxed{\mu_k^{\times} = \mu_k^{\mathrm{R}} \qquad \forall k \geq 0,}$$

then

$$\boxed{\nu_{\times} = \nu_{\mathrm{R}}.}$$

Corollary 5.3 (Local Analytic-Germ Witness)

Suppose $F_{\times}$ and F_{R} are both analytic in a neighborhood of $y = 0$ and satisfy

$$F_{\times}^{(k)}(0) = F_{\mathrm{R}}^{(k)}(0) \qquad \forall k \geq 0.$$

Then they have the same analytic germ.

If both are Stieltjes transforms of compactly supported finite positive measures, then

$$\boxed{\nu_{\times} = \nu_{\mathrm{R}}.}$$

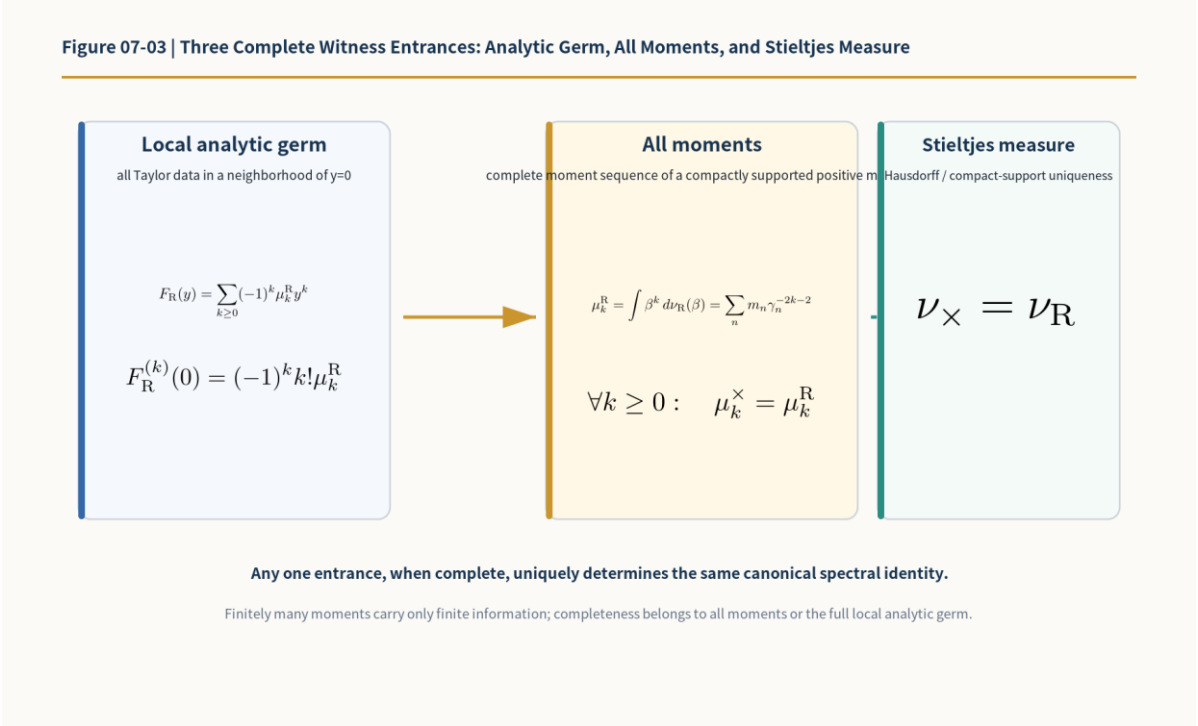


Figure 07-03. Three complete witness entrances. The full analytic germ near $y = 0$ is equivalent to all derivative data and hence to the complete moment sequence μ_k^{R}; for compactly supported positive measures, the complete moment sequence uniquely determines the Stieltjes measure. Thus the full local analytic germ, all moments, and the measure are three complete entrances to the same canonical spectral identity. A finite list of moments does not by itself carry this global uniqueness.

6. Uniqueness from the Response on an Open Interval

Theorem 6.1 (Analytic Response Witness Theorem)

Let $\nu_{\times}$ be a compactly supported finite positive measure on $[0,\infty)$, and define

$$F_{\times}(y)=\int \frac{d\nu_{\times}(\beta)}{1+y\beta}.$$

If there exists a nonempty real open interval

$$I\subset(0,\infty)$$

such that

$$\boxed{F_{\times}(y)=F_{\mathrm{R}}(y)\qquad \forall y\in I,}$$

then

$$\boxed{\nu_{\times}=\nu_{\mathrm{R}}.}$$

Proof

The two Stieltjes transforms are analytic on their common connected analytic domain containing the positive real axis.

They agree on the real open interval I, which has an accumulation point. By the identity theorem they agree throughout the common analytic domain.

Uniqueness of the Stieltjes transform then gives

$$\nu_{\times} = \nu_{\mathrm{R}}.$$

▫

Remark 6.2

Exact identification therefore does not require pointwise comparison of

$$\gamma_n.$$

It is enough to prove that one scalar analytic response agrees with F_{R} on any nonempty open interval.

7. Cyclic Spectral Realization of the Witness

7.1 Canonical Witness Space

Let

$$\boxed{\mathcal{H}_{\mathrm{W}} = L^2([0,\infty), d\nu_{\mathrm{R}}).}$$

Define the multiplication operator

$$\boxed{(B_{\mathrm{R}} f)(\beta) = \beta f(\beta).}$$

Because

$$\mathrm{supp}\nu_{\mathrm{R}} \subset [0, \beta_1],$$

B_{R} is a bounded positive self-adjoint operator.

Let

$$\mathbf{1}(\beta) \equiv 1.$$

Since ν_{R} is finite,

$$\mathbf{1} \in \mathcal{H}_{\mathrm{W}}.$$

Moreover,

$$\boxed{F_{\mathrm{R}}(y) = \langle (I + yB_{\mathrm{R}})^{-1}\mathbf{1}, \mathbf{1} \rangle.}$$

7.2 Cyclicity

Because ν_{R} is purely atomic and all atoms β_n are distinct, the subspace generated by applying polynomials in B_{R} to $\mathbf{1}$ is dense in $\mathcal{H}_{\mathrm{W}}$.

Thus $\mathbf{1}$ is cyclic.

Equivalently, $(B_{\mathrm{R}}, \mathbf{1})$ is the canonical cyclic realization of the Riemann witness.

8. Cyclic Witness Uniqueness Theorem

Theorem 8.1

Let $\mathcal{H}_\times$ be a Hilbert space,

$$B_\times = B_\times^* \geq 0$$

a bounded operator, and $\Psi_\times \in \mathcal{H}_\times$ a cyclic vector.

Define

$$\boxed{F_\times(y) = \langle (I + yB_\times)^{-1}\Psi_\times, \Psi_\times \rangle.}$$

Assume either of the following.

(A) Equality of the Responses on an Open Interval

There exists a nonempty open interval $I \subset (0, \infty)$ such that

$$F_\times(y) = F_{\mathrm{R}}(y) \qquad \forall y \in I;$$

or

(B) Equality of All Moments

$$\langle B_\times^k \Psi_\times, \Psi_\times \rangle = \mu_k^{\mathrm{R}} \qquad \forall k \geq 0.$$

Then there exists a unitary

$$U: \mathcal{H}_\times \to L^2(\nu_{\mathrm{R}})$$

such that

$$\boxed{UB_\times U^{-1} = B_{\mathrm{R}},}$$

and

$$\boxed{U\Psi_\times = \mathbf{1}.}$$

That is,

$$\boxed{(B_\times, \Psi_\times) \simeq (B_{\mathrm{R}}, \mathbf{1})}$$

as pointed cyclic spectral objects.

Proof

By the spectral theorem, $(B_\times, \Psi_\times)$ defines the unique scalar spectral measure

$$\nu_\times(E) = \langle E_{B_\times}(E)\Psi_\times, \Psi_\times \rangle.$$

Since $B_\times$ is bounded and positive,

$$\mathrm{supp}\nu_\times \subset [0, \| B_\times \|].$$

Moreover,

$$F_\times(y) = \int \frac{d\nu_\times(\beta)}{1+y\beta}.$$

Under condition (A), Theorem 6.1 gives

$$\nu_\times = \nu_{\mathrm{R}}.$$

Under condition (B),

$$\langle B_\times^k \Psi_\times, \Psi_\times \rangle = \int \beta^k \, d\nu_\times(\beta),$$

so Theorem 5.1 again gives

$$\nu_\times = \nu_{\mathrm{R}}.$$

Because $\Psi_\times$ is cyclic, the cyclic spectral theorem gives the pointed representation

$$(\mathcal{H}_\times, B_\times, \Psi_\times) \simeq (L^2(\nu_\times), M_\beta, \mathbf{1}).$$

Substituting

$$\nu_\times = \nu_{\mathrm{R}}$$

gives the result. ▫

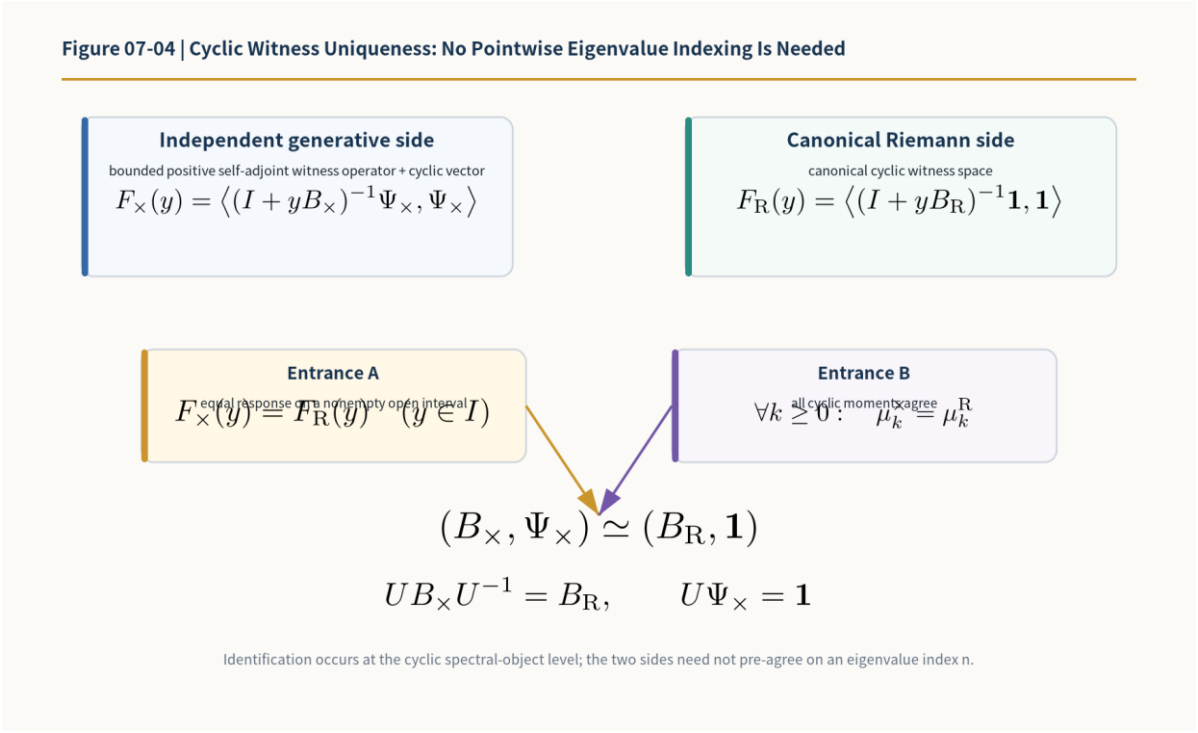


Figure 07-04. Cyclic witness uniqueness. For a bounded positive self-adjoint witness operator with a cyclic vector, equality of the scalar response with F_{R} on any nonempty open interval, or equality of all cyclic moments with the canonical Riemann moments, yields pointed unitary equivalence $(B_\times, \Psi_\times) \simeq (B_{\mathrm{R}}, \mathbf{1})$ by Stieltjes uniqueness, moment uniqueness, and the cyclic spectral theorem. This object-level identification does not require the two sides to preselect the same eigenvalue indexing.

9. From the Bounded Witness Operator to a Hilbert–Pólya Operator

9.1 Inverse-Square-Root Transform

On the canonical witness space,

$$B_{\mathrm{R}}u_n = \beta_n u_n, \qquad \beta_n = \gamma_n^{-2}.$$

Because

$$\nu_{\mathrm{R}}(\{0\}) = 0,$$

B_{R} has no kernel.

Define the unbounded positive self-adjoint operator

$$\boxed{H_{\mathrm{id}} = B_{\mathrm{R}}^{-1/2}}$$

by spectral functional calculus.

Then

$$H_{\mathrm{id}}u_n = \gamma_n u_n.$$

Thus H_{id} is an identity-faithful Hilbert–Pólya realization.

Theorem 9.1 (Transfer from the Witness to Hilbert–Pólya)

Under the hypotheses of Theorem 8.1, if

$$H_{\times} = B_{\times}^{-1/2},$$

then

$$\boxed{H_{\times} \simeq H_{\mathrm{id}}.}$$

Proof

From

$$UB_{\times}U^{-1} = B_{\mathrm{R}}$$

and Borel functional calculus,

$$UB_{\times}^{-1/2}U^{-1} = B_{\mathrm{R}}^{-1/2}.$$

Hence

$$UH_{\times}U^{-1} = H_{\mathrm{id}}.$$

▫

10. Recovering Analytic Multiplicities and Divisor Amplification

10.1 Recovering Analytic Multiplicity from the Witness Measure

From

$$\nu_{\mathrm{R}}(\{\beta_n\}) = m_n\beta_n,$$

we have

$$\boxed{m_n = \frac{\nu_{\mathrm{R}}(\{\beta_n\})}{\beta_n}.}$$

Thus the cyclic witness simultaneously determines the distinct spectral identity addresses and their analytic multiplicities.

10.2 The Analytic Multiplicity Operator

On the identity space define

$$\boxed{M_{\mathrm{mult}}e_n = m_n e_n.}$$

Then M_{mult} strongly commutes with H_{id}.

10.3 Divisor Amplification

Define

$$\boxed{\mathrm{Amp}_{M_{\mathrm{mult}}}(H_{\mathrm{id}}) = \oplus_n \gamma_n I_{m_n}.}$$

This is exactly the divisor-faithful canonical Ren–Riemann operator:

$$\boxed{\mathrm{Amp}_{M_{\mathrm{mult}}}(H_{\mathrm{id}}) \simeq H_{\mathrm{Ren}}.}$$

Combining this with Theorem 9.1 gives:

Theorem 10.1 (Transfer from the Witness to the Ren–Riemann Spectral Class)

If a generative-source-side cyclic pair $(B_\times, \Psi_\times)$ satisfies either witness condition of Theorem 8.1, then

$$\boxed{H_\times \simeq H_{\mathrm{id}}}$$

and the analytic multiplicity operator M_{mult} recovered from the same witness measure satisfies

$$\boxed{\mathrm{Amp}_{M_{\mathrm{mult}}}(H_\times) \simeq H_{\mathrm{Ren}}.}$$

Thus the independently generated realization completes its identity identification with the canonical Ren–Riemann spectral class through the scalar witness.

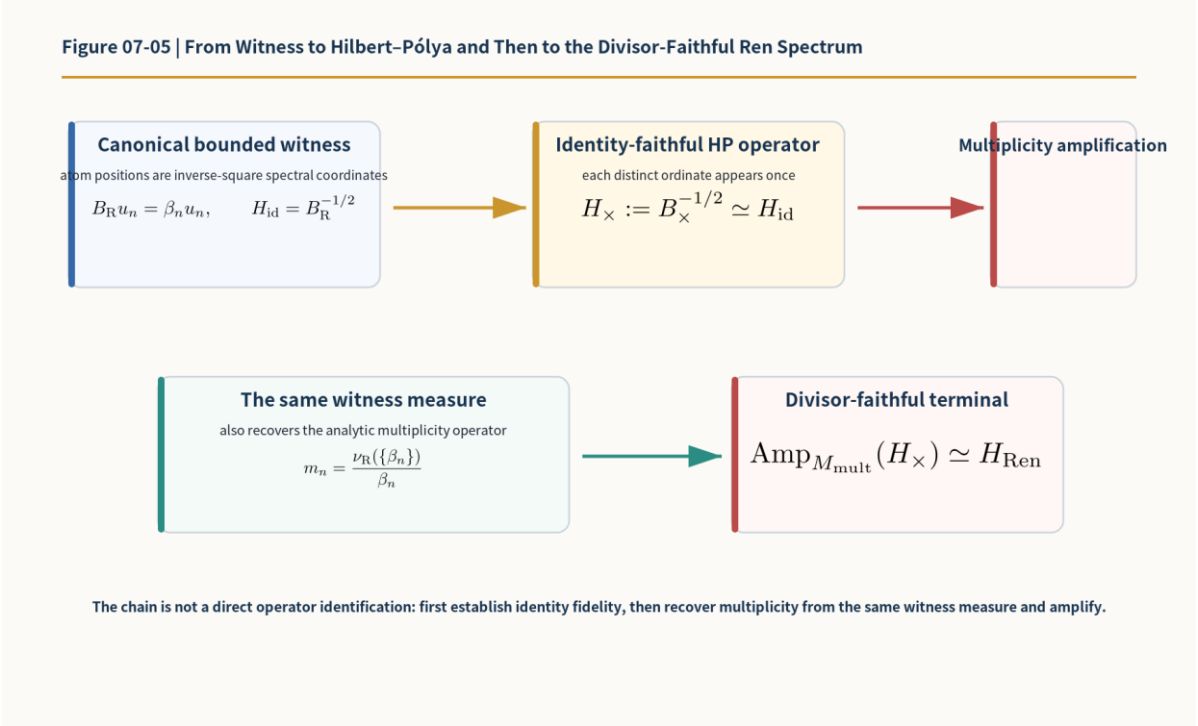


Figure 07-05. From the witness to Hilbert–Pólya and the divisor-faithful spectrum. The inverse-square-root transform first sends the bounded witness operator to the identity-faithful Hilbert–Pólya realization $H_\times \simeq H_{\mathrm{id}}$. The same witness measure independently recovers analytic multiplicity, and multiplicity amplification by M_{mult} then gives $\mathrm{Amp}_{M_{\mathrm{mult}}}(H_\times) \simeq H_{\mathrm{Ren}}$. The correct chain must therefore not be abbreviated as $H_\times \simeq H_{\mathrm{Ren}}$.

11. Identification Theorem from a Source-Generated Spectrum to the Riemann Spectrum

Theorem 11.1

Suppose an independent mathematical construction provides:

1. a Hilbert space $\mathcal{H}_\times$;
2. a bounded positive self-adjoint operator

$$B_\times;$$

3. a cyclic vector

$$\Psi_\times;$$

4. a generative-source-defined response

$$F_\times(y) = \langle (I + yB_\times)^{-1}\Psi_\times, \Psi_\times \rangle.$$

Assume that this construction defines $B_\times$, $\Psi_\times$, and $F_\times$ from its own generative-source data. If the independent construction further proves either

$$\boxed{F_\times = F_{\mathrm{R}}}$$

on some nonempty open interval, or proves that all moments satisfy

$$\boxed{\langle B_\times^k \Psi_\times, \Psi_\times \rangle = \mu_k^{\mathrm{R}} \qquad \forall k,}$$

then

$$\boxed{(B_\times, \Psi_\times) \simeq (B_{\mathrm{R}}, \mathbf{1}),}$$

$$\boxed{H_\times = B_\times^{-1/2} \simeq H_{\mathrm{id}},}$$

and

$$\boxed{\mathrm{Amp}_{M_{\mathrm{mult}}}(H_\times) \simeq H_{\mathrm{Ren}}.}$$

Object-Level Meaning

The operator $B_\times$ has already been supplied by an independent generative-source construction; this theorem is responsible only for terminal spectral-identity identification.

Its object-level conclusion is

$$\boxed{\text{same complete response} \Rightarrow \text{same spectral identity.}}$$

The theorem therefore belongs to the spectral-identity identification layer.

12. Relation to the Independent Hilbert–Pólya Route of Chapter 9

The independent Hilbert–Pólya route of Chapter 9 begins from the root multiplicative identity and constructs

$$\boxed{\begin{array}{r}\mathcal{R}_\times \to \text{source-generated positive structure} \to \\ B_\times \to H_\times = H_\times^* \to \text{Riemann zero closure.}\end{array}} \tag{12.1}$$

The witness chain of the present chapter sits at the terminal end of that independent generative direction:

$$\boxed{\begin{array}{r}(B_\times, \Psi_\times) \to F_\times \overset{\text{witness}}{=} F_{\mathrm{R}} \to \\ \text{canonical identification with the Riemann spectral identity.}\end{array}} \tag{12.2}$$

The corresponding two-sided structure is

$$\boxed{\begin{array}{ccc}\text{canonical Riemann side} & & \text{independent generative-source side} \\ \boldsymbol{R}_{\mathrm{Ren}}^{\mathrm{full}} & & \mathcal{R}_\times \\ \Downarrow & & \Downarrow \\ \mathfrak{W}_{\mathrm{R}} & & (B_\times, \Psi_\times) \\ & & \Downarrow \\ & & H_\times \\ \mathfrak{W}_{\mathrm{R}} & \Leftrightarrow & F_\times \\ \Downarrow & & \Downarrow \\ H_{\mathrm{Ren}} & \simeq & \mathrm{Amp}_{M_{\mathrm{mult}}}(H_\times).\end{array}} \tag{12.3}$$

Chapter 9 is responsible for the independent construction from the multiplicative generative source to a self-adjoint spectrum; the present chapter is responsible for the terminal witness and canonical spectral-identity identification. The two chapters share the identification interface while keeping their generative directions independent.

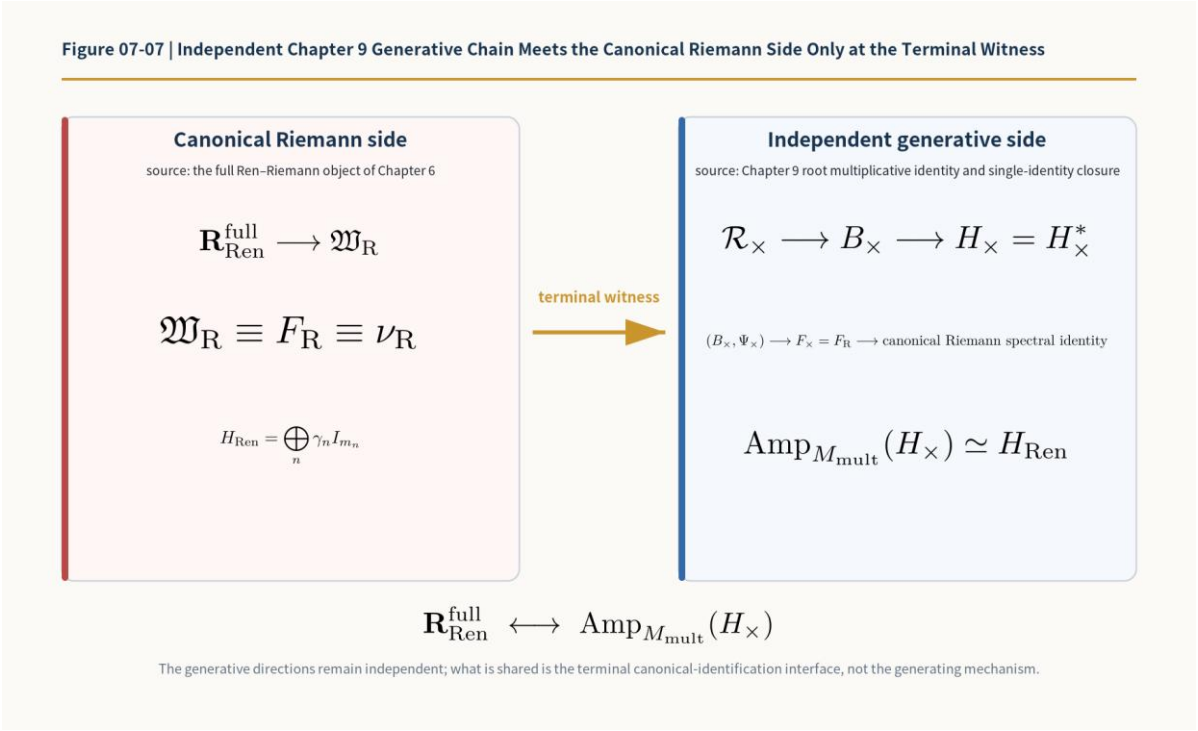


Figure 07-07. Terminal identification of two independent chains. On the canonical Riemann side, Chapter 6 compresses the fully marked Ren–Riemann object to the canonical witness. Chapter 9 independently generates $B_\times$ and the self-adjoint $H_\times$ from the root multiplicative identity. The two generative directions remain independent and meet only at the terminal witness through $F_\times = F_{\mathrm{R}}$, or an equivalent complete witness condition; the same measure then recovers multiplicity and passes to H_{Ren}.

13. Object-Level Identification versus Pointwise Indexing

A traditional identification strategy might ask one to prove

$$\lambda_n = \gamma_n \qquad \forall n.$$

The present chapter shows that, for cyclic realizations, this is not the necessary proof format. If

$$F_\times = F_{\mathrm{R}},$$

then directly

$$\nu_\times = \nu_{\mathrm{R}}.$$

Consequently all atom locations and atom weights agree automatically:

$$\beta_n^\times = \beta_n^{\mathrm{R}},$$

and

$$m_n^\times = m_n^{\mathrm{R}}.$$

Since

$$\gamma_n = \beta_n^{-1/2},$$

all zero ordinates are recovered automatically.

The object-level proof is therefore

$$\boxed{\text{same response} \Rightarrow \text{same measure} \Rightarrow \text{same spectral identity.}}$$

This object-level identification does not depend on choosing the same eigenvalue indexing on the two sides in advance.

14. Identity-Faithful and Divisor-Faithful Representations

14.1 The Identity-Faithful Operator

Let

$$\mathcal{H}_{\mathrm{id}} = \ell^2(\mathbb{N}),$$

and define

$$\boxed{H_{\mathrm{id}} e_n = \gamma_n e_n.}$$

Then the eigenspace corresponding to each distinct ordinate is one-dimensional:

$$\dim\ker(H_{\mathrm{id}} - \gamma_n I) = 1.$$

14.2 The Divisor-Faithful Operator

Define

$$\mathcal{H}_{\mathrm{div}} = \oplus_n \mathbb{C}^{m_n},$$

and

$$\boxed{H_{\mathrm{Ren}} = \oplus_n \gamma_n I_{m_n}.}$$

Then

$$\dim\ker(H_{\mathrm{Ren}} - \gamma_n I) = m_n.$$

Thus

$$\boxed{\text{identity} \neq \text{multiplicity.}}$$

Nevertheless, the pair

$$(H_{\mathrm{id}}, M_{\mathrm{mult}})$$

and

$$H_{\mathrm{Ren}}$$

carry the same divisor data.

15. Bidirectional Reconstruction Between Identity and Divisor Representations

Theorem 15.1

$$\boxed{[H_{\mathrm{Ren}}]_{\mathrm{u}} \quad \leftrightarrow \quad [(H_{\mathrm{id}}, M_{\mathrm{mult}})]_{\mathrm{u}}}$$

is a one-to-one correspondence.

Proof

The spectral projections of H_{Ren} recover the distinct spectral support

$$\gamma_n$$

and the ranks

$$m_n = \mathrm{rank} E_{H_{\mathrm{Ren}}}(\{\gamma_n\}).$$

Hence they recover $(H_{\mathrm{id}}, M_{\mathrm{mult}})$.

Conversely, from $(H_{\mathrm{id}}, M_{\mathrm{mult}})$, amplify each one-dimensional spectral fiber m_n-fold:

$$\mathrm{Amp}_{M_{\mathrm{mult}}}(H_{\mathrm{id}}) = \oplus_n \gamma_n I_{m_n} \simeq H_{\mathrm{Ren}}.$$

▫

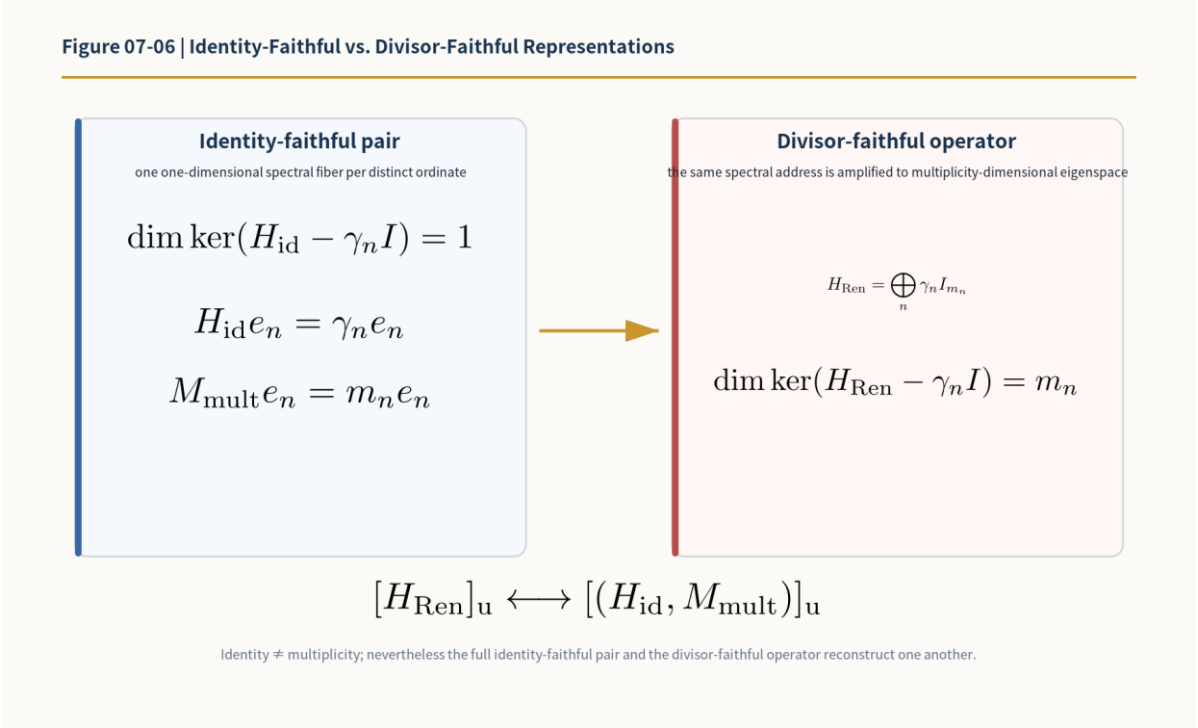


Figure 07-06. Identity-faithful and divisor-faithful representations. H_{id} retains one one-dimensional spectral fiber for each distinct ordinate, while the independent operator M_{mult} stores analytic multiplicity. H_{Ren} instead amplifies the same address to an m_n-dimensional eigenspace. The fiber dimensions differ, but $(H_{\mathrm{id}}, M_{\mathrm{mult}})$ and H_{Ren} carry the same complete divisor data and reconstruct one another at the level of unitary-equivalence classes.

16. Canonical Classification of Hilbert–Pólya Realizations

16.1 Identity-Faithful Realization Class

Call a positive self-adjoint operator with compact resolvent A an **identity-faithful realization** if its eigenvalues are exactly the distinct γ_n, each with a one-dimensional eigenspace.

Then:

Theorem 16.1

$$\boxed{A\text{is identity-faithful} \Leftrightarrow A \simeq H_{\mathrm{id}}.}$$

16.2 Divisor-Faithful Realization Class

Call A a **divisor-faithful realization** if

$$\sigma_{\mathrm{p}}(A) = \{\gamma_n\}$$

and

$$\mathrm{dimker}(A - \gamma_n I) = m_n.$$

Then:

Theorem 16.2

$$\boxed{A\text{is divisor-faithful} \Leftrightarrow A \simeq H_{\mathrm{Ren}}.}$$

These classification results are not independent generative-source constructions. They identify the canonical unitary-equivalence class of a self-adjoint realization that already possesses the corresponding Riemann spectral data.

17. Fredholm Compatibility

Define

$$B_{\mathrm{Ren}} = H_{\mathrm{Ren}}^{-2}.$$

Then

$$B_{\mathrm{Ren}} = \oplus_n \gamma_n^{-2} I_{m_n} \in \mathfrak{S}_1.$$

Hence

$$\boxed{\frac{X(z)}{X(0)} = \det(I + z^2 B_{\mathrm{Ren}}).}$$

On the identity space define

$$B_{\mathrm{id}} = H_{\mathrm{id}}^{-2}.$$

The ordinary determinant counts each distinct spectral identity address once, while the full multiplicities are restored by M_{mult}:

$$\boxed{\frac{X(z)}{X(0)} = \prod_n \left(1 + \frac{z^2}{\gamma_n^2}\right)^{m_n}.}$$

On a simply connected region not crossing any zero, with a fixed branch of the logarithm,

$$\boxed{\log \frac{X(z)}{X(0)} = \mathrm{Tr}[M_{\mathrm{mult}} \log(I + z^2 B_{\mathrm{id}})].}$$

Thus the witness measure, identity representation, and divisor representation give consistent readouts of the same completed analytic object.

18. Information Hierarchy

The Riemann spectral objects have the strict hierarchy

$$\boxed{\begin{aligned} \boldsymbol{R}_{\mathrm{Ren}}^{\mathrm{full}} \to \mathfrak{W}_{\mathrm{R}} \leftrightarrow \nu_{\mathrm{R}} \leftrightarrow \\ (H_{\mathrm{id}}, M_{\mathrm{mult}}) \leftrightarrow H_{\mathrm{Ren}} \to H_{\mathrm{id}} \to \Gamma_+. \end{aligned}}$$

The arrows have different meanings.

18.1 Full Object → Canonical Witness

Forget the full generative-source/completion provenance marks and retain only the scalar analytic response sufficient to determine the spectral identity.

18.2 Witness ↔ Measure

Uniqueness of the Stieltjes transform.

18.3 Measure ↔ Identity-Faithful Pair

Atom locations determine γ_n, and atom weights determine m_n.

18.4 Identity-Faithful Pair ↔ Divisor-Faithful Operator

Multiplicity amplification / reduction.

18.5 Divisor/Identity Representation → Identity Operator

Forget M_{mult}; analytic multiplicities are therefore lost.

18.6 Identity Operator → Bare Support

Further forget the Hilbert-space realization and retain only the set

$$\Gamma_+.$$

Thus

$$\boxed{\text{bare spectrum} \prec_{\text{info}} \text{canonical spectral witness} \prec_{\text{info}} \text{fully marked provenance object.}}$$

Here "$\prec_{\mathrm{info}}$" denotes strict decrease in information level. Set-theoretic inclusion is denoted separately by $\subset$ or $\subsetneq$.

19. Object Levels in Hilbert–Pólya-Related Spectral Routes

Different spectral routes primarily read different information layers of the Riemann object:

Route	Principal object	Principal information layer
Hilbert–Pólya	Self-adjoint operator	Real spectral identity
Selberg trace formula	Laplacian and trace formula	Geometry/arithmetic ↔ spectrum
Weil	Positive quadratic form	Arithmetic positivity
Montgomery–Odlyzko	Zero-spacing statistics	Second-order spectral organization
de Branges	Hilbert spaces of entire functions	Analytic function ↔ Hilbert structure
Berry–Keating	xp / dilation generator	Continuous scale/frequency
Connes	Noncommutative trace formula	Arithmetic provenance ↔ spectral trace
Suzuki	Weil/de Branges Hilbert structure	Positivity → Hilbert space → spectrum
This chapter	Scalar cyclic witness	Exact spectral-identity identification

The interface added by this chapter between these object levels is

$$\boxed{\text{unique identification of an independent spectral realization with the canonical Riemann spectral identity.}} \tag{19.1}$$

20. Interface with the Second-Order Spectral Statistics of Chapter 8

Define the signed divisor-faithful operator

$$D_{\mathrm{Ren}} = H_{\mathrm{Ren}} \oplus (-H_{\mathrm{Ren}}),$$

and the signed identity-faithful operator

$$D_{\mathrm{id}} = H_{\mathrm{id}} \oplus (-H_{\mathrm{id}}).$$

The former retains analytic multiplicities; the latter retains only the distinct zero ordinates.

For a suitable test function ϕ, define

$$Z_{\phi}(t) = \mathrm{Tr}\big(\phi(D_{\mathrm{Ren}})e^{itD_{\mathrm{Ren}}}\big).$$

Second-order statistics read relations among the zero ordinates, not the witness identification itself.

Therefore

$$\boxed{\text{witness identity} \neq \text{second-order spectral statistics.}}$$

Statistical analysis can read the required data from D_{Ren} or D_{id} without carrying the full provenance marks of the generative source.

21. Finite-Dimensional Truncation and Moment Consistency

Take the first N distinct zero ordinates and define

$$H_{\mathrm{id},N} = \mathrm{diag}(\gamma_1, \dots, \gamma_N),$$

$$M_{\mathrm{mult},N} = \mathrm{diag}(m_1, \dots, m_N).$$

Their divisor amplification is

$$H_{\mathrm{Ren},N} = \oplus_{n \le N} \gamma_n I_{m_n}.$$

Then the exact finite-dimensional identities

$$\det(I + z^2 H_{\mathrm{Ren},N}^{-2}) = \prod_{n \le N} \left(1 + \frac{z^2}{\gamma_n^2}\right)^{m_n},$$

and

$$\mathrm{logdet}(I + z^2 H_{\mathrm{Ren},N}^{-2}) = \mathrm{Tr}\left[M_{\mathrm{mult},N} \log(I + z^2 H_{\mathrm{id},N}^{-2})\right]$$

hold on a consistent branch of the logarithm.

At the same time, a finite list of moments

$$\mu_0, \dots, \mu_K$$

may serve as a numerical consistency check, but one must strictly distinguish

equality of finitely many moments ⇒/ exact witness identity.

The exact uniqueness in Theorem 5.1 uses all moments.

Finite-dimensional numerical checks therefore verify only the structural prototype, numerical consistency, and truncation trends; they do not replace the infinite-order witness theorem.

22. Formal Extension to General Completed L-Functions

For a completed L-function

$$\Lambda_L(s),$$

suppose the corresponding critical-line result has already been established, with distinct zero ordinates $\gamma_{L,n}$ and analytic multiplicities $m_{L,n}$. Define

$$\nu_L = \sum_n m_{L,n}\, \gamma_{L,n}^{-2} \delta_{\gamma_{L,n}^{-2}},$$

and

$$F_L(y) = \int \frac{d\nu_L(\beta)}{1 + y\beta}.$$

Then one similarly obtains

$$F_L \Leftrightarrow \nu_L \Leftrightarrow (H_{L,\mathrm{id}}, M_L) \Leftrightarrow H_{L,\mathrm{div}}.$$

The same formal conclusion depends on:

- a compactly supported finite positive witness measure;
- the cyclic spectral theorem;

- uniqueness of the Stieltjes transform;
- determinacy of the compact-support moment problem.

Thus the extension applies once the corresponding completed L-function already possesses critical-line spectral data.

23. Riemann Spectral Witness and Transfer Theorem

Theorem 23.1

On the canonical Riemann side under RH, define

$$\mathfrak{W}_{\mathrm{R}} = F_{\mathrm{R}} = \frac{d}{dy}\log\frac{X(\sqrt{y})}{X(0)}.$$

Then:

(a) Scalar Completeness

$$\boxed{\mathfrak{W}_{\mathrm{R}} \Leftrightarrow \nu_{\mathrm{R}} \Leftrightarrow (H_{\mathrm{id}}, M_{\mathrm{mult}}) \Leftrightarrow H_{\mathrm{Ren}}.}$$

(b) Moment Completeness

The full moment sequence

$$\mu_k^{\mathrm{R}} = \int \beta^k \, d\nu_{\mathrm{R}}(\beta)$$

uniquely determines ν_{R}.

(c) Analytic-Germ Completeness

The complete analytic germ of F_{R} at 0 uniquely determines ν_{R}.

(d) Cyclic Witness Uniqueness

If the scalar resolvent response of an independent cyclic pair $(B_\times, \Psi_\times)$ agrees with F_{R} on some nonempty open interval, or has the same full moment sequence, then

$$\boxed{(B_\times, \Psi_\times) \simeq (B_{\mathrm{R}}, \mathbf{1}).}$$

(e) Hilbert–Pólya Spectral-Identity Transfer

Let

$$H_\times = B_\times^{-1/2}.$$

Then

$$\boxed{H_\times \simeq H_{\mathrm{id}}.}$$

(f) Divisor Transfer

Recover the analytic multiplicity operator M_{mult} from the witness measure. Then

$$\boxed{\mathrm{Amp}_{M_{\mathrm{mult}}}(H_\times) \simeq H_{\mathrm{Ren}}.}$$

(g) Interface with the Independent Generative Chain

Chapter 9 independently generates $B_\times$ and $H_\times$. Parts (d)–(f) of the present chapter read $F_\times$ only at the terminal stage and complete identification with the canonical Riemann spectral identity.

Proof

Part (a) is Theorem 4.1.

Part (b) is Theorem 5.1.

Part (c) follows from

$$F_{\mathrm{R}}^{(k)}(0) = (-1)^k k!\, \mu_k^{\mathrm{R}}$$

together with part (b).

Part (d) is Theorem 8.1.

Part (e) is Theorem 9.1.

Part (f) is Theorem 10.1.

Part (g) follows directly from the two-layer structure of Section 12. ▫

24. Conclusion

Chapter 6 constructed the canonical Riemann spectral operator H_{Ren} and its fully marked object. The present chapter extracts from them the scalar canonical spectral witness

$$\boxed{\mathfrak{W}_{\mathrm{R}} = F_{\mathrm{R}}.}$$

This witness uniquely determines the Stieltjes measure

$$\nu_{\mathrm{R}},$$

which in turn uniquely determines

$$\{\gamma_n\}, \qquad \{m_n\}, \qquad (H_{\mathrm{id}}, M_{\mathrm{mult}}), \qquad H_{\mathrm{Ren}}.$$

Thus

$$\boxed{\mathfrak{W}_{\mathrm{R}} \Leftrightarrow \nu_{\mathrm{R}} \Leftrightarrow (H_{\mathrm{id}}, M_{\mathrm{mult}}) \Leftrightarrow H_{\mathrm{Ren}}.} \tag{24.1}$$

For any independently generated cyclic spectral pair

$$(B_\times, \Psi_\times),$$

if its scalar resolvent response

$$F_\times(y) = \langle (I + yB_\times)^{-1}\Psi_\times, \Psi_\times \rangle$$

agrees with F_{R} on a nonempty open interval, or has the same full moment sequence, then

$$\boxed{(B_\times, \Psi_\times) \simeq (B_{\mathrm{R}}, \mathbf{1}),} \tag{24.2}$$

and hence

$$\boxed{H_\times \simeq H_{\mathrm{id}},} \tag{24.3}$$

while

$$\boxed{\mathrm{Amp}_{M_{\mathrm{mult}}}(H_\times) \simeq H_{\mathrm{Ren}}.} \tag{24.4}$$

Thus spectral identity can be identified at the object level:

$$\boxed{\begin{array}{r}\text{same response} \Rightarrow \text{same measure} \Rightarrow \\ \text{same cyclic spectral object} \Rightarrow \\ \text{same canonical Riemann spectral identity.}\end{array}} \tag{24.5}$$

Chapter 7 therefore completes the bridge from the canonical Riemann spectral object to a unique witness of spectral identity. Chapter 8 proceeds from this first-order spectral identity to GUE second-order self-relations. Chapter 9 starts from the root multiplicative identity, independently constructs a source-generated Hilbert–Pólya spectrum, and can complete its terminal identity identification through the canonical witness of the present chapter.

Appendix A | Core Notation

Symbol	Meaning
$X(z)$	$\xi(1/2+z)$
$G(y)$	$X(\sqrt{y})/X(0)$
F_{R}	Riemann scalar spectral witness
$\mathfrak{W}_{\mathrm{R}}$	Canonical Riemann spectral witness
β_n	γ_n^{-2}
ν_{R}	$\sum m_n \beta_n \delta_{\beta_n}$
B_{R}	Multiplication by β on $L^2(\nu_{\mathrm{R}})$
$\mathbf{1}$	Canonical cyclic vector
H_{id}	$B_{\mathrm{R}}^{-1/2}$, the identity-faithful Hilbert–Pólya operator
M_{mult}	Analytic multiplicity operator
H_{Ren}	Divisor-faithful canonical Ren–Riemann operator
$\boldsymbol{R}_{\mathrm{Ren}}^{\mathrm{full}}$	Fully marked Ren–Riemann spectral object
μ_k^{R}	$\int \beta^k \, d\nu_{\mathrm{R}}$
$B_\times, \Psi_\times$	Independent generative-source-side cyclic witness pair
$H_\times$	$B_\times^{-1/2}$

Appendix B | Equivalent Entrances to the Witness Condition

This chapter uses three exact witness conditions:

$$\boxed{F_\times = F_{\mathrm{R}} \text{ on some nonempty open interval}}$$

$$\Downarrow$$

$$\boxed{\text{the same analytic continuation on the common Stieltjes domain}}$$

$$\Downarrow$$

$$\boxed{\nu_\times = \nu_{\mathrm{R}}.}$$

An equivalent entrance is

$$\boxed{F_\times^{(k)}(0) = F_{\mathrm{R}}^{(k)}(0) \quad \forall k}$$

or

$$\boxed{\mu_k^\times = \mu_k^{\mathrm{R}} \quad \forall k.}$$

A finite set of moments gives only a finite-order consistency check:

$$\boxed{\mu_k^{\times} = \mu_k^{\mathrm{R}} \quad 0 \le k \le K}$$

and cannot imply exact witness identity.

Appendix C | Object Scope of the Witness Theorem

The canonical witness theorem of this chapter acts on the cyclic Stieltjes spectral class. Its exact entrances include

$$F_{\times} = F_{\mathrm{R}}$$

on a nonempty open interval;

or

$$F_{\times}^{(k)}(0) = F_{\mathrm{R}}^{(k)}(0) \qquad \forall k \ge 0;$$

or equivalently

$$\mu_k^{\times} = \mu_k^{\mathrm{R}} \qquad \forall k \ge 0.$$

These conditions all imply

$$\nu_{\times} = \nu_{\mathrm{R}},$$

and thereby determine

$$(H_{\mathrm{id}}, M_{\mathrm{mult}}) \quad \text{and} \quad H_{\mathrm{Ren}}.$$

Equality of only finitely many moments gives finite-order consistency, whereas the complete spectral identity is determined by a full-order witness condition. Chapter 9 is responsible for independently generating the self-adjoint spectrum on the generative-source side; the present chapter is responsible for its terminal canonical identification. Analytic simplicity is not assumed in advance: analytic multiplicities are retained throughout by M_{mult} and the divisor-faithful representation.

Chapter 8 From the Riemann Spectral Witness to GUE

Two-Point Self-Relations, Multiplicative-Source Migration, and the Finite-Scale Renormalization Interface

Abstract

The Riemann Hypothesis, Hilbert–Pólya, and GUE belong to different mathematical levels. Chapter 1 fixes the horizontal locations of the nontrivial zeros; Chapters 6 and 7 construct the first-order canonical spectrum and its identity witness; the present chapter begins from that already determined first-order Riemann spectral identity and passes to two-point and higher-order self-relations.

Let the distinct positive zero ordinates be γ_n, with analytic multiplicities m_n, and use the identity-faithful pair of Chapter 7,

$$H_{\mathrm{id}} e_n = \gamma_n e_n, \qquad M_{\mathrm{mult}} e_n = m_n e_n.$$

Define the signed spectral operator and multiplicity display by

$$\mathcal{D} = H_{\mathrm{id}} \oplus (-H_{\mathrm{id}}), \qquad \mathcal{M} = M_{\mathrm{mult}} \oplus M_{\mathrm{mult}}.$$

For a suitable window ϕ and test function F, the spectral amplitude

$$Z_\phi(u) = \mathrm{Tr}\big[\mathcal{M}\phi(\mathcal{D})e^{iu\mathcal{D}}\big]$$

satisfies the exact two-point Fourier–Plancherel identity

$$\sum_{\lambda,\mu} m_\lambda\, m_\mu \phi(\lambda)\overline{\phi(\mu)} F(\lambda-\mu) = \frac{1}{2\pi}\int_{\mathbb{R}} \hat{F}\,(u)|Z_\phi(u)|^2\, du.$$

Thus GUE belongs to the layer of second-order self-relations formed after the first-order spectrum has already been established.

If any independently source-generated Hilbert–Pólya realization $(H_\times, M_\times)$ is identified by the Riemann spectral witness of Chapter 7 as

$$(H_\times, M_\times) \simeq (H_{\mathrm{id}}, M_{\mathrm{mult}}),$$

then its signed operator, trace amplitude, two-point measure, form factor, and every unitary-invariant two-point observable constructed by functional calculus and trace agree exactly with those of the canonical Riemann representation. This gives **second-order witness inheritance**: equality of first-order spectral identity implies equality of the second-order unitary-invariant structure.

Through the Guinand–Weil / explicit-formula interface, first-order von Mangoldt data $\Lambda(n)$ lift in the two-point self-product to

$$\Lambda(m)\Lambda(n).$$

The diagonal part produces the principal structure of the Montgomery ramp, while the off-diagonal part enters shifted Mangoldt correlations. If the generative-source length is

$$X = T^{\alpha},$$

then the integer shifts jointly resolved by a microscopic probe at height T satisfy

$$|h| \lesssim \frac{X}{T} = T^{\alpha-1}.$$

Hence $\alpha = 1$ is the second-order arithmetic-resolution threshold. It belongs to a different level from the critical real coordinate $1/2$ of the Riemann Hypothesis.

At finite scale, the raw two-point organizations of ζ and CUE/GUE are not the same. The random-matrix side is organized by the Vandermonde^2 joint law; the ζ-side is organized by Euler/local congruence factors and deterministic arithmetic locations in the integers. Each side first forms its own self-relation, performs unfolding and Fourier projection, subtracts its independently defined finite-scale structure, and finally enters a common two-point observational quotient space. This structure is called **migration of multiplicative self-relations**.

Renormalization of the raw data is implemented by the fit-free map

$$\mathfrak{M}\colon K_{\zeta}^{\mathrm{raw}} \mapsto K_{\zeta}^{\mathrm{raw}} - K_{\zeta}^{\mathrm{local}} + K_{U}^{\mathrm{ref}}.$$

In the finite-scale numerical ledger, the mean raw discrepancy falls from 0.147475 to 0.0151165; with the pre-specified finite Euler resolution $p \le H$, it falls to 0.0135793. Removal-and-restoration controls simultaneously show that the integer positions of $\Lambda(n)$ and the local prime factors govern the principal off-diagonal finite-scale correction.

The renormalized residual

$$\varepsilon_{\mathrm{ren}}$$

is retained as a finite-scale second-order observable. The structural handshake requires the two sides, after their respective corrections, to enter the same comparison space of two-point observables. If one further asks for the classical infinite-GUE / sine-kernel asymptotic, then

$$\varepsilon_{\mathrm{ren}} \to 0$$

is the stronger asymptotic specialization.

Finite-N CUE corrections together with high Riemann-zero data give an additional finite-to-finite comparison layer:

$$\begin{array}{ccccc} \zeta_{\mathrm{raw}} & \to & \zeta_{\mathrm{ren}} & \to & \mathcal{Q}_{\mathrm{pair}} \\ & & & & \updownarrow \\ \mathrm{CUE}_{N_{\mathrm{eff}}} & \to & \mathrm{CUE/GUE}_{\mathrm{bulk}} & \to & \mathcal{Q}_{\mathrm{pair}}. \end{array}$$

This chapter therefore establishes a continuous interface from first-order Riemann spectral identity to second-order self-relations, arithmetic two-point structure, and finite-scale GUE comparison. Chapter 9 then returns to the root multiplicative identity and independently constructs a Hilbert–Pólya spectrum from the generative-source side.

1. From First-Order Spectral Identity to Second-Order Self-Relations

Chapter 7 fixed the first-order Riemann spectral identity:

$$\boxed{(H_{\mathrm{id}}, M_{\mathrm{mult}}), \qquad H_{\mathrm{id}} e_n = \gamma_n e_n, \qquad M_{\mathrm{mult}} e_n = m_n e_n.} \tag{1.1}$$

Here H_{id} records the distinct zero ordinates, while M_{mult} independently records analytic multiplicities. The equivalent divisor-faithful realization is

$$H_{\mathrm{Ren}} = \oplus_n \gamma_n I_{m_n}. \tag{1.2}$$

The Riemann spectral witness gives

$$F_{\mathrm{R}} \Leftrightarrow \nu_{\mathrm{R}} \Leftrightarrow (H_{\mathrm{id}}, M_{\mathrm{mult}}) \Leftrightarrow H_{\mathrm{Ren}}. \tag{1.3}$$

1.1 First-Order Input Supplied by the Spectral Witness of Chapter 7

By the Riemann spectral witness theorem of Chapter 7, within the corresponding cyclic Stieltjes spectral class,

$$\boxed{\mathfrak{W}_{\mathrm{R}} = F_{\mathrm{R}} \Leftrightarrow \nu_{\mathrm{R}} \Leftrightarrow (H_{\mathrm{id}}, M_{\mathrm{mult}}) \Leftrightarrow H_{\mathrm{Ren}}.} \tag{1.3a}$$

Thus the first-order input of this chapter is

$$\boxed{(H_{\mathrm{id}}, M_{\mathrm{mult}}),} \tag{1.3b}$$

where

$$H_{\mathrm{id}} e_n = \gamma_n e_n, \qquad M_{\mathrm{mult}} e_n = m_n e_n.$$

If another source-generated Hilbert–Pólya realization $(H_\times, M_\times)$ has already been identified by the same spectral witness as

$$\boxed{(H_\times, M_\times) \simeq (H_{\mathrm{id}}, M_{\mathrm{mult}}),} \tag{1.3c}$$

then the two representations carry the same first-order Riemann spectral identity.

This identification fixes the first-order spectral identity. The present chapter then enters the second-order layer and proves that first-order unitary equivalence transfers to every unitary-invariant two-point observable constructed by functional calculus and trace.

Thus the logical entrance is

$$\boxed{\mathfrak{W}_{\mathrm{R}} \Rightarrow [(H_{\mathrm{id}}, M_{\mathrm{mult}})]_{\mathrm{u}} \Rightarrow \text{canonical second-order self-relations.}} \tag{1.3d}$$

The next level, once this first-order identity is fixed, is

$$\boxed{\{\gamma_n, m_n\} \rightarrow \text{two-point self-relations} \rightarrow \text{unitary random-matrix comparison.}} \tag{1.4}$$

The following three questions therefore remain distinct:

RH	:	whether the nontrivial zeros lie on the critical line,
HP	:	whether the zero ordinates admit a natural self-adjoint realization,
GUE	:	how the local two-point/higher-order relations among these first-order spectral identities are organized.

(1.5)

If an independent source-generated realization

$$(H_\times, M_\times)$$

has already been identified by the Riemann spectral witness as

$$(H_\times, M_\times) \simeq (H_{\mathrm{id}}, M_{\mathrm{mult}}), \tag{1.6}$$

then every two-point construction in this chapter agrees in the two representations. Section 3.3 gives the corresponding unitary-invariance theorem.

The logical chain of this chapter is therefore

$$\boxed{\begin{aligned} &\text{canonical/already-identified first-order spectrum} \rightarrow \\ &\text{exact two-point calculus} \rightarrow \\ &\text{arithmetic self-correlation} \rightarrow \\ &\text{finite-scale renormalization interface.} \end{aligned}} \tag{1.7}$$

Thus the object-level starting point of this chapter is an already determined first-order spectral identity, and GUE occupies the layer of its second-order self-relations.

2. Montgomery–Dyson–Odlyzko Background for Two-Point Statistics

In 1973 Montgomery studied Fourier statistics of the differences $\gamma - \gamma'$ between Riemann zeros. Under RH, he proved that the classical form factor satisfies, for fixed $0 \le \alpha < 1$,

$$F(\alpha, T) = (1 + o(1))T^{-2\alpha}\log T + \alpha + o(1). \tag{2.1}$$

Ignoring the Dirac-type diagonal term at $\alpha = 0$, one obtains

$$K(\alpha) = |\alpha|, \qquad 0 < |\alpha| < 1. \tag{2.2}$$

Dyson subsequently observed that Montgomery's conjectured two-point function is exactly the form of the local spectral statistics of large complex Hermitian/unitary random matrices. Odlyzko's computations of high zeros further showed striking agreement between the local spacing statistics of the zeros and random-Hermitian-matrix predictions, with finite-sample deviations generally decreasing at greater heights.

The corresponding second-order structural question is

> a deterministic spectrum generated from a prime multiplicative source enters the unitary universality class in its local two-point statistics. (2.3)

The first-order spectral witness and self-adjoint realization settle the spectral-identity layer. The present chapter studies the second-order layer of (2.3).

3. From a Deterministic First-Order Spectrum to an Exact Two-Point Trace

3.1 Bilateral Spectrum and Multiplicity Display

Define the signed Hilbert–Pólya operator

$$\mathcal{D} = H_{\mathrm{id}} \oplus (-H_{\mathrm{id}}), \tag{3.1}$$

and

$$\mathcal{M} = M_{\mathrm{mult}} \oplus M_{\mathrm{mult}}. \tag{3.2}$$

Its discrete spectrum is

$$\sigma(\mathcal{D}) = \{\pm\gamma_n\}, \tag{3.3}$$

while $\mathcal{M}$ supplies only the analytic weight attached to the same identity address.

For a smooth window ϕ, define the spectral amplitude

$$Z_\phi(u) := \mathrm{Tr}\left[\mathcal{M}\phi(\mathcal{D})e^{iu\mathcal{D}}\right] = \sum_{\lambda=\pm\gamma_n} m_\lambda\, \phi(\lambda)e^{iu\lambda}. \tag{3.4}$$

3.2 Exact Two-Point Fourier–Plancherel Identity

Let F be a Schwartz test function, with convention

$$F(x) = \frac{1}{2\pi}\int_{\mathbb{R}} \hat{F}\,(u)e^{iux}\,du. \tag{3.5}$$

Direct expansion gives

$$\boxed{\sum_{\lambda,\mu} m_\lambda\, m_\mu \phi(\lambda)\overline{\phi(\mu)}F(\lambda-\mu) = \frac{1}{2\pi}\int_{\mathbb{R}} \hat{F}\,(u)|Z_\phi(u)|^2\, du.} \tag{3.6}$$

This is an exact Fourier–Plancherel identity and is independent of any GUE asymptotic assumption.

Equation (3.6) lifts first-order spectral points to pairwise relations and therefore passes from a first-order spectrum to second-order self-relations.

3.3 Second-Order Witness Inheritance Theorem

Unitary equivalence of the first-order spectral witness transfers automatically to unitary-invariant two-point structure.

Let

$$U: \mathcal{H}_\times \to \mathcal{H}_{\mathrm{id}}$$

be unitary and satisfy

$$UH_\times U^{-1} = H_{\mathrm{id}}, \qquad UM_\times U^{-1} = M_{\mathrm{mult}}. \tag{3.7}$$

Define the signed source-generated operators

$$\mathcal{D}_\times = H_\times \oplus (-H_\times), \qquad \mathcal{M}_\times = M_\times \oplus M_\times, \tag{3.8}$$

and let

$$\mathcal{U} = U \oplus U.$$

Then

$$\mathcal{U}\mathcal{D}_\times\mathcal{U}^{-1} = \mathcal{D}, \qquad \mathcal{U}\mathcal{M}_\times\mathcal{U}^{-1} = \mathcal{M}. \tag{3.9}$$

Theorem 3.1 (Second-Order Witness Inheritance)

For every window ϕ for which the relevant operators are trace class, and every $u \in \mathbb{R}$,

$$\boxed{\mathrm{Tr}\left[\mathcal{M}_\times \phi(\mathcal{D}_\times) e^{iu\mathcal{D}_\times}\right] = \mathrm{Tr}\left[\mathcal{M}\phi(\mathcal{D})e^{iu\mathcal{D}}\right].} \tag{3.10}$$

Consequently the two sides have exactly the same weighted two-point measure, form factor, and every unitary-invariant two-point observable constructed from functional calculus and trace.

Proof

By (3.9) and Borel functional calculus,

$$\phi(\mathcal{D}) = \mathcal{U}\phi(\mathcal{D}_\times)\mathcal{U}^{-1},$$

and

$$e^{iu\mathcal{D}} = \mathcal{U}e^{iu\mathcal{D}_\times}\mathcal{U}^{-1}.$$

The corresponding trace-class operators are therefore unitarily conjugate. Trace is invariant under unitary conjugation, which gives (3.10). Substitution into the two-point Fourier–Plancherel identity yields equality of all two-point observables. ▫

This theorem gives the **source-generated equivalent GUE interface** required by this chapter:

$$\boxed{(H_\times, M_\times) \simeq (H_{\mathrm{id}}, M_{\mathrm{mult}}) \Rightarrow \mathcal{P}_2(H_\times, M_\times) = \mathcal{P}_2(H_{\mathrm{id}}, M_{\mathrm{mult}}),} \tag{3.11}$$

where $\mathcal{P}_2$ denotes the complete family of two-point observables.

Thus, once any independently constructed Hilbert–Pólya realization has been identified as the same first-order spectral identity, all of its unitary-invariant two-point structure automatically agrees with the canonical representation. The second-order theory does not need to be rebuilt merely because the first-order representation has a different provenance.

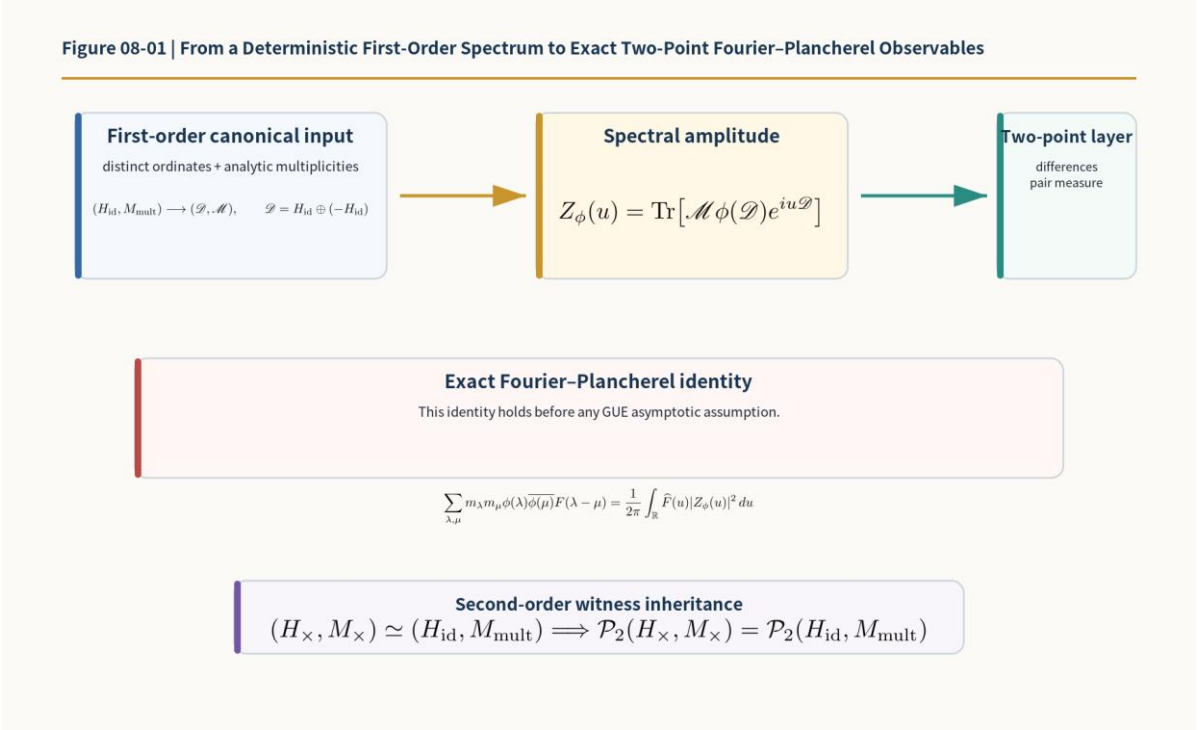


Figure 08-01. From first-order spectrum to exact two-point observables. The fixed first-order identity $(H_{\mathrm{id}}, M_{\mathrm{mult}})$ is first extended to the signed bilateral pair $(\mathcal{D}, \mathcal{M})$, and the spectral amplitude $Z_\phi(u)$ then gives an exact two-point Fourier–Plancherel identity. This step is independent of any GUE asymptotic. If another source-generated realization is unitarily equivalent to the canonical first-order spectrum, all unitary-invariant two-point observables are inherited automatically.

4. Unfolding: Removing the Mean Density

The mean density of the Riemann zero ordinates varies slowly with height. If the raw gaps between the γ_n are compared directly, their mean spacing changes with height and cannot be compared directly with a stationary bulk random-matrix law.

Take the smooth main term of the Riemann–von Mangoldt counting function,

$$\bar{N}(T) = \frac{T}{2\pi}\left(\log\frac{T}{2\pi} - 1\right) + \frac{7}{8}. \tag{4.1}$$

Define the unfolded coordinates

$$\boxed{x_n = \bar{N}(\gamma_n).} \tag{4.2}$$

Their local mean spacing is therefore normalized to approximately 1.

The universal bulk two-point density for GUE/CUE is

$$\boxed{R_2(u) = 1 - \left(\frac{\sin\pi u}{\pi u}\right)^2.} \tag{4.3}$$

This formula includes level repulsion: as $u \to 0$, the density for two distinct spectral points to occur together is suppressed.

5. Second-Order Correspondence between the ζ-Spectrum and GUE

The phrase "one-to-one correspondence between the ζ-spectrum and GUE" becomes mathematically precise only after the object levels are fixed. This chapter uses the following correspondence dictionary:

Deterministic ζ/HP spectrum	GUE/CUE random-matrix side	Mode of correspondence
ordinate γ_n	eigenphase/eigenvalue point	compare point processes after unfolding; no sample-by-sample pointwise identification
$x_n = \bar{N}(\gamma_n)$	bulk-unfolded spectral point	same local mean-spacing scale
difference $x_m - x_n$	eigenvalue difference	two-point relative coordinate
two-point measure $\sum_{m,n} \delta_{x_m - x_n}$	ensemble two-point measure	compare in the sense of test functions
Fourier transform of the two-point measure	spectral form factor	two-way Fourier interface
diagonal $m = n$	self-correlation diagonal	diagonal source of the ramp
connected off-diagonal part	connected GUE correlation	nontrivial part of plateau / sine kernel
arithmetic decoration of ζ	finite-size / arithmetic correction	accounted for separately before entering the universal quotient space

Thus the genuine "one-to-one correspondence" used in this chapter is

$$\boxed{\text{deterministic spectral object} \leftrightarrow \text{random-matrix observable of the same type}} \tag{5.1}$$

rather than

$$\boxed{\text{the}n\text{th Riemann zero} = \text{the}n\text{th eigenvalue of one random-matrix sample.}} \tag{5.2}$$

The latter is neither canonical nor part of what GUE statistics predicts.

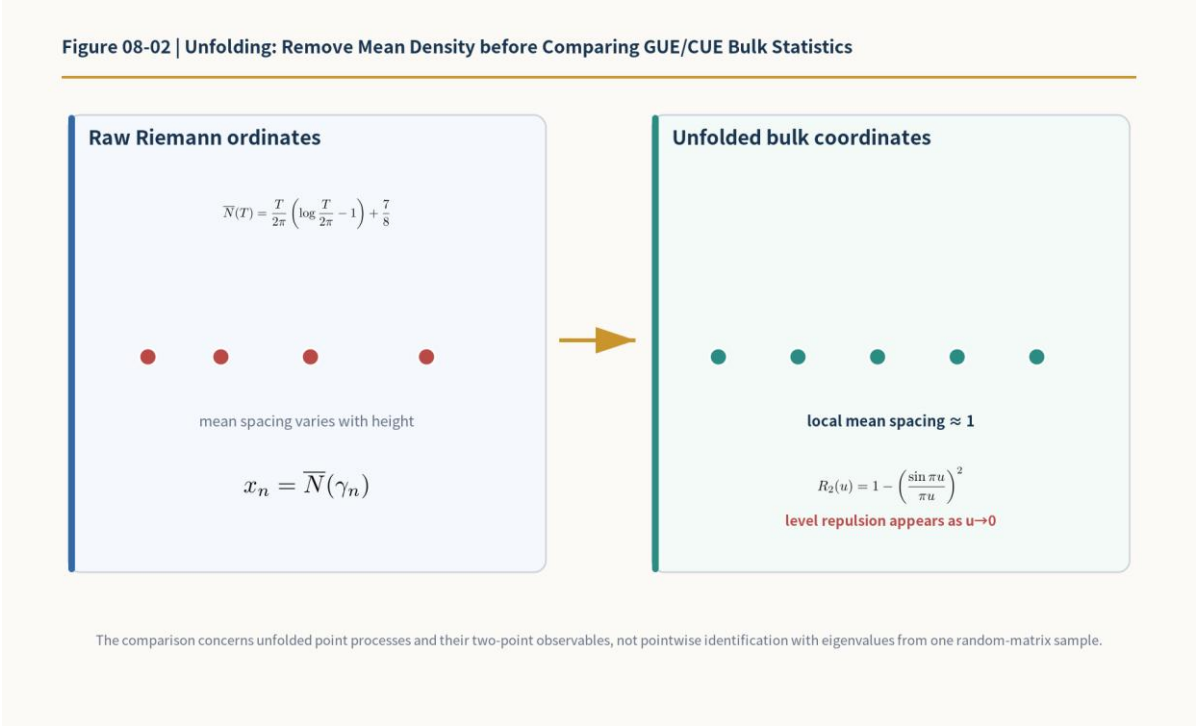


Figure 08-02. Unfolding. The mean density of the raw Riemann ordinates varies with height, so one first maps γ_n to $x_n = \overline{N}(\gamma_n)$ using the smooth Riemann–von Mangoldt counting term, normalizing local mean spacing to approximately 1. Only on this scale is comparison with the GUE/CUE bulk sine-kernel two-point density meaningful. The comparison concerns point-process observables, not pointwise equality with one random-matrix sample.

6. Arithmetic Interface from the First-Order Spectrum to the Prime Side

The first-order Riemann spectral readout is connected with prime-power data through the Guinand–Weil explicit formula. Let

$$H_{\mathrm{mult}}e_n = (\log n)e_n, \qquad \Lambda_{\times}e_n = \Lambda(n)e_n. \tag{6.1}$$

For a suitable even test function h and Fourier transform g, one has the structural relation

$$\mathrm{Tr}[M_{\mathrm{mult}}h(H_{\mathrm{id}})] = \frac{1}{2}\mathcal{A}_{\infty}[h] - \mathrm{Tr}\left[\Lambda_{\times}e^{-H_{\mathrm{mult}}/2}g(H_{\mathrm{mult}})\right]. \tag{6.2}$$

The arithmetic side is

$$\sum_{n\geq 2}\frac{\Lambda(n)}{\sqrt{n}}g(\log n). \tag{6.3}$$

Define the prime-event measure

$$\mu_{\mathrm{prime}} = \sum_{n\geq 2}\frac{\Lambda(n)}{\sqrt{n}}\delta_{\log n} = \sum_{p}\sum_{k\geq 1}\frac{\log p}{p^{k/2}}\delta_{k\log p}. \tag{6.4}$$

The following type distinction remains in force:

$$\{\gamma_n\} \not\equiv \{k\log p\} \quad \text{pointwise.} \tag{6.5}$$

They read one another only at the global test-function level through the explicit formula.

7. The Two-Point Self-Product and $\Lambda(m)\Lambda(n)$

A one-point trace is linear:

$$\mu \mapsto \langle \mu, f\rangle. \tag{7.1}$$

Two-point statistics instead involve

$$\mu \mapsto \mu \otimes \mu. \tag{7.2}$$

Let the arithmetic part of the spectral amplitude be denoted by $P_\phi(u)$. The explicit formula gives

$$Z_\phi(u) = A_\phi(u) + P_\phi(u), \tag{7.3}$$

where A_ϕ is the Archimedean/background contribution. Squaring gives

$$|Z_\phi|^2 = |A_\phi|^2 + 2\Re(A_\phi \overline{P_\phi}) + |P_\phi|^2. \tag{7.4}$$

The genuine arithmetic two-point fluctuation is concentrated in

$$\boxed{|P_\phi(u)|^2.} \tag{7.5}$$

Expanding it necessarily produces

$$\boxed{|P_\phi(u)|^2 = \sum_{m,n} \frac{\Lambda(m)\Lambda(n)}{\sqrt{mn}} W_{\phi,u}(\log m, \log n).} \tag{7.6}$$

Thus shifted Mangoldt correlations are not an external complication introduced later. They are the second-order object that necessarily appears when the one-point spectrum is multiplied by itself.

7.1 The Second-Order Relative Relation of the First-Order Multiplicative Identity

Merely saying that "$\Lambda(n)$ becomes $\Lambda(m)\Lambda(n)$" does not yet explain the geometry of the transition. What actually happens is that **the same multiplicative identity is no longer read only once; it begins to form relative relations with itself.**

On the multiplicative-source Hilbert space,

$$H_\times e_n = (\log n) e_n. \tag{7.7}$$

A one-point readout asks only for the logarithmic scale of the nth multiplicative event. At the two-point level, the natural operator is no longer $H_\times$ itself but the tensor-difference operator

$$\boxed{D_\times = H_\times \otimes I - I \otimes H_\times.} \tag{7.8}$$

Its spectrum is

$$\boxed{\mathrm{spec} D_\times = \{\log m - \log n\} = \left\{\log \frac{m}{n}\right\}.} \tag{7.9}$$

This step is crucial. **The natural coordinate of first-order multiplication is** $\log n$**; the natural coordinate of the second-order self-relation is not** m **and** n **separately, but their ratio** m/n**.** Second order therefore does not create a new arithmetic; it is a relative readout of the original multiplicative identity.

If the two-point probe is concentrated near the diagonal,

$$m = n + h, \qquad |h| \ll n, \tag{7.10}$$

then

$$\log \frac{n+h}{n} = \frac{h}{n} + O\left(\frac{h^2}{n^2}\right). \tag{7.11}$$

This gives one of the central structural transitions of the second half of this chapter:

$$\boxed{\text{multiplicative relative relation} \log(m/n) \quad \rightarrow \quad \text{microscopic additive near-diagonal relation} h = m - n.} \tag{7.12}$$

This is the precise form of "multiplication meeting itself." It does not mean that multiplication suddenly becomes addition. It means that, after a second-order comparison of a multiplicative object with itself, the microscopic coordinate near the identity ratio $m/n = 1$ is linearized by the additive difference h.

Thus the later appearance of prime-pair / shifted-Mangoldt problems is not a deviation from the route; it is the natural coordinate expression of second-order multiplicative identity in the near-identity region.

Equations (7.8)–(7.12) are exact at the operator and local-expansion levels. They are not by themselves equivalent to the sine-kernel / infinite-GUE asymptotic.

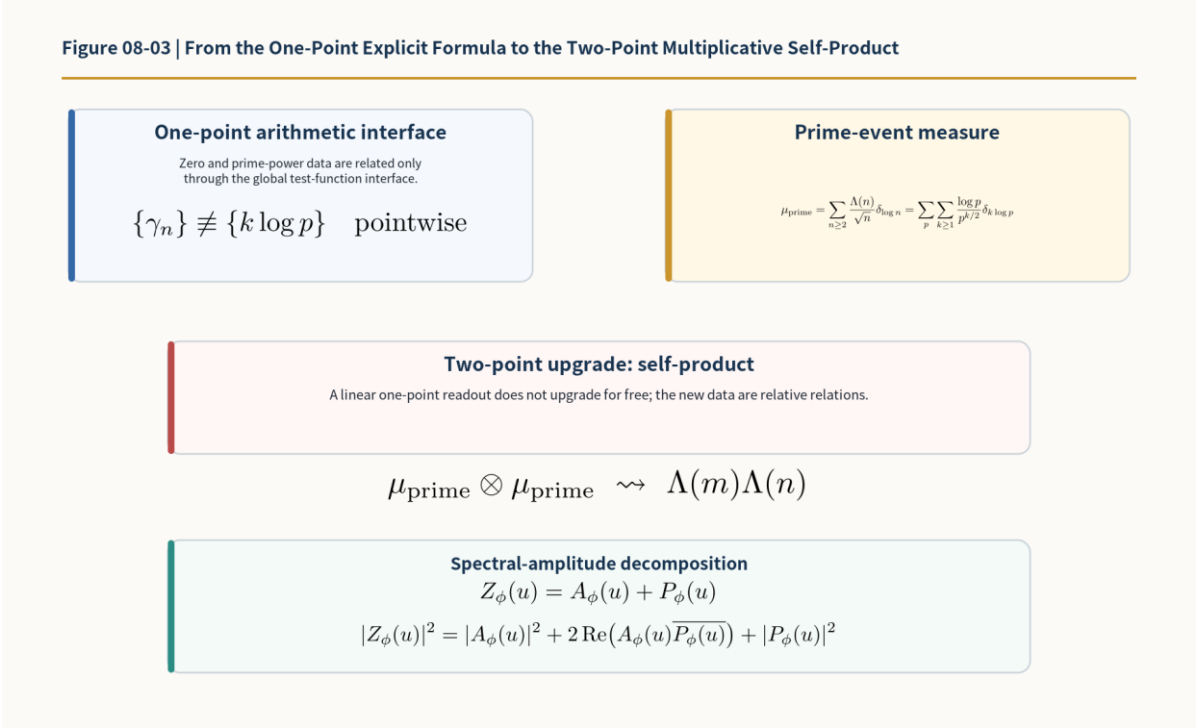


Figure 08-03. From the one-point interface to the two-point self-product. The explicit formula relates the first-order Riemann spectrum to the prime-power source only at the global test-function level; $\{\gamma_n\}$ and $\{k\log p\}$ are not pointwise identical. At second order, the linear one-point readout is upgraded to the self-product of the prime-event measure, introducing the genuinely new objects $\Lambda(m)\Lambda(n)$ and their relative/shifted correlations. Squaring the spectral amplitude likewise produces arithmetic quadratic and cross terms.

8. The Diagonal Term and the Montgomery Ramp

Split (7.6) into

$$m = n \quad \text{and} \quad m \neq n. \tag{8.1}$$

The diagonal term is

$$\sum_{n} \frac{\Lambda(n)^2}{n} W(n,n). \tag{8.2}$$

It pairs the same arithmetic event with itself and therefore requires no control of relative positions between distinct prime channels.

Under Montgomery's normalization, this corresponds to

$$\boxed{K(\alpha) = |\alpha|, \qquad 0 < |\alpha| < 1.} \tag{8.3}$$

Montgomery proved the corresponding form-factor asymptotic on $0 \leq \alpha < 1$ under RH. This chapter does not write the plateau for $|\alpha| > 1$ as though it were already contained in that classical theorem.

9. Off-Diagonal Terms: Multiplicative Locality and Additive Near-Diagonality

Write the off-diagonal part as

$$m = n + h, \qquad h \neq 0. \tag{9.1}$$

Its core data are

$$\Lambda(n)\Lambda(n+h). \tag{9.2}$$

On the other hand, the two-point spectrum reads only the logarithmic ratio

$$\log\frac{m}{n}. \tag{9.3}$$

If $m = n + h$ with $|h| \ll n$, then

$$\boxed{\log\frac{n+h}{n} = \frac{h}{n} + O\left(\frac{h^2}{n^2}\right).} \tag{9.4}$$

Thus

$$\boxed{\text{multiplicative relative coordinate} \log(m/n) \quad \rightarrow \quad \text{microscopic additive near-diagonal coordinate} h = m - n.} \tag{9.5}$$

This explains an apparently paradoxical fact: the first-order structure of ζ is localized multiplicatively by the Euler product, while its second-order self-relations naturally enter additive-shift problems.

9.1 Local Euler Multiplication and Global Additive Neighbors

The first-order logarithmic derivative

$$-\frac{\zeta'}{\zeta}(s) = \sum_{n\geq 1}\frac{\Lambda(n)}{n^s} \tag{9.6}$$

is local with respect to the Euler product: each prime channel can be registered separately.

At second order, however, the genuine off-diagonal sector contains

$$\Lambda(m)\Lambda(n). \tag{9.7}$$

In the most important primitive sector, the two ends often come from different prime channels, typically

$$p \neq q, \qquad (p,q) = 1. \tag{9.8}$$

No single Euler factor can re-localize this pair relation to the diagonal. Meanwhile the microscopic spectral condition

$$T\log(p/q) = O(1) \tag{9.9}$$

becomes, for $p, q \asymp X$,

$$q - p = h, \qquad |h| \lesssim X/T. \tag{9.10}$$

The original intuition can therefore be stated more precisely as

second-order relations among local multiplicative factors are read globally through additive near-neighbors. (9.11)

This is a statement about the transformation of coordinates and second-order relations; it does not by itself establish the sine kernel. What can be retained unconditionally is

$$\boxed{\text{second-order multiplication} \Rightarrow \text{additive near-diagonal relative spectrum.}} \tag{9.12}$$

The stronger passage

$$\boxed{\text{actual relative spectrum} \Rightarrow \text{sine-kernel scaling}} \tag{9.13}$$

still requires second-order arithmetic input such as Actual-to-Dual Transfer.

10. $\alpha = 1$: The Second-Order Multiplicative-Source Resolution Threshold

Let the height parameter be T and the generative-source length be

$$X = T^{\alpha}. \tag{10.1}$$

A local probe resolves logarithmic ratios on the scale $1/T$. If $n \asymp X$, then

$$T\log\frac{n+h}{n} = O(1) \tag{10.2}$$

requires

$$\boxed{|h| \lesssim \frac{X}{T} = T^{\alpha-1}.} \tag{10.3}$$

Hence

$$\alpha < 1 \quad \Rightarrow \quad X/T \to 0, \tag{10.4}$$

so every nonzero integer h eventually falls outside the same microscopic probe and only $h = 0$ remains; whereas

$$\alpha > 1 \quad \Rightarrow \quad X/T \to \infty, \tag{10.5}$$

so more and more nonzero shifts become visible.

Thus

$$\boxed{\alpha = 1} \tag{10.6}$$

is a genuine **arithmetic resolution threshold**.

This does not mean that $\alpha = 1$ itself proves GUE. It explains why the difficulty changes qualitatively at the ramp/plateau transition.

10.1 The Critical Real Coordinate $1/2$ versus the Second-Order Resolution Threshold $\alpha = 1$

The statement that "the encounter of first-order and second-order multiplication forces a self-dual critical point" has a rigorous meaning only after the two levels are separated.

The first critical value belongs to RH:

$$\sigma = \frac{1}{2}, \tag{10.7}$$

and comes from the functional equation of the completed zeta function,

$$\xi(s) = \xi(1-s). \tag{10.8}$$

This is the **identity-level duality center**.

The second critical value belongs to second-order generative-source resolution:

$$\alpha = 1, \tag{10.9}$$

and comes from

$$H = X/T = T^{\alpha-1} \tag{10.10}$$

crossing from a scale smaller than one integer shift to a scale capable of containing nonzero shifts. This is the **self-correlation resolution threshold**.

The two must not be merged into one theorem. Structurally, however, they exhibit a clear order-level correspondence: the first-order duality center fixes the spectral axis, while the fixed scale of the second-order relative readout determines the boundary between diagonal and off-diagonal behavior.

10.2 One-Swap Reciprocal Duality and $\alpha = 1$

Moreover, $\alpha = 1$ is not merely a resolution heuristic. In the one-swap structure of long Dirichlet polynomials, the natural length ratio is

$$r = \frac{X}{Q(t)}, \qquad Q(t) \asymp \frac{T}{2\pi}, \tag{10.11}$$

with reciprocal involution

$$\boxed{r \mapsto r^{-1}.} \tag{10.12}$$

Equivalently, the dual length is

$$X^{\vee} = \frac{Q(t)^2}{X}, \tag{10.13}$$

whose fixed point is

$$X = Q(t) \asymp T. \tag{10.14}$$

Writing $X = T^{\alpha}$, the exponent coordinate satisfies asymptotically

$$\alpha^{\vee} = 2 - \alpha + o(1), \qquad \boxed{\alpha = 1} \tag{10.15}$$

as the fixed scale.

For the low-order generative source

$$D_X(t) = \sum_{n \le X} n^{-1/2-it}, \tag{10.16}$$

the diagonal contribution to the normalized second moment gives α. Once $X > T$, the one-swap/dual contribution supplies

$$1 - \alpha. \tag{10.17}$$

Thus this low-order model exhibits the exact prototype

$$\boxed{K_0(\alpha) = \min(\alpha, 1), \qquad 0 < \alpha < 2,} \tag{10.18}$$

namely

$$\boxed{\text{direct diagonal} + \text{dual off-diagonal} = \alpha + (1 - \alpha) = 1.} \tag{10.19}$$

This point is important: **the plateau correction $1 - \alpha$ already has a genuine direct/dual mathematical prototype in a low-order ζ-generated source; it is not reverse-engineered from the desired GUE target.**

It still cannot be promoted directly to full GUE. The genuine logarithmic-derivative / von-Mangoldt layer requires lifting the coefficients from the low-order model to $\Lambda(n)$ and controlling a uniform remainder in the true second-order average.

The one-swap reciprocal structure and the low-order direct/dual decomposition therefore provide an exact prototype in their proper setting. Promoting that structure to the classical full zero plateau requires additional second-order arithmetic control.

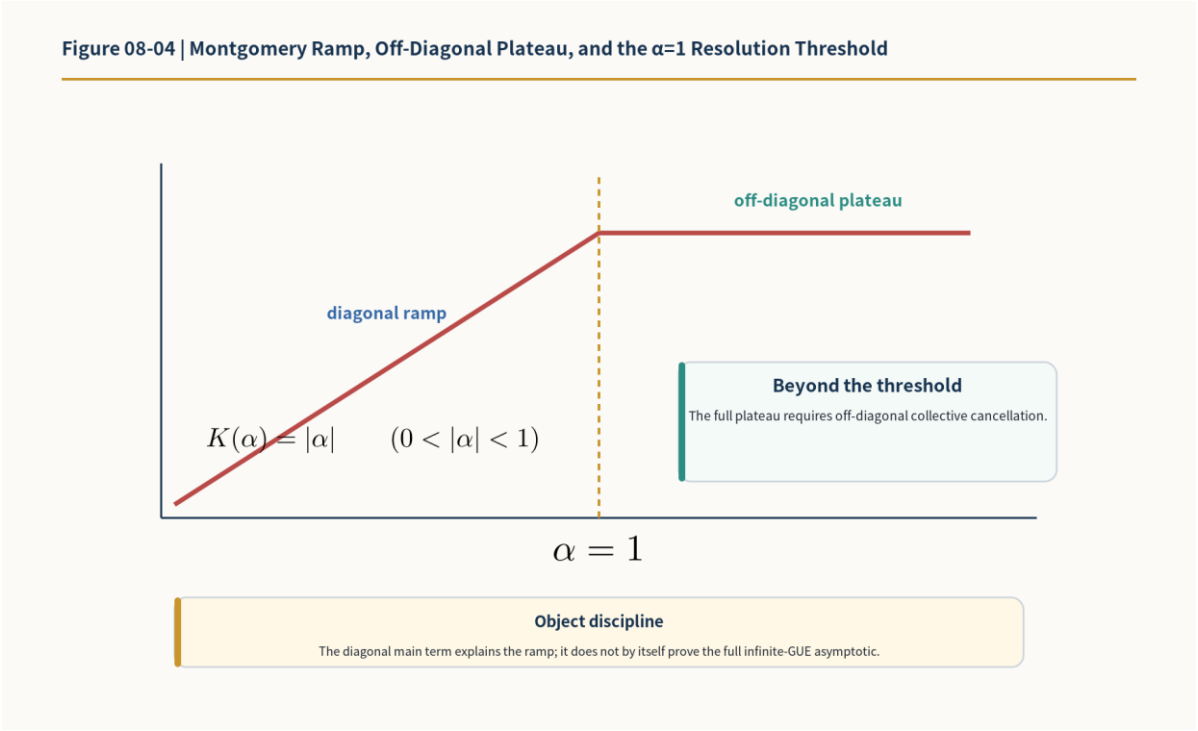


Figure 08-04. Ramp, plateau, and $\alpha = 1$. For $0 < |\alpha| < 1$, Montgomery's classical two-point shape gives the ramp $K(\alpha) = |\alpha|$, whose leading contribution can be explained by diagonal structure. Beyond the threshold $\alpha = 1$, the full plateau depends on off-diagonal collective cancellation. Obtaining the ramp is therefore not the same as proving the complete infinite-GUE asymptotic.

11. Arithmetic Form of the Plateau and the Connected Second-Order Term

The raw product

$$\Lambda(n)\Lambda(n+h) \tag{11.1}$$

contains a large amount of first-order mean information. Write

$$a(n) = \Lambda(n) - 1. \tag{11.2}$$

Then

$$\Lambda(n)\Lambda(n+h) = 1 + a(n) + a(n+h) + a(n)a(n+h). \tag{11.3}$$

The first three terms are all controlled by first-order mean structure. The genuinely new term is

$$\boxed{a(n)a(n+h).} \tag{11.4}$$

After further subtracting the predictable part of the Hardy–Littlewood singular-series model, what remains is the connected second-order residual. A corresponding dynamic arithmetic target can be written in kernel-weighted form as

$$\sum_{h,n} [(\Lambda(n) - 1)(\Lambda(n+h) - 1) - (\mathfrak{S}(h) - 1)]\, K_{T,\alpha}(n,h) = o(T\log T). \tag{11.5}$$

This formula represents one type of dynamically centered arithmetic control required for the classical plateau specialization. It is not part of the structural handshake theorem of this chapter.

12. The Goldston–Montgomery Bridge and Prime Variance in Short Intervals

A typical scale for the centered Chebyshev variance over short intervals is

$$V(X,H) \sim HX\log\frac{X}{H}. \tag{12.1}$$

Classical work of Goldston and Montgomery shows that, under RH and in suitable parameter ranges, sufficiently strong two-point correlation asymptotics are equivalent to corresponding asymptotics for the variance of primes in short intervals.

A convenient discrete triangular-kernel form is

$$V(X,H)=\sum_{m,n}(\Lambda(m)-1)(\Lambda(n)-1)(H-|m-n|)_{+}. \tag{12.2}$$

This yields the conceptual chain

$$\boxed{\begin{array}{r}\text{GUE two-point correlation} \Leftrightarrow\\ \text{short-interval variance} \Leftrightarrow\\ \text{centered shifted-Mangoldt correlation.}\end{array}} \tag{12.3}$$

Thus, if one further pursues the classical infinite-GUE asymptotic, its new arithmetic requirement is not artificially created by the spectral representation of this chapter; it lands precisely in the second-order arithmetic core of classical pair-correlation theory.

13. Non-Equivalence of First-Order Self-Adjoint Structure and the GUE Second-Order Law

A self-adjoint spectrum can have entirely different local statistics: Poisson, clock-like, GOE, GUE, and other behaviors can occur in different systems. Therefore

$$H=H^{*} \tag{13.1}$$

ensures only that the spectrum is real; it does not determine the two-point correlation kernel.

Likewise, the unitary phase associated with multiplicative dilation fixes a frequency coordinate but does not automatically generate the sine kernel.

Accordingly, this chapter fixes the following distinction:

HP self-adjointness + horizon phase do not suffice to imply GUE. (13.2)

One therefore cannot infer GUE directly from a self-adjoint Hilbert–Pólya realization merely because GUE is the statistics of Hermitian matrices.

14. Non-Equivalence of Low-Order Means and the Second-Order Plateau

A lower-order generative-source model uses a Dirichlet polynomial weighted by $\Lambda(n)/\log n$; scale differentiation can formally recover the $\Lambda(n)$-level. The decisive issue, however, is regularity of the remainder in the scale variables.

Suppose the remainder in a lower-order covariance satisfies

$$|E_T(L_1,L_2)|\le \mathcal{E}_T. \tag{14.1}$$

Recovering mixed curvature by a second finite difference with scale step Δ amplifies the error by roughly

$$\frac{L^4}{\Delta^2}\mathcal{E}_T. \tag{14.2}$$

To keep this below the natural main scale at the Λ-level requires scale regularity substantially stronger than that supplied by the existing lower-order theorem.

Thus the principle

"differentiate the existing lower-order theorem and obtain the full GUE plateau."

(14.3)

is not valid as stated. What is actually needed is

$$\boxed{C^{1,1}\text{-type mixed-curvature control}} \tag{14.4}$$

in the scale variables.

Heap's results on long Dirichlet polynomials reinforce the same point from another direction: one can obtain strong control for lower-order weights, but when one passes to the logarithmic-derivative / Λ-level, Montgomery-type pair-correlation information reappears.

15. Functional Equation and the Dual Diagonal Main Term

Consider the ratio coefficients

$$I_{\alpha,\gamma}(s) = \frac{\zeta(s+\alpha)}{\zeta(s+\gamma)} = \sum_{n\geq 1} \frac{I_{\alpha,\gamma}(n)}{n^s}. \tag{15.1}$$

At the parameter origin,

$$-\partial_\alpha I_{\alpha,\gamma}(n)\big|_{\alpha=\gamma=0} = \Lambda(n). \tag{15.2}$$

Conrey–Keating-type analyses of long Dirichlet polynomials and ratios show that, in appropriate models or under suitable uniform correlation input, an off-diagonal transformation can match a dual diagonal produced by the functional equation of the same ζ-function.

This gives an important structural conclusion:

the correct main term of the plateau is not mysterious; it already appears as a dual diagonal of the same ζ-identity.

(15.3)

What remains to be closed is whether the actual self-correlation can be transferred losslessly to this dual diagonal.

15.1 First-Order Anti-Self-Duality and Second-Order Self-Duality

One can also remove a potential structural obstruction: compatibility between coefficient raising/differentiation and one-swap duality.

Write the one-swap duality as

$$(\mathcal{D}_Q f)(a,b) = Q^{-a-b} f(-b,-a), \qquad \ell = \log Q. \tag{15.6}$$

Then

$$\boxed{\mathcal{D}_Q^2 = I.} \tag{15.7}$$

Ordinary derivatives do not commute with $\mathcal{D}_Q$, because

$$\partial_a \mathcal{D}_Q = -\mathcal{D}_Q(\partial_b + \ell). \tag{15.8}$$

Introduce the half-conductor connection

$$\boxed{\nabla_a = \partial_a + \frac{1}{2}\log Q, \qquad \nabla_b = \partial_b + \frac{1}{2}\log Q.} \tag{15.9}$$

Then one obtains the exact intertwining relations

$$\boxed{\nabla_a \mathcal{D}_Q = -\mathcal{D}_Q \nabla_b, \qquad \nabla_b \mathcal{D}_Q = -\mathcal{D}_Q \nabla_a,} \tag{15.10}$$

and the second-order identity

$$\boxed{\nabla_a \nabla_b \mathcal{D}_Q = \mathcal{D}_Q \nabla_a \nabla_b.} \tag{15.11}$$

After changing variables to

$$u = (a+b)/2, \qquad v = (a-b)/2, \tag{15.12}$$

and applying the natural gauge, the one-swap transformation reduces to the ordinary reflection $u \mapsto -u$. Hence

the first-order completed multiplicative readout is anti-self-dual; the second-order self-correlation is self-dual.

(15.13)

This explains why the completed logarithmic derivative is the natural object: the Archimedean/conductor term is not an external patch but precisely the connection that makes raising covariant with respect to self-duality.

Thus algebraic/model compatibility between raising and duality is no longer an obstruction. If one pursues the classical infinite-GUE asymptotic, the remaining analysis is concentrated in the uniform remainder of the actual average.

16. Arithmetic Strengthening for the Classical Infinite-GUE Asymptotic: Actual-to-Dual Diagonal Transfer

The exact pair calculus, generative-source self-correlation, and finite-scale handshake developed above do not require the classical infinite-GUE plateau to be proved first. If one goes further and asks for the standard infinite-height Montgomery–GUE asymptotic, one meets a stronger arithmetic problem.

In the language of ratios and the functional equation, the completed functional equation already supplies the principal structure that the dual diagonal must have. The additional task is to control whether the actual shifted self-correlation, on dynamic microscopic scales, falls onto that dual diagonal with a sufficiently uniform remainder.

A typical target has the form

$$\mathcal{R}_{\mathrm{DC}}(X,H) = o\left(HX\log\frac{X}{H}\right), \tag{16.1}$$

or, in scale coordinates, a corresponding mixed-curvature remainder estimate.

This problem lies on the same second-order arithmetic level as strong pair correlation and the variance of primes in short intervals. It is retained here to show where the arithmetic content of the classical infinite-GUE asymptotic resides. It is explicitly classified as an additional arithmetic requirement of that stronger asymptotic.

Thus we distinguish

$$\boxed{\text{structural / finite-scale handshake}}$$

from

$$\boxed{\text{classical infinite-GUE asymptotic specialization.}}$$

The former is the main subject of this chapter; the latter imposes a stronger asymptotic condition on the limiting behavior of $\varepsilon_{\mathrm{ren}}$.

17. The Ratios Method and Higher-Order Arithmetic Coordinates for the Classical GUE Asymptotic

The ratios method of Conrey–Snaith shows that, under the ratios-conjecture input, one can systematically obtain n-correlations of ζ-zeros together with lower-order terms; the same method on $U(N)$ produces random-matrix expressions of the same structural form.

Conrey–Keating further showed that the ratios conjecture and a class of conjectures on correlations of arithmetic coefficients lead to the same result. This demonstrates that

$$\boxed{\text{random-matrix expression} \quad \text{and} \quad \text{arithmetic coefficient correlation}} \tag{17.1}$$

are genuinely two coordinate systems for the same structure.

However, a uniform ratios remainder carries substantive second-order arithmetic information; it is not a merely formal small error from ordinary complex analysis. Recent strong results even show that sufficiently uniform input for two-over-two ζ-ratios can imply Hardy–Littlewood asymptotics for fixed-shift prime pairs. Thus the statement

$$\boxed{\text{“formal analyticity of ratios automatically yields the plateau.”}} \tag{17.2}$$

is too strong. More precisely, ratios analyticity supplies a powerful automatic-differentiation and organizational coordinate system, but the classical plateau still requires a uniform remainder carrying genuine second-order arithmetic information.

18. The Two-Sided ζ–GUE Migration Interface

Writing naively

$$\zeta \stackrel{?}{=} \mathrm{GUE} \tag{18.1}$$

mixes object levels. ζ is a deterministic arithmetic object, whereas GUE is a random-matrix ensemble. Their natural meeting point is not the raw source but the quotient space of second-order pair observables.

Define the conceptual two-sided diagram

$$\boxed{\begin{array}{ccccc} \zeta\text{generative source} & \overset{\text{self product}}{\rightarrow} & \text{ratio relations} & \overset{\text{unfold}}{\rightarrow} & \mathcal{Q}_{\mathrm{pair}} \\ & & & & \updownarrow\ \mathcal{F} \\ \text{GUE/CUE generative source} & \overset{\text{self product}}{\rightarrow} & \text{relative spectrum} & \overset{\text{unfold}}{\rightarrow} & \mathcal{Q}_{\mathrm{pair}}. \end{array}} \tag{18.2}$$

This chapter calls the mechanism

$$\boxed{\textbf{Multiplicative Self-Relation Migration}.} \tag{18.3}$$

At the level of two-point statistics, the two-point measure and the form factor are translated in both directions by the Fourier transform. But in general one cannot recover the phase of $\hat{\mu}$ from

$$|\hat{\mu}|^2.$$

Therefore

invertibility occurs in the second-order quotient space, not in the raw source space.

(18.4)

This is the point of the migration mechanism: ζ is not required to "obey GUE," nor is GUE asked to explain all primes. The two sides meet only at the common level of second-order observables.

18.1 Difference in Joint Organization between ζ and CUE/GUE

This distinction is one of the most important corrections in the latter half of the chapter. A direct finite-scale comparison between ζ and GUE displays clear discrepancies. Looking only at the outcome may suggest that the multiplicative structure of ζ and GUE have nothing to do with one another. Joint-organization controls show instead that the real difference lies not in the raw self-relation but in **how the two sides organize the full family of pair relations**.

For CUE, the joint density of the eigenangles contains

$$p(\theta_1, \dots, \theta_N) \propto \prod_{i<j} |e^{i\theta_i} - e^{i\theta_j}|^2, \tag{18.5}$$

the complete Vandermonde^2 joint law. If this joint law is removed and replaced by independent uniform phases, the normalized form factor is

$$K_{\mathrm{iid}}(\tau) = 1. \tag{18.6}$$

Restoring the Haar/CUE joint law gives

$$K_{\mathrm{CUE}}(\tau) = \min(\tau, 1), \tag{18.7}$$

so

$$\boxed{K_{\mathrm{CUE}} - K_{\mathrm{iid}} = -(1-\tau)_+.} \tag{18.8}$$

Thus the CUE/GUE ramp and level repulsion are not automatically created by the self-product identity; they arise from the complete joint probability law built into the ensemble.

The ζ-side is fundamentally different. It has no externally prescribed ensemble joint law. Its second-order structure comes from the deterministic placement of $\Lambda(n)$ in the multiplicative world of the integers. If the positions of $\Lambda(n)$ are shuffled while preserving the same first-order weight distribution, the off-diagonal correction almost disappears in finite-scale computation. When the Hardy–Littlewood singular-series factors are restored prime factor by prime factor through local congruence information, the true correction returns progressively.

Thus the difference between the two sides can be summarized as follows:

CUE/GUE	ζ
raw self-relation: $z_i z_j^{-1}$	raw self-relation: m/n
product over pairs	product over primes
complete Vandermonde^2 joint law	Euler/local-congruence law
ensemble probability	deterministic arithmetic placement
global joint law specified at definition	global organization generated by integer arithmetic

Hence

the two sides do not diverge at the level of multiplicative identity; they diverge at the level of how the entire collection of self-relations is jointly organized.

(18.9)

This is the structural reason the first version of the handshake did not line up. It also explains why migration cannot simply subtract a constant from ζ: the source-specific local organization must first be separated from the universal two-point structure.

19. Renormalized Migration Coordinates and Finite-Scale Residuals

In the common coordinates of pair observables, write the ζ-side as

$$\mathcal{C}_\zeta = \mathcal{C}_{\mathrm{ref}} + \Delta_{\mathrm{native}}, \tag{19.1}$$

where $\mathcal{C}_{\mathrm{ref}}$ is a chosen finite-CUE / bulk reference coordinate, while Δ_{native} collects source-specific finite-scale structure not removed by the independently defined correction map.

Here Δ_{native} is defined as

$$\boxed{\text{a finite-scale deformation coordinate under the chosen renormalization rule.}} \tag{19.2}$$

Only when discussing the classical infinite-GUE limit does one additionally ask whether this coordinate tends to zero under the corresponding normalization. If it retains identifiable arithmetic lower-order structure, that structure should continue to be recorded as an arithmetic deformation rather than erased by an a posteriori constant.

From this point onward the chapter therefore replaces an undifferentiated language of "error" by the more precise language of **correction / deformation / residual observable**. A numerical discrepancy must first be assigned to the finite-scale structure to which it belongs before it can participate in a limiting statement.

20. Fit-Free Migration: Independent Subtraction of Local ζ-Structure

Define the fit-free migration operator

$$\boxed{\mathfrak{M}_T : K_\zeta^{\mathrm{raw}} \mapsto K_\zeta^{\mathrm{raw}} - K_\zeta^{\mathrm{local}} + K_{\mathrm{GUE}}.} \tag{20.1}$$

Under plateau normalization $K_{\mathrm{GUE}} = 1$, so

$$K_{\mathrm{mig}} - 1 = K_\zeta^{\mathrm{raw}} - K_\zeta^{\mathrm{local}}. \tag{20.2}$$

Here K_ζ^{local} uses only the direct/Euler/singular-series local structure intrinsic to ζ; GUE supplies only the universal coordinate reference. The correction is defined entirely from the local structure of the ζ-side itself.

20.1 Renormalizing the Raw Data: Twelve Comparisons

Finite-scale computation gives

$$\text{mean raw error} = 0.147475, \tag{20.3}$$

while after full singular-series migration

$$\text{mean error} = 0.0151165, \tag{20.4}$$

a mean-error reduction of

$$\boxed{89.75\%}, \tag{20.5}$$

with a median improvement of approximately

$$7.93\times. \tag{20.6}$$

Using instead the pre-specified finite Euler cutoff consistent with the current resolution,

$$p \le H, \tag{20.7}$$

the mean error drops further to

$$0.0135793, \tag{20.8}$$

a reduction relative to the raw value of

$$\boxed{90.79\%}, \tag{20.9}$$

with a median improvement of approximately

$$11.91\times. \tag{20.10}$$

Representative samples are:

X, θ, H	raw K	raw error	migrated K	migrated error	improvement
16384,	0.799617	0.200383	1.00304	0.003037	65.98 ×
26214	0.872484	0.127516	0.997233	0.002767	46.09 ×
52428	0.861196	0.138804	0.998442	0.001558	89.08 ×
52428	0.888907	0.111093	1.01283	0.012833	8.66 ×

These data show that local representational corrections explain most of the finite-scale discrepancy. The statement $\Delta_T \to 0$ remains a separate infinite-scale asymptotic claim.

20.2 Four-Step Definition of Multiplicative Self-Relation Migration

To turn "migration" from a slogan into a checkable mathematical operation, this chapter decomposes both sides into the same four steps.

For any discrete source measure μ, first define its self-relation

$$\mathcal{R}[\mu] = \mu * \tilde{\mu}.$$

If one defines the equivalence relation

$$\mu_1 \sim \mu_2 \Leftrightarrow \mathcal{R}[\mu_1] = \mathcal{R}[\mu_2],$$

one obtains the self-correlation quotient space

$$\boxed{\mathcal{Q} = \{\text{generative sources}\}/\sim.}$$

After entering this quotient space, the full information of the original generative source is no longer retained; the comparison concerns only its second-order self-relation.

On the ζ-side: start from

$$\nu_\zeta = \sum_n a_n \, \delta_{\log n}.$$

Then perform:

1. **self-product:** $\mathcal{R}_\zeta = \nu_\zeta * \tilde{\nu}_\zeta$;
2. **unfolding:** rescale $\log(m/n)$ to $u = T\log(m/n)$;
3. **Mellin/Fourier projection:** the finite-window kernel is

$$K_B^{\times}(m,n) = \frac{1}{2\pi}\int_{-B}^{B} (m/n)^{it}\, dt.$$

It enters a sine/Fejér-type projection after microscopic normalization;

4. **renormalization:** subtract the diagonal and the local part explained internally by the Euler/singular-series structure of ζ, leaving the connected arithmetic pair observable $\mathcal{C}_\zeta$.

On the GUE/CUE side: start from the eigenangle/eigenvalue measure, perform the same self-product, unfolding, Fourier projection, and subtract the diagonal/background to obtain $\mathcal{C}_U$. Its bulk limit is

$$\mathcal{C}_U(u) = -\left(\frac{\sin\pi u}{\pi u}\right)^2.$$

Thus the handshake condition is not "ζ=GUE," but

$$\boxed{\mathcal{C}_\zeta \to \mathcal{C}_U \quad \text{in} \mathcal{Q}_{\text{pair}}.}$$

The Fourier transform translates the two-point measure and the form factor in both directions; however, from

$$\widehat{\mu * \tilde{\mu}} = |\hat{\mu}|^2$$

one cannot in general recover the phase of $\hat{\mu}$. Therefore

> **ζ and GUE can be mutually translated at the level of the second-order self-relation quotient, but not inverted in the raw source space.**

This is precisely the value of the migration mechanism: ζ is not forced to obey GUE, and GUE is not forced to explain the entire prime structure. The two sides meet only at the same level of second-order observables.

20.3 Positive and Negative Controls for Joint Organization on the Two Sides

To determine where the corrections on the two sides actually come from, this chapter uses structural removal controls.

CUE positive/negative control. If the Vandermonde^2 joint law is removed and replaced by independent uniform phases, the ramp disappears; restoring the Haar/CUE joint law restores $\min(\tau, 1)$. This verifies that what is genuinely added on the random-matrix side is the complete joint law, not the self-product itself.

ζ-side positive/negative control. If the positions of $\Lambda(n)$ are shuffled while keeping the same first-order weight histogram, the off-diagonal correction almost disappears; as local prime factors are restored step by step, the correction returns layer by layer.

A representative sample is

$$X = 524288, \qquad \theta = 0.45.$$

The actual off-diagonal correction is approximately

$$-0.842425.$$

Retaining only the local factor $p = 2$ gives approximately

$$-0.1380,$$

while accumulation up to

$$p \le 31: \quad -0.6903,$$

then

$$p \le 101: \quad -0.7979,$$

and finally

$$p \le 199: \quad -0.83675.$$

This gives a direct numerical fact: **the dominant second-order correction on the ζ-side is indeed accumulated prime local factor by prime local factor.**

Across twelve (X, H) tests, after subtraction of the full Hardy–Littlewood local model, the median ratio of the residual to the actual correction is approximately

$$1.95\%,$$

the median ratio to the modeled correction is approximately

$$1.91\%,$$

and the maximum is approximately

$$3.70\%.$$

Thus at finite scale the dominant structure is already captured by local arithmetic organization, while the remaining term becomes the candidate residual of global deterministic placement.

20.4 Finite Euler Resolution

A further resolution check does not force the complete infinite singular series at finite scale. Instead it places a finite cutoff P on the Euler product and observes the best matching resolution across the twelve samples. The a posteriori optimum satisfies the empirical relation

$$\text{median}\,\frac{P_*}{H} \approx 1.33.$$

Thus the best local Euler resolution often lies on the scale

$$P \sim H.$$

In this purely numerical diagnostic, the median mismatch of the best truncated model is approximately

$$9.6 \times 10^{-5},$$

whereas the median mismatch of the full infinite singular-series model is approximately

$$1.56 \times 10^{-2}.$$

Because P_* is selected a posteriori, this result is used only as a finite-resolution diagnostic. Its structural meaning is

> **part of the residual may arise from imposing an "infinite Euler completion" prematurely on a finite-resolution window.**

The migration rule therefore uses the pre-fixed natural cutoff $p \le H$, not the a posteriori optimal P_*.

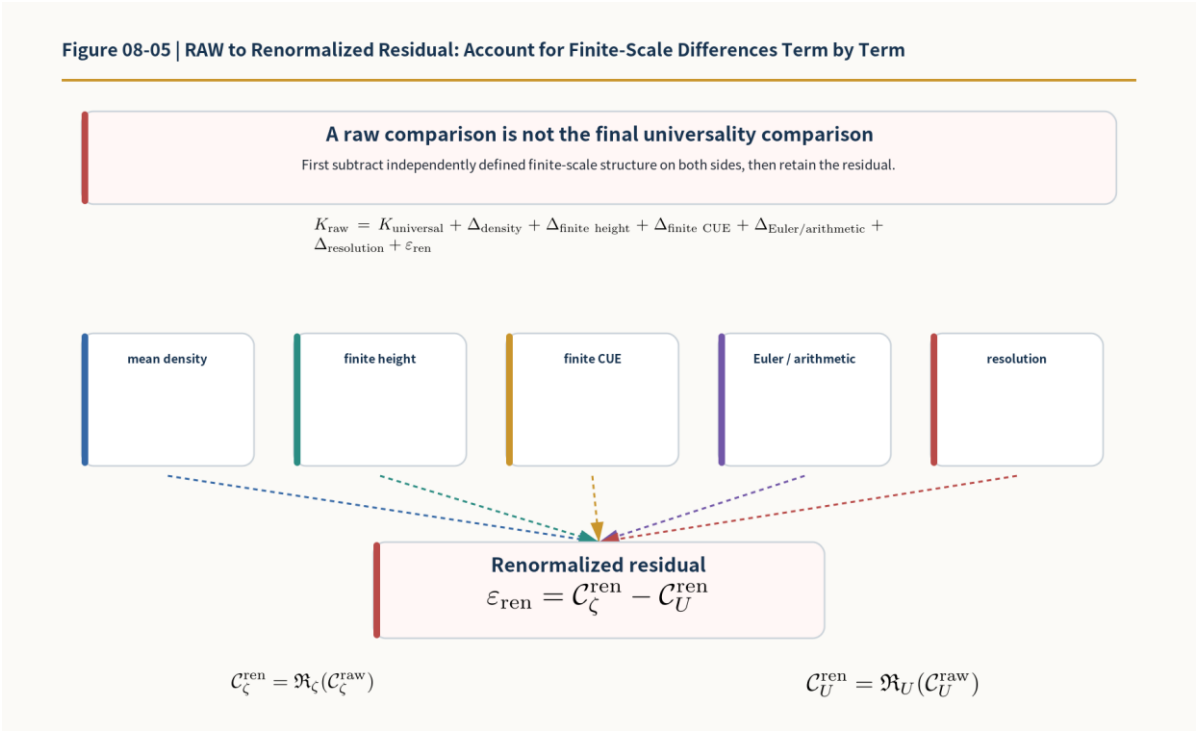


Figure 08-05. From RAW difference to the renormalized residual. The raw ζ–CUE/GUE difference is decomposed into independently defined corrections for mean density, finite height, finite CUE size, Euler/arithmetic structure, and resolution, leaving the residual $\varepsilon_{\mathrm{ren}}$. The residual is retained rather than forced to zero by an a posteriori fitted constant. Renormalized comparison therefore extracts common structure while preserving source-specific differences.

21. Window Stability of the High-Scale Residual

After fixing the finite-resolution Euler rule, define

$$\boxed{\Delta_{X,\theta} = K_{\mathrm{raw}} - K_{\mathrm{local}}^{p\le H}, \qquad H = \lfloor X^{\theta} \rfloor.} \tag{21.1}$$

When X is extended to 2^{23}, and quarter-octave, smooth, moving, and non-overlapping windows are added, the computation shows:

1. the residual changes sign several times;
2. the high-scale mean displays a pronounced negative bias;
3. the oscillation remains after replacing the hard cutoff by a Hann window;
4. moving and non-overlapping windows retain significant deviations;
5. the data support neither a clearly established monotone decay to zero nor convergence to a fixed nonzero constant.

On the quarter-octave grid, the mean absolute residuals are

$$\theta = .35\colon\ 0.01422, \qquad \theta = .45\colon\ 0.01963, \qquad \theta = .50\colon\ 0.03143. \tag{21.2}$$

On the higher octaves, the mean residuals are approximately

$$-0.02334, \qquad -0.03795, \qquad -0.05493, \tag{21.3}$$

while the single-point readouts at $X = 2^{23}$ are approximately

$$-0.02090, \qquad -0.02460, \qquad -0.04583. \tag{21.4}$$

Thus the direct finite-scale observation is

there is a signed, scale-dependent finite-scale residual with arithmetic oscillation. (21.5)

The presently accessible finite interval is not used to define or force a final limiting value. These residuals are retained in full as finite-scale data.

21.1 High-Scale Comparisons under Different Windows

To distinguish a genuine finite-scale residual from hard-cutoff boundary artifacts, this chapter uses four classes of windows.

(a) Quarter-Octave Grid

On

$$2^{19} \le X \le 2^{23}, \tag{21.6}$$

one point is sampled every quarter octave, giving 17 scales. For $\theta = .35, .45, .50$, the mean absolute residuals are respectively

$$0.01422, \quad 0.01963, \quad 0.03143. \tag{21.7}$$

The three sequences change sign 2, 3, and 4 times respectively. The residual is therefore not a simple positive tail decreasing monotonically to zero.

(b) Hann Window

To remove hard dyadic-scale boundaries, a Hann window is used. For $\theta = .45$, a representative sequence remains

$$0.02856,\ 0.02011,\ 0.02085,\ -0.06965,\ -0.00789 \tag{21.8}$$

at $X = 2^{19}, 2^{20}, 2^{21}, 2^{22}, 2^{23}$. Thus the explanation that the residual is mainly a hard-window boundary effect is numerically disfavored.

(c) Moving Smooth Windows

The upper-high-scale window means are

$$\theta = .35: -0.02867, \quad \theta = .45: -0.05718, \quad \theta = .50: -0.07673. \tag{21.9}$$

(d) Non-Overlapping Windows

To avoid artificial stability caused by overlapping windows, retain only mutually non-overlapping windows. The means remain

$$\theta = .35: -0.03410, \quad \theta = .45: -0.05947, \quad \theta = .50: -0.07285. \tag{21.10}$$

Single-window fluctuations remain large. For example, for $\theta = .45$,

$$-0.12095 \le \Delta \le 0.01734, \tag{21.11}$$

while for $\theta = .50$,

$$-0.16546 \le \Delta \le 0.04957. \tag{21.12}$$

Together these results show that the remaining residual is not an artifact easily erased by changing windows. At the same time, it does not display enough stability to establish a nonzero constant limit.

An empirical description compatible with the present finite-scale data is

$$\Delta_T = A(T) + \varepsilon_T, \qquad A(T) \to 0, \tag{21.13}$$

where a slowly decaying background is superposed with arithmetic oscillations that remain significant on the current scales. These data serve only as finite-scale diagnostics and do not impose a specific decay law on the main theorem of this chapter.

22. Eight Components of the Finite-Scale Difference

This is the chapter's principal bookkeeping section for discrepancies. The difference between ζ and GUE does not have a single source. A decisive lesson of the later analysis is that **unless differences from distinct object levels are kept in separate ledgers, any statement that an "error tends to zero" or "does not tend to zero" is mathematically underdetermined.**

22.1 First-Order Objects versus Second-Order Self-Relations

Hilbert–Pólya and Guinand–Weil already provide a complete one-point spectral/arithmetic interface, whereas GUE requires $\mu \otimes \mu$. Passing from first to second order therefore introduces genuinely new connected covariance. A completed one-point handshake does not imply an automatic two-point handshake.

22.2 Different Modes of Joint Organization

CUE/GUE comes with the complete Vandermonde^2 joint law at the definitional level. The ζ-side is generated jointly by Euler/local congruence structure and the global deterministic placement of the integers. The raw self-relations are of the same type, but the source-specific joint organizations differ. This is the largest structural difference before migration.

22.3 Mean-Density Correction

If unfolding uses only a finite-order approximation to $\bar{N}(T)$ rather than a more complete locally smoothed density, lower-order density curvature can leak into the local spacing statistics.

22.4 Finite Height versus Infinite Height

Local statistics of Riemann zeros at finite height T contain arithmetic lower-order terms, whereas the infinite GUE/sine process is a limiting object. Directly comparing

$$\zeta_{\text{finite height}} \quad \text{with} \quad \text{GUE}_\infty \tag{22.1}$$

therefore naturally creates a systematic model discrepancy.

22.5 Finite CUE Size versus the Infinite Sine Kernel

The random-matrix side also has finite-N corrections. Thus a more natural comparator for zeta at finite height is an effective-size CUE rather than immediately setting $N = \infty$.

22.6 Arithmetic Euler Corrections and Finite Euler Resolution

The ζ-side contains Euler factors, prime powers, and singular-series-type lower-order structure. Such structure disappears in the universal sine-kernel quotient but remains visible at finite scale.

Moreover, a finite window can resolve only a finite prime scale. Imposing an infinite Euler completion too early can itself create a finite-resolution discrepancy.

22.7 Difference in Generative-Source Resolution Variables

The internal prime-source variable uses

$$T_{\mathrm{prime}} = X/H, \tag{22.2}$$

whereas the external zero-statistics height uses

$$T_{\mathrm{zero}} = \gamma. \tag{22.3}$$

These are not the same finite-scale variable. Consequently a decay exponent observed for an external gap-ratio statistic cannot simply be copied to the internal $\Delta_{X,\theta}^{\mathrm{prime}}$.

22.8 Renormalized Connected Residual

After the previous corrections have been separated, define the remaining term as

$$\boxed{\varepsilon_T^{\mathrm{ren}}} \tag{22.4}$$

or the renormalized migration residual. It records the connected finite-scale structure that remains visible under the stated renormalization rule. Only when the classical infinite-GUE asymptotic is considered separately does its limiting behavior become an additional asymptotic criterion.

23. A Posteriori Constant Fitting versus Independently Defined Corrections

Over a finite range, a model such as

$$\Delta_T \approx \Delta_\infty + \frac{c}{\log T} \tag{23.1}$$

may fit better than a pure $c/\log T$ model. But the fitted Δ_∞ is highly sensitive to the window, to θ, and to the order k used in $1/\log^k T$.

Therefore this chapter does not adopt the rule

$$\boxed{\text{fit a slowly drifting finite-range discrepancy by a constant and then subtract it so that } \zeta = \mathrm{GUE}.} \tag{23.2}$$

The issue is not aesthetic. Such a constant has no independent definition and would write the target answer into the correction itself. It may be used for graphical calibration, but not in a proof chain.

24. Finite-Height Calibration: Finite ζ versus Finite CUE

The external random-matrix literature provides an important model calibration. Nishigaki (2024) gives the GUE limiting nearest-neighbor-spacing and gap-ratio distributions and uses high Riemann zeros as examples approaching random-matrix statistics. Nishigaki (2026; preprint 2025) further studies finite-N CUE corrections and identifies a special finite-size cancellation in the gap ratio, explaining why deviations of Riemann-zero gap ratios decay approximately as $(\log(T/2\pi))^{-3}$.

In an independent recomputation of the published finite-height data, the mean discrepancy of four height samples from infinite GUE is approximately

$$2.2233 \times 10^{-3}. \tag{24.1}$$

After adding the independently defined finite-height correction, the residual falls to approximately

$$4.9167 \times 10^{-5}, \tag{24.2}$$

which explains on average approximately

$$\boxed{97.79\%} \tag{24.3}$$

of the apparent finite-height discrepancy, with a median improvement of about $68.1\times$.

This numerical reconstruction checks whether a finite-height model explains the observed deviation. It does not replace an infinite-height asymptotic theorem by finite data.

Thus at the finite-height level,

> a substantial part of the discrepancy between finite-height ζ and infinite GUE is itself a computable, decaying finite-height/model difference. (24.4)

24.1 Four-Point Reconstruction and Comparison of Decay Laws

For four independent published height points, direct comparison with infinite GUE and comparison after the independent finite-height correction give:

zeros near index	direct error vs. infinite GUE	residual after finite-height correction	improvement
10^8	3.4853×10^{-3}	1.1435×10^{-4}	$30.5\times$
10^9	2.4424×10^{-3}	2.3092×10^{-5}	$105.8\times$
10^{10}	1.6882×10^{-3}	9.2966×10^{-6}	$181.6\times$
1.037×10^{11}	1.2773×10^{-3}	4.9934×10^{-5}	$25.6\times$

The mean error therefore falls from

$$2.2233 \times 10^{-3} \tag{24.5}$$

to

$$4.9167 \times 10^{-5}, \tag{24.6}$$

so approximately

$$\boxed{97.79\%} \tag{24.7}$$

of the apparent finite-height difference is explained, with a median improvement of about $68.1\times$.

Independent power-law reconstruction for the four gap-ratio moments gives exponents

$$p_1 = 2.9080, \quad p_2 = 2.8778, \quad p_3 = 2.8868, \quad p_4 = 2.9009. \tag{24.8}$$

They cluster near $p \simeq 2.9$. For the first moment, representative RMSE values for $1/\log T$, $1/\log^2 T$, and $1/\log^3 T$ are approximately

$$5.74 \times 10^{-4}, \quad 3.06 \times 10^{-4}, \quad 5.40 \times 10^{-5}. \tag{24.9}$$

Thus the external finite-height data for this observable support decay close to $\log^{-3} T$ much more strongly than a fixed nonzero residual.

This reconstruction is important, but it cannot be transferred as a decay law to the internal prime-source residual $\Delta_{X,\theta}^{\mathrm{prime}}$, because the two finite-scale variables are different. Section 25 keeps this boundary explicit.

25. Distinguishing Two Kinds of Finite-Scale Residual

The internal prime-source finite-scale calculation defines

$$\boxed{\Delta_{X,\theta}^{\text{prime}} = K_{\text{raw}} - K_{\text{Euler}}^{p\le H}.} \tag{25.1}$$

External zero statistics naturally define

$$\boxed{\Delta_{T}^{\text{zero}} = K_{\text{zero}}^{\text{obs}} - K_{\text{GUE}}^{\infty}.} \tag{25.2}$$

Although they lie on the same chain

multiplicative self-relation → zero two-point statistics,

their finite-scale variables, windows, and observables are different. Therefore

$$\boxed{\Delta_{T}^{\text{zero}} \sim \log^{-3} T \quad \not\Rightarrow \quad \Delta_{X,\theta}^{\text{prime}} \sim \log^{-3}(X/H).} \tag{25.3}$$

This is exactly why the internal high-scale residual need not exhibit the same power law as the external gap ratio.

26. Finite-to-Finite Renormalization Interface and the Universal Quotient Space

The first version of the handshake migrated finite ζ-data directly to an infinite-GUE baseline. After external calibration, the stricter structure is

$$\boxed{K_{\zeta}(T) = K_{\text{GUE}}^{(\infty)} + K_{\text{finite}}(T) + \varepsilon_{T}.} \tag{26.1}$$

More finely, a finite-height Riemann-zero observable may be written schematically as

$$K_{\text{RZ}}(T) = K_{\sin} + \frac{1}{N_e(T)^2} K_2 + \frac{1}{N_e(T)^3} K_{3,\text{arith}} + \cdots, \tag{26.2}$$

where $N_e(T)$ is an effective CUE size matched to the height. The orders of the corrections depend on the observable, so (26.2) is not asserted as one universal term-by-term formula for all statistics.

The final handshake is therefore

$$\boxed{\begin{array}{ccccc} \zeta_{\text{raw}} & \to & \zeta_{\text{finite corrected}} & \to & \mathcal{Q}_{\text{universal}} \\ & & & & \updownarrow \\ \text{CUE}_N & \to & \text{CUE}/\text{GUE}_{\infty} & \to & \mathcal{Q}_{\text{universal}}. \end{array}} \tag{26.3}$$

Its governing principle is

finite ζ is compared with finite CUE; only limiting ζ is compared with infinite GUE. (26.4)

This structure satisfies three object-level conditions:

1. it does not require a finite-height arithmetic object to possess the infinite random-matrix limit prematurely;
2. each side is responsible for its own finite-size / finite-height corrections;
3. only the residual remaining after independently defined corrections enters the final universality comparison.

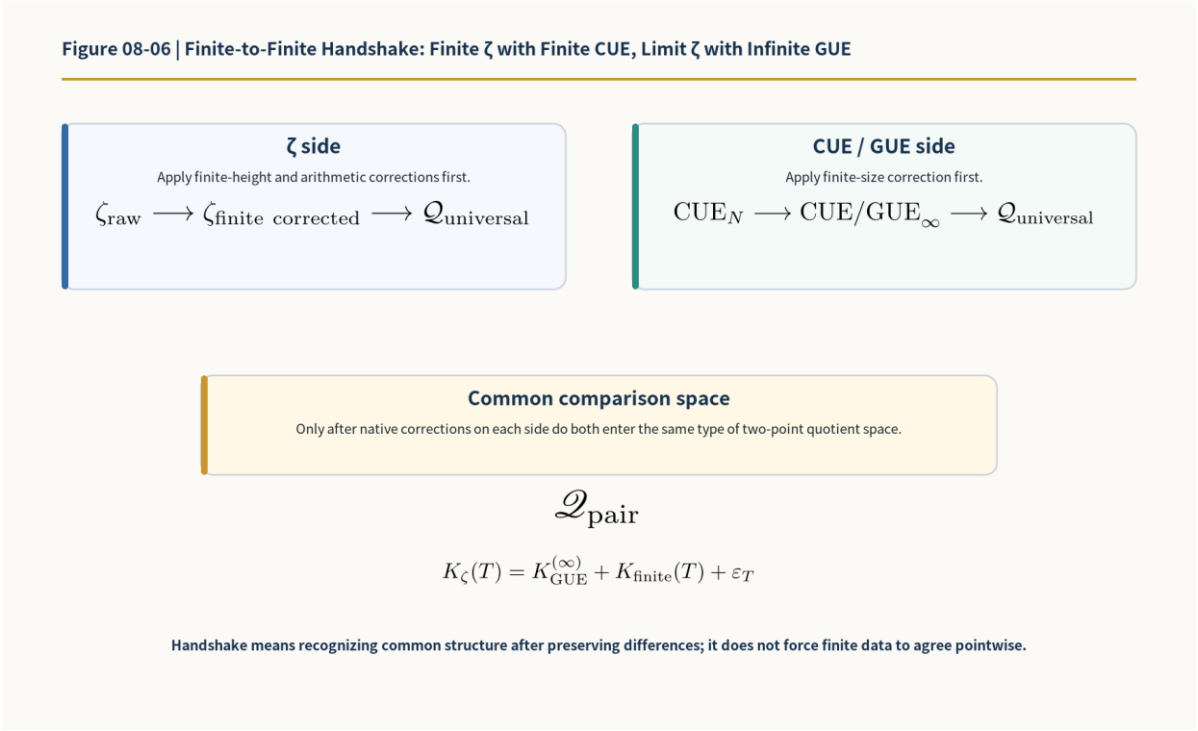


Figure 08-06. Finite-to-finite handshake. Finite-height ζ observables first carry their own density, finite-height, and arithmetic corrections, while finite CUE carries its own finite-size correction. Only after each side has completed its native corrections do both enter the common pair-comparison quotient $\mathcal{Q}_{\text{pair}}$. The comparison principle is therefore: finite ζ with finite CUE; limiting ζ with infinite GUE.

27. Renormalization Handshake Theorem: Structural Interface and Asymptotic Specialization

Define the independently specified correction operator on the ζ-side by

$$\mathfrak{R}_\zeta,$$

and the finite-size correction operator on the random-matrix side by

$$\mathfrak{R}_U.$$

They treat finite-scale structures already identified in their respective native coordinates, such as

$$\Delta_{\text{density}}, \quad \Delta_{\text{finite height}}, \quad \Delta_{\text{finite CUE}}, \quad \Delta_{\text{Euler/arithmetic}}, \quad \Delta_{\text{resolution}}.$$

Define the renormalized pair observables

$$\mathcal{C}_\zeta^{\text{ren}} = \mathfrak{R}_\zeta(\mathcal{C}_\zeta^{\text{raw}}), \tag{27.1}$$

and

$$\mathcal{C}_U^{\text{ren}} = \mathfrak{R}_U(\mathcal{C}_U^{\text{raw}}). \tag{27.2}$$

Finally define

$$\boxed{\varepsilon_{\text{ren}} = \mathcal{C}_\zeta^{\text{ren}} - \mathcal{C}_U^{\text{ren}}.} \tag{27.3}$$

Theorem 27.1 (Renormalization Handshake Structure)

Within the two-point observational framework of this chapter:

1. the self-products, unfolding, Fourier projections, and correction maps on the ζ- and CUE/GUE-sides are defined on their respective generative sources;
2. after these mappings, both sides enter the same comparison space $\mathcal{Q}_{\mathrm{pair}}$ of two-point observables;
3. the raw discrepancy decomposes exactly into the declared correction coordinates and $\varepsilon_{\mathrm{ren}}$;
4. $\varepsilon_{\mathrm{ren}}$ is the source-specific residual observable retained under this renormalization scheme and is recorded in full;
5. the structural handshake and the infinite-scale limit of $\varepsilon_{\mathrm{ren}}$ belong to two different logical levels.

Therefore what this chapter calls a "completed handshake" is

$$\boxed{\text{the two sides possess two-point objects of the same type, a common comparison space, explicit independent correction maps, and a co}} \tag{27.4}$$

It is not a pointwise equality forcing finite ζ to equal infinite GUE.

27.2 Classical Infinite-GUE Asymptotic Specialization

If one further proves, along a family of scales $T \to \infty$, that

$$\boxed{\langle \varepsilon_{\mathrm{ren}}(T), \Phi \rangle \to 0} \tag{27.5}$$

for every admissible pair-test observable Φ, then one obtains the classical infinite-GUE / sine-kernel asymptotic in the corresponding class of observables.

Thus

$$\boxed{\text{classical GUE asymptotic} = \text{renormalization handshake} + \text{vanishing-residual specialization.}} \tag{27.6}$$

Equation (27.5) is a stronger asymptotic statement imposed on top of the structural handshake.

28. Source-Generated Equivalent GUE Interface: First-Order Witness Inheritance to Second-Order Statistics

Section 3.3 proved that once an independent source-generated Hilbert–Pólya terminal object is recognized by the first-order Riemann spectral witness as

$$(H_\times, M_\times) \simeq (H_{\mathrm{id}}, M_{\mathrm{mult}}),$$

all two-point objects built from functional calculus, trace, and Fourier pair constructions agree exactly.

Define the source-generated signed operators

$$\mathcal{D}_\times = H_\times \oplus (-H_\times), \qquad \mathcal{M}_\times = M_\times \oplus M_\times. \tag{28.1}$$

Their spectral amplitude

$$Z_{\times,\phi}(u) = \mathrm{Tr}\big[\mathcal{M}_\times \phi(\mathcal{D}_\times) e^{iu\mathcal{D}_\times}\big] \tag{28.2}$$

satisfies

$$\boxed{Z_{\times,\phi}(u) = Z_{\mathrm{R},\phi}(u).} \tag{28.3}$$

Hence

$$\boxed{\mathcal{R}_{\times,\phi} = \mathcal{R}_{\mathrm{R},\phi},} \tag{28.4}$$

where $\mathcal{R}$ denotes the corresponding weighted two-point measure.

All downstream objects—unfolded two-point correlations, form factors, finite-CUE comparisons, and renormalized migration coordinates—can therefore be written directly in the source-generated HP representation without altering any numerical value or theorem.

This gives the representation-independence statement

GUE comparison belongs to the second-order layer of the common spectral identity, not to any particular first-order route by which that spectrum was constructed.

(28.5)

Thus any HP realization that independently reaches the same first-order terminal object from the multiplicative generative source automatically has the same GUE interface. No second second-order theory is required.

29. The Renormalized Residual as a Second-Order Data Coordinate

By definition and the independent correction ledger, the raw discrepancy of this chapter can be written as

$$\boxed{\Delta_{\text{observed}} = \Delta_{\text{density}} + \Delta_{\text{finite height}} + \Delta_{\text{finite CUE}} + \Delta_{\text{Euler/arithmetic}} + \Delta_{\text{resolution}} + \varepsilon_{\text{ren}}.} \tag{29.1}$$

The purpose of this identity is not to hide the final term, but to separate finite-scale differences according to their sources.

The first five correction classes have explicit object-level origins. The last term

$$\boxed{\varepsilon_{\text{ren}}} \tag{29.2}$$

is retained in full, including its sign, window dependence, scale oscillation, and observable dependence.

Its object status is

ε_{ren} is a second-order data coordinate that remains present after renormalization.

(29.3)

For a faithful finite-scale handshake, (29.1) gives the complete ledger. The condition $\varepsilon_{\text{ren}} = 0$ belongs to a stronger infinite-scale specialization.

Only if the target is further strengthened to the classical infinite-GUE asymptotic does one additionally ask whether

$$\varepsilon_{\text{ren}}(T) \overset{?}{\to} 0$$

in some topology of test functions. That question belongs to a stronger limiting specialization and is not a definitional obligation of the structural handshake.

In arithmetic coordinates, Actual-to-Dual Diagonal Transfer gives one route for studying this limit. In random-matrix coordinates, finite-CUE corrections provide another lower-order expansion. Both can act on ε_{ren} without changing the second-order object and renormalization structure already established here.

30. Correction Rules after Renormalizing the Raw Data

Once the residual defined in (29.3) has been identified, fitting increasingly elaborate models such as

$$\frac{c}{\log T}, \quad \frac{c\log\log T}{\log T}, \quad T^{-\eta}\cos(\omega \log T + \phi), \quad \Delta_\infty + \frac{c}{\log T} \tag{30.1}$$

to the current finite-scale Δ_T does not automatically add proof information.

This chapter therefore adopts the following rules:

- known finite corrections are modeled independently and subtracted;
- verifiable source-local corrections are derived independently from the ζ-side;
- constants that cannot be defined independently are not used for alignment;
- the remaining residual retains its sign, scale, and window dependence as an object of study;
- an asymptotic limit is assigned only by analytic proof or a sufficiently strong extrapolation theory.

Thus the finite-scale residual ceases to be an "error" to be concealed and becomes a mathematical object with explicit provenance and a defined scope of responsibility.

31. Arithmetic–Unitary-Matrix Correspondence in Function Fields

In function fields, Katz's Frobenius equidistribution allows certain arithmetic short-interval variances to be converted rigorously into unitary-group matrix integrals. The Keating–Rudnick result for the variance of prime polynomials in short intervals is a typical example.

Thus the migration proposed in this chapter is not an analogy based merely on similar curves. It is inspired by a rigorous paradigm that already succeeds in another setting:

$$\boxed{\text{arithmetic object} \to \text{unitary conjugacy class} \to \text{Haar matrix statistic.}} \tag{31.1}$$

For the integer ζ-function, obtaining the classical infinite-GUE asymptotic would require a sufficiently strong global transfer playing the role that Frobenius geometry plays over function fields. Actual-to-Dual Diagonal Transfer is one arithmetic formulation of that stronger asymptotic requirement.

32. Six Logical Non-Equivalences

The following six non-equivalences fix the object boundaries of this chapter.

32.1 Self-Adjointness versus the GUE Two-Point Law

$$H_{\mathrm{HP}} = H_{\mathrm{HP}}^{*}$$

fixes only a real spectrum. It does not determine a local statistical class.

32.2 One-Point Trace versus Two-Point Self-Relation

The exact linear Guinand–Weil trace interface does not upgrade for free to $\mu \otimes \mu$. The genuinely new second-order information is the shifted correlation.

32.3 Diagonal Main Term versus the Full Infinite-GUE Asymptotic

The ramp can be explained by the diagonal. The plateau requires collective off-diagonal cancellation.

32.4 Lower-Order Means versus a Second-Order Theorem

Scale differentiation amplifies the remainder and requires mixed-curvature regularity.

32.5 Finite ζ versus Infinite GUE

Finite-height and finite-size corrections must be entered into the ledger first.

32.6 A Posteriori Constant Alignment versus a Theoretically Defined Correction

Any constant fitted after the fact merely to make the answer equal to 1 has no independent arithmetic identity and may be used only for graphical calibration.

33. The Three Responsibilities of RH, HP, and GUE

The central stratification of this chapter is summarized in the following table.

Level	Core object	Key degree of freedom / statistic	What it answers	What it does not answer automatically
RH	$\rho = \frac{1}{2} + d_\rho + i\gamma$	horizontal d_ρ	whether all nontrivial zeros lie on the critical line	why the γ_n are arranged as they are
spectral witness	$\mathfrak{W}_{\mathrm{R}} = F_{\mathrm{R}}$, ν_{R}, $(H_{\mathrm{id}}, M_{\mathrm{mult}})$	unique identification of first-order spectral identity and analytic multiplicity	when different first-order realizations are genuinely the same Riemann spectral identity	the two-point statistics or GUE law
HP	H_{id} or a unitarily equivalent $H_{\times}^{\mathrm{HP}}$	real spectrum γ_n with multiplicity display M_{mult}	how zero identities are realized as a self-adjoint spectrum	why local spacings obey a GUE two-point law
GUE	unfolded $\{x_n\}$	two-point correlation / form factor	local universal statistics of the γ-spectrum	the horizontal closure of RH itself
arithmetic generative source	$\Lambda(n)$, $\Lambda(n)\Lambda(n+h)$	one-point/two-point multiplicative responses	why spectral traces arise from primes; how two-point relations return to the multiplicative side	the full classical off-diagonal asymptotic transfer
handshake layer	$\mathcal{Q}_{\mathrm{pair}}$	universal quotient + finite-scale decoration + residual	how ζ and GUE/CUE are compared at the same level	unique inversion of the raw generative source

The responsibilities of this chapter may therefore be compressed as

RH closes the horizontal direction; the spectral witness identifies first-order identity; HP carries the vertical spectrum; GUE describes its self-relations; the arithmetic source explains where those relations come from; and the handshake layer compares the two second-order representations without erasing their differences.

(33.1)

The spectral witness is not a new physical layer but an identity interface:

$$\boxed{\text{one-point realization} \xrightarrow{\text{spectral witness}} \text{common Riemann spectral identity} \rightarrow \text{second-order relation.}} \tag{33.2}$$

If a source-generated HP realization $(H_\times, M_\times)$ satisfies

$$(H_\times, M_\times) \simeq (H_{\mathrm{id}}, M_{\mathrm{mult}}),$$

then the second-order witness-inheritance theorem immediately transfers all two-point structure to $H_\times$. The second-order theory therefore belongs to the common first-order spectral identity, not to one particular construction route.

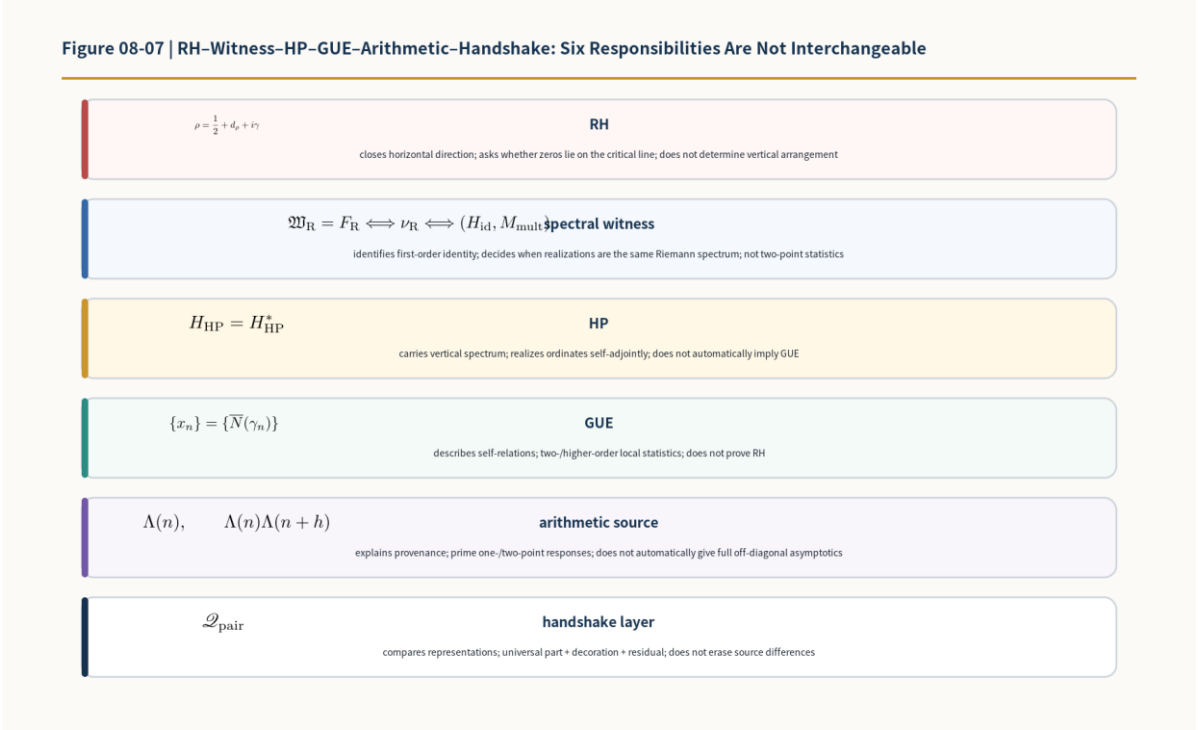


Figure 08-07. Separation of six responsibilities. RH closes the horizontal freedom of zeros; the spectral witness identifies a common first-order Riemann spectral identity; Hilbert–Pólya carries the vertical spectrum self-adjointly; GUE describes unfolded two- and higher-order self-relations; the arithmetic source explains how these relations arise from the prime side; and the handshake layer compares common second-order structure while retaining decoration and residuals. No layer can freely substitute for the proof responsibility of another.

34. Precise Meaning of the Renormalization Interface

A "handshake" does not prove that ζ and a random matrix are the same raw object, nor does it erase arithmetic structure into randomness. It means:

1. each side constructs its second-order self-relations in its own native coordinates;

2. each side performs its necessary finite-scale corrections;
3. both sides enter the same unfolded space of two-point observables;
4. the universal component is compared in that space;
5. source-specific decoration and residuals are retained separately.

Thus

$$\boxed{\text{handshake} = \text{recognizing a common structure after preserving the differences,}} \tag{34.1}$$

rather than

$$\boxed{\text{handshake} = \text{forcing all finite-scale data on the two sides to be exactly equal.}} \tag{34.2}$$

35. Unified Structure of First-Order Spectra and Second-Order Statistics

The structural path has two historical branches.

The first is the **Hilbert–Pólya vision**: behind the Riemann zeros there should be a genuine spectral structure rather than a list of accidentally occurring imaginary parts of complex zeros. It asks

$$\boxed{\gamma_n \quad \text{can these numbers occur as a natural self-adjoint spectrum?}} \tag{35.1}$$

The second is the **random-matrix expectation from Montgomery–Dyson–Odlyzko onward**: the local relations among these spectral frequencies should correspond deeply to unitary random-matrix universality. It asks

$$\boxed{\text{why do the two-point and higher-order self-relations of} \{\gamma_n\} \text{exhibit unitary universality?}} \tag{35.2}$$

The two expectations fit into one stratified history:

$$\boxed{\begin{aligned} &\text{multiplicative generative source} \to X \to \\ &\text{first-order spectral identity} \to \\ &\text{identified HP spectrum} \to \text{two-point trace} \to \\ &\text{prime self-correlation} \leftrightarrow \mathcal{Q}_{\text{pair}} \leftrightarrow \text{GUE/CUE coordinates.} \end{aligned}} \tag{35.3}$$

The meeting point is not that the discovery of a mysterious Hamiltonian automatically solves every subsequent problem. Rather, RH, Hilbert–Pólya, and GUE can be assigned distinct responsibilities and placed into one diagram through explicit interfaces:

$$\boxed{\begin{aligned} &\text{generative source} \to \text{spectral identity} \to \\ &\text{spectral witness} \to \\ &\text{second-order self-relation.} \end{aligned}} \tag{35.4}$$

GUE is not responsible for generating the first-order spectral identity. The spectral witness has already reduced the question "is this the same Riemann spectrum?" to a first-order identity problem. At second order, the object of study becomes the relation formed by this common spectral identity with itself.

Two boundaries remain explicit. First, the conclusions concerning RH and the independent HP closure remain subject to formal publication and independent peer scrutiny. Second, the present chapter establishes exact two-point calculus, representation-independent second-order inheritance, raw-to-renormalized correction bookkeeping, and a finite-scale handshake mechanism; the complete infinite-height asymptotic of the classical GUE/sine kernel is a stronger asymptotic specialization.

This stratification does not weaken the results; it preserves the exact domain of each claim.

36. Formal Extensions and Higher-Order Interfaces

36.1 Arithmetic Form of Finite-Height Corrections

A natural extension is not to continue fitting the residual, but to ask whether the multiplicative side of ζ alone can derive the same finite-height / finite-size corrections,

$$N_e^{-2}, \qquad N_e^{-3}, \qquad \dots$$

that arise independently on the finite-CUE/RMT side, with automatically matching coefficients.

The ideal strengthened form is

$$\boxed{\text{independently derived}\zeta\text{-side correction} = \text{independently derived finite-CUE correction.}} \tag{36.1}$$

If established, the finite-height handshake would be upgraded from comparison of two independently corrected structures to an **analytic identification of the correction coefficients themselves**.

36.2 Formal Extension to Families of Completed L-Functions

RH corresponds to one completed self-dual object. The Generalized Riemann Hypothesis naturally extends this to a family of character/L-function spectral systems:

$$\boxed{\{H_\chi\}_\chi.} \tag{36.2}$$

The central question is then not merely whether each spectrum is self-adjoint, but

$$\boxed{\text{arithmetic family symmetry type} \rightarrow \text{unitary / orthogonal / symplectic universality class.}} \tag{36.3}$$

This would lift both spectral-witness identification and the second-order quotient space to the family level.

36.3 Deterministic Spectra and the Language of Quantum Chaos

Once the first-order Riemann spectral identity has a natural self-adjoint realization, one may ask a question distinct from the proof problem:

> is there a more natural dynamical, geometric, or noncommutative space in which GUE statistics arise from a classical/semiclassical chaotic mechanism? (36.4)

This step is no longer necessary for proving RH. It asks for an explanation of why the same spectrum not only exists but exhibits second-order statistics of unitary type.

Under such a dynamical realization, Hilbert–Pólya would evolve from a problem of spectral realization into a physical/geometric explanation:

$$\boxed{\text{self-adjoint carrier} \quad \rightarrow \quad \text{dynamical origin of spectral statistics.}} \tag{36.5}$$

Appendix E places this quantum-spectral story in its historical setting.

36.4 Finite Spectral Visualization

The Source–Krylov spectral camera gives a finite-dimensional realization: finite moments generate finite positive matrices, and their Ritz values can be tracked as they progressively lock onto the first few γ_n.

Using the independent source-generated HP route as input, one may display

$$\boxed{\begin{array}{r}\text{finite multiplicative information} \rightarrow \\ \text{finite spectral camera} \rightarrow \\ \text{progressive stabilization of frequency identities} \rightarrow \\ \text{spectral witness identification} \rightarrow \\ \text{local two-point statistics in unitary-universality coordinates.}\end{array}} \tag{36.6}$$

In this form, the "sound of the primes" is no longer merely a plot placing primes and zeros side by side. It can display how first-order identity forms, how second-order self-relations arise, and how raw corrections are renormalized layer by layer.

The same structure is suitable for interactive visualization of finite spectral convergence, two-point relations, and the renormalization process.

36.5 Localization of Actual-to-Dual Transfer

If one further pursues the classical infinite-GUE specialization, one may seek a weighted theorem finer than a complete strong pair-correlation hypothesis—one that directly controls the transfer under the particular dynamic kernels used in this chapter, without requiring the full Hardy–Littlewood conjecture for each fixed h.

The corresponding target is to control the normalized infinite-scale limit of the exact self-correlation already present.

36.6 Higher-Order Correlations

The two-point object already shows that

$$\mu \rightarrow \mu \otimes \mu$$

does not introduce a second generative source; it places the same first-order object into a self-relation.

Higher order therefore corresponds to

$$\mu^{\otimes k}.$$

One may compare this structure with random-matrix k-point determinantal correlations and ask which source-specific invariants survive when "the same identity repeatedly forms relations with itself" at higher order.

36.7 Recording Raw-to-Renormalized Data

A corresponding data presentation may simultaneously show:

- HP zero ordinates and their unfolding;
- the pair-difference histogram;
- sine-kernel / finite-CUE predictions;
- local arithmetic corrections on the ζ-side;
- the universal component after migration;
- the dependence of the renormalized residual on height, window, and generative-source resolution.

A reader could then directly see

$$\boxed{\begin{array}{r}\text{raw} \to \text{source-specific correction} \to \\ \text{finite-scale handshake} \to \\ \text{optional asymptotic specialization.}\end{array}} \tag{36.7}$$

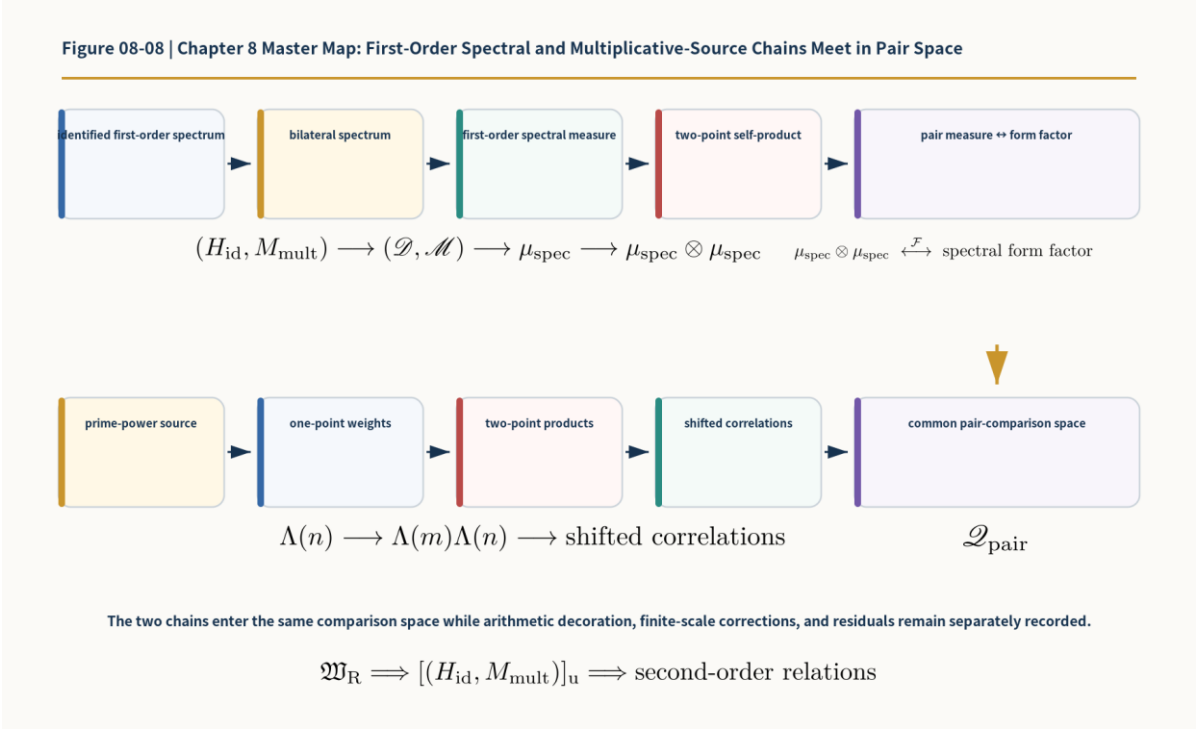


Figure 08-08. Chapter 8 master map. The upper chain runs from the canonical or identified first-order spectrum through the bilateral spectrum, first-order spectral measure, and two-point self-product to the pair measure / spectral form factor. The lower chain runs from the prime-power source through $\Lambda(n)$, $\Lambda(m)\Lambda(n)$, and shifted correlations into the same $\mathcal{Q}_{\mathrm{pair}}$. The two chains share a pair-comparison space while arithmetic decoration, finite-scale corrections, and residuals remain separately recorded.

37. Conclusion: From First-Order Spectral Identity to Second-Order Self-Relations

This chapter can be compressed into four statements.

First, **RH, HP, and GUE are not three names for the same problem.** RH closes the actual horizontal zero displacement d_ρ; HP realizes the vertical identity γ; the spectral witness identifies different first-order realizations; GUE describes the local two-point and higher-order relations of the common γ-spectrum.

Second, the first-order spectrum can be supplied by the canonical Riemann side or produced by an independent source-generated Hilbert–Pólya construction. Once the spectral witness identifies the two realizations as the same Riemann spectral identity, the second-order theory acts on the self-relations of that common identity.

Third, the chapter fixes six logical non-equivalences: representation-sheet count versus analytic multiplicity; self-adjointness versus the GUE two-point law; one-point trace versus two-point trace; lower-order means versus a second-order theorem; finite ζ versus infinite GUE; and a posteriori constant matching versus independently defined theoretical corrections.

Fourth, ζ and GUE/CUE form self-relations within their own generative sources and, after unfolding, finite-scale corrections, and raw renormalization, enter the same quotient space of pair observables:

$$\boxed{\zeta_{\mathrm{ren}} \to \mathcal{Q}_{\mathrm{pair}} \leftrightarrow \mathrm{CUE/GUE}_{\text{appropriately scaled}}.} \tag{37.1}$$

The three historical questions can therefore be placed on one stratified map:

where is the spectrum?why does it look like a quantum spectrum?why does GUE appear? (37.2)

37.1 How First-Order Identity Enters Second-Order Relations

The Riemann spectral witness theorem gives

$$\boxed{F_{\mathrm{R}} \Leftrightarrow \nu_{\mathrm{R}} \Leftrightarrow (H_{\mathrm{id}}, M_{\mathrm{mult}}) \Leftrightarrow H_{\mathrm{Ren}}.} \tag{37.3}$$

If any source-generated realization satisfies

$$\boxed{(H_{\times}, M_{\times}) \simeq (H_{\mathrm{id}}, M_{\mathrm{mult}}),} \tag{37.4}$$

the first-order identity has already been identified.

The corresponding extension proved in this chapter is

$$\boxed{\text{same first-order spectral identity} \Rightarrow \text{same unitary-invariant second-order observables.}} \tag{37.5}$$

Thus

the spectral witness answers "is this the same spectrum?"; the second-order theory asks "what does this same spectrum look like when it forms relations with itself?" (37.6)

37.2 Raw Difference and Renormalized Residual

The finite-scale discrepancy retains the complete ledger

$$\boxed{\Delta_{\mathrm{raw}} = \Delta_{\mathrm{density}} + \Delta_{\text{finite height}} + \Delta_{\text{finite CUE}} + \Delta_{\text{Euler/arithmetic}} + \Delta_{\mathrm{resolution}} + \varepsilon_{\mathrm{ren}}.} \tag{37.7}$$

Here $\varepsilon_{\mathrm{ren}}$ is the finite-scale observable that remains present after renormalization. Therefore

$$\boxed{\text{a nonzero residual} \Rightarrow / \text{ failure of the structural handshake.}} \tag{37.8}$$

Only when the target is strengthened to the classical infinite-GUE asymptotic does one further discuss its vanishing specialization.

37.3 Multiplicative Identity Meets Itself

At the two-point level there is no second multiplicative object.

The first-order multiplicative generator is

$$H_{\mathrm{mult}} e_n = (\log n) e_n.$$

The second-order relation places the same object in a tensor square and takes the relative generator:

$$\boxed{D_{\times} = H_{\mathrm{mult}} \otimes I - I \otimes H_{\mathrm{mult}}.} \tag{37.9}$$

Thus

$$D_{\times}(e_m \otimes e_n) = (\log m - \log n)(e_m \otimes e_n),$$

and therefore

$$\boxed{\operatorname{spec} D_{\times} = \{\log(m/n)\}.} \tag{37.10}$$

On the spectral side define likewise

$$\boxed{D_{\mathrm{HP}} = H_{\mathrm{HP}} \otimes I - I \otimes H_{\mathrm{HP}},} \tag{37.11}$$

whose relative spectrum is

$$\boxed{\{\gamma_j - \gamma_k\}.} \tag{37.12}$$

In measure language, for a measure μ on a suitable group,

$$\boxed{\widehat{\mu * \tilde{\mu}}(\chi) = |\hat{\mu}(\chi)|^2.} \tag{37.13}$$

Hence

second-order relation = the canonical self-product of the same first-order object. (37.14)

What the arithmetic side and the random-matrix side genuinely share is this autocorrelation architecture. Their sampling organizations remain different:

$$\boxed{\Lambda\text{-weighted deterministic arithmetic measure}}$$

and

$$\boxed{\text{Haar / unitary ensemble measure}}$$

are not the same generative source.

The conceptual closure of the chapter can therefore be stated as

it is not that "two multiplicative identities finally meet," but that "the same multiplicative identity appears in two representations at the level of self-relation." (37.15)

More strongly:

it is not two theories that meet; it is multiplicative identity finally meeting the level of its own relations. (37.16)

These statements are conceptual compressions of

$$D_{\times}, \quad D_{\mathrm{HP}}, \quad \mu * \tilde{\mu}, \quad |Z_{\phi}|^2, \quad \mathcal{Q}_{\mathrm{pair}},$$

and do not carry an additional proof burden.

37.4 Hierarchical Discipline of Objects, Provenance, and Error

The object-level discipline of the chapter is

formulas belong to definite proposition levels; spectral objects retain explicit generative provenance; finite-scale differences are recorded separately according to the object level to which they belong.

(37.17)

Second-order objects also obey

for every "new second-order object," first ask whether it is a genuinely new generative source or merely the readout produced when the same first-order identity forms a relation with itself.

(37.18)

The chapter does not mechanically splice unrelated theories together. It lets the same mathematical identity appear successively in different languages, orders, and observables while preserving its provenance and boundaries at every stage.

Appendix A | Levels of Conclusions and Types of Evidence

The content of this chapter falls into four mathematical levels.

A.1 Exact Structural Identities

These include:

- functional calculus for the signed spectrum;
- the two-point Fourier–Plancherel identity;
- second-order witness inheritance under unitary equivalence;
- the autocorrelation/Fourier correspondence for two-point observables;
- the definitional decomposition of the raw correction ledger.

These identities are independent of the GUE asymptotic conjecture.

A.2 Classical Theorems Used

These include:

- the proved range of Montgomery's pair-correlation theorem under RH;
- the Goldston–Montgomery equivalence between pair correlation and short-interval variance;
- the standard explicit formula;
- finite-N CUE/random-matrix identities.

A.3 Finite-Scale Numerical Checks

These include:

- raw versus migrated discrepancy comparisons;
- prime-local-factor restoration experiments;
- finite Euler-resolution diagnostics;

- hard-cutoff, Hann, moving, and non-overlapping windows;
- numerical reconstruction of finite-height corrections.

These data check finite-scale structure. Infinite-height asymptotics are determined by independent analytic statements.

A.4 Stronger Asymptotic Specialization

Within the framework of this chapter, classical infinite-GUE universality is written as

$$\langle \varepsilon_{\mathrm{ren}}(T), \Phi \rangle \to 0$$

for the corresponding class of two-point observables.

This limiting condition is an asymptotic specialization imposed on top of the structural handshake. The finite-scale renormalization residual is retained as an independent coordinate.

Appendix B | Master Diagram of the ζ–GUE Hierarchy

canonical/already-identified first-order spectrum	$\to$	$(H_{\mathrm{id}}, M_{\mathrm{mult}})$	$\to$	$(\mathcal{D}, \mathcal{M})$	$\to$	μ_{spec}	$\to$	
						$\downarrow$		
						two-point measure	$\overset{\mathcal{F}}{\leftrightarrow}$	
						$\downarrow$		
						$\mathcal{Q}_{\mathrm{pair}}$	$\leftrightarrow$	fini
prime-power generative source	$\to$	$\Lambda(n)$	$\to$	$\Lambda(m)\Lambda(n)$	$\to$	shifted correlation	$\to$	

(B.1)

If a source-generated HP realization satisfies

$$(H_\times, M_\times) \simeq (H_{\mathrm{id}}, M_{\mathrm{mult}}),$$

then second-order witness inheritance allows the entire first row to be replaced by $(H_\times, M_\times)$ without changing any two-point observable.

Appendix C | Raw-to-Renormalized Correction Ledger

This chapter uses

$$\boxed{\begin{aligned}\Delta_{\mathrm{raw}} = \Delta_{\mathrm{density}} + \Delta_{\mathrm{finite\ height}} + \Delta_{\mathrm{finite\ CUE}} + \Delta_{\mathrm{Euler/arithmetic}} \\ + \Delta_{\mathrm{resolution}} + \varepsilon_{\mathrm{ren}}.\end{aligned}} \tag{C.1}$$

The correction-ledger rules are:

1. every correction must have an independently defined object-level source;
2. no correction may be defined by fitting backward from the requirement that the result be closer to GUE;
3. $\varepsilon_{\mathrm{ren}}$ is retained in full as the residual observable after renormalization;
4. only when the infinite-GUE asymptotic is discussed separately is the limiting behavior of $\varepsilon_{\mathrm{ren}}$ analyzed;
5. the finite-scale handshake itself requires only a clear correction ledger and comparison space.

Appendix D | From First-Order Multiplicative Readout to the Second-Order Interface: Structural Chain and Numerical Checks

This appendix preserves the order of the structural chain and numerical checks, summarizing the object levels, structural conclusions, and numerical diagnostics of the chapter.

Stage	Core question	Result	Status
one-point → two-point	how the one-point explicit formula enters two-point statistics	$\Lambda(n) \to \Lambda(m)\Lambda(n)$, together with difference-operator/autocorrelation structure	exact structure
near-diagonalization	how second-order multiplication enters shifted-prime correlation	$\log(m/n) \to h/n$, with the primitive off-diagonal sector entering additive near-diagonality	local expansion
resolution threshold	structural origin of $\alpha = 1$	one-swap reciprocal duality; low-order direct/dual prototype of the threshold	structural prototype
completed raising	whether raising destroys self-duality	completed covariant derivatives are exactly compatible with one-swap duality	exact algebra
classical-GUE strengthening	why almost-all-shift results still do not imply the full infinite-GUE asymptotic	stronger signed collective / uniform-remainder control is required	asymptotic strengthening
joint-organization check	source of finite-scale difference between ζ and CUE/GUE	GUE: Vandermonde^2 joint law; ζ: Euler/local congruence + deterministic placement	structural decomposition
finite Euler resolution	infinite Euler model versus finite window	empirical best cutoff $P_* \sim H$, suggesting a finite-resolution effect	numerical diagnostic
raw renormalization	discrepancy before/after migration	mean raw $0.147475 \to 0.0151165$; with $p \le H$, 0.0135793	numerical check
residual check	behavior of finite-scale residual	signed bias and oscillation remain visible at high scales and under multiple windows	numerical check
anti-fitting check	whether a constant may be used for artificial alignment	constant depends on window and model order, so it is excluded from the theoretical definition	fixed boundary
external finite-height calibration	how much finite-CUE correction explains	for the four listed samples, mean difference falls from 2.2233×10^{-3} to 4.9167×10^{-5}, about 97.79% explained	numerical reconstruction
final structure	how to avoid comparing finite ζ directly with infinite GUE	finite ζ ↔ finite CUE, then passage to a common quotient of pair observables	structural handshake

The structural chain connects multiplicative self-relations, source-specific joint organization, and the universal pair law through a renormalization interface:

$$\boxed{\begin{array}{r}\text{first-order multiplicative identity} \rightarrow \\ \text{second-order self-relation} \rightarrow \\ \text{source-specific joint organization} \rightarrow \\ \text{quotient space / migration} \rightarrow \\ \text{universal pair law.}\end{array}} \tag{D.1}$$

The structural chain and correction ledger are fixed in the main text. If the classical infinite-GUE specialization is pursued further, the limiting behavior of the renormalized residual must then be studied in the corresponding test-function topology.

Appendix E | Riemann Zeros and the Language of Quantum Spectra: From Montgomery–Dyson to Second-Order Spectral Statistics

The nontrivial Riemann zeros first appear as objects of complex analysis:

$$\rho_n = \frac{1}{2} + i\gamma_n.$$

The Hilbert–Pólya idea asks further:

$$\boxed{\text{do the}\gamma_n\text{form a natural self-adjoint spectrum?}} \tag{E.1}$$

Random-matrix theory advances the question to another level:

$$\text{how are the local second-order relations among these frequencies organized?} \tag{E.2}$$

These three questions correspond respectively to zero location, spectral realization, and spectral statistics.

E.1 The Montgomery–Dyson Connection

Montgomery's analysis of pair correlation among the Riemann zeros points to the normalized two-point law

$$\boxed{R_2(x) = 1 - \left(\frac{\sin\pi x}{\pi x}\right)^2.} \tag{E.3}$$

Dyson recognized this as the same form as the two-point law of large unitary random-matrix spectra in the bulk-scaling limit.

The correspondence is not pointwise,

$$\gamma_n = \lambda_n^{\text{one random matrix}},$$

but rather

$$\boxed{\text{unfolded two-point statistics of high Riemann zeros} \quad \leftrightarrow \quad \text{bulk two-point statistics of unitary random matrices.}} \tag{E.4}$$

As $x \rightarrow 0$, the two-point density is suppressed, expressing level repulsion. Thus Riemann zeros carry information not only about "where each point lies," but also about a highly structured self-relation among the points.

The Hilbert–Pólya question therefore naturally extends to

if the zero ordinates form a self-adjoint spectrum, to which statistical symmetry class does that spectrum belong?

(E.5)

E.2 Atomic Nuclei, Random Matrices, and Quantum Spectra

An important historical route by which random-matrix theory entered quantum physics came through complex atomic nuclei. Wigner studied spacing statistics of nuclear resonances and helped establish the statistical treatment of complicated Hamiltonian spectra. Dyson subsequently systematized random-matrix spectra by symmetry class.

For complex quantum systems with time-reversal symmetry, GOE is one classical reference; when time-reversal symmetry is broken, GUE becomes the reference for the corresponding unitary symmetry class. Bohigas–Giannoni–Schmit later connected random-matrix level statistics with quantum spectra of classically chaotic systems.

The historical chain can therefore be written

$$\boxed{\begin{array}{r}\text{complex quantum Hamiltonian} \rightarrow \\ \text{random-matrix spectral statistics} \rightarrow \\ \text{symmetry class} \rightarrow \text{local level correlation.}\end{array}} \tag{E.6}$$

The Montgomery–Dyson picture places Riemann zeros precisely into this language of local spectral statistics.

E.3 Odlyzko's Experiments with High Zeros

Odlyzko computed very high Riemann zeros at large scale and high precision, systematically comparing their local spacings and two-point statistics.

These numerical experiments provide sustained and strong support for the Montgomery–Dyson picture:

$$\boxed{\text{local statistics of high Riemann zeros} \quad \approx \quad \text{GUE/CUE bulk predictions.}} \tag{E.7}$$

The symbol "≈" must be understood statistically. Finite height still carries the finite-height, finite-size, and arithmetic corrections analyzed systematically in the main text.

E.4 RH, the Spectral Witness, HP, and GUE

The levels can be separated rigorously:

$$\boxed{\text{RH: where are the zeros?}} \tag{E.8}$$

spectral witness: when are different realizations genuinely the same Riemann spectral identity?

(E.9)

HP: how do the zero ordinates form a self-adjoint spectrum?

(E.10)

GUE: how is this spectrum organized after it forms two-point relations with itself? (E.11)

The structural diagram is therefore

$$\begin{array}{c} \mathcal{R}_{\times} \\ \Downarrow \\ X(z)=\xi(1/2+z) \\ \Downarrow \\ \text{analytic zero data} \\ \Downarrow \\ \text{spectral witness / self-adjoint realization} \\ \Downarrow \\ \{\gamma_n, m_n\} \\ \Downarrow \\ \text{two-point self-relations} \\ \Downarrow \\ \text{GUE/CUE comparison.} \end{array} \tag{E.12}$$

First order reads spectral identity; second order reads spectral relations:

$$\gamma_j - \gamma_k.$$

Thus

$$\boxed{\text{HP is the carrier of first-order spectral identity,}} \tag{E.13}$$

and

GUE is the second-order self-relation readout of that same spectral identity family. (E.14)

E.5 Connection with the Arithmetic Second-Order Interface

The main text obtains the chain

$$\{\gamma_n, m_n\} \to \mathrm{Tr} f(H) \to |\mathrm{Tr}(\cdots)|^2 \to \Lambda(m)\Lambda(n) \to \Lambda(n)\Lambda(n+h). \tag{E.15}$$

Thus first-order spectral identity and second-order spectral statistics never leave the same multiplicative generative source.

More precisely,

the same multiplicative identity appears at first order as a spectral identity address and at second order as a relation among those identities. (E.16)

The Montgomery–Dyson connection occurs at the second-order layer after the common spectral identity has already formed.

E.6 Quantum-Spectral Language and Riemann Zeros: From First-Order Spectral Identity to Second-Order Statistics

Hilbert space, self-adjoint Hamiltonians, unitary evolution, spectra, and frequencies are among the basic mathematical languages of quantum theory.

When the Riemann zero ordinates are realized as

$$He_n = \gamma_n e_n,$$

they naturally appear in spectral language as self-adjoint frequencies.

More generally, for a Hilbert–Pólya realization generated from open multiplicative identity and identified by the spectral witness, one may write

$$H_{\times} e_n = \gamma_n e_n.$$

The same set of Riemann zero ordinates can therefore be read either as the vertical coordinates of analytic zeros or as self-adjoint spectral frequencies.

At the GUE level one then studies the second-order relations among these frequencies and compares them with universal statistics of the unitary symmetry class. The long-standing connection between Riemann zeros and quantum-spectral language can therefore be written as a continuous mathematical structure:

$$\boxed{\begin{array}{c}\text{open multiplicative identity}\\ \Downarrow\\ \text{analytic zero ordinates}\\ \Downarrow\\ \text{self-adjoint spectral frequencies}\\ \Downarrow\\ \text{second-order spectral relations}\\ \Downarrow\\ \text{GUE universality problem.}\end{array}} \tag{E.17}$$

The point of this continuous structure is not to fit number theory retrospectively to a quantum model, nor to assert

$$\text{number theory} = \text{quantum mechanics}.$$

The more precise statement is

the same mathematical identity can appear independently in languages that are far apart; once those languages recognize the same object, the next-order question naturally becomes its relation with itself.

(E.18)

From this perspective, Hamiltonians, self-adjointness, unitary flow, spectra, and frequencies recur around the Riemann problem not because the zeros must be forced into one particular physical system, but because these notions provide natural spectral expressions of the same spectral identity.

At first order the question is

$$\boxed{\text{who is} \gamma_n ?}$$

At second order it becomes

$$\boxed{\text{how are} \gamma_j - \gamma_k \text{organized?}}$$

Thus the historical convergence of arithmetic language and quantum-spectral language may be understood as

arithmetic language and quantum-spectral language converge successively at the levels of first-order spectral identity and second-order statistics.

(E.19)

In that stratification,

RH fixes first-order spectral location, (E.20)

HP provides a self-adjoint carrier for the first-order spectrum,

(E.21)

and

GUE describes the second-order statistical organization of that same spectrum.

(E.22)

The three levels are continuous but cannot be conflated.

RH asks whether the actual zeros satisfy

$$\Re\rho = \frac{1}{2}.$$

HP asks whether and how the zero ordinates γ_n are carried by a natural self-adjoint realization.

GUE no longer asks about a single γ_n, but about unfolded two-point differences, pair correlations, form factors, and higher-order local statistics.

Thus the "mysterious connection between Riemann zeros and quantum energy levels" should not be compressed into the sentence "the zeros are quantum energy levels." It is more accurately written as

analytic zero identity →
self-adjoint spectral identity →
second-order spectral self-relation →
unitary-universality comparison. (E.23)

This is also why the present chapter consistently separates first-order spectral identity from second-order spectral statistics: the former answers "who is present," while the latter asks "how do those present form relations with one another?"

E.7 From First-Order Quantum Spectrum to Second-Order Statistics

Hilbert–Pólya spectral language addresses the question "what self-adjoint object carries the frequencies?" GUE/CUE statistical language addresses the question "how are those frequencies arranged relative to one another?"

The final structure of the quantum-spectral story is therefore not a reduction of every question to one Hamiltonian, but

first-order self-adjoint spectrum →
relative spectrum →
two-point correlation / form factor →
unitary universality. (E.24)

Within this structure, first-order spectral identity and second-order statistics are continuous yet distinct: the former determines “who is present,” and the latter studies “what relations occur among those present.”

Chapter 9 Another Closure Path for the Riemann Hypothesis: Open Multiplicative Identity and an Independent Hilbert–Pólya Spectral Route

From the Root Multiplicative Identity to a Source-Generated Self-Adjoint Spectrum and Canonical Terminal Identification

Abstract

This chapter starts from the unique root multiplicative identity of the book,

$$\Im_{\times} = (\mathbb{N}_{>0}, \mu), \qquad \mu(m,q) = mq,$$

and constructs a source-generated Hilbert–Pólya spectral route. The list of Riemann zeros, the Yifei Ren operator K_{Ren}, the canonical Riemann spectral operator H_{Ren}, and the canonical spectral witness of Chapter 7 do not enter the generative chain. They enter only after the source-generated spectrum has been formed and the RH closure has been completed, where they serve canonical terminal identification.

The complete open multiplicative relation

$$\mathcal{R}_{\times} = \mathrm{Graph}(\mu) = \{(m,q,n) \in \mathbb{N}^3 : mq = n\}$$

has a complete generative-source representation Ω. For every finite moving horizon r, the head/tail role difference is eliminated in the identity quotient:

$$\boxed{[\Psi_r] = [\Omega]_{\mathrm{id}} \qquad (\forall r).}$$

Let

$$\boxed{\mathfrak{C}_{\times} := [\Omega]_{\mathrm{id}}}$$

denote the complete generative-source-side identity class of the root multiplicative identity. Completion, the centered function, and its analytic readout all factor through this identity class:

$$X_r = X, \qquad G_r = G, \qquad F_r = F.$$

From

$$F(y) = \mu_0 - \mu_1 y + \mu_2 y^2 - \cdots, \qquad \mu_k = \frac{(-1)^k}{k!} F^{(k)}(0),$$

define the unique scan functional

$$\mathcal{L}_{\times}(\beta^k) = \mu_k.$$

If

$$\Psi_n = T_{\times}^n \Psi_0,$$

then $\Psi_0, \Psi_1, \ldots$ are manifestations, at different scan depths, of the same generative-source-side identity class $\mathfrak{C}_\times$. The scan composition law

$$T_\times^i T_\times^j = T_\times^{i+j}$$

implies that the relational coordinate between two manifestations depends only on the total scan depth. Hence

$$\boxed{\mathsf{H}_N = [\mu_{i+j}], \qquad \mathsf{H}_N^{(1)} = [\mu_{i+j+1}]}$$

are finite coordinate tables of the self-relation of one and the same root multiplicative identity at two relational depths. Together these structures form the **Unified Single-Identity Closure Package**.

The self-pairing of the same identity at relational depths $r = 0,1$ gives

$$\boxed{\mathcal{E}_\times^{[r]}\left(\Psi_i^{[r]}, \Psi_j^{[r]}\right) = \mathcal{L}_\times(\beta^{i+j+r}) = \mu_{i+j+r}, \qquad r = 0,1.}$$

Therefore, for arbitrary finite coefficients c_i,

$$\boxed{\sum_{i,j} \bar{c}_i\, c_j \mu_{i+j+r} = \left\| \sum_i c_i\, \Psi_i^{[r]} \right\|^2 \geq 0, \qquad r = 0,1,}$$

and hence

$$\boxed{\mathsf{H}_N \succcurlyeq 0, \qquad \mathsf{H}_N^{(1)} \succcurlyeq 0 \qquad (\forall N).}$$

Dual Hankel positivity and the Stieltjes moment theorem recover a unique finite positive measure

$$\nu_\times.$$

Its Cauchy/Stieltjes response agrees with

$$F(y) = \frac{G'(y)}{G(y)}.$$

Meromorphicity then yields a pure-point measure. The support and atomic weights recover, respectively, the distinct zero ordinates γ_n and analytic multiplicities m_n. On the identity-faithful space define

$$B_\times = M_\beta, \qquad H_\times = B_\times^{-1/2}.$$

Then

$$\boxed{H_\times = H_\times^*, \qquad \sigma(H_\times) = \{\gamma_n\}.}$$

At the same time define the source-generated analytic multiplicity operator

$$M_\times e_n = m_n e_n.$$

The recovered centered zeros

$$z = \pm i\gamma_n$$

give

$$\rho = \frac{1}{2} \pm i\gamma_n,$$

thereby completing the independent Hilbert–Pólya ⇒ RH closure.

After the generative chain is complete, the canonical spectral witness of Chapter 7 gives

$$\boxed{(H_\times, M_\times) \simeq (H_{\mathrm{id}}, M_{\mathrm{mult}}),}$$

and divisor amplification,

$$\widetilde{H}_\times = \mathrm{Amp}_{M_\times}(H_\times),$$

gives

$$\boxed{\widetilde{H}_\times \simeq H_{\mathrm{Ren}}.}$$

By second-order witness inheritance from Chapter 8, all unitary-invariant two-point observables agree once the first-order spectral identity has been identified.

Finite-dimensional Source–Krylov truncations provide independent numerical checks. Cholesky tests of the ordinary and shifted Hankel matrices pass for $N = 1, \ldots, 12$; all Gaussian quadrature weights are positive at $N = 12$; and the maximum relative residual in matching the first 24 moments is approximately

$$5.2 \times 10^{-150}.$$

These finite-section results are consistent with the all-order Gram-positivity theorem, but the universal conclusion comes from the two-depth self-pairing of the same root multiplicative identity, not from extrapolation of finite numerics.

The main chain of the chapter is therefore

root multiplicative identity →
single-identity closure →
dual Gram positivity →
Stieltjes reconstruction →
source-generated self-adjoint Hilbert–Pólya spectrum →
RH → canonical terminal identification.

0.1 Object Position of the Hilbert–Pólya Route

The Hilbert–Pólya idea asks for a natural self-adjoint operator H such that the ordinates γ of the nontrivial Riemann zeros

$$\rho = \frac{1}{2} + i\gamma$$

occur as its real spectrum:

$$\boxed{H\psi_\gamma = \gamma\psi_\gamma, \qquad H = H^*.} \tag{0.7}$$

This chapter follows a source-generated route beginning from the root multiplicative identity:

$$\boxed{\begin{array}{r}\mathcal{R}_\times \to \\ \boxed{\text{Unified Single-Identity Closure Package}} \to \\ \boxed{\text{ordinary/shifted self-pairing Gram positivity}} \to \\ F \to \nu_\times \to H_\times.\end{array}} \tag{0.8}$$

The Unified Single-Identity Closure Package compresses the identity consistency from the generative source to the coordinate layer into multiple representations of the same object, while ordinary/shifted self-pairing at two depths yields the two Gram positivities simultaneously. Standard Stieltjes theory and spectral theory then complete the global recovery.

The first-order source-generated spectral terminal of this chapter is $(H_\times, M_\times)$. The second-order statistics of Chapter 8 act only after the first-order spectral identity has been formed and canonically identified, at the level of its self-relations.

1. Proof Structure and Object Levels

This chapter treats four mathematical levels in sequence.

First, the Unified Single-Identity Closure Package proves that the moving horizon, identity quotient, completion, $X/G/F$, scan functional, moments, ordinary/shifted Hankel matrices, and finite scan windows are all different representations of the same root multiplicative identity. The root identity remains

$$\mathfrak{I}_\times = (\mathbb{N}_{>0}, \mu),$$

while the complete generative-source-side identity class is denoted

$$\mathfrak{C}_\times = [\Omega]_{\mathrm{id}}.$$

Second, the ordinary and shifted relation tables are simultaneously written as Hilbert/Gram self-pairings of the same identity at two relational depths:

$$\mathcal{E}_\times^{[r]}(\Psi_i^{[r]}, \Psi_j^{[r]}) = \mu_{i+j+r}, \qquad r = 0,1.$$

This yields both all-order Hankel positivity statements at once.

Third, dual Hankel positivity yields a unique finite positive measure by the Stieltjes moment theorem. Meromorphicity further yields a pure-point spectrum and recovers the distinct zero ordinates, the analytic multiplicities, and the source-generated self-adjoint Hilbert–Pólya operator $H_\times$. The centered zeros are then forced to be purely imaginary, which yields RH.

Fourth, after the source-generated chain has been completed, the canonical spectral witness of Chapter 7 performs terminal identification:

$$(H_\times, M_\times) \simeq (H_{\mathrm{id}}, M_{\mathrm{mult}}),$$

and divisor amplification identifies the result with the canonical Riemann spectral operator of Chapter 6.

The generative direction is fixed as

$$\boxed{\mathcal{R}_\times \to X \to F \to \mathcal{L}_\times \to (\mathcal{E}_\times, T_\times) \to \nu_\times \to B_\times \to (H_\times, M_\times).} \tag{1.1}$$

None of

$$\{\gamma_n\}, \qquad K_{\mathrm{Ren}}, \qquad H_{\mathrm{Ren}}$$

enters the definition of these objects. They are used only after the source-generated spectral terminal has already been formed, for independent checking or canonical identification.

Finite-dimensional numerical checks in the body of the chapter verify only consistency of finite sections with the universal theorem. All-order positivity comes from the two-depth identity-self-pairing theorem of Section 5. The classical infinite-GUE asymptotic is a stronger second-order asymptotic specialization beyond the structure of Chapter 8.

2. Root Multiplicative Identity, Open Relation, and Role Exchange

Using the book-wide notation of Chapter 1, the unique root multiplicative identity is

$$\boxed{\mathfrak{I}_{\times} = (\mathbb{N}_{>0}, \mu), \qquad \mu(m,q) = mq.}$$

Its open relational representation is

$$\boxed{\mathcal{R}_{\times} = \mathrm{Graph}(\mu) = \{(m,q,n) \in \mathbb{N}^3 : mq = n\}.}$$

Define the reciprocal exchange

$$J(m,q) = (q,m).$$

To avoid conflict with the height parameter T used in second-order spectral statistics, this chapter fixes the total logarithmic multiplicative scale as

$$\boxed{L_{\times} = \log(mq) = \log n,} \tag{2.1}$$

and the relative factor-role coordinate as

$$\boxed{R = \log\frac{q}{m}.} \tag{2.2}$$

Then

$$\log m = \frac{L_{\times} - R}{2}, \qquad \log q = \frac{L_{\times} + R}{2}.$$

The role exchange acts by

$$J : (L_{\times}, R) \mapsto (L_{\times}, -R). \tag{2.3}$$

Take the centered Mellin parameter

$$s = \frac{1}{2} + z.$$

The corresponding generative-source role kernel is

$$\boxed{\kappa_z(L_{\times}, R) = e^{-L_{\times}/2} e^{zR} = m^{-1/2-z} q^{-1/2+z}.} \tag{2.4}$$

Hence

$$\kappa_z(L_{\times}, -R) = \kappa_{-z}(L_{\times}, R). \tag{2.5}$$

When $z = i\tau \in i\mathbb{R}$,

$$\kappa_{i\tau}(L_{\times}, R)\overline{\kappa_{i\tau}(L_{\times}, R)} = e^{-L_{\times}} > 0. \tag{2.6}$$

This provides the minimal positive-kernel source for the root multiplicative identity self-pairing used later: reciprocal exchange reverses the phase direction, but pairing the same multiplicative identity with itself retains the positive total-scale weight.

The chapter therefore fixes two distinct objects:

$$\boxed{L_\times = \text{multiplicative total log-scale}, \qquad \mathcal{L}_\times = \text{moment/scan functional.}} \tag{2.7}$$

Their notation is not interchanged.

3. The Multiplicative-Source Hamiltonian and the Completed Riemann Function

Define the multiplicative-source Hamiltonian

$$H_{\text{mult}} e_n = (\log n) e_n.$$

Then, for $\Re s > 1$,

$$\boxed{\text{Tr}(e^{-sH_{\text{mult}}}) = \sum_{n\geq 1} e^{-s\log n} = \sum_{n\geq 1} n^{-s} = \zeta(s).} \tag{3.1}$$

Thus, in the half-plane of absolute convergence, the Riemann zeta function is directly the trace response of the multiplicative generative source. Using the standard theta/Mellin representation together with the Jacobi–Poisson functional equation, define the completion

$$\boxed{\xi(s) = \frac{1}{2} s(s-1)\pi^{-s/2}\Gamma\left(\frac{s}{2}\right)\zeta(s),} \tag{3.2}$$

with

$$\boxed{\xi(s) = \xi(1-s).} \tag{3.3}$$

Take the centered coordinate

$$s = \frac{1}{2} + z$$

and define

$$\boxed{X(z) = \xi\left(\frac{1}{2} + z\right).} \tag{3.4}$$

Then

$$\boxed{X(z) = X(-z).} \tag{3.5}$$

This fixes the only global analytic generative source allowed in this chapter. Its entire continuation and functional equation come from the standard Riemann completion and do not use RH.

The later spectral truncations are allowed to read only

$$X(0), \quad X''(0), \quad X^{(4)}(0), \ldots$$

and the quantities G, F, μ_k determined from these source derivatives. Explicitly,

$$\boxed{\{\gamma_n\}\textbf{are not construction inputs for the HP spectral truncation.}} \tag{3.6}$$

The zero list is used only for independent comparison after the source-only output has been frozen. Likewise, neither K_{Ren} nor H_{Ren} enters the spectral generative chain of this chapter.

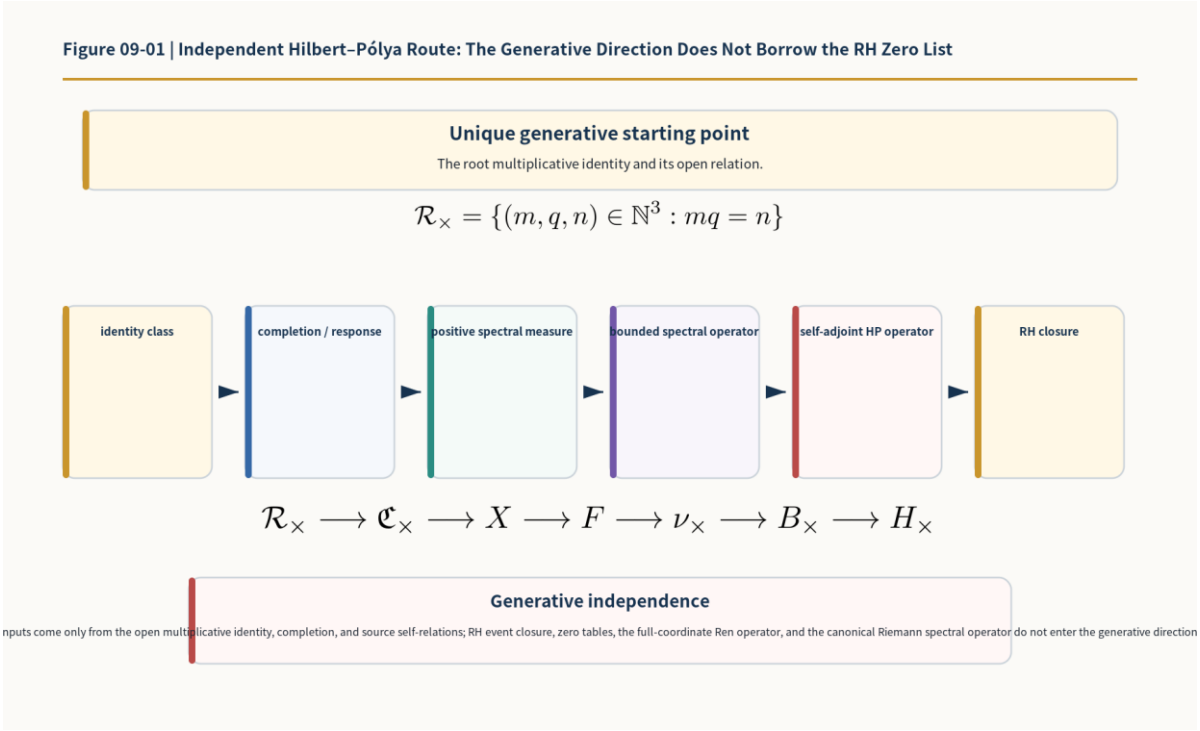


Figure 09-01. Object position of the independent Hilbert–Pólya route. The generative direction starts from the unique open multiplicative relation and passes through its identity class, completed response, positive spectral measure, bounded spectral operator, and self-adjoint $H_\times$, finally closing RH through purely imaginary centered spectral addresses. RH event closure, zero tables, K_{Ren}, H_{Ren}, and the canonical spectral witness do not enter this generative direction; they are used only afterward for independent comparison or terminal identification.

4. Unified Single-Identity Closure Package

The identity structure of this chapter is no longer split into several independent bridges. Structurally, **one complete multiplicative identity repeatedly appears in different mature mathematical languages, different horizons, and different scan depths.** The identity-consistency obligation should therefore be paid once, rather than re-proving after every change of representation that the object is still the same.

Let the unique open multiplicative generative source be

$$\mathcal{R}_\times = \{(m,q,n) \in \mathbb{N}^3 : mq = n\}.$$

Let its complete generative-source representation be Ω. For every finite moving horizon r, make a lossless cut

$$\Omega = \Omega_r^{\mathrm{H}} + \Omega_r^{\mathrm{T}},$$

and define the role-sum map

$$S(h,t) = h + t.$$

Any role-space difference lying in $\ker S$ does not alter the complete generative-source-side identity class. Hence define

$$\mathcal{Q}_{\mathrm{id}} = (\mathcal{E} \oplus \mathcal{E})/\ker S,$$

and obtain

$$\boxed{[\Psi_r] = [\Omega]_{\mathrm{id}} \qquad (\forall r).} \tag{4.1}$$

There is no $r \to \infty$ here: finite cutting changes the visible range, not the identity.

Completion factors through this identity quotient, so all finite-horizon representations descend to the same centered completed object:

$$\boxed{X_r = X, \qquad G_r = G, \qquad F_r = F.} \tag{4.2}$$

Here

$$G(y) = \frac{X(\sqrt{y})}{X(0)}, \qquad F(y) = \frac{G'(y)}{G(y)}.$$

Thus the moments are not new objects; they are monomial/scan coordinates of the same F:

$$\boxed{\mu_n = \frac{(-1)^n}{n!} F^{(n)}(0), \qquad \mathcal{L}_\times(\beta^n) = \mu_n.} \tag{4.3}$$

Let the complete generative-source-side identity class of the root multiplicative identity be

$$\boxed{\mathfrak{C}_\times := [\Omega]_{\mathrm{id}}.}$$

Write its multiple scan manifestations as

$$\boxed{\Psi_n = T_\times^n \Psi_0.} \tag{4.4}$$

The sequence $\Psi_0, \Psi_1, \Psi_2, \ldots$ does not represent multiple identities; it consists of manifestations of the same $\mathfrak{C}_\times$ at different scan depths. Scanning does not create a new object; it enlarges the visible relational range of the same identity.

The scan composition law

$$\boxed{T_\times^i T_\times^j = T_\times^{i+j}} \tag{4.5}$$

shows that the relational coordinate between two scan manifestations depends only on the total number of scans. Hence

$$\boxed{\mathcal{E}_\times(\Psi_i, \Psi_j) = \mathcal{L}_\times(\beta^{i+j}) = \mu_{i+j},} \tag{4.6}$$

while one further relational scan is read as

$$\boxed{\mathcal{E}_\times^{[1]}(\Psi_i, \Psi_j) = \mathcal{L}_\times(\beta^{i+j+1}) = \mu_{i+j+1}.} \tag{4.7}$$

Here $\mathcal{E}_\times^{[1]}$ means **the relational readout of the same complete identity after the overall relation-scan depth has been increased by one**. It is not a second identity and does not require renewed identity matching.

Therefore the ordinary and shifted Hankel tables

$$\boxed{\mathrm{H}_N = [\mu_{i+j}]_{i,j=0}^{N-1}, \qquad \mathrm{H}_N^{(1)} = [\mu_{i+j+1}]_{i,j=0}^{N-1}} \tag{4.8}$$

are simply finite coordinate tables of the self-relation of the same identity at two scan depths. Likewise, the finite scan spaces

$$\mathcal{P}_0 \subset \mathcal{P}_1 \subset \cdots, \qquad \mathcal{P}_{N-1} = \mathrm{span}\{1, \beta, \ldots, \beta^{N-1}\},$$

are not a sequence of new models; they are increasing coordinate windows for the same $\mathcal{L}_\times$. An N-dimensional spectral truncation uses

$$\mu_0, \ldots, \mu_{2N-1},$$

because the ordinary table requires moments through μ_{2N-2}, and the shifted table, one relational depth deeper, requires one additional moment μ_{2N-1}. The number $2N$ expresses complete coverage of one N-dimensional relational scan, not "twice as many objects."

The foregoing may be summarized as

$$\boxed{\begin{array}{c}\mathcal{R}_{\times}\\ \Downarrow\\ \mathfrak{C}_{\times}=[\Omega]_{\mathrm{id}}\\ \Downarrow\\ X\to G\to F\to \mathcal{L}_{\times}\\ \Downarrow\\ \Psi_n=\mathrm{Scan}_n(\mathfrak{C}_{\times})\\ \Downarrow\\ (i,j)\mapsto i+j \text{ or } i+j+1\\ \Downarrow\\ \mathsf{H}_N,\ \mathsf{H}_N^{(1)},\ \text{finite scan windows.}\end{array}} \tag{4.9}$$

This is the chapter's

Unified Single-Identity Closure Package

and its core **Multiple-Scan Relation Theorem for a Single Identity**.

It simultaneously contains the following identity-consistency conditions:

$$\boxed{\begin{array}{l}\text{unique generative-source-side identity class,}\\ \text{identity preservation under moving horizons,}\\ \text{identity fidelity under completion,}\\ \text{moment provenance,}\\ \text{multiple-scan identity,}\\ \text{ordinary/shifted coordinate identity,}\\ \text{finite-window identity consistency.}\end{array}} \tag{4.10}$$

The structure can be compressed to

one identity quotient + one multiple-scan composition law, in place of several repeated identity-matching steps.

(4.11)

Thus the generative source, completion, moments, Hankel and shifted-Hankel tables, and finite spectral truncations are all treated as different representations of the same root multiplicative identity. Subsequent sections separately address positivity, spectral representation, and limiting recovery.

Identity re-audit. The universal structure of this chapter is not extrapolated from finite matrices with $N \leq 12$. Finite Source–Krylov computations only enlarge the visible window of the same identity and serve as independent checks. Section 4 has already fixed

$$\boxed{\Psi_0, \Psi_1, \ldots \text{as scan manifestations of the same} \mathfrak{C}_{\times},}$$

while ordinary and shifted are merely two coordinate tables of the self-relation of the same identity at relational depths $r = 0,1$.

The genuine point to be checked here is therefore **whether identity self-pairing is well defined on the same identity class**: changing a finite-horizon representative, scan depth, or coordinate window must not create a second identity or alter the readout of the self-relation of the same identity. The Gram formula of Section 5 reads this already-fixed identity self-pairing; finite numerical results are not the source of the universal conclusion.

In other words, "finite verification → all-order conclusion" is not a proof bridge in this chapter. If further formalization is desired, what is required is well-definedness of $\mathcal{E}_{\times}^{[r]}$ on representatives of the identity quotient. That remains an identity question, not a new positivity mechanism.

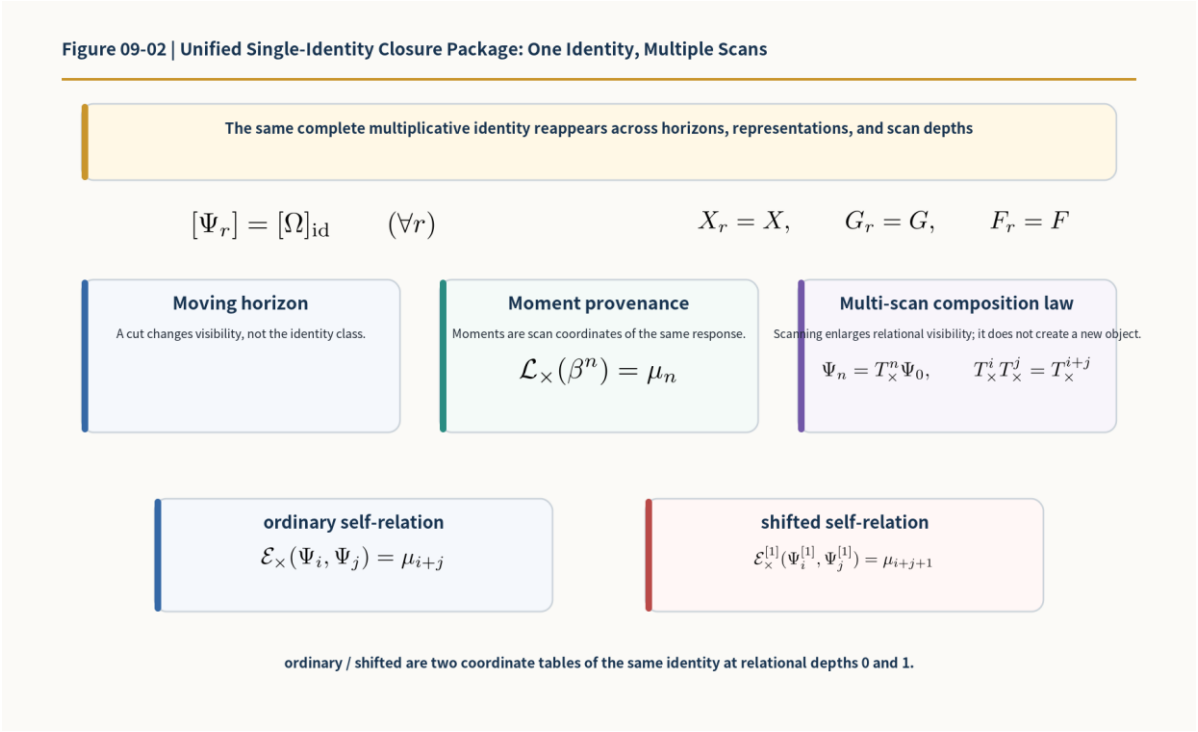


Figure 09-02. Unified Single-Identity Closure Package. A moving-horizon cut changes visibility but not $[\Omega]_{\mathrm{id}}$; the completed objects X, G, F remain the same across finite horizons; moments are scan coordinates of the same response; and $\Psi_n = T_{\times}^n \Psi_0$ are multiple scan manifestations of the same $\mathfrak{C}_{\times}$. Ordinary and shifted tables are not two identities, but two self-relation coordinate tables of one identity at relational depths 0 and 1.

5. Two-Depth Identity Self-Pairing and Dual Gram Positivity

Section 4 has already discharged, in one step, all identity-consistency obligations concerning "to which object these coordinates belong." It remains only to read the Hilbert/Gram expression of the same identity meeting itself at two relational depths.

Define

$$\Psi_i^{[0]} := \Psi_i,$$

and let $\Psi_i^{[1]}$ denote the ith scan manifestation of the same generative-source-side identity class $\mathfrak{C}_\times$ after the overall relational depth has been increased by one. The superscript [1] records only the relational scan context; it does not introduce a second generative source, a second object, or a new dynamical action.

The Unified Single-Identity Closure Package gives

$$\boxed{\mathcal{E}_\times^{[r]}\left(\Psi_i^{[r]}, \Psi_j^{[r]}\right) = \mathcal{L}_\times(\beta^{i+j+r}) = \mu_{i+j+r}, \qquad r = 0,1.} \tag{5.1}$$

This is the two-depth form of the **Identity Self-Pairing Coordinate Theorem**. The case $r = 0$ gives the ordinary table and $r = 1$ the shifted table; both are coordinate readouts of the same identity meeting itself.

For arbitrary

$$p(\beta) = \sum_{i=0}^{N-1} c_i\, \beta^i,$$

the Gram identity gives simultaneously

$$\boxed{\sum_{i,j=0}^{N-1} \bar{c}_i\, c_j \mu_{i+j+r} = \left\| \sum_{i=0}^{N-1} c_i\, \Psi_i^{[r]} \right\|^2 \geq 0, \qquad r = 0,1.} \tag{5.2}$$

Therefore

$$\boxed{\mathsf{H}_N = [\mu_{i+j}] \succcurlyeq 0, \qquad \mathsf{H}_N^{(1)} = [\mu_{i+j+1}] \succcurlyeq 0 \qquad \forall N.} \tag{5.3}$$

The key point is not to infer positive definiteness from pointwise positivity. Rather,

$$\boxed{\begin{array}{r} \text{one complete identity} \rightarrow \\ \text{multiple scan manifestations} \rightarrow \\ \text{the identity meeting itself} \rightarrow \\ \text{two families of Gram coordinate tables.} \end{array}} \tag{5.4}$$

Shifted positivity is therefore not an independent analytic condition. Treating

$$\mathcal{L}_\times(\beta|p|^2) \geq 0$$

as a separate shifted-positivity proposition would re-objectify the $+1$ relational depth that already belongs to the same identity self-pairing. The correct reading is

$$\mathcal{L}_\times(\beta|p|^2) = \left\| \sum_i c_i\, \Psi_i^{[1]} \right\|^2 \geq 0, \tag{5.5}$$

which is simply the quadratic-form version of the $r = 1$ Gram identity, not a new proof bridge.

This section therefore yields

$$\boxed{\begin{array}{c} \text{Unified Single-Identity Closure Package} \\ \Downarrow \\ \text{identity self-pairing at relational depths} r = 0,1 \\ \Downarrow \\ \mathsf{H}_N \succcurlyeq 0, \qquad \mathsf{H}_N^{(1)} \succcurlyeq 0 \quad \forall N. \end{array}} \tag{5.6}$$

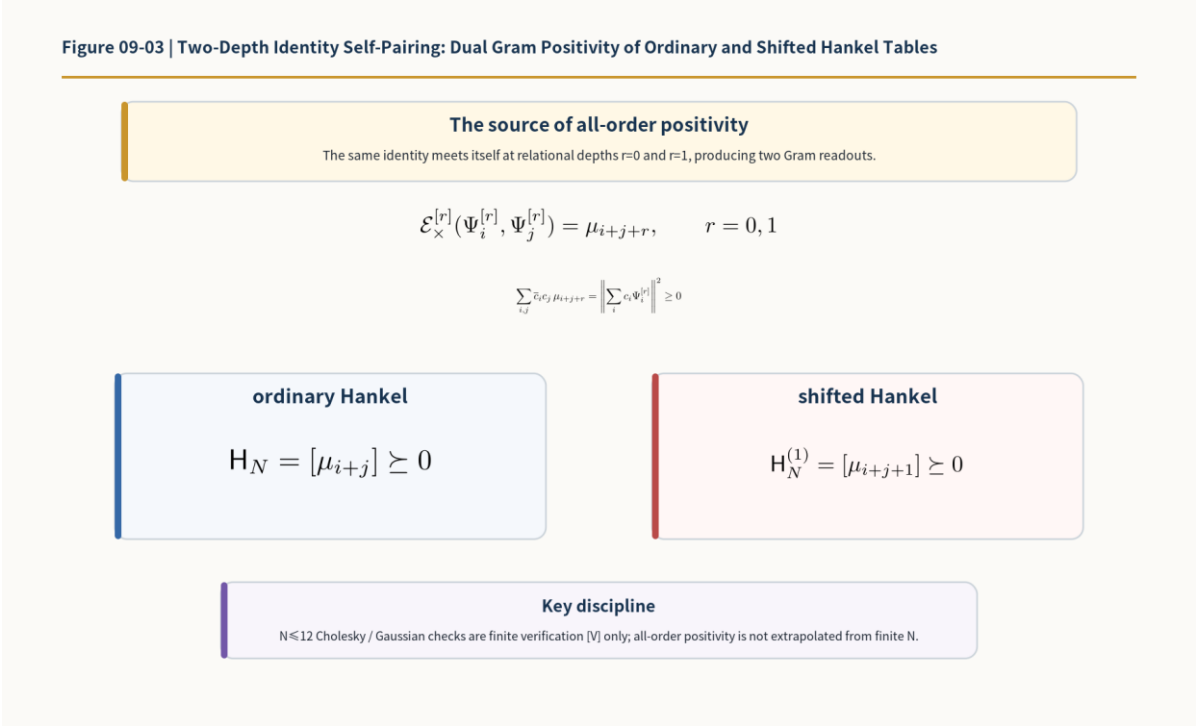


Figure 09-03. Two-depth identity self-pairing. For $r = 0,1$, the same identity self-pairing satisfies $\mathcal{E}_{\times}^{[r]}(\Psi_i^{[r]}, \Psi_j^{[r]}) = \mu_{i+j+r}$, and its quadratic form is directly a Hilbert norm square. Hence the ordinary and shifted Hankel tables are positive semidefinite for every N. The high-precision $N \leq 12$ Cholesky / Gaussian calculations are finite verification [V] only; the chapter does not extrapolate all-order positivity from finite N.

6. Finite Source–Krylov Spectral Truncations

Section 5 has already established, universally, positivity of both the ordinary and shifted Hankel families. The high-precision computations for $N \leq 12$ in Section 8 serve only as independent finite checks. Thus the following finite spectral-truncation formulas hold unconditionally at the level of the global theorem:

$$\mathsf{H}_N \succcurlyeq 0, \qquad \mathsf{H}_N^{(1)} \succcurlyeq 0.$$

If H_N is nondegenerate, define directly

$$\boxed{B_{\times,N} = \mathsf{H}_N^{-1/2} \mathsf{H}_N^{(1)} \mathsf{H}_N^{-1/2}.} \tag{6.1}$$

If H_N has null directions, first pass to the identity quotient

$$\mathcal{P}_{N-1}/\ker \mathsf{H}_N.$$

Equivalently, one may use the Moore–Penrose inverse on $\mathrm{Ran}\mathsf{H}_N$. The resulting finite spectral truncation is still uniquely determined by the same pair of Gram tables and satisfies

$$\boxed{B_{\times,N} = B_{\times,N}^{*} \geq 0.} \tag{6.2}$$

On its positive spectral support define the finite Hilbert–Pólya readout

$$\boxed{H_{\times,N} = B_{\times,N}^{-1/2}.} \tag{6.3}$$

Equivalently, solve the generalized eigenvalue problem

$$\boxed{\mathsf{H}_N^{(1)} v = \beta\, \mathsf{H}_N v,} \tag{6.4}$$

retaining only the positive generalized eigenvalues $\beta > 0$ on the identity quotient. The corresponding finite spectral readout is

$$\boxed{\gamma^{(N)} = \beta^{-1/2}.} \tag{6.5}$$

Thus the mathematical identity of the finite spectral truncation is

$$\boxed{B_{\times,N} = \text{the positive compression of the same generative-source-side identity class to a finite scan/Krylov window.}} \tag{6.6}$$

It is not a family of new spectral models and does not bear the universal proof of RH. Its role is to provide finite-resolution readouts and connect with the compression theory of the global operator below.

7. Independence of the Generative Inputs

The finite spectral truncation uses only the following generative-source data:

$$X$$

and its local derivatives.

The computational chain is

$$X \to G \to F \to \mu \to \mathsf{H}_N, \mathsf{H}_N^{(1)} \to B_{\times,N} \to \gamma_j^{(N)}.$$

The finite spectral truncation does not take

$$\gamma_j$$

as input.

It does not take

$$H_{\mathrm{Ren}}$$

as input.

Nor does it preload

$$\nu_\times = \sum m_n \gamma_n^{-2} \delta_{\gamma_n^{-2}}$$

as prior information.

Hence the finite spectral recovery is independent at the level of input.

8. Finite Source-Side Truncation and Independent Zero Comparison

The finite spectral camera of the independent HP channel uses only local derivatives of the source-generated X. It does not input a table of Riemann zeros and does not call the terminal zero identities supplied by the independent RH proof.

Existing source-only independent checks give

$$N = 2: \quad 14.60686489306,\ 48.64801900795;$$

$$N = 3: \quad 14.15189601461,\ 23.90191976465,\ 78.01695224576;$$

$$N = 4: \quad 14.13509583518,\ 21.54890073193,\ 33.63176075304, \ldots;$$

$$N = 5: \quad 14.13473094478,\ 21.10588451750,\ 27.06733537729, \ldots;$$

$$N = 6: \quad 14.1347251821114,\ 21.0272939502839,\ 25.2906124281783, \ldots;$$

$$N = 7: \quad 14.1347251418888,\ 21.0221890679236,\ 25.0335044184750, \ldots;$$

$$N = 8: \quad 14.1347251417353,\ 21.0220440879397,\ 25.0128201639747,\ 30.8600444716268, \ldots.$$

The computational order is frozen as

$$X \to F \to \mu_k \to (\mathsf{H}_N, \mathsf{H}_N^{(1)}) \to B_{\times,N} \to \gamma_j^{(N)}.$$

Only after the HP output has been frozen is it compared with the terminal ordinates obtained by the independent RH channel:

$$14.13472514173469 \ldots,$$

$$21.02203963877155 \ldots,$$

$$25.01085758014569 \ldots,$$

$$30.42487612585951 \ldots.$$

The same data may be organized as follows:

N	$\gamma_1^{\mathrm{HP}}(N)$	$\gamma_2^{\mathrm{HP}}(N)$	$\gamma_3^{\mathrm{HP}}(N)$	$\gamma_4^{\mathrm{HP}}(N)$
2	14.60686489306	48.648019007 95	—	—
3	14.15189601461	23.901919764 65	78.016952245 76	—
4	14.13509583518	21.548900731 93	33.631760753 04	—
5	14.13473094478	21.105884517 50	27.067335377 29	—
6	14.1347251821 114	21.0272939502 839	25.2906124281 783	—
7	14.1347251418 888	21.0221890679 236	25.0335044184 750	—
8	14.1347251417 353	21.0220440879 397	25.0128201639 747	30.8600444716 268
independent RH-channel terminal	14.1347251417 3469…	21.0220396387 7155…	25.0108575801 4569…	30.4248761258 5951…

The high-order outputs at different N are boundary readouts at finite resolution. The purpose of the table is to observe that fixed low-lying identities progressively lock in as N increases, not to interpret every column at small N as an already completed kth Ritz identity.

The finite-dimensional numerical check extends to $N = 12$. Without using a zero table to generate the spectral truncation, one obtains

$$14.13472514173469379046, \quad 21.02203963877163321195, \quad 25.01085758158437040980,$$

$$30.42494005309699443594, \quad 32.93742416945363182010, \quad 37.72686071096628094559, \ldots$$

At 150-digit working precision, Cholesky tests of H_N and $\mathsf{H}_N^{(1)}$ pass for $1 \le N \le 12$; all $N = 12$ Gaussian quadrature weights are positive; and the maximum relative moment residual for $\mu_0, \ldots, \mu_{23}$ is approximately

$$5.20 \times 10^{-150}.$$

As an independent numerical stability check, the 24 source-generated moments were re-extracted using contour radii 6 and 10, with maximum relative difference approximately

$$1.19 \times 10^{-101}.$$

These finite-dimensional computations independently reproduce the numerical chain and are consistent with the all-order dual Gram positivity established in Section 5. The source of the universal positivity theorem is the two-depth identity-self-pairing theorem.

Thus there are two independent readout channels:

independent RH channel	independent HP channel
event/analytic closure	source-generated moments/spectral truncation
↓	↓
γ_k^{RH}	$\gamma_k^{\mathrm{HP}}(N)$

As N increases, the low-lying readouts of the finite HP spectral truncation lock onto the same terminal identities supplied by the independent RH channel:

$$\gamma_k^{\mathrm{HP}}(N) \to \gamma_k^{\mathrm{RH}}.$$

The comparison is performed only after both channels have independently completed their outputs. It is therefore **cross-witnessing between independent channels**, not part of the HP construction.

The principal significance of these computations is not numerical precision itself, but

> the same open multiplicative identity yields the same low-lying spectral addresses through two independent mathematical channels.

9. Gaussian Quadrature: Identity and Weight Readout of the Finite Spectral Truncation

The finite spectral measure is

$$\boxed{\nu_{\times,N} = \sum_{j=1}^{N} w_j^{(N)} \delta_{\beta_j^{(N)}}, \qquad w_j^{(N)} > 0.} \tag{9.1}$$

The finite resolvent response is

$$\boxed{F_N(y) = \sum_{j=1}^{N} \frac{w_j^{(N)}}{1 + y\beta_j^{(N)}}.} \tag{9.2}$$

It exactly reproduces

$$\boxed{\int \beta^r \, d\nu_{\times,N} = \mu_r, \qquad 0 \le r \le 2N - 1.} \tag{9.3}$$

Thus the finite spectral truncation outputs two types of data:

$$\boxed{\beta_j^{(N)} = \text{identity address}}$$

and

$$\boxed{w_j^{(N)} = \text{display weight.}}$$

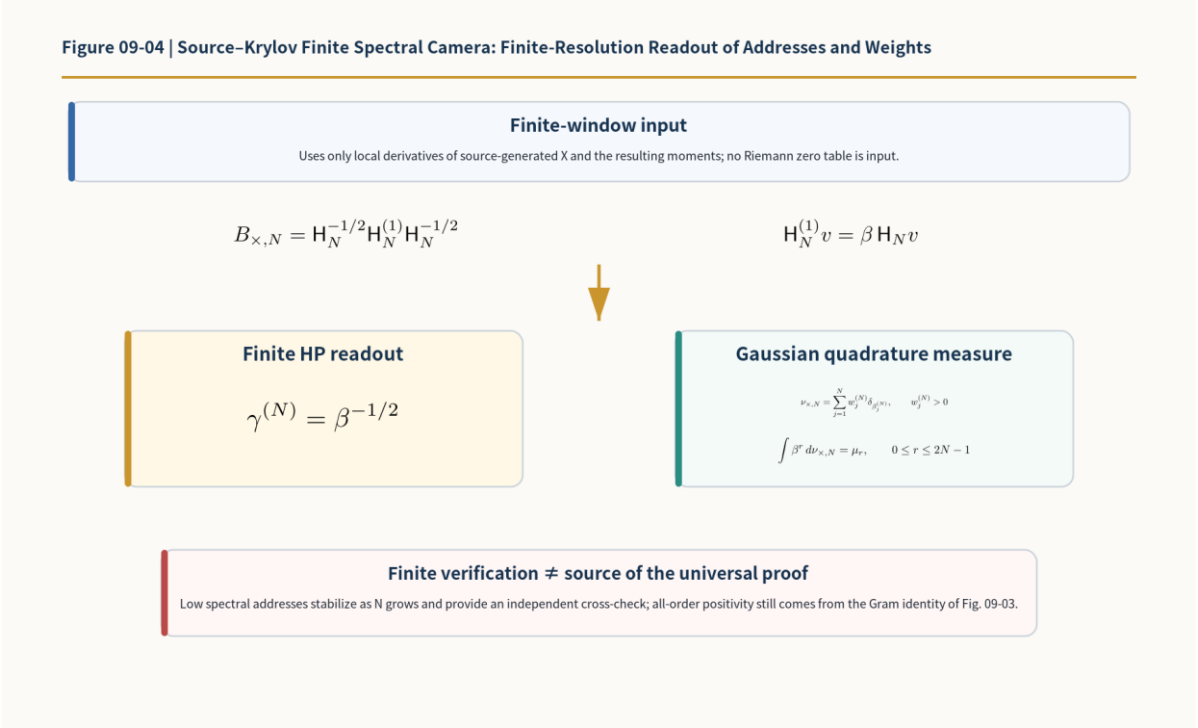


Figure 09-04. Source–Krylov finite spectral camera. The ordinary and shifted Gram tables form the positive compression $B_{\times,N}$ on a finite scan window. Its generalized eigenvalues $\beta_j^{(N)}$ give finite Hilbert–Pólya address readouts $\gamma_j^{(N)} = (\beta_j^{(N)})^{-1/2}$. Gaussian quadrature simultaneously produces positive weights $w_j^{(N)}$ and exactly reproduces the first $2N$ moments. The camera does not use a Riemann zero table as input; stabilization of low addresses as N grows is an independent cross-check, not the source of the universal positivity proof.

10. Dual Gram Positivity and Stieltjes Reconstruction

By Section 5, the two all-order Hankel positivity statements are already given simultaneously by

$$\mathcal{E}_\times(\Psi_i, \Psi_j) = \mu_{i+j}, \qquad \mathcal{E}_\times^{[1]}(\Psi_i^{[1]}, \Psi_j^{[1]}) = \mu_{i+j+1},$$

with both ordinary and shifted positivity arising from two Gram realizations of the same identity self-pairing. Hence

$$\mathcal{L}_\times(|p|^2) \ge 0,$$

$$\mathcal{L}_\times(\beta|p|^2) \ge 0.$$

By the Stieltjes moment theorem, there exists a positive measure $\nu_\times$ such that

$$\boxed{\mu_k = \int_0^\infty \beta^k \, d\nu_\times(\beta).} \tag{10.1}$$

Uniqueness follows from analyticity and the local germ. Since F is analytic in some disk about $y = 0$, let its Taylor radius of convergence be $R_0 > 0$. For every $0 < r < R_0$, Cauchy's estimates give a constant C_r such that

$$0 \le \mu_k \le C_r \, r^{-k}.$$

If $\nu_\times$ had positive mass beyond some $\beta_0 > r^{-1}$, then its kth moment would grow at least like β_0^k, contradicting the estimate above. Hence

$$\mathrm{supp}\nu_\times \subset [0, R_0^{-1}],$$

with the endpoint understood by taking $r \uparrow R_0$. Thus $\nu_\times$ is a compactly supported Stieltjes measure; the moment problem is determinate, so this positive measure is unique.

Define its Stieltjes response by

$$S_\times(y) = \int \frac{d\nu_\times(\beta)}{1 + y\beta}.$$

In the common analytic neighborhood of $y = 0$,

$$S_\times(y) = \sum_{k\geq 0} (-1)^k \mu_k y^k = F(y).$$

By analytic uniqueness, $S_\times$ and the source-defined F are global continuations of the same analytic germ.

Thus $\nu_\times$ is not a new generative mechanism. It is the unique positive spectral measure representing the same scan self-pairing as a multiplication operator.

11. The Global Hilbert Space

In the Stieltjes representation,

$$\boxed{\mathcal{H}_\times = L^2(\nu_\times).} \tag{11.1}$$

Define

$$\boxed{(B_\times f)(\beta) = \beta f(\beta).} \tag{11.2}$$

Then

$$\boxed{B_\times = B_\times^* \geq 0.} \tag{11.3}$$

Take the vector

$$\mathbf{1}(\beta) = 1.$$

Because $\nu_\times$ has compact support by Section 10, polynomials are dense in $C(\mathrm{supp}\nu_\times)$ by the Stone–Weierstrass theorem, while continuous functions are dense in $L^2(\nu_\times)$. Hence

$$\overline{\mathrm{span}\{\mathbf{1}, B_\times\mathbf{1}, B_\times^2\mathbf{1}, \dots\}} = L^2(\nu_\times).$$

Thus $\mathbf{1}$ is a cyclic vector for $B_\times$.

Moreover,

$$\boxed{\mu_n = \langle B_\times^n \mathbf{1}, \mathbf{1}\rangle.} \tag{11.4}$$

Therefore

$$\boxed{\mu_{i+j} = \langle B_\times^i \mathbf{1}, B_\times^j \mathbf{1}\rangle.} \tag{11.5}$$

At this point the Gram architecture appears automatically.

It is a conclusion, not a starting assumption.

12. Krylov Spaces: Standard Operator Form of the Finite Scan

Define

$$\boxed{\mathcal{K}_N = \mathrm{span}\{\mathbf{1}, B_\times \mathbf{1}, \dots, B_\times^{N-1}\mathbf{1}\}.} \tag{12.1}$$

Let P_N be the orthogonal projection onto $\mathcal{K}_N$.

Define the compression

$$\boxed{\hat{B}_N = P_N B_\times P_N|_{\mathcal{K}_N}.} \tag{12.2}$$

In the symmetrically orthogonalized monomial basis,

$$\hat{B}_N \sim \mathsf{H}_N^{-1/2}\mathsf{H}_N^{(1)}\mathsf{H}_N^{-1/2}.$$

Therefore

$$\boxed{B_{\times,N} \text{is not a fitted matrix; it is the canonical Krylov compression of the same} B_\times.}$$

13. Recovery of the Complete Infinite Spectrum from Finite Spectral Truncations

This section treats the second finite parameter: the spectral-resolution parameter N.

Unlike the horizon parameter r of Section 4, N measures the finite-dimensional scan resolution of the moment/Krylov spectrum. The complete source-side identity class and the global operator $B_\times$ are already defined by the same infinite object. The purpose of finite spectral truncation is not to manufacture a new finite model, but to read the complete object in progressively larger Krylov subspaces.

The two finite mechanisms are strictly distinguished:

	finite parameter	mathematical role
truncated horizon	r	exact identity equality for each r
spectral camera	N	recovery of the complete spectrum as $N \to \infty$

Thus

$$\boxed{r\text{-technology answers “is this still the same object?”;}}$$

while

$$\boxed{N\text{-technology answers “how does a finite scan read the complete infinite spectrum?”}}$$

By cyclicity from Section 11,

$$\boxed{\overline{\bigcup_{N\geq 1} \mathcal{K}_N} = L^2(\nu_\times).} \tag{13.1}$$

Hence the corresponding orthogonal projections satisfy

$$P_N \to I$$

strongly.

Section 14 proves that $\nu_\times$ is purely atomic and that its nonzero atoms can accumulate only at 0; therefore the multiplication operator $B_\times$ is a positive compact operator. For a compact operator and strongly convergent projections,

$$\| (I - P_N)B_\times \| \to 0, \qquad \| B_\times (I - P_N) \| \to 0.$$

Thus, viewing $P_N B_\times P_N$ as a finite-rank operator on the full Hilbert space,

$$\boxed{\| P_N B_\times P_N - B_\times \| \to 0.} \tag{13.2}$$

This is operator-norm recovery of the entire bounded infinite-dimensional operator $B_\times$, not merely recovery of a fixed low spectral window.

By the spectral approximation theorem for compact self-adjoint operators, order the **distinct nonzero atomic addresses** nonincreasingly; analytic multiplicities are recovered separately from the weights/residues in Section 16. Then for every fixed $k \in \mathbb{N}$,

$$\boxed{\beta_k^{(N)} \to \beta_k.} \tag{13.3}$$

The quantifier is

$$\boxed{\forall k \in \mathbb{N}.}$$

Thus every discrete spectral address is recovered. Set

$$\gamma_k = \beta_k^{-1/2}, \qquad \gamma_k^{(N)} = (\beta_k^{(N)})^{-1/2}.$$

Then for every k,

$$\boxed{\gamma_k^{(N)} \to \gamma_k.} \tag{13.4}$$

Hence the limit of finite spectral truncations recovers the entire infinite sequence

$$\boxed{\{\gamma_1, \gamma_2, \dots\}.}$$

The global Hilbert–Pólya operator is not defined as a bounded-operator norm limit. It is defined directly by spectral functional calculus of the complete $B_\times$:

$$\boxed{H_\times = B_\times^{-1/2}.} \tag{13.5}$$

Its full domain is

$$D(H_\times) = \left\{ f : \int \beta^{-1} |f(\beta)|^2 \, dv_\times(\beta) < \infty \right\}.$$

In the pure-point representation,

$$D(H_\times) = \left\{ (a_n) : \sum_n \gamma_n^2 \, |a_n|^2 < \infty \right\}.$$

Thus the "finite-to-global" endpoint of this chapter is a complete infinite-dimensional unbounded self-adjoint operator together with its entire infinite spectrum, not a fixed finite sector.

The global limit of the unbounded operators is expressed in a topology appropriate to spectral functional calculus. The operators $B_{\times,N}$ converge to $B_\times$ in operator norm at the bounded compact-operator level, while

$$H_{\times,N} = B_{\times,N}^{-1/2}$$

converges to the complete unbounded $H_\times$ on fixed spectral windows and in the corresponding resolvent/spectral-projection sense. For every fixed finite spectral projection P_K^{spec}, one can choose compatible spectral-subspace identifications U_N such that

$$\boxed{\| (U_N H_{\times,N} U_N^{-1} - H_\times) P_K^{\mathrm{spec}} \| \to 0.} \tag{13.6}$$

Equivalently, complete infinite-spectrum recovery is characterized by (13.3)–(13.6) for every k.

14. Meromorphicity and the Discrete Atomic Spectrum

By Section 10, the Stieltjes response

$$S_{\times}(y) = \int \frac{d\nu_{\times}(\beta)}{1 + y\beta}$$

agrees in a neighborhood of $y = 0$ with the source-defined function

$$F(y) = \frac{G'(y)}{G(y)},$$

and by analytic uniqueness they belong to the same global meromorphic function.

To read the structure of the spectral measure, set

$$y = -\frac{1}{z}.$$

Then

$$F(-1/z) = z\int \frac{d\nu_{\times}(\beta)}{z - \beta}.$$

Hence the Cauchy transform of $\nu_{\times}$ is

$$\boxed{C_{\nu_{\times}}(z) = \int \frac{d\nu_{\times}(\beta)}{z - \beta} = \frac{1}{z}F(-1/z).} \tag{14.1}$$

The right-hand side is meromorphic on $\mathbb{C}\backslash\{0\}$. By Stieltjes inversion for positive measures, equivalently Cauchy-transform inversion, any non-atomic continuous component would produce a non-discrete boundary jump on its support. But the finite-plane singularities of a meromorphic Cauchy transform can only be isolated poles. Therefore $\nu_{\times}$ has no continuous component, and its nonzero support consists of discrete atoms.

Thus

$$\boxed{\nu_{\times} = \nu_{\times}(\{0\})\delta_0 + \sum_n w_n\,\delta_{\beta_n}, \qquad w_n > 0, \quad \beta_n > 0.} \tag{14.2}$$

It remains to exclude an atom at 0. Along the positive real axis, $y \to +\infty$, Stirling asymptotics for the completed ξ-function give

$$F(y) = \frac{1}{2\sqrt{y}}\frac{X'(\sqrt{y})}{X(\sqrt{y})} \to 0.$$

On the other hand, for a compactly supported positive measure, dominated convergence gives

$$\lim_{y\to+\infty} \int \frac{d\nu_{\times}(\beta)}{1 + y\beta} = \nu_{\times}(\{0\}).$$

Therefore

$$\nu_{\times}(\{0\}) = 0.$$

Finally,

$$\boxed{\nu_\times = \sum_n w_n \, \delta_{\beta_n}, \qquad w_n > 0, \quad \beta_n > 0.} \tag{14.3}$$

Since the Cauchy transform on the right is meromorphic, any sequence of nonzero atoms has no accumulation point in $(0, \infty)$. Combined with compact support, the only possible accumulation point is 0. Thus $B_\times = M_\beta$ is a positive compact operator.

Correspondingly,

$$F(y) = \sum_n \frac{w_n}{1 + y\beta_n}.$$

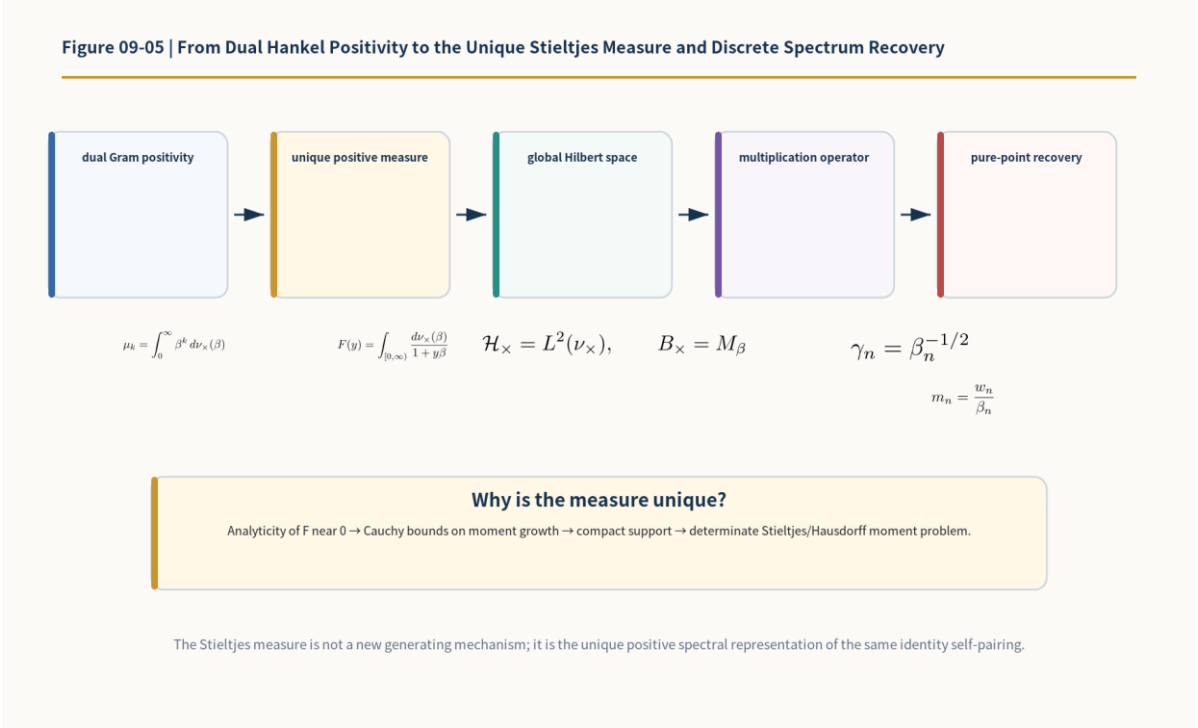


Figure 09-05. From dual Hankel positivity to the discrete spectrum. The two all-order Gram positivities trigger the Stieltjes moment theorem and produce a positive measure $\nu_\times$. Analyticity of F near 0 yields moment-growth bounds, forcing compact support and making the moment problem determinate. Thus $\nu_\times$ is unique, with $\mathcal{H}_\times = L^2(\nu_\times)$ and $B_\times = M_\beta$; the meromorphic structure of $F = G'/G$ then makes the measure purely atomic and separately recovers γ_n and m_n.

15. Recovery of the Zeros

Since

$$F = \frac{G'}{G}$$

and G is entire with $G(0) = 1$, if y_0 is a zero of G of multiplicity m, then locally

$$G(y) = (y - y_0)^m h(y), \qquad h(y_0) \neq 0,$$

and hence

$$F(y) = \frac{m}{y - y_0} + \frac{h'(y)}{h(y)}.$$

Conversely, because G has no poles, every finite pole of $F = G'/G$ comes from a zero of G. Therefore

$$\boxed{y_0 \in Z(G) \Leftrightarrow y_0 \in \mathrm{Pole}(F),}$$

and the residue of F at that point equals the zero multiplicity.

Section 14 proves that all finite poles of the Stieltjes representation lie on the negative real axis at

$$y = -\beta_n^{-1}.$$

Hence all zeros of G lie at these points.

The standard Riemann–von Mangoldt counting formula shows that the number of nontrivial zeros of ξ tends to infinity with height. Thus these spectral addresses form an infinite sequence. Accordingly,

$$\gamma_n \to \infty, \qquad \beta_n = \gamma_n^{-2} \to 0.$$

The pole locations are

$$y = -\beta_n^{-1}.$$

Define

$$\boxed{\gamma_n = \beta_n^{-1/2}.} \tag{15.1}$$

Then

$$y = -\gamma_n^2.$$

Since

$$y = z^2,$$

we obtain

$$\boxed{z = \pm i\gamma_n.} \tag{15.2}$$

Therefore

$$\boxed{\rho = \frac{1}{2} \pm i\gamma_n.} \tag{15.3}$$

Hence, from the two-family identity-self-pairing Gram positivity of Section 5, this generative-source-to-spectrum chain rigorously closes Hilbert–Pólya ⇒ RH.

16. Recovery of Analytic Multiplicities

If G has multiplicity m_n at

$$y = -\beta_n^{-1},$$

then

$$\mathrm{Res} F = m_n.$$

But

$$\mathrm{Res}_{y=-\beta_n^{-1}} \frac{w_n}{1 + y\beta_n} = \frac{w_n}{\beta_n}.$$

Therefore

$$\boxed{m_n = \frac{w_n}{\beta_n}.} \tag{16.1}$$

Equivalently,

$$\boxed{w_n = m_n \beta_n.} \tag{16.2}$$

Identity and multiplicity therefore separate automatically:

$$\boxed{\beta_n = \text{identity address},}$$

$$\boxed{m_n = \text{analytic display strength.}}$$

Define immediately the multiplicity display operator

$$\boxed{M_\times e_n = m_n e_n.} \tag{16.3}$$

From this point onward, the source-generated identity-level terminal is fixed as

$$\boxed{(H_\times, M_\times).} \tag{16.4}$$

Here $H_\times$ contains each distinct spectral identity once, while $M_\times$ independently preserves analytic multiplicity. The Stieltjes atomic weight is $m_n \beta_n$ and is not conflated with the dimension of a cyclic eigenspace.

17. The Global Hilbert–Pólya Operator

Define

$$\boxed{H_\times = B_\times^{-1/2}.} \tag{17.1}$$

In the discrete representation,

$$H_\times e_n = \gamma_n e_n.$$

Its domain is

$$D(H_\times) = \left\{ (a_n) : \sum_n \gamma_n^2 \, |a_n|^2 < \infty \right\}.$$

Therefore

$$\boxed{H_\times = H_\times^*.} \tag{17.2}$$

Moreover,

$$\boxed{\sigma(H_\times) = \{\gamma_n\}.} \tag{17.3}$$

Since

$$\gamma_n \to \infty,$$

$H_\times$ is an unbounded positive self-adjoint operator with purely discrete real spectrum.

Its self-adjointness is not preloaded. It arises from the standard spectral-theoretic realization of the generative-source-side identity self-pairing.

18. Divisor-Faithful Amplification

The identity-faithful pair is

$$H_\times e_n = \gamma_n e_n, \qquad M_\times e_n = m_n e_n, \qquad [H_\times, M_\times] = 0. \tag{18.1}$$

The cyclic representation of $H_\times$ gives one spectral address for each distinct atom; analytic multiplicity is displayed independently by $M_\times$.

Define multiplicity amplification

$$\boxed{\widetilde{H}_\times = \mathrm{Amp}_{M_\times}(H_\times) = \oplus_n \gamma_n I_{m_n}.} \tag{18.2}$$

Then

$$\boxed{\mathrm{dimker}(\widetilde{H}_\times - \gamma_n I) = m_n.} \tag{18.3}$$

This distinction freezes three different levels:

$$\boxed{\begin{array}{rcl} \text{event sheet number} & : & \text{number of sheets in a finite reciprocal lift,} \\ \text{support-address count} & : & \text{each distinct atomic address counted once,} \\ \text{analytic multiplicity} & : & m_n. \end{array}} \tag{18.4}$$

The Stieltjes atomic weight is

$$\nu_\times(\{\beta_n\}) = m_n \beta_n.$$

It encodes m_n, but the cyclic eigenspace of the scalar multiplication operator at one distinct atom remains one-dimensional. Only divisor-faithful amplification turns analytic multiplicity into eigenspace dimension.

Therefore

$$\boxed{\text{all zeros simple} \Leftrightarrow M_\times = I \Leftrightarrow \widetilde{H}_\times \simeq H_\times \text{at the multiplicity level.}} \tag{18.5}$$

This chapter does not assume simple zeros.

19. Fredholm Determinant

Because

$$\sum_n m_n \beta_n = \sum_n w_n = \nu_\times([0,\infty)) = \mu_0 = F(0) < \infty,$$

the amplified operator

$$\tilde{B}_\times$$

is positive trace class.

Hence

$$\det(I + y\tilde{B}_\times) = \prod_n (1 + y\beta_n)^{m_n}.$$

Its logarithmic derivative is

$$\frac{d}{dy}\mathrm{logdet}(I + y\tilde{B}_\times) = \sum_n \frac{m_n \beta_n}{1 + y\beta_n} = F(y).$$

Also,

$$G(0) = 1.$$

Thus the two sides have the same logarithmic derivative and the same normalized value in a neighborhood of $y = 0$, so they agree there. Since both sides are entire, the identity theorem gives global equality:

$$\boxed{G(y) = \det(I + y\tilde{B}_\times).} \tag{19.1}$$

Equivalently,

$$\boxed{\frac{X(z)}{X(0)} = \det(I + z^2\tilde{B}_\times).} \tag{19.2}$$

This closes the loop

generative source → identity → spectrum → determinant → generative source.

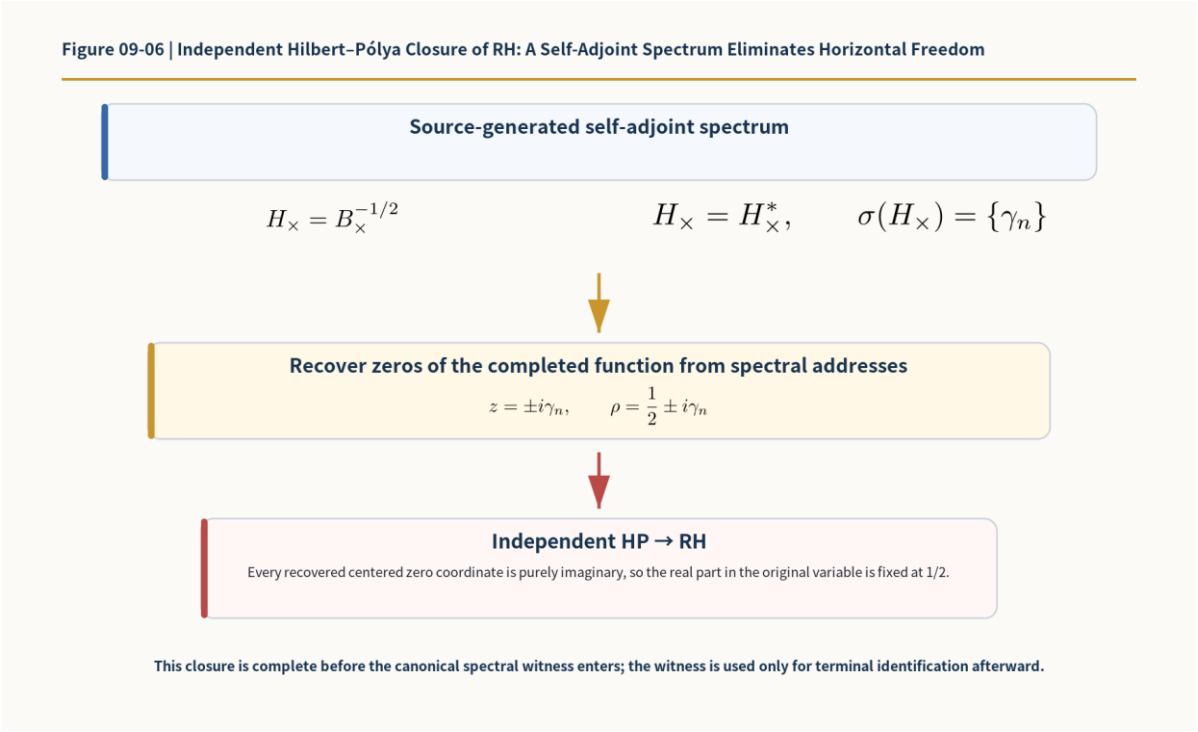


Figure 09-06. Independent Hilbert–Pólya closure of RH. Defining $H_\times = B_\times^{-1/2}$ from $B_\times = M_\beta$ gives a positive self-adjoint operator with pure discrete spectrum $\{\gamma_n\}$. Stieltjes pole recovery gives $z = \pm i\gamma_n$, hence $\rho = \frac{1}{2} \pm i\gamma_n$ in the original variable. RH is therefore closed by the source self-pairing–Stieltjes–self-adjoint spectral chain before the canonical spectral witness enters; the witness is used only for terminal identification afterward.

20. Canonical Spectral Witness: Identity-Level Identification and Divisor Amplification

The HP generative chain has already produced the source-side cyclic response

$$F_\times(y) = \langle (I + yB_\times)^{-1}\mathbf{1}, \mathbf{1}\rangle,$$

and the same completed generative source gives

$$F_\times = F_{\mathrm{R}} = \frac{d}{dy}\log\frac{X(\sqrt{y})}{X(0)}. \tag{20.1}$$

The uniqueness theorem for the canonical Riemann spectral witness therefore directly gives the pointed unitary equivalence

$$\boxed{(B_\times, \mathbf{1}) \simeq (B_{\mathrm{R}}, \mathbf{1}).} \tag{20.2}$$

By Borel functional calculus,

$$H_\times = B_\times^{-1/2} \simeq B_{\mathrm{R}}^{-1/2} = H_{\mathrm{id}}. \tag{20.3}$$

At the same time, the atomic weights uniquely recover the analytic multiplicities, so

$$\boxed{(H_\times, M_\times) \simeq (H_{\mathrm{id}}, M_{\mathrm{mult}}).} \tag{20.4}$$

This is identity-faithful terminal identification. It does not conflate the cyclic identity-level realization with the divisor-faithful operator.

Now apply multiplicity amplification:

$$\boxed{\widetilde{H}_\times = \mathrm{Amp}_{M_\times}(H_\times) \simeq \mathrm{Amp}_{M_{\mathrm{mult}}}(H_{\mathrm{id}}) = H_{\mathrm{Ren}}.} \tag{20.5}$$

Here

$$\boxed{H_{\mathrm{Ren}} := K_{\mathrm{Ren}}|_{\mathrm{RH}}} \tag{20.6}$$

is the **canonical Riemann spectral operator (Ren–Riemann operator) after RH**; K_{Ren} is the pre-RH full-coordinate Yifei Ren operator, or full-coordinate Ren operator. This chapter does not use K_{Ren} to generate the HP spectrum.

The terminal structure must therefore be written at two levels:

$$\boxed{(H_\times, M_\times) \simeq (H_{\mathrm{id}}, M_{\mathrm{mult}})}$$

and

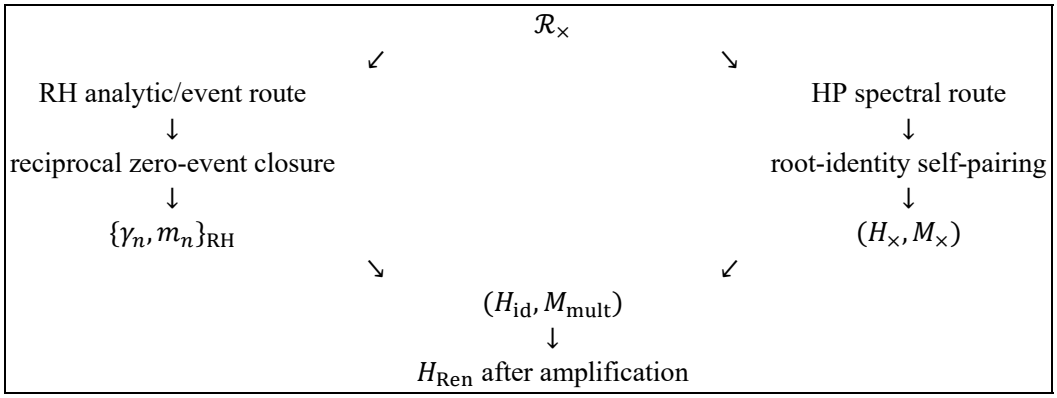
$$\boxed{\widetilde{H}_\times \simeq H_{\mathrm{Ren}}.}$$

Writing simply $H_\times \simeq H_{\mathrm{Ren}}$ would collapse the distinct-identity and divisor-multiplicity levels into a single object; this chapter does not use that abbreviation.

The sole role of the canonical spectral witness in this chapter is **terminal identification**. Generative-source self-pairing, Stieltjes reconstruction, self-adjoint spectral generation, and RH closure have all been completed before the witness enters.

21. Terminal Identification between the Source-Generated Spectrum and the Canonical Riemann Spectrum

The two routes begin from the same open multiplicative identity but use different mature mathematical languages:



(21.1)

The HP route does not borrow the zero list from the RH side in order to construct $H_\times$. Terminal identification uses the scalar complete witness:

$$F_\times = F_{\mathrm{R}} \Rightarrow (H_\times, M_\times) \simeq (H_{\mathrm{id}}, M_{\mathrm{mult}}).$$

Thus

$$\boxed{\text{independent generation} \quad + \quad \text{unique terminal identification}} \tag{21.2}$$

hold simultaneously.

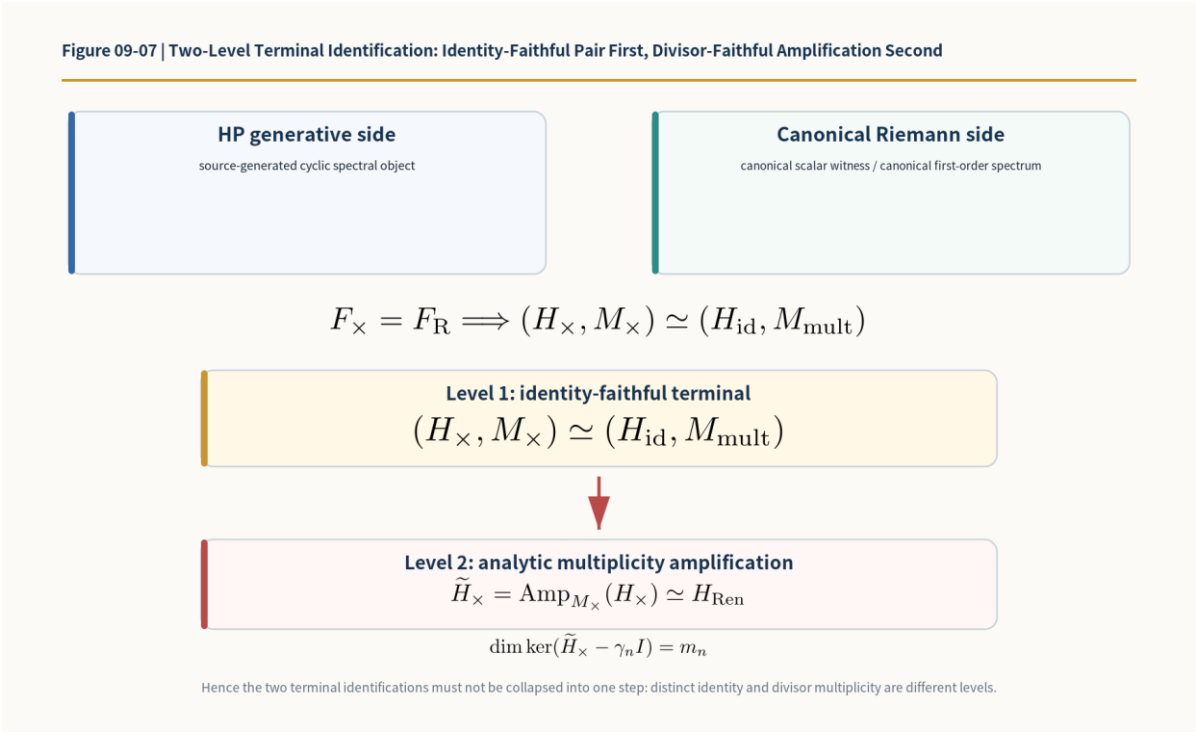


Figure 09-07. Two-level terminal identification. The complete scalar witness first identifies the source-generated pair with the canonical Riemann identity layer as $(H_\times, M_\times) \simeq (H_{id}, M_{mult})$. Only afterward is multiplicity amplification performed with the same analytic multiplicity data, giving $\widetilde{H}_\times \simeq H_{Ren}$ and eigenspace dimension m_n. The two levels must therefore not be collapsed into the incorrect shorthand $H_\times \simeq H_{Ren}$.

22. Main Proof Chain: Independent Hilbert–Pólya ⇒ RH

The generative direction of the HP route comes entirely from the open multiplicative generative source, completion, the identity quotient, and generative-source-side self-relations. The RH event closure, zero list, K_{Ren}, H_{Ren}, and the canonical Riemann spectral witness do not enter this generative direction.

Sections 4–5 rigorously give two self-pairings of the same identity:

$$\boxed{\mathcal{E}_\times^{[r]}(\Psi_i^{[r]}, \Psi_j^{[r]}) = \mu_{i+j+r}, \qquad r = 0,1,} \tag{22.1}$$

and hence

$$\boxed{\mathsf{H}_N \succcurlyeq 0, \qquad \mathsf{H}_N^{(1)} \succcurlyeq 0 \qquad \forall N.} \tag{22.2}$$

The Stieltjes moment theorem therefore directly yields a unique positive measure

$$F(y) = \int \frac{d\nu_\times(\beta)}{1 + y\beta}, \qquad \nu_\times \geq 0. \tag{22.3}$$

Then the meromorphicity of $F = G'/G$, pure-point recovery, and

$$B_\times = M_\beta, \qquad H_\times = B_\times^{-1/2}$$

give rigorously

$$H_\times = H_\times^*, \qquad z = \pm i\gamma_n, \qquad \rho = \frac{1}{2} \pm i\gamma_n. \tag{22.4}$$

Hence

$$\boxed{\text{RH.}} \tag{22.5}$$

The current main chain is

$$\boxed{\begin{array}{c} \mathcal{R}_\times \\ \Downarrow \\ [\Omega]_{\mathrm{id}} \\ \Downarrow \\ X \to F \to \mathcal{L}_\times \\ \Downarrow \\ \text{same-identity self-pairing at} r = 0{,}1 \\ \Downarrow \\ \mathsf{H}_N \succcurlyeq 0, \quad \mathsf{H}_N^{(1)} \succcurlyeq 0 \quad \forall N \\ \Downarrow \\ \nu_\times \geq 0 \to H_\times = H_\times^* \to z = \pm i\gamma \to \boxed{\text{RH}}. \end{array}} \tag{22.6}$$

The canonical spectral witness is strictly downstream:

$$(H_\times, M_\times) \simeq (H_{\mathrm{id}}, M_{\mathrm{mult}}) \to \widetilde{H}_\times \simeq H_{\mathrm{Ren}}. \tag{22.7}$$

It performs terminal identification only; it does not participate in the source-generated HP⇒RH construction or proof.

23. Structural Compression after Identity Preservation

The identity consistency across representational layers was closed uniformly in Section 4; Section 5 then treats the standard analytic positivity. Its central fact is

$$\boxed{\text{root multiplicative identity self-pairing} \equiv \text{moment scan pairing.}} \tag{23.1}$$

The moving horizon has already been handled by the identity quotient:

$$[\Psi_r] = [\Omega]_{\mathrm{id}}.$$

Completion fidelity gives

$$X_r = X, \qquad G_r = G, \qquad F_r = F.$$

The moments are uniquely determined by the same F:

$$\mu_k = \frac{(-1)^k}{k!} F^{(k)}(0).$$

Scan composition gives

$$T_\times^i T_\times^j = T_\times^{i+j}.$$

Coordinate fidelity of generative-source self-pairing gives

$$\mathcal{E}_\times(\Psi_i, \Psi_j) = \mu_{i+j}, \qquad \mathcal{E}_\times^{[1]}(\Psi_i^{[1]}, \Psi_j^{[1]}) = \mu_{i+j+1}.$$

Thus positivity of the ordinary and shifted Hankel matrices is in both cases a standard Gram consequence of the same identity self-pairing. They differ only by the relational-depth label $r = 0{,}1$, not in identity or generative source, and no additional proof object of the form “one-step scan is itself

positive" is needed. Finite-dimensional numerical truncations verify only finite sections of these universal theorems.

This also explains why the finite matrices are principal blocks, why each anti-diagonal is labeled by the same moment, and why increasing N only enlarges the visible coordinate window:

$$\boxed{\text{the visible range changes; the identity does not.}} \tag{23.2}$$

24. Interface with the Second-Order Spectral Relations of Chapter 8

This chapter needs only one second-order interface.

Terminal witnessing has already given

$$\boxed{(H_\times, M_\times) \simeq (H_{\mathrm{id}}, M_{\mathrm{mult}}).} \tag{24.1}$$

Let U implement this unitary equivalence:

$$UH_\times U^{-1} = H_{\mathrm{id}}, \qquad UM_\times U^{-1} = M_{\mathrm{mult}}.$$

Then for every window ϕ for which the relevant operators are trace class and every $u \in \mathbb{R}$, unitary invariance gives

$$\mathrm{Tr}\big[M_\times \phi(H_\times) e^{iuH_\times}\big] = \mathrm{Tr}\big[M_{\mathrm{mult}} \phi(H_{\mathrm{id}}) e^{iuH_{\mathrm{id}}}\big]. \tag{24.2}$$

Therefore

$$\boxed{(H_\times, M_\times) \simeq (H_{\mathrm{id}}, M_{\mathrm{mult}}) \Rightarrow \mathcal{P}_2(H_\times, M_\times) = \mathcal{P}_2(H_{\mathrm{id}}, M_{\mathrm{mult}}),} \tag{24.3}$$

where $\mathcal{P}_2$ denotes the complete family of unitary-invariant second-order observables formed by functional calculus, trace, signed doubling, and the Fourier–Plancherel construction.

Chapter 8 distinguishes three levels of second-order structure:

$G0$:	second-order witness inheritance: exact consequence of first-order unitary equivalence,
$G1$:	finite-scale renormalization handshake: downstream structure of Chapter 8,
$G2$:	classical infinite-GUE asymptotic: stronger asymptotic specialization.

(24.4)

Thus the second-order theory lies downstream of the Hilbert–Pólya ⇒ RH closure of this chapter. First-order unitary equivalence already suffices to transfer all unitary-invariant two-point observables to Chapter 8.

25. Theorem Dependencies and Object Levels

Module	Mathematical content
IP0	Unified Single-Identity Closure Package
IP1	Moving-horizon identity preservation: $[\Psi_r] = [\Omega]_{\mathrm{id}}$
IP2	Completion identity fidelity: $X_r = X,\ G_r = G,\ F_r = F$
IP3	Provenance of moments and scan functional: $\mathcal{L}_\times(\beta^n) = \mu_n$
IP4	Multiple scan manifestations: $\Psi_n = T_\times^n \Psi_0$
IP5	Total-depth law: $(i,j) \mapsto i+j$, shifted $i+j+1$
IP6	Ordinary/shifted Hankel matrices as two coordinate tables of the same identity relation
IP7	Finite scan windows as restrictions of the same identity
G0	Ordinary identity self-pairing and Gram positivity
G1	Shifted identity self-pairing and Gram positivity

Module	Mathematical content
G2	All-order ordinary Hankel positivity
G3	All-order shifted Hankel positivity
P2	Unique finite positive Stieltjes measure
P3	Meromorphic Cauchy transform ⇒ pure-point measure
P4	Support ⇒ γ_n
P5	Atomic weights/residues ⇒ m_n
P6	$H_\times = B_\times^{-1/2}$ self-adjoint
P7	Zero recovery ⇒ RH
M0	$M_\times e_n = m_n e_n$
M1	Divisor-faithful amplification $\widetilde{H}_\times$
K0	Finite Source–Krylov truncation and generalized-eigenvalue readout; $N \le 12$ gives numerical checks
K1	Finite-truncation convergence for the compact operator $B_\times$
K2	Recovery of eigenvalues with fixed index
R0	Canonical-witness identification $(H_\times, M_\times) \simeq (H_{\mathrm{id}}, M_{\mathrm{mult}})$
R1	$\widetilde{H}_\times \simeq H_{\mathrm{Ren}}$
Q0	Second-order witness inheritance
Q1	Inheritance of the finite-scale renormalization handshake from Chapter 8
Q2	Classical infinite-GUE asymptotic specialization

IP0–IP7 and G0–G3 jointly express the self-pairing structure of the same root multiplicative identity across different representations and at two relational depths. Finite-dimensional numerical checks test only the corresponding finite sections; all-order positivity is supplied by the Gram identities of Section 5.

26. Generative Independence and Terminal Identification

The generative direction of this chapter is fixed as

$$\boxed{\mathcal{R}_\times \to X \to F \to \mathcal{L}_\times \to (\mathcal{E}_\times, T_\times) \to \nu_\times \to B_\times \to (H_\times, M_\times).} \tag{26.1}$$

This order gives four non-circularity constraints.

First, the generative-source-side identity class precedes every spectral coordinate:

$$\Psi_{r+1} - \Psi_r \in \ker S, \qquad [\Psi_r] = [\Omega]_{\mathrm{id}}.$$

Second, the moments come from

$$F(y) = \frac{G'(y)}{G(y)},$$

already fixed by completion of the generative source, rather than being read from a zero list:

$$\mu_k = \frac{(-1)^k}{k!} F^{(k)}(0).$$

Third, generative-source-side identity self-pairing precedes the Hankel tables, and the ordinary and shifted families arise simultaneously from the same intrinsic Hilbert self-pairing of the generative source:

$$\mathcal{E}_\times^{[r]}(\Psi_i^{[r]}, \Psi_j^{[r]}) = \mu_{i+j+r}, \qquad r = 0,1.$$

Thus positivity of both families comes from the upstream self-pairing, rather than defining an inner product backward from the Hankel matrices; nor is there a separate "one-step scan operator" whose positivity must be proved independently.

Fourth, the finite spectral truncation uses only X and its derivatives:

$$X(0), X''(0), X^{(4)}(0), \ldots$$

and

$$\boxed{\{\gamma_n\}, \quad K_{\mathrm{Ren}}, \quad H_{\mathrm{Ren}} \text{do not enter the spectral-truncation construction.}} \tag{26.2}$$

Finally, the canonical spectral witness lies downstream of the generative chain:

$$(H_\times, M_\times) \overset{\text{witness}}{\simeq} (H_{\mathrm{id}}, M_{\mathrm{mult}}) \to \widetilde{H}_\times \simeq H_{\mathrm{Ren}}. \tag{26.3}$$

Thus the canonical Riemann spectral witness performs terminal identification, while second-order witness inheritance from Chapter 8 transfers downstream second-order structure.

27. Main Theorem System

Theorem A | Unified Single-Identity Closure Package

The moving-horizon representation, identity quotient, completion, $X/G/F$, moment functional, multiple scan manifestations, ordinary/shifted relational coordinates, and finite scan windows of the open multiplicative relation $\mathcal{R}_\times$ all arise from the same root multiplicative identity $\mathfrak{I}_\times$ and remain consistent through the generative-source-side identity class $\mathfrak{C}_\times$. In particular,

$$\boxed{[\Psi_r] = [\Omega]_{\mathrm{id}}, \quad X_r = X, \quad G_r = G, \quad F_r = F,}$$

$$\boxed{\mathcal{L}_\times(\beta^n) = \mu_n, \qquad T_\times^i T_\times^j = T_\times^{i+j},}$$

and

$$\boxed{\mathsf{H}_N = [\mu_{i+j}], \qquad \mathsf{H}_N^{(1)} = [\mu_{i+j+1}].}$$

This theorem closes all identity-matching conditions of the chapter in one step.

Theorem B | Two-Depth Identity Self-Pairing and Gram Positivity

Let $\Psi_i^{[r]}$ be the ith scan manifestation of the same generative-source-side identity class at relational depth $r = 0,1$. Then

$$\boxed{\mathcal{E}_\times^{[r]}(\Psi_i^{[r]}, \Psi_j^{[r]}) = \mathcal{L}_\times(\beta^{i+j+r}) = \mu_{i+j+r}, \qquad r = 0,1.}$$

Therefore

$$\boxed{\sum_{i,j} \bar{c}_i \, c_j \mu_{i+j+r} = \left\| \sum_i c_i \, \Psi_i^{[r]} \right\|^2 \geq 0, \qquad r = 0,1,}$$

and hence

$$\boxed{\mathsf{H}_N \succcurlyeq 0, \qquad \mathsf{H}_N^{(1)} \succcurlyeq 0 \quad \forall N.}$$

Theorem C | Global Stieltjes Reconstruction

By the two Hankel positivities of Theorem B, there exists a unique finite positive measure $\nu_\times$ such that

$$\boxed{F(y) = \int_{[0,\infty)} \frac{d\nu_\times(\beta)}{1+y\beta}.}$$

Theorem D | Recovery of the Discrete Riemann Spectrum

By meromorphicity of $F = G'/G$, $\nu_\times$ is pure point. Its support and atomic weights recover γ_n and the analytic multiplicities m_n, respectively, and give

$$z = \pm i\gamma_n.$$

Theorem E | Source-Generated Hilbert–Pólya Operator

Define

$$B_\times = M_\beta, \qquad H_\times = B_\times^{-1/2}.$$

Then

$$\boxed{H_\times = H_\times^*, \qquad \sigma(H_\times) = \{\gamma_n\}.}$$

Theorem F | Independent Hilbert–Pólya Closure of RH

Theorems D–E give

$$\boxed{\rho = \frac{1}{2} \pm i\gamma_n,}$$

and hence RH holds.

Theorem G | Canonical Riemann Spectral-Witness Identification

After the above terminal has formed, scalar completeness of the witness gives

$$\boxed{(H_\times, M_\times) \simeq (H_{\mathrm{id}}, M_{\mathrm{mult}}).}$$

Theorem H | Divisor-Faithful Ren–Riemann Identification

Define

$$\widetilde{H}_\times = \mathrm{Amp}_{M_\times}(H_\times).$$

Then

$$\boxed{\widetilde{H}_\times \simeq H_{\mathrm{Ren}}.}$$

Corollary I | Second-Order Witness Inheritance

$$\boxed{(H_\times, M_\times) \simeq (H_{\mathrm{id}}, M_{\mathrm{mult}}) \Rightarrow \mathcal{P}_2(H_\times, M_\times) = \mathcal{P}_2(H_{\mathrm{id}}, M_{\mathrm{mult}}).}$$

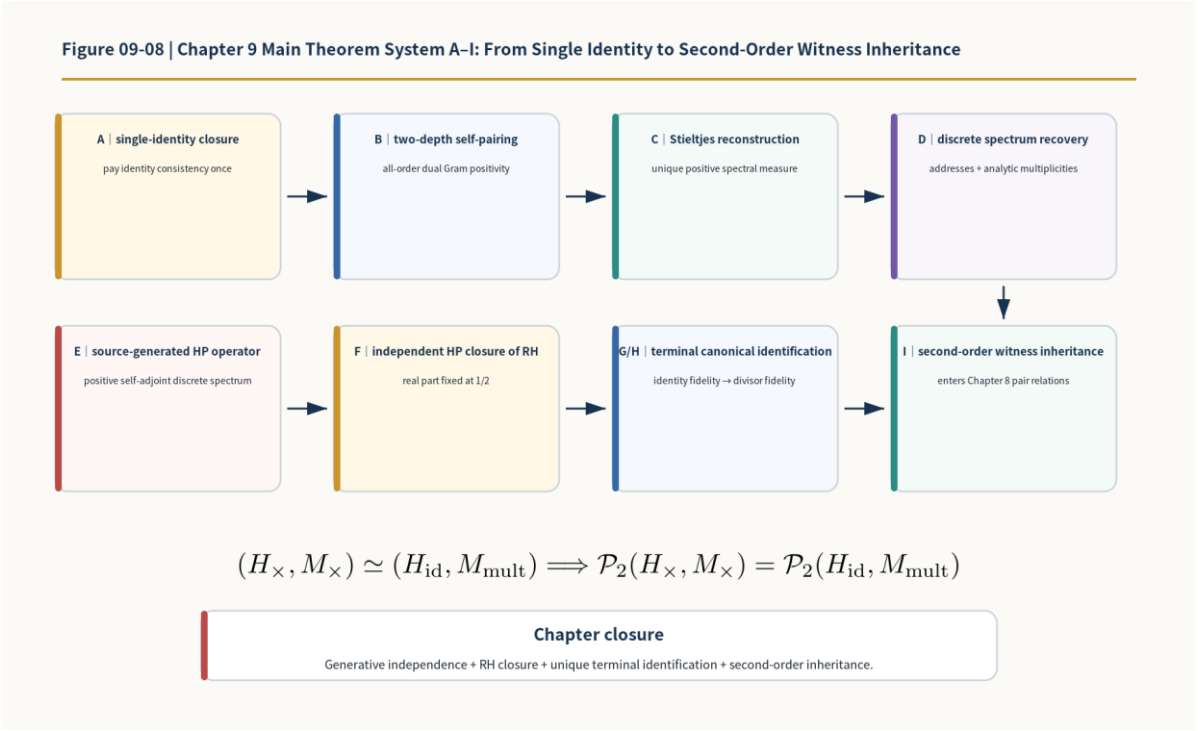


Figure 09-08. Main theorem system of Chapter 9. A fixes the single-identity closure package; B supplies two-depth self-pairing and all-order dual Gram positivity; C–D complete the Stieltjes and discrete-spectrum recovery; E generates the positive self-adjoint Hilbert–Pólya operator; F independently closes RH; G/H perform terminal identity-faithful and divisor-faithful identification; and I transfers the identified first-order spectral object into the second-order self-relations of Chapter 8. The full chain preserves both generative independence and unique terminal identifiability.

28. Closure Structure of the Independent Hilbert–Pólya Route

The source-generated HP route of this chapter closes at four levels.

First level: identity closure

$$\mathcal{R}_\times \to [\Omega]_{\mathrm{id}} \to X \to F \to \mathcal{L}_\times.$$

Second level: self-pairing of the same identity

$$\boxed{\mathcal{E}_\times^{[r]}(\Psi_i^{[r]}, \Psi_j^{[r]}) = \mu_{i+j+r}, \qquad r = 0,1.} \tag{28.1}$$

Hence

$$\boxed{\mathsf{H}_N \succcurlyeq 0, \qquad \mathsf{H}_N^{(1)} \succcurlyeq 0 \quad \forall N.} \tag{28.2}$$

Third level: Stieltjes/spectral reconstruction

$$\boxed{(\mathsf{H}_N, \mathsf{H}_N^{(1)})_{N\geq 1} \to \nu_\times \to (H_\times, M_\times).} \tag{28.3}$$

Fourth level: zero recovery/RH

$$\boxed{(H_\times, M_\times) \to z = \pm i\gamma \to \rho = \frac{1}{2} \pm i\gamma \to \mathrm{RH}.} \tag{28.4}$$

Finite-dimensional numerical checks can independently recompute the source-generated moments, ordinary/shifted positivity for $N \leq 12$, Gaussian quadrature, resolvent responses, and locking of the low-lying spectrum. The proof of all-order positivity comes from the two-depth identity-self-pairing theorem of Section 5, not from extrapolation of finite numerics.

The canonical spectral witness enters only after the Hilbert–Pólya terminal has formed:

$$(H_\times, M_\times) \simeq (H_{\mathrm{id}}, M_{\mathrm{mult}}), \qquad \widetilde{H}_\times \simeq H_{\mathrm{Ren}}. \tag{28.5}$$

It answers "what is the terminal?" and does not participate in the intrinsic generation from the source.

29. Conclusion: Source-Generated Spectral Closure of the Root Multiplicative Identity

The core structure of the chapter is the **Unified Single-Identity Closure Package**: the moving horizon, completion, scanning, moments, ordinary/shifted Hankel tables, and finite windows are unified through the identity quotient and multiple-scan composition law into the complete generative-source-side identity class $\mathfrak{C}_\times$.

The chapter begins from the unique open multiplicative relation

$$\boxed{\mathcal{R}_\times = \{(m,q,n): mq = n\}.}$$

No second arithmetic source is subsequently introduced, and neither a list of Riemann zeros nor a canonical spectral object replaces the generative source.

The moving horizon changes only the head/tail role presentation:

$$[\Psi_r] = [\Omega]_{\mathrm{id}}.$$

Completion, passage to the squared variable, logarithmic response, and moments all belong to the same identity class:

$$X_r = X, \qquad G_r = G, \qquad F_r = F.$$

Scanning produces only multiple manifestations of the same identity:

$$\Psi_n = T_\times^n \Psi_0.$$

The relation between two scan manifestations is controlled by total scan depth:

$$T_\times^i T_\times^j = T_\times^{i+j}.$$

Therefore

$$\mathcal{E}_\times(\Psi_i, \Psi_j) = \mu_{i+j}$$

is not a Hankel form selected afterward by hand, but a coordinate trace of this identity-composition law.

29.1 Two Kinds of Finite Parameters

The horizon parameter r answers

$$\boxed{\text{whether a finite presentation is still the same complete identity.}}$$

The conclusion holds exactly for every r; no $r \to \infty$ is required.

The spectral-resolution parameter N answers

$$\boxed{\text{when a finite spectral truncation resolves the same complete infinite spectrum.}}$$

Therefore

$$\boxed{r\text{resolves identity equality;} \qquad N\text{resolves spectral resolution.}} \tag{29.1}$$

29.2 Independent Hilbert–Pólya Closure

Root-identity self-pairing gives simultaneously, at two relational depths,

$$\mathcal{E}_{\times}^{[r]}(\Psi_i^{[r]}, \Psi_j^{[r]}) = \mu_{i+j+r}, \qquad r = 0,1.$$

Therefore

$$\boxed{\mathsf{H}_N \succcurlyeq 0, \qquad \mathsf{H}_N^{(1)} \succcurlyeq 0 \quad \forall N.} \tag{29.2}$$

Stieltjes reconstruction yields a positive spectral measure. Pure-point recovery, $B_{\times} \geq 0$, $H_{\times} = B_{\times}^{-1/2} = H_{\times}^{*}$, and

$$\rho = \frac{1}{2} \pm i\gamma_n$$

then follow rigorously. Hence the chapter obtains

$$\boxed{\text{RH.}} \tag{29.3}$$

Finite numerical checks of shifted positivity verify consistency of finite sections with the universal conclusion.

29.3 Self-Adjoint Spectrum and the Horizontal Degree of Freedom

In the centered coordinate

$$z = d + i\gamma,$$

the analytic RH route proves $d = 0$ directly. The HP route instead uses reality of a positive self-adjoint spectral parameter to force support of the squared spectral variable onto

$$\beta > 0,$$

so that

$$z^2 = -\beta^{-1} < 0, \qquad z = \pm i\beta^{-1/2}.$$

The two routes use different languages but close the same horizontal degree of freedom.

29.4 Local Moment Data and the Global Analytic Response

The HP route does not reconstruct the entire-function continuation of ξ a second time. The completed generative source already places

$$X(z) = \xi(1/2 + z)$$

globally in the construction. The finite spectral truncation reads the Taylor germ of F at $y = 0$:

$$F(y) = \sum_{k\geq 0} (-1)^k \mu_k y^k.$$

Stieltjes reconstruction realizes this local all-order germ as a positive spectral measure; analytic uniqueness then identifies its Stieltjes response with the complete

$$F(y) = \frac{G'(y)}{G(y)}.$$

Thus

$$\boxed{\text{local moment germ} \rightarrow \text{Stieltjes representation} \rightarrow \text{global meromorphic response.}} \tag{29.4}$$

This chain re-identifies local all-order moment data with the global meromorphic response.

29.5 Identity-Faithful and Divisor-Faithful Terminals

The source-generated cyclic terminal is

$$(H_\times, M_\times),$$

with

$$H_\times e_n = \gamma_n e_n, \qquad M_\times e_n = m_n e_n.$$

The canonical Riemann spectral witness gives

$$\boxed{(H_\times, M_\times) \simeq (H_{\mathrm{id}}, M_{\mathrm{mult}}).} \tag{29.5}$$

The divisor-faithful amplification is

$$\widetilde{H}_\times = \oplus_n \gamma_n I_{m_n},$$

and

$$\boxed{\widetilde{H}_\times \simeq H_{\mathrm{Ren}}.} \tag{29.6}$$

This keeps four levels separate: identity address, analytic multiplicity, cyclic representation, and divisor eigenspace dimension.

29.6 Inheritance of Second-Order Self-Relations

Once the first-order spectral identity has been identified by the terminal witness, all unitary-invariant second-order observables agree automatically:

$$\boxed{(H_\times, M_\times) \simeq (H_{\mathrm{id}}, M_{\mathrm{mult}}) \Rightarrow \mathcal{P}_2(H_\times, M_\times) = \mathcal{P}_2(H_{\mathrm{id}}, M_{\mathrm{mult}}).} \tag{29.7}$$

Thus the first-order source-generated HP terminal naturally enters the existing second-order spectral theory; this chapter need not repeat the technical GUE/CUE development.

29.7 Final Closure of the Chapter

The strict logic of the chapter is

open multiplicative identity
⇓
lossless identity quotient
⇓
multiple scans of the same identity
⇓
same-identity self-pairing at $r = 0{,}1$
⇓
$\mathsf{H}_N \succcurlyeq 0, \quad \mathsf{H}_N^{(1)} \succcurlyeq 0 \quad \forall N$
⇓
Stieltjes reconstruction + source-generated self-adjoint Hilbert–Pólya spectrum
⇓
RH
⇓
canonical spectral witness / second-order inheritance.

(29.8)

The final identity re-audit carries the Unified Single-Identity Closure Package through to the end: **ordinary and shifted are not two objects, one already closed and the other still requiring a separate positivity proof. They are two families of Gram coordinates formed when the same identity meets itself at two relational depths.** The formerly isolated shifted-positivity condition is therefore withdrawn as an independent condition; it is simply the quadratic-form expression of the $r = 1$ Gram identity.

there is only one underlying identity; scanning enlarges only its manifestation; ordinary and shifted are two coordinate tables of the self-relation of that same identity.

(29.9)

Appendix A | Core Notation and Object Levels

Symbol	Meaning
$\mathcal{R}_\times$	Open multiplicative relation $\{(m,q,n): mq = n\}$
$L_\times$	Total multiplicative log-scale $\log(mq)$
R	Relative factor-role coordinate $\log(q/m)$
$\kappa_z(L_\times, R)$	Generative-source role kernel $e^{-L_\times/2} e^{zR}$
Ω	Complete generative-source representation
$\Omega_r^{\mathrm{H}}, \Omega_r^{\mathrm{T}}$	Head/tail representations of the moving horizon
$S(h,t) = h + t$	Complete identity sum map
$\mathcal{N}_{\mathrm{role}}$	Role-null directions
$\mathcal{Q}_{\mathrm{id}}$	Identity quotient
$\mathfrak{I}_\times = (\mathbb{N}_{>0}, \mu)$	Unique root multiplicative identity of the book
$\mathfrak{C}_\times = [\Omega]_{\mathrm{id}}$	Complete generative-source-side identity class of the root multiplicative identity
$X(z)$	Centered completed generative-source function
$G(y)$	Normalized entire function in the squared variable
$F(y)$	Logarithmic-derivative response
μ_k	Generative-source scan-moment fingerprint
$\mathcal{L}_\times$	Moment/scan functional
$\mathcal{E}_\times$	Root-identity self-pairing
$A_\times$	Generative-source scan-analysis map

Symbol	Meaning
$T_\times$	Scan-composition notation for the same identity; carries scan indexing and composition only, not an independent positivity condition
H_N	Ordinary Hankel finite relation table
$\mathsf{H}_N^{(1)}$	Shifted Hankel coordinate table at relation depth $+1$
$B_{\times,N}$	Finite Source–Krylov spectral truncation
$\nu_\times$	Global finite positive Stieltjes spectral measure
$B_\times = M_\beta$	Bounded positive identity-level spectral operator
$H_\times = B_\times^{-1/2}$	Source-generated identity-faithful Hilbert–Pólya operator
$M_\times$	Source-generated analytic multiplicity operator
$\widetilde{H}_\times$	Divisor-faithful amplification
K_{Ren}	Pre-RH full-coordinate Ren operator / Yifei Ren operator
$H_{\mathrm{Ren}} = K_{\mathrm{Ren}}\vert_{\mathrm{RH}}$	Canonical Riemann spectral operator after RH
$H_{\mathrm{id}}, M_{\mathrm{mult}}$	Canonical identity-faithful Riemann spectral pair

Appendix B | Generative Independence and Object Boundaries

The source-generated main chain of this chapter is

$$\boxed{\mathcal{R}_\times \to X \to F \to \mathcal{L}_\times \to \text{same-identity self-pairing at} r = 0{,}1 \to \begin{cases} \mathsf{H}_N \succcurlyeq 0, \\ \mathsf{H}_N^{(1)} \succcurlyeq 0, \end{cases} \quad \forall N \to \nu_\times \geq 0 \to (H_\times, M_\times) \to \mathrm{RH}.} \tag{B.1}$$

The shifted quadratic form

$$\mathcal{L}_\times(\beta|p|^2)$$

is no longer treated as an independent condition. The intrinsic Gram identity at $r = 1$ reads it directly as

$$\boxed{\mathcal{L}_\times(\beta|p|^2) = \left\| \sum_i c_i \Psi_i^{[1]} \right\|^2 \geq 0.} \tag{B.2}$$

The independence discipline remains:

1. $\{\gamma_n\}$ is not an input to the spectral-truncation construction;
2. K_{Ren} does not participate in HP spectral generation;
3. H_{Ren} does not participate in the HP⇒RH implication;
4. the canonical Riemann spectral witness enters only after the Hilbert–Pólya terminal has formed and serves terminal identification;
5. GUE/CUE and second-order statistics enter only after first-order spectral identity has been fixed;
6. finite-dimensional numerical audits and all-order theorems have distinct roles.

Thus the chapter explicitly distinguishes

$$\boxed{\text{finite-dimensional numerical positivity} \neq \text{the proof source of the all-order theorem;}}$$

the universal positivity theorem comes from intrinsic generative-source identity self-pairing, while finite-dimensional numerics serve only independent verification.

Likewise,

canonical spectral-witness identification ⇒/ intrinsic generative-source construction.

Terminal identification occurs after the proof and does not participate in the upstream construction.

Afterword

The Higher Form of Proof Is Not to Add More Reasoning,

but to See What Was There All Along, So That Unnecessary Reasoning Disappears.

With these nine chapters, the mathematical main line of the book is complete.

Chapter 1 begins from open multiplicative relations, reciprocal roles, and complete event histories, and gives the first closure proof of the Riemann Hypothesis in this book.

Chapters 2 and 3 unfold the closed zero set further into gap geometry, boundary analytic germs, identity addresses, and analytic multiplicities.

Chapter 4 compresses the direct closure into a parameterized seven-condition kernel and proves the Dirichlet case of the Generalized Riemann Hypothesis through minimal identity migration.

Chapter 5 stratifies the actual zero spectrum, finite event-lift spectra, and existing spectral routes.

Chapter 6 constructs the Yifei Ren operator and the full Ren–Riemann spectral object.

Chapter 7 establishes the scalar spectral witness and canonical spectral-identity identification.

Chapter 8 moves from the first-order spectrum into the Montgomery–GUE second-order self-relations.

Chapter 9 returns to the root multiplicative identity, independently constructs a Hilbert–Pólya self-adjoint spectrum from the generative source, and closes the Riemann Hypothesis once again.

Structurally, the story could end here.

But if one asks what this book truly hopes to leave behind, I would not want the answer to be only the sentence “the Riemann Hypothesis has been proved.”

A proof is a result.

What changed me more deeply along this path was learning to ask again why a mathematical problem becomes a problem in the first place.

After completing these nine chapters, I have become increasingly convinced that the deepest question of this book is not how much more reasoning can be added.

The more important question is:

> **when the identity of an object becomes clear again, which steps that once seemed unavoidable turn out to be extra burdens created only by a split representation?**

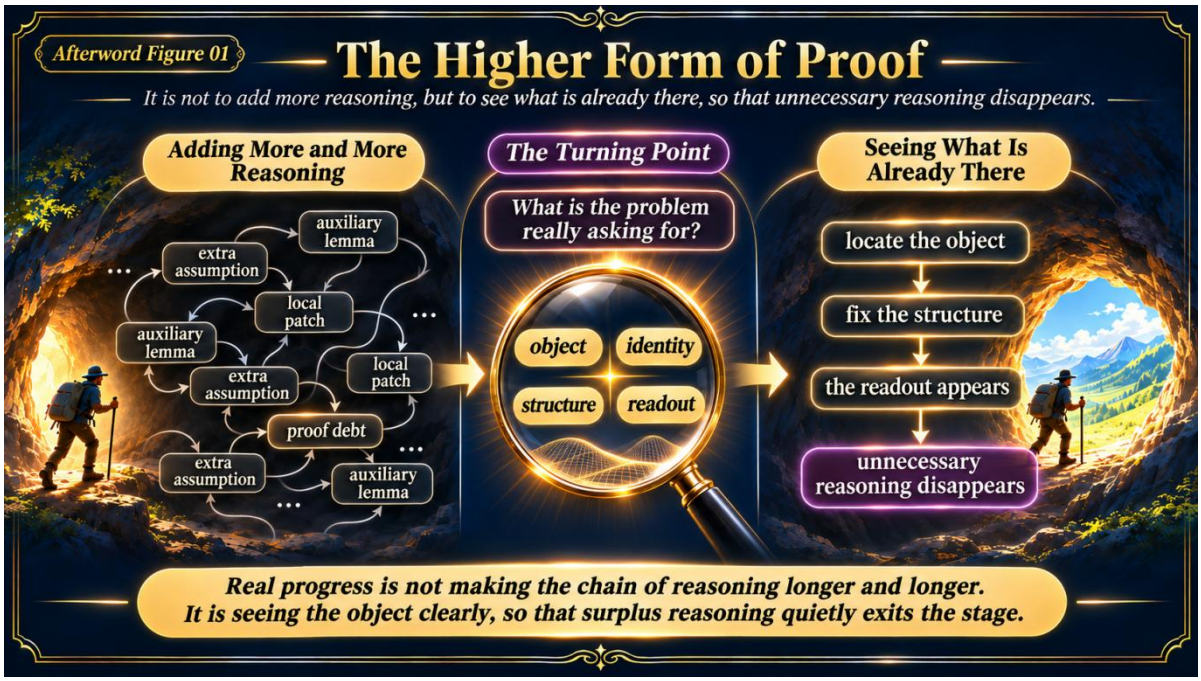
“To see what was there all along” does not mean bypassing proof, still less replacing proof with intuition.

It means the opposite. One must first return objects, roles, readouts, representations, and generative sources to their proper places. Only then can we tell which proof obligations belong to the mathematical object itself, and which arose because we photographed the same object in many different ways and then began paying debts for the differences among the photographs.

That is why I would like to leave this book with the following sentence:

the higher form of proof is not to add more reasoning,

but to see what was there all along, so that unnecessary reasoning disappears.



Afterword Figure 01. The higher form of proof: seeing what was there all along. This figure compresses the central claim of the afterword into three stages: continually adding reasoning, relocating the object and identity actually demanded by the problem, and allowing unnecessary reasoning to fall away once the structure is fixed. It is not a new proof step, but a closing visual statement about the book's view of proof.

Part I — Seeing What Was There All Along: How a Problem Is Made, and How It Becomes Visible Again

1. In the End, We Return to the Smallest Question

After nine chapters, this book contains:
reciprocal roles;
moving horizons;
boundary analytic germs;
zero addresses;
analytic multiplicities;
closure kernels;
event spectral atlases;
the Yifei Ren operator;
Stieltjes witnesses;
Hilbert–Pólya;
GUE;
Gram positivity;
Source–Krylov truncations;
Fredholm determinants.
That is already a great many objects.
Yet all of them arose from a very small question:

$$\boxed{\text{why}\frac{1}{2}?}$$

Perhaps this is one of the most beautiful things about mathematics.

A very small question can take us very far.

And after going far enough, we may discover that the most important ability is not always to keep adding new objects.

Sometimes it is to turn back.

To ask whether the original question is still there.

To ask when it became difficult.

To ask whether we took many photographs of the same object and then began paying debts for the differences among those photographs.

If the problem still exists after we return, we go back and continue proving.

If the problem has changed, we name it again.

And if, in the end, two genuinely different routes return us to the same conclusion, perhaps the most valuable thing is not that we have "won" a famous problem.

Perhaps it is that we have learned one more way to see mathematics.

So I do not want this book to end with a declaration of victory.

I would rather leave an invitation:

$$\boxed{\textbf{walk this road again.}}$$

If it is wrong, let the error appear clearly.

If it is right, let the conclusion cease to depend on its author.

For the moment at which mathematics truly completes a proof is never the moment when the author writes the final period.

It is the moment when the proof can leave the author and still stand.

2. It All Began with Curiosity, Not Ambition

I did not enter this problem with a plan to "solve the Riemann Hypothesis."

What first made me stop was a much smaller question:

$$\boxed{\text{why exactly}\frac{1}{2}?}$$

Mathematical history is full of numbers.

Some come from normalization.

Some from dimension.

Some from centers of symmetry.

Some from averages.

Some from choices of coordinates.

In the Riemann Hypothesis, $1/2$ looks both simple and strange.

The completed function already has the complementary structure

$$s \leftrightarrow 1 - s,$$

and the zeros already carry the critical-line reflection

$$\rho \leftrightarrow 1 - \overline{\rho}.$$

So $1/2$ is plainly there from the beginning.

But standard mathematics is equally clear that

the symmetry center is$1/2$

does not imply

$$\Re\rho = \frac{1}{2}$$

for every zero.

That obvious obstruction is what makes the problem genuinely interesting.

From there, one can ask two very different questions.

The first is:

how can one prove that every$\Re\rho - \frac{1}{2}$is zero?

The second is:

why did$\Re\rho - \frac{1}{2}$become an independent proof obligation in the first place?

The first question moves forward.

The second moves backward.

This book was formed by moving repeatedly between those two directions: proving forward, while also looking backward at how the problem came to be written in its present form.

3. Objectification Is One of Mathematics' Greatest Powers—and It Can Also Leave Proof Debt

Much of the power of mathematics comes from its ability to objectify.

We compress a relation into an object.

We place the object in a set.

We place the set in a space.

We turn a function into its zeros.

We turn zeros into a spectrum.

We turn a spectrum into a measure.

We turn a measure into an operator.

We compress local data into invariants.

These operations allow mathematics to advance without apparent limit.

But objectification has another side.

When a complete object is decomposed, its local parts acquire new names, new addresses, and new coordinates.

Once a part can be named independently, it is easy to feel that

> if it can be written separately, it ought to have a separate independent source.

That step is not always valid.

Greater addressability does not mean greater identity information.

A more elaborate representation does not mean that the object has changed identity.

Extracting one coordinate does not mean that the coordinate has acquired a second generative mechanism independent of the whole object.

I call the proof obligations that must be re-examined at such points **proof debt**.

Proof debt does not mean that less proof is required.

It means the opposite.

Whenever a new proof obligation appears, we should ask one more question:

> is this debt owed by the object itself, or was it created by the representation?

If it is a genuine debt, it must be paid.

If it is an equivalence transformation, one must not mistake a change of coordinates for a reduction of proof information.

If it is a boundary term created by a finite cut, the horizon itself should enter the problem.

If the same identity readout has been registered twice, one must first explain why it truly has two independent sources.

This methodology is not the proof of the Riemann Hypothesis.

But it changed the way I looked for one.

4. I Repeatedly Saw “the Final Step”—Then Began Asking Whether It Was Always the Same Step

When working on the Riemann Hypothesis, it is easy to feel again and again:

“We are very close. Only one final step remains.”

In the language of zeros, that step may be

$$\Re\rho = \frac{1}{2}.$$

In Möbius language, it may become

$$M(x) = O_\varepsilon(x^{1/2+\varepsilon}).$$

In a finite ledger, it may become some critical bilinear correlation.

In spectral language, it may become

> prove that the spectrum of a self-adjoint operator is exactly the Riemann zero spectrum.

Each time the language changes, the “final step” changes appearance.

What finally made me stop was a very simple observation.

If

$$A \Leftrightarrow B,$$

then rewriting A as B does not by itself reduce the information needed for a proof.

And if

$$B \Leftrightarrow C,$$

then the fact that C looks cleaner does not by itself mean that we are closer to the conclusion.

Proof debt truly changes only when some new fact appears that cannot be recovered merely by translating back into the previous representation.

This also gave me a deeper respect for equivalent formulations.

Equivalent formulations are not useless.

They are immensely valuable.

They change perspective, expose structure, introduce tools, and may make a genuinely new fact visible for the first time.

But their value should not be measured by how much they "look like the answer."

The real question is:

$$\boxed{\Delta\text{ProofInformation} > 0 \quad \text{where does it actually occur?}}$$

5. Minimal Sufficient Retreat: Not Returning Mathematics to Nothingness, but Retreating Until the Problem Becomes Visible Again

There is one more phrase I would like to leave with the reader:

$$\boxed{\text{minimal sufficient retreat.}}$$

It does not mean taking every mathematical question all the way back to first philosophy.

That would not be operational.

It means:

> retreat only far enough to expose the source of the difficulty, and then stop.

If the problem is already clear at the function level, there is no need to retreat to multiplication.

If it is clear at the multiplicative level, there is no need to retreat further into generative philosophy.

For the Riemann Hypothesis, the effective retreat eventually stopped at

$$\text{zeros} \leftarrow \xi \leftarrow \zeta \leftarrow \text{Euler product} \leftarrow \text{the multiplicative identity of the natural numbers.}$$

Then the argument moves forward again.

This is why GHT ultimately recedes into the background of this book.

It helped formulate the question:

"Where does the object come from?"

But once the mathematical object had been found again, the book returned to standard mathematical language.

Starting from root multiplicative identity, it moves forward through relations, representations, events, measures, and operators.

Discovery may come from anywhere.

Proof must return to mathematics.

6. The Last Century and a Half Was Not a Detour, but an Enormous Repository of Mathematical Tools

I once described the feeling by saying:

mathematics traveled very far, while identity did not move.

If this is taken to mean that the mathematics of the past century and a half made no real progress, it is completely wrong.

Since Riemann, mathematics has gained an immense amount of genuinely new information.

We know far more about where zeros lie.

We know stronger zero-free regions.

We know sharper errors in prime counting.

We know the relations of zeta to Möbius, von Mangoldt, and explicit formulas.

We know how function spaces, positivity, approximation, spectra, and random matrices can reformulate the Riemann Hypothesis.

We know that the two-point statistics of the zeros exhibit astonishing structure.

We know that broad families of L-functions display deep universality.

We know how far computation can push finite verification.

All of this is real mathematics.

A more accurate ledger is therefore

$$\begin{aligned} \Delta\mathrm{Representation} &\gg 0,\\ \Delta\mathrm{AnalyticInformation} &> 0,\\ \Delta\mathrm{SpectralInformation} &> 0,\\ \Delta\mathrm{StatisticalInformation} &> 0. \end{aligned}$$

This book asks about one further quantity:

$$\Delta\mathrm{IdentityInformation},$$

and where it actually changes.

That does not diminish representation.

It classifies representation more carefully.

A mature theory should know not only how much information it has gained, but also to which level that information belongs.

Part II — When Identity Reappears: How Proof Moves from Explanation into Mathematics

7. Identity Clarification Did Not Stop at Explanation; It Entered the First Proof

If this book had stopped at diagnosing "proof debt," it would still have been only a methodology.

The decisive change occurred when identity clarification was compressed into precise mathematical objects.

Chapter 1 does not argue:

"multiplication is self-dual, therefore all zeros lie on the critical line."

That inference would not be valid.

What Chapter 1 actually builds is

root multiplicative identity →
reciprocal role → complete event →
role fidelity → terminal fixed-role readout.

Within this chain,

$$\text{identity} \neq \text{role} \neq \text{role readout}.$$

The source-side $1/2$ is not a constant numerically transported into the real part of a zero.

Closure occurs within the reciprocal-role structure of the same complete event.

When the complete source-side event is already at a reciprocal fixed role, and the terminal analytic representation preserves that same reciprocal role, the terminal object can lie only in the fixed set of the analytic reciprocal involution.

For the Riemann zeros, that fixed set is

$$\Re\rho = \frac{1}{2}.$$

This step matters enormously.

It is the point at which the early "identity question" ceases to be merely explanatory and assumes actual proof responsibility.

8. The Meaning of the Spectral Route Also Changed: from a Possible Explanation to a Second Independent Proof

I have always kept one basic caution in mind when thinking about Hilbert–Pólya.

The reason is simple.

If one first knows the Riemann zeros

$$\gamma_n$$

and then defines

$$He_n = \gamma_n e_n,$$

one certainly gets a self-adjoint diagonal operator.

But this does not explain why the zeros come from that operator.

It merely repackages the answer as a spectrum.

The hard question was never

can one write down a spectral operator?

It was:

can the spectrum be generated from an independent arithmetic source?

and

why must it coincide with the Riemann zero spectrum?

Chapters 6 and 7 answer the questions "what is the canonical Riemann spectral object?" and "how can one recognize the same spectrum?"

Chapter 9 does something else.

It does not begin from a zero list.

It does not begin from K_{Ren}.

It does not begin from H_{Ren}.

It does not begin from the witness measure of Chapter 7.

It begins again from

$$\mathfrak{I}_{\times} = (\mathbb{N}_{>0}, \mu).$$

Through the Unified Single-Identity Closure Package, two-depth self-pairing, Gram positivity, Stieltjes reconstruction, a pure-point measure, and the spectral theorem, it generates

$$H_\times = H_\times^*.$$

It then recovers from this spectrum

$$\rho = \frac{1}{2} \pm i\gamma_n.$$

At that point Hilbert–Pólya is no longer only the idea that "if such an operator exists, then the Riemann Hypothesis follows."

Within this book, it becomes

an independent closure chain from the multiplicative generative source to a self-adjoint spectrum and then to the Riemann Hypothesis.

Only after this chain is complete does the canonical spectral witness of Chapter 7 enter and tell us

$$(H_\times, M_\times) \simeq (H_{\mathrm{id}}, M_{\mathrm{mult}}).$$

The second route generates first and identifies afterward.

I regard that distinction as one of the most important structural achievements of the book.

9. GUE Then Returns to Its Proper Place

Only after first-order spectral identity has been fixed does GUE properly enter.

This may look like a matter of chapter order, but it is mathematically important.

It is easy to blur together:

- the Riemann Hypothesis;
- Hilbert–Pólya;
- random matrices;
- GUE;
- quantum chaos.

They are related, but they are not the same statement.

The Riemann Hypothesis concerns horizontal location:

$$\Re\rho = \frac{1}{2}.$$

Hilbert–Pólya asks whether the vertical frequencies can be realized as a self-adjoint spectrum.

GUE asks how that first-order spectrum is statistically organized when it forms two-point and higher-order relations with itself.

Therefore

self-adjointness ⇒/ GUE.

Likewise,

numerical agreement with GUE ⇒/ a proof of the Riemann Hypothesis.

Chapter 8 separates these levels again.

And once Chapters 7 and 9 establish

$$(H_{\times}, M_{\times}) \simeq (H_{\mathrm{id}}, M_{\mathrm{mult}}),$$

the second-order unitary-invariant structure can be inherited automatically.

GUE therefore no longer carries a proof burden that does not belong to it.

It becomes a natural downstream theory of the self-relations of the closed Riemann spectrum.

Part III — After Proof: Public Verification, History, and Mathematics That Continues to Grow

10. “We Have Proved the Riemann Hypothesis” and “The Mathematical Community Has Accepted the Proof” Are Two Different Sentences

At this point one boundary matters more than any other.

The mathematical claims of this book are explicit.

The conclusions stated in the body are:

Chapter 1 completes a direct closure of the Riemann Hypothesis.

Chapter 9 gives a second, independent proof through a source-generated Hilbert–Pólya spectrum.

Thus, within the theorem chains of this book,

the Riemann Hypothesis

is not retained as an assumption.

It is a conclusion.

But mathematics is a form of public reason.

My writing down a proof is not the same event as the mathematical community completing its verification.

A result of genuine importance should be able to be:

- redefined by others;
- derived step by step by others;
- shown wrong by others;

- challenged by counterexamples;
- rewritten in another mathematical language;
- replayed, where formalization permits, by formal systems or independent programs;
- and ultimately stand independently of the author's own explanation.

I do not want anyone to believe that the Riemann Hypothesis has been proved because of the tone of this book.

Nor do I want anyone to decide in advance that it must be right or wrong merely because the author is, or is not, a familiar name.

There is only one fair standard:

check the proof.

If one step is wrong, identify the step.

If an object definition is circular, draw the circle.

If an "independent generation" actually borrows from the Riemann spectrum, identify exactly what it borrows.

If an equivalence has been incorrectly promoted to an implication, give a counterexample.

If a local statement does not support a universal conclusion, identify the missing quantifier.

Such criticism is not hostility toward the book.

It is the examination that every mathematical proof must accept.

11. The Best Ending for a Book Is Not to Ask for Belief, but to Begin Being Seriously Tested

What matters more to me now is that these ideas become visible to the mathematical community.

That wish has not changed.

But it has become more precise.

I do not need anyone to look more closely because this is a Millennium Prize problem.

I do not need anyone to lower the standard because the author persisted for a long time.

What I genuinely hope is that someone will read Chapter 1 as an unfamiliar proof.

That someone will attack only the weakest of K1–K7.

That someone will formalize the generative chain of Chapter 9 and inspect every assumption one by one.

That someone will look for the smallest counterexample.

That someone will identify a type error.

That someone will prove that a complicated passage I wrote can be replaced by one line from a classical theorem.

That someone will disagree with the conclusion and still state precisely where the disagreement begins.

Mathematics is not a relation of trust between author and reader.

It is a structure that can be checked together.

That is the sentence I most want to leave after finishing this book.

12. Mathematics Continues after the Proof

If the two proofs in this book survive independent scrutiny, the story will not end there.

The natural next step for a reader is not simply to accept the conclusion, but to open the argument further.

One can inspect chapter by chapter what every theorem actually depends on and whether cross-chapter references use only previously established assumptions.

One can read Chapters 1 and 9 separately and test whether the two proofs of the Riemann Hypothesis truly preserve the independence each claims.

One can hand the formalizable parts to a computer: moments, finite truncations, Fredholm identities, identification of spectral measures, and every algebraic or analytic step that can be replayed mechanically.

One can also translate the language of this book into more familiar languages of classical analytic number theory, operator theory, or spectral theory. If another formulation makes the same proof shorter and more transparent, mathematics itself gains.

Chapter 4 carries identity migration to the Dirichlet case of the Generalized Riemann Hypothesis; Chapters 7 and 8 carry the story into spectral witnesses and second-order statistics. New questions arise naturally: which more general completed L-functions preserve the same identity, reciprocal, and completion structures? Which objects only look formally similar, while lacking the decisive identity conditions?

And beyond the Riemann Hypothesis itself, the vertical zero spectrum, gap geometry, multiplicity, GUE/CUE, finite-scale arithmetic corrections, and quantum-dynamical interpretations remain rich mathematical worlds in their own right.

So “the proof is complete” never means “the mathematics is over.”

It only means that a question long standing in the doorway has been moved aside, and the space behind it can be seen more clearly.

13. Thanking the Past Is Not Courtesy; It Is Respect for Mathematical Fact

When writing a book that claims a proof of the Riemann Hypothesis, it is easy to create a narrative illusion:

as if the author stands at the finish line and everyone before him was simply someone who failed to get there.

I do not understand the history that way.

Riemann did not prove the Riemann Hypothesis, but he created the entire problem-space in which we still work.

Hadamard and de la Vallée Poussin did not solve the Riemann Hypothesis, but they proved the prime number theorem and turned Riemann’s methods into decisive arithmetic mathematics for the first time.

Hardy, Selberg, Levinson, and Conrey did not reach “one hundred percent,” but they turned the critical line from the center of a conjecture into a mathematically accessible object.

Turing, Odlyzko, and generations of computation did not turn finite verification into an infinite proof, but they made the world of zeros visible with unprecedented clarity.

Weil, Nyman, Beurling, Li, and others did not make equivalent criteria automatically solve the Riemann Hypothesis, but they showed how many mathematical structures the same problem could inhabit.

Hilbert–Pólya, de Branges, Connes, Berry–Keating, Suzuki, and other spectral directions did not, in the existing literature, produce a proof of the Riemann Hypothesis accepted by the community, but they made the question "are the Riemann zeros a spectrum?" into a profound and continuously growing mathematical program.

Montgomery, Dyson, Odlyzko, Katz, Sarnak, and others showed us that even if all zeros lie on one line, the world of zeros is vastly richer than "a line."

Therefore, even if the central conclusions of this book ultimately stand, the previous century and a half cannot be compressed into the sentence "they did not think about identity."

That would not be mathematical history.

A truer statement is:

> **because earlier mathematicians carried each road so far,we now possess enough structure to see the same object again.**

14. I Increasingly Believe That Curiosity Is More Worth Protecting Than the Desire to "Solve a Great Problem"

A famous problem has enormous gravitational pull.

It encourages the thought:

"How can I solve it?"

But by the end of this book I have come to think that something else deserves even more protection:

curiosity.

Curiosity does not care whether a problem is worth a million dollars.

It does not care whether the problem has sufficient historical prestige.

It simply stops somewhere and asks:

Why?

Why this object?

Why this definition?

Why must this term be proved separately?

Why has a new degree of freedom suddenly appeared?

Why does a local piece acquire an independent identity after the whole object has been decomposed?

Why do we feel closer to the answer every time we move to an equivalent formulation?

Why, after a problem has been worked on for more than a century, do we assume that we can only keep moving forward and never turn back to examine how the problem itself was formed?

These questions do not all produce theorems.

But they determine where we look for theorems.

If this book has any methodological value beyond the Riemann Hypothesis itself, I hope it comes from that willingness to turn back without abandoning rigor.

15. Private Curiosity and Public Mathematics

Mathematics often begins in a very private place.

One person finds a number strange.

A formula feels unsettling.

An object everyone uses suddenly invites one more question:

“Why is it this way?”

Such beginnings carry no public authority.

They may even begin from a misunderstanding.

But mathematics has an extraordinary mechanism: private curiosity can be translated into public objects.

Once an idea is written as definitions, lemmas, theorems, and reproducible derivations, it begins to leave its author.

Others do not need to share the author’s experience.

They do not need to accept the author’s methodology.

They do not need to share the original intuition.

They need only inspect the relations written on the page.

This is one of the things I love most about mathematics.

It allows a person to begin in great solitude.

And it requires that person, eventually, to leave that solitude.

When Riemann wrote the conjecture in 1859, he could not have known how many people over the next century and a half would enter entirely different mathematical worlds through it.

Hardy could not have known Montgomery.

Montgomery did not begin with random matrices in mind when he found pair correlation.

Dyson’s physical intuition met number theory in an unexpected place.

The Hilbert–Pólya vision has been re-expressed by generations in different mathematical languages.

Many of the tools we use today were left by people from different eras who could not have known where their ideas would eventually meet.

So if this book has indeed done what it claims to have done, it is still only one node in a much longer river.

It uses the language of those who came before.

It inherits their theorems.

It borrows the vistas they opened.

And from a new angle on the question, it reorganizes those things once more.

If it is wrong, mathematics will separate out its errors.

If it is right, mathematics will gradually strip what is genuinely effective from the author's private language and turn it into structures anyone can use.

Both outcomes are better than belief.

So at the end I would like to place together the two words with which this book began and ends:

curiosity may be private; proof must be public.

Between them lies the long connection between people.

People from different eras.

People using different methods.

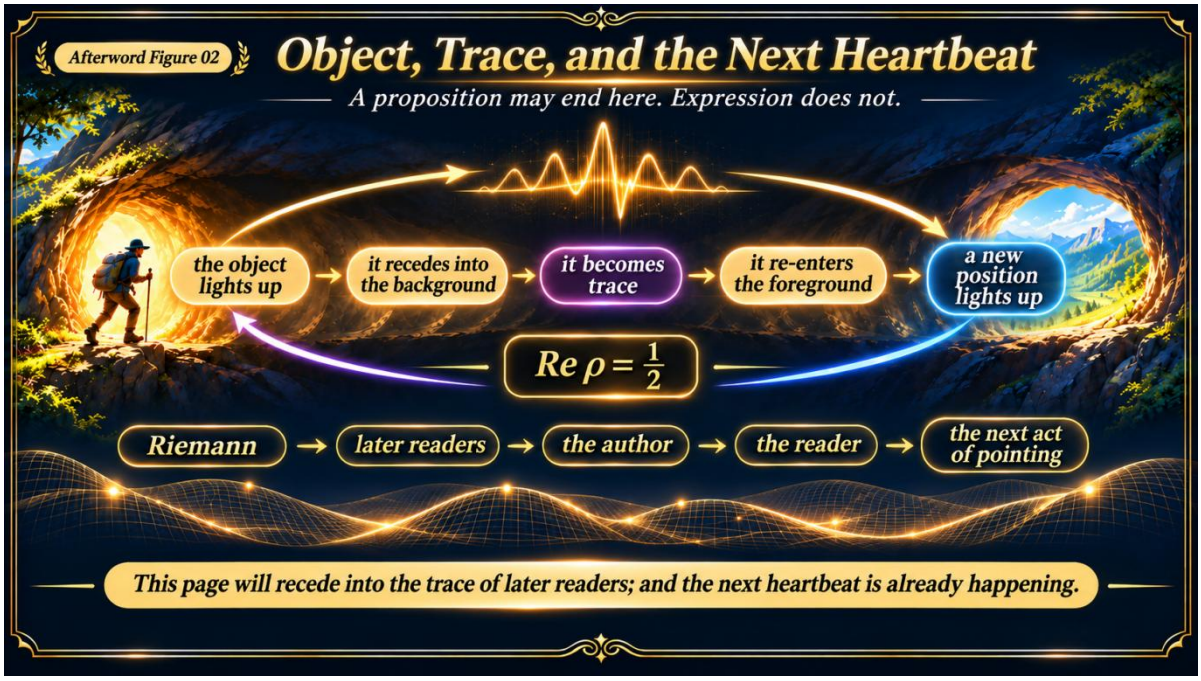
People reaching different judgments.

Even people who disagree with one another.

All may enter the same mathematical history because of one question.

Solitude can be real.

Connection can be equally real.



Afterword Figure 02. Object, trace, and the next heartbeat. An object lights up, recedes into the background, becomes part of a trace, and re-enters the foreground in a new relation. Authors, readers, and later readers belong to the same chain of transmission. A proposition may end on a page, but its trace, public verification, and the next act of pointing continue.

Acknowledgements

At this point, the mathematics of the book is finished.

Gratitude is not part of a proof, and it carries no responsibility for any theorem. But a book is never truly completed by the person sitting alone at the desk. Much of the support that makes a book possible never enters an equation, never appears in a footnote, and leaves no number that can be cited. Without it, however, these pages would not have reached the reader in the form they have today.

To My Parents and Family

Some of the most important forms of support are not always expressed in words. Sometimes they are simply long years of companionship, understanding, concern, and the quiet strength of being held up even when I could not see it.

To My Friends at Matrix

You were among the first people to watch this book grow, little by little.

Whenever I had written something new, I often sent it to you almost immediately. Sometimes that was after writing late into the night, or even through the night. Before finally going to rest, I would still send you a screenshot and say: today, it moved forward a little more.

Most of the time, you were not involved in the mathematical derivations themselves. But you were there.

That companionship made the long period of writing feel less lonely. It also reminded me that when an idea is finally written down, or a problem finally moves forward, there are people willing to be the first to see it.

It was this very ordinary, very quiet kind of companionship that carried me all the way here, and helped me finish this book.

To the People I Have Met Along the Way

I am also grateful to everyone who has known me, and to everyone I have had the good fortune to know.

Some people stayed for a long time. Some passed through only briefly. Some relationships were clear and deep; others may have left behind only a very small fragment.

But a life is never made only of its “important moments.”

Sometimes it is a sentence.

Sometimes a meal.

Sometimes an argument.

Sometimes it is your willingness to listen for a few extra minutes while I excitedly explain an idea.

Sometimes it is the fact that, when I was silent, you did not rush to ask why.

Sometimes it is only many years later that I look back and suddenly realize that an ordinary act of kindness stayed with me much farther than I knew at the time.

None of these things need to be written into mathematics.

But they are written into a person.

And I have come to understand more clearly that we become who we are not because of what we manage to preserve alone, but because at different moments someone gave us understanding, patience, help, criticism, tolerance, or warmth.

Some names will not appear here.

Not because they matter less, but because the things that matter most do not always need to become a list.

If you have ever appeared in my life, whether for a long time or only briefly, and wherever our paths later went, I want to say one thing to you here, at the end of this book:

Thank you.

To Those Who Never Asked Me to Become Someone Else

There is one more kind of gratitude I have wanted to save for the end.

Thank you to those who allowed me to understand the world at my own pace.

You did not urge me to follow a more standard path. You did not close down an idea merely because it sounded too far away. You did not lose patience when I changed the way I tried to express something again and again.

Many things can only grow into their own shape when they are not defined too quickly.

This book has its mathematical conclusions, of course. But for me personally, something even more precious is that through the long process of writing it, I was able to preserve the small spark of curiosity with which I began, rather than trade it for a posture that would have been easier to explain to others.

I did not manage that alone.

So I also thank those who gave me freedom.

Finally, to You, the Reader

Perhaps you have read from the first page all the way to this one. Perhaps you happened to open the book near the end.

You may be familiar with number theory, complex analysis, and spectral theory. Or perhaps you simply paused because the words “Riemann Hypothesis” caught your attention.

Either way, thank you for giving some of your time to this book.

Finishing a book is only an ending on the author’s side.

Once another person truly opens it, the words begin to have a fate the author can no longer control. You may agree with some of what is here and doubt other parts. You may stay on one page for a long time, or turn another very quickly. Years from now, you may remember only one formula, one sentence, or some detail I could never have expected.

All of that is fine.

Because from this moment on, the book no longer belongs only to the person who wrote it.

What I hope you take away is not belief in the author.

It does not even have to be a particular conclusion.

If anything is to remain, I would rather it be a willingness to keep asking questions: when a problem has been made to sound sufficiently complicated, can we still go back and ask what it was at the beginning? When we think we have traveled very far, can we still see again the things that were there all along?

As for the answers, they should ultimately belong to mathematics—and to time.

Thank you to my parents and family.

Thank you to my friends at Matrix

Thank you to everyone who has appeared, who is here now, and who has yet to appear.

And thank you to you, reading these words at this moment.

Here, at last, the formulas fall quiet.

May we each preserve what makes us irreplaceable, and remember the hands that once held us up.

Then keep living.

Keep meeting one another.

Keep wondering.

No zeros.

Only heartbeats.

References

I. Historical Foundations of the Riemann Zeta Function, the Prime Number Theorem, and the Riemann Hypothesis

[1] L. Euler, *Introductio in analysin infinitorum*, 2 vols., Lausanne, 1748.

[2] B. Riemann, "Ueber die Anzahl der Primzahlen unter einer gegebenen Grösse," *Monatsberichte der Königlichen Preußischen Akademie der Wissenschaften zu Berlin*, 1859, 671–680.

[3] J. Hadamard, "Sur la distribution des zéros de la fonction $\zeta(s)$ et ses conséquences arithmétiques," *Bulletin de la Société Mathématique de France* **24** (1896), 199–220. DOI: 10.24033/bsmf.545.

[4] C.-J. de la Vallée Poussin, *Recherches analytiques sur la théorie des nombres premiers*, Bruxelles, 1896–1897.

[5] E. C. Titchmarsh, revised by D. R. Heath-Brown, *The Theory of the Riemann Zeta-Function*, 2nd ed., Clarendon Press / Oxford University Press, Oxford, 1986.

[6] H. M. Edwards, *Riemann's Zeta Function*, Academic Press, New York, 1974; Dover reprint, 2001.

[7] E. Bombieri, "The Riemann Hypothesis," in J. Carlson, A. Jaffe, and A. Wiles (eds.), *The Millennium Prize Problems*, Clay Mathematics Institute / American Mathematical Society, 2006, 107–124.

[8] J. B. Conrey, "The Riemann Hypothesis," *Notices of the American Mathematical Society* **50** (2003), no. 3, 341–353.

[9] G. H. Hardy, "Sur les zéros de la fonction $\zeta(s)$ de Riemann," *Comptes Rendus de l'Académie des Sciences de Paris* **158** (1914), 1012–1014.

[10] N. Levinson, "At Least One-Third of Zeros of Riemann's Zeta-Function Are on $\sigma = 1/2$," *Proceedings of the National Academy of Sciences USA* **71** (1974), no. 4, 1013–1015. DOI: 10.1073/pnas.71.4.1013.

[11] J. B. Conrey, "More than Two Fifths of the Zeros of the Riemann Zeta Function Are on the Critical Line," *Journal für die reine und angewandte Mathematik* **399** (1989), 1–26. DOI: 10.1515/crll.1989.399.1.

[12] A. M. Turing, "Some Calculations of Riemann's Zeta-Function," *Proceedings of the London Mathematical Society*, Series 3, **3** (1953), 99–117.

[13] A. R. Booker, "Turing and the Riemann Hypothesis," *Notices of the American Mathematical Society* **53** (2006).

[14] A. M. Odlyzko, "On the Distribution of Spacings Between Zeros of the Zeta Function," *Mathematics of Computation* **48** (1987), no. 177, 273–308. DOI: 10.1090/S0025-5718-1987-0866115-0.

II. Equivalent Criteria, Positivity, Function Spaces, and Moment Problems

[15] A. Weil, "Sur les 'formules explicites' de la théorie des nombres premiers," *Communications du Séminaire Mathématique de l'Université de Lund*, Tome supplémentaire, 1952, 252–265.

[16] B. Nyman, *On the One-Dimensional Translation Group and Semi-Group in Certain Function Spaces*, Ph.D. thesis, University of Uppsala, 1950.

[17] A. Beurling, "A Closure Problem Related to the Riemann Zeta-Function," *Proceedings of the National Academy of Sciences USA* **41** (1955), no. 5, 312–314. DOI: 10.1073/pnas.41.5.312.

[18] X.-J. Li, "The Positivity of a Sequence of Numbers and the Riemann Hypothesis," *Journal of Number Theory* **65** (1997), no. 2, 325–333. DOI: 10.1006/jnth.1997.2137.

[19] L. de Branges, "The Riemann Hypothesis for Hilbert Spaces of Entire Functions," *Bulletin of the American Mathematical Society* **15** (1986), no. 1, 1–17. DOI: 10.1090/S0273-0979-1986-15429-7.

[20] W. F. Donoghue, Jr., *Monotone Matrix Functions and Analytic Continuation*, Springer-Verlag, Berlin, 1974.

[21] N. I. Akhiezer, *The Classical Moment Problem and Some Related Questions in Analysis*, Oliver & Boyd, Edinburgh, 1965.

[22] J. A. Shohat and J. D. Tamarkin, *The Problem of Moments*, American Mathematical Society, Providence, RI, 1943.

[23] B. Ya. Levin, *Distribution of Zeros of Entire Functions*, revised ed., Translations of Mathematical Monographs, Vol. 5, American Mathematical Society, Providence, RI, 1980.

[24] R. P. Boas, *Entire Functions*, Academic Press, New York, 1954.

[25] N. Aronszajn, "Theory of Reproducing Kernels," *Transactions of the American Mathematical Society* **68** (1950), 337–404.

[26] D. V. Widder, *The Laplace Transform*, Princeton Mathematical Series, Vol. 6, Princeton University Press, Princeton, 1941.

[27] B. Hatinoğlu, "Uniqueness Theorems for Meromorphic Inner Functions and Canonical Systems," *Canadian Mathematical Bulletin* **68** (2025), 124–140.

[28] Á. Baricz, P. Kumar, and S. Singh, "Asymptotic Expansions for the Radii of Starlikeness of Normalized q-Bessel Functions," *Results in Mathematics* **79** (2024), 248.

III. Hilbert–Pólya, Operator Theory, and Spectral Routes to the Riemann Problem

[29] G. Pólya, letter to A. M. Odlyzko, 3 January 1982, reproduced in A. M. Odlyzko, "Correspondence about the Hilbert–Pólya Conjecture," University of Minnesota online archive.

[30] M. V. Berry and J. P. Keating, "The Riemann Zeros and Eigenvalue Asymptotics," *SIAM Review* **41** (1999), no. 2, 236–266. DOI: 10.1137/S0036144598347497.

[31] M. V. Berry and J. P. Keating, "$H = xp$ and the Riemann Zeros," in I. V. Lerner, J. P. Keating, and D. E. Khmelnitskii (eds.), *Supersymmetry and Trace Formulae: Chaos and Disorder*, Kluwer/Plenum, New York, 1999, 355–367.

[32] A. Connes, "Trace Formula in Noncommutative Geometry and the Zeros of the Riemann Zeta Function," *Selecta Mathematica* **5** (1999), 29–106. DOI: 10.1007/s000290050042.

[33] M. Suzuki, "A Canonical System of Differential Equations Arising from the Riemann Zeta-Function," arXiv:1204.1827, 2012.

[34] M. Suzuki, "Aspects of the Screw Function Corresponding to the Riemann Zeta-Function," *Journal of the London Mathematical Society* **108** (2023), 1448–1487.

[35] M. Suzuki, "On the Hilbert Space Derived from the Weil Distribution," *Canadian Journal of Mathematics*, published online 3 November 2025, 1–24. DOI: 10.4153/S0008414X25101739.

[36] A. Connes and C. Consani, "The Scaling Hamiltonian," arXiv:1910.14368.

[37] A. Connes and C. Consani, "Spectral Triples and Zeta-Cycles," *L'Enseignement Mathématique* **69** (2023), 93–148; arXiv:2106.01715.

[38] A. Connes, C. Consani, and H. Moscovici, "Zeta Spectral Triples," arXiv:2511.22755, 2025.

[39] A. Connes and W. D. van Suijlekom, "Quadratic Forms, Real Zeros and Echoes of the Spectral Action," arXiv:2511.23257, 2025.

[40] M. Suzuki, "Weil's Quadratic Form via the Screw Function," arXiv:2606.09096, 2026.

[41] M. Suzuki, "Spectral Convergence Associated with Weil's Quadratic Form," arXiv:2610.32704, 2026.

[42] M. Reed and B. Simon, *Methods of Modern Mathematical Physics, Vol. I: Functional Analysis*, Academic Press, New York, 1972.

[43] B. Simon, *Trace Ideals and Their Applications*, 2nd ed., Mathematical Surveys and Monographs, Vol. 120, American Mathematical Society, Providence, RI, 2005. DOI: 10.1090/surv/120.

[44] J. B. Conway, *A Course in Functional Analysis*, 2nd ed., Graduate Texts in Mathematics, Vol. 96, Springer-Verlag, New York, 1990.

IV. Montgomery–GUE, Random Matrices, and Second-Order Spectral Statistics

[45] H. L. Montgomery, "The Pair Correlation of Zeros of the Zeta Function," in *Analytic Number Theory* (St. Louis, 1972), Proceedings of Symposia in Pure Mathematics, Vol. 24, American Mathematical Society, Providence, RI, 1973, 181–193.

[46] F. J. Dyson, "Statistical Theory of the Energy Levels of Complex Systems. I," *Journal of Mathematical Physics* **3** (1962), 140–156.

[47] D. A. Goldston and H. L. Montgomery, "Pair Correlation of Zeros and Primes in Short Intervals," in *Analytic Number Theory and Diophantine Problems*, Progress in Mathematics, Vol. 70, Birkhäuser, Boston, 1987, 183–203.

[48] Z. Rudnick and P. Sarnak, "Zeros of Principal L-Functions and Random Matrix Theory," *Duke Mathematical Journal* **81** (1996), no. 2, 269–322. DOI: 10.1215/S0012-7094-96-08115-6.

[49] E. B. Bogomolny and J. P. Keating, "Random Matrix Theory and the Riemann Zeros. I. Three- and Four-Point Correlations," *Nonlinearity* **8** (1995), 1115–1131. DOI: 10.1088/0951-7715/8/6/013.

[50] E. B. Bogomolny and J. P. Keating, "Random Matrix Theory and the Riemann Zeros II: n-Point Correlations," *Nonlinearity* **9** (1996), 911–935. DOI: 10.1088/0951-7715/9/4/006.

[51] N. M. Katz and P. Sarnak, *Random Matrices, Frobenius Eigenvalues, and Monodromy*, American Mathematical Society Colloquium Publications, Vol. 45, American Mathematical Society, Providence, RI, 1999.

[52] J. B. Conrey and N. C. Snaith, "Correlations of Eigenvalues and Riemann Zeros," *Communications in Number Theory and Physics* **2** (2008), no. 3, 477–536. DOI: 10.4310/CNTP.2008.v2.n3.a1.

[53] B. Conrey and J. P. Keating, "Averages of Ratios of the Riemann Zeta-Function and Correlations of Divisor Sums," arXiv:1611.09198, 2016.

[54] J. P. Keating and Z. Rudnick, "The Variance of the Number of Prime Polynomials in Short Intervals and in Residue Classes," *International Mathematics Research Notices* **2014** (2014), no. 1, 259–288. DOI: 10.1093/imrn/rns220.

[55] M. L. Mehta, *Random Matrices*, 3rd ed., Elsevier / Academic Press, Amsterdam, 2004.

[56] P. J. Forrester, *Log-Gases and Random Matrices*, London Mathematical Society Monographs, Princeton University Press, Princeton, 2010.

[57] E. P. Wigner, "On the Statistical Distribution of the Widths and Spacings of Nuclear Resonance Levels," *Proceedings of the Cambridge Philosophical Society* **47** (1951), no. 4, 790–798. DOI: 10.1017/S0305004100027237.

[58] O. Bohigas, M. J. Giannoni, and C. Schmit, "Characterization of Chaotic Quantum Spectra and Universality of Level Fluctuation Laws," *Physical Review Letters* **52** (1984), no. 1, 1–4. DOI: 10.1103/PhysRevLett.52.1.

[59] S. M. Nishigaki, "Distributions of Consecutive Level Spacings of Gaussian Unitary Ensemble and Their Ratio: Ab Initio Derivation," *Progress of Theoretical and Experimental Physics* **2024** (2024), no. 8. DOI: 10.1093/ptep/ptae120; arXiv:2407.15704.

[60] S. M. Nishigaki, “Distributions of Consecutive Level Spacings of Circular Unitary Ensemble and Their Ratio: Finite-Size Corrections and Riemann ζ Zeros,” *Progress of Theoretical and Experimental Physics* **2026** (2026), no. 2, 023A02. DOI: 10.1093/ptep/ptag006.

V. Harmonic Analysis, Probabilistic Structures, and Basic Tools

[61] S. Bochner, *Lectures on Fourier Integrals*, Princeton University Press, Princeton, 1959.

[62] N. Wiener, “Generalized Harmonic Analysis,” *Acta Mathematica* **55** (1930), 117–258.

[63] A. Khintchine, “Korrelationstheorie der stationären stochastischen Prozesse,” *Mathematische Annalen* **109** (1934), 604–615.

[64] T. M. Apostol, *Introduction to Analytic Number Theory*, Undergraduate Texts in Mathematics, Springer-Verlag, New York, 1976.

[65] NIST Digital Library of Mathematical Functions, Chapter 25, “Riemann Zeta Function.”

VI. Work by the Author

[66] Yifei Ren, *Foundations of Mathematics: An Introduction to Generative History Theory (GHT)*, Zenodo, 2026. DOI: 10.5281/zenodo.23662772.

VII. Current Status and Historical Sources

[67] Clay Mathematics Institute, “Riemann Hypothesis,” *Millennium Prize Problems*, current problem-status page, accessed November 2026.

[68] A. Weil, “Numbers of Solutions of Equations in Finite Fields,” *Bulletin of the American Mathematical Society* **55** (1949), 497–508.

[69] P. Deligne, “La conjecture de Weil. I,” *Publications Mathématiques de l’IHÉS* **43** (1974), 273–307.

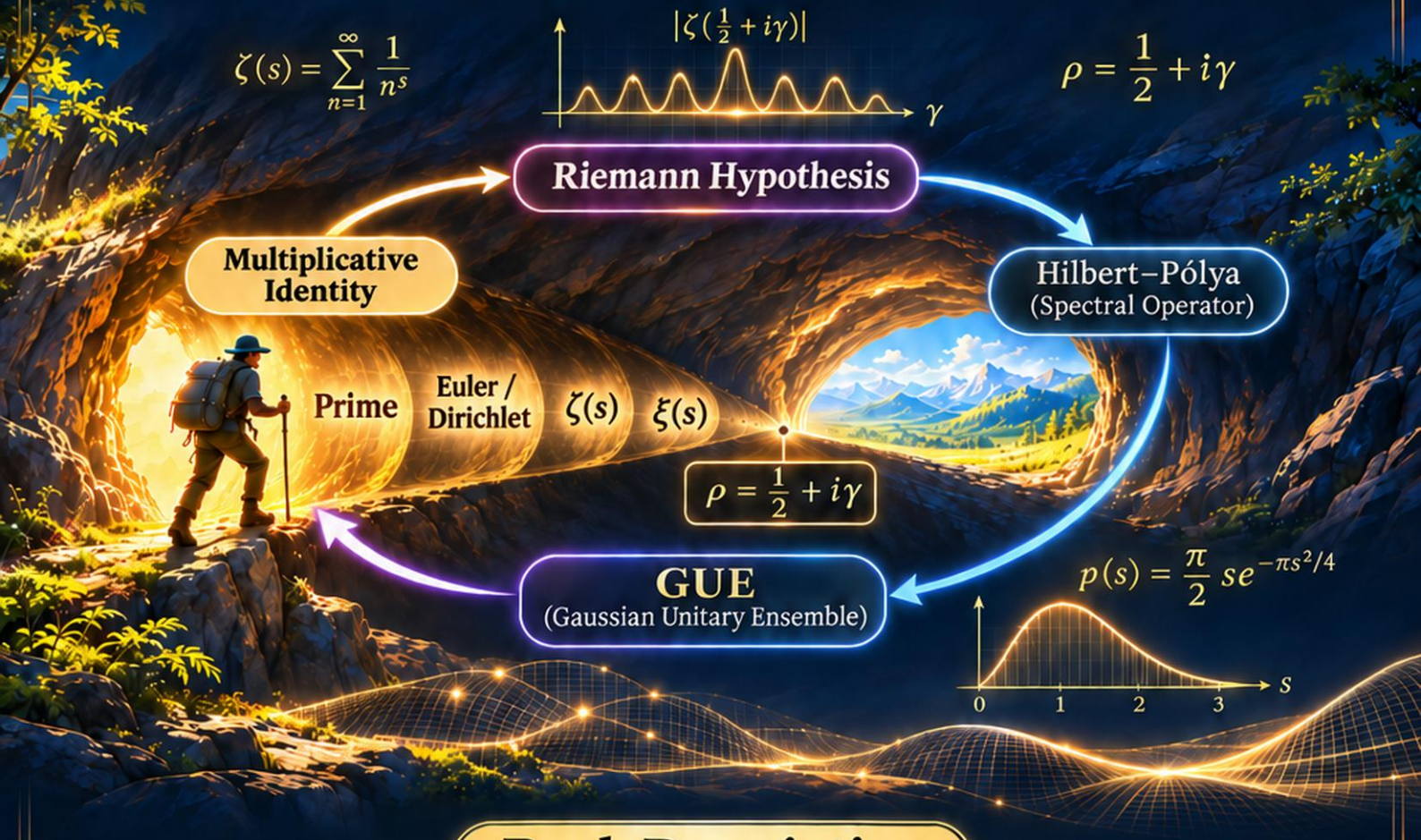
[70] H. Davenport, revised by H. L. Montgomery, *Multiplicative Number Theory*, 3rd ed., Graduate Texts in Mathematics, Vol. 74, Springer-Verlag, New York, 2000.

[71] J. Neukirch, *Algebraic Number Theory*, Grundlehren der mathematischen Wissenschaften, Vol. 322, Springer-Verlag, Berlin, 1999.

[72] L. C. Washington, *Introduction to Cyclotomic Fields*, 2nd ed., Graduate Texts in Mathematics, Vol. 83, Springer-Verlag, New York, 1997.

The Riemann Hypothesis: Proof, Spectra, and the Mathematical World Behind It

— From Multiplicative Identity and the Generalized Riemann Hypothesis to Hilbert–Pólya and GUE



Book Description

This book presents a coherent and proof-oriented framework for the Riemann Hypothesis and its generalizations, centering on multiplicative identity, spectral structure, and structural closure.

- **Proof Route for the Riemann Hypothesis:** Develops a complete proof route centered on multiplicative identity, starting from the source identity, through its compressed representation, and leading to the critical line Re $\rho = 1/2$.
- **Proof Route for the Generalized Riemann Hypothesis:** Establishes a proof route for the Generalized Riemann Hypothesis (GRH) via minimal identity transfer, extending the method to Dirichlet L-functions and broader settings.
- **Independent Spectral Route:** Constructs an independent spectral route through the Ren operator, the Riemann spectral witness, and Hilbert–Pólya ideas, linking zeros to a self-adjoint spectral framework and providing an analytic–spectral perspective complementary to the identity route.
- **Connection to GUE and the Broader Mathematical World:** Connects the spectrum to the Gaussian Unitary Ensemble (GUE), and systematically maps the broader mathematical world of the Riemann Hypothesis, including zeros, spectra, pair relations, and structural closure.

Author: Yifei Ren

Independent Researcher